Faculty of Science and Engineering

Department of Applied Geology

Evolution of the Lower Palaeozoic Nanhua Foreland Basin and Nature of the Wuyi–Yunkai Orogeny, South China

Wei-Hua Yao

This thesis is presented for the Degree of

Doctor of Philosophy

of

Curtin University

March 2014

Declaration

To the best of my knowledge and belief this thesis contains no material previously published by any other person except where due acknowledgement has been made.

This thesis contains no material which has been accepted for the award of any other degree or diploma in any university.

WEI-HUA YAO

Date: 18-03-2014

ABSTRACT

The early Palaeozoic Wuyi–Yunkai orogen in the South China Block (SCB) is > 2000 km long, and its evolution was linked to, and recorded by, the lower Palaeozoic Nanhua Basin. Understanding the orogenic processes and driving mechanism for the Wuyi–Yunkai orogeny is important for understanding the tectonic history of the SCB and its possible interactions with other continents during the early Palaeozoic, and for assessing the palaeopositions of South China during the transition from the break-up of Rodinia to the assembly of Gondwanaland. Sedimentary rocks in the Nanhua Basin may also record the nature and tectonic history of adjacent continents at the time. However, it is still debated whether the Wuyi–Yunkai orogeny represents a continent collision involving ocean closure between the Yangtze and Cathaysia blocks, or intracontinental tectonism. Equally, opinions vary regarding whether the lower Palaeozoic Nanhua Basin was a back-arc/marginal basin, retro-arc foreland basin, or a peripheral foreland basin. This thesis reports results of a combined sedimentological, stratigraphic, detrital provenance, geochronological, isotopic and geochemical study of early Palaeozoic South China to reveal the nature of the Wuyi–Yunkai orogeny, and the sedimentary and provenance evolution of the lower Palaeozoic Nanhua Basin. It further explores the tectonic relationship between the SCB and northern India during the late Neoproterozoic to early Palaeozoic.

The first mafic–intermediate volcanic succession near the edge of the Wuyi–Yunkai orogenic core was reported in this study, and it was used to explore any mantle–crust interaction during the orogeny. The volcanic succession, dated at *ca.* 435 Ma, unconformably overlies strongly deformed Cambro-Ordovician strata, but is in low-angle unconformable contact with overlying post-orogenic mid-Devonian strata. It is younger than peak-orogenic metamorphism (*ca.* 460–445 Ma) but synchronous with widespread late-orogenic granitic intrusions (*ca.* 440–415 Ma). Geochemical and isotopic results indicate that the mafic magma was likely generated from partial melting of sub-continental lithospheric mantle (SCLM), whereas the intermediate rocks were differentiated from the same mafic magma. A late-orogenic lithospheric delamination model and subsequent orogenic collapse are proposed to explain the melting of the SCLM that generated the mafic–intermediate volcanic rocks and the

widespread granitic intrusions in the orogen.

A detrital provenance analysis of Ediacaran–Cambrian sandstone/metasandstone samples in the southern Nanhua Basin revealed zircon geochronological and isotopic signatures of the source region distinctly different from the known tectonomagmatic record of the SCB, but match well with those of the Ediacaran–Cambrian clastic rocks and granitic intrusions in northern India. The SCB–northern India provenance linkage appears to have started from the Ediacaran. It is thus proposed that after breaking away from central Rodinia, the SCB collided with northern India of eastern Gondwanaland during the Ediacaran–Ordovician, causing the Bhimphedian orogeny at the northern Indian margin (the Northern Indian orogen), as well as foreland basins on both sides of the collision zone. Ediacaran–Cambrian sandstones in the southern Nanhua Basin are interpreted as foreland deposits received from the Northern Indian and other adjacent orogens.

Based on a sedimentary-stratigraphic analysis of four stratigraphic sections across the Nanhua Basin, it is interpreted that the entire lower Palaeozoic Nanhua Basin was a peripheral foreland basin which started to receive foreland deposits from the Cambrian or as early as the Ediacaran, after its *ca.* 860–600 Ma stage of continental rifting and failed rift deposition. The sedimentary evolution of the lower Palaeozoic Nanhua Basin can be subdivided into two stages: (1) The Cambrian (also Ediacaran?) to earliest-Ordovician underfilled to filled stage with shallow marine clastic deposition, fed by an exotic orogen outboard the SCB; and (2) the early-Ordovician to Silurian overfilled stage with subaerial clastic deposits, fed by the local Wuyi–Yunkai orogen in the SCB. The first stage was likely related to the Bhimphedian orogeny along the northern margin of Indian due to the SCB–northern India collision, and the second stage was related to the intraplate Wuyi–Yunkai orogeny, which was caused by the far-field stress of that collision.

A systematic detrital provenance analysis of Ediacaran–Silurian clastic samples across the entire Nanhua Basin supports a similar two-stage evolution of the Nanhua foreland basin: (1) the Ediacaran–Cambrian sediments in the Nanhua foreland basin were mainly sourced externally – northern India and adjacent orogens, and (2) the Ordovician–Silurian sediments were derived from internal sources – both locally

recycled Ediacaran–Cambrian rocks and eroded Cathaysian basement rocks. The Wuyi–Yunkai syn- to late-orogenic magmatic rocks only contributed to Silurian sediments in the basin, possibly during orogenic collapse. The upper-Ordovician to Silurian samples in northeast Yangtze, on the other hand, received higher proportions of eroded local Cryogenian rift-related magmatic rocks which were uplifted during late-Ordovician to Silurian time. Again, the first stage of sedimentation is interpreted to be related to the collisional orogeny between the SCB and northern India, and the second stage of sedimentation is interpreted to be related to the intraplate Wuyi–Yunkai orogeny in South China.

Cambrian provenance analysis further supports the idea that there was no broad ocean between the Yangtze and Cathaysia blocks since the Neoproterozoic, and that the Ordovician–Silurian Wuyi–Yunkai orogeny was an intraplate orogeny in South China. The post-kinematic lithospheric delamination of the Wuyi–Yunkai orogen led to a late orogenic collapse, which may have produced a graben (also a piggy-back basin?) within the orogenic core, receiving thick Silurian marine sedimentation in the so-called “Qinfang Tough” in the southwestern Cathaysia Block.

ACKNOWLEDGEMENTS

Almost four years ago I quit from a petroleum industry job in Beijing and travelled to Perth to start this PhD, and now it is finally finished. I owe many thanks to a large number of people who helped me on my long four-year PhD journey, but can only mention a few individuals below. To all of you, I say thank you!

First and foremost, I would like to express my sincere appreciation to my principle supervisor Prof. Zheng-Xiang Li. Thank you for your professional guidance and supervision, which has lead me into the real world of geology and taught me ways of thinking/seeing the "big pictures". As one of the top geoscientists in the world, your academic excellence has inspired me to always aim for higher standard in research. I also very much appreciate your emphasis on critical thinking, and being honest with field observations and laboratory data.

To Prof. Xian-Hua Li, thank you for your help with all things geochemical. As one of my associate supervisors, your assistance in getting me access to experimental facilities and commenting on my manuscripts have been critical for timely data acquisition and publication of my research. To my other associate supervisor Prof. Bryan Krapez, thank you for teaching me sedimentology in the field as well as data interpretation.

To all Chinese academic staff that helped me through my PhD project, I would have not accomplished it without your encouragement and assistance during the fieldtrips and in the laboratories. Thank you Prof. Wu-Xian Li, you have been very helpful and patient with me during my fieldtrips and lab work. Thank you Prof. Jin-Hui Yang, Dr. Li Su, Dr. Yueheng Yang, Dr. Qiuli Li, Dr. Yafei Wang, Hongxia Ma, Yu Liu, Guoqiang Tang, Yuya Gao, and the many more whose names I could not list here, all your help made my staying in Beijing labs very efficient and enjoyable.

Thanks to all Curtin staff and fellow PhD students that helped me to survive the sometime intense academic stress in a not-so-familiar world. In particular, I express my sincere thanks to Prof. Chris Elders, who helped me during my final days of

thesis writing. Thanks are also delivered to Prof. Simon Wilde, Dr. Xuan-Ce Wang, Dr. Katy Evans, Dr. Leslie Almberg and Dr. Milo Barham, who helped with manuscript revision and editing. To my fellow PhDs at Curtin, forgive me for not listing all your names here because of limited pages, but your unselfish assistance through these years have been indispensable to me for both the pursuing the research degree and for living an enjoyable life here. Many thanks also go to the rest of the Department of Applied Geology — you all have been so great. Appreciation also goes to Prof. Galen Halverson from McGill University Canada, for help on editing my manuscript during his stay in Perth.

Living abroad and being so far away from home has made this PhD period a challenge for me sometimes, and life has changed much since I first stepped onto this mysterious continent. But I feel lucky to be supported by such a great family who helped me to survive all the ups and downs of my age. Dad, you have always been my rock even though I did not follow your advice to get a job soon after my first degree. Mum, you are a traditional Chinese mother who always cares about my life beyond academia, and please trust me that I will live the life as you like to see soon.

My PhD research has been jointly supported by the Chinese Scholarship Council (CSC) and a Curtin International Postgraduate Research Scholarship (CIPRS). I also received funding support from The Institute for Geoscience Research (TIGeR) at Curtin University. I would therefore like to thank them supporting me.

List of Publications Included as Part of this Thesis

This thesis compiles a collection of five research papers that were either published, in press or nearly ready for submission at the time of writing this document. The objectives and relationships amongst the different papers are described in the introductory chapter. The final chapter summarises the five papers and places them into a coherent wider context.

The five research papers contained within this thesis are given below.

Yao, W.H., Li, Z.X., Li, W.X., Wang, X.C., Li, X.H., and Yang, J.H., 2012. Post-kinematic lithospheric delamination of the Wuyi–Yunkai orogen in South China: Evidence from *ca.* 435 Ma high-Mg basalts. Lithos 154, 115–129.

Yao, W.H., Li, Z.X., Li, W.X., Li, X.H., and Yang, J.H., 2014. From Rodinia to Gondwanaland: a tale of detrital zircon provenance analyses from the southern Nanhua Basin, South China. American Journal of Science 314, 278–313.

Yao, W.H., and Li, Z.X., 2014 (to be submitted). Stratigraphic history of the lower Palaeozoic Nanhua foreland basin in South China: Response to two successive orogenies.

Yao, W.H., Li, Z.X., Li, W.X., Su, L., and Yang, J.H., 2014 (to be submitted). Detrital provenance evolution of the lower Palaeozoic Nanhua foreland basin, South China.

Yao, W.H., Li, Z.X., and Li, W.X., 2014 (in press). Was there a Cambrian ocean in South China? – Insight from detrital provenance analyses. Geological Magazine, doi: 10.1017/S0016756814000338

The formatting of each chapter within this thesis varies according to the requirements and formatting guidelines of each individual journal and this thesis. As a result of this, there is also a degree of repetition throughout.

Statement of Contributions of Others

This thesis has been supported by the Department of Applied Geology, Curtin University. The individual chapters of this thesis, notably those comprising the published or to-be-submitted papers listed above, were conducted under the supervision of Prof. Zheng-Xiang Li at Curtin University. Fieldtrips of stratigraphic logging, sample collection, laboratory sample preparation, mineral separation, data acquisition and processing were undertaken through collaboration between Curtin University, Guangzhou Institute of Geochemistry (Chinese Academy of Sciences), Institute of Geology and Geophysics (Chinese Academy of Sciences), and China University of Geosciences. As the author of this thesis, and the first author of all published or in-preparation manuscripts contained within, I declare that I have been primarily responsible for all subsequent research, analysis, data interpretation and writing up of these papers/chapters. A written statement of co-author contributions is provided in Appendix E at the end of this thesis.

WEI-HUA YAO

Date: 18-03-2014

TABLE OF CONTENTS

LIST OF FIGURES

CL images have diameters of ~40 μm or ~25 μm, representing the sites for the LA-ICP-MS analyses and SHRIMP analyses, respectively. a: andesitic sample 10GD23-1 LA-ICP-MS age plots; b: andesitic sample 10GD23-1 SHRIMP age plots; c: dacitic sample 10GD25 LA-ICP-MS age plots; d: dacitic sample 10GD25 SHRIMP age plots.

Figure 2.3. (a) Cumulative plot of zircon Hf model ages for samples 10GD23-1 (andesite) and 10GD25 (dacite). (b) Plot of *in-situ* zircon $\varepsilon_{Hf}(t)$ versus $\delta^{18}O$ values for samples 10GD23-1 (andesite) and 10GD25 (dacite) from the Chayuanshan volcanic succession, northern Guangdong.

Figure 2.4. Plot of the Chayuanshan volcanic samples in the $Zr/TiO_2 \times 0.0001$ versus Nb/Y diagram (Winchester and Floyd, 1976).

Figure 2.5. Primitive mantle-normalized trace element spider diagrams for the 10GD23 (andesite) and 10GD25 (dacite) sample groups (a), and the 10GD21 (basalts) sample group (b); Chondrite-normalized REE spider diagrams for the 10GD23 and 10GD25 sample groups (c) and the 10GD21 sample group (d). Normalization values for the primitive mantle and chondrite, as well as values for OIB, N-MORB and E-MORB, are from Sun and McDonough (1989).

Figure 2.6. Bivariation plots of Sm/Nd (a), La/Sm (b), $\varepsilon_{Nd}(t)$ (e), and Zr/Nb (f) versus Nb/La, respectively, and plots of Nb/La vs. MgO (c) and Nb/U vs. SiO_2/MgO (d) for samples from the Chayuanshan volcanic succession.

Figure 2.7. Variations diagrams of selected major oxides MgO and FeO^T versus SiO_2 (wt.%) (a–b), and bivariation plots of trace element Ni (c), Cr (d), Sc (e), CaO/Al_2O_3 (f), SiO_2 (g), and FeO^T (h) versus Mg#. $Mg^{\#}=100\times Mg/(Mg+Fe^{2+})$, assuming $Fe^{2+}/Fe_{total}=0.85$, cation ratio.

Figure 2.8. Plot of La/Nb versus $\varepsilon_{Nd}(435\ Ma)$ of the Chayuanshan volcanic samples. The asthenosphere (Basin and Range, USA) area is modified after DePalo and Daley (2000). The South China SCLM (sub-continental lithospheric mantle) area is after Fang et al. (2002) and Zhang et al. (2008).

and Permian samples from the Tethyan Himalaya. (C) Enlarged plot of zircon $\varepsilon_{Hf}(t)$ values versus U-Pb ages as in (B) for the 900–400 Ma range, where the dashed arrow indicates more negative $\varepsilon_{Hf}(t)$ values after *ca.* 580 Ma. The depleted mantle (DM) and new continental crust (NCC) evolution lines were extrapolated after Griffin and others (2000) and Dhuime and others (2011), respectively. Light grey bands in (A)-(B) highlight potential episodes of new continental crustal growth. Potential crustal evolution lines at 3.0 Ga, 2.5 Ga and 1.0 Ga were calculated for the mean continental crust of $^{176}Lu/^{177}Hf$ value of 0.015 after Griffin and others (2000).

Figure 3.5. Q-F-L diagram (parameters after Dickinson, 1970, 1985; Dickinson and others, 1983) of Cambrian sandstone/metasandstone samples from Guangdong, western Cathaysia, with a photomicrograph of each of the sample. Sample (1) 10GD16, (2) 10GD17 and (3) 10GD19 are from sandstone samples from the Oujiadong section of the northern Guangdong Province, whereas samples (4) 10GD48 and (5) 10DG49-1 are from meta-sandstone samples from southwestern Guangdong Province (see figure 3.1 for sample locations).

Figure 3.6. Detrital zircon age spectra of Cambrian sandstone samples in different localities in the western Cathaysia Block (see text for details). n = total number of analyses. All zircon U-Pb ages are within 90% concordance.

Figure 3.7. Summary provenance plots of U-Pb zircon age spectra of sedimentary rocks in Cathaysia, and comparisons with both the basement age spectra and provenance data for western Laurentia. (A) Western Cathaysia Cambrian strata (this study; Wang and others, 2010b; Wu and others, 2010); (B) Western Cathaysia Ediacaran strata (Yu and others, 2008, 2010; Wu and others, 2010); (C) Mid-Neoproterozoic Nanhua Rift Basin (Wang and others, 2010a; Wang and others, 2012a); (D) Eastern Cathaysia late Palaeozoic to Mesozoic strata (X.H. Li and others, 2012; Yao and others, 2012); (E) Eastern Cathaysia Neoproterozoic metasediments and Precambrian crystalline basement rocks (X.H. Li, 1997; Z.X. Li and X.H Li., 2007; Wan and others, 2007; Liu and others, 2009; Yu and others, 2009; Z.X. Li and others, 2010); (F) Western Cathaysia Mesoproterozoic metasediments and Precambrian crystalline basement rocks (Z.X. Li and others, 2002, 2008a); (G) Western Laurentia (Smith and Gehrels, 1994; Stewart and others, 2001;

Vega-Granillo and others, 2008). N = number of samples, n = total number of analyses. All zircon U-Pb ages are within 90% concordance.

Figure 3.8. Provenance variations of Ediacaran–Cambrian sedimentary rocks along the northern margin of India, and comparisons with provenance results from possible adjacent continents/terranes in Gondwanaland, Age spectra in (A)–(H) correspond to data points A–H in the location cartoon (I), where data points C_1–C_3 and D represent western North Indian margin, data points E represent central North Indian margin, and data points F_1 and F_2 represent eastern North Indian margin. Sources of detrital zircon age spectra: A — this study, Yu and others (2008, 2010), Wang and others (2010b) and Wu and others (2010); B — Dong and others (2011), Pullen and others, (2011) and Zhu and others (2011); C_1 — Myrow and others (2010); C_2 — Myrow and others (2010) and Webb and others (2011); C_3 — Myrow and others (2010); D — Myrow and others (2010); E — Martin and others (2005) and Gehrels and others (2011); F_1 — Myrow and others (2010) and Gehrels and others (2011); F_2 — McQuarrie and others (2008), Myrow and others (2010) and Hughes and others (2011); G — Leier and others (2007), Gehrels and others (2011) and Zhu and others (2011); H — Cawood and Nemchin (2000) and Veevers and others (2005). Inset in (I) shows palaeocurrent directions, with data sources being as follows: (1) Tethyan Himalaya, lower–middle Cambrian rocks in the Spiti and Zanskar valleys (Myrow and others, 2006a, 2006b; Bagati and others, 1991); (2) Tethyan Himalaya, lower and upper Cambrian rocks in the Zanskar Valley (Garzanti and others, 1986); (3) Greater Himalaya, lower Cambrian rocks at Keylong (Draganits, 2000); (4) Lesser Himalaya, Ediacaran rocks at Simla (Valdiya, 1970). The positions of South Qiangtang and Lhasa terranes relative to Indo-Australia in Gondwanaland, as shown in (I), follow that of Zhu and others (2011).

Figure 3.9. Palaeogeographic reconstructions showing palaeoposition of the SCB (A) before the break-up of Rodinia in the mid-Neoproterozoic (750 Ma), (B) after Rodinia break up, but prior to its collision with India during the assembly of Gondwanaland (635 Ma), (C) beginning of collision with NW India at *ca.* 580 Ma during the assembly of Gondwanaland, and (D) colliding with India to become part of Gondwanaland (515 Ma). Active orogens, and speculated drainage directions for Ediacaran–Cambrian time, are shown (see text for detailed discussion).

Palaeogeographic reconstructions follow that of Zhu and others (2012) for relative positions of the Lhasa and Qiangtang terranes, and Z.X. Li and others (2013) for the rest. The cartoon palaeo-drainage patterns are modified after Myrow and others (2010). North China is notional shown close to northern Australia in the Cambrian because of some bioprovince and detrital zircon provenance similarities (for example, McKenzie and others, 2011), but there is no evidence to suggest that it was a coherent part of Gondwanaland at that time (for example, Z.X. Li and Powell, 2001; Cocks and Torsvik, 2013).

Figure 4.1. (A) A simplified regional map of the South China Block (SCB), highlighting the regional extent of the lower Palaeozoic Wuyi–Yunkai orogen including the distribution of metamorphic rocks and granites, interpreted early Palaeozoic structural trends and extent of the remnant Nanhua Basin. The inset shows the Cathaysia and Yangtze blocks as parts of the SCB. (B) Distribution of Palaeozoic sedimentary outcrops in the SCB, highlighting the Cambrian, Ordovician and Silurian rocks. Localities of the four logged stratigraphic sections are marked by yellow stars.

Figure 4.2. (A) Regional geological map of central South China highlighting the early Palaeozoic sedimentary outcrops and granitic intrusions. (B) Geological map of the Rongxian county, showing a part of the Yulin Section; (C) Geological map of the Cenxi county, showing a part of the Yulin Section; (D) Geological map of the Beiliu county, showing a part of the Yulin Section; (E) Geological map of the Shaoguan Section; (F) Geological map of the Dongkou Section; (G) Geological map of the Zhangjiajie Section (revised after RGMRGD, 1962; RGMRGX-a, 1966; RGMRGX-b, 1968; RGMRHN-a, 1965; RGMRHN-b, 1968).

Figure 4.3. Synthesized early Palaeozoic stratigraphic chart of the Yulin, Shaoguan, Dongkou and Zhangjiajie sections in the South China Block (revised after RGMRGD, 1962; RGMRGX-a, 1966; RGMRHN-a, 1965, RGMRHN-b, 1968).

Figure 4.4. Cambro-Silurian lithostratigraphic column of the Yulin Section. Lithologic scale: m = mudstone/shale, ss = siltstone, fs = fine-grained sandstone, ms = medium-grained sandstone, cs = coarse-grained sandstone, g =

gravel/conglomerate. Field photos: (A) medium-grained sandstone beds in lower Ordovician strata, with a hammer (30 cm long) for scale; (B) rhythmical intercalations of thick-bedded fine sandstone and thin-bedded shale in the lower Ordovician strata; (C) muddy conglomerates with oriented pebbles in the lowest Silurian strata with a pen (15 cm long) for scale; (D) folded, thin-layered shales in the mid- to upper-Silurian strata, with a hammer (30 cm long) for scale.

Figure 4.5. Cambro-Ordovician lithostratigraphic column of the Shaoguan Section. Lithologic scale and information are the same as in Figure 4.4.

Figure 4.6. Cambro-Silurian lithostratigraphic column of the Dongkou Section. Lithologic scale and information are the same as in Figure 4.4. Field photos: (A) lower Cambrian horizontal-laminated black carbonaceous shale, with a pen (15 cm long) for scale; (B) thick-bedded fine sandstone intercalated with thin-bedded yellowish shale packages in mid-Ordovician strata; (C) a series of flute casts on sandstone surface with a notebook (18 cm in length) for scale, and (c) an enlarged flute cast, with a hammer (30 cm long); (D) Asymmetrical ripple marks on the topmost Silurian sandstones with a notebook (18 cm long) for scale.

Figure 4.7. Cambro-Silurian lithostratigraphic column of the Zhangjiajie Section. Lithologic scale and information are the same as figure 4.4. Field photos: (A) lower-Ordovician crystalline limestone, with a pen (15 cm long) for scale; (B) lower-Silurian green and purple shale interlayers; (C) thick- to medium-bedded fine sandstones intercalated with thin-layered shales; (D) mid-Devonian brick-red fine-grained quartz sandstone disconformably overlying Silurian sandstones. The notebook is 18 cm in length for scale.

Figure 4.8. Palaeogeographic maps of the South China Block showing the evolution of the Nanhua foreland basin and the Wuyi–Yunkai orogen through the (A) mid-Cambrian, (B) mid-Ordovician and (C) early-Silurian (revised after Liu and Xu, 2004).

Figure 4.9. Time-space diagram of the Cambro–Silurian South China Block, covering the Zhangjiajie, Dongkou, Yulin and Shaoguan sections across the Nanhua

Figure 5.6. Plots of zircon $\varepsilon_{Hf}(t)$ values versus U–Pb ages from (a) Cambrian, (b) Ordovician and (c) Silurian sandstone samples in the Nanhua foreland basin. Data sources for published Hf isotopic data: (a) Xu et al. (2014); Yao et al. (2014a); (b) Yao et al. (2011). The depleted mantle (DM) and new continental crust (NCC) evolution lines were extrapolated after Griffin et al. (2000) and Dhuime et al. (2011), respectively.

Figure 5.7. Relative probability plots of detrital zircon U–Pb ages (with concordance of 90–110%) for sample subgroup 2-3 from the Nanning–Yulin area. Samples 11FS-1, -3, -6 and -11 are from Xu et al. (2014).

Figure 5.8. Palaeogeographic maps of South China in seven time intervals (revised after Wang, 1985; Liu and Xu, 1994) and relative probability plots of detrital zircon U–Pb ages from corresponding strata from the four sample groups: (a) – Ediacaran (late-Neoproterozoic); (b) – early-Cambrian; (c) – mid- to late-Cambrian; (d) – early-Ordovician; (e) – mid- to late-Ordovician; (f) – early-Silurian; (g) – mid- to late-Silurian. U–Pb ages are within 90–110% concordance, and N = number of samples, n = numbers of concordant analyses. A compilation plot of age constitutes from Cathaysia basement rocks and pre-Devonian magmatic events is presented for provenance comparison, and the data are referred from Li, 1997, Wan et al. (2007), Li et al. (2002, 2003b, 2008a, 2008b, 2008c, 2010a), Liu et al. (2009), Yu et al., (2009), Wang et al. (2006, 2007a, 2007b; 2011), and Yao et al. (2012).

Figure 6.1. (a) Distribution of Cambrian strata in the South China Block, highlighting the inferred boundary between the Yangtze and Cathaysia blocks. JSF = the Jiaoshan–Shaoxing Fault. (b) Geological map of central South China, highlighting three Cambrian sampling regions from central Yangtze, southeastern Yangtze and northern Cathaysia. Red stars are samples from this study, and white stars are samples reported in previous studies.

Figure 6.2. (a)–(b) Palaeogeographic maps of the South China Block (revised after Liu & Xu, 1994): (a) early Cambrian, (b) middle- to late-Cambrian. (c)–(e) Stratigraphic columns of Cambrian strata and sandstone samples from (c) the Xinhuang section of central Yangtze (RGMRHN-b, 1972), (d) the Xinning section of

LIST OF TABLES

CHAPTER 1 INTRODUCTION

1.1 Pre-Devonian Geology of the South China Block: The Nanhua Basin and the Wuyi–Yunkai Orogeny

The South China Block (SCB) in East Asia is bounded by the North China Block to the north, the Tibet Plateau to the west, the South China Sea to the south and the Pacific Ocean/East China Sea to the east (Figure 1.1). It consists of the Yangtze Block in the northwest and the Cathaysia Block in the southeast, with the present boundary between the two blocks in eastern South China running approximately along the northeasterly trending Jiangshan–Shaoxing fault (Figure 1.2). However, the southwestern extension of the boundary is unclear due to poor exposure and younger tectonic modifications (e.g., Ren, 1991; Chen, 2004; Li et al., 2010a).

1.1.1 Pre-Ediacaran Geology of the South China Block

The Yangtze and Cathaysia blocks exhibit different pre-Ediacaran crustal growth histories with contrasting crystalline basement rocks. The Yangtze basement consists predominantly of Proterozoic rocks with minor outcrops of Archean rocks found in the Kongling Complex in northern Yangtze (the Kongling "Group", dated at *ca.* 3.3–3.2 Ga and *ca.* 2.95–2.90 Ga; Qiu et al., 2000; Zheng et al., 2006; Jiao et al., 2009; Gao et al., 2011). Along the southeastern Yangtze margin, scattered outcrops of Mesoproterozoic metasedimentary rocks ($\leqslant$1.53 Ga) that experienced 1.04–0.94 Ga metamorphism/reworking (Li et al., 2007), and some 1.16–0.88 Ga magmatic rocks (Ye et al., 2007; Li et al., 2008a, 2009, 2013) are present. More widespread outcrops of *ca.* 1.7–0.9 Ga volcanic and sedimentary rocks, or their metamorphosed equivalents, are found along the southwestern Yangtze margin (Li et al., 2002; Greentree et al., 2006; Greentree and Li, 2008; Sun et al., 2009; Zhao et al., 2010). Widespread mid- to late-Neoproterozoic igneous rocks (860–750 Ma) and volcaniclastic successions are well developed in rift basins along the Yangtze margins (e.g., Zhou et al., 2002a, 2002b, 2006; Li et al., 2003a, 2003b; Wang et al., 2006; Li et al., 2010b).

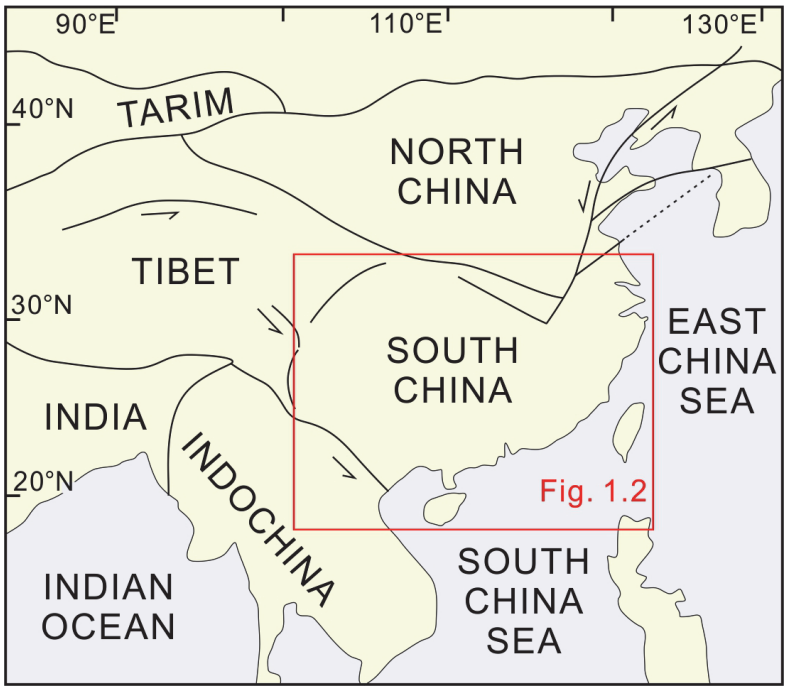

Figure 1.1. A sketch map showing major tectonic units in East Asia and the present geographical position of the South China Block.

The Cathaysia Block has less Precambrian basement exposed, with most regions covered by Phanerozoic (particularly Mesozoic) sedimentary and/or volcanic rocks. Although Archean zircons have been reported from either Cathaysian sedimentary rocks (e.g., Li, 1997; Wan et al., 2007; Xu et al., 2007; Yu et al., 2009; Li et al., 2010a; Yao et al., 2011) or as xenocrysts in volcanic rocks (Zheng et al., 2011), no Archean rocks have been identified so far. The oldest known crystalline basement rocks are the *ca.* 1.89–1.77 Ga granites and amphibolite facies metamorphic rocks in western Zhejiang and northwestern Fujian Provinces in the northeast part of Cathaysia (Li, 1997; Li and Li, 2007; Xiang et al., 2008; Zeng et al., 2008; Yu et al., 2011). On Hainan Island in southwestern Cathaysia (Figure 1.2), the known Precambrian basement rocks include the *ca.* 1.43 Ga Baoban Complex gneissic granitoids, adjacent coeval Shilu Group metavolcaniclastic succession and the overlying *ca.*1.0 Ga Shihuiding Formation metasedimentary rocks (Ma et al., 1998; Li et al., 2002, 2008b). Mid- to late-Neoproterozoic (860–750 Ma) bimodal magmatic rocks and volcaniclastic successions (e.g., Li et al., 2005; Shu et al., 2011) are also widely exposed on the Cathaysian side of the mid-Neoproterozoic Nanhua rift basin (Figure 1.2).

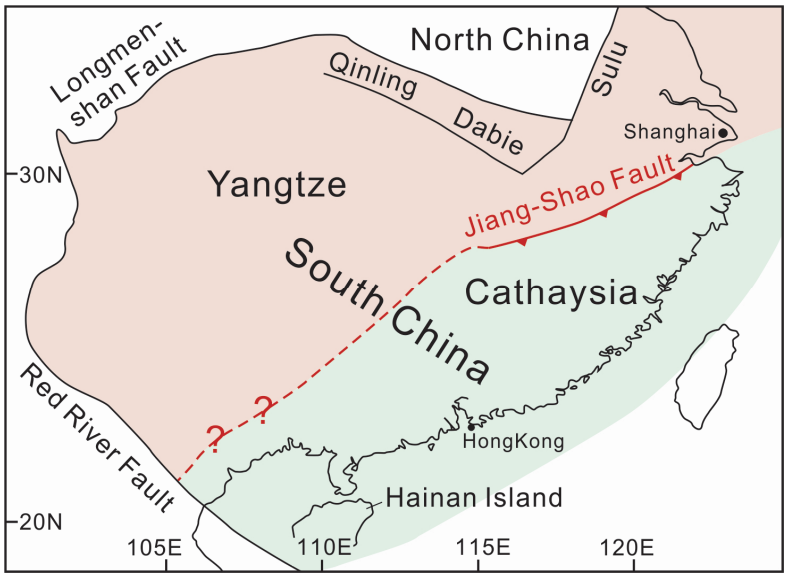

Figure 1.2. A sketch map showing the relationship between the Yangtze and Cathaysia blocks in South China.

1.1.2 Models for the Amalgamation of the South China Block

There has been an ongoing debate regarding the formation and evolution of the South China Block. The research can be divided into two periods: before 1990s and since 1990s.

Before 1990s, tectonic models regarding the formation of the SCB can be generally called the "Phanerozoic ocean" models proposed by Shui (1988) and Hsü et al. (1988; 1990, 1994). These models suggest that there was an ocean between the Yangtze and Cathaysia blocks during late Precambrian to earliest Palaeozoic (Figure 1.3a-c) (Shui, 1988) or until mid-Mesozoic (Figure 1.3d-e) (Hsü et al., 1988, 1990). Hsü and co-workers considered that the collision of the Yangtze and Cathaysia blocks which led to the ocean closure was a two-plate Alps-style collision, and the ocean was closed during the Jurassic (Figure 1.3e) (Hsü et al., 1988, 1990, 1994). This model has largely been discarded by the research community because the key argument in his model, the existence of a Mesozoic "Banxi mélange", was later proven to be late Precambrian in age. Nonetheless, that model was adopted by some subsequent workers (e.g., Xiao and He, 2005; Chen et al., 2006). Shui (1988), on the other hand, suggested that the Yangtze and Cathaysia blocks first amalgamated at their eastern ends with a remnant ocean open to the west (Figure 1.3a). Further amalgamation totally closed the ocean during late Ordovician to Silurian and caused intense

deformation and widespread metamorphic events in the region (Figure 1.3b–c) — traditionally called the "Caledonian" orogeny (Huang et al., 1980; Shui, 1988, Ren, 1991). This model was later adopted by Liu and Xu (1994). However, so far no evidence has been found for the existence of such an ocean or an Ordovician–Silurian ocean closure.

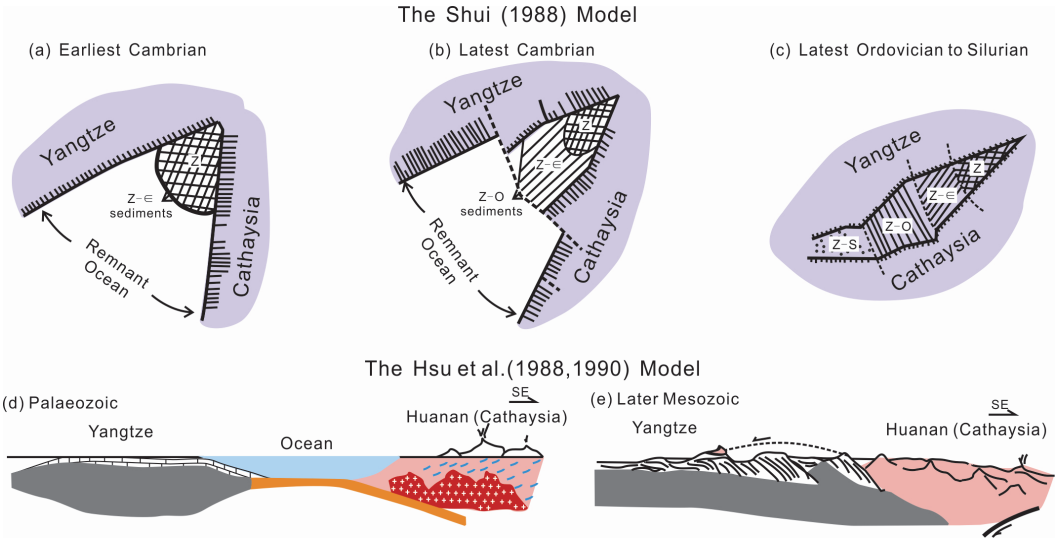

Figure 1.3. Schematic diagrams showing the two "Phanerozoic ocean" tectonic models for South China (revised after Hsü et al., 1988, 1990; Shui, 1988).

After the 1990s, many new studies, aided by high-precision geochronological and geochemical data, continued this scientific debate. Although most researchers now accept a Precambrian amalgamation of the SCB, there are still two main schools of thoughts. One suggests that the Cathaysia and Yangtze blocks collided between 1100 and 900 Ma (e.g., Li et al., 2002, 2008c, 2009), whereas the other suggests that the collision did not occur until 820–750 Ma (Zhou et al., 2002a; 2002b; Wang et al., 2004). This PhD thesis is primarily concerned with events after the Precambrian formation of the SCB, and will therefore not elaborate more on the aforementioned debate regarding the precise age of the amalgamation.

The presence of major Neoproterozoic continental rifting systems in South China after its amalgamation has long been recognized (e.g., Dong and Liu, 1991). Li and colleagues (Li, 1998; Li et al., 1999; Wang and Li, 2003) formalize the geographic position, geometry and evolution history of the rift basin that developed on top of the late Precambrian orogen between the Cathaysia and Yangtze blocks, and named it the Nanhua Rift. They argued that the Nanhua rift basin was a failed rift active between

>820 Ma to *ca.* 750 Ma. The Nanhua failed rift basin was eventually turned into a foreland basin (Figure 4.1a) during the late Ordovician–Silurian "Caledonian" orogeny (Li, 1998; Wang and Li, 2003), which Li et al. (2010a) renamed the Wuyi–Yunkai orogeny. This orogeny was an intense tectonic event that influenced much of the Cathaysia Block. Although many researchers (e.g., Li, 1998; Li et al., 2010a; Charvet et al., 2010) discussed the possibility that the Nanhua foreland basin could also had been a retro-arc foreland basin (Liu and Xu, 1994) before it was turned a peripheral foreland basin, no early Palaeozoic arc or arc-signaled rock has been found between the Yangtze and Cathaysia blocks. Little systematic analysis has been conducted on the stratigraphic and sedimentary evolution of the early Palaeozoic Nanhua basin, which would have kept clues regarding the nature of this basin and the evolution history of the Wuyi–Yunkai orogeny.

The early Palaeozoic Wuyi–Yunkai orogeny stretches for ~2000 km in a northeasterly direction (Ren et al., 1997; Li et al., 2010a). It could have extended as far as the Korean Peninsula (Kim et al., 2006) and to the Indochina block (Roger et al., 2007). It was firstly recognized because of the existence of an angular unconformity between deformed Silurian and older strata and overlying Devonian and younger strata in the southeastern part of South China (Huang et al., 1980; Liu and Xu, 1994; Li et al., 2010a). This orogeny produced voluminous early Palaeozoic magmatic and metamorphic rocks, and left strong tectonic deformation on the thick sedimentary and volcaniclastic cover successions in the Cathaysia Block and the southeastern Yangtze Block (Huang et al., 1980; Ren, 1991). The Wuyi–Yunkai orogeny was traditionally regarded as being active in late Ordovician–Silurian (Liu and Xu, 1994), while recent metamorphic and petrogenetic analyses led Li et al. (2010a) to conclude that it occurred between middle Ordovician (>460 Ma) and latest Silurian (415 Ma). However, Li et al.'s (2010) work were unable to provide a precise age constraint on the prograde stage of the metamorphism during the onset of the orogeny, which left the initiation time of the orogeny an open question. Furthermore, geodynamic mechanism for the Wuyi–Yunkai orogeny is also a fundamental question yet to be satisfactorily answered.

This study is thus designed to answer the following scientific questions. (1) When did the Wuyi–Yunkai orogenic event start and what geodynamic mechanism

generated this orogeny? (2) What type of basin was the lower Palaeozoic Nanhua Basin, and how did the basin evolved in terms of stratigraphy and sedimentary evolution, detrital provenance evolution? (3) Was there an ocean between the Yangtze and Cathaysia blocks in the early Palaeozoic? (4) Where was the South China Block located during the assembly of Gondwanaland?

1.2 Objectives

This thesis aims at the following objectives:

(1) To understand the nature of the Wuyi–Yunkai orogeny

In this study, volcanic and volcaniclastic rocks will be examined among lower Palaeozoic clastic strata. Such volcanic rocks probably represent syn-orogenic magmatism during the Wuyi–Yunkai orogeny, and would thus provide precise zircon U–Pb ages for the magmatic events related to the orogeny. Hf–O isotope and geochemical characteristics of the volcanic rocks will help to define chemical compositions of primary melts, thus further determine the source and physical-chemical conditions of the melts, possibly leading to new understandings regarding the geodynamics of the Wuyi–Yunkai orogeny.

(2) To characterize the sedimentary evolution of the lower Palaeozoic Nanhua Basin as a record of the Wuyi–Yunkai orogeny

The Nanhua Basin once covered much of the Cathaysia Block and the southeastern Yangtze Block. Because of the intense deformation, variable metamorphism and erosion of the strata on the Cathaysia side of the basin, the currently preserved strata represent a rather incomplete record of the basin history. Although the basin is generally thought to be a foreland basin, it is unclear if it was also a back-arc basin at the same time, or even once an oceanic basin (e.g., Pan, 1984; Guo et al., 1989). This study will focus on stratigraphic correlation across the basin, documenting the variations in strata thickness, compositions and grain sizes, and sedimentary structures in time and space.

(3) To characterize the provenance evolution of the lower Palaeozoic Nanhua Basin

Besides the sedimentary evolution, provenance evolution is another important aspect of basin analysis to reveal the nature of the lower Palaeozoic Nanhua Basin. Sandstone samples were collected across the basin, from Cambrian strata to Silurian strata. This study will establish a temporal and spatial framework of provenance evolution for the basin. Combined with palaeogeographic maps of South China, this study will explore variations in the provenance during depostion of the Nanhua Basin strata, which presumably reflect the evolution of the Wuyi–Yunkai orogeny.

(4) To determine the relationship between the Yangtze and Cathaysia blocks in the early Palaeozoic, and to verify whether an ocean existed between them

Some previous workers thought that there was an early Palaeozoic ocean between the Yangtze and Cathaysia blocks (Shui, 1988; Xu and Qiao, 1989; Liu and Xu, 1994; Xu et al., 1996; Chen et al., 2006). Debates on the existence of such an ocean have been going on for decades. This project will use provenance analysis of Cambrian sandstones on both sides of the proposed ocean, to test whether there was once a wide ocean (thus a barrier for clastic sediments) between the two blocks.

(5) To understand the position of the South China Block during the breakup of the Neoproterozoic supercontinent Rodinia and the assembly of Gondwanaland

This study will compare provenance analysis results of the SCB, along with other geotectonic records, with that of other continents, particularly the margin of eastern Gondwanaland. The aim is to explore the roles that the SCB played during the global transition from the breakup of the Neoproterozoic supercontinent Rodinia and the assembly of Gondwanaland. This will help to answer the questions of (a) the position of South China in Rodinian, (b) whether South China was a part of Gondwanaland, and (c) what drive the early Palaeozoic Wuyi–Yunkai orogeny in South China.

1.3 Research Methods

This thesis is based on extensive field work and laboratory analyses.

1.3.1 Field work

Geological fieldwork forms the foundation of this study and six field excursions with a total of 66 days were spent in the field. Tasks for the fieldwork include stratigraphic logging, sedimentary structures analysis, palaeocurrent measurements and collecting sandstone/volcanic rock samples. To study the evolution of the lower Palaeozoic Nanhua Basin, four representative stratigraphic sections have been logged using compasses and meter sticks; sandstone/metasandstone samples were collected for provenance analysis; volcanic samples were collected for geochronological and geochemical analyses.

During stratigraphic logging, detailed clastic grain sizes, lithologic colours, bed thicknesses and sedimentary structures were documented. Palaeocurrent data were measured on structures of trough cross-bedding, planar cross-bedding, gutter cast and ripple marks. Basin geometry was constrained by analysing facies patterns of lower Palaeozoic sedimentary strata.

Cambrian–Silurian sandstone samples were collected from the four different sections for the analysis of basin-wide provenance changes within time. Provenance results of the Cambrian sandstone samples across the Yangtze–Cathaysia boundary were also used to test the existence of a Cambrian ocean as proposed by some researchers. Early Palaeozoic volcanic rocks were sampled in the core zone of the Wuyi–Yunkai orogenic core to analyse the nature of the orogeny.

1.3.2 Laboratory studies

Laboratory studies include rock crushing, thin-section preparation, mineral separation and extraction, reflect-light and transmitted-light imaging of zircons by optical microscope, cathodoluminescence (CL) imaging of zircons by SEM (Scanning Electron Microscopy), LA-ICP-MS (Laser Ablation Inductively Coupled

Plasma Mass Spectrometry) zircon U–Pb dating, SHRIMP (Sensitive High Resolution Ion MicroProbe) zircon U–Pb dating, Cameca IMS-1280 SIMS zircon U–Pb dating and oxygen isotope analysis, and LA-MC-ICP-MS (Multi-Collector Inductively Coupled Plasma Mass Spectrometry attached with a laser ablation system) zircon Hf isotope analysis. Additional geochemical analyses were conducted on volcanic samples, including loss on ignition (LOI) determination, major element determination by XRF (X-ray Fluorescence Spectrometer), trace element determination by ICP-MS (Inductively Coupled Plasma Mass Spectrometry), Sr–Nd isotope determination by MC-ICP-MS (Multi-Collector Inductively Coupled Plasma Mass Spectrometry). Detailed analytical procedures and facilities used are given in the "Analytical Methods" sections of Chapters 2, 3, 5 and 6.

1.4 Thesis Structure

This thesis starts with an introduction (Chapter one) that reviews the geological settings of the early Palaeozoic South China Block and history of the Precambrian crystalline basements, raises scientific questions that this study aims to address, and outline the major approaches taken. It is followed by Chapters two, three, four, five and six, each consisting of a published or drafted journal article. Within each of the five manuscripts there are sections on relevant literature review and geological background, analytical methodologies, results, discussions of new findings with reference to the previous studies, and references cites. Two of these manuscripts are published (Chapter 2 in *Lithos,* and Chapter 3 in *American Journal of Science*), one is in-press (Chapter 6 in *Geological Magazine*), and two are to-be-submitted. The thesis finishes with a synthesis chapter (Chapter 7) that summarises the major outcomes of this research.

The following is a brief introduction on the contents of Chapters 2 to 7.

Chapter 2 is a manuscript published in *Lithos:*

Yao, W.H., Li, Z.X., Li, W.X., Wang, X.C., Li, X.H., and Yang, J.H., 2012. Post-kinematic lithospheric delamination of the Wuyi–Yunkai orogen in South China: Evidence from *ca.* 435 Ma high-Mg basalts. *Lithos* **154**,

115–129.

This study reports geochronological, geochemical and isotopic data for the first lower Palaeozoic mafic–intermediate volcanic succession found in the Ordovician–Silurian (>460 Ma to 420 Ma) Wuyi–Yunkai orogen in the South China Block. The manuscript places new constraints on the timing of late-orogenic magmatism (*ca.* 435 Ma), and supports the model of post-kinematic lithospheric delamination and orogenic collapse in South China. The delamination in the Wuyi–Yunkai orogen likely caused partial melting near the edge of the remaining sub-continental lithospheric mantle by upwelling asthenosphere, which produced the Silurian mafic–intermediate volcanic rocks. Heat from the upwelling asthenosphere as well as possible basaltic underplating, and regional decompression caused by orogenic collapse, can best explain the widespread and synchronous granites along the orogen.

Chapter 3 is a manuscript published in *American Journal of Science:*

Yao, W.H., Li, Z.X., Li, W.X., Li, X.H., and Yang, J.H., 2014. From Rodinia to Gondwanaland: a tale of detrital zircon provenance analyses from the southern Nanhua Basin, South China. *American Journal of Science* **314**, 278–313.

This study reports *in-situ* U–Pb ages and Hf–O isotope results of detrital zircons from Cambrian sedimentary rocks in the southwestern SCB, and examines the provenance characteristics and implications to South China's positions during the breakup of the supercontinent Rodonia and the assembly of Gondwanaland. The data demonstrate a provenance record different from the known tectonomagmatic record of the SCB, or that of western Australia or western Laurentia, but similar to that of northern India. It has thus been proposed that the SCB collided with NW India during the Ediacaran–Ordovician time, causing the “Pan-African” orogeny at the northern Indian margin as well as the intraplate Wuyi–Yunkai orogeny in South China. Ediacaran–Ordovician clastic rocks in the Nanhua Basin are therefore interpreted to be foreland basin deposits formed during this collision.

Chapter 4 is a manuscript close to submission, formatted for *Tectonics:*

Yao, W.H., and Li, Z.X., 2014 (to be submitted). Stratigraphic history of the lower Palaeozoic Nanhua foreland basin in South China: Response to two successive orogenies.

This study presents sedimentary evolution of the lower Palaeozoic Nanhua foreland basin and explores the relationship between clastic sedimentation of the basin and advance of the Wuyi–Yunkai Orogen. Sedimentary facies include turbiditic, shallow marine and fluvial-dominated deltaic facies in an ascending order, and feature diachronous lateral facies changes from southeast to northwest. The study divides the evolution of the Nanhua foreland basin into two stages: (1) during the Cambrian to early Ordovician, it was in an underfilled to filled stage with shallow marine clastic deposits, fed by a detritus source outboard the Cathaysia Block; (2) during the middle Ordovician to Silurian, the basin was in an overfilled stage with subaerial clastic deposits, fed by the northwestward-advancing Wuyi–Yunkai Orogen. The Cambro-Ordovician orogenic event is speculated to be related to the SCB–India collision, and the Ordovician–Silurian Wuyi–Yunkai orogenic event within the SCB was caused by the far-field stress of that collision.

Chapter 5 is a manuscript close to submission, formatted for *Gondwana Research:*

Yao, W.H., Li, Z.X., Li, W.X., Su, L., and Yang, J.H., 2014 (to be submitted). Detrital provenance evolution of the lower Palaeozoic Nanhua foreland basin, South China.

This study reports integrated *in-situ* U–Pb and Hf isotopic analyses of detrital zircons from Cambrian–Silurian clastic samples across the Nanhua foreland basin. Together with published data from Ediacaran–Silurian sandstones in the region, the study establishes a temporal and spatial evolution of provenance across the basin. Utilizing the lower Palaeozoic basin history and palaeogeography of South China, this study concludes that Ediacaran–Cambrian sediments were mainly sourced from northern India, and Ordovician–Silurian sediments were derived from both locally recycled Ediacaran–Cambrian strata and possibly uplifted Cathaysian basement. The

Wuyi–Yunkai magmatic rocks contributed to Silurian sediments.

Chapter 6 is a manuscript published in *Geological Magazine:*

Yao, W.H., Li, Z.X., and Li, W.X., 2014 (in press). Was there a Cambrian ocean in South China? – Insight from detrital provenance analyses. *Geological Magazine*, doi:10.1017/S0016756814000338

This study reports two distinctly different detrital zircon age patterns for Cambrian sandstones from central Yangtze and northwestern Cathaysia blocks, and a mixing of the two at southeastern Yangtze. Provenance analyses suggest that northwestern Cathaysia sandstones were likely sourced from northern India, whereas central Yangtze sandstones were sourced from the western Yangtze Block. The mixed provenances in southeastern Yangtze indicate that detritus can travel across the Yangtze–Cathaysia boundary during the Cambrian, arguing against the existence of a broad Cambrian ocean between the two blocks at that time.

Chapter 7 presents a summary of the evolution of the lower Palaeozoic Nanhua foreland basin and the nature of the Ordovician–Silurian Wuyi–Yunkai orogeny. This chapter utilises research results presented in the previous five chapters to provide an overall interpretation regarding the basin evolution and orogen propagation in the early Palaeozoic South China, as well as to explore the geodynamics of the South China Block during the assembly of Gondwanaland.

Appendices lie at the end of this thesis. U–Pb ages and Hf–O isotopic data tables for volcanic and clastic sedimentary samples, as reported in the chapters, are also given. (1) Co-author contribution statement for the five manuscripts (Chapters 2, 3, 4, 5 and 6) and (2) permission of copyright from third parties where Chapters 2 and 3 were published, are given at the end of the thesis, as the final two appendix documents.

1.5 References

Charvet, J., Shu, L., Faure, M., Choulet, F., Wang, B., Lu, H., Breton, N.L., 2010. Structural development of the Lower Paleozoic belt of South China: Genesis

of an intracontinental orogen. Journal of Asian Earth Sciences 39, 309–330.

Chen, X., Rong, J.Y., Li, Y., Boucot, A.J., 2004. Facies patterns and geography of the Yangtze region, South China, through the Ordovician and Silurian transition. Palaeogeography, Palaeoclimatology, Palaeontology 204, 353–372.

Chen, H., Hou, M., Xu, X., Tian, J., 2006. Tectonic evolution and sequence stratigraphic framework in South China during Caledonian. Journal of Chengdu University of Technology 33, 1–8 (in Chinese with English abstract).

Dong, R., Liu, H., 1991. Regional stratigraphy. In: Liu, H. (Eds.), The Sinian System in China. Science Press, Beijing, pp. 11–114 (in Chinese).

Gao, S., Yang, J., Zhou, L., Li, M., Hu, Z., Guo, J., Yuan, H., Gong, H., Xiao, G., Wei, J., 2011. Age and growth of the Archean Kongling terrain, South China, with emphasis on 3.3 Ga granitoid gneisses. American Journal of Science 311, 153–182.

Greentree, M.R., Li, Z.X., Li, X.H., Wu, H., 2006. Late Mesoproterozoic to earliest Neoproterozoic basin record of the Sibao orogenesis in western South China and relationship to the assembly of Rodinia. Precambrian Research 151, 79–100.

Greentree, M.R., Li, Z.X., 2008. The oldest known rocks in south-western China: SHRIMP U–Pb magmatic crystallisation age and detrital provenance analysis of the Paleoproterozoic Dahongshan Group. Journal of Asian Earth Sciences 33, 289–302.

Guo, L.Z., Shi, Y.S., Lu, H.F., Ma, R.S., Dong, H.G., Yang, S.F., 1989. The pre-Devonian tectonic patterns and evolution of South China. Journal of Southeast Asian Earth Science 3, 87–93.

Hsü, K.J., Shu, S., Jiliang, L., Haihong, C., Haipo, P., Sengor, A.M.C., 1988. Mesozoic overthrust tectonics in south China. Geology 16, 418–421.

Hsü, K.J., Li, J., Chen, H., Wang, Q., Sun, S., Sengr, A.M.C., 1990. Tectonics of South China: Key to understanding West Pacific geology. Tectonophysics 183, 9–39.

Hsü, K.J., 1994. Tectonic facies in an archipelago model of intraplate orogenesis. GSA today 4, 289–293.

Huang, J., Ren, J., Jiang, C., Zhang, Z., Qin, D., 1980. The geotectonic evolution of China. Science Press, Beijing (in Chinese with English abstract).

Jiao, W., Wu, Y., Yang, S., Peng, M., Wang, J., 2009. The oldest basement rock in the Yangtze Craton revealed by zircon U–Pb age and Hf isotope composition. Science in China Series D: Earth Sciences 52, 1393–1399.

Kim, S.W., Oh, C.W., Williams, I.S., Rubatto, D., Ryu, I.C., Rajesh, V.J., Kim, C.B., Guo, J., Zhai, M., 2006. Phanerozoic high-pressure eclogite and intermediate-pressure granulite facies metamorphism in the Gyeonggi Massif, South Korea: Implications for the eastward extension of the Dabie–Sulu continental collision zone. Lithos 92, 357–377.

Li, X.H., 1997. Timing of the Cathaysia Block formation: Constraints from SHRIMP U–Pb zircon geochronology. Episodes 20, 188–192.

Li, Z. X., 1998. Tectonic history of the major East Asian lithospheric blocks since the mid-Proterozoic – a synthesis. In: Flower, M.J., Chung, S.L., Lo, C.H., Lee, T.Y. (Eds.), Mantle dynamics and plate interactions in East Asia. American Geophysical Union, Washington, DC, pp. 221–243.

Li, Z.X., 1999. 830–820 Ma Mafic to felsic igneous activity in South China and the breakup of Rodinia. Gondwana Research 2, 591–591.

Li, Z.X., Li, X.H., Zhou, H., Kinny, P.D., 2002. Grenvillian continental collision in south China: New SHRIMP U–Pb zircon results and implications for the configuration of Rodinia. Geology 30, 163–166.

Li, X.H., Li, Z.X., Ge, W., Zhou, H., Li, W.X., Liu, Y., Wingate, M.T.D., 2003a. Neoproterozoic granitoids in South China: crustal melting above a mantle plume at *ca.* 825 Ma? Precambrian Research 122, 45–83.

Li, Z.X., Li, X.H., Wang, J., Zhang, S., 2003b. A tectonic overview of the South China Block. In: Li, Z.X., Wang, J., Li, X.H., Zhang, S. (Eds.), From Sibao Orogenesis to Nanhua Rifting: Late Precambrian Tectonic History of Eastern South China. Geological Publishing House, Beijing, pp.1–13.

Li, W.X., Li, X.H., Li, Z.X., 2005. Neoproterozoic bimodal magmatism in the Cathaysia Block of South China and its tectonic significance. Precambrian Research 136, 51–66.

Li, Z.X., Li, X.H., 2007. Formation of the 1300-km-wide intracontinental orogen and postorogenic magmatic province in Mesozoic South China: A flat-slab subduction model. Geology 35, 179–182.

Li, Z.X., Wartho, J.A., Occhipinti, S., Zhang, C.L., Li, X.H., Wang, J., Bao, C., 2007. Early history of the eastern Sibao Orogen (South China) during the assembly

of Rodinia: New mica $^{40}Ar/^{39}Ar$ dating and SHRIMP U–Pb detrital zircon provenance constraints. Precambrian research 159, 79–94.

Li, W.X., Li, X.H., Li, Z.X., Lou, F.S., 2008a. Obduction-type granites within the NE Jiangxi Ophiolite: Implications for the final amalgamation between the Yangtze and Cathaysia Blocks. Gondwana Research 13, 288–301.

Li, Z.X., Li, X.H., Li, W.X., Ding, S., 2008b. Was Cathaysia part of Proterozoic Larentia? – new data from Hainan Island, south China. Terran Nova 20, 154–164.

Li, Z.X., Bogdanova, S.V., Collins, A.S., Davidson, A., De Waele, B., Ernst, R.E., Fitzsimons, I.C.W., Fuck, R.A., Gladkochub, D.P., Jacobs, J., Karlstrom, K.E., Lu, S., Natapov, L.M., Pease, V., Pisarevsky, S.A., Thrane, K., Vernikosky, V., 2008c. Assembly, configuration, and break-up history of Rodinia: a synthesis. Precambrian Research 160, 179–210.

Li, X.H., Li, W.X., Li, Z.X., Lo, C.H., Wang, J., Ye, M.F., Yang, Y.H., 2009. Amalgamation between the Yangtze and Cathaysia Blocks in South China: Constraints from SHRIMP U–Pb zircon ages, geochemistry and Nd–Hf isotopes of the Shuangxiwu volcanic rocks. Precambrian research 174, 117–128.

Li, Z.X., Li, X.H., Wartho, J.A., Clark, C., Li, W.X., Zhang, C.L., Bao, C., 2010a. Magmatic and metamorphic events during the early Palaeozoic Wuyi–Yunkai orogeny, southeastern South China: New age constraints and pressure–temperature conditions. Geological Society of America Bulletin 122, 772–793.

Li, W.X., Li, X.H., Li, Z.X., 2010b. *Ca.* 850 Ma bimodal volcanic rocks in northeastern Jiangxi Province, South China: Initial extension during the breakup of Rodinia?: American Journal of Science 310, 951–980.

Li, L., Lin, S., Xing, G., Davis, D.W., Davis, W.J., Xiao, W., Yin, C., 2013. Geochemistry and tectonic implications of late Mesoproterozoic alkaline bimodal volcanic rocks from the Tieshajie Group in the southeastern Yangtze Block, South China. Precambrian Research 230, 179–192.

Liu, B., Xu, X., 1994. Altas of Lithofacies and Paleogeography of South China. Science Press, Beijng.

Ma, D., Huang, X., Xiao, Z., Chen, Z., Zhang, W., Zhong, S., 1998. The crystalline basement of the Hainan Island – stratigraphy and geochronology of the

Baoban group. China University of Geosciences Press, Wuhan (in Chinese).

Pan, G., 1984. The late Precambrian and early Paleozoic marginal basin of South China. In: Kokelaor, B.P., Howell, M.F. (Eds.), Marginal Basin Geology. Blackwell Scientific, Oxford, pp. 279–283.

Qiu, Y.M., Gao, S., McNaughton, N.J., Groves, D.I., Ling, W., 2000. First evidence of >3.2 Ga continental crust in the Yangtze craton of south China and its implications for Archean crustal evolution and Phanerozoic tectonics. Geology 28, 11–14.

Ren, J., 1991. On the geotectonics of southern China. Acta Geologica Sinica 4, 111–130.

Ren, J., Wang, Z., Chen, B., Jiang, C.F., Niu, B.G., 1997. Tectonic maps of China and adjacent regions. Geological Publishing House, Beijing, scale 1:5,000,000.

Roger, F., Maluski, H., Leyreloup, A., Lepvrier, C., Troung Thi, P., 2007. U–Pb dating of high temperature metamorphic episodes in the Kon Tum Massif (Vietnam). Journal of Asian Earth Sciences 30, 565–572.

Shu, L.S., Faure, M., Yu, J.H., Jahn, B.M., 2011. Geochronological and geochemical features of the Cathaysia block (South China): New evidence for the Neoproterozoic breakup of Rodinia. Precambrian Research 187, 263–276.

Shui, T., 1988. Tectonic framework of the continental basement of southeast China. Science in China (B) 31, 24–34.

Sun, W.H., Zhou, M.F., Gao, J.F., Yang, Y.H., Zhao, X.F., Zhao, J.H., 2009. Detrital zircon U–Pb geochronological and Lu–Hf isotopic constraints on the Precambrian magmatic and crustal evolution of the western Yangtze Block, SW China. Precambrian Research 172, 99–126.

Wan, Y., Liu, D., Xu, M., Zhuang, J., Song, B., Shi, Y., Du, L., 2007. SHRIMP U–Pb zircon geochronology and geochemistry of metavolcanic and metasedimentary rocks in Northwestern Fujian, Cathaysia block, China: Tectonic implications and the need to redefine lithostratigraphic units. Gondwana Research 12, 166–183.

Wang, J., Li, Z.X., 2003. History of Neoproterozoic rift basins in South China: implications for Rodinia break-up. Precambrian Research, 122, 141–158.

Wang, X., Zhou, J., Qiu, J., Gao, J., 2004. Geochemistry of the Meso- to Neoproterozoic basic–acid rocks from Hunan Province, South China: implications for the evolution of the western Jiangnan orogen. Precambrian

Research 135, 79–103.

Wang, X.L., Zhou, J.C., Qiu, J.S., Zhang, W.L., Liu, X.M., Zhang, G.L., 2006. LA-ICP-MS U–Pb zircon geochronology of the Neoproterozoic igneous rocks from Northern Guangxi, South China: Implications for tectonic evolution. Precambrian Research 145, 111–130.

Xiang, H., Zhang, L., Zhou, H., Zhong, Z., Zeng, W., Liu, R., Jin, S., 2008. U–Pb zircon geochronology and Hf isotope study of metamorphosed basic-ultrabasic rocks from metamorphic basement in southwestern Zhejiang: The response of the Cathaysia Block to Indosinian orogenic event. Science in China Series D: Earth Sciences 51, 788–800.

Xiao, W., He, H., 2005. Early Mesozoic thrust tectonics of the northwest Zhejiang region (Southeast China). Geological Society of America Bulletin 117, 945–961.

Xu, B., Qiao, G.S., 1989. Sm–Nd isotopic age and tectonic setting of the Late Proterozoic ophiolites in northeastern Jiangxi province. Journal of Nanjing University (Science and Technology) 3, 108–114.

Xu, X., O'Reilly, S.Y., Griffin, W.L., Wang, X., Pearson, N.J., He, Z., 2007. The crust of Cathaysia: Age, assembly and reworking of two terranes. Precambrian Research 158, 51–78.

Xu, X., Xu, Q., Pan, G., 1996. The continental evolution of southern China and its global comparison. Geological, Beijing.

Yao, J., Shu, L., Santosh, M., 2011. Detrital zircon U–Pb geochronology, Hf-isotopes and geochemistry — New clues for the Precambrian crustal evolution of Cathaysia Block, South China. Gondwana Research 20, 553–567.

Ye, M.F., Li, X.H., Li, W.X., Liu, Y., Li, Z.X., 2007. SHRIMP zircon U–Pb geochronological and whole-rock geochemical evidence for an early Neoproterozoic Sibaoan magmatic arc along the southeastern margin of the Yangtze Block. Gondwana Research 12, 144–156.

Yu, J.H., Wang, L., O'Reilly, S.Y., Griffin, W.L., Zhang, M., Li, C., Shu, L., 2009. A Paleoproterozoic orogeny recorded in a long-lived cratonic remnant (Wuyishan terrane), eastern Cathaysia Block, China. Precambrian Research 174, 347–363.

Yu, J.H., O'Reilly, S.Y., Zhou, M.F., Griffin, W., Wang, L., 2011. U–Pb geochronology and Hf–Nd isotopic geochemistry of the Badu Complex,

Southeastern China: Implications for the Precambrian crustal evolution and paleogeography of the Cathaysia Block. Precambrian Research 222–223, 424–449.

Zeng, W., Zhang, L., Zhou, H., Zhong, Z., Xiang, H., Liu, R., Jin, S., Lü, X., Li, C., 2008. Caledonian reworking of Paleoproterozoic basement in the Cathaysia Block: Constraints from zircon U–Pb dating, Hf isotopes and trace elements. Chinese Science Bulletin 53, 895–904.

Zhao, X.F., Zhou, M.F., Li, J.W., Sun, M., Gao, J.F., Sun, W.H., Yang, J.H., 2010. Late Paleoproterozoic to early Mesoproterozoic Dongchuan Group in Yunnan, SW China: Implications for tectonic evolution of the Yangtze Block. Precambrian Research 182, 57–69.

Zheng, J., Griffin, W., O'Reilly, S.Y., Zhang, M., Pearson, N., Pan, Y., 2006. Widespread Archean basement beneath the Yangtze craton. Geology 34, 417–420.

Zheng, J.P., Griffin, W.L., Li, L.S., O'Reilly, S.Y., Pearson, N.J., Tang, H.Y., Liu, G.L., Zhao, J.H., Yu, C.M., Su, Y.P., 2011. Highly evolved Archean basement beneath the western Cathaysia Block, South China. Geochimica et Cosmochimica Acta 75, 242–255.

Zhou, M.F., Yan, D.P., Kennedy, A.K., Li, Y., Ding, J., 2002a. SHRIMP U–Pb zircon geochronological and geochemical evidence for Neoproterozoic arc-magmatism along the western margin of the Yangtze Block, South China. Earth and Planetary Science Letters 196, 51–67.

Zhou, M.F., Kennedy, A.K., Sun, M., Malpas, J., Lesher, C.M., 2002b. Neoproterozoic Arc-related mafic intrusions along the northern margin of South China: Implications for the Accretion of Rodinia. The Journal of Geology 110, 611–618.

Zhou, M.F., Ma, Y., Yan, D.P., Xia, X., Zhao, J.H., Sun, M., 2006. The Yanbian Terrane (Southern Sichuan Province, SW China): A Neoproterozoic arc assemblage in the western margin of the Yangtze Block. Precambrian Research 144, 19–38.

CHAPTER 2 POST-KINEMATIC LITHOSPHERIC DELAMINATION OF THE WUYI–YUNKAI OROGEN IN SOUTH CHINA: EVIDENCE FROM CA. 435 MA HIGH-MG BASALTS

Wei-Hua Yao[a,b], Zheng-Xiang Li[a*], Wu-Xian Li[c], Xuan-Ce Wang[a], Xian-Hua Li[d], Jin-Hui Yang[d]

[a]ARC Center of Excellence for Core to Crust Fluid Systems (CCFS) and The Institute for Geoscience Research (TIGeR), Department of Applied Geology, Curtin University, Perth, WA 6845, Australia

[b]Faculty of Earth Resource, China University of Geosciences, Wuhan, 430074, China

[c]Key Laboratory of Isotope Geochronology and Geochemistry, Guangzhou Institute of Geochemistry, China Academy of Sciences, Guangzhou, 510640, China

[d]State Key Laboratory of Lithospheric Evolution, Institute of Geology and Geophysics, Chinese Academy of Sciences, Beijing, 100029, China

* Corresponding author: z.li@exchange.curtin.edu.au

Abstract

Understanding the processes responsible for the intra-plate early Palaeozoic Wuyi–Yunkai orogeny (>460 Ma to 420–415 Ma) in the South China Block (SCB) is important for deducing the interactions of this block with other continents at that time, as well as the tectonic evolution of East Asia. One salient feature of the orogen is that despite the wide occurrence of syn- to late-orogenic (440 Ma to 420–415 Ma) granites in the orogen, neither syn- to late-orogenic volcanic rocks nor mafic rocks of any type have been reported. Such mafic rocks could shed clues about any mantle–crust interaction during such a major orogeny, thus help to understand the dynamics of the orogenic event. We present here, for the first time, geochronological, isotopic and geochemical data for a mafic–intermediate volcanic succession in northern Guangdong, near the edge of the metamorphic core of the orogen. The volcanic rocks unconformably

overlie strongly deformed Cambro-Ordovician strata, but are in low-angle unconformable contact with overlying post-orogenic mid-Devonian strata. LA-ICP-MS and SHRIMP U–Pb dating of zircons from two andesitic and dacitic samples gives a consistent crystallization age of *ca.* 435 Ma, younger than the 460–445 Ma peak metamorphism of the orogeny but synchronous with the widespread late-orogenic (*ca.* 440–415 Ma) granitic intrusions. Nine least crustally-contaminated basaltic samples are characterized by high MgO (12.3–19.2 wt.%), Ni (214–715 ppm) and Cr (724–1107 ppm), but low TiO_2 (0.6–0.8 wt.%), Al_2O_3 (10.2–12.8 wt.%) and $Fe_2O_3^T$ (total Fe as Fe_2O_3) (8.7–11.4 wt.%) contents. The basalts also exhibit low Nb/La ratios (0.4–0.8) and constant $\varepsilon_{Nd}(t)$ values (–8.0 to –8.4) with variable SiO_2 (44.8–51.5 wt.%) contents, suggesting a likely sub-continental lithospheric mantle origin. These high-magnesian basalts have chemical compositions similar to their primary magma, which was estimated using geochemical modeling at $SiO_2 \approx 50\%$, MgO $\approx 14\%$ and $FeO^T \approx 9\%$. The estimated potential temperature for the melts is >1300 °C, much higher than that of a normal sub-continental lithosphere. This implies that the magma was likely generated from partial melting of lithospheric peridotite heated by hot upwelling asthenosphere. The high-magnesian andesites are interpreted as the products of differentiation and AFC processes from the same basaltic magma source, as supported by their negative zircon $\varepsilon_{Hf}(t)$ values (–21.7 to –6.3) and high zircon $\delta^{18}O$ values (7.3–9.0‰). Overall, we interpret that these post-kinematic basalts, plus andesites and dacites as differentiates, resulted from a late-orogenic lithospheric delamination which led to an orogenic collapse, melting of the SCLM, and widespread late-orogenic granitic intrusions in the orogen.

Key words: South China, Wuyi–Yunkai orogeny, geochemistry, Silurian basalts, orogenic collapse, delamination

2.1 Introduction

Orogenic events often entail syn-kinematic crustal thickening followed by late-kinematic gravitational collapse (Dewey, 1988). The transition from crustal thickening to thinning related to orogenic collapse is often triggered by the transformation of overthickened lower crust into eclogite, leading to the removal of

both the eclogitic lower crust and the peridotitic sub-continental lithospheric mantle, and subsequent asthenosphere upwelling (Lustrino, 2005). Such a tectonothermal event would induce widespread post-kinematic felsic to mafic magmatism. Well-studied examples include the Cenozoic Central Andes in South America (Kay and Kay, 1993) and the early Cretaceous Sulu–Dabie orogen in central China (Li et al., 2002).

Delamination of lithospheric mantle and the lowermost crust is also one of the principal mechanisms for recycling the lithosphere into the deeper mantle, as required by mass balance considerations in orogenic environments (Ducea, 2011). Seismic tomographic imaging of the deeper Earth provides snapshots of modern ongoing lithospheric delamination/dripping (Fillerup et al., 2010; Zandt et al., 2004), but for ancient orogenic belts such as the early Palaeozoic Wuyi–Yunkai orogen in the South China Block (Li et al., 2010c), we can only identify such events through the combination of surface geological observation (e.g., structural and basin records of orogenic collapse) and the analyses of the magmatic record (e.g., Ducea, 2011).

Primary melts of basalts are often used for probing the chemical composition and thermal state of the mantle (e.g., Langmuir et al., 1992; Lee et al., 2011; Wang et al., 2007a; Wang et al., 2008; Wang et al., 2012; White and McKenzie, 1989), thus shedding light on mantle processes such as lithosphere delamination, asthenosphere upwelling and plume activities (Lee et al., 2011). High-Mg basalts represent the least evolved samples which have the potential to record the mantle thermochemical state. For instance, secular changes in Nd isotopic composition of basaltic rocks in the Iberian Massif from an ancient enriched lithospheric mantle (with low $\varepsilon_{Nd}(t)$ values) to a young and depleted asthenospheric mantle (with high $\varepsilon_{Nd}(t)$ values) were interpreted as reflecting lithospheric delamination (Guttierez-Alonso et al., 2011).

The Wuyi–Yunkai orogen is an early Palaeozoic intra-plate orogen in the South China Block (SCB) that lasted from >460 Ma to 420–415 Ma (Li, 1998; Charvet et al., 2010; Li et al., 2010c). It was broadly synchronous with the Caledonian orogeny in Europe, and represents an important tectonic event for understanding the interactions of the SCB with other continents (e.g., northwestern margin of Gondwanaland; Li, 1998; Li and Powell, 2001) at that time, and the tectonic

evolution of East Asia in general. However, the >2000 km-long orogen remains one of the least studied ancient mountain belts in the world. The orogen features high-grade metamorphism along its core, and widespread post-kinematic granites (Figure 2.1a), which have been interpreted as the results of dehydration melting of heated Proterozoic crustal materials during orogenic collapse (e.g., Li et al., 2010c; Zeng et al., 2008). However, so far no synchronous mafic rocks have been reported in the published literature, which are crucial for understanding the petrogenesis of those granites and mantle–crust evolution beneath the orogen. We report here both geochronological and geochemical characteristics of the first post-kinematic mafic volcanic succession identified by regional geological mapping (GDRGMR, 1962; GDBGMR, 1988). The results allow us to interpret the post-kinematic magmatic province in terms of lithospheric delamination during orogenic collapse.

2.2 Geological Background and Sampling

The SCB consists of the Yangtze Block in the northwest and the Cathaysia Block in the southeast (Figure 2.1a insert). The Yangtze basement consists predominantly of Proterozoic rocks with a small outcrop area of Archean rocks known as the Kongling Complex (locally known as the Kongling "Group", dated at *ca.* 3.2 Ga and *ca.* 2.95–2.90 Ga; Qiu et al., 2000; Zheng et al., 2006; Jiao et al., 2009). Outcrops of the Precambrian Cathaysian basement are more scattered. Palaeoproterozoic outcrops (1.89–1.77 Ga) are found mainly in the northeastern section of the block (Li, 1997; Li and Li, 2007a; Li et al., 2010c; Xiang et al., 2008; Yu et al., 2009), whereas Mesoproterozoic (1.43 Ga) crystalline rocks are found on Hainan Island only (Li et al., 2008b). These two blocks amalgamated in early Neoproterozoic by *ca.* 900 Ma (e.g., Li et al., 2007, 2008a, 2009).

A widespread angular unconformity between the overlying upper Palaeozoic terrestrial deposits (Devonian and younger) and the lower Palaeozoic meta-sedimentary successions (typically Silurian and older) was recognized in the southeast part of the SCB. This angular unconformity, together with the widespread, dominantly Silurian granitic intrusions, defines the regional extent of the Wuyi–Yunkai orogen (e.g., Charvet et al., 2010; Huang et al., 1980; Li et al., 2010c; Ren, 1991; Figure 2.1a). The core of the Wuyi–Yunkai orogen is defined by a zone of

northeast-trending, upper greenschist to amphibolite-facies metamorphic complexes (Figure 2.1a). The ages of the granites in the orogeny mostly fall within the 440–415 Ma range (Chen et al., 2008; Li and Gui, 1992; Li et al., 1989, 2010c; Liu et al., 2008; Roger et al., 2000; Wan et al., 2010; Wang et al., 1998; Wang et al., 2007b; Wang et al., 2011; Xu et al., 2005; Yang et al., 2010; Zeng et al., 2008; Zhang et al., 2011, 2012).

The Silurian Chayuanshan volcanic succession is located near Fengwan with a mean geographic coordinate of N24°49′, E113°54′, close to the northern margin of the orogenic core (Figure 2.1). The outcrops cover an area of about 260 km^2. The volcanic rocks unconformably overlie strongly-deformed Cambro-Ordovician strata (deformed by the Wuyi–Yunkai orogeny before the eruption of the Silurian volcanic rocks), but are overlain, with a low-angle angular unconformity, by the post-orogenic mid-Devonian strata (Figure 2.1b). The volcanic rocks are therefore post-kinematic with respect to the main compressional phase of the Wuyi–Yunkai orogeny. The volcanic succession was previously described as discrete and discontinuous porphyrite layers intruding the Ordovician sandstones (GDRGMR, 1962), but the latest regional geological mapping identified it as a volcanic succession sitting below the post-orogenic Devonian sandstone (with basal conglomerate) unit (GDBGMR, 1988).

The lenticular-shaped volcanic succession has a maximum thickness of *ca*. 450 m, consisting of basalts, andesites, dacites (see section 4.3 for geochemical classifications), andesitic ignimbrite, dacitic ignimbrite, and tuffaceous sandstone (Figure 2.1c). Some volcanic units exhibit typical porphyritic textures with dominantly plagioclase and clinopyroxene phenocrysts, suggesting that the succession probably consists of a mixture of volcanic and sub-volcanic rocks. Thirteen least-altered samples were collected from the Chayuanshan volcanic rocks (Figure 2.1b–c). Samples 10GD21–1 to –9 were collected from the upper part of the succession, and samples 10GD23–1 to –3 and 10GD25 from the lower part of the succession. Petrographic examination shows that most of the phenocrysts are altered, with some small fresh olivine crystals still preserved. Geochemical analyses were conducted for all the samples, whereas zircon U–Pb age dating and Hf–O isotopic analyses were conducted on representative samples 10GD23–1 and 10GD25.

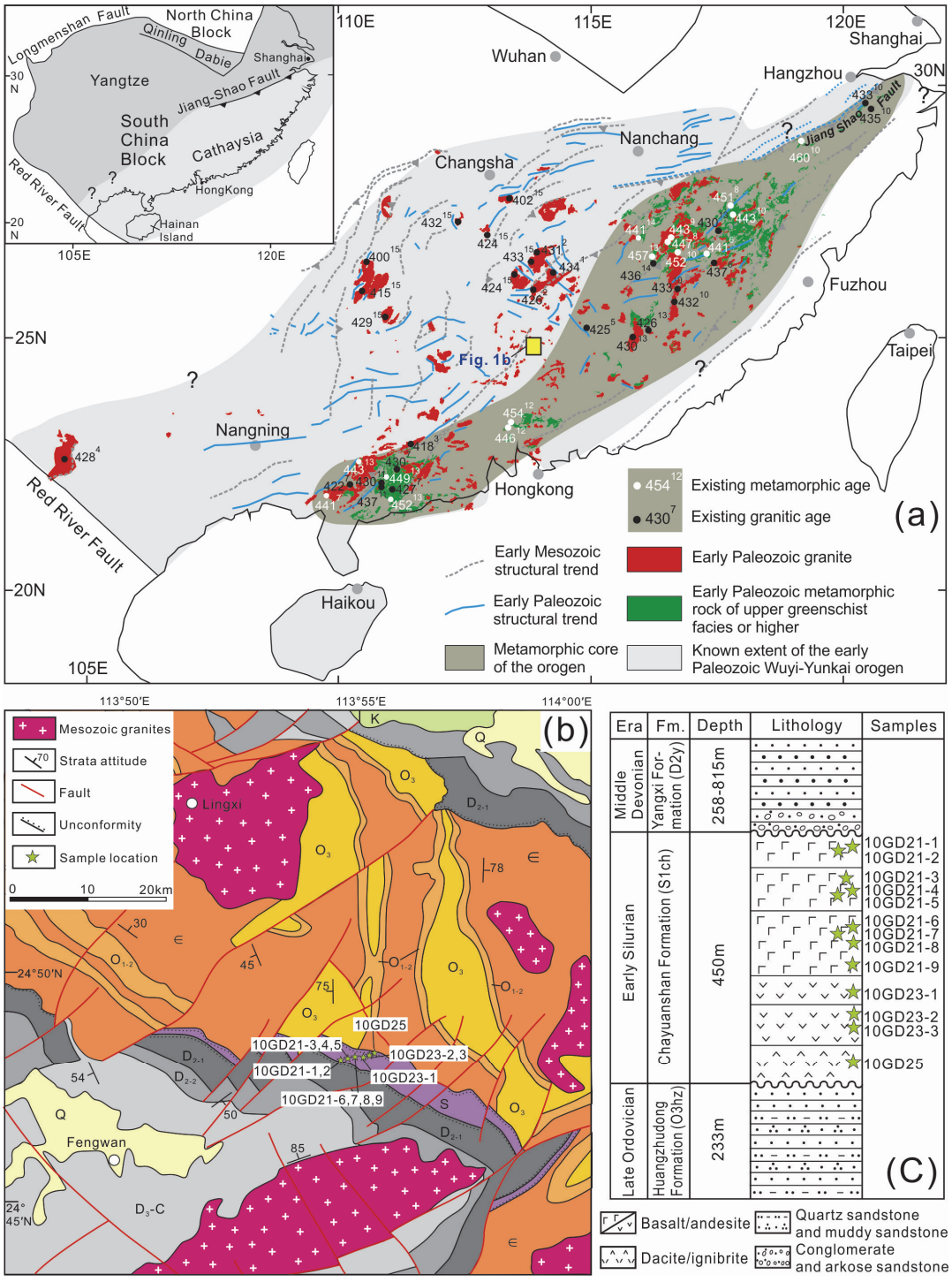

Figure 2.1. (a) Simplified regional geological map highlighting the known extent of the early Palaeozoic Wuyi–Yunkai orogen, the metamorphic core of the orogen, distributions of early Palaeozoic magmatic and metamorphic rocks, and early Palaeozoic structural trends overprinted by Mesozoic structures (modified after Li et al., 2010c). Sources for existing metamorphic (shown in white dots and numbers) and granitic (shown in black dots and numbers) ages as shown in the figure are: 1 — Li et al. (1989); 2 — Li (1991); 3 — Wang et al. (1998); 4 — Roger et al. (2000); 5 — Xu et al. (2005); 6 — Liu et al. (2008); 7 — Wang et al. (2007b); 8 — Chen et al. (2008); 9 — Zeng et al. (2008); 10 — Li et al. (2010c); 11 — Wan et al. (2010); 12 — Yang et al. (2010); 13 — Wang et al. (2011); 14 — Zhang et al. (2011); 15 — Zhang et al. (2012). The insert in (a) shows the relationship between the Yangtze and Cathaysia blocks. (b) Simplified geological map of the study area showing distribution of the

Silurian Chayuanshan volcanic succession in northern Guangdong (revised after GDRGMR, 1962; GDBGMR, 1988) and sampling locations. Symbols for strata ages in (b) are: — Cambrian; O — Ordovician; S — Silurian; D — Devonian; C — Carboniferous; K — Cretaceous; Q — Quaternary. (c) A composite stratigraphic column with sampling locations of the Chayuanshan volcanic succession.

2.3 Analytical Methods

2.3.1 Zircon U–Pb age

Zircons crystals were extracted from bulk-rocks using standard density and magnetic separation techniques. Zircon grains, together with zircon U–Pb standard 91500 and Plešovice, zircon oxygen standard Penglai, were cast in an epoxy mount and then polished to section the crystal in half for analyses. All analyzed zircon grains were imaged in transmitted and reflected light as well as cathodoluminescence (CL) to better reveal their internal structures. U–Th–Pb concentrations were measured using a LA-ICP-MS facility at the Institute of Geology and Geophysics (IGG), Chinese Academy of Sciences. External zircon standard 91500 with $^{207}U/^{206}Pb$ age of 1065.4 ± 0.6 Ma (Wiedenbeck et al., 1995; 2004) and GJ-1 with $^{206}U/^{238}Pb$ age of 608.5 ± 0.4 Ma (Jackson et al., 2004) were introduced to calibrate U–Th–Pb ratios of unknown zircon grains. The detailed analytical procedure can be found in Xie et al. (2008). Data reduction was carried out using Glitter v4.0, ComPbCorr#3_151 (Anderson, 2002) and Isoplot/Ex v2.49 (Ludwig, 2001b) packages.

To further check the reliability of the laser ages, the SHRIMP-II facility at Curtin University Australia was employed for additional zircon U–Pb dating. Standard operation conditions of 2 nA O_2^- primary beam, 20 μm spot size and *ca.* 5000 mass resolution were followed, and six scans were made for each age determination. U abundance was calibrated using zircon 91500 (Wiedenbeck et al., 1995), and $^{206}Pb/^{238}U$ ratio was constraint by zircon Plešovice (Sláma et al., 2008). Data reduction was carried out using Squid v2.50 (Ludwig, 2001a) and Isoplot/Ex v2.49 (Ludwig, 2001b) packages.

2.3.2 Zircon Hf–O isotopes

Zircon oxygen analyses were undertaken before laser dating, using the Cameca IMS

1280 SIMS facility at IGG and the spot locations are identical to the laser dating sites. Zircon standard Penglai with $\delta^{18}O$ = 5.31 ± 0.10‰ (2σ) (Li et al., 2010b) was used for monitoring and correcting measurements on unknown zircon grains. The entire analytical procedure is similar as that described in Li et al. (2010a).

Laser ablation zircon Lu-Hf isotopic analyses were carried out at IGG, using a ThermoFinnigan Neptune MC-ICP-MS equipped with a 193 nm laser. Zircon 91500 and GJ-1 were used as reference standards, with a recommended $^{176}Hf/^{177}Hf$ ratio of 0.282307 ± 0.000031 (2σ) (e.g., Wu et al., 2006) and 0.282000 ± 0.000005 (2σ) (Morel et al., 2008), respectively. Laser ablation Hf sites were centered as close as possible to the spots for U–Pb dating and oxygen analyses. More details on analytical procedures could be found in Wu et al. (2006). A decay constant for ^{176}Lu of 1.867×10^{-11}/year (Soderlund et al., 2004), the present-day chondritic ratios of $^{176}Hf/^{177}Hf$ = 0.282772 and $^{176}Lu/^{177}Hf$ = 0.0332 (Blichert-Toft and Albarède, 1997) were accepted for calculating $\varepsilon_{Hf}(t)$ values. One-stage model ages (T_{DM}) were calculated relative to depleted mantle with a present-day $(^{176}Hf/^{177}Hf)_{DM}$ = 0.28325 and $(^{176}Lu/^{177}Hf)_{DM}$ = 0.0384 (Griffin, et al., 2000). Two-stage model ages (T_{DM}^{C}) were calculated by forcing a growth-curve through the zircon initial ratio with an assumed $(^{176}Lu/^{177}Hf)_{C}$ value of 0.0093 corresponding to the upper continental crust (Amelin, 1999).

2.3.3 Whole-rock major and trace elements

Whole-rock geochemical analyses were carried out at Guangzhou Institute of Geochemistry (GIG), Chinese Academy of Sciences. Major element oxides were obtained using a Rigaku ZSK100e XRF on a fused glass bead. Loss-of-ignition (LOI) measurements were undertaken on dried sample powder by heating in a pre-ignition silica crucible to 1000°C for 1 h and recording the percentage of weight loss. Calibration lines used in quantification were produced by bivariate regression of data from 36 reference materials covering a wide range of silicate compositions (Li et al., 2005), with analytical uncertainties ranging from 1% to 5%.

Trace element concentrations were measured using a ThermoFisher X2 ICP-MS. About 50 mg of each powdered sample was dissolved in a high-pressure Teflon

bomb for 24 h using a HF + HNO_3 mixture. An internal standard solution of Rh was used to monitor signal drift during analysis. The International standards SY-4, AGV-2, W-2Q, SARM-4 and BHVO-2 were used for calibrating the measured element concentrations, and analytical precision was better than 3%.

2.3.4 Whole-rock Nd isotopes

Nd isotopic analyses were carried out at GIG. The isotope measurements were performed on a NEPTUNE PLUS (Thermo Fisher Scientific, MA, USA) multi-collection mass spectrometry equipped with nine Faraday cup collectors and eight ion counters. The analytical procedure was similar to that of Yang et al. (2007). Normalizing factors used to correct the mass fractionation of Nd during the measurements was $^{143}Nd/^{144}Nd = 0.7219$. Analyses of standard Shin Etsu JNdi-1 standard over the measurement period gave $^{143}Nd/^{144}Nd = 0.512099 \pm 0.000004$ (2σ) (n = 4).

2.4 Analytical Results

2.4.1 Zircon U–Pb age

The LA-ICP-MS and SHRIMP zircon U–Pb dating results are listed in Appendix A1 and A2, respectively. Zircon crystals from andesitic sample 10GD23-1 are euhedral and display magmatic growth zonation. On the LA-ICP-MS facility, 42 spots were analyzed on 42 zircon grains (Appendix A1). Thirty-three of the analyses on zircon rims gave Palaeozoic $^{206}Pb/^{238}U$ ages, and among the remaining nine analyses, six on zircon cores had Proterozoic ages of *ca.* 730 Ma (n = 1), *ca.* 1000 Ma (n = 3), *ca.* 1700 Ma (n = 1) and *ca.* 2400 Ma (n = 1), while three crossed core–rim boundaries gave Proterozoic age of *ca.* 730 Ma (n = 1), *ca.* 1000 Ma (n = 1) and *ca.* 1300 Ma (n = 1) (Figure 2.2A). Thirty-one out of the 33 concordant analyses that gave Palaeozoic ages yielded Th/U ratios of >0.4 and a concordant age of 434 ± 7 Ma (MSWD of concordance = 1.1), which is the same as the weighted mean $^{206}Pb/^{238}U$ age of 435 ± 6 Ma (MSWD = 1.0) within errors. The additional 26 analyses on magmatic rims of 26 zircon grains using the Curtin SHRIMP facility (Appendix A2) gave Th/U ratios of 0.5–1.1, implying a magmatic origin (Möller et

al., 2003). The results yielded a concordant age of 434 ± 6 Ma (MSWD of concordance = 12) from 23 analyses (Figure 2.2B), identical to the weighted mean $^{206}Pb/^{238}U$ age of 433 ± 6 Ma (MSWD = 4.0) and the age obtained using LA-ICP-MS. We therefore use the weighted mean $^{206}Pb/^{238}U$ age of 435 ± 6 Ma based on 30 LA-ICP-MS analyses as the crystallization age of sample 10GD23-1.

Most zircon grains from the dacitic sample 10GD25 are euhedral to subhedral and show concentric magmatic zoning in CL images. Forty-two analyses were conducted on 42 zircon grains using the LA-ICP-MS facility (Appendix A1). Thirty-three of them were on magmatic rims that gave a weighted mean $^{206}Pb/^{238}U$ age of 433 ± 6 Ma (MSWD = 0.99), and thirty-one out of the 33 analyses gave a concordant age of 431 ± 6 Ma (MSWD of concordance = 4.0, Figure 2.2C). The remaining nine analyses on zircon cores gave scattered Proterozoic ages of *ca.* 800 Ma (n = 2), *ca.* 1000 Ma (n = 2), *ca.* 1200 Ma (n = 1), *ca.* 1600 Ma (n = 1), *ca.* 2500 Ma (n = 2) and *ca.* 3400 Ma (n = 1) (Figure 2.2C). Additional 20 analyses were conducted on 20 zircon grains at Curtin SHRIMP-A facility (Appendix A2), all on magmatic rims. The 20 analyses yield a weighted mean $^{206}Pb/^{238}U$ age of 435 ± 6 Ma (MSWD = 2.6) and 16 of them give a Concordia age of 438 ± 6 Ma (MSWD of concordance = 6.9, Figure 2.2D). All the 53 analyses on sample 10GD25 that gave Palaeozoic ages (33 LA-ICP-MS analyses and 20 SHRIMP analyses) gave Th/U ratios of 0.2–1.1, suggesting a likely magmatic origin. Therefore, 435 ± 6 Ma is taken as the magmatic crystallization age of sample 10GD25.

Figure 2.2. Laser ablation inductively coupled plasma mass spectrometry (LA-ICP-MS) zircon U–Pb Concordia age plots and sensitive high-resolution ion microprobe (SHRIMP) zircon U–Pb Concordia age plots of the Silurian volcanic samples, with cathodoluminescence (CL) images of zircons. The white circles in the CL images have diameters of ~40 μm or ~25 μm, representing the sites for the LA-ICP-MS analyses and SHRIMP analyses, respectively. a: andesitic sample 10GD23-1 LA-ICP-MS age plots; b: andesitic sample 10GD23-1 SHRIMP age plots; c: dacitic sample 10GD25 LA-ICP-MS age plots; d: dacitic sample 10GD25 SHRIMP age plots.

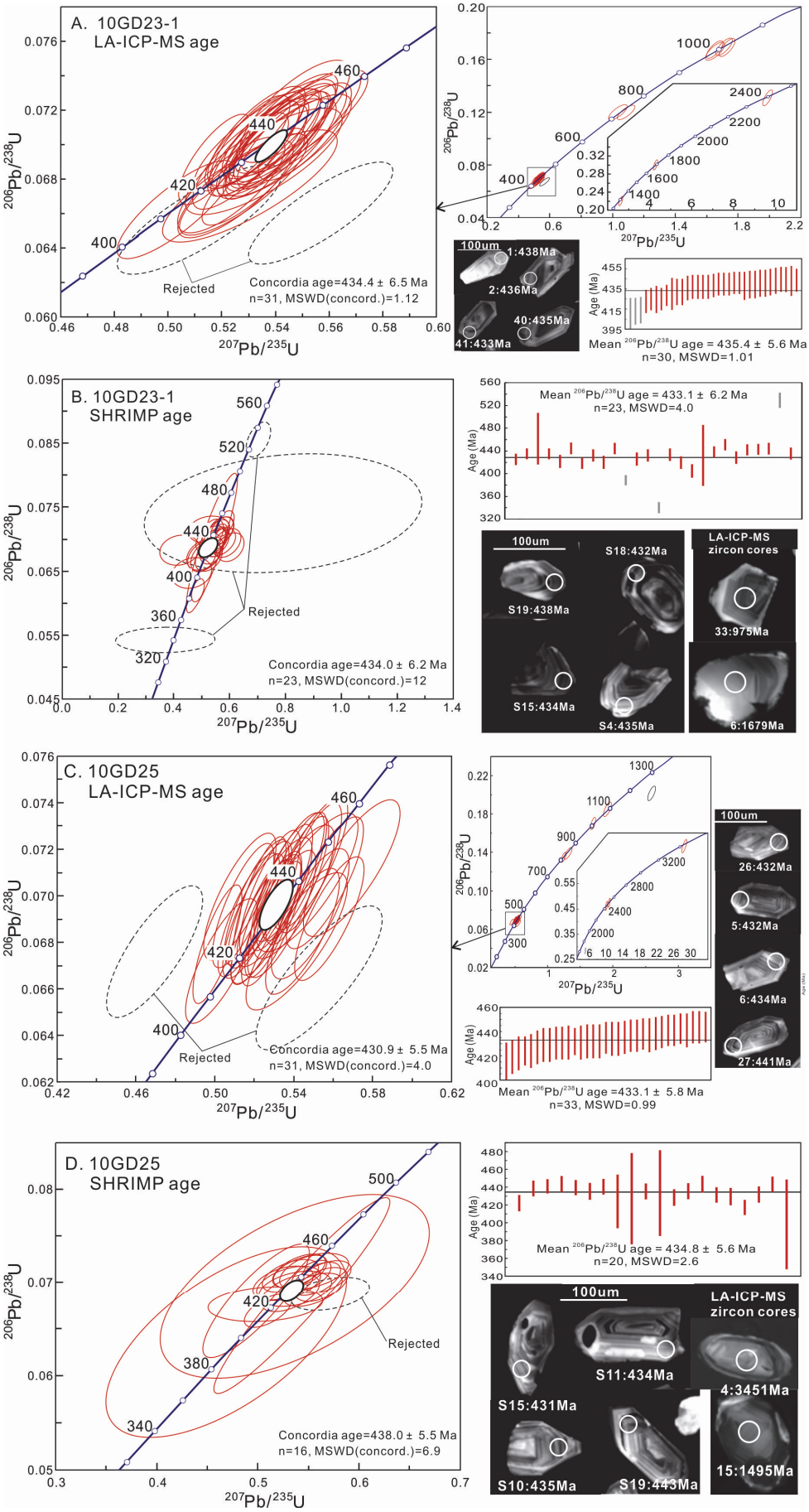
A. 10GD23-1
LA-ICP-MS age
Rejected
Concordia age=434.4 ± 6.5 Ma
n=31, MSWD(concord.)=1.12
100um
1:438Ma
2:436Ma
40:435Ma
41:433Ma
Mean 206Pb/238U age = 435.4 ± 5.6 Ma
n=30, MSWD=1.01
B. 10GD23-1
SHRIMP age
Rejected
Concordia age=434.0 ± 6.2 Ma
n=23, MSWD(concord.)=12
Mean 206Pb/238U age = 433.1 ± 6.2 Ma
n=23, MSWD=4.0
100um
S18:432Ma
S19:438Ma
S15:434Ma
S4:435Ma
LA-ICP-MS
zircon cores
33:975Ma
6:1679Ma
C. 10GD25
LA-ICP-MS age
Rejected
Concordia age=430.9 ± 5.5 Ma
n=31, MSWD(concord.)=4.0
Mean 206Pb/238U age =433.1 ± 5.8 Ma
n=33, MSWD=0.99
100um
26:432Ma
5:432Ma
6:434Ma
27:441Ma
D. 10GD25
SHRIMP age
Rejected
Concordia age=438.0 ± 5.5 Ma
n=16, MSWD(concord.)=6.9
Mean 206Pb/238U age = 434.8 ± 5.6 Ma
n=20, MSWD=2.6
100um
LA-ICP-MS
zircon cores
S11:434Ma
S15:431Ma
4:3451Ma
S10:435Ma
S19:443Ma
15:1495Ma
207Pb/235U
206Pb/238U
Age (Ma)

2.4.2 Zircon Hf–O isotopes

Forty-two oxygen and hafnium isotopic analyses each were conducted on zircons from sample 10GD25 and 10GD23-1, and the results are given in Appendix A3. Excluding the 18 spots with Proterozoic ages, 66 analyses with Palaeozoic ages (~435Ma) yielded variable $^{176}Hf/^{177}Hf$ ratios (0.28190–0.28233) and negative $\varepsilon_{Hf}(t)$ values (–21.7 to –6.3). The calculated two-stage model ages (T_{DM}^{C}) range from 1.57 Ga to 2.32 Ga, with a peak of 1.7 Ga for both sample 10GD23-1 and sample 10GD25 (Figure 2.3A). The $\delta^{18}O$ values for these analyses (~435Ma) are in the range of 7.3‰ to 9.0‰ with a weighted mean value of 8.2 ± 0.2 ‰ (2σ), much higher than the mantle zircon $\delta^{18}O$ value of 5.3‰ ± 0.6 (2σ) (Valley et al., 1998). The 18 analyses on Proterozoic (>700 Ma) xenocryst zircons yielded two main clusters in their zircon $\varepsilon_{Hf}(t)$ versus $\delta^{18}O$ plot. One cluster gives dominant positive $\varepsilon_{Hf}(t)$ values and $\delta^{18}O$ of ~8‰. The other cluster falls into the mantle zircon $\delta^{18}O$ range and offers both positive and negative $\varepsilon_{Hf}(t)$ values (Figure 2.3B).

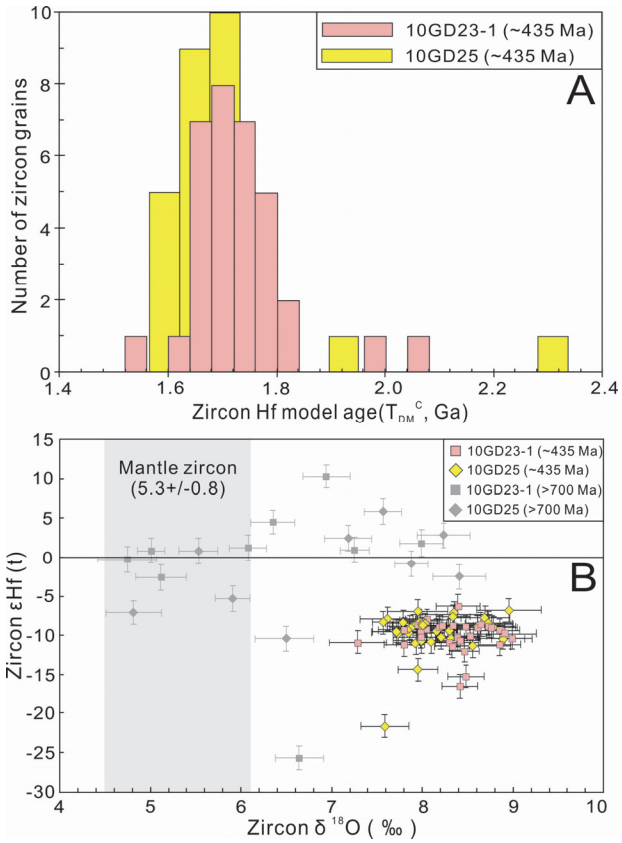

Figure 2.3. (a) Cumulative plot of zircon Hf model ages for samples 10GD23-1 (andesite) and 10GD25 (dacite). (b) Plot of *in-situ* zircon $\varepsilon_{Hf}(t)$ versus $\delta^{18}O$ values for samples 10GD23-1 (andesite) and 10GD25 (dacite) from the Chayuanshan volcanic succession, northern Guangdong.

2.4.3 Whole-rock major and trace element compositions

Based on the petrological examination, thirteen least-altered samples were selected for major and trace element composition measurements, and the results are presented in Table 2.1. The 10GD21 samples show a mafic affinity with SiO_2 = 45–51 wt.%, Mg# = 75–80 and Al_2O_3 = 10.2–12.8 wt.%. The 10GD23 samples are intermediate in composition with SiO_2 = 61–63 wt.%, Mg# = 54–62 and Al_2O_3 = 14.8–16.2 wt.% (volatile-free). Sample 10GD25 has the highest silicate content with SiO_2 = 65 wt.%, Mg# = 44 and Al_2O_3 = 16.4 wt.%. On the Zr/Ti versus Nb/Y diagram (Winchester and Floyd, 1976), the 10GD21 sample group plots in the sub-alkaline basalt fields, while the 10GD23 sample group and sample 10GD25 plot in the andesite and dacite fields, respectively (Figure 2.4). We also notice that the basalts have extremely high MgO content (12.3–19.2 wt.%).

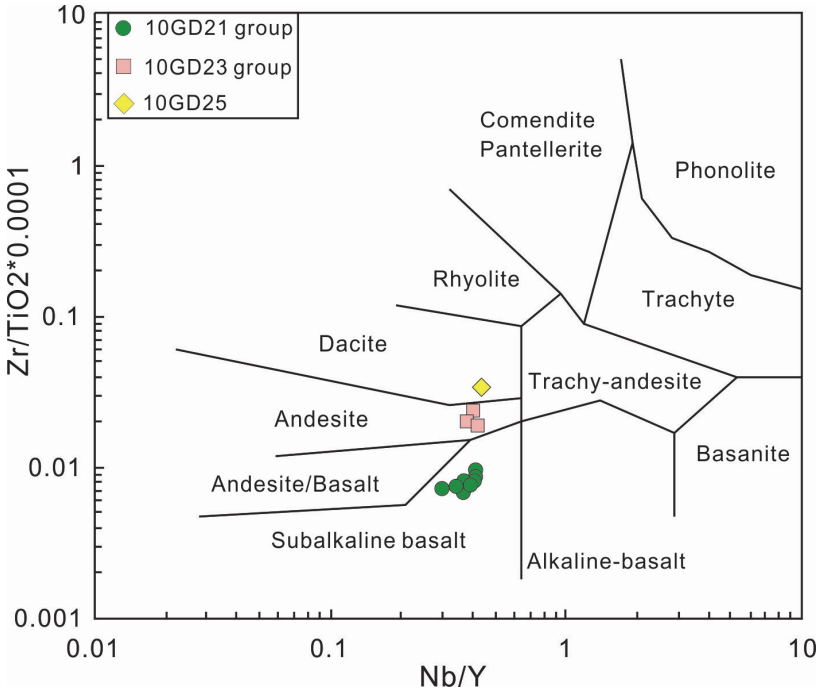

Figure 2.4. Plot of the Chayuanshan volcanic samples in the Zr/TiO_2×0.0001 versus Nb/Y diagram (Winchester and Floyd, 1976).

The incompatible trace element patterns of the Chayuanshan basalts are characterized by significant depletions in Nb, Ta, Zr, Hf and Ti and enrichments in U, Th, La and Nd (Figure 2.5a), with relatively low contents in REE (total REE = 39.5–78.4 ppm, average 59.8 ppm) and LREE/HREE ratios (4.0–5.9, average 4.9; $(La/Yb)_N$ = 3.4–6.2). The chondrite-normalized REE patterns of the basalts are distinctively different from that of OIB or MORB (Figure 2.5b), and show negative

Eu anomalies (Eu* = 0.65–0.91, average 0.77). They also have higher LREE concentrations and lower HREE concentrations compared to N-MORB (Figure 2.5b). $(La/Sm)_N$ ratios of the basalts are in the range of 1.8–2.9 (average 2.4). Compatible elements Cr (724–1107 ppm, average 918 ppm) and Ni (214–715 ppm, average 416 ppm) are typically higher in the basalts compared to N-MORB.

The 10GD23 andesitic samples and the 10GD25 dacitic samples are depleted in high field strength elements (HFSEs: Nb, Ti, Ta and Zr) and enriched in U, Th and LREE (Figure 2.5c). They have $(La/Yb)_N$ ratios of 6.2–10.5 (Table 2.1). They also show nearly constant $(La/Sm)_N$ ratios (3.1–3.8; average 3.5), and slightly depletion in Eu with Eu* = 0.6–0.8 (average 0.7) (Figure 2.5d).

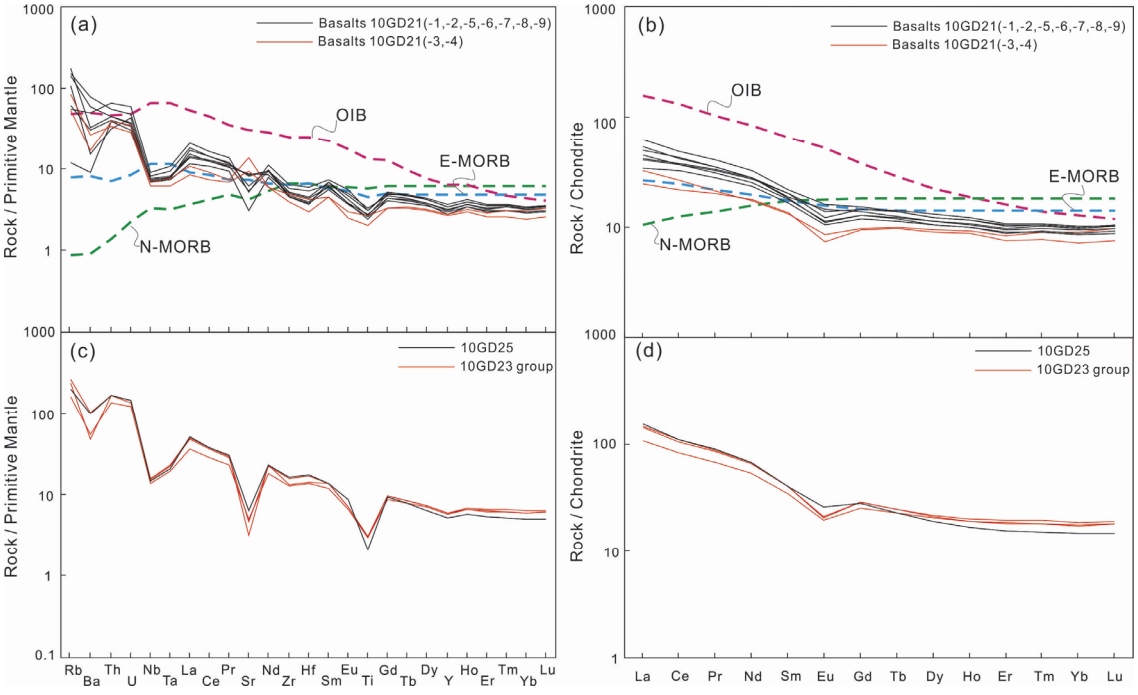

Figure 2.5. Primitive mantle-normalized trace element spider diagrams for the 10GD23 (andesite) and 10GD25 (dacite) sample groups (a), and the 10GD21 (basalts) sample group (b); Chondrite-normalized REE spider diagrams for the 10GD23 and 10GD25 sample groups (c) and the 10GD21 sample group (d). Normalization values for the primitive mantle and chondrite, as well as values for OIB, N-MORB and E-MORB, are from Sun and McDonough (1989).

Table 2.1. Major and trace element results for the volcanic samples from the Chayuanshan volcanic succession, northern Guangdong

Sample#	10GD21-1	10GD21-2	10GD21-3	10GD21-4	10GD21-5	10GD21-6	10GD21-7	10GD21-8	10GD21-9	10GD23-1	10GD23-2	10GD23-3	10GD25
rock-type	basalt	basalt	basalt	basalt	basalt	basalt	basalt	basalt	basalt	andesite	andesite	andesite	dacite
Latitute	N 24°49'14.6"		N 24°49'14.7''			N 24°49'14.8''			N 24°49'18.3''	N 24°49'15.1''	N 24°49'11.7"	N 24°49'08.8"	N 24°49'25.1''
Longitute	E 113°54'33.9''		E 113°54'34.0''			E 113°54'32.9''			E 113°54'35.1''	E 113°54'39.3''	E 113°54'47.8''	E 113°54'47.7''	E 113°55'08.8''
Major oxides (wt.%)													
SiO_2	44.8	51.5	50.2	48.8	47.5	49.6	50.7	46.2	51.1	61.3	61.5	63.4	65.0
TiO_2	0.69	0.77	0.64	0.71	0.69	0.79	0.61	0.65	0.74	0.74	0.70	0.68	0.53
Al_2O_3	10.5	12.4	10.7	11.7	11.4	12.8	10.3	10.2	11.5	16.2	14.8	14.8	16.4
$Fe_2O_3^T$	11.3	8.69	8.83	9.81	10.0	9.70	9.62	11.4	9.53	6.59	6.52	6.70	5.48
MnO	0.20	0.15	0.17	0.15	0.16	0.15	0.18	0.20	0.17	0.07	0.10	0.10	0.08
MgO	19.2	12.3	13.8	14.2	15.6	12.5	12.7	17.6	14.2	4.64	3.26	3.63	1.87
CaO	7.76	7.68	10.72	9.95	8.73	6.56	11.69	7.31	6.88	3.59	5.07	3.79	4.19
Na_2O	0.34	1.55	0.37	0.64	0.59	1.35	0.51	0.53	0.55	0.31	2.26	1.98	1.51
K_2O	0.14	2.47	1.40	0.72	1.98	2.54	1.18	1.05	0.75	3.25	2.22	3.20	3.07
P_2O_5	0.17	0.19	0.18	0.18	0.18	0.21	0.17	0.17	0.21	0.16	0.16	0.16	0.12
LOI	4.69	1.85	2.52	2.65	2.68	3.47	1.76	4.38	4.03	2.69	3.08	0.98	1.16
Total	99.8	99.6	99.5	99.5	99.5	99.7	99.4	99.7	99.7	99.5	99.7	99.4	99.4
Mg#	80	77	78	77	78	75	76	78	78	62	54	56	44
Trace elements (ppm)													
Sc	29.7	35.6	19.3	31.5	28.7	32.5	9.5	28.2	27.6	18.4	20.0	19.0	14.2
V	3466	4057	2680	3558	3577	4376	3190	3381	3969	3999	3836	3817	2787
Cr	197	228	150	211	200	224	176	191	192	126	134	130	77.5
Mn	1015	938	745	1107	914	724	977	931	913	146	167	145	123
Co	1345	1006	927	1024	1123	1083	1267	1412	1156	524	732	697	618
Ni	32.7	38.9	22.1	71.0	59.1	47.2	33.6	62.5	44.4	37.4	27.1	15.3	11.7
Cu	452	345	303	715	503	214	304	537	373	36.7	29.6	35.6	26.8
Zn	27.3	31.5	31.3	96.2	77.2	42.6	33.1	70.2	52.3	31.5	102	24.0	38.6
Rb	7.70	90.8	54.7	33.8	111	97.3	68.1	39.1	35.8	151	104	172	129

Sr	113	176	201	293	186	170	132	66.0	109	66.5	106	100	137
Y	16.6	15.9	12.1	12.8	14.2	14.6	12.6	13.6	15.8	27.3	26.1	27.1	23.7
Zr	50.5	57.8	43.7	54.4	56.6	65.7	53.4	51.4	72.2	152	143	177	186
Nb	4.93	5.38	4.43	5.00	5.22	5.88	5.14	4.93	6.43	11.6	9.97	10.8	10.4
Cs	3.70	31.1	12.4	4.50	67.6	12.4	10.8	10.2	12.9	26.7	7.78	19.3	19.9
Ba	63.2	412	184	120	230	550	108	218	348	337	382	717	701
La	9.52	9.90	5.80	7.59	10.5	12.4	11.7	8.06	14.7	35.0	25.4	33.4	36.1
Ce	22.1	22.9	13.3	16.3	22.3	25.4	25.6	19.5	29.3	66.4	50.3	64.2	68.1
Pr	3.04	3.11	1.92	2.00	2.89	3.24	3.27	2.61	3.83	8.26	6.43	7.98	8.41
Nd	12.6	13.0	8.12	8.07	11.7	12.9	13.0	10.8	15.1	31.1	24.9	30.3	31.4
Sm	3.06	3.02	2.04	1.99	2.67	2.83	2.76	2.51	3.26	6.08	5.26	6.14	6.15
Eu	0.71	0.80	0.42	0.50	0.65	0.84	0.64	0.61	0.92	1.19	1.12	1.21	1.49
Gd	2.94	3.00	1.95	2.01	2.61	2.79	2.64	2.42	3.14	5.82	5.18	5.88	5.71
Tb	0.53	0.51	0.36	0.37	0.45	0.47	0.44	0.42	0.52	0.92	0.86	0.92	0.85
Dy	3.29	3.09	2.25	2.37	2.83	2.83	2.68	2.63	3.11	5.52	5.20	5.35	4.79
Ho	0.68	0.66	0.49	0.52	0.59	0.60	0.57	0.55	0.65	1.14	1.08	1.08	0.95
Er	1.78	1.70	1.25	1.39	1.56	1.61	1.48	1.45	1.72	3.21	3.00	3.04	2.57
Tm	0.28	0.27	0.19	0.23	0.25	0.26	0.23	0.23	0.27	0.49	0.46	0.46	0.39
Yb	1.72	1.69	1.21	1.51	1.58	1.66	1.43	1.48	1.69	3.15	2.96	2.93	2.46
Lu	0.26	0.27	0.19	0.24	0.25	0.26	0.22	0.23	0.27	0.48	0.46	0.46	0.38
Hf	1.15	1.42	0.91	1.30	1.34	1.66	1.24	1.18	1.85	4.46	4.22	5.19	5.46
Ta	0.32	0.34	0.25	0.32	0.33	0.39	0.32	0.31	0.44	0.97	0.80	0.91	0.88
Pb	11.7	8.24	7.38	9.62	8.77	9.31	6.17	7.22	6.48	14.4	29.8	16.7	30.0
Th	3.30	3.88	2.94	3.30	3.88	4.80	2.75	3.51	5.71	14.3	11.8	14.6	14.6
U	0.65	0.78	0.59	0.74	0.79	1.01	0.91	0.73	1.26	2.84	2.57	3.07	3.07
∑REE	62.5	64.0	39.5	45.1	60.8	68.1	66.7	53.5	78.4	169	133	163	170
Eu*	0.72	0.81	0.65	0.76	0.75	0.91	0.73	0.76	0.88	0.61	0.66	0.62	0.77
$(La/Yb)_N$	3.98	4.19	3.43	3.60	4.77	5.37	5.88	3.90	6.22	7.95	6.15	8.18	10.5

Mg# = 100*Mg/(Mg+Fe^{2+}), assuming Fe^{2+}/Fe^{total} = 0.85; LOI = loss of ignition; $Fe_2O_3^T$ = total Fe oxides as Fe_2O_3; footnote N means chondrite normalization.

2.4.4. Whole-rock Nd isotopes

The bulk-rock Nd isotope data are listed in Table 2.2. The Chayuanshan basalts have $(^{143}Nd/^{144}Nd)_i$ values ranging from 0.51165 to 0.51167 and nearly constant corresponding $\varepsilon_{Nd}(t)$ values (–8.0 to –8.4), while the andesitic and dacitic samples have slightly lower $(^{143}Nd/^{144}Nd)_i$ values ranging from 0.51158 to 0.51160 and corresponding lower $\varepsilon_{Nd}(t)$ values (–9.4 to –9. 8).

Table 2.2. Whole-rock Nd-isotope data for the volcanic samples from the Chayuanshan volcanic succession, northern Guangdong

Sample#	Lithology	Sm	Nd	$^{147}Sm/^{144}Nd$	$^{143}Nd/^{144}Nd$	$2\sigma(10^{-7})$	$(^{143}Nd/^{144}Nd)_i$	$\varepsilon_{Nd}(t)$
10GD21-1	basalt	3.06	12.6	0.1471	0.512082	32	0.511663	-8.1
10GD21-2	basalt	3.02	13.0	0.1404	0.512050	29	0.511650	-8.4
10GD21-4	basalt	1.99	8.07	0.1489	0.512090	37	0.511666	-8.0
10GD21-7	basalt	2.76	13.0	0.1279	0.512012	32	0.511648	-8.4
10GD21-8	basalt	2.51	10.8	0.1401	0.512067	35	0.511668	-8.0
10GD23-1	andesite	6.08	31.1	0.1182	0.511914	35	0.511577	-9.8
10GD23-2	andesite	5.26	24.9	0.1278	0.511951	47	0.511587	-9.6
10GD23-3	andesite	6.14	30.3	0.1227	0.511946	35	0.511596	-9.4
10GD25	dacite	6.15	31.4	0.1183	0.511929	32	0.511592	-9.5

t = 435 Ma, crystallization age of zircon.

$(^{143}Nd/^{144}Nd)_i=(^{143}Nd/^{144}Nd)_{sample}-(^{147}Sm/^{144}Nd)_m\times(e^{\lambda t}-1)$,
$\varepsilon_{Nd}(t)=[(^{143}Nd/^{144}Nd)_{sample}/(^{143}Nd/^{144}Nd)_{CHUR}(t)-1]\times10^4$,
$(^{143}Nd/^{144}Nd)_{CHUR}(t)=0.512638-0.1967\times(e^{\lambda t}-1)$, $\lambda=1.42\times10^{-11}$ year^{-1}

2.5 Discussions

2.5.1 Timing of the Chayuanshan volcanism during the Wuyi–Yunkai orogeny

The Silurian Chayuanshan volcanic succession sits on top of highly-deformed Cambro-Ordovician meta-quartz arkose with a high-angle unconformity. On the other hand, it is at a low-angle contact with mid-Devonian post-orogenic quartz sandstones with terrestrial polymictic basal conglomerate. The volcanic rocks are therefore regarded to have formed post-kinematic during the later stage of the Ordovician–Silurian Wuyi–Yunkai orogeny (Li et al., 2010c). Our zircon U-Pb dating of andesitic sample 10GD23-1 and dacitic sample 10GD25 gave consistent magmatic ages of 434 ± 6 Ma (2σ) and 435 ± 6 Ma (2σ), respectively. Such ages are younger than the peak metamorphic ages of 460–440 Ma for the orogeny, but synchronous with the widespread, commonly non-deformed late-orogenic felsic

magmatism dated mostly at the 440–415 Ma range (Li et al., 2010c and references therein). This age relationship is therefore consistent with aforementioned field constraints.

2.5.2 Effects of alteration, crustal contamination and crystal fractionation

The basaltic samples underwent variable degrees of alteration as evidenced by the existence of secondary minerals and variable LOI values (1.8–4.7%). The lack of meaningful correlations between Al_2O_3, SiO_2, $Fe_2O_3^T$, MgO and TiO_2 with LOI indicates that these elements were essentially immobile during alteration. Zirconium, one of the most immobile elements during low-degree metamorphism and alteration, could be an alteration-independent index to test the mobility of other trace elements (e.g., Wang et al., 2010 and references therein). We therefore used bivariate plots of Zr against selected trace elements to evaluate the mobility of such elements during alteration (figures not shown). The contents of high field strength elements (HFSEs, such as Nb, Ta, Zr, Hf, Th, U, and Y), rare earth elements (REEs) and Y correlate well with Zr contents, suggesting that these elements were essentially immobile during alteration. In contrast, large iron lithosphile elements (LILEs, such as Cs, Rb, Sr, and Ba), and other elements such as Mn, K, Na, and Ca, show no correlation with Zr, indicating variable degrees of mobility during alteration. In the following discussions, only immobile elements are used for evaluating primary magma sources and petrogenesis of the volcanic rocks.

To evaluate the effect of crustal contamination, we examined correlations among selected trace element ratios such as La/Sm, Nb/La, Th/Ta, Sm/Nd, and Nb/U. The correlations between these ratios could be caused by crustal contamination or contributions from an enriched sub-continental lithospheric mantle (SCLM), but the latter should not produce correlations between major elements (such as MgO, SiO_2 and $Fe_2O_3^T$), isotope ratios and above-mentioned trace element ratios. The basaltic samples exhibit clear correlations between Sm/Nd vs. Nb/La and La/Sm vs. Nb/La (Figure 2.6a–b), likely indicating crustal contamination and/or the involvement of SCLM components. No clear correlation is found in the bivariation diagrams of Nb/U vs. SiO_2/MgO and Nb/La vs. MgO (Figure 2.6c–d), ruling out the possibility of significant crustal contamination (e.g., Wang et al., 2008). Although the basalts

display a large range of SiO_2 (44.8–51.5 wt.%), MgO (12.3–19.2 wt.%), and Al_2O_3 (10.2–12.8 wt.%) contents, they have nearly constant $\varepsilon_{Nd}(t)$ values (–8.0 to –8.4). This suggests that crustal contamination, often introducing a wider range of $\varepsilon_{Nd}(t)$ values due to complex crustal compositions, was insignificant in the generation of the basalts. The lack of clear correlation in $\varepsilon_{Nd}(t)$ vs. Nb/La and Zr/Nb vs. Nb/La (Figure 2.6e–f) further supports this interpretation.

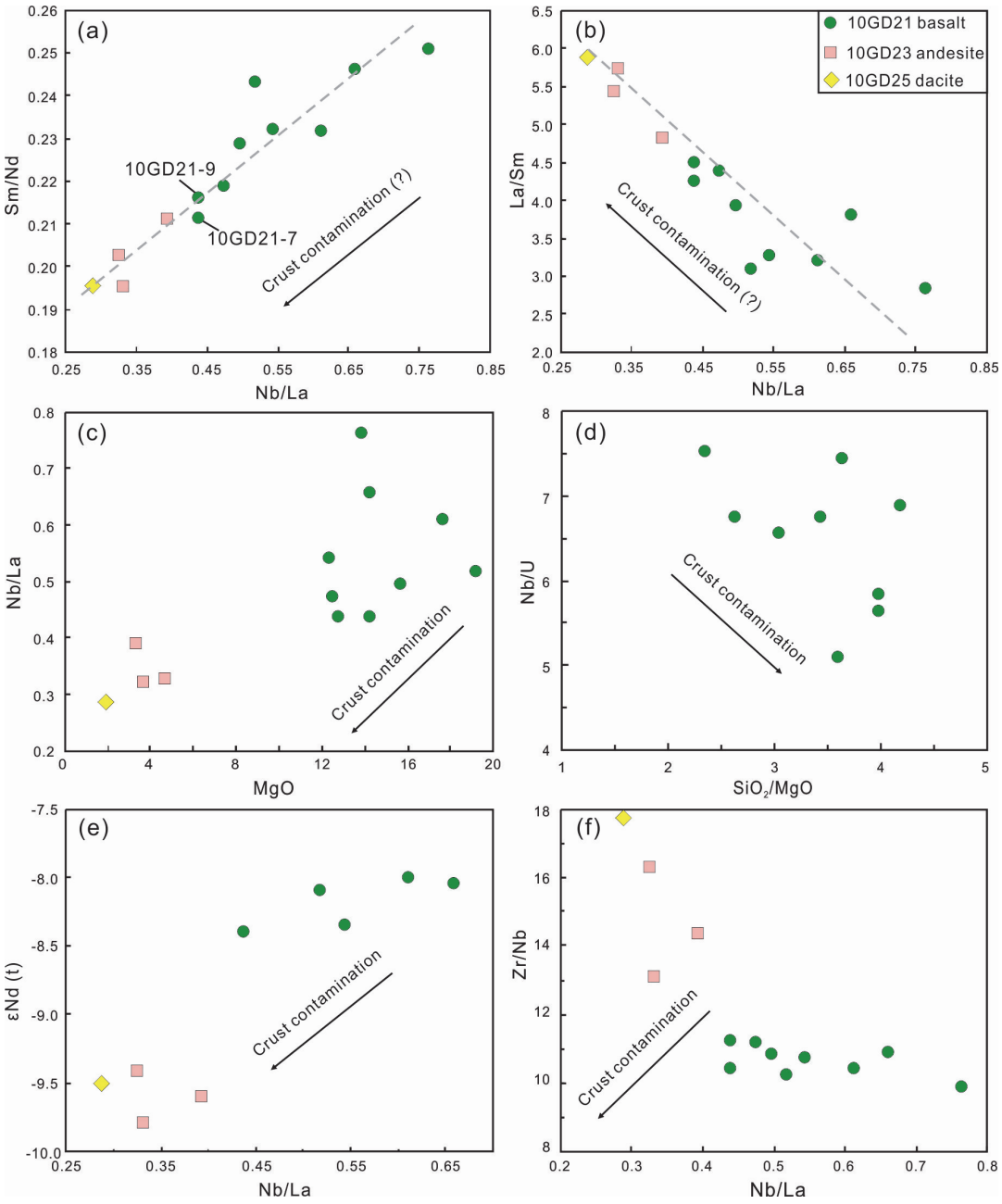

Figure 2.6. Bivariation plots of Sm/Nd (a), La/Sm (b), $\varepsilon_{Nd}(t)$ (e), and Zr/Nb (f) versus Nb/La, respectively, and plots of Nb/La vs. MgO (c) and Nb/U vs. SiO_2/MgO (d) for samples from the Chayuanshan volcanic succession.

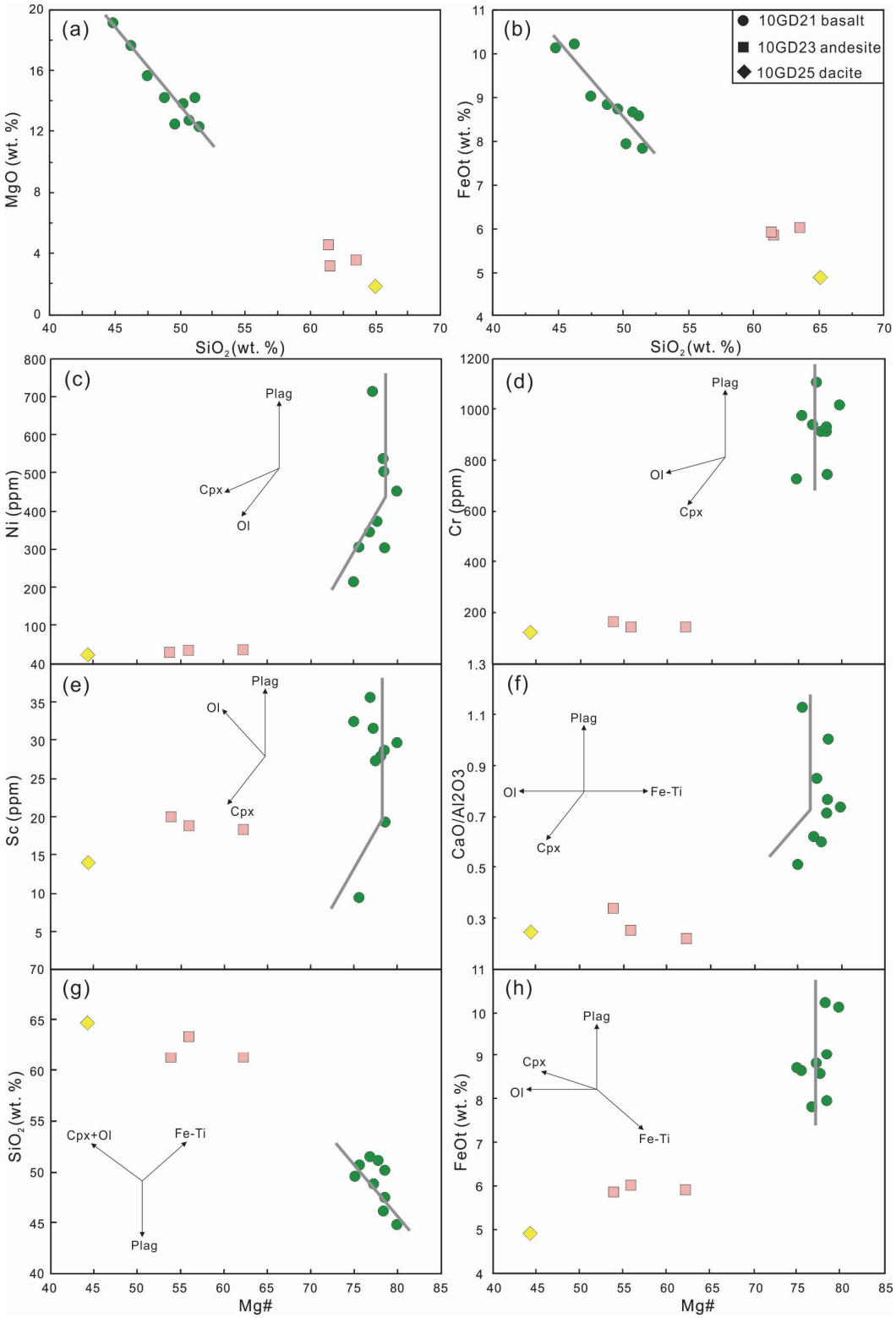

Figure 2.7. Variations diagrams of selected major oxides MgO and FeO^T versus SiO_2 (wt.%) (a–b), and bivariation plots of trace element Ni (c), Cr (d), Sc (e), CaO/Al_2O_3 (f), SiO_2 (g), and FeO^T (h) versus Mg#. $Mg^{\#} = 100\times Mg/(Mg+Fe^{2+})$, assuming $Fe^{2+}/Fe_{total}=0.85$, cation ratio.

For the Chayuanshan basalts, decreases in MgO and FeO^T with increasing SiO_2 indicate possible crystal fractionation/accumulation of olivine in the magma chamber,

or during magma ascent (Figure 2.7a–b). The high MgO content (12.3–19.2 wt.%) suggests likely olivine accumulation as the magma was ascending. Variation trends in the plots of Mg# vs. Cr, Ni, Sc, SiO_2, CaO/Al_2O_3 and FeO^T (Figure 2.7c–h) suggest that the basalts may have experienced olivine fractionation/accumulation first, followed by low-pressure fractionation of clinopyroxene and plagioclase as the magma rose through the upper mantle and the continental crust. The fact that phenocrysts in the basalts are mainly clinopyroxene and plagioclase is consistent with such an interpretation.

In summary, the Chayuanshan basalts experienced olivine fractionation followed by mainly clinopyroxene and plagioclase fractionation during magma ascent. Chemical alteration did not have impact on most incompatible trace elements, but did affect a few compatible elements such as Mn, K, Na and Ca.

2.5.3 Primary melts of the Chayuanshan basalts

Chemical composition of primary melts could reflect chemical and thermal conditions of the magma sources (e.g., Herzberg et al., 2007; Langmuir et al., 1992; McKenzie and Bickle, 1988). Basaltic primary melts generally have Ni > 400 ppm, Cr > 1000 ppm (Wilson, 1989), and Mg# = 73–81 (Sharma, 1997 and references therein). The Chayuanshan basalts have an average Ni content of 416 ppm (214–715 ppm), Cr of 918 ppm (724–1107 ppm) and Mg# of 75–80, similar to those of primary melts. To further constrain the composition of the primary magma, and to compensate for the effect of crystallization, all samples with least crustal contamination were used for the calculation and correction following the steps below: (1) the composition of equilibrium olivine was obtained using KD $(Fe / Mg)^{oliv/liq}$ = 0.31 (Putirka, 2005) and $D_{Ni}^{oliv/liq}$ (Beattie et al., 1991), assuming that $Fe^{2+} / \sum Fe$ = 0.90 in the melt (Putirka, 2005); (2) a more primitive basalt composition was calculated as a mixture of the basalt in equilibrium with olivine in a weight ratio of 99.9 : 0.1; (3) repeating the first two steps using the calculated primitive basalt to obtain a more primitive basalt composition (Langmuir et al., 1992; Wang et al., 2008; Wang et al., 2012). The calculated results are presented in Table 2.3. The major uncertainty of the method comes from the value of KD, the redox state ($Fe^{3+} / \sum Fe$) and the mantle Mg# (Wang et al., 2012).

Table 2.3. Calculated major elements and thermal parameters for selected samples from the Chayuanshan volcanic succession, northern Guangdong

Sample #	10GD21-1	10GD21-2	10GD21-3	10GD21-4	10GD21-5	10GD21-6	10GD21-7	10GD21-8
SiO_2	48.5	53.2	52.8	51.1	50.0	51.7	51.9	49.5
TiO_2	0.83	0.80	0.70	0.75	0.76	0.81	0.62	0.74
Al_2O_3	12.6	12.9	11.8	12.5	12.6	13.1	10.5	11.6
FeO^T	10.3	7.54	7.68	8.62	8.81	8.63	7.58	10.3
MnO	0.24	0.15	0.18	0.16	0.18	0.16	0.18	0.22
MgO	16.6	12.2	12.4	14.0	14.2	14.0	13.5	16.6
CaO	9.30	8.04	11.8	10.6	9.65	6.71	11.9	8.27
Na_2O	0.41	1.62	0.41	0.68	0.65	1.38	0.52	0.60
K_2O	0.17	2.59	1.54	0.77	2.19	2.60	1.20	1.19
H_2O	0.50	0.47	0.28	0.34	0.48	0.50	0.51	0.42
Fo	0.90	0.90	0.90	0.90	0.90	0.90	0.90	0.90
F	0.89	0.99	0.95	0.98	0.94	1.03	1.01	0.94
T (°C)	1450	1306	1323	1370	1377	1355	1313	1444
P (GPa)	1.62	0.95	0.65	0.98	1.40	1.28	1.32	1.66

Major elements and H_2O are in wt.%.
Fo = $Mg/(Mg + Fe + Mn)_{molar} \times 100$.
F represents the final mass portion relative to the original melt mass.
T (°C) represents the melting temperature, P(GPa) represents the effective melting pressure, both calculated following Lee et al. (2009).

In the case of our calculations, the major uncertainty arises from the mantle Mg#. The Nd isotope and trace element compositions of the Chayuanshan basalts indicate that these high-Mg basalts were most likely derived from an ancient sub-continental lithospheric mantle (SCLM), which is generally depleted in basaltic melts in comparison with the asthenospheric mantle, resulting in high mantle Mg# values. To minimize the effect of clinopyroxene fractionation, only samples with $SiO_2 < 53$ wt.%, CaO ≥ 9 wt.%, LOI < 3 wt.%, Ni > 400 ppm, and Cr > 1000 ppm were chosen as initial materials to constrain the composition of the primary melts, and under such conditions, we chose two least-evolved basaltic samples (10GD21-4 and 10GD21-5) for the calculation. The calculated primary basaltic melt has ~50.5 wt.% SiO_2, ~14.1 wt.% MgO and ~8.7 wt.% FeO^T.

Melting conditions and mantle potential temperatures can be estimated using primary melt compositions (Wang et al., 2012 and references therein). Effective melting pressure (P_f), an average equilibration pressure, is estimated at 1.0–1.4 GPa for the Chayuanshan basalts using the method of Lee et al. (2009). The estimated pressure is

consistent with the flat HREE patterns of the basalts (Figure 2.5b), indicating that partial melting occurred within the spinel stability field. The estimated melting temperature (T) is about 1370 ^{o}C using the method in Lee et al (2009). MgO concentrations of primary basaltic melts are directly related to melt temperatures (e.g., Albarède, 1992; Herzberg et al., 2007). The melt temperature of the Chayuanshan basalts is calculated at 1400 ± 40 °C (2σ) using the equation T (°C) = 2000 × MgO wt.% / (MgO wt.% + SiO_2 wt.%) + 969 (Albarède, 1992), consistent within error, with the estimation of 1370 ± 45 °C (2σ) using the alternative approach of Lee et al. (2009). The mantle potential temperature (T_p) is estimated at about 1430 ^{o}C (Herzberg et al., 2007).

It is noteworthy that neither of the two estimation models takes into account the effect of water, which is another factor that influences the melting temperatures and pressures. H_2O concentrations in melts were estimated using their primary Ce, assuming that the studied basalts have the same H_2O/Ce ratios of ~200 as oceanic basalts (Herzberg et al., 2007). The calculated H_2O concentrations are constant at 0.5 wt.% based on the Ce contents of all nine basaltic samples. However, this may represent an underestimation of the water concentration because the high Si–Mg and low Fe concentrations associated with the significant depletions of Nb, Ta, Zr, Hf and Ti indicate that the source of the basalts was enriched in fluids (Wang et al., 2008 and references therein). There may have been other fluid phases (such as CO_2 and Cl), or higher H_2O/Ce ratios, in the melts compared with that in oceanic basalts. If we accept the highest value of H_2O/Ce (~300) from oceanic basalts (Dixon et al., 2002; Michael, 1995), the calculated H_2O concentration is ~0.75 wt.%. The effect of H_2O on olivine liquidus temperature was demonstrated as liquidus depression temperature (^{o}C) = 74.403 × (H_2O wt.%)$^{0.352}$ (Falloon and Danyushevsky, 2000). About 0.75 wt.% H_2O would suppress the melt temperature by ~70 °C relative to the anhydrous system. Therefore, both the estimated melting temperature and mantle potential temperature for the melting region of the SCLM are ~1300 ^{o}C, similar to that of a MORB-like asthenospheric mantle (McKenzie and Bickle, 1988).

2.5.4 Origin of the Chayuanshan basalts and andesites

Mantle convection normally involves the mobility of the viscous asthenosphere

rather than the solid sub-continental lithospheric mantle (e.g., Hager, 1981; Morgan, 1972). Sub-continental lithospheric mantle thus could be a distinct geochemical reservoir that provides significant impact on the trace elements and isotope concentrations of intra-plate basalts (e.g., Murphy and Dostal, 2007; Sprung et al., 2007; Wilson et al., 1995). The SCLM could also contain metasomatized veins that preserve geochemical signatures of ancient subduction events or record previous infiltration of asthenospheric melts (e.g., Sprung et al., 2007; Wang et al., 2008). Recent experiments show that subduction-derived fluids are characterized by low Nb/La and Nb/Th ratios but high Th/Ta and LREE/HREE ratios (e.g., Kessel et al., 2005). Such tectonic processes likely lead to the sub-continental lithospheric mantle becoming selectively enriched in incompatible elements and hydrous phases, and basalts consequently derived from such sources would thus be enriched in Th, LREE, but relatively depleted in HFSEs (such as Nb, Ta, Zr and Hf).

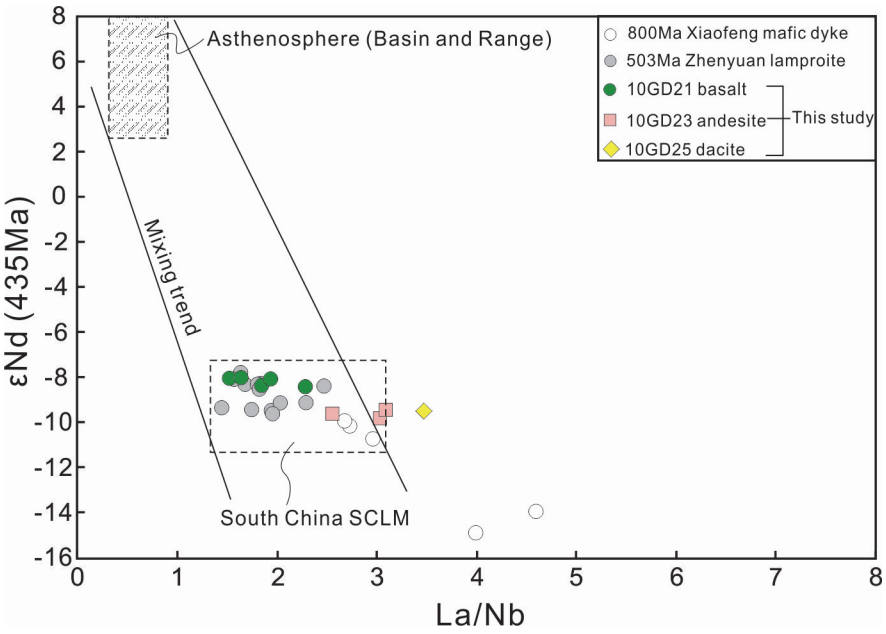

Figure 2.8. Plot of La/Nb versus εNd(435 Ma) of the Chayuanshan volcanic samples. The asthenosphere (Basin and Range, USA) area is modified after DePalo and Daley (2000). The South China SCLM (sub-continental lithospheric mantle) area is after Fang et al. (2002) and Zhang et al. (2008).

The following lines of evidence argue for the Chayuanshan basalts being derived from a metasomatized sub-continental lithospheric mantle. First, their low Nb/La ratios (0.4–0.8) and negative $\varepsilon_{Nd}(t)$ values (–8.0 to –8.4) fit the characteristics of melts from the sub-continental lithospheric mantle as summarized in DePalo and Daley (2000). The Chayuanshan basalts plot into the field of South China

sub-continental lithospheric mantle back-corrected to 435 Ma (Figure 2.8) using data from previous studies (e.g., Fang et al., 2002; Li et al., 2006; Wang et al., 2008; Xiao et al., 2004; Zhang et al., 2001; Zhang et al., 2008) and time evolution trend of ε_{Nd} values (DePalo and Daley, 2000; Murphy et al., 2008). Second, extremely low yet nearly constant Nd isotopic compositions in the nine basaltic samples imply that these basalts originated from an ancient sub-continental lithospheric mantle. Depletions in Nb–Ta and Zr–Hf–Ti suggest that the magma source may have experienced melt/fluid interaction before partial melting, which could be caused by previous subduction.

Andesites can be generated by differentiation of coeval basaltic magma melts followed by the assimilation and fractionation crystallization (AFC) processes during interactions with the crust (e.g., Mcbirney et al., 1987; Tatsumi, 2006). The Chayuanshan andesites and dacites have geochemical characteristics of constant and negative $\varepsilon_{Nd}(t)$ values (–9.4 to –9.8), and relatively low Nb/La ratios (0.3–0.4). The andesitic and dacitic samples share the same evolution trend as the basalts on the bivariation plots of Sm/Nd vs. Nb/La and La/Sm vs. Nb/La (Figure 2.6a–b), suggesting that the andesites and dacites were likely derived from the highly evolved basaltic end-member. Their relatively lower $\varepsilon_{Nd}(t)$ values, compared with the basalts, imply that they were generated by a basaltic magma which has assimilated with evolved crustal materials. This is consistent with their relatively high zircon $\delta^{18}O$ values of 7–9‰ and highly variable and negative $\varepsilon_{Hf}(t)$ values of –22 to –6.

2.5.5 The Chayuanshan volcanic succession: a product of post-kinematic lithospheric delamination?

As discussed above, the Chayuanshan volcanic rocks were probably derived from a metasomatized sub-continental lithospheric mantle (SCLM) with saturated water content and a MORB-like potential temperature. We also notice that the basalt outcrops occur close to the edge of the high-grade metamorphic core of the Wuyi–Yunkai orogen (Figure 2.1a). There are a number of scenarios in which the SCLM as part of a young intra-plate orogenic root can melt. One is lithosphere extension and decompression, which may occur in the late-orogenic stage. However, numerical modeling indicates that it is difficult to melt shallow lithospheric peridotite

(< 60 km) through extension alone at pressures less than about 2.0 GPa, even if hydrated, because ascent paths for the lithospheric mantle during extension do not move the mantle materials into supersolidus conditions (Harry and Leeman, 1995).

An orogenic cycle typically involves three stages of development (Froidevaux and Ricard, 1987): (1) crustal shortening leading to a thick crust and high topography at the orogenic core, (2) the thickened crust resisting further shortening, crustal root experiencing eclogite facies metamorphism, with the possibility of causing the delamination of both the eclogitic lower crustal and the attached lithospheric mantle, (3) late-orogenic tectonic collapse as a result of mantle–crust isostatic re-equilibrium (Leech, 2001; Schott and Schmeling, 1998). Crustal delamination requires that the crustal root undergoes mineral equilibration under eclogite facies, and becomes denser than the underlying mantle (Arndt and Goldstein, 1989). The delaminated eclogitic lower crust, along with the attached SCLM, would drop into the hotter asthenosphere, promoting regional asthenospheric upwelling.

Here we use the orogenic root delamination model (Figure 2.9), as proposed by Li et al. (2010c), to explain the generation of the Chayuanshan volcanic rocks. The model is supported by the following evidence and arguments. (1) Geochemical analyses on the basalts indicate that the basaltic magma was likely derived from an ancient hydrated sub-continental lithosphere mantle, whereas the andesites and dacites were the products of AFC processes with interactions between the basaltic magma and evolved crustal materials. (2) Melting of a hydrated SCLM requires it to be heated and elevated to a level with significantly lower pressure. The delamination of an orogenic root would bring a significant elevation of temperature at the edge of the remaining SCLM by asthenosphere upwelling. It would also reduce the pressure of the region by orogenic collapse as a consequence of the root delamination (Figure 2.9). (3) The melting temperature for the basaltic magma and the calculated mantle potential temperature are both ~1300 ^{o}C, similar to that of a MORB-like asthenospheric mantle, supporting the hypothesis that the partially molten SCLM was heated up by upwelling asthenosphere triggered by the dropping of the delaminated lithosphere (Figure 2.9). (4) The Chayuanshan volcanic rocks unconformably overlie the strongly deformed Cambro-Ordovician succession with a high-angle contact, but is in nearly parallel depositional contact with the overlying,

post-orogenic Devonian succession (Figure 2.1b), indicating that the magmatic event occurred after peak deformation in the region but prior to the end of the orogeny, consistent with these volcanic rocks being formed during post-kinematic orogenic root delamination. (5) The *ca.* 435 Ma age of the volcanism post-dates the high-grade metamorphism at *ca.* 460–440 Ma, but synchronous with the widespread, dominantly post-kinematic felsic magmatism at *ca.* 440–415 Ma (Li et al., 2010c and references therein), making the underplating of such mafic magmatism, in combination with heat from the upwelling asthenosphere and decompression due to orogenic collapse, a plausible cause for the widespread post-kinematic felsic magmatism (Figure 2.9). (6) The location of the Chayuanshan volcanic rocks near the margin of the orogenic core is consistent with the model prediction in which the delaminated orogenic root was primarily from the region below the core of the orogen (Figure 2.9).

The model also predicts asthenospheric melts due to decompression after the delamination. Such melts likely contributed to the basaltic underplating beneath the orogen. However, outcrop of such magmatism has not yet been identified, possibly due to the poor outcropping conditions and the lack of detailed studies on the Wuyi–Yunkai orogen.

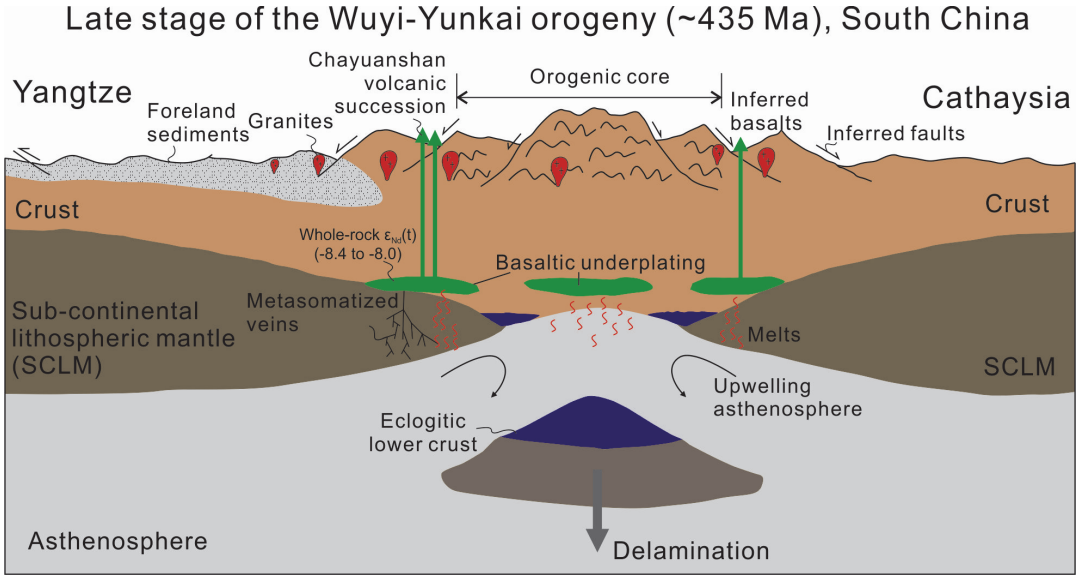

Figure 2.9. A cartoon diagram showing the sub-continental lithospheric mantle (SCLM) and lower crust delamination after crustal thickening during the Wuyi–Yunkai orogeny at ~435 Ma. Cartoons for the early evolution of the Wuyi–Yunkai orogeny can be found in Li et al. (2010c).

2.6 Conclusions

We report here geochronological, geochemical and isotopic data for the first lower Palaeozoic mafic-intermediate volcanic succession found in the Ordovician–Silurian (>460 Ma to *ca.* 420 Ma) Wuyi–Yunkai orogen in the South China Block. Our results place new constraints on the timing of the late-orogenic magmatism, and support the model of post-kinematic lithospheric delamination and orogenic collapse for the generation of widespread post-kinematic Silurian magmatism in South China. Our main findings are the followings:

(1) The Chayuanshan volcanic succession, consisting of high-Mg basalts, andesites and dacites with a crystallization age of ~435 Ma (early Silurian), is the first syn- to late-orogenic mafic to intermediate volcanic succession found in the lower Palaeozoic Wuyi–Yunkai orogen. It occurred after the major regional deformation as well as the high-grade metamorphism at *ca.* 460–440 Ma in the orogenic core but prior to the formation of the post-orogenic mid-Devonian succession;

(2) The basalts are characterized by high Mg contents (MgO = 12.3–19.2 wt.%), low $\varepsilon_{Nd}(t)$ values (–8.0 to –8.4), and low Nb/La ratios (0.4–0.8). The andesites and dacites are characterized by high Mg (MgO = 1.9–4.6 wt.%), slightly lower $\varepsilon_{Nd}(t)$ values (–9.4 to –9.8), lower Nb/La ratios (0.3–0.4), negative zircon $\varepsilon_{Hf}(t)$ values (–21.7 to –6.3) and positive zircon $\delta^{18}O$ values (7.3–9.0‰);

(3) The basalts were likely derived from partial melting of an ancient hydrated and metasomatized sub-continental lithospheric mantle with potential melting temperature of ~1300 °C. The andesites and dacites were likely generated from the same basaltic magma by AFC processes;

(4) Post-kinematic lithospheric delamination in the Wuyi–Yunkai orogen likely caused partial melting near the edge of the remaining sub-continental lithospheric mantle by upwelling asthenosphere, which produced the Chayuanshan volcanic rocks. Heat from the upwelling asthenosphere as well as possible basaltic underplating, and regional decompression caused by orogenic collapse, can best explain the widespread and synchronous granites along the orogen.

2.7 Acknowledgment

We thank L.F. Meng, J.H. Tao, L. Wang and W.Q. Yang for helps during the field work. Q.L. Li, Y.H. Yang and H.X. Ma are thanked for their assistance in SIMS oxygen analyses, LA(MC)-ICP-MS U–Pb dating/Hf analyses and mount making, respectively. Z.Y. Ren, Y. Liu and X.L. Tu are thanked for their assistance in geochemical and Nd isotopic analyses, and L. Almberg for proofreading the paper. Constructive reviews by J.B. Murphy and an anonymous reviewer improved the quality of this paper. This study was supported by the Chinese Academy of Sciences SAFEA International Partnership Program for Creative Research Teams grant (KZCX2-YW-Q04-06), National Natural Sciences Foundation of China (40973025) and the Australian Research Council (DP110104799). This is TIGeR (The Institute for Geoscience Research) publication #421, and contribution 193 from the ARC Center of Excellence for Core to Crust Fluid Systems (http://www.ccfs.mq.edu.au/).

2.8 References

Albarède, F., 1992. How deep do common basaltic magmas form and differentiate? Journal of Geophysical Research 97, 10997–11009.

Amelin, Y., Lee, D.C., Halliday, A.N., Pidgeon, R.T., 1999. Nature of the Earth's earliest crust from hafnium isotopes in single detrital zircons. Nature 399, 252–255.

Anderson, T., 2002. Correction of common lead in U–Pb analyses that do not report ^{204}Pb. Chemical Geology 192, 59–79.

Arndt, N.T., Goldstein, S.L., 1989. An open boundary between lower continental crust and mantle: its role in crust formation and crustal recycling. Tectonophysics 161, 201–212.

Beattie, P., Ford, C., Russell, D., 1991. Partition coefficients for olivine–melt and orthopyroxene–melt systems. Contributions to Mineralogy and Petrology 109, 212–224.

Blichert Toft, J., Albarède, F., 1997. The Lu–Hf isotope geochemistry of chondrites and the evolution of the mantle–crust system. Earth and Planetary Science Letters 148, 243–258.

Charvet, J., Shu, L.S., Faure, M., Choulet, F., Wang, B., Lu, H.F., Breton, N.L., 2010.

Structural development of the Lower Paleozoic belt of South China: Genesis of an intracontinental orogen. Journal of Asian Earth Sciences 39, 309–330.

Chen, C.H., Lee, C.Y., Hsieh, P.S., Zeng, W., Zhou, H.W., 2008. Approaching the age problem for some metamorphosed Precambrian basement rocks and Phanerozoic granitic bodies in the Wuyi area: the application of EMP monazite age dating. Geological Journal of China University 14, 1–15 (in Chinese with English abstract).

DePalo, D.J., Daley, E.E., 2000. Neodymium isotopes in basalts of the southwest basin and range and lithospheric thinning during continental extension. Chemical Geology 169, 157–185.

Dewey, J.F., 1988. Extensional collapse of orogens. Tectonics 7, 1123–1139.

Dixon, J.E., Leist, L., Langmuir, C., Schilling, J.G., 2002. Recycled dehydrated lithosphere observed in plume-influenced mid-ocean-ridge basalt. Nature 420, 385–389.

Ducea, M.N., 2011. Fingerprinting orogenic delamination. Geology 39, 191–192.

Falloon T.J., Danyushevsky, L.V., 2000. Melting of refractory mantle at 1.5, 2 and 2.5 GPa under anhydrous and H_2O-undersaturated conditions: implications for the petrogenesis of high-Ca boninites and the influence of subduction components on mantle melting. Journal of Petrology 41, 257–283.

Fang, W.X., Hu, R.Z., Su, W.C., Xiao, R.F., Qi, L., Jiang, G.H., 2002. Emplacement age of Zhenyuan lamproite in Guizhou. China Science Bulletin 47, 307–312 (in Chinese with English abstract).

Fillerup, M.A., Knapp, J.H., Knapp, C.C., Raileanu, V., 2010. Mantle earthquakes in the absence of subduction? Continental delamination in the Romanian Carpathians. Lithosphere 2, 333–340.

Froidevaux, C., Ricard, Y., 1987. Tectonic evolution of high plateaus. Tectonophysics 134, 227–238.

GDRGMR, 1962. Regional Geological Mapping and Report of Guangdong Province – 1:200,000 Shaoguan Sheet. Institute of Geoscience, Ministry of Geology, Beijing (in Chinese).

GDBGMR, 1988. Bureau of Geology and Mineral Resources of Guangdong Province. Geology Publishing House, Beijing (in Chinese with English abstract).

Griffin, W.L., Pearson, N.J., Belousova, E., Jackson, S.E., Achterbergh, E.V.,

O'Reilly, S.Y., Shee, S.R., 2000. The Hf isotope composition of cratonic mantle: LAM-MC-ICPMS analysis of zircon megacrysts in kimberlites. Geochimica et Cosmochimica Acta 64, 133–147.

Gutierrez-Alonso, G., Murphy, J.B., Fernández-Suárez, J., Weil, A.B., Franco, M.P., Gonzalo, J.P., 2011. Lithospheric delamination in the core of Pangea: Sm–Nd insights from the Iberian mantle. Geology 39, 155–158.

Hager, B.H., 1981. A simple global model of plate dynamics and mantle convection. Journal of Geophysical Research 86, 4843–4867.

Harry, D.L., Leeman, W.P., 1995, Partial melting of melt metasomatized subcontinental mantle and the magma source potential of the lower lithosphere. Journal of Geophysical Research 100, 255–269.

Herzberg, C., Asimow, P.D., Arndt, N., Niu, Y., Lesher, C.M., Fitton, J.G., Saunders, A.D., 2007. Temperature in ambient mantle and plumes: constraints from basalts, picrites and komatiites. Geochemistry Geophysics Geosystems 8, 1–34.

Huang J., Ren J., Jiang C., Zhang Z., Qin D., 1980. The Geotectonic Evolution of China. Science Press, Beijing (in Chinese with English abstract).

Jackson, S.E., Pearson, N.J., Griffin, W.L, Belousova, E.A., 2004. The application of laser ablation-inductively coupled plasma-mass spectrometry to *in-situ* U–Pb zircon geochronology. Chemical Geology 211, 47–69.

Jiao, W.F., Wu, Y.B., Yang, S.H., Peng, M., Wang, J., 2009. The oldest basement rock in the Yangtze Craton revealed by zircon U–Pb age and Hf isotope composition. Science in China Series D: Earth Sciences 52, 1393–1399.

Kay, R.W., Kay, S.M., 1993. Delamination and delamination magmatism. Tectonophysics 219, 177–189.

Kessel, R., Schmidt, M.W., Ulmer, P., Pettke, T., 2005. Trace element signature of subduction-zone fluids, melts and supercritical liquids at 120–180 km depth. Nature 437, 724–727.

Langmuir, C.H., Klein, E.M., Plank, T., 1992. Petrological systematics of mid-ocean ridge basalts: Constraints on melt generation beneath ocean ridges, in: Morgan, J.P., Blackman, D.K., Sinton, J.M. (Eds.), Mantle Flow and Melt Generation at Mid-Ocean Ridges. American Geophysical Union Geophysical Monograph, New York, pp. 183–280.

Lee, C.T., Luffi, P., Plank, T., Dalton, H., Leeman, W. P., 2009. Constraints on the

depths and temperatures of basaltic magma generation on Earth and other terrestrial planets using new thermobarometers for mafic magmas. Earth and Planetary Science Letters 279, 20–33.

Lee, C.T., Luffi, P., Chin, E.J., 2011. Building and Destroying Continental Mantle. Annual Review of Earth and Planetary Sciences 39, 59–90.

Leech, M.L., 2001. Arrested orogenic development: eclogitization, delamination, and tectonic collapse. Earth and Planetary Science Letters 185, 149–159.

Li, X.H., 1997. Timing of the Cathaysia Block formation: constraints from SHRIMP U–Pb zircon geochronology. Episodes 20, 188–192.

Li, Z.X., 1998. Tectonic history of the major East Asian lithospheric blocks since the mid-Proterozoic — a synthesis. In: Flower, M.J., Chung, S.L., Lo, C.H., Lee, T.Y. (Eds.), Mantle Dynamics and Plate Interactions in East Asia. American Geophysical Union, Washington, DC, pp. 221–243.

Li, X.H., 1991. Geochronology of the Wanyangshan-Zhuguangshan granitoid batholith: implication for the crust development. Science in China. Series B 34, 620–629.

Li, X.H., Gui, X.T., 1992. Source rocks of Wanyangshan–Zhuguangshan Caledonian granitic batholith, South China: evidence from Sr–Nd–Pb–O isotopic constraints. Science in China. Series B 5, 533–540 (in Chinese with English abstract).

Li, Z.X., Li, X.H., 2007. Formation of the 1300-km-wide intracontinental orogen and postorogenic magmatic province in Mesozoic South China: a flat-slab subduction model. Geology 35, 179–182.

Li, Z.X., Powell, C.M., 2001. An outline of the palaeogeographic evolution of the Australasian region since the beginning of the Neoproterozoic. Earth-Science Reviews 53, 237–277.

Li, X.H., Tatsumoto, M., Premo, W.R., 1989. Age and origin of the Tanghu granite, southeast China: results from U–Pb single zircon and Nd isotopes. Geology 17, 395–399.

Li, S.G., Huang, F., Li, H., 2002. Post-collisional lithosphere delamination of the Dabie–Sulu orogen. Chinese Science Bulletin 47, 259–263.

Li, X.H., Qi, C.S., Liu, Y., Liang, X.R., Tu, X.L., Xie, L.W., Yang, Y.H., 2005. Petrogenesis of the Neoproterozoic bimodal volcanic rocks along the western margin of the Yangtze Block: new constraints from Hf isotopes and Fe/Mn

ratios. Chinese Science Bulletin 50, 2481–2486.

Li, X.H., Li, Z.X., Sinclair, J.A., Li, W.X., Carter, G., 2006. Revisiting the "Yanbian Terrane": implications for Neoproterozoic tectonic evolution of the western Yangtze Block, South China. Precambrian Research 151, 14–30.

Li, Z.X., Wartho, J.A., Occhipinti, S., Zhang, C.L., Li, X.H., Wang, J., Bao, C.M., 2007. Early history of the eastern Sibao Orogen (South China) during the assembly of Rodinia: new mica $^{40}Ar/^{39}Ar$ dating and SHRIMP U–Pb detrital zircon provenance constraints. Precambrian Research 159, 79–94.

Li, W.X., Li, X.H., Li, Z.X., Lou, F.S., 2008a. Obduction-type granites within the NE Jiangxi Ophiolite: implications for the final amalgamation between the Yangtze and Cathaysia Blocks. Gondwana Research 13, 288–301.

Li, Z.X., Li, X.H., Li, W.X., Ding, S., 2008b. Was Cathaysia part of Proterozoic Laurentia? —New data from Hainan Island, south China. Terra Nova 20, 154–164.

Li, X.H., Li, W.X., Li, Z.X., Lo, C.H., Wang, J., Ye, M.F., Yang, Y.H., 2009. Amalgamation between the Yangtze and Cathaysia Blocks in South China: constraints from SHRIMP U–Pb zircon ages, geochemistry and Nd–Hf isotopes of the Shuangxiwu volcanic rocks. Precambrian Research 174, 117–128.

Li, X.H., Li, W.X., Li, Q.L., Wang, X.C., Liu, Y., Yang, Y.H., 2010a. Petrogenesis and tectonic significance of the 850 Ma Gangbian alkaline complex in South China: evidence from *in-situ* zircon U–Pb dating, Hf–O isotopes and whole-rock geochemistry. Lithos 114, 1–15.

Li, X.H., Long, W.G., Li, Q.L., Liu, Y., Zheng, Y.F., Yang, Y.H., Chamberlain, K.R., Wan, D.F., Guo, C.H., Wang, X.C., Tao, H., 2010b. Penglai zircon megacrysts: a potential new working reference material for microbeam determination of Hf–O isotopes and U–Pb age. Geostandards and Geoanalytical Research 34, 117–134.

Li, Z.X., Li, X.H., Wartho, J.A., Clark, C., Li, W.X., Zhang, C.L., Bao, C.M., 2010c. Magmatic and metamorphic events during the early Paleozoic Wuyi–Yunkai orogeny, southeastern South China: new age constraints and pressure–temperature conditions. Geological Society of America Bulletin 122, 772–793.

Liu, R., Zhang, L., Zhou, H.W., Zhong, Z.Q., Zeng, W., Xiang, H., Ji, S., Lv, X.Q.,

Li, C.Z., 2008. Petrogenesis of the Caledonian migmatites and related granites in northwestern Fujian Province, South China: syndeformational crustal anatexis. Acta Petrologica Sinica 24, 1205–1222.

Ludwig, K.R., 2001a. Squid version 1.02 – A geochronological toolkit for Microsoft Excel. Berkley Geochronological Centre Special Publication, Berkley.

Ludwig, K.R., 2001b. Isoplot/Ex version 2.49 – A geochronological toolkit for Microsoft Excel. Berkley Geochronological Centre Special Publication, Berkley.

Lustrino, W., 2005. How the delamination and detachment of lower crust can influence basaltic magmatism. Earth Science Reviews 72, 21–38.

McBirney, A.R., Taylor, H.P., Armstrong, R.L., 1987. Paricutin re-examined: a classic example of crustal assimilation in calc-alkaline magma. Contributions to Mineralogy and Petrology 95, 4–20.

McKenzie, D., Bickle, M.J., 1988. The volume and composition of melt generated by extension of the lithosphere. Journal of Petrology 29, 625–679.

Michael, P., 1995. Regionally distinctive sources of depleted MORB: evidence from trace elements and H_2O. Earth and Planetary Science Letters 131, 301–320.

Möller, A., O'Brien, J.P., Kennedy, A., Kröner, A., 2003. Linking growth episodes of zircon and metamorphic textures to zircon chemistry: an example from the ultrahigh-temperature granulites of Rogaland (SW Norway). EMU Notes in Mineralogy 5, 65–82.

Morel, M.L.A., Nebel, O., Nebel-Jacobsen, Y.J., Miller, J.S., Vroon, P.Z., 2008. Hafnium isotope characterization of the GJ-1 zircon reference material by solution and laser-ablation MC-ICPMS. Chemical Geology 255, 231–235.

Morgan, W.J., 1972. Deep mantle convection plumes and plate motions. AAPG Bulletin 56, 203–213.

Murphy, J.B., Dostal, J., 2007. Continental mafic magmatism of different ages in the same terrane: Constraints on the evolution of an enriched mantle source. Geology 35, 335–338.

Murphy, J.B., Dostal, J., Keppie, J.D., 2008. Neoproterozoic–Early Devonian magmatism in the Antigonish Highlands, Avalon terrane, Nova Scotia: Tracking the evolution of the mantle and crustal sources during the evolution of the Rheic Ocean. Tectonophysics 461, 181–201.

Putirka, K.D., 2005. Mantle potential temperatures at Hawaii, Iceland, and the

mid-ocean ridge system, as inferred from olivine phenocrysts: Evidence for thermally driven mantle plume. Geochemistry Geophysics Geosystems 6, 1–14.

Qiu, Y.M., Gao, S., McNaughton, N.J., Groves, D.I., Ling, W.L., 2000. First evidence of >3.2 Ga continental crust in the Yangtze craton of south China and its implications for Archean crustal evolution and Phanerozoic tectonics. Geology 28, 11–14.

Ren, J.S., 1991. On the geotectonics of southern China. Acta Geologica Sinica 2, 111–130.

Roger, F., Leloup, P.H., Jolivet, M., Lacassin, R., Trinh, P.T., Brunel, M., Seward, D., 2000. Long and complex thermal history of the Song Chay metamorphic dome (northern Vietnam) by multi-system geochronology. Tectonophysics 321, 449–466.

Schott, B, Schmeling, H, 1998. Delamination and detachment of a lithospheric root. Tectonophysics 296, 225–247.

Sharma, M., 1997. Siberian traps, in: Mahoney, J.J., Coffin, M.F. (Eds.), Large Igneous Provinces: Continental, Oceanic and Planetary Flood Volcanism. American Geophysical Union Geophysical Monograph, New York, pp. 273–295.

Sláma, J., Košler, J., Condon, D.J., Crowley, J.L., Gerdes, A., Hanchar, J.M., Horstwood, M.S.A., Morris, G.A., Nasdala, L., Norberg, N., Schaltegger, U., Schoene, B., Tubrett, M.N., Whitehouse, M.J., 2008. Plesovice zircon – A new natural reference material for U–Pb and Hf isotopic microanalysis. Chemical Geology 249, 1–35.

Soderlund, U., Patchett, P.J., Vervoort, J.D., Isachsen, C.E., 2004. The ^{176}Lu decay constant determined by Lu–Hf and U–Pb isotope systematics of Precambrian mafic intrusions. Earth and Planetary Science Letters 219, 311–324.

Sprung, P., Schuth, S., Munker, C., Hoke, L., 2007. Intraplate volcanism in New Zealand: the role of fossil plume material and variable lithospheric properties. Contributions to Mineralogy and Petrology 153, 669–687.

Sun, S.S., McDonough, W.F., 1989. Chemical and isotopic systematics of oceanic basalt: implications for mantle composition and processes, in: Saunders, A.D., Norry, M.J. (Eds.), Magmatism in the Ocean Basins. Geological Society Special Publication, London, pp. 528–548.

Tatsumi, Y., 2006. High-Mg andesites in the Setouchi volcanic belt, southwestern Japan: Analogy to Archean magmatism and continental crust formation? Annual Review of Earth and Planetary Sciences 34, 467–499.

Valley, J.W., Kinny, P.D., Schulze, D.J., Spicuzza, M.J., 1998. Zircon megacrysts from kimberlite: oxygen isotope variability among mantle melts. Contributions to Mineralogy and Petrology 133, 1–11.

Wan, Y.S., Liu, D.Y., Wilde, S.A., Cao, J.J., Chen, B., Dong, C.Y., Song, B., Du, L.L., 2010. Evolution of the Yunkai Terrane, South China: Evidence from SHRIMP zircon U-Pb dating, geochemistry and Nd isotope. Journal of Asian Earth Sciences 37, 140–153.

Wang, J., Sun, D., Chang, X., Deng, S., Zhang, H., Zhou, H., 1998. U–Pb dating of the Napeng granite at the NW margin of the Yunkai block, Guangdong, South China. Acta Mineralogica Sinica 18, 130–133 (in Chinese with English abstract).

Wang, X.C., Li, X.H., Li, W.X., Li, Z.X., 2007a. *Ca.* 825 Ma komatiitic basalts in South China: first evidence for >1500 ^{o}C mantle melts by a Rodinian mantle plume. Geology 35, 1103–1106.

Wang, Y.J., Fan, W.M., Zhao, G.C., Ji, S.C., Peng, T.P., 2007b. Zircon U–Pb geochronology of gneissic rocks in the Yunkai massif and its implications on the Caledonian event in the South China Block. Gondwana Research 12, 404–416.

Wang, X.C., Li, X.H., Li, W.X., Li, Z.X., Liu, Y., Yang, Y.H., Liang, X.R., Tu, X.L., 2008. The Bikou basalts in the northwestern Yangtze block, South China: Remnants of 820–810 Ma continental flood basalts? Geological Society of America Bulletin 120, 1478–1492.

Wang, X.C., Li, X.H., Li, Z.X., Liu, Y., Yang, Y.H., 2010. The Willouran basic province of South Australia: Its relation to the Guibei large igneous province in South China and the breakup of Rodinia. Lithos 119, 569–584.

Wang, Y.J., Zhang, A.M., Fan, W.M., Zhao, G.C., Zhang, G.W., Zhang, F.F., Zhang, Y.Z., Li, S.Z., 2011. Kwangsian crustal anatexis within the eastern South China Block: Geochemical, zircon U–Pb geochronological and Hf isotopic fingerprints from the gneissoid granites of Wugong and Wuyi–Yunkai Domains. Lithos 127, 239–260.

Wang, X.C., Li, Z.X., Li, X.H., Li, J., Liu, Y., Long, W.G., Zhou, J.B., Wang, F., 2012.

Temperature, pressure, and composition of the mantle source region of late Cenozoic basalts in Hainan Island, SE Asia: a consequence of a young thermal mantle plume close to subduction zones? Journal of Petrology 53, 177–233.

White, R., McKenzie, D., 1989. Magmatism at rift zones: the generation of volcanic continental margins and flood basalts. Journal of Geophysical Research 94, 7685–7729.

Wiedenbeck, M., Alle, P., Corfu, F., Griffin, W.L., Meer, M., Oberli, F., Vonquadt, A., Roddick., J.C., Spegel, W., 1995. Three natural zircon standards for U–Th–Pb, Lu–Hf, trace element and REE analysis. Geostandards and Geoanalytical Research 19, 1–23.

Wiedenbeck, M., Hanchar, J.M., Peck, W.H., Sylvester, P., Valley, J., Whitehouse, M., Kronz, A., Morishita, Y., Nasdala, L., Fiebig, J., Franchi, I., Girard, J.P., Greenwood, R.C., Hinton, R., Kita, N., Mason, P.R.D., Norman, M., Ogasawara, M., Piccoli, P.M., Rhede, D., Satoh, H., Schulz-Dobrick, B., Spicuzza, M.J., Terada, K., Tindle, A., Togashi, S., Vennemann, T., Xie, Q., Zheng, Y.F., 2004. Further characterisation of the 91500 zircon crystal. Geostandards Newsletter 28, 9–39.

Wilson, M., 1989. Igneous Petrogenesis. Chapman and Hall, London.

Wilson, M., Rosenbaum, J.M., Dunworth, E.A., 1995. Melilitites: partial melts of the thermal boundary layer? Contribution to Mineral Petrology 119, 181–196.

Winchester, J.A., Floyd, P.A., 1976. Geochemical magma type discrimination: application to altered and metamorphosed basic igneous rocks. Earth and Planetary Science Letters 28, 459–469.

Wu, F.Y., Yang, Y.H., Xie, L.W., Yang, J.H., Xu, P., 2006. Hf isotopic compositions of the standard zircons and baddeleyites used in U–Pb geochronology. Chemical Geology 234, 105–126.

Xiang, H., Zhang, L., Zhou, H.W., Zhong, Z.Q., Zeng, W., Liu, R., Jin, S., 2008. U–Pb zircon geochronology and Hf isotope study of metamorphosed basic–ultrabasic rocks from metamorphic basement in southwestern Zhejiang: The response of the Cathaysia Block to Indosinian orogenic event. Science in China Series D: Earth Sciences 51, 788–800.

Xiao, L., Xu, Y.G., Mei, H.J., Zheng, Y.F., He, B., Pirajno, F., 2004. Distinct mantle sources of low-Ti and high-Ti basalts from the western Emeishan large

igneous province, SW China: implications for plume–lithosphere interaction. Earth and Planetary Science Letters 228, 525–546.

Xie, L.W., Zhang, Y.B., Zhang, H.H., Sun, J.F., Wu, F.W., 2008. *In-situ* simultaneous determination of trace elements, U–Pb and Lu–Hf isotopes in zircon and baddeleyite. Chinese Science Bulletin 53, 1565–1573.

Xu, X.S., O'Reilly, S.Y., Griffin, W.L., Deng, P., Pearson, N.J., 2005. Relict Proterozoic basement in the Nanling Mountains (SE China) and its tectonothermal overprinting. Tectonics 24, 1–16.

Yang, Y.H., Zhang, H.F., Xie, L.W., Wu, F.Y. 2007. Accutate measurement of Neodymium isotopic composition using Neptune multiple collector inductively coupled plasma mass spectrometry. Chinese Journal of Analytical Chemistry 35, 71–74.

Yang, D.S., Li, X.H., Li, W.X., Liang, X.Q., Long, W.G., Xiong, X.L., 2010. U–Pb and $^{40}Ar/^{39}Ar$ geochronology of the Baiyunshan gneiss (central Guangdong, South China): constraints on the timing of early Paleozoic and Mesozoic tectonothermal events in the Wuyun (Wuyi–Yunkai) Orogen. Geological Magazine 147, 481–496.

Yu, J.H., Wang, L.J., O'Reilly, S.Y., Griffin, W.L., Zhang, M., Li, C.Z., Shu, L.S., 2009. A Paleoproterozoic orogeny recorded in a long-lived cratonic remnant (Wuyishan terrane), eastern Cathaysia Block, China. Precambrian Research 174, 347–363.

Zandt, G., Gilbert, H., Owens, T.J., Ducea, M., Saleeby, J., Jones, C.H., 2004. Active foundering of a continental arc root beneath the southern Sierra Nevada in California. Nature 431, 41–46.

Zeng, W., Zhang, L., Zhou, H.W., Zhong, Z.Q., Xiang, H., Liu, R., Jin, S., Lu, X.Q., Li, C.Z., 2008. Caledonian reworking of Paleoproterozoic basement in the Cathaysia Block: Constraints from zircon U–Pb dating, Hf isotopes and trace elements. Chinese Science Bulletin 53, 895–904.

Zhang, H.F., Sun, M., Lu, F.X., Zhou, X.H., Zhou, M.F., Liu, Y.S., Zhang, G.W., 2001. Geochemical significance of a garnet lherzolite from the Dahongshan kimberlite, Yangtze Craton, southern China. Geochemical Journal 35, 315–331.

Zhang, S.B., Zheng, Y.F., Zhao, Z.F., Wu, Y.B., Yuan, H.L., Wu, F.Y., 2008. Neoproterozoic anatexis of Archean lithosphere: Geochemical evidence from

felsic to mafic intrusions at Xiaofeng in the Yangtze Gorge, South China. Precambrian Research 163, 210–238.

Zhang, A.M., Wang, Y.J., Fan, W.M., Zhang, F.F., Zhang, Y.Z., 2011. LA-ICPMS zircons U–Pb geochronology and Hf isotopic composition of the Taoxi migmatite (Wuping): constrains on the formation age of the Taoxi complex and the Yu'nan event. Geotectonica et Metallogenia 35, 64–72.

Zhang, F.F., Wang, Y.J., Zhang, A.M., Fan, W.M., Zhang, Y.Z., Zi, J.W., 2012. Geochronological and geochemical constraints on the petrogenesis of Middle Paleozoic (Kwangsian) massive granits in the eastern South China Block. Lithos 150, 188–208.

Zheng, J.P., Griffin, W.L., O'Reilly, S.Y., Zhang, M., Pearson, N., Pan, Y.M., 2006. Widespread Archean basement beneath the Yangtze craton. Geology 34, 417–420.

CHAPTER 3 FROM RODINIA TO GONDWANALAND: A TALE OF DETRITAL ZIRCON PROVENANCE ANALYSES FROM THE SOUTHERN NANHUA BASIN, SOUTH CHINA

WEI-HUA YAO[*,**,†], ZHENG-XIANG LI[*,†], WU-XIAN LI[***], XIAN-HUA LI[****], JIN-HUI YANG[****]

* ARC Center of Excellence for Core to Crust Fluid Systems (CCFS), The Institute for Geoscience Research (TIGeR), Department of Applied Geology, Curtin University, Perth, WA 6845, Australia

** Faculty of Earth Resource, China University of Geosciences, Wuhan 430074, China

*** Key Laboratory of Isotope Geochronology and Geochemistry, Guangzhou Institute of Geochemistry, Chinese Academy of Sciences, Guangzhou 510640, China

**** State Key Laboratory of Lithospheric Evolution, Institute of Geology and Geophysics, Chinese Academy of Sciences, Beijing 100029, China

† Corresponding authors: weihua.yao@postgrad.curtin.edu.au; z.li@curtin.edu.au

Abstract

The palaeogeographic positions of the South China Block (SCB) during the Neoproterozoic and early Palaeozoic are important for understanding the transition from the break-up of the supercontinent Rodinia to the formation of Gondwanaland. Integrated *in situ* U–Pb ages and Hf–O isotope analyses of detrital zircons from Cambrian sedimentary rocks in the southwestern SCB reveal major age populations at 2500 Ma, 1100 to 900 Ma, 850 to 750 Ma and 650 to 500 Ma, with a predominant group at ~980 Ma that counts for ~50 percent of all analyses. Zircon Hf–O isotopic results suggest three Precambrian episodes of juvenile crustal growth for the source area(s) (3.0 Ga, 2.5 Ga and 1.0 Ga), with major crustal reworking at 580 to 500 Ma. The source provenance as defined by the U–Pb and Hf analyses is distinctly different from the known

tectonomagmatic record of the SCB, or that of western Australia or western Laurentia, but matches well with that of the Ediacaran (latest Neoproterozoic)–Cambrian clastic sedimentary rocks and granitic intrusions in the NW Indian Himalaya. The SCB–NW India provenance linkage appears to have started from the Ediacaran. We propose that after breaking away from central Rodinia, the SCB collided with NW India during the Ediacaran–Ordovician time, causing the "Pan-African" Kurgiakh/Bhimphedian orogeny at the northern margin of India as well as the intraplate Wuyi–Yunkai orogeny (>460 Ma – 415 Ma) in South China. The Ediacaran–lower Palaeozoic clastic sedimentary rocks in the Nanhua Basin are therefore interpreted to be foreland deposits formed during the collision of the SCB with Gondwanaland.

Key words: Detrital zircon, Cambrian, Cathaysia Block, South China, North India, Rodinia, Gondwanaland

3.1 Introduction

The South China Block (SCB; Figure 3.1A inset) has featured prominently in studies of Earth history during the Precambrian–Cambrian transition, including the Neoproterozoic extreme global palaeoclimate (for example, Jiang and others, 2003), the rapid explosion of complex life (for example, Zhu and others, 2007), and the closely linked issue of global palaeogeography between the break-up of the Neoproterozoic supercontinent Rodinia and the formation of Gondwanaland (for example, Hoffman, 1991; Z.X. Li and others, 1996; Zhou and others, 2002). It has been suggested that the Cathaysia Block of the SCB was once connected to western Laurentia during the Mesoproterozoic, and joined with the Yangtze Block and Australia by *ca.* 900 Ma to become a central part of the early Neoproterozoic supercontinent Rodinia (Z.X. Li and others, 2008a). The coherent SCB broke away during the break-up of Rodinia in the mid- to late-Neoproterozoic (750–650 Ma), and then drifted toward the margin of eastern Gondwanaland by the Cambrian (Z.X. Li and others, 1996; Z.X. Li and Powell, 2001). Alternatively, it has been suggested that the SCB started its western Australia–northern India connection since Rodinia time or earlier (Zhang and Piper, 1997; Jiang and others, 2003; Yang and others, 2004; Yu and others, 2008; Cawood and others, 2013), or was on the margin of northwestern Australia at that time (Zhou and others, 2002, 2006; Wang and others, 2004). The

main reason for the existence of such diverse views is the current poor knowledge of the Precambrian evolution of the Cathaysia Block and that of the SCB in general, due to its extensive Phanerozoic reworking and poor outcrops of basement rocks (for example, Gan and others, 1995; X.H. Li, 1997; Chen and Jahn, 1998; Wan and others, 2007; Xu and others, 2007; Yu and others, 2010).

Detrital zircons from siliciclastic sedimentary rocks have proven to provide a good record of geological information about their source regions (for example, Barth and others, 2000; Neves, 2003). U–Pb age spectra of such detrital zircons can indicate provenance characteristics, including possible magmatic events that the source region experienced and affinity with other terranes/blocks (for example, Condie and others, 2009; Zhu and others, 2011). *In situ* Hf–O isotopic results for detrital zircons can further reveal tectonothermal events involving either mantle input to existing continental crust and/or reworking of pre-existing crustal materials (for example, Griffin and others, 2004; Hawkesworth and Kemp, 2006; Kemp and others, 2006; Belousva and others, 2010). Integrated detrital zircon U–Pb ages and Hf–O isotopic analyses have therefore become a powerful tool for deciphering the evolution of continental crust (for example, Zhang and others, 2006; Condie and others, 2009), for reconstructing continental block/terrane assemblages (for example, Stewart and others, 2001; Zhu and others, 2011) – particularly for terranes like the Cathaysia Block where basement bedrock is poorly exposed, and for analyzing transportation processes and provenance mixing (Zhang and others, 2012).

In this study, we report detrital zircon U–Pb ages and Hf–O isotopes for Cambrian marine sandstones/metasandstones that were deposited in Guangdong Province, western Cathaysia (Figure 3.1). Together with published detrital zircon U–Pb/Hf data of latest Neoproterozoic (Ediacaran)–Cambrian clastic sedimentary rocks from nearby regions, these data offer new insights on the late Precambrian to early Palaeozoic tectonic evolution of the SCB and shed light on its interactions with other continents from the break-up of Rodinia to the assembly of Gondwanaland.

3.2 Geological Background and Sampling

The SCB, consisting of the Yangtze Block in the northwest and the Cathaysia Block

in the southeast, is bounded by the Mesozoic Qinling–Dabie–Sulu orogenic belt to the north, the Mesozoic–Cenozoic Longmenshan orogenic belt to the northwest, the Cenozoic Red River Fault to the southwest, and the Cenozoic continental slope of the East and South China seas to the southeast (Figure 3.1). The present boundary between the Yangtze and Cathaysia blocks in eastern South China is approximately the northeasterly trending Jiangshan–Shaoxing Fault (Figure 3.1A). However, the southwestern extension of this boundary is unclear due to poor exposure and tectonic modifications (Ren, 1991; Z.X. Li and others, 2010).

The Yangtze and Cathaysia blocks exhibit different pre-Neoproterozoic crustal growth histories with contrasting crystalline basement rocks. The Yangtze basement consists predominantly of Proterozoic rocks with minor outcrops of Archean rocks found in the Kongling Complex in northern Yangtze (locally known as the Kongling "Group", dated at *ca.* 3.3 to 3.2 Ga and *ca.* 2.95 to 2.90 Ga; Qiu and others, 2000; Zheng and others, 2006; Jiao and others, 2009; Gao and others, 2011). Along the southeastern Yangtze margin, scattered outcrops of Mesoproterozoic metasedimentary rocks (≤1.53 Ga) that experienced 1.04 to 0.94 Ga metamorphism/reworking (Z.X. Li and others, 2007), and some 1.16 to 0.88 Ga magmatic rocks (Ye and others, 2007; W.X. Li and others, 2008; X.H. Li and others, 2009; L. Li and others, 2013), are present. More widespread outcrops of *ca.* 1.7 to 0.9 Ga volcanic and sedimentary rocks, or their metamorphosed equivalents, are found along the southwestern Yangtze margin (Z.X. Li and others, 2002; Greentree and others, 2006; Greentree and Z.X. Li, 2008; Sun and others, 2009; Zhao and others, 2010). Widespread mid- to late-Neoproterozoic igneous rocks (860 to 750 Ma) and volcaniclastic successions are well developed in rift basins along the Yangtze margins (for example, Zhou and others, 2002, 2006; Z.X. Li and others, 2003; X.H. Li and others, 2003; Wang and others, 2006; W.X. Li and others, 2010).

The Cathaysia Block has even less Precambrian basement exposed, with most regions covered by Phanerozoic (particularly Mesozoic) sedimentary and/or volcanic rocks. Although Archean zircons have been reported from either Cathaysian sedimentary rocks (for example, X.H. Li, 1997; Wan and others, 2007; Xu and others, 2007; Yu and others, 2009; Z.X. Li and others, 2010; Yao and others, 2011) or as xenocrysts in volcanic rocks (Zheng and others, 2011), no Archean rocks have been

identified so far. The oldest known crystalline basement rocks are the *ca.* 1.89 to 1.77 Ga granites and amphibolite facies metamorphic rocks in western Zhejiang and northwestern Fujian Provinces in the northeast part of Cathaysia (X.H. Li, 1997; Z.X. Li and X.H. Li, 2007; Xiang and others, 2008; Zeng and others, 2008; Yu and others, 2011). On Hainan Island in southwestern Cathaysia (Figure 3.1A), known Precambrian basement rocks include the *ca.* 1.43 Ga Baoban Complex gneissic granitoids, adjacent coeval Shilu Group metavolcaniclastic succession and the overlying *ca.* 1.0 Ga Shihuiding Formation metasedimentary rocks (Ma and others, 1998; Z.X. Li and others, 2002, 2008a). Mid- to late-Neoproterozoic (860–750 Ma) bimodal magmatic rocks and volcaniclastic successions (for example, W.X. Li and others, 2005; Shu and others, 2011) are also widely exposed on the Cathaysian side of the mid-Neoproterozoic Nanhua rift basin (Figure 3.1A).

Rifting in the mid- to late-Neoproterozoic Nanhua Basin ceased at *ca.* 700 Ma (Wang and Li, 2003), with the failed rift continuing to receive the uppermost Neoproterozoic (Ediacaran) to early Palaeozoic (Cambrian) sedimentary successions (Figure 3.1B; BGMRJX, 1984; BGMRGX, 1985; BGMRGD, 1988; BGMRGZ, 1988; BGMRHN, 1988; Ren, 1991; Ren and others, 1997; Yu and others, 2009). However, the sedimentation patterns of the Yangtze and Cathaysia blocks during the Ediacaran–Cambrian were quite different (Liu and Xu, 1994). The Yangtze Block was dominated by the precipitation of carbonate, argillaceous carbonate/dolomite, arenaceous carbonate, with siliciclastic intercalations found in the lower Cambrian strata in western Yangtze (BGMRGX, 1985; BGMRGZ, 1988; BGMRHN, 1988). It indicates that for much of the Ediacaran–Cambrian time the Yangtze Block was covered by shallow seas with no major elevated land areas to provide significant terrestrial detritus. In contrast, the Cathaysia Block received massive siliciclastic sedimentation (BGMRJX, 1984; BGMRGX, 1985; BGMRGD, 1988; BGMRHN, 1988), consisting of shale, siltstone, arkosic sandstone, quartz sandstone and minor pebbly sandstone (Figure 3.1B).

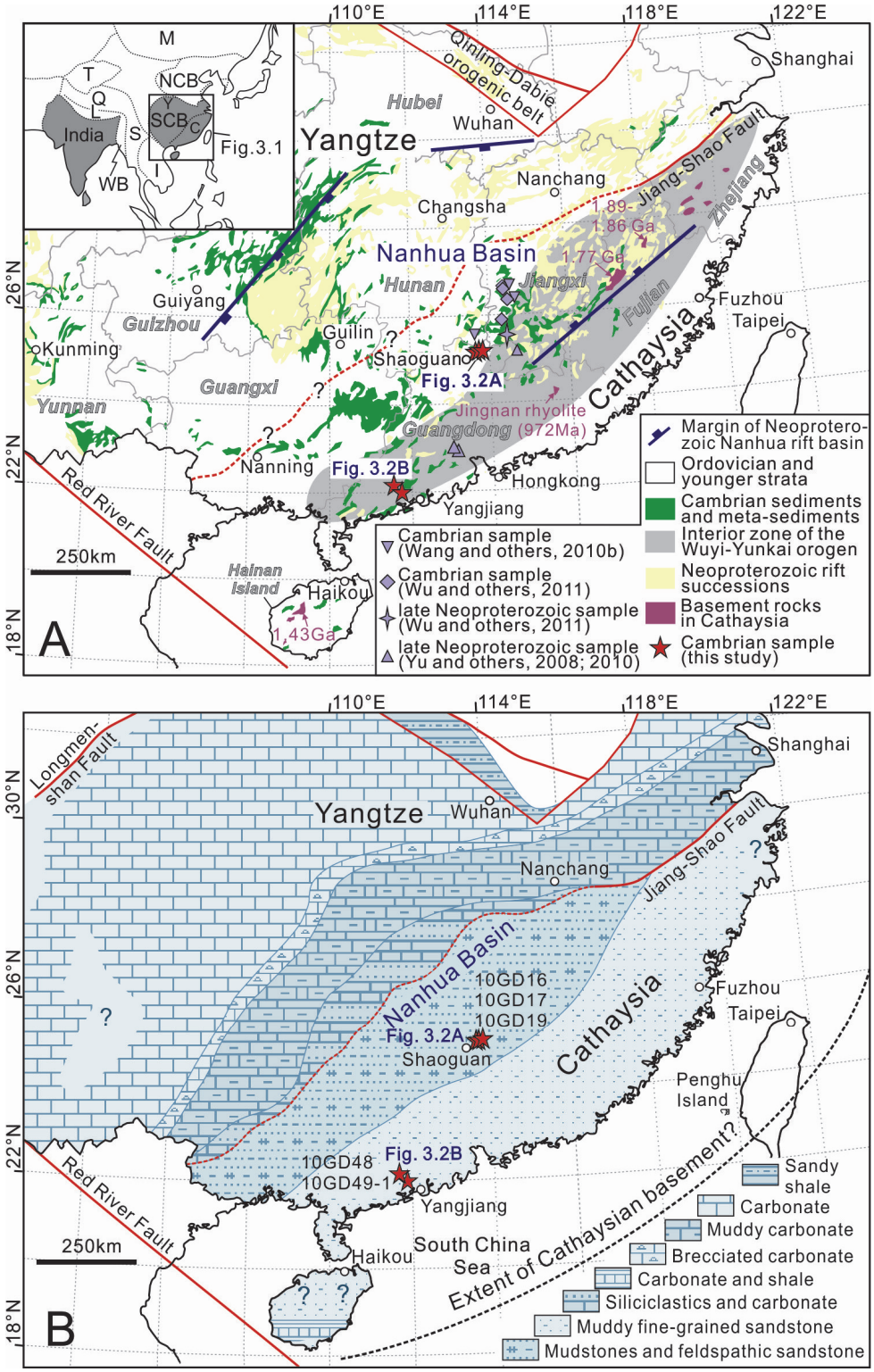

Figure 3.1. (A) Distribution of Precambrian and Cambrian rocks in the South China Block (SCB) and sample locations for both this study and previous studies. Inset figure in figure 3.1A shows the current geographic sketch of major continental blocks/terranes in the Southeast Asia. In which: NCB – North China Block, SCB – South China Block, Y – Yangtze, C – Cathaysia, M – Mongolian terranes, T – Tarim, L – Lhasa, S – Subumasu (including the Qiangtang terrane, shown as "Q"), I – Indochina, WB – West Burma. (B) Mid- to late-Cambrian palaeogeographic map of the SCB (revised after Wang, 1985 and Liu and Xu, 2004) with sample locations for this study. Some facies boundaries are truncated by younger thrust faults (red lines).

The Cambrian strata in Guangdong Province of western Cathaysia are generally referred to as the Bacun Group (BGMRGD, 1988), exhibiting marine clastic sedimentation. Its lower boundary is defined by a conformably underlying cherty unit at the top of the Ediacaran succession; this cherty unit is well developed and regionally correlatable through much of the Nanhua Basin (Liu and Xu, 1994). The upper boundary of the Cambrian strata is defined by conformably overlying Ordovician strata that contain early-Ordovician graptolites (BGMRGD, 1988; Zhang and He, 1993, and references therein). The Bacun Group in the northern Guangdong Province has been divided into three formations (Zhang and He, 1993). The bottom one is the Xiazhai Formation, consisting of quartz sandstone interlayered with carbonaceous shale and a few 'stone coal' (carbon-rich rocks that can be mined as fuels) units, and exhibiting characteristics of turbiditic marine facies. No Cambrian fossils have been found from this formation. The middle Bacun Group is called the Oujiadong Formation, featuring a series of transgression sequences. This formation hosts inarticulate brachiopod fossils *Acrothele* sp., *Homotreta* cf. *venia* (Walcott) and *Obolus* sp., and sponge fossil *Protospongia* sp. (Zhang and He, 1993, and references therein). The upper Bacun Group is called the Laoshuzhai Formation, consisting dominantly arkosic sandstone with muddy shale interlayers. It contains inarticulate brachiopod fossils *Lingulella* cf. *liui* Sun*, Homotreta* cf. *venia, Obolus* sp. and *Palaeobolus* cf. *rotulus* Wang, and the sponge fossil *Protospongia* sp. (Zhang and He, 1993). The three formations have therefore been given the ages of lower-, mid- and upper-Cambrian, respectively (BGMRGD, 1988; Zhang and He, 1993).

The Cambrian strata are best preserved in northern Guangdong Province, where the clastic successions are generally non-metamorphosed, but are complexly deformed and fault-interrupted with no single succession preserving the complete Cambrian strata. Here we examined and sampled the Oujiadong succession near Shaoguan, which is the type section for the Oujiadong and Laoshuzhai formations (Figure 3.2A and C; for location see Figure 3.1). The lower Cambrian Xiazhai Formation is missing from this succession as the Oujiadong Formation is in fault contact with either Neoproterozoic or Devonian strata (Figure 3.2A) (Zhang and He 1993). The succession is exposed along a small mountain track in a densely vegetated area. The lower part of the Oujiadong Formation consists of thick siltstone, fine-grained feldspathic quartz sandstone, and thin grey and purple mudstone. Horizontal

laminations are present in muddy sedimentary rocks (Figure 3.2D), indicating that transport energy was not high. The middle part of the Oujiadong Formation consists of packages of fine- to medium-grained thick quartz sandstone and thin shale units, with local low-angle cross-laminations observed in sandy units (Figure 3.2E). Local thin cherty units (Figure 3.2F) are present in the upper part of the Laoshuzhai Formation, which shares similar lithological associations with the underlying Oujiadong Formation. Three sandstone samples were collected from this stratigraphic section for detrital zircon provenance analysis, with samples 10GD16 and 10GD17 from the lower and upper parts of the Oujiadong Formation, respectively. Sample 10GD19 was taken from the upper part of the Laoshuzhai Formaiton according to Zhang and He (1993).

The Bacun Group in the southwestern Guangdong Province (Figure 3.2B) has generally been metamorphosed to greenschist facies. Although regional lithological correlations and fossils found in the metasedimentary rocks (for example, *Lingulella* cf. *Liui, Homotreta* cf. *venia, H.* cf. *shantungenesis, Acrothele* sp., *Acrothele* cf. *asiatica,* and *Protospongia* sp.) point to a Cambrian age for the metasedimentary rocks, unequivocal stratigraphic subdivision has not been possible (RGMRGD, 1964; BGMRGD, 1988). Here we collected two meta-sandstone samples for detrital zircon provenance analysis because of the approximation of the locality to the basin margin (Figure 3.1B): sample 10GD48 was from a locality ~50 km northwestern of Yangjiang city, and sample 10GD49-1 was from a locality ~20 km western of Yangjiang (Figure 3.2B).

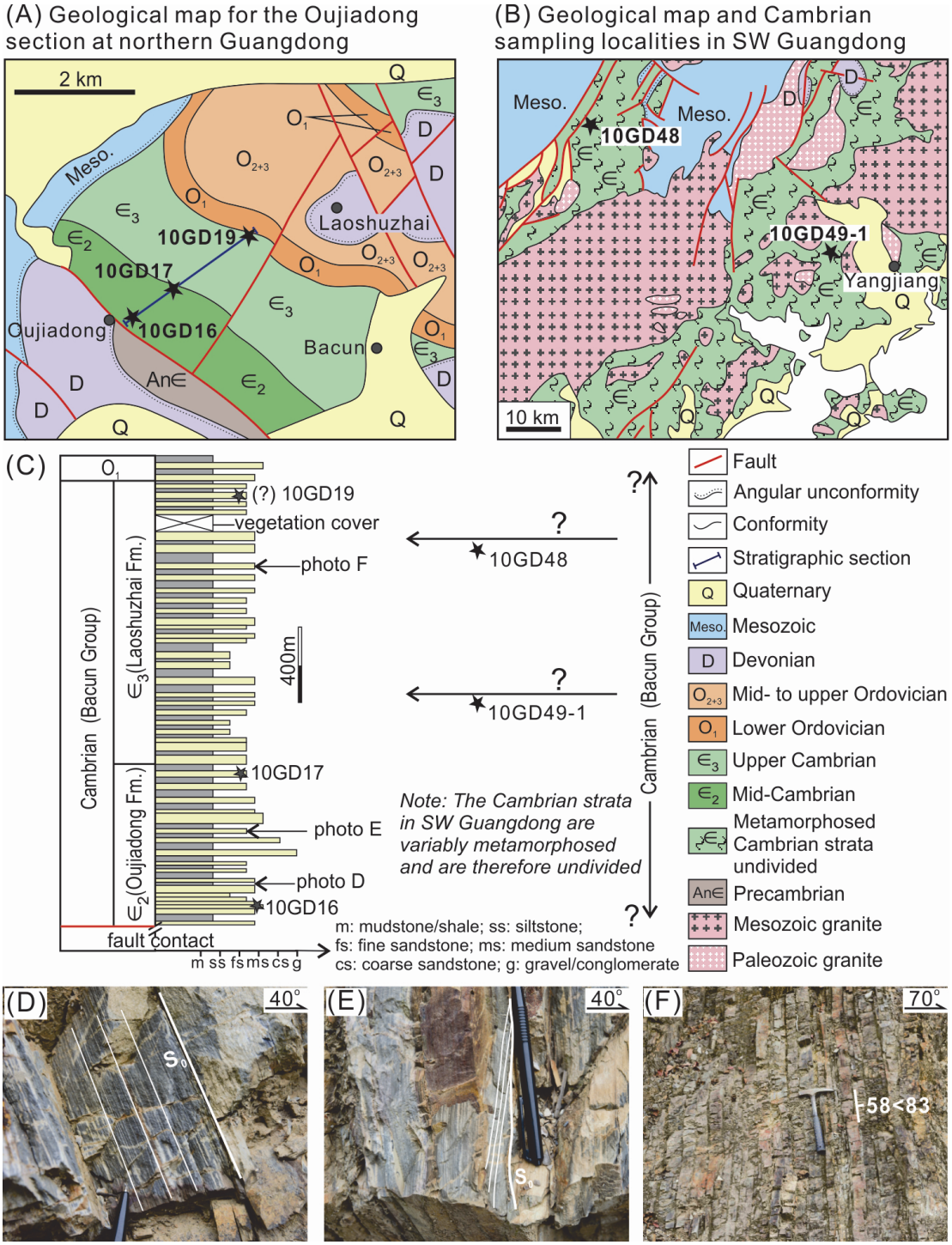

Figure 3.2. (A) Regional geological map and sampling localities along the Oujiadong section near Shaoguan, northern Guangdong Province (after Zhang and He, 1993). (B) Regional geological map and sampling localities in the southwestern Guangdong Province (after RGMRGD, 1964). See figure 3.1 for map locations of both (A) and (B). (C) Stratigraphy of the Oujiadong section (see location in (A)) with sampling positions. Note that the stratigraphic positions of the two metasedimentary samples from southwestern Guangdong can not be precisely located. (D) Horizontal laminations in grey-black muddy shale. (E) Low-angle cross-laminations (marked as "S_1") in siltstone layers. (F) Cherty layers with high dip angles. The hammer is 28 cm in length, and the pencil is 15 cm in length, for scale.

3.3 Analytical Methods

3.3.1 Sample Preparation

Mineral separation of the five samples was conducted at the Institute of Hebei Regional Geology and Mineral Survey in Langfang, China. The crushed samples were washed with water and then with alcohol to extract the denser components. Magnetic and heavy liquid separation techniques were adopted for concentrating heavy minerals. Zircon grains were hand-picked under a binocular microscope, and then mounted in epoxy resin with zircon U–Pb standards 91500 and Plešovice, and zircon oxygen standard Penglai. The mounts were polished to expose the internal structure of the zircon grains. We analyzed at least 100 grains for each sample. All analyzed zircon grains were imaged in transmitted and reflected light, as well as by cathodoluminescence (CL) to reveal their internal structure. For those grains with rim–core structures, we analyzed their rims only, since these ages record the most recent tectonothermal events.

3.3.2 Zircon U–Pb Geochronology

3.3.2.1 LA-ICP-MS U–Pb dating

Detrital zircon analyses for samples 10GD48 and 10GD49-1 were conducted at the Institute of Geology and Geophysics (IGG), Chinese Academy of Sciences (CAS) in Beijing, using an Agilent 7500a multicollector-inductively coupled plasma-mass spectrometer (MC-ICP-MS). Each analysis included a ~30s background measurement with laser off and a ~60s measurement at peak intensity. The ablation pits were generally ~45 μm in diameter and 30 to 40 μm in depth. External zircon standards 91500 with a $^{207}U/^{206}Pb$ age of 1065.4 ± 0.6 Ma (Wiedenbeck and others, 1995, 2004) and GJ-1 with a $^{206}U/^{238}Pb$ age of 608.5 ± 0.4 Ma (Jackson and others, 2004) were employed to correct for mass bias affecting U–Th–Pb ratios of the unknown zircon grains. NIST 610 glass was used for concentration information and the U/Th ratio determination. Detailed analytical procedures follow that of Xie and others (2008). Detrital zircon U–Pb analyses of samples 10GD16, 10GD17 and 10GD19 were conducted using the LA-ICP-MS facility at the Geological Laboratory

Center, China University of Geosciences (Beijing), following the analytical procedure of Song and others (2010). Calibration of U–Th–Pb concentrations was carried out using zircon 91500 (Wiedenbeck and others, 1995) as an external standard. Zircon standards TEMORA (Black and others, 2003) and Plešovice (Sláma and others, 2008) were also used as additional monitors for ratio measurements and age calculations. Fractionation correction and age results were calculated using the GLITTER v. 4.0 (Van Achterbergh and others, 2001) and ISOPLOT/Ex v. 2.49 (Ludwig, 2001a) software packages. Common lead was corrected following the methods described by Anderson (2002). The analytical LA-ICP-MS U–Pb data are present in Appendix B1. The U–Pb ages are based on $^{206}Pb/^{238}U$ for ages younger than 1000 Ma and $^{207}Pb/^{206}Pb$ for ages older than 1000 Ma, with uncertainties for both at the 1σ level.

3.3.2.2 SHRIMP U–Pb dating

Additional zircon U–Pb analyses on samples 10GD48 and 10GD49-1 were carried out at Curtin University, Australia, using the Sensitive High Resolution Ion Micro Probe (SHRIMP) facility. Standard operation conditions of 2 nA O_2^- primary beam and spot size of ~25 μm in diameter and ~20 μm in depth were followed and each U–Th–Pb measurement consisted of six cycles. U abundances were calibrated using zircon 91500 (Wiedenbeck and others, 1995), and $^{206}Pb/^{238}U$ ratios were constrained by zircon Plešovice (Sláma and others, 2008). The detailed analytical procedure follows that of Williams (1998). Data reduction was carried out using the SQUID v. 2.50 (Ludwig, 2001b) and ISOPLOT/Ex v. 2.49 (Ludwig, 2001a) packages. The interpreted U–Pb ages are based on $^{206}Pb/^{238}U$ for ages younger than 1000 Ma and $^{207}Pb/^{206}Pb$ for ages older than 1000 Ma, with uncertainties at the 1σ level, whereas the weighted mean ages are quoted at the 95% confidence interval (2σ). The SHRIMP U–Pb data are present in Appendix B2.

3.3.3 Zircon Oxygen Isotopic Analyses

Zircon oxygen isotopic analyses were conducted on the Cameca IMS 1280 large radius SIMS facility at IGG–CAS. The Cs^+ primary ion beam was accelerated to 10 kV with an intensity of 2 nA. The analytical spots were the same as the U–Pb sites,

with U–Pb analyses conducted after the oxygen isotope measurements. Zircon standard Penglai with $\delta^{18}O = 5.31 \pm 0.10‰$ (2σ) (X.H. Li and others, 2010a) was adopted for monitoring and correcting oxygen isotope measurements on unknown zircon grains. The detailed analytical procedure follows that described by X.H. Li and others (2010b). The zircon oxygen isotopic data for the samples from southwest Guangdong are given in Appendix B3.

3.3.4 Zircon Lu–Hf Isotopic Analyses

Zircon Lu–Hf isotopic analyses were carried out at IGG–CAS, using a ThermoFinnigan Neptune MC-ICP-MS equipped with a 193 nm laser. Zircon standards 91500 and GJ-1 were used as reference standards, with a recommended $^{176}Hf/^{177}Hf$ ratio of 0.282307 ± 0.000031 (2σ) (for example, Wu and others, 2006) and 0.282000 ± 0.000005 (2σ) (Morel and others, 2008), respectively. Laser ablation Hf analytical spots were placed as closely as possible on the previously analyzed U–Pb sites guided by their zircon CL images, with spots of 60 μm in diameter and 45 μm in depth. Details of the analytical and calculation procedures follow that of Wu and others (2006). Lu–Hf isotope data for all samples are given in Appendix B3.

3.3.5 Sandstone Modal Compositions

Modal compositions of sandstone samples were analyzed using the following procedure. Sandstone thin-sections were made from hand specimen, and mounted with epoxy resin. Six hundred grains were counted per thin-section using the Gazzi–Dickinson method (Gazzi, 1966; Dickinson, 1970; Ingersoll and others, 1984; Dickinson, 1985). The mineral types were identified and tabulated following the methods of Ingersoll and others (1984) and Dickinson (1985). Only quartz (Q), feldspar (F) and lithic fragments (L) were counted in our analyses to determine the first-order trend of sand composition.

3.4 Analytical Results

3.4.1 Zircon U–Pb Geochronology

A total of 655 zircon grains from five Cambrian clastic sedimentary samples was analyzed in this study. Apart from 25 measurements that gave Th/U <0.10, all the remaining 630 zircon grains have Th/U ratios ranging from 0.10 to 3.01. Except for a few Archean grains which are rounded in shape with no clear internal structures, most detrital zircons have subhedral shapes and show oscillatory zoning in CL images (Figure 3.3). These features suggest that most detrital zircons are of magmatic origin (for example, Corfu and others, 2003). For the following provenance analyses, we filtered the U–Pb results using a discordance cut-off <10% at the 1σ level.

3.4.1.1 Sample 10GD16, northern Guangdong

Sample 10GD16 was collected from the lower Oujiadong Formation in northern Guangdong (Figures 3.1 and 3.2). We analyzed 100 U–Pb spots on 100 zircon grains, all of which are concordant within uncertainties (that is, the 1σ ellipses overlap the concordia line). The measured $^{206}Pb/^{238}U$ (<1000 Ma) and $^{207}Pb/^{206}Pb$ (≥1000 Ma) ages range from 490 Ma to 3480 Ma, but the majority is between 500 and 1080 Ma, with a major peak at ~920 Ma and a minor one at ~520 Ma (Figure 3.3A). The four youngest grains give a weighted mean $^{206}Pb/^{238}U$ age of 499 ± 8 Ma (Figure 3.3A inset), defining the maximum depositional age.

3.4.1.2 Sample 10GD17, northern Guangdong

Sample 10GD17 was collected from the top part of the Oujiadong Formation in northern Guangdong (Figures 3.1 and 3.2). We analyzed 100 U–Pb spots on 100 zircon grains, and all 100 results are concordant within uncertainties (Figure 3.3B). The ages of detrital zircons range from 500 Ma to 3310 Ma with two major peaks at ~530 Ma and ~1000 Ma. The three youngest zircon grains give a weighted mean $^{206}Pb/^{238}U$ age of 502 ± 7 Ma (Figure 3.3B inset), defining the maximum depositional age of the sample.

3.4.1.3 Sample 10GD19, northern Guangdong. –Sample 10GD19 was collected from the upper Laoshuzhai Formation in northern Guangdong (Figures 3.1 and 3.2). Of the 100 analyses on 100 zircon grains from this sample, 97 are concordant within uncertainties (Figure 3.3C). Most analyses define a Neoproterozoic age peak at ~960 Ma. The six youngest grains give a weighted mean $^{206}Pb/^{238}U$ age of 533 ± 7 Ma (Figure 3.3C inset), defining the maximum depositional age.

3.4.1.4 Sample 10GD48, southwestern Guangdong. –Sample 10GD48 was collected from the metamorphosed Cambrian Bacun Group in southwestern Guangdong. We analyzed 170 U–Pb spots (120 LA-ICP-MS analyses and 50 SHRIMP analyses) on 170 zircon grains, and 165 U–Pb results are concordant within uncertainties (Appendix B1 and B2; Figure 3.3D). The largest age population is ~1000 Ma, with minor clusters between 500 and 3000 Ma. There are six analyses with $^{206}Pb/^{238}U$ ages younger than the Cambrian chronostratigraphic age, including three discordant and three concordant ones (236, 244 and 339 Ma) (Figure 3.3D inset, shown in grey). The six young analyses likely reflect the metamorphic influences of post-Cambrian metamorphic event(s), particularly the Permo-Triassic Indosinian orogeny (for example, Z.X. Li and X.H. Li, 2007). Indeed, this sampling region is within the crystalline interior zones of both the Ordovician–Silurian Wuyi–Yunkai orogen (for example, Charvet and others, 2010; Z.X. Li and others, 2010) (Figure 3.1A) and the Indosinian orogen, where widespread Palaeozoic and Mesozoic metamorphic and magmatic events have been reported (for example, Wang and others, 2007; Wan and others, 2010). Excluding these six results, the two youngest grains in the remaining analyses give a weighted mean $^{206}Pb/^{238}U$ age of 489 ± 7 Ma (Figure 3.3D inset), defining the maximum depositional age for the protolith of the metasedimentary rock.

3.4.1.5 Sample 10GD49-1, southwestern Guangdong. –Sample 10GD49-1 was also collected from the Cambrian Bacun Group in the western Cathaysia Block. We analyzed 185 U–Pb spots (120 LA-ICP-MS analyses and 65 SHRIMP analyses) on 185 zircon grains, and 176 U–Pb results are concordant within uncertainties (Figure 3.3E). There is one zircon with a $^{206}Pb/^{238}U$ age of ~350 Ma (Figure 3.3E inset), which is again interpreted as being resulted from the Wuyi–Yunkai and/or the Indosinian orogenies (see previous paragraph) The remaining 175 concordant

analyses form a major cluster around 1000 Ma, and several minor clusters between 600 and 3100 Ma. The youngest zircon gives a $^{206}Pb/^{238}U$ age of 500 ± 15 Ma, defining the maximum depositional age for the protolith of the metasedimentary rock.

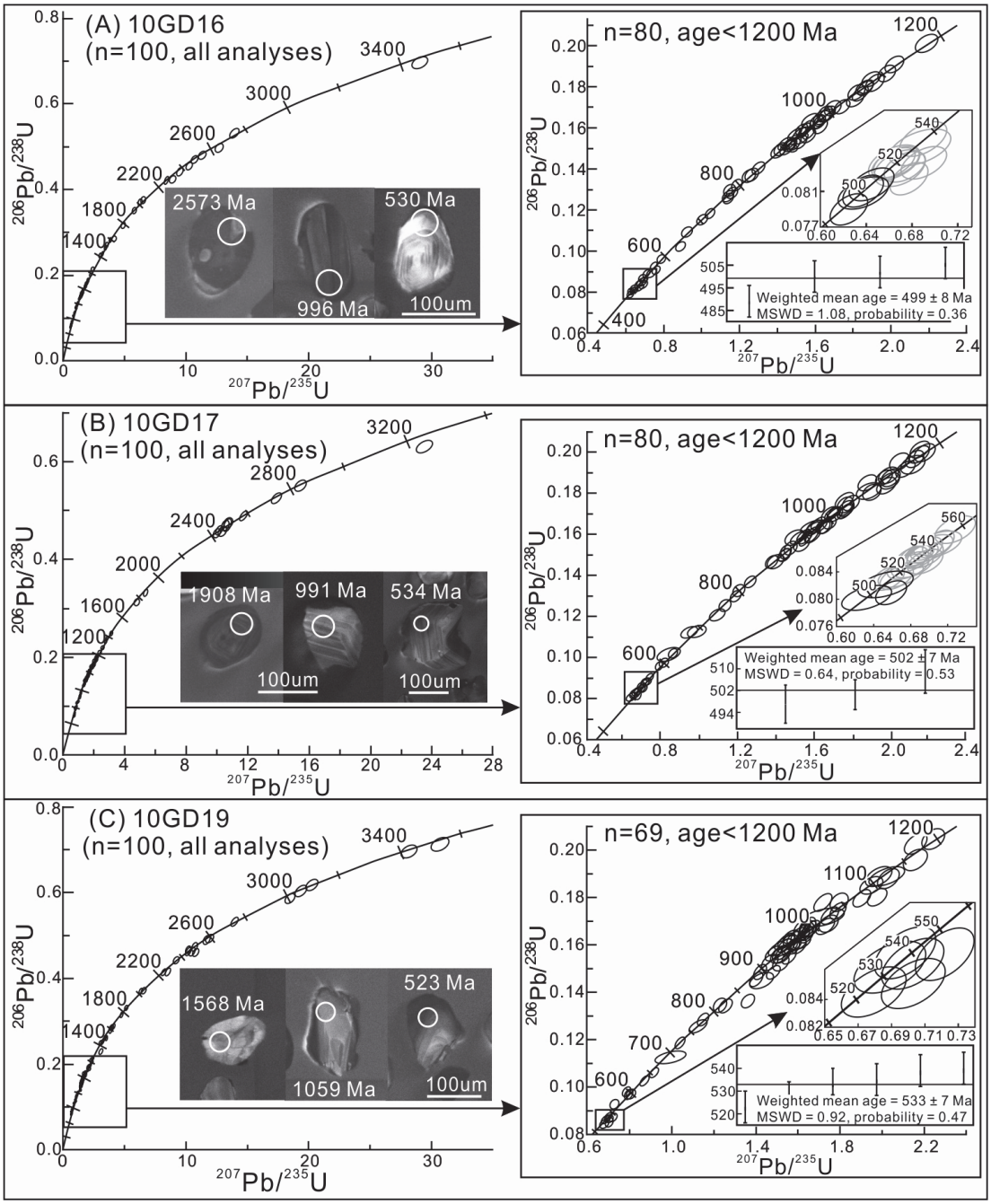

Figure 3.3. U–Pb concordia plots of detrital zircons from the five Cambrian sandstone samples in northern and southwestern Guangdong. Representative CL images with analytical spots are also present.

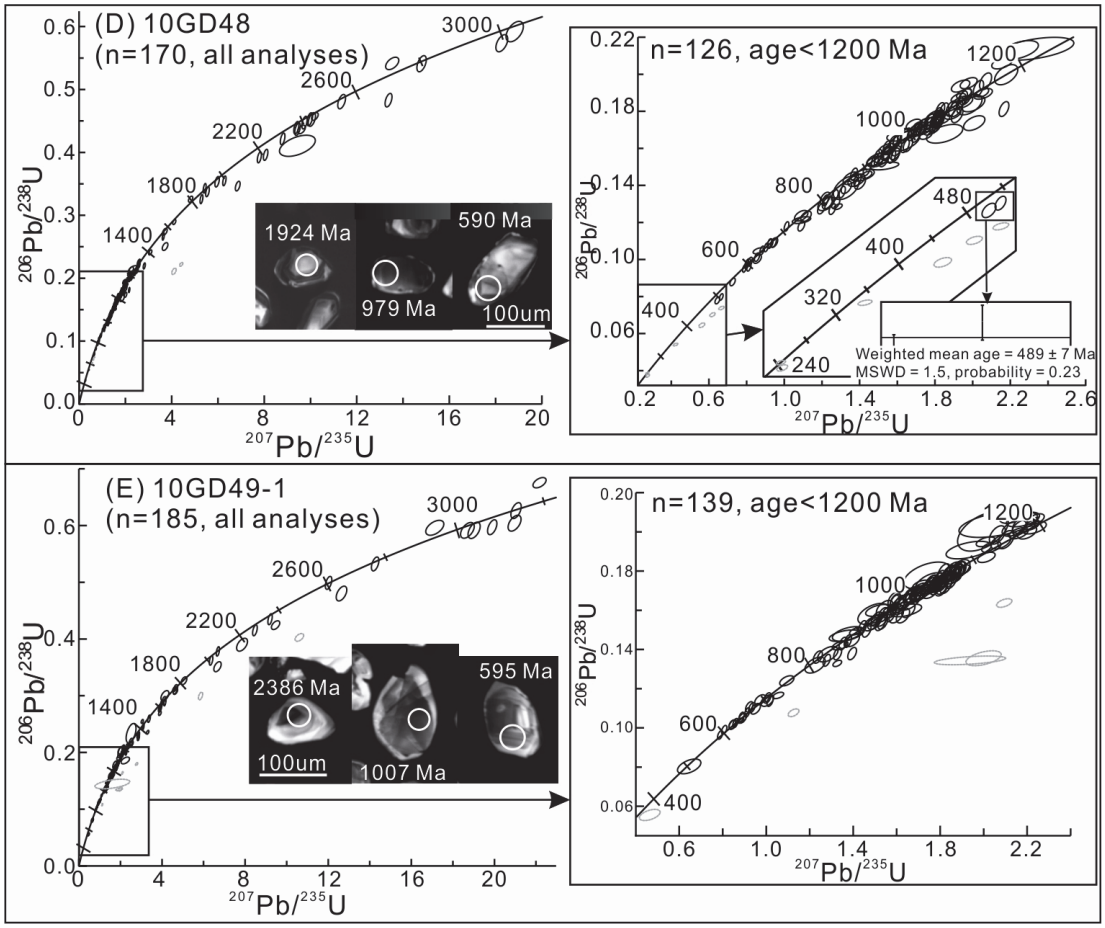

Figure 3.3. (continued)

3.4.2 Zircon Oxygen Isotopes

A total of 239 dated detrital zircons from samples 10GD48 and 10GD49-1 was selected for oxygen isotopic analysis. The $\delta^{18}O$ values range from 4.5 permil to 11.9 permil (Figure 3.4A), and the minimum values for both samples are 4.5 to 5.0 permil, consistent with mantle-derived zircon values (5.3 ± 0.6‰, Valley and others, 1998), whereas the maximum values increase from 7.6 permil in the Archean zircons to 11.9 permil in the Palaeozoic zircons, following a trend similar to that documented by Valley and others (2005).

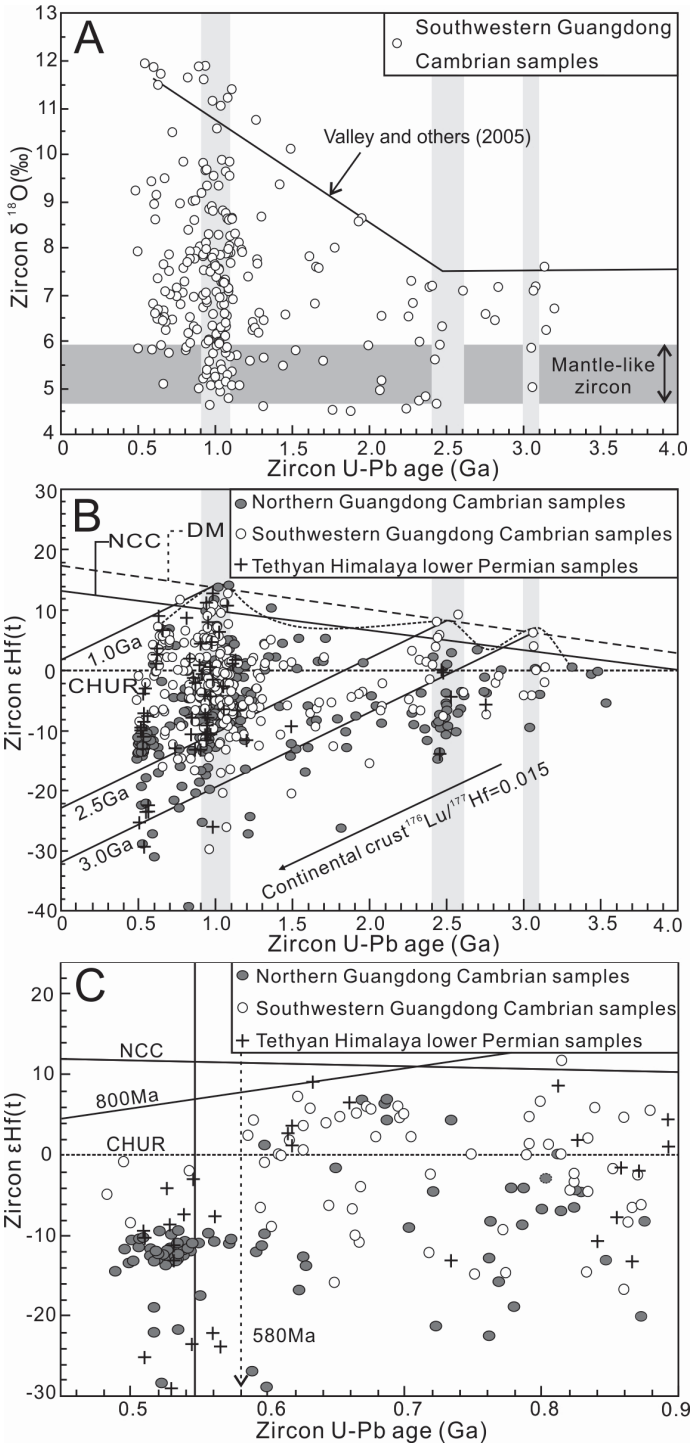

Figure 3.4. (A) Plot of detrital zircon $\delta^{18}O$ values versus U–Pb ages for Cambrian samples in southwestern Guangdong. The highlighted dark grey band represents the mantle-like zircon $\delta^{18}O$ value range (4.7–5.9‰, 2σ; Valley and others, 1998). (B) Plot of zircon $\varepsilon_{Hf}(t)$ values versus U–Pb ages for Cambrian samples from Cathaysia and Permian samples from the Tethyan Himalaya. (C) Enlarged plot of zircon $\varepsilon_{Hf}(t)$ values versus U–Pb ages as in (B) for the 900–400 Ma range, where the dashed arrow indicates more negative $\varepsilon_{Hf}(t)$ values after *ca.* 580 Ma. The depleted mantle (DM) and new continental crust (NCC) evolution lines were extrapolated after Griffin and others (2000) and Dhuime and others (2011), respectively. Light grey bands in (A)–(B) highlight potential episodes of new continental crustal growth. Potential crustal evolution lines at 3.0 Ga, 2.5 Ga and 1.0 Ga were calculated for the mean continental crust of $^{176}Lu/^{177}Hf$ value of 0.015 after Griffin and others (2000).

3.4.4 Sandstone Modal Compositions

Modal composition analyses show that the northern Guangdong samples (10GD16, 10GD17 and 10GD19) plot in the field of dissected arc in the Q-F-L diagram (Figure 3.5; Table 3.1). Quartz and other detrital grains in the thin sections of these samples show primary sedimentary textures (Figure 3.5, microphotos 1-3). The southwestern Guangdong metasedimentary samples (10GD48 and 10GD49-1), on the other hand, have lost their primary sedimentary textures, with quartz grains show secondary interlocking grain boundaries rather than their primary detrital grain boundaries (Figure 3.5, microphotos 4 and 5). Although these two samples plot in the field of "continental block" with abundant quartz but few lithic fragments (Figure 3.5), the Q-F-L plot is unlikely to give a valid interpretation on the tectonic environment of the source region(s) because of the metamorphic modification.

Table 3.1. Modal composition of Cambrian sandstone samples

Sample name	Component counts				Component percentage (%)		
	Q	F	L	Total	Q	F	L
10GD16	206	289	105	600	34.3	48.2	17.5
10GD17	243	247	110	600	40.5	40.2	18.3
10GD19	244	254	102	600	40.7	42.3	17.0
10GD48	353	234	13	600	58.8	39.0	2.2
10GD49-1	398	200	2	600	66.3	33.3	0.4

Note: Q = Quartz, F = Feldspar, L = Lithic fragment

3.5 Interpretation and Discussion

3.5.1 Results of Statistical Analysis to Determine Cambrian Provenance Variation within Cathaysia

Here we summarize all published detrital U–Pb zircon age data of Cambrian clastic sedimentary rocks in the western Cathaysia Block (Wang and others, 2010b; Wu and others, 2010) and compare them with our new results (see Table 3.2 and Figure 3.1 for sample localities). All our analyzed samples have similar age spectra, with a large population of zircons falling in the 1100 to 900 Ma age range (Figure 3.6), suggesting that they may have been derived from similar sources. To further determine the degree of similarity in the detrital sources between these samples, we ran the two–sample Kolmogorov–Smirnov (K–S) test (Kolmogorov, 1933; Smirnov,

1944). In the K–S test, the largest vertical difference between the cumulative probabilities of two tested samples is defined as the D value, and a critical D value for a test with 95% confidence ($P_0 = 0.05$) is given by $D_{critical} = 1.36\ ([M+N]/[MN])^{1/2}$ where M and N are the numbers of dated zircons with concordant ages from the two compared samples. If D value > $D_{critical}$ ($P_0 = 0.05$), the null hypothesis (H_0) that the two samples were derived from the same population can be rejected at a 95 percent confidence level. Otherwise, it would suggest that the two tested samples could have shared the same source. Alternatively, the probability level (P) at which the null hypothesis can be rejected is calculated following Schervish (1996). If the P value for a pair of samples is larger than 0.05, the null hypothesis cannot be rejected at a 95 percent confidence; in other words, detritus of the two samples have not been shown to have difference provenances.

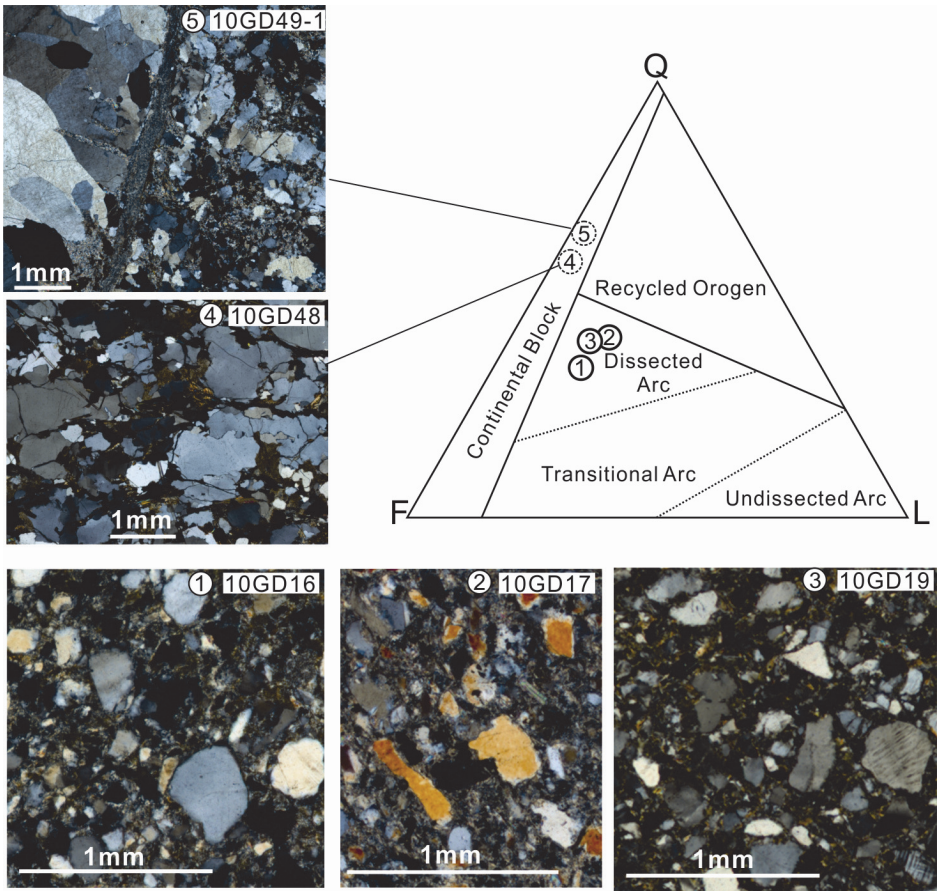

Figure 3.5. Q–F–L diagram (parameters after Dickinson, 1970, 1985; Dickinson and others, 1983) of Cambrian sandstone/metasandstone samples from Guangdong, western Cathaysia, with a photomicrograph of each of the sample. Sample (1) 10GD16, (2) 10GD17 and (3) 10GD19 are from sandstone samples from the Oujiadong section of the northern Guangdong Province, whereas samples (4) 10GD48 and (5) 10DG49-1 are from meta-sandstone samples from southwestern Guangdong Province (see Figure 3.1 for sample locations).

The zircon number for each tested Cambrian sample is given in table 3.2, and their calculated P and D ($D_{critical}$) values are given in table 3.3. The samples can be divided into three groups according to their paired P values. The northern Guangdong samples (10GD16, 10GD17 and 10GD19) have P values > 0.05 when compared between them, implying that these three samples likely shared the same provenance. The southwestern Guangdong samples (10GD48 and 10GD49-1) have a P value of 0.739 (> 0.05), also suggesting a common source. Of these two groups of samples, 10GD19 is statistically indistinguishable from 10GD48 (P = 0.314) and 10GD49-1 (P = 0.309). Therefore, the Cambrian samples from northern and southwestern Guangdong Province can be regarded as being derived from the same provenance.

Table 3.2. Summary of all Cambrian sample names and locations

Sample name	Location	Latitude (N)	Longitude (E)	Zircons numbers (concordant)	Data source
Northern Guangdong, Western Cathaysia Block					
10GD16	Renhua, Guangdong	25°01′19.9″	113°47′55.5″	100	This study
10GD17	Renhua, Guangdong	25°01′27.6″	113°48′12.1″	100	This study
10GD19	Renhua, Guangdong	25°01′45.6″	113°48′45.2″	97	This study
Southwestern Guangdong, Western Cathaysia Block					
10GD48	Yangjiang, Guangdong	22°04′28.2″	111°26′44.9″	162*	This study
10GD49-1	Yangjiang, Guangdong	21°52′53.0″	111°49′35.1″	175*	This study
Western Jiangxi, Western Cathaysia Block					
J186	Jinggangshan, Jiangxi	26°49′36.6″	114°37′16.4″	117	Wu et al. (2010)
J188	Jinggangshan, Jiangxi	26°48′50.0″	114°26′16.4″	116	Wu et al. (2010)
J192	Suichuan, Jiangxi	26°27′15.6″	114°12′49.0″	125	Wu et al. (2010)
J200	Chongyi, Jiangxi	25°24′27.1″	114°18′36.4″	107	Wu et al. (2010)
JX12	Jinggangshan, Jiangxi	26°25′14.6″	114°13′48.4″	40	Wang et al. (2010b)
JX16	Suichuan, Jiangxi	26°21′43.0″	114°27′09.2″	41	Wang et al. (2010b)
HU37	Rucheng, Hunan	25°32′47.5″	113°51′50.2″	40	Wang et al. (2010b)

* number of zircons with concordant ages, excluding zircons showing lead loss (see "analytical results")

The western Jiangxi samples (J186, J188, J192, J200, JX12, JX16 and HU37 — note that sample HU37 is located in the easternmost Hunan Province near Jiangxi, and is

here treated as part of the western Jiangxi sample group) have P values >0.05 when any two of them are compared, and P values mostly >0.05 when compare any one of them with Guangdong samples 10GD19, 10GD48, and 10GD49-1 (Table 3.3). This indicates that the western Jiangxi samples likely share a similar provenance with these Guangdong samples. However, when comparing any one of the western Jiangxi samples with Guangdong samples 10GD16 and 10GD17, the P values are <0.05 (Table 3.3), indicating a difference between them.

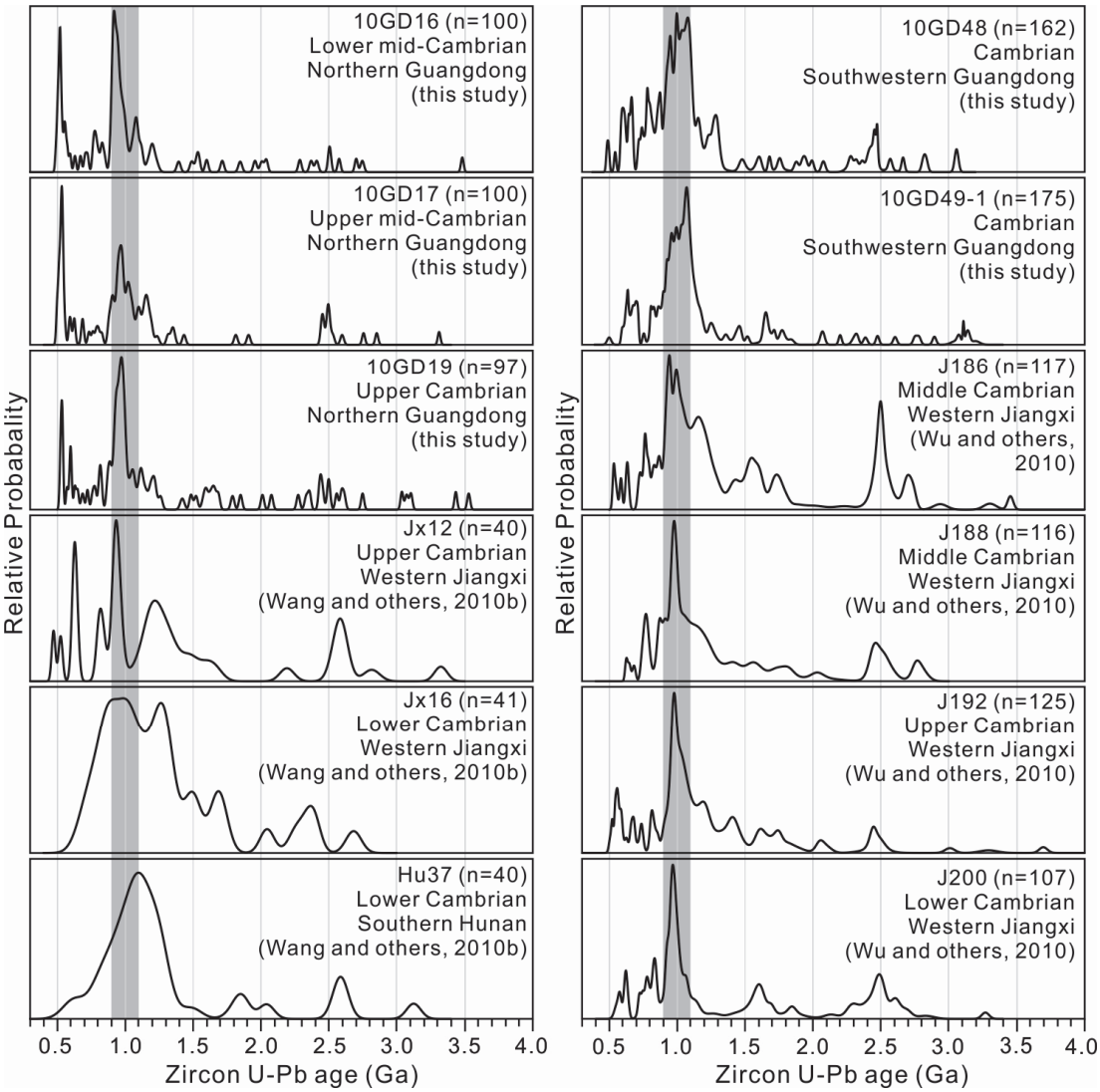

Figure 3.6. Detrital zircon age spectra of Cambrian sandstone samples in different localities in the western Cathaysia Block (see text for details). n = total number of analyses. All zircon U–Pb ages are within 90% concordance.

We observe that all three northern Guangdong samples (10GD16, 10GD17 and 10GD19) contain large zircon population with peaks between 535 and 520 Ma (~13% of all analyses), which are not as prominent in the other samples (Figure 3.6). This dissimilarity can be caused by a number of reasons. One is that three of the

previously reported samples from western Jiangxi (samples JX12, JX16 and HU37) only have about 40 concordant analyses each, and there is therefore a high probability that the datasets are missing some zircon populations. The other is that as the ages of the sampled rocks spread from lower to upper Cambrian, they may thus contain different peaks related to syn-depositional magmatic activity. Excluding analyses younger than 540 Ma from all samples, a re-run of the K-S test revealed that the majority of the samples from the western Jiangxi and the northern Guangdong samples can no longer be distinguished from each other. Therefore, we conclude that the Guangdong samples and the western Jiangxi samples probably contained detritus from the same source(s).

3.5.2 Transport Processes Affecting Age Distribution of Detrital Zircons

Sediments carrying zircon grains are considered to be eroded from topographic highs, being washed and selected by stream action in drainage systems, and finally deposited in sedimentary basins (Reading, 1996; Nichols, 2009). Therefore, processes like recycling, dilution and temporal variation of drainage geometry are all important factors contributing to the age distribution of detrital zircons in a sedimentary rock (for example, Stewart and others, 2001; Gehrels and others, 2011). For modern sedimentation, it is possible to reconstruct the drainage system and transport processes (for example, Zhang and others, 2012). However, it is often difficult to do so for ancient sedimentary rocks due to the loss of palaeotopography and the fragmented record of palaeo-drainages (for example, Veevers and others, 2005; Myrow and others, 2010). Indirect information such as palaeocurrents (indicating stream directions in palaeo-drainage; for example, Myrow and others, 2006a, 2006b; Wang and others, 2010b), and sandstone compositions (suggesting transport distance away from source areas; for example, Ingersoll and others, 1984) can then be utilized for determining ancient transport processes affecting the sediments.

Based on systematic regional data compilation and facies analyses, it has been established that the Cathaysia Block was a NW-deepening (in present coordinates) continental shelf/slope that experienced marine clastic deposition in Cambrian time (for example, Wang, 1985; Liu and Xu, 1994; Chen and others, 1995, 1997) (Figure

3.1B). As the grain sizes of clastic sediments increase to the southeast (BGMRJX, 1984; BGMRFJ, 1985; BGMRGD, 1988; BGMRHN, 1988; Chen and others, 1997), this may suggest a potential source region to the southeast. However, with almost the entire region beneath the sea during the Cambrian, we speculate that the sediments might have been transported from their source region(s) and deposited first as major deltaic systems (like the Cenozoic Bengal delta system, for example), and then carried by shore-parallel currents, with little local addition. This is similar to the case suggested for Cambrian–Triassic eastern Australia where the sediments were considered to have been mainly derived from neighboring East Antarctica within Gondwanaland (Veevers and others, 2006).

To analyze the effect of recycling from underlying sedimentary successions on the age distribution of detrital zircons in the Cambrian samples, we compared the age spectra of detrital zircons with those of Ediacaran (Yu and others, 2008, 2010; Wu and others, 2010) and Cryogenian (Wang and others, 2010a, 2012a) sedimentary rocks in the Nanhua Basin (Figure 3.7A-C). The Cambrian and Ediacaran sedimentary rocks, both from the Cathaysia side of the Nanhua Basin, share similar age spectra, with a common age peak at ~980 Ma (K–S test P = 0.101, greater than 0.05), but they differ significantly from the Cryogenian rifting-related sedimentary rocks (peaking at ~800 Ma; K–S test P = 0.00 for both tests, smaller than 0.05). Furthermore, the Ediacaran sedimentary facies are similar to those of the Cambrian sedimentary rocks in the Cathaysia Block (Liu and Xu, 1994). These observations indicate that the Cathaysia Block received continuous turbiditic to shallow marine siliciclastic sedimentation throughout Ediacaran–Cambrian time, which is in stark contrast to the dominantly carbonate platform deposition over the Yangtze Block (Figure 3.1B). The Ediacaran–Cambrian clastic sedimentary rocks exhibit a common provenance (Figure 3.7A-B) that is different from the underlying Cryogenian sedimentary rocks (Figure 3.7C). This suggests that recycling of pre-existing local sedimentary rocks contributed little to the provenance of the Ediacaran–Cambrian sedimentary rocks. Furthermore, the almost complete water coverage of the region for the entire Ediacaran–Cambrian period (Wang, 1985; Liu and Xu, 1994; Figure 3.1B for mid-Cambrian time) means that no known local pre-existing sedimentary rocks were exposed or eroded into the Nanhua Basin at that time.

Table 3.3. P and D values of two-sample Kolmogorov-Smirnov (K-S) Tests

	10GD16	10GD17	10GD19	10GD48	10GD49-1	J186	J188	J192	J200	JX12	JX16	HU37
10GD16	–	0.106 *(0.192)*	0.184 *(0.194)*	0.209 *(0.173)*	0.262 *(0.170)*	0.337 *(0.185)*	0.310 *(0.186)*	0.298 *(0.182)*	0.245 *(0.189)*	0.306 *(0.254)*	0.310 *(0.252)*	0.343 *(0.254)*
10GD17	**0.622**	–	0.159 *(0.194)*	0.171 *(0.173)*	0.196 *(0.170)*	0.283 *(0.185)*	0.225 *(0.186)*	0.196 *(0.182)*	0.262 *(0.189)*	0.292 *(0.254)*	0.274 *(0.252)*	0.270 *(0.254)*
10GD19	**0.070**	**0.167**	–	0.123 *(0.175)*	0.122 *(0.172)*	0.203 *(0.187)*	0.145 *(0.187)*	0.132 *(0.184)*	0.111 *(0.191)*	0.164 (0.256)	0.182 (0.253)	0.211 (0.256)
10GD48	0.009	**0.054**	**0.314**	–	0.074 (0.148)	0.242 (0.165)	0.173 (0.165)	0.132 (0.162)	0.228 (0.169)	0.239 (0.240)	0.225 (0.238)	0.193 (0.240)
10GD49-1	0.000	0.015	**0.309**	**0.739**	–	0.254 (0.162)	0.186 (0.163)	0.149 (0.159)	0.225 (0.167)	0.259 (0.238)	0.240 (0.236)	0.195 (0.238)
J186	0.000	0.000	0.025	0.001	0.000	–	0.068 (0.178)	0.132 (0.175)	0.137 (0.182)	0.130 (0.249)	0.155 (0.247)	0.183 (0.249)
J188	0.000	0.009	**0.218**	0.034	0.016	**0.948**	–	0.096 (0.175)	0.109 (0.182)	0.129 (0.249)	0.109 (0.247)	0.119 (0.249)
J192	0.000	0.028	**0.296**	**0.174**	**0.078**	**0.243**	**0.632**	–	0.174 (0.179)	0.129 (0.247)	0.093 (0.245)	0.093 (0.247)
J200	0.004	0.002	**0.557**	0.002	0.002	**0.245**	**0.522**	**0.060**	–	0.131 (0.252)	0.168 (0.250)	0.210 (0.252)
JX12	0.010	0.015	**0.434**	**0.051**	0.025	**0.694**	**0.708**	**0.690**	**0.701**	–	0.146 (0.302)	0.132 (0.304)
JX16	0.008	0.026	**0.297**	**0.074**	**0.044**	**0.461**	**0.862**	**0.953**	**0.374**	**0.781**	–	0.111 (0.302)
HU37	0.002	0.031	**0.159**	**0.182**	**0.169**	**0.268**	**0.796**	**0.957**	**0.150**	**0.876**	**0.964**	–

P value

D value ($D_{critical}$ value)

Note: The software (K-S test 1.0.xls) used in this study is from the University of Arizona, USA

3.5.3 Crustal History of the Source Region for the Cambrian Sandstones

The overall age spectra of all available Cambrian sandstone samples in the western Cathaysia Block show a dominant population of 1100 to 900 Ma, peaking at ~980 Ma, and minor age populations of *ca.* 2500, 850 to 750 and 650 to 500 Ma (Figure 3.7A). The data suggest that the source region(s) possibly experienced four broad episodes of tectono-magmatic events. Specifically, Archean–Palaeoproterozoic zircons account for 9% of all analyzed zircon grains, with a peak at ~2.5 Ga. Most zircons of this age group are round in shape and show signs of abrasion, suggesting multiple episodes of sedimentary recycling. These zircons have relatively low $\delta^{18}O$ values of 4.6–7.3 permil (Figure 3.4A) and variable $\varepsilon_{Hf}(t)$ values of –14.8 to +9.2 (Figure 3.4B), indicating that both mantle-derived melts and remelted old crustal components were involved. Grenvillian (1100–900 Ma) zircons make up 50 percent of the population with a pronounced peak at ~980 Ma (Figure 3.7A). Variable $\delta^{18}O$ values (4.6–11.8‰) and $\varepsilon_{Hf}(t)$ values (–30 to +14) (Figure 3.4A-B) suggest contributions from both juvenile and reworked crustal materials. Zircons form a subordinate population at 850–750 Ma (7% out of all analyses) with $\delta^{18}O$ values of 5.7 to11.6 permil and $\varepsilon_{Hf}(t)$ values of –40 to +11 (Figure 3.4A-B), suggesting crystallization from reworked older crust, with minor new mantle input. The age of this population coincides with widespread continental rifting events related to the break-up of the Rodinia supercontinent (for example, Hoffman, 1991; Z.X. Li and others, 2008b). Zircons with ages of 650 to 500 Ma (~15% of all analyses) have $\delta^{18}O$ values mostly falling outside the range for mantle-like zircons (Figure 3.4A) and negative $\varepsilon_{Hf}(t)$ values (Figure 3.4C), suggesting that these zircons were mainly derived from remelting and recycling of ancient crustal materials. Within this population, there is a dramatic shift in zircon Hf isotopes at ~580 Ma (Figure 3.4C). A large number of pre-580 Ma zircons have positive $\varepsilon_{Hf}(t)$ values, whereas post-580 Ma zircons exclusively record negative $\varepsilon_{Hf}(t)$ values, hinting at a possible change of tectonic environment in the source region(s).

In summary, zircon Hf isotopic data indicate that the source region(s) of the Cambrian sandstones probably experienced three Precambrian episodes of juvenile crustal growth, at 3.0 Ga, 2.5 Ga and 1.0 Ga, and two possible minor events at 1.35

Ga and 850 to 580 Ma (Figure 3.4B), which is consistent with the mantle-like $\delta^{18}O$ values (Figure 3.4A). Zircon Hf–O isotope results also suggest that the source region(s) underwent extensive crustal remelting and reworking without new crustal addition at 580 to 500 Ma.

3.5.4 Provenance of the Cambrian Sedimentary Rocks in the Cathaysia Block

3.5.4.1 Not sourced from the Cathaysia or the Yangtze blocks

Some previous work typically viewed the lower Palaeozoic clastic rocks along the Cathaysian margin as sourced from the Cathaysia Block itself, and suggested that these rocks can reflect the crustal history of Cathaysia (for example, Yao and others, 2011). However, a closer examination of the available data suggests that the provenance interpretation of these clastic rocks may not be that straightforward. If we ignore the post-540 Ma grains in the Cambrian samples, the age spectra of detrital zircons from the Cambrian and Ediacaran clastic samples in western Cathaysia are consistent (Figure 3.7A–B), suggesting common sources for the continuous sedimentation on the Cathaysian side of the Nanhua Basin during Ediacaran to Cambrian time (Figure 3.1B). The *ca.* 540 to 490 Ma grains in the Cambrian samples are interpreted as input from newly formed magmatic rocks in the source region(s).

We have already ruled out recycling of local underlying sedimentary rocks as a source for the Ediacaran–Cambrian sedimentation in Cathaysia. Known basement rocks from Cathaysia are also unlikely to have contributed to the sedimentation for two reasons. First, most of the known Cathaysian pre-Neoproterozoic bedrock areas were covered by sea water and marine deposits during much of Ediacaran to Cambrian time (Figure 3.1B; Wang, 1985; Liu and Xu, 1994), and thus could not have served as a source of detritus for the Ediacaran–Cambrian sedimentary rocks. Second, the age spectra of the sedimentary rocks are different from that of the basement. We show in figure 3.7E–F age spectra of known Cathaysian basement rocks, and in figure 3.7D younger provenance data from eastern Cathaysia that mimics the basement data. Eastern Cathaysia has a dominant 1.89 to 1.86 Ga age peak in its crystalline basement (Figures 3.1A and 3.7E), which is reflected in the age spectra of the late Palaeozoic to Mesozoic sandstones found in the region (Figure

3.7D). Western Cathaysia, on the other hand, has a prominent *ca.* 1.43 Ga age peak in the basement that crops out in Hainan Island (Figures 3.1A and 3.7F). Clearly neither peak from the basement rocks is clearly shown in the provenance data for the Ediacaran–Cambrian strata (Figure 3.7A–B). Rare Grenville-age magmatic rocks have been reported within Cathaysia (for example, the ~972 Ma Jingnan rhyolites in eastern Guangdong by Shu and others, 2008; Figure 3.1A) that fit the prominent 980 Ma peak of the Ediacaran–Cambrian deposits (Figure 3.7A–B), but, as stated above, the extensive sedimentary and sea-water coverage of the entire region rule out such rocks as a potential detritus source.

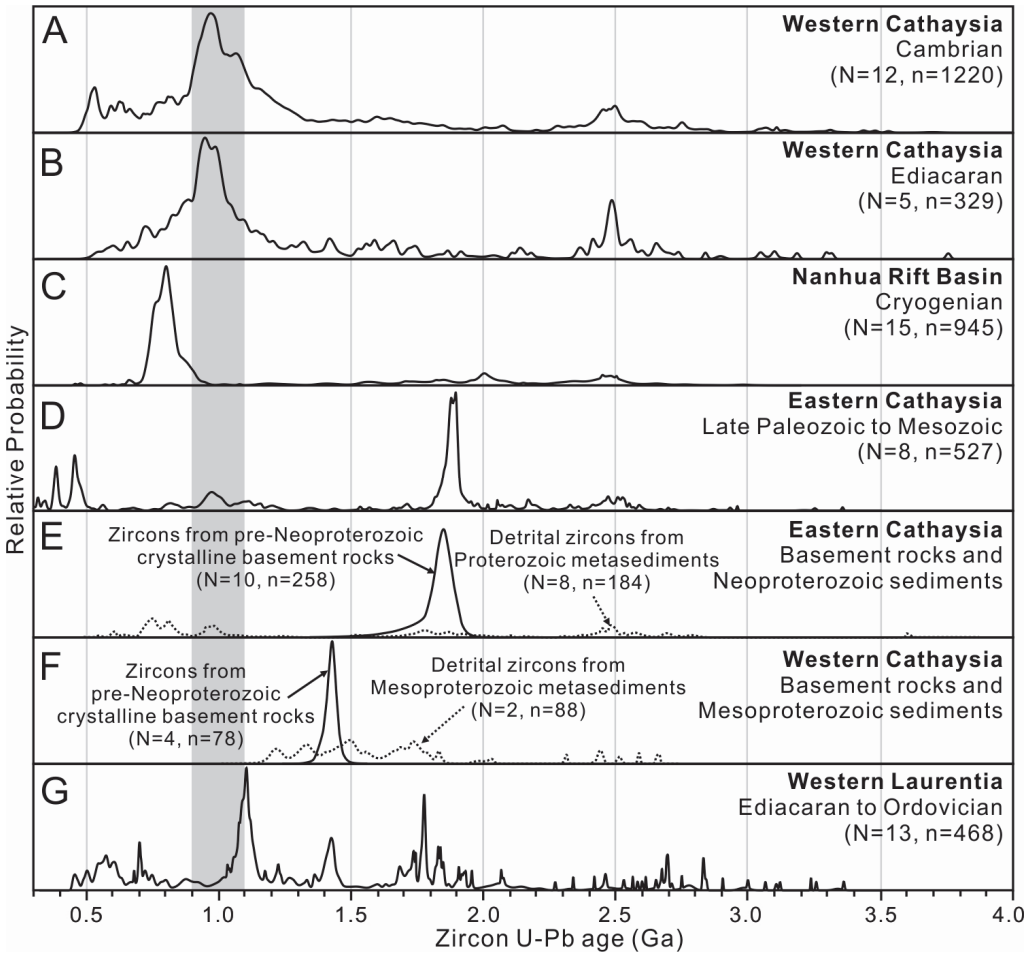

Figure 3.7. Summary provenance plots of U–Pb zircon age spectra of sedimentary rocks in Cathaysia, and comparisons with both the basement age spectra and provenance data for western Laurentia. (A) Western Cathaysia Cambrian strata (this study; Wang and others, 2010b; Wu and others, 2010); (B) Western Cathaysia Ediacaran strata (Yu and others, 2008, 2010; Wu and others, 2010); (C) Mid-Neoproterozoic Nanhua Rift Basin (Wang and others, 2010a; Wang and others, 2012a); (D) Eastern Cathaysia late Palaeozoic to Mesozoic strata (X.H. Li and others, 2012; Yao and others, 2012); (E) Eastern Cathaysia Neoproterozoic metasediments and Precambrian crystalline basement rocks (X.H. Li, 1997; Z.X. Li and X.H Li., 2007; Wan and others, 2007; Liu and others, 2009; Yu and others, 2009; Z.X. Li and others, 2010); (F) Western Cathaysia Mesoproterozoic metasediments and Precambrian crystalline

basement rocks (Z.X. Li and others, 2002, 2008a); (G) Western Laurentia (Smith and Gehrels, 1994; Stewart and others, 2001; Vega-Granillo and others, 2008). N = number of samples, n = total number of analyses. All zircon U–Pb ages are within 90% concordance.

The neighboring Yangtze Block is another potential source for the clastic sedimentary rocks. There are some 1100 to 900 Ma magmatic rocks along the margins of the Yangtze Block (Z.X. Li and others, 2002; Ling and others, 2003; Greentree and others, 2006; Ye and others, 2007; X.H. Li and others, 2009), which are the same age as the prominent peak in the Cambrian samples (Figure 3.7A). However, the large-scale carbonate deposition over the Yangtze Block (Figure 3.1B) makes it an unlikely source region for the vast amount of clastic sediments on the Cathaysia side of the Nanhua Basin. In addition, no *ca.* 600 to 500 Ma magmatism has been reported from the Yangtze Block.

Consequently, the prominent Grenvillian zircon population would have to be from areas outboard of the known Cathaysian basement, either in the concealed part of the South China continental crust along the South China Sea margin (Figure 3.1B), or an exotic terrane once connected to the Cathaysia Block during Ediacaran–Cambrian time, but subsequently drifted away. In the former scenario, the concealed source area along the current continental margin would have been an elevated region striking NE–SW along the present-day continental margin (Figure 3.1B). The dominant 1100 to 900 Ma zircon population and subordinate 850 to 750 Ma and 650 to 500 Ma populations in the Ediacaran–Cambrian sedimentary rocks demand the concealed source area to be part of a Grenville-aged orogenic belt that not only experienced 850 to 750 Ma continental rifting similar to the Nanhua Basin (for example, Z.X. Li and others, 2003; Wang and Li, 2003), but also underwent prominent 580 to 500 Ma crustal melting. However, there is no such outcrop of basement rocks in the speculated offshore region. A study of xenoliths from Cenozoic basalts in Penghu Island (Figure 3.1B) reported sulphide T_{RD} age peaks of 1.9 Ga, 1.7 to 1.6 Ga, 1.4 to 1.3 Ga and 0.9 to 0.8 Ga, which were interpreted to represent the timing of melt extraction and/or metasomatic events in the sub-continental lithospheric mantle beneath the region (Wang and others, 2009). Such inferred events correlate well with tectonothermal events in the exposed Cathaysia Block, including the 1.9 to 1.8 Ga event in eastern Cathaysia and the 1.4 Ga event on Hainan Island. It is thus likely that known basement components in

mainland Cathaysia extend to the Taiwan region (at least to Penghu Island). On the other hand, almost no record of magmatic events at 1100 to 900 Ma or 580 to 500 Ma, as demanded by the Ediacaran–Cambrian clastic sedimentary provenance data (Figure 3.7A–B), has been reported from either the coastal area of the Cathaysia Block or its offshore extension (except for some *ca.* 1.3–1.0 Ga metamorphic ages from Hainan Island; Z.X. Li and others, 2002, 2008a). Therefore, although the possibility of the concealed offshore extension area being the source region cannot be totally ruled out, it appears unlikely.

3.5.4.2 Possible exotic sources from the East African Orogen and the northern Indian margin

To test the possibility of exotic sources for the detritus, we compared the zircon age spectra of the Ediacaran–Cambrian samples from western Cathaysia with those from several potential continental blocks that were suggested to be adjacent to the SCB during that time interval (for example, Zhang and Piper, 1997; Z.X. Li and Powell, 2001; Zhou and others, 2002; Jiang and others, 2003; Yang and others, 2004; Z.X. Li and others, 2008b; Yu and others, 2008, 2009; Cook and Torsvik, 2013). Most of the detrital zircons were derived from siliciclastic successions coeval with the studied rocks in the Cathaysia Block. The prominent age peaks at 1.1 Ga, 1.4 Ga and 1.8 Ga in Ediacaran–Ordovician sedimentary rocks from western Laurentia (Figure 3.7G) (Smith and Gehrels, 1994; Stewart and others, 2001; Vega-Granillo and others, 2008) bear no similarity to those of the western Cathaysia samples (Figure 3.7A–B). Likewise, the distinct 1.2 Ga age peak from western Australian Ordovician and Permian sedimentary rocks (Figure 3.8H) (Cawood and Nemchin, 2000; Veevers and others, 2005) has no counterpart in the Cathaysian provenance data (Figure 3.8A). These differences indicate that during the Ediacaran–Cambrian time interval, the Cathaysia Block was unlikely to have had a direct connection with either western Australia or western Laurentia, both of which were previously suggested to be connected to the southeast margin of the Cathaysia Block sometime during the Proterozoic (for example, Yang and others (2004) for a Cathaysia–western Australia connection, and Z.X. Li and others (2008a) for a Cathaysia–western Laurentia connection) and/or the lower Palaeozoic (for example, Zhang and Piper (1997) and Yang and others (2004) for a Cathaysia–western Australia connection).

To examine a possible SCB–northern India connection, as previously speculated based on (1) their comparative Ediacaran–Cambrian tectonostratigraphic records (Kumar, 1984; Jiang and others, 2003), (2) their Cambrian faunal affinities (for example, Jell and Hughes, 1997; Peng and others, 2009), (3) palaeomagnetism (Z.X. Li and others, 2004; Zhang, 2004), and (4) similarities in their Ediacaran detrital zircon provenance data and tectonomagmatic records (Yu and others, 2008), we first look at the tectonic framework and provenance data for northern India.

The Palaeozoic northern Indian margin (that is, the Himalaya region; Figure 3.8) includes three modern tectonic units from north to south: the Tethyan Himalaya (TH), the Greater Himalaya (GH) and the Lesser Himalaya (LH) (for example, Le Fort, 1975). Although there are models arguing for an exotic origin for some of the tectonic units (for example, Liu and others, 2012), here we follow the view that these tectonic units are all part of the northern margin of the Indian craton that were dismembered and reworked during the India–Asia collision. This is because they: (1) exhibit coherent continental shelf–slope litho-facies, tectonostratigraphy and palaeoenvironment in the late Precambrian–Palaeozoic (for example, Brookfield, 1993; Pogue and others, 1999; Myrow and others, 2003); (2) share a similar bioprovince (Peng and others, 2009); and (3) have similar detrital zircon age distribution patterns (for example, Myrow and others, 2003, 2010).

Precambrian crystalline basement rocks are poorly exposed along the northern margin of India, with the oldest being 1.8 to 1.6 Ga igneous rocks reported in the eastern Himalaya (Cottle and others, 2009; Yin and others, 2010a) and around the Shillong Plateau (Ameen and others, 2007; Yin and others, 2010b), 1.9 to 1.8 Ga magmatic rocks in the central Himalaya (Nepal) (Kohn and others, 2010), and 2.0 to 1.84 Ga granites and 1.8 Ga mafic igneous rocks in the western Himalaya (Miller and others, 2000; Singh and others, 2006). In addition, *ca.* 1.1 to 1.0 Ga, 880 to 820 Ma, and 550 to 470 Ma tectono-magmatic events have been reported from the region (for example, Schärer and others, 1986; Brookfield, 1993; Miller and others, 2001; Singh and others, 2002; Cawood and others, 2007; Liu and others, 2007; Cottle and others, 2009; Yin and others, 2010a, 2010b).

Figure 3.8 shows that the age spectra of the Cathaysia detrital zircons match well

with similar-aged clastic sedimentary rocks from the northern margin of India. In particular, the Cathaysia age spectra with a distinct age peak of 980 Ma (Figure 3.8A) match well with the similar-aged sedimentary rocks from the western part of the northern Indian margin (Myrow and others, 2003, 2009, 2010; Webb and others, 2011) (Figure 3.8C–D). Similar age spectra persisted in the central and eastern segment of the northern Indian margin, although *ca.* 1.2 to 1.1 Ga age populations in general become more prominent in this region (Figure 3.8E–F) (Gehrels and others, 2003, 2006a, 2006b; Martin and others, 2005; McQuarrie and others, 2008; Myrow and others, 2010; Hughes and others, 2011). These correlations indicate that the Cathaysia Block possibly shared a similar provenance with the northern Indian margin during the Ediacaran–Cambrian time. The comparable zircon Hf isotopic characteristics between the Cathaysian Cambrian sedimentary rocks (this study) and the Tethyan Himalayan Permian sedimentary rocks (Zhu and others, 2011) that share a similar age spectrum to the Ediacaran–Cambrian samples, including the common lack of any zircon with a positive $\varepsilon_{Hf}(t)$ value after 580 Ma, also support such a speculation (Figure 3.4B–C).

Figure 3.8 further illustrates that the similarities between the age spectra of the Cathaysian sedimentary rocks and those from the Indo-Australian Gondwana margin gradually decrease toward Australia, with a prominent Grenvillian age peak shifting from *ca.* 980 Ma for Cathaysia (Figure 3.8A), Qiangtang (Figure 3.8B) and western Himalaya (Figure 3.8C–D), to *ca.* 1100 Ma for much of central–eastern Himalaya (Figure 3.8E–F, with F still showing a prominent *ca.* 980 Ma peak), and finally to nearly 1200 Ma for the Lhasa terrane and western Australia (Figure 3.8G–H). It thus indicates that western Cathaysia (SCB) likely shared the same detritus provenance as the northwestern Indian Himalaya, and the provenance connection appears to gradually weaken toward western Australia.

3.5.5 The South China Block (SCB): from Central Rodinia in the Early Neoproterozoic to Northeastern Gondwanan Margin in the Cambrian?

As discussed in the introduction section, the palaeo-position of the SCB in the Neoproterozoic supercontinent Rodinia and its subsequent connection with Gondwanaland in the early Palaeozoic has been a subject of ongoing debate.

Although current palaeomagnetic results permit the SCB to be on either side of the Australian continent in Rodinia (for example, Z.X. Li and others, 2004; Yang and others, 2004; Z.X. Li and Evans, 2011), some previous studies prefer the SCB to be adjacent to either western Australia or northern India in Rodinia (Zhang and Piper, 1997; Jiang and others, 2003; Yang and others, 2004; Yu and others, 2008). Z.X. Li and others (2008b), on the other hand, preferred the so-called "missing-link" model, where the SCB is placed between Australia and western Laurentia in Rodinia because such a configuration: (1) explains the close similarities in both basement geology and possible late Mesoproterozoic provenance connections between southern Cathaysia and southern Laurentia (Z.X. Li and others, 2008a); (2) allows the SCB to be above a Neoproterozoic plume-center as indicated by dyke swarms in both Australia and western Laurentia and corresponding plume-centers in the SCB (Z.X. Li and others, 2003); (3) explains the Grenvillian metamorphic/magmatic events in both eastern Australia and western Laurentia (Z.X. Li and others, 2008b and references therein; Nesheim and others, 2012); and (4) provides a solution for geological mismatch between Laurentia and Australia–East Antarctica during Rodinian time and fills the gap between them as required by the palaeomagnetic results (Z.X. Li and others, 2008b; Z.X. Li and Evans, 2011). Following this scenario, the SCB was considered to have drifted adjacent to the northwestern margin of Gondwanaland by the Cambrian (Z.X. Li and others, 1996; Z.X. Li and Powell, 2001; Metcalfe, 1996). In addition, as we will discuss in the following paragraphs, the "missing-link" model and the following scenario (Figure 3.9) is not only consistent with our provenance analyses, but it also permits the northern margin of India to develop an active margin during Ediacaran to Cambrian time (for example, DeCelles and others, 2000; Cawood and others, 2007), and provides a driving mechanism for the early Palaeozoic Wuyi–Yunkai orogeny in the SCB (for example, Charvet and others, 2010; Z.X. Li and others, 2010).

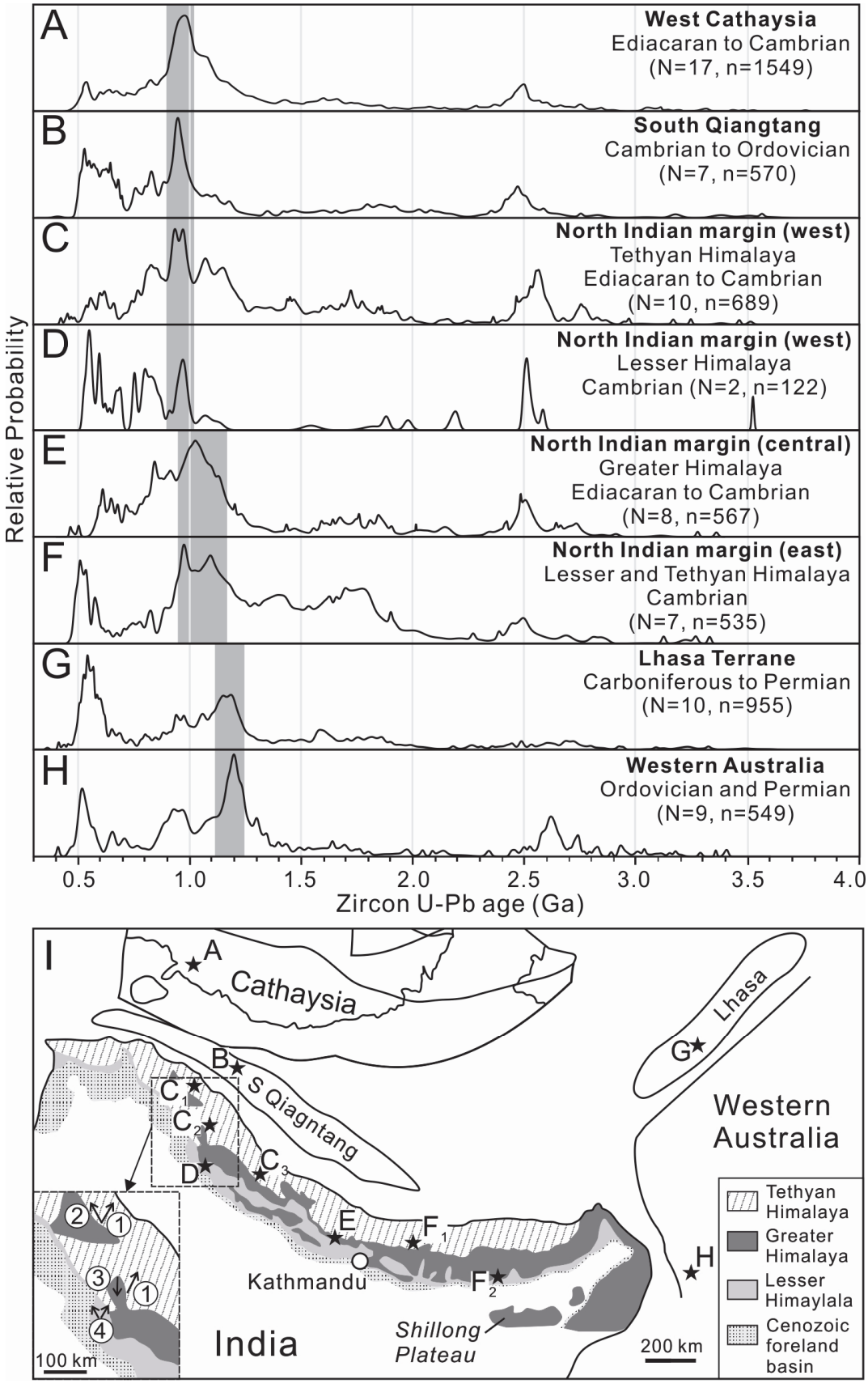

Figure 3.8. Provenance variations of Ediacaran–Cambrian sedimentary rocks along the northern margin of India, and comparisons with provenance results from possible adjacent continents/terranes in Gondwanaland, Age spectra in (A)–(H) correspond to data points A–H

in the location cartoon (I), where data points C_1–C_3 and D represent western North Indian margin, data points E represent central North Indian margin, and data points F_1 and F_2 represent eastern North Indian margin. Sources of detrital zircon age spectra: A — this study, Yu and others (2008, 2010), Wang and others (2010b) and Wu and others (2010); B — Dong and others (2011), Pullen and others, (2011) and Zhu and others (2011); C_1 — Myrow and others (2010); C_2 — Myrow and others (2010) and Webb and others (2011); C_3 — Myrow and others (2010); D — Myrow and others (2010); E — Martin and others (2005) and Gehrels and others (2011); F_1 — Myrow and others (2010) and Gehrels and others (2011); F_2 — McQuarrie and others (2008), Myrow and others (2010) and Hughes and others (2011); G — Leier and others (2007), Gehrels and others (2011) and Zhu and others (2011); H — Cawood and Nemchin (2000) and Veevers and others (2005). Inset in (I) shows palaeocurrent directions, with data sources being as follows: (1) Tethyan Himalaya, lower–middle Cambrian rocks in the Spiti and Zanskar valleys (Myrow and others, 2006a, 2006b; Bagati and others, 1991); (2) Tethyan Himalaya, lower and upper Cambrian rocks in the Zanskar Valley (Garzanti and others, 1986); (3) Greater Himalaya, lower Cambrian rocks at Keylong (Draganits, 2000); (4) Lesser Himalaya, Ediacaran rocks at Simla (Valdiya, 1970). The positions of South Qiangtang and Lhasa terranes relative to Indo-Australia in Gondwanaland, as shown in (I), follow that of Zhu and others (2011).

Wang and others (2010a, 2012a) documented the provenance of middle Neoproterozoic successions in the central Nanhua Basin (the region between Shaoguan and Guilin in Figure 3.1B), and revealed a dominant early Neoproterozoic zircon age population with a peak at *ca.* 800 Ma, and a small number of older grains between 2.5 and 1.5 Ga (Figure 3.7C). A similar detrital provenance is identified in metasedimentary rift successions (protolith ages of 840–720 Ma) in eastern Cathaysia (Figure 3.7E, Wan and others, 2007; Z.X. Li and others, 2010). Such age patterns can be explained by local sources inside the SCB without invoking exotic sources, as one would expect of rift basin deposits sourced predominantly from elevated rift shoulders and syn-rifting volcanic rocks (Z.X. Li and others, 2003; Wang and Li, 2003).

The provenance of the clastic sediments on the Cathaysia side of the Nanhua Basin changed dramatically during the Ediacaran, as shown by the lack of a 2.1 to 1.8 Ga zircon population and the dominance of a 1.1 to 0.9 Ga zircon population (Figure 3.7B). A similar provenance continued to at least the Cambrian, but with the addition of 540 to 500 Ma magmatic zircons (Figure 3.7A). This potential exotic provenance matches well with that of northwestern Indian Himalaya (see discussion in the previous sections; Figure 3.8A, C–D). We thus suggest that the SCB drifted north of Australia (current configuration) to approach northern India during the Ediacaran (Figure 3.9B–C), which is consistent with available 650 to 580 Ma palaeomagnetic

constraints (Z.X. Li and others, 2013). The older end of the 588 ± 33 to 423 ± 7 Ma monazite $^{208}Pb^{*}/^{232}Th$ metamorphic age spectrum reported from schists in the northwestern Indian section of the western Himalaya (Webb and others, 2011) may thus reflect the onset of the SCB–India collision. In such a palaeogeographic configuration (Figure 3.9C), western Cathaysia and the northwestern margin of the Indian continent started to receive dominantly siliciclastic deposits from that time, probably from a common source such as the giant East African orogen (for example, Myrow and others, 2010; McQuarrie and others, 2013).

The SCB possibly rotated clockwise relative to Gondwanaland during Cambro-Ordovician time (Figure 3.9D), leading to the closure of the V-shaped ocean during the Ordovician (*ca.* 470 Ma). Apart from their strong sedimentary provenance and bioprovenance connections as discussed above, and palaeomagnetic evidence for the SCB to join Gondwanaland adjacent to northern India during the Cambrian (Zhang and others, 2013), such a collisional event is also consistent with a number of other observations across India and the SCB. First, the model can accommodate the development of an Andean-type active plate margin during the Cambrian, resulting in the formation of a trans-Himalaya granitic belt between *ca.* 550 Ma and *ca.* 470 Ma (for example, DeCelles and others, 2000; Miller and others, 2001; Gehrels and others, 2003; Cawood and others, 2007; Yin and others, 2010b; Webb and others, 2011; Wang and others, 2012b). The granites of this belt are commonly reported to be the result of continental crustal melts, with the Cambrian ones possibly forming in a back-arc environment associated with slab roll-back, whereas the younger, Cambro-Ordovician ones are associated with terrane accretion/collision after the ocean closure (for example, Cawood and others, 2007; Yin and others, 2010b; Wang and others, 2012b). Here we interpret that "accreted" terrane to be the SCB which completely accreted/collided with northern India by *ca.* 470 Ma. Second, the *ca.* 580(?)–420 Ma metamorphic ages reported from the northwestern Indian Himalaya (Webb and others, 2011), and the 500 to 450 Ma metamorphism and deformation prior to 490 to 470 Ma granitic intrusions in the central Himalaya (Gehrels and others, 2003), are consistent with a diachronous collision with the SCB. Third, a Cambro-Ordovician hiatus has been recognised across the Himalaya range between the more deformed and metamorphosed Ediacaran to mid-Cambrian sedimentary strata (with some Cambro-Ordovician(?) granites intruding the strata being exposed

and eroded), and a widespread overlying Cambrian(?)–Ordovician conglomerate unit (for example, Gehrels and others, 2003; McQuarrie and others, 2013 and references therein), noting that the overlying conglomerate unit could be as young as mid- to late-Ordovician (Torsvik and others, 2009). This tectonism has been interpreted as indicating a trans-Himalaya Cambro-Ordovician mountain-building event (the Kurgiakh orogeny, Srikantia, 1977, as quoted in Bhargava and others, 2011; also known as the Bhimphedian orogeny, with the orogen called the North India orogen, Cawood and others, 2007) featuring south-verging thrusting. We speculate here that the orogenic event possibly started at the northwestern margin of the Indian craton when it collided with the SCB (Figure 3.9D), with a fold-and-thrust belt propagating to the south during the Ordovician (Gehrels and others, 2003; McQuarrie and others, 2013). Fourth, the model can account for the presence of both north-directed and south-directed palaeo-flow directions observed in the Ediacaran to Ordovician clastic strata in the Himalaya range (Valdiya, 1970; Garzanti and others, 1986; Bagati and others, 1991; Draganits, 2000; Myrow and others, 2006a, 2006b; McQuarrie and others, 2013) (see Figure 3.8I inset for western Himalaya dataset), driven by palaeo-topography away from northern India, and the emerging North India orogen (Figure 3.9C–D). Fifth, continuing convergence between the SCB and India (as part of Gondwanaland) after the ocean closure by *ca.* 470 Ma can explain the driving force for the intraplate orogenic event in South China — the >460 to 415 Ma Wuyi–Yunkai orogeny (Z.X. Li and others, 2010) in a similar way as the Cenozoic India–Eurasia collision causing the intraplate orogeny along the Tianshan (Yin and others, 1998).

Models that have South China connected to western Australia–northern India since Rodinia time (Zhang and Piper, 1997; Jiang and others, 2003; Yang and others, 2004; Yu and others, 2008; Cawood and others, 2013), on the other hand, would have difficulties in accounting for a number of geotectonic observations and events: the development of a "Pan-African" continental margin in northern India and possibly northwestern Australia (for example, Decelles and others, 2000; Cawood and others, 2007; Yin and others, 2010b; Zhu and others, 2011, 2012; Wang and others, 2012b); the notably closer provenance connection between Cathaysia and northwestern India rather than with northeastern India or Lhasa–western Australia (Figure 3.8); palaeomagnetic evidence that South China was in different positions with respect to

India and Australia before it joined Gondwanaland in the Cambro-Ordovician (Zhang and others, 2013); the development of the intraplate Wuyi–Yunkai orogeny in southeastern South China during the early Palaeozoic; and the lack of any early Palaeozoic active margin along the northwestern and northern SCB continental margin as would be expected had the SCB been a coherent part of northern India or western Australia before that time.

In our preferred model, the Cathaysia side of the Nanhua Basin (Figure 3.1B) probably largely received sediments from a similar source to the northern margin of India during the early stage of the SCB–India suturing/collision (Figure 3.9C), when the entire northern margin of the Indian craton was under water and receiving similar sediments (for example, Myrow and others, 2010). However, as the proposed diachronous collision progressed, part of the Indian margin would have been uplifted and eroded, and could have therefore provided both recycled Ediacaran–Cambrian sediments and detritus from exposed Cambro-Ordovician granites, that typically intruded the Ediacaran–Cambrian strata, to foreland basins on both sides of the new orogen (Figure 3.9D). In both cases, the source regions (that is, the East African orogen, and/or the new North India orogen) appear to satisfy the characteristics of the Ediacaran–Cambrian Cathaysian sediments as being derived from dissected arc(s) and including post-580 Ma magmatism sourced from an old continental crust [see low $\varepsilon_{Hf}(t)$ values of zircons in figure 3.4C and sandstone model compositions in Figure 3.5].

In addition, our model of having the SCB joining Gondwanaland during a Cambro-Ordovician collisional event is consistent with the palaeomagnetic argument that the SCB started to share a common apparent polar wander path with Gondwanaland from Cambro-Ordovician time until the Early Devonian (Zhang, 2004; Zhang and others, 2013). It can also account for the lack of clastic deposition on the Yangtze side of the SCB during much of the Cambrian (Figure 3.1B), as it was separated by the Nanhua foreland basin from the Ediacaran–Ordovician orogens. The propagation of the Wuyi–Yunkai orogeny from the Cathaysia Block toward the Yangtze Block eventually pushed the remnant Nanhua foreland basin to the Yangtze side by the Silurian (Liu and Xu, 1994; Z.X. Li, 1998). The foreland basin ceased to develop by the Early Devonian, when the entire SCB started to develop a platformal

marine transgression leading to the formation of an upper Palaeozoic platform cover sequence (Liu and Xu, 1994).

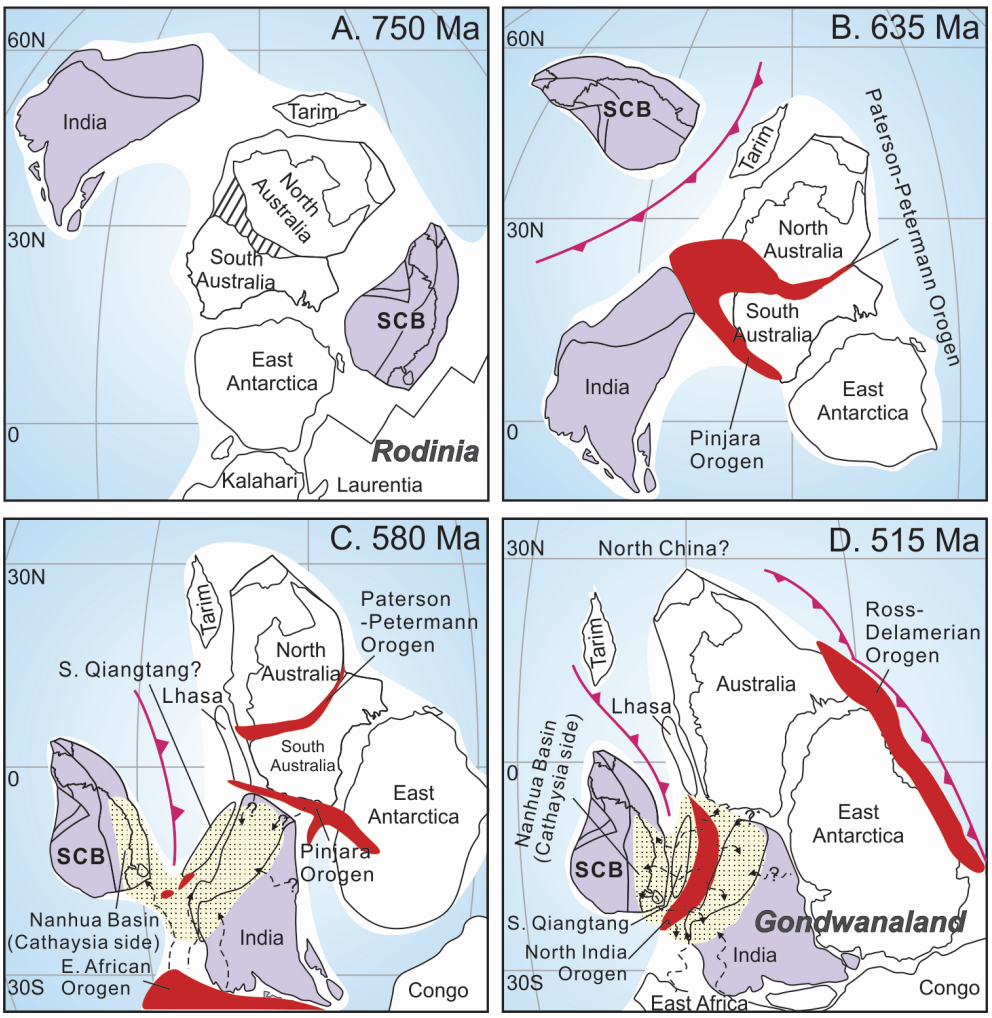

Figure 3.9. Palaeogeographic reconstructions showing palaeoposition of the SCB (A) before the break-up of Rodinia in the mid-Neoproterozoic (750 Ma), (B) after Rodinia break up, but prior to its collision with India during the assembly of Gondwanaland (635 Ma), (C) beginning of collision with NW India at *ca.* 580 Ma during the assembly of Gondwanaland, and (D) colliding with India to become part of Gondwanaland (515 Ma). Active orogens, and speculated drainage directions for Ediacaran–Cambrian time, are shown (see text for detailed discussion). Palaeogeographic reconstructions follow that of Zhu and others (2012) for relative positions of the Lhasa and Qiangtang terranes, and Z.X. Li and others (2013) for the rest. The cartoon palaeo-drainage patterns are modified after Myrow and others (2010). North China is notional shown close to northern Australia in the Cambrian because of some bioprovince and detrital zircon provenance similarities (for example, McKenzie and others, 2011), but there is no evidence to suggest that it was a coherent part of Gondwanaland at that time (for example, Z.X. Li and Powell, 2001; Cocks and Torsvik, 2013).

3.6 Conclusions

Integrated U–Pb and Hf–O isotopic analyses of zircons from Cambrian sandstones /

metasandstones from the western Cathaysia Block of South China reveal an exotic source region(s) that experienced three Precambrian episodes of juvenile crustal growth at 3.0, 2.5 and 1.0 Ga, and which underwent extensive crustal remelting and reworking at 580 to 500 Ma. This provenance shows remarkable similarities to that of the NW Indian Himalaya during Ediacaran–Cambrian time. The two regions also share similarities in terms of Ediacaran–Cambrian tectonostratigraphy and Cambrian bioprovinces. We consider that the SCB (including Cathaysia) drifted away from central Rodinia during supercontinent break-up after *ca.* 750 Ma. Its collision with the NW Indian Himalaya between the late Ediacaran (*ca.* 580 Ma) and the Ordovician as part of Gondwana assembly led to the formation of a "Pan-African" orogenic belt along the Himalaya at the northern Indian margin. The Cathaysia side of the Nanhua Basin possibly received sediments similar to northern India, dominantly shed from the East African orogen, during the late Ediacaran. As the collision progressed, the Nanhua Basin was transformed into a fully-developed foreland basin, probably receiving both recycled sediments and eroded detritus from 550 to 470 Ma granites in the Cambro-Orodvician trans-Himalaya North India orogen. Far-field tectonic stress of the SCB–India collision eventually caused the Ordovician–Silurian intraplate Wuyi–Yunkai orogeny (>460–415 Ma) in southeastern South China that resulted in closure of the Nanhua Basin.

3.7 Acknowledgement

We thank L.F. Meng and J.H. Tao for help during the field work, Y.F. Wang, L. Su and Y.H. Yang for assistances in LA (MC)-ICP-MS U–Pb dating/Hf isotope analyses, H.X. Ma for help in mount making, G. Li and C. Zhou for assisting with fossil descriptions, and S.A. Wilde and K.A. Evans for commenting on the manuscript. Review comments from Robert Rainbird, Nigel Hughes, guest editors Sun-Lin Chung and William Griffin, and four anonymous reviewers helped to improve the paper. This study was supported by the Australian Research Council (DP110104799), the Chinese Academy of Sciences SAFEA International Partnership Program for Creative Research Teams grant (KZCX2-YW-Q04-06) and the National Natural Sciences Foundation of China (41173039). This is TIGeR (The Institute for Geoscience Research) publication #495, and contribution 366 from the ARC Centre of Excellence for Core to Crust Fluid Systems (http://www.ccfs.mq.edu.au/).

3.8 References

Ameen, S. M. M., Wilde, S. A., Kabir, Z., Akon, E., Chowdhury, K. R., and Khan, S. H., 2007, Paleoproterozoic granitoids in the basement of Bangladesh: A piece of the Indian shield or an exotic fragment of the Gondwana jigsaw?: Gondwana Research, v. 12, p. 380–387, http://dx.doi.org/10.1016/j.gr.2007.02.001

Anderson, T., 2002, Correction of common lead in U–Pb analyses that do not report ^{204}Pb: Chemical Geology, v. 192, p. 59–79, http://dx.doi.org/10.1016/S0009-2541(02)00195-X

Bagati, T. N., Kumar, R., and Ghosh, S. K., 1991, Regressive–transgressive sedimentation in the Ordovician sequence of the Spiti (Tethys) basin, Himachal Pradesh, India: Sedimentary Geology, v. 73, p. 171–184, http://dx.doi.org/10.1016/0037-0738(91)90029-D

Barth, A. P., Wooden, J. L., Coleman, D. S., and Fanning, C. M., 2000, Geochronology of the Proterozoic basement of southwesternmost North America, and the orogin and evolution of the Mojave crustal province: Tectonics, v. 19, p. 616–629, http://dx.doi.org/10.1029/1999TC001145

Belousova, E.A., Kostitsyn, Y.A., Griffin, W.L., Begg, G.C., O'Reilly, S.Y., and Pearson, N.J., 2010, The growth of the continental crust: constraints from zircon Hf–isotope data: Lithos, v. 119, p. 457–466, http://dx.doi.org/10.1016/j.lithos.2010.07.024

BGMRFJ (Bureau of Geology and Mineral Resources of Fujian Province), 1985, Regional Geology of the Fujian Province: Beijing, Geological Publishing House, 671 p. (in Chinese with English abstract).

BGMRGD (Bureau of Geology and Mineral Resources of Guangdong Province), 1988, Regional Geology of the Guangdong Province: Beijing, Geological Publishing House, 971 p. (in Chinese with English abstract).

BGMRGX (Bureau of Geology and Mineral Resources of Guangxi Province), 1985, Regional Geology of the Guangxi Province: Beijing, Geological Publishing House, 853 p. (in Chinese with English abstract).

BGMRGZ (Bureau of Geology and Mineral Resources of Guizhou Province), 1988, Regional Geology of the Guizhou Province: Beijing, Geological Publishing House, 698 p. (in Chinese with English abstract).

BGMRHN (Bureau of Geology and Mineral Resources of Hunan Province), 1988, Regional Geology of the Hunan Province: Beijing, Geological Publishing House, 719 p. (in Chinese with English abstract).

BGMRJX (Bureau of Geology and Mineral Resources of Jiangxi Province), 1984, Regional Geology of the Jiangxi Province: Beijing, Geological Publishing House, 921 p. (in Chinese with English abstract).

Bhargava, O. N., Frank, W., and Bertle, R., 2011, Late Cambrian deformation in the Lesser Himalaya: Journal of Asian Earth Sciences, v. 40, p. 201–212, http://dx.doi.org/10.1016/j.jseaes.2010.07.015

Black L. P., Kamo, S. L., Allen, C. M., Aleinikoff, J. N., Davis, D. W., Korsch, R. J., and Foudoulis, C., 2003, TEMORA1: a new zircon standard for Phanerozoic U–Pb geochronology: Chemical Geology, v. 200, p. 155–170, http://dx.doi.org/10.1016/S0009-2541(03)00165-7

Brookfield, M. E., 1993, The Himalayan passive margin from Precambrian to Cretaceous: Sedimentary Geology, v. 84, p. 1–35, http://dx.doi.org /10.1016/0037-0738(93)90042-4

Cawood, P. A., and Nemchin, A. A., 2000, Provenance record of a rift basin: U/Pb ages of detrital zircons from the Perth Basin, Western Australia: Sedimentary Geology, v. 134, p. 209–234, http://dx.doi.org/10.1016/S0037-0738(00)00044-0

Cawood, P. A., Johnson, M. R. W., and Nemchin, A. A., 2007, Early Palaeozoic orogenesis along the Indian margin of Gondwana: Tectonic response to Gondwana assembly: Earth and Planetary Science Letters, v. 255, p. 70–84, http://dx.doi.org /10.1016/j.epsl.2006.12.006

Cawood, P. A., Wang, Y. J., Xu, Y. J., and Zhao, G. C., 2013, Locating South China in Rodinia and Gondwana: A fragment of greater India lithosphere?: Geology, v. 41, p. 903–906, http://dx.doi.org/10.1130/G34395.1

Charvet, J., Shu, L., Faure, M., Choulet, F., Wang, B., Lu, H., and Breton, N. L., 2010, Structural development of the Lower Paleozoic belt of South China: Genesis of an intracontinental orogen: Journal of Asian Earth Sciences, v. 39, p. 309–330, http://dx.doi.org/10.1016/j.jseaes.2010.03.006

Chen, X., Rong, J., Rowley, D. B., Zhang, J., Zhang, Y. D., and Zhan, R. B., 1995, Is the early Paleozoic Banxi Ocean in South China necessary?: Geological Review, v. 41, p. 389–400 (in Chinese with English abstract).

Chen, X., Rowley, D. B., Rong, J., Zhang, J., Zhang, Y. D., and Zhan, R. B., 1997, Late Precambrian through Early Paleozoic stratigraphic and tectonic evolution of the Nanling region, Hunan Province, South China: International Geology Review, v. 39, p. 469–478, http://dx.doi.org/10.1080/00206819709465285

Chen, J., and Jahn, B. M., 1998, Crustal evolution of southeastern China: Nd and Sr isotopic evidence: Tectonophysics, v. 284, p. 101–133, http://dx.doi.org/10.1016/S0040-1951(97)00186-8

Chen, Z. H., Xing, G. F., Guo, K. Y., Dong, Y. G., Chen, R., Zeng, Y., Li, L. M., He, Z. Y., and Zhao, L., 2009, Petrogenesis of keratophyes in the Pingshui Group, Zhejiang: Constraints from zircon U–Pb ages and Hf isotopes: Chinese Science Bulletin, v. 54, p. 1570–1578, http://dx.doi.org/10.1007/s11434-009-0081-y

Cocks, L. R. M., and Torsvik, T. H., 2013, The dynamic evolution of the Palaeozoic geography of eastern Asia: Earth-Science Reviews, v. 117, p. 40–79, http://dx.doi.org/10.1016/j.earscirev.2012.12.001

Condie, K. C., Belousova, E., Griffin, W. L., and Sircombe, K. N., 2009, Granitoid events in space and time: Constraints from igneous and detrital zircon age spectra: Gondwana Research, v. 15, p. 228–242, http://dx.doi.org /10.1016/j.gr.2008.06.001

Corfu, F., Hanchar, J. M., Hoskin, P. W. O., and Kinny, P., 2003, Altas of zircon textures: Reviews in Mineralogy and Geochemistry, v. 53, p. 469–500, http://dx.doi.org/10.2113/0530469

Cottle, J. M., Jessup, M. J., Newell, D. L., Horstwood, M. S. A., Noble, S. R., Parrish, R. R., Waters, D. J., and Searle, M. P., 2009, Geochronology of granulitized eclogite from the Ama Drime Massif: Implications for the tectonic evolution of the South Tibetan Himalaya: Tectonics, v. 28, no. 1, http://dx.doi.org/10.1029/2008TC002256

DeCelles, P. G., Gehrels, G. E., Quade, J., Lareau, B., and Spurlin, M., 2000, Tectonic implications of U–Pb zircon ages of the Himalayan orogenic belt in Nepal: Science, v. 288, p. 497–499, http://dx.doi.org/10.1126/science.288.5465.497

Dhuime, B., Hawkesworth, C., and Cawood, P., 2011, When continents formed: Science, v. 331, p. 154–155, http://dx.doi.org/10.1126/science.1201245

Dickinson, W. R., 1970, Interpreting detrital modes of greywacke and arkose: Journal

of Sedimentary Research, v. 40, p. 695–707, http://dx.doi.org/10.1306/74D72018-2B21-11D7-8648000102C1865D

Dickinson, W. R., Beard, L. S., Brakenridge, G. R., Erjavec, J. L., Ferguson, R. C., Inman, K. F., Knepp, R. A., Lindberg, F. A., and Ryberg, P. T., 1983, Provenance of North American Phanerozoic sandstones in relation to tectonic setting: Geological Society of America Bulletin, v. 94, p. 222–235, http://dx.doi.org/10.1130/0016-7606(1983)94<222:PONAPS>2.0.CO;2

Dickinson, W. R., 1985, Interpreting provenance relations from detrital modes of sandstones, *in* Zuffa, G.G., editors, Provenance of arenites: NATO ASI series C: 148: Dordrecht/Boston/Lancaster, D. Reidel Publishing Company, p. 333–361.

Dong, C. Y., Li, C., Wan, Y. S., Wang, W., Wu, Y. W., Xie, H. Q., and Liu, D. Y., 2011, Detrital zircon age model of Ordovician Wenquan quartzite south of Lungmuco–Shuanghu suture in the Qiangtang area, Tibet: Constraint on tectonic affinity and source regions: Science China, Earth Sciences, v. 54, p. 1034–1042, http://dx.doi.org/10.1007/s11430-010-4166-x

Draganits, E., 2000, The Muth Formation in the Pin Valley (Spiti, N-India): Depositional environment and Ichnofauna of a Lower Devonian barrier island system: Ph.D. thesis, University of Viena, Viena, 144 p.

Gan, X. C., Li, H. M., and Sun, D. Z., 1995, A geochronological study on early Proterozoic granitic rocks, Southwestern Zhejiang: Acta Petrologica et Mineralogica, v. 14, p. 1–8 (in Chinese with English abstract).

Gao, S., Yang, J., Zhou, L., Li, M., Hu, Z., Guo, J., Yuan, H., Gong, H., Xiao, G., and Wei, J., 2011, Age and growth of the Archean Kongling terrain, South China, with emphasis on 3.3 Ga granitoid gneisses: American Journal of Science, v. 311, p. 153–182, http://dx.doi.org/10.2475/02.2011.03

Garzanti, E., Casnedi, R., and Jadoul, F., 1986, Sedimentary evidence of a Cambro-Ordovician orogenic event in the northwestern Himalaya: Sedimentary Geology, v. 48, p. 237–265, http://dx.doi.org/10.1016/0037-0738(86)90032-1

Gazzi, P., 1966, Le arenarie del flysch sopracretaceo dell'Appennino modenese; correlazioni con il flysch di Monghidoro: Acta Mineralogica-Peteographica, v. 12, p. 69–97.

Gehrels, G. E., DeCelles, P. G., Matin, A., Ojha, T. P., and Pinhassi, G., 2003,

Initiation of the Himalayan orogen as an early Paleozoic thin-skinned thrust belt: GSA today, v. 13, no. 9, p. 4–9.

Gehrels, G. E., DeCelles, P. G., Ojha, T. P., and Upreti, B. N., 2006a, Geologic and U–Th–Pb geochronologic evidence for early Paleozoic tectonism in the Kathmandu thrust sheet, central Nepal Himalaya: Geological Society of America Bulletin, v. 118, p. 185–198, http://dx.doi.org/10.1130/B25753.1

Gehrels, G. E., DeCelles, P. G., Ojha, T. P., and Upreti, B. N., 2006b, Geologic and U–Pb geochronologic evidence for early Paleozoic tectonism in the Dadeldhura thrust sheet, far-west Nepar Himalaya: Journal of Asian Earth Sciences, v. 28, p. 386–408, http://dx.doi.org/10.1016/j.jseaes.2005.09.012

Gehrels, G. E., Kapp, P., DeCelles, P., Pullen, A., Blakey, R., Weislogel, A., Ding, L., Guynn, J., Martin, A., McQuarrie, N., and Yin, A., 2011, Detrital zircon geochronology of pre-Tertiary strata in the Tibetan–Himalayan orogen: Tectonics, v. 30, p. 1–27, http://dx.doi.org/10.1029/2011TC002868

Greentree, M. R., Li, Z. X., Li, X. H., and Wu, H. C., 2006, Late Mesoproterozoic to earliest Neoproterozoic basin record of the Sibao orogenesis in western South China and relationship to the assembly of Rodinia: Precambrian Research, v. 151, p. 79–100, http://dx.doi.org/10.1016/j.precamres.2006.08.002

Greentree, M. R., and Li, Z. X., 2008, The oldest known rocks in south-western China: SHRIMP U–Pb magmatic crystallisation age and detrital provenance analysis of the Paleoproterozoic Dahongshan Group: Journal of Asian Earth Sciences, v. 33, p. 289–302, http://dx.doi.org/10.1016/j.jseaes.2008.01.001

Griffin, W. L., Pearson, N. J., Belousova, E., Jackson, S. E., Achterbergh, E. V., O'Reilly, S. Y., and Shee, S. R., 2000, The Hf isotope composition of cratonic mantle: LAM-MC-ICPMS analysis of zircon megacrysts in kimberliters: Geochimica et Cosmochimica Acta, v. 64, p. 133–147, http://dx.doi.org/10.1016/S0016-7037(99)00343-9

Griffin, W.L., Belousova, E.A., Shee, S.R., Pearson, N.J., and O'Reilly, S.Y., 2004, Archean crustal evolution in the northern Yilgarn Craton: U–Pb and Hf–isotope evidence from detrital zircons: Precambrian Research, v. 131, p. 231–282, http://dx.doi.org/10.1016/j.precamres.2003.12.011

Hawkesworth, C. J., and Kemp, A. I. S., 2006, Using hafnium and oxygen isotopes in zircons to unravel the record of crustal evolution: Chemical Geology, v. 226, p. 144–162, http://dx.doi.org/10.1016/j.chemgeo.2005.09.018

Hoffman, P. F., 1991, Did the breakout of Laurentia turn Gondwanaland inside-out? Science, v. 252, p. 1409–1412.

Hughes, N. C., Myrow, P. M., Mckenzie, N. R., Harper, D. A. T., Bhargava, O. N., Tangri, S. K., Ghalley, K. S., and Fanning, C. M., 2011, Cambrian rocks and faunas of the Wachi La, Black Mountains, Bhutan: Geological Magazine, v. 148(3), p. 351–379, http://dx.doi.org/10.1017/S0016756810000750

Ingersoll, R. V., Bullard, T. P., Ford, R. L., Grimm, P., Pickle, L. D., and Sares, S. W., 1984, The effect of grain size on detrital modes: A test of the Gazzi–Dickinson point-counting method: Sedimentary Petrology, v. 54, p. 103–116, http://dx.doi.org/10.1306/212F83B9-2B24-11D7-8648000102C1865D

Jackson, S. E., Pearson, N. J., Griffin, W. L., and Belousova, E. A., 2004, The application of laser ablation-inductively coupled plasma-mass spectrometry to *in situ* U–Pb zircon geochronology: Chemical Geology, v. 211, p. 47–69, http://dx.doi.org/10.1016/j.chemgeo.2004.06.017

Jell, P. A., and Hughes, N. C., 1997, Himalayan Cambrian trilobites: Special Papers in Palaeontology, v. 58, p. 1–113.

Jiang, G., Sohl, L. E., and Christie-Blick, N., 2003, Neoproterozoic stratigraphic comparison of the Lesser Himalaya (India) and Yangtze block (south China): Paleogeographic implications: Geology, v. 31, p. 917–920, http://dx.doi.org/10.1130/G19790.1

Jiao, W. F., Wu, Y. B., Yang, S. H., Peng, M., and Yang, J., 2009, The oldest basement rock in the Yangtze Craton revealed by zircon U–Pb age and Hf isotope composition: Science in China Series D: Earth Sciences, v. 52, p. 1393–1399, http://dx.doi.org/10.1007/s11430-009-0135-7

Kemp, A. I. S., Hawkerworth, C. J., Paterson, B. A., and Kinny, P. D., 2006, Episodic growth of the Gondwana supercontinent from hafnium and oxygen isotopes in zircon: Nature, v. 439, p. 580–583, http://dx.doi.org/10.1038/nature04505

Kohn, M. J., Pau, S. K., and Corrie, S. L., 2010, The lower Lesser Himalayan sequence: a Paleoproterozoic arc on the northern margin of the Indian plate: Geological Society of America Bulletin, v. 122, p. 323–335, http://dx.doi.org/10.1130/B26587.1

Kolmogorov, A. N., 1933, Sulla determinazione empirica di una legge di distribuzione: Giornale dell'Istituto Italiano degli Attuari, v. 4, p. 83–91.

Kumar, G., 1984, The Precambrian–Cambrian boundary beds, northwest Himalaya, India, and boundary problems, *in* Proceedings of the Fifth Indian Geophytological Conference, Lucknow, November 1983. Palaeobotanical Society of India, Special Publications, Lucknow, p. 98–111.

Le Fort, P., 1975, Himalayas: collided range. Present knowledge of continental arc: American Journal of Science, v. 275, p. 1–44.

Leier, A. L., Kapp, P., Gehrels, G. E., and DeCelles, P. G., 2007, Detrital zircon geochronology of Carboniferous–Cretaceous strata in the Lhasa terrane, Southern Tibet: Basin Research, v. 19, p. 361–378, http://dx.doi.org/10.1111/j.1365-2117.2007.00330.x

Li, L., Lin, S., Xing, G., Davis, D. W., Davis, W. J., Xiao, W., and Yin, C., 2013, Geochemistry and tectonic implications of late Mesoproterozoic alkaline bimodal volcanic rocks from the Tieshajie Group in the southeastern Yangtze Block, South China: Precambrian Research, v. 230, p. 179–192, http://dx.doi.org/10.1016/j.precamres.2013.02.004

Li, W. X., Li, X. H., and Li, Z. X., 2005, Neoproterozoic bimodal magmatism in the Cathaysia Block of South China and its tectonic significance: Precambrian Research, v. 136, p. 51–66, http://dx.doi.org/10.1016/j.precamres.2004.09.008

Li, W. X., Li, X. H., Li, Z. X., and Lou, F. S., 2008, Obduction-type granites within the NE Jiangxi Ophiolite: Implications for the final amalgamation between the Yangtze and Cathaysia Blocks: Gondwana Research, v. 13, no. 3, p. 288-301, http://dx.doi.org/10.1016/j.gr.2007.12.010

Li, W. X., Li, X. H., and Li, Z. X., 2010, *Ca.* 850 Ma bimodal volcanic rocks in northeastern Jiangxi Province, South China: Initial extension during the breakup of Rodinia?: American Journal of Science, v. 310, p. 951–980, http://dx.doi.org/10.2475/09.2010.08

Li, X. H., 1997, Timing of the Cathaysia block formation: constraints from SHRIMP U–Pb zircon geochronology: Episodes, v. 20, p. 188–192.

Li, X. H., Li, Z. X., Ge, W. C., Zhou, H. W., Li, W. X., Liu, Y., and Wingate, M. T. D., 2003, Neoproterozoic granitoids in South China: crustal melting above a mantle plume at *ca.* 825 Ma? Precambrian Research, v. 122, p. 45–83, http://dx.doi.org/10.1016/S0301-9268(02)00207-3

Li, X. H., Li, W. X., Li, Z. X., Lo, C. H., Wang, J., Ye, M. F., and Yang, Y. H., 2009,

Amalgamation between the Yangtze and Cathaysia blocks in South China: Constraints from SHRIMP U–Pb zircon ages, geochemistry and Nd–Hf isotopes of the Shuangxiwu volcanic rocks: Precambrian Research, v. 174, p. 117–128, http://dx.doi.org/10.1016/j.precamres.2009.07.004

Li, X. H., Long, W. G., Li, Q. L., Liu, Y., Zheng, Y. F., Yang, Y. H., Chamberlain, K. R., Wan, D. F., Guo, C. H., Wang, X. C., and Tao, H., 2010a, Penglai zircon megacrysts: a potential new working reference material for microbeam determination of Hf–O isotopes and U–Pb age: Geostandards and Geoanalytical Research, v. 34, p. 117–134, http://dx.doi.org/10.1111/j.1751-908X.2010.00036.x

Li, X. H., Li, W. X., Li, Q. L., Wang, X. C., Liu, Y., and Yang, Y. H., 2010b, Petrogenesis and tectonic significance of the ca 850Ma Gangbian alkaline complex in South China: evidence from *in situ* zircon U–Pb dating, Hf–O isotopes and whole rock geochemistry: Lithos, v. 114, p. 1–15, http://dx.doi.org/10.1016/j.lithos.2009.07.011

Li, X. H., Li, Z. X., He, B., Li, W. X., Li, Q. L., Gao, Y. Y., and Wang, X. C., 2012, The Early Permian active continental margin and crustal growth of the Cathaysia Block: *In situ* U–Pb, Lu–Hf and O isotope analyses of detrital zircons: Chemical Geology, v. 328, p. 195–207, http://dx.doi.org/10.1016/j.chemgeo.2011.10.027

Li, Z. X., Zhang, L. H., and Powell, C. M., 1996, Positions of the East Asian cratons in the Neoproterozoic supercontinent Rodinia: Australian Journal of Earth Science, v. 43, p. 593–604, http://dx.doi.org/10.1080/08120099608728281

Li, Z. X., 1998, Tectonic history of the major East Asian lithospheric blocks since the mid-Proterozoic – a synthesis, *in* Flower, M. J., Chung, S. L., Lo, C. H., and Lee, T. Y., editors, Mantle dynamics and plate interactions in East Asia: Washington, DC, United States, American Geophysical Union, p. 221–243, http://dx.doi.org/10.1029/GD027p0221

Li, Z. X., and Powell, C. M., 2001, An outline of the Palaeogeographic evolution of the Australasian region since the beginning of the Neoproterozoic: Earth-Science Reviews, v. 53, p. 237–277, http://dx.doi.org/10.1016/S0012-8252(00)00021-0

Li, Z. X., Li, X. H., Zhou, H. W., and Kinny, P. D., 2002, Grenvillian continental collision in south China: new SHRIMP U–Pb zircon results and implications

for the configuration of Rodinia: Geology, v. 30, p. 163–166, http://dx.doi.org/10.1130/0091-7613(2002)030<0163:GCCISC>2.0.CO;2

Li, Z. X., Li, X. H., Kinny, P. D., Wang, J., Zhang, S., and Zhou, H. W., 2003, Geochronology of Neoproterozoic syn-rift magmatism in the Yangtze Craton, South China and correlations with other continents: evidence for a mantle superplume that broke up Rodinia: Precambrian Research, v. 122, p. 85–109, http://dx.doi.org/10.1016/S0301-9268(02)00208-5

Li, Z. X., Evans, D. A. D., and Zhang, S. H., 2004, A 90º Spin on Rodinia: Possible causal links between the Neoproterozoic supercontinent, superplume, true polar wander and low-latitude glaciation: Earth and Planetary Science Letters, v. 220, p. 409–421, http://dx.doi.org/10.1016/S0012-821X(04)00064-0

Li, Z. X., and Li, X. H., 2007, Formation of the 1300 km-wide intracontinental orogen and postorogenic magmatic province in Mesozoic South China: a flat-slab subduction model: Geology, v. 35, p. 179–182, http://dx.doi.org/10.1130/G23193A.1

Li, Z. X., Wartho, J. A., Occhipinti, S., Zhang, C. L., Li, X. H., Wang, J., and Bao, C. M., 2007, Early history of the eastern Sibao Orogen (South China) during the assembly of Rodinia: New mica $^{40}Ar/^{39}Ar$ dating and SHRIMP U–Pb detrital zircon provenance constraints: Precambrian Research, v. 159, p. 79–94, http://dx.doi.org/10.1016/j.precamres.2007.05.003

Li, Z. X., Li, X. H., Li, W. X., and Ding, S., 2008a, Was Cathaysia part of Proterozoic Larentia? – new data from Hainan Island, south China: Terran Nova, v. 20, p. 154–164, http://dx.doi.org/10.1111/j.1365-3121.2008.00802.x

Li, Z. X., Bogdanova, S. V., Collins, A. S., Davidson, A., De Waele, B., Ernst, R. E., Fitzsimons, I. C. W., Fuck, R. A., Gladkochub, D. P., Jacobs, J., Karlstrom, K. E., Lu, S., Natapov, L. M., Pease, V., Pisarevsky, S. A., Thrane, K., and Vernikosky, V., 2008b, Assembly, configuration, and break-up history of Rodinia: a synthesis: Precambrian Research, v. 160, p. 179–210, http://dx.doi.org/ 10.1016/j.precamres.2007.04.021

Li, Z. X., Li, X. H., Wartho, J. A., Clark, C., Li, W. X., Zhang, C. L., and Bao, C. M., 2010, Magmatic and metamorphic events during the early Paleozoic Wuyi–Yunkai orogeny, southeastern South China: New age constraints and pressure–temperature conditions: Geological Society of America Bulletin, v. 122, p. 772–793, http://dx.doi.org/10.1130/B30021.1

Li, Z. X., and Evans, D. A. D., 2011, Late Neoproterozoic 40° intraplate rotation within Australia allows for a tighter-fitting and longer-lasting Rodinia: Geology, v. 39, p. 39–42, http://dx.doi.org/10.1130/G31461.1

Li, Z. X., Evans, D. A. D., and Halverson, G. P., 2013, Neoproterozoic glaciations in a revised global paleogeography from the breakup of Rodinia to the assembly of Gondwanaland: Sedimentary Geology, v. 294, p. 219–232, http://dx.doi.org/10.1016/j.sedgeo.2013.05.016

Ling, W., Gao, S., Zhang, B., Li, H., Liu, Y., 2003, Neoproterozoic tectonic evolution of Yangtze craton, South China: implications for amalgamation and break-up of Rodinia Supercontinent: Precambrian Research, v. 122, p. 111–140, http://dx.doi.org/10.1016/S0301-9268(02)00222-X

Liu, B., and Xu, X., 1994, Atlas of Lithofacies and Paleogeography of South China: Beijing, Science Press, 188 p.

Liu, R., Zhou, H. W., Zhang, L., Zhong, Z. Q., Zeng, W., Xiang, H., Jin, S., Lu, X. Q., and Li, C. Z., 2009, Paleoproterozoic reworking of ancient crust in the Cathaysia Block, South China: Evidence from zircon trace elements, U–Pb and Lu–Hf isotopes: Chinese Science Bulletin, v. 54, p. 1543–1554, http://dx.doi.org/10.1007/s11434-009-0096-4

Liu, X., Hsü, K.J., Ju, Y., Li, G., Liu, X., Wei, L., Zhou, X., and Zhang, X., 2012, New interpretation of tectonic model in south Tibet: Journal of Asian Earth Sciences, v. 56, p. 147–159, http://dx.doi.org/10.1016/j.jseaes.2012.05.005

Liu, Y., Siebel, W., Massonne, H., and Xiao, X., 2007, Geochronological and petrological constraints for tectonic evolution of the central Greater Himalayan sequence in the Kharta area, southern Tibet: The Journal of Geology, v. 115, p. 215–230, http://dx.doi.org/10.1086/510806

Ludwig, K. R., 2001a, ISOPLOT/EX version 2.49 – A geochronological toolkit for Microsoft excel: Berkley Geochronological Centre Special Publication No. 1, 56 p.

Ludwig, K. R., 2001b, SQUID version 1.02 – A geochronological toolkit for Microsoft excel: Berkley Geochronological Centre Special Publication No. 2, 19 p.

Ma, D., Huang, X., Xiao, Z., Chen, Z., Zhang, W., and Zhong, S., 1998, The crystalline basement of the Hainan Island – stratigraphy and geochronology of the Baoban group: Wuhan, China University of Geosciences Press, 60 p.

(In Chinese).

Martin, A. J., DeCelles, P. G., Gehrels, G. E., Patchett, P. J., and Isachsen, C., 2005, Isotopic and structural constraints on the location of the main Central thrust in the Annapurna Range, central Nepal Himalaya: Geological Society of America Bulletin, v. 117, p. 926–944, http://dx.doi.org/10.1130/B25646.1

McKenzie, N. R., Hughes, N. C., Myrow, P. M., Choi, D. K., and Park, T.-y., 2011, Trilobites and zircons link north China with the eastern Himalaya during the Cambrian: Geology, v. 39, no. 6, p. 591–594, http://dx.doi.org/10.1130/G31838.1

McQuarrie, N., Robinson, D., Long, S., Tobgay, T., Grujic, D., Gehrels, G., and Duce, M., 2008, Preliminary stratigraphic and structural architecture of Bhutan: Implications for the alongstrike architecture of the Himalayan system: Earth and Planetary Science Letters, v. 272, p. 105–117, http://dx.doi.org/10.1016/j.epsl.2008.04.030

McQuarrie, N., Long, S. P., Tobgay, T., Nesbit, J. N., Gehrels, G., and Ducea, M. N., 2013, Documenting basin scale, geometry and provenance through detrital geochemical data: Lessons from the Neoproterozoic to Ordovician Lesser, Greater, and Tethyan Himalayan strata of Bhutan: Gondwana Research, v. 23, p. 1491–1510, http://dx.doi.org/10.1016/j.gr.2012.09.002

Metcalfe, I., 1996, Gondwanaland dispersion, Asian accretion and evolution of eastern Tethys: Australian Journal of Earth Sciences, v. 43, p. 605–623, http://dx.doi.org/10.1080/08120099608728282

Miller, C., Klotzli, U., Frank, W., Thoni, M., and Grasemann, B., 2000, Proterozoic crustal evolution in the NW Himalaya (India) as recorded by circa 1.80 Ga mafic and 1.84 Ga granitic magmatism: Precambrian Research, v. 103, p. 191–206, http://dx.doi.org/10.1016/S0301-9268(00)00091-7

Miller, C., Thoni, M., Frank, W., Grasemann, B., Klotzli, U., Guntli, P., and Draganits, E., 2001, The early Palaeozoic magmatic event in the Northwest Himalaya, India: source, tectonic setting and age of emplacement: Geological Magazine, v. 138, p. 237–251, http://dx.doi.org/10.1017/S0016756801005283

Morel, M. L. A., Nebel, O., Nebel-Jacobsen, Y. J., Miller, J. S., and Vroon, P. Z., 2008, Hafnium isotope characterization of the GJ-1 zircon reference material by solution and laser ablation MC-ICPMS: Chemical Geology, v. 255, p. 231–235, http://dx.doi.org/10.1016/j.chemgeo.2008.06.040

Myrow, P. M., Hughes, N. C., Paulsen, T. S., Williams, I. S., Parcha, S. K., Thompson, K. R., Bowring, S. A., Peng, S. C., and Ahluwalia, A. D., 2003, Intergrated tectonostratigraphic analysis of the Himalaya and implications for its tectonic reconstruction: Earth and Planetary Science Letters, v. 212, p. 433–441, http://dx.doi.org/10.1016/S0012-821X(03)00280-2

Myrow, P. M., Snell, K. E., Hughes, N. C., Paulsen, T. S., Heim, N. A., and Parcha, S. K., 2006a, Cambrian depositional history of the Zanskar Valley region of the Indian Himalaya: tectonic implications: Journal of Sedimentary Research, v. 76, p. 364–381, http://dx.doi.org/10.2110/jsr.2006.020

Myrow, P. M., Thompson, K. R., Hughes, N. C., Paulsen, T. S., Sell, B. K., and Parcha, S. K., 2006b, Cambrian stratigraphy and depositional history of the northern Indian Himalaya, Spiti Valley, north-central India: Geological Society of America Bulletin, v. 118, p. 491–510, http://dx.doi.org/10.1130/B25828.1

Myrow, P. M., Hughes, N. C., Searle, M. P., Fanning, C. M., Peng, S. C., and Parcha, S. K., 2009, Stratigraphic correlation of Cambrian–Ordovician deposits along the Himalaya: Implications for the age and nature of rocks in the Mount Everest region: Geological Society of America Bulletin, v. 120, p. 323–332, http://dx.doi.org/10.1130/B26384.1

Myrow, P. M., Hughes, N. C., Goodge, J. W., Fanning, C. M., Williams, I. S., Peng, S. C., Bhargava, O. N., Parcha, S. K., and Pogue, K. R., 2010, Extraordinary transport and mixing of sediment across Himalayan central Gondwana during the Cambrian–Ordovician: Geological Society of America Bulletin, v. 122, p. 1660–1670, http://dx.doi.org/10.1130/B30123.1

Nesheim, T. O., Vervoort, J. D., McClelland, W. C., Gilotti, J. A., and Lang, H. M., 2012, Mesoproterozoic syntectonic garnet within Belt Supergroup metamorphic tectonites: Evidence of Grenville-age metamorphism and deformation along northwest Laurentia: Lithos, v. 134–135, p. 91–107, http://dx.doi.org/10.1016/j.lithos.2011.12.008

Neves, S. P., 2003, Proterozoic history of the Borborema province (NE Brazil): correlations with neighboring cratons and Pan-African belts and implications for the evolution of western Gondwana: Tectonics, v. 22, p. 1031–1044, http://dx.doi.org/10.1029/2001TC001352

Nichols, G., 2009, Sedimentology and Stratigraphy (second edition): London,

Blackwell Science Publishing, 419 p.

Peng, S., Hughes, N. C., Heim, N. A., Sell, B. K., Zhu, X. J, Myrow, P. M., and Parcha, S. K., 2009, Cambrian trilobites from the Parahio and Zanskar Valleys, Indian Himalaya: Paleontological Society Memoirs (Journal of Paleontology Supplement), v. 71, p. 1–95.

Pogue, K. R., Hylland, M. D., Yeats, R. S., Khattak, W. U., and Hussain, A., 1999, Stratigraphic and structural framework of Himalayan foothills, northern Pakistan, *in* Macfarlane, A., Sorkhabi, R.B., and Quade, J., editors, Himalaya and Tibet: Mountain Roots to Mountain Tops: Geological Society of America Special Papers, v. 328, p. 257–274.

Pullen, A., Kapp, P., Gehrels, G. E., Ding, L., and Zhang, Q., 2011, Metamorphic rocks in central Tibet: Lateral variations and implications for crustal structure: Geological Society of America Bulletin, v. 123, p. 585–600, http://dx.doi.org/10.1130/B30154.1

Qiu, Y., Gao, S., McNaughton, N. J., Groves, D. I., and Ling, W., 2000, First evidence of >3.2 Ga continental crust in the Yangtze craton of south China and its implications for Archean crustal evolution and Phanerozoic tectonic: Geology, v. 28, p. 11–14, http://dx.doi.org/10.1130/0091-7613(2000)028<0011:FEOGCC>2.0.CO;2

Reading, H. G., 1996, Sedimentary Environments: Processes, Facies and Stratigraphy: London, Blackwell Science Publishing, 687 p.

Ren, J., 1991, On the geotectonics of southern China: Acta Geologica Sinica, v. 4, p. 111–130.

Ren, J., Wang, Z., Chen, B., Jiang, C., and Niu, B., 1997, Tectonic map of China and adjacent regions: Beijing, Geological Publishing House, scale 1:5,000,000.

RGMRGD, 1964, Regional Geological Mapping and Report of Guangdong Province –Yangjiang Sheet: Beijing, Institute of Geoscience, Ministry of Geology (in Chinese), scale 1:200,000.

Schärer, U., Xu, R. H., and Allègre1, C. J., 1986, U–(Th) –Pb systematics and ages of Himalayan leucogranites, South Tibet: Earth and Planetary Science Letters, v. 77, p. 35–48, http://dx.doi.org/10.1016/0012-821X(86)90130-5

Schervish, M. J., 1996, P values: what they are and what they are not: The American Statistician, v. 50, no. 3, p. 203–206.

Shu, L. S., Deng, P., Yu, J. H., Wang, Y. B., and Jiang, S. Y., 2008, The age and

tectonic environment of the rhyolitic rocks on the western side of Wuyi Mountain, South China: Science in China, Series D: Earth Sciences, v.51, p. 1053–1063, http://dx.doi.org/ 10.1007/s11430-008-0078-4

Shu, L. S., Faure, M., Yu, J. H., and Jahn, B. M., 2011, Geochronological and geochemical features of the Cathaysia block (South China): New evidence for the Neoproterozoic breakup of Rodinia: Precambrian Research, v. 187, p. 263–276, http://dx.doi.org/10.1016/j.precamres.2011.03.003

Singh, S., Barley, M. E., Brown, S. J., Jain, A. K., and Manickavasagam, R. M., 2002, SHRIMP U–Pb in zircon geochronology of the Chor granitoid: evidence for Neoproterozoic magmatism in the Lesser Himalayan granite belt of NW India: Precambrian Research, v. 118, p. 285–292, http://dx.doi.org/10.1016/S0301-9268(02)00107-9

Singh, S., Claesson, S., Jain, A. K., Gee, D. G., Andreasson, P. G., and Manickavasagam, R. M., 2006, 2.0 Ga granite of the lower package of the Higher Himalayan crystallines, Maglad Khad, Sutlej Valley, Himachal Pradesh: Journal of the Geological Society of India, v. 67, p. 295–300.

Sláma, J., Kosler, J., Condon, D. J., Crowley, J. L., Gerdes, A., Hanchar, J. M., Horstwood, M. S. A., Morris, G. A., Nasdala, L., Norberg, N., Schaltegger U., Schoene, B., Tubrett, M. N., and Whitehouse, M. J., 2008, Plesovice zircon: a new natural reference material for U–Pb and Hf isotopic microanalysis: Chemical Geology, v. 249, p. 1–35, http://dx.doi.org/10.1016/j.chemgeo.2007.11.005

Smirnov, N. V., 1944, Approximate laws of distribution of random variables from empirical data: Uspekhi Matematicheskikh Nauk, v. 10, p. 179–206 (In Russian).

Smith, M., and Gehrels, G., 1994, Detrital zircon geochronology and the provenance of the Harmony and Valmy Formations, Roberts Mountains allochthon, Nevada: Geological Society of America Bulletin, v. 106, p. 968–979, http://dx.doi.org/10.1130/0016-7606(1994)106<0968:DZGATP>2.3.CO;2

Song, S., Niu, Y., Wei, C., Ji, J., and Su, L., 2010, Metamorphis, anatexis, zircon ages and tectonic evolution of the Gongshan block in the northern Indochina continent – an eastern extension of the Lhasa Block: Lithos, v. 120, p. 327–346, http://dx.doi.org/10.1016/j.lithos.2010.08.021

Srikantia, S. V., 1977, Sedimentary cycles in the Himalaya and their significance on

the Orogenic evolution of the mountain belt: International Colloquium Centre National de la Recherche Scientiques, v. 268, p. 395–407.

Stewart, J. H., Gehrels, G. E., Barth, A. P., Link, P. K., Christie-Blick, N., and Wrucke, C. T., 2001, Detrital zircon provenance of Mesoproterozoic to Cambrian arenites in the western United States and northwestern Mexico: Geological Society of America Bulletin, v. 113, p. 1343–1356, http://dx.doi.org/10.1130/0016-7606(2001)113<1343:DZPOMT>2.0.CO;2

Sun, W. H., Zhou, M. F., Gao, J. F., Yang, Y. H., Zhao, X. F., and Zhao, J. H., 2009, Detrital zircon U–Pb geochronological and Lu–Hf isotopic constraints on the Precambrian magmatic and crustal evolution of the western Yangtze Block, SW China: Precambrian Research, v. 172, p. 99–126, http://dx.doi.org/10.1016/j.precamres.2009.03.010

Torsvik, T. H., Paulsen, N. C., Hughes, P. M., Myrow, M., and Ganerod, 2009, The Tethyan Himalaya: palaeogeographical and tectonic constraints from Ordovician palaeomagnetic data: Journal of the Geological Society, v. 166, p. 679–687, http://dx.doi.org/10.1144/0016-76492008-123

Valdiya, K. S., 1970, Simla slate: the Precambrian flysch of the Lesser Himalaya, its turbidites, sedimentary structures and paleocurrents: Geological Society of America Bulletin, v. 81, p. 451–468, http://dx.doi.org/10.1130/0016-7606(1970)81[451:SSTPFO]2.0.CO;2

Valley, J. W., Kinny, P. D., Schulze, D. J., and Spicuzza, M. J., 1998, Zircon megacrysts from kimberlite: oxygen isotope variability among mantle melts: Contribution to Mineralogy and Petrology, v. 133, p. 1–11, http://dx.doi.org/10.1007/s004100050432

Valley, J. W., Lackey, J. S., Cavosie, A. J., Clechenko, C. C., Spicuzza, M. J., Basei, M. A. S., Bindeman, I. N., Ferreira, V. P., Sial, A. N., King, E. M., Peck, W. H., Sinha, A. K., and Wei, C. S., 2005, 4.4 billion years of crustal maturation; oxygen isotope ratios of magmatic zircon: Contributions to Mineralogy and Petrology, v. 150, p. 561–580, http://dx.doi.org/10.1007/s00410-005-0025-8

Van Achterbergh, E., Ryan, C. G., Jackson, S. E., and Griffin,W. L., 2001, Data reduction software for LA-ICP-MS: appendix, *in* Sylvester, P.J., editors, Laser Ablation-ICP-Mass Spectrometry in the Earth Sciences: Principles and Applications: Ottawa, Canada, Mineralogist Association Canada (MAC) Short Course Series, v. 29, p. 239–243.

Veevers, J. J., Saeed, A., Belousova, E. A., and Griffin, W. L., 2005, U–Pb ages and source composition by Hf–isotope and trace–element analysis of detrital zircons in Permian sandstone and modern sand from southwestern Australia and a review of the paleogeographical and denudational history of the Yilgarn Craton: Earth-Science Reviews, v. 68, p. 245–279, http://dx.doi.org/10.1016/j.earscirev.2004.05.005

Veevers, J. J., Belousova, E. A., Saeed, A., Sircombe, K., Cooper, A. F., and Read, S. E., 2006, Pan-Gondwanaland detrital zircons from Australia analysed for Hf–isotopes and trace elements reflect an ice-covered Antarctic provenance of 700–500 Ma age, TDM of 2.0–1.0 Ga, and alkaline affinity: Earth-Science Reviews, v. 76, no. 3–4, p. 135–174, http://dx.doi.org/10.1016/j.earscirev.2005.11.001

Vega-Granillo, R., Salgado-Souto, S., Herrera-Urbina, S., Valencia, V., Ruiz, J., Meza-Figueroa, D., and Talavera-Mendoza, O., 2008, U–Pb detrital zircon data of the Rio Fuerte Formation (NW Mexico): Its peri-Gondwanan provenance and exotic nature in relation to southwestern North America: Journal of South American Earth Sciences, v. 26, p. 343–354, http://dx.doi.org/10.1016/j.jsames.2008.08.011

Wan, Y., Liu, D., Xu, M., Zhuang, J., Song, B., Shi, Y., and Du, L., 2007, SHRIMP U–Pb zircon geochronology and geochemistry of metavolcanic and metasedimentary rocks in Northwestern Fujian, Cathaysia block, China: Tectonic implications and the need to redefine lithostratigraphic units: Gondwana Research, v. 12, p. 166–183, http;//dx.doi.org/10.1016/j.gr.2006.10.016.

Wan, Y., Liu, D., Wilde, S. A., Cao, J., Chen, B., Dong, C., Song, B., and Du, L., 2010, Evolution of the Yunkai Terrane, South China: Evidence from SHRIMP zircon U–Pb dating, geochemistry and Nd isotope: Journal of Asian Earth Sciences, v. 37, p. 140–153, http://dx.doi.org/10.1016/j.jseaes.2009.08.002

Wang, H. (Chief Compiler), 1985, Atlas of the Palaeogeography of China. Cartographic Publishing House, Beijing, 281 p.

Wang, J., and Li, Z. X., 2003, History of Neoproterozoic rift basins in South China: implications for Rodinia break-up: Precambrian Research, v. 122, p. 141–158, http://dx.doi.org/10.1016/S0301-9268(02)00209-7

Wang, X., Zhou, J., Qiu, J., and Gao, J., 2004, Geochemistry of the Meso- to

Neoproterozoic basic–acid rocks from Hunan Province, South China: implications for the evolution of the western Jiangnan orogen: Precambrian Research, v. 135, p. 79–103, http://dx.doi.org/10.1016/j.precamres.2004.07.006

Wang, X. L., Zhou, J. C., Qiu, J. S., Zhang, W. L., Liu, X. M., and Zhang, G. L., 2006, LA-ICP-MS U–Pb zircon geochronology of the Neoproterozoic igneous rocks from Northern Guangxi, South China: implications for tectonic evolution: Precambrian Research, v. 145, p. 111–130, http://dx.doi.org/10.1016/j.precamres.2005.11.014

Wang, Y., Fan, W., Zhao, G., Ji, S., and Peng, T., 2007, Zircon U–Pb geochronology of gneissic rocks in the Yunkai massif and its implications on the Caledonian event in the South China Block: Gondwana Research, v. 12, p. 404–416, http://dx.doi.org/10.1016/j.gr.2006.10.003

Wang, K. L., O'Reilly, S. Y., Griffin, W. L., Pearson, N. J., and Zhang, M., 2009, Sulfides in mantle peridotites from Penghu Islands, Taiwan: Melt percolation, PGE fractionation, and the lithospheric evolution of the South China block: Geochimica et Cosmochimica Acta, v. 73, p. 4531–4557, http://dx.doi.org/10.1016/j.gca.2009.04.030

Wang, L. J., Griffin, W. L., Yu, J. H., and O'Reilly, S. Y., 2010a, Precambrian crustal evolution of the Yangtze Block tracked by detrital zircons from Neoproterozoic sedimentary rocks: Precambrian Research, v. 177, p. 131–144, http://dx.doi.org/10.1016/j.precamres.2009.11.008

Wang, Y., Zhang, F., Fan, W., Zhang, G., Chen, S., Cawood, P. A., and Zhang, A., 2010b, Tectonic setting of the South China Block in the early Paleozoic: Resolving intracontinental and ocean closure models from detrital zircon U–Pb geochronology: Tectonics, v. 29, http://dx.doi.org/10.1029/2010TC002750.

Wang, X. C., Li, X. H., Li, Z. X., Li, Q. L., Tang, G. Q., Gao, Y. Y., Zhang, Q. R., and Liu, Y., 2012a, Episodic Precambrian crust growth: evidence from U–Pb ages and Hf–O isotopes of zircon in the Nanhua Basin, central South China: Precambrian Research, v. 222–223, p. 386–403, http://dx.doi.org/10.1016/j.precamres.2011.06.001

Wang, X., Zhang, J., Santosh, M., Liu, J., Yan, S., and Guo, L., 2012b, Andean-type orogeny in the Himalayas of south Tibet: Implications for early Paleozoic

tectonics along the Indian margin of Gondwana: Lithos, v. 154, p. 248–262, http://dx.doi.org/10.1016/j.lithos.2012.07.011

Webb, A. A. G., Yin, A., Harrison, T. M., Celerier, J., Gehrels, G. E., Manning, C. E., and Grove, M., 2011, Cenozoic tectonic history of the Himachal Himalaya (northwestern India) and its constraints on the formation mechanism of the Himalayan orogen: Geosphere, v. 7, p. 1013–1061, http://dx.doi.org/10.1130/GES00627.1

Wiedenbeck, M., Alle, P., Corfu, F., Griffin, W. L., Meier, M., Oberli, F., Von Quadt, A., Roddick, J. C., and Spiegel, W., 1995, Three natural zircon standards for U–Th–Pb, Lu–Hf, trace element and REE analyses: Geostandards newsletter, v. 19, p. 1–23.

Wiedenbeck, M., Hanchar, J. M., Peck, W. H., Sylvester, P., Valley, J., Whitehouse, M., Kronz, A., Morishita, Y., Nasdala, L., Fiebig, J., Franchi, I., Girard, J. P., Greenwood, R. C., Hinton, R., Kita, N., Mason, P. R. D., Norman, M., Ogasawara, M., Piccoli, P. M., Rhede, D., Satoh, H., Schulz-Dobrick, B., Skar, O., Spicuzza, M. J., Terada, K., Tindle, A., Togashi, S., Vennemann, T., Xie, Q., and Zheng, Y. F., 2004, Further characterization of the 91500 zircon crystal: Geostandards newsletter, v. 28, p. 9–39.

Williams, I. S., 1998, U–Th–Pb geochronology by ion microprobe, *in* McKibben, M. A., Shanks III, W. C., and Ridley, W. I., editors, Applications of microanalytical techniques to understanding mineralizing processes: Reviews in Economic Geology, v. 7, p. 1–35.

Wu, F. Y., Yang, Y. H., Xie, L. W., Yang, J. H., and Xu, P., 2006, Hf isotopic compositions of the standard zircons and baddeleyites used in U–Pb geochronology: Chemical Geology, v. 234, p. 105–126, http://dx.doi.org/10.1016/j.chemgeo.2006.05.003

Wu, L., Jia, D., Li, H., Deng, F., and Li, Y., 2010, Provenance of detrital zircons from the late Neoproterozoic to Ordovician sandstones of South China: implications for its continental affinity: Geological Magazine, v. 147, p. 974–980, http://dx.doi.org/10.1017/S0016756810000725

Xiang, H., Zhang, L., Zhou, H. W., Zhong, Z. Q., Zeng, W., Liu, R., and Jin, S., 2008, U–Pb zircon geochronology and Hf isotope study of metamorphosed basic–ultrabasic rocks from metamorphic basement in southwestern Zhejiang: The response of the Cathaysia Block to Indosinian orogenic event: Science in

China Series D: Earth Sciences, v. 51, p. 788–800, http://dx.doi.org/10.1007/s11430-008-0053-0

Xie, L. W., Zhang, Y. B., Zhang, H. H., Sun, J. F., and Wu, F. Y., 2008, *In situ* simultaneous determination of trace elements, U–Pb and Lu–Hf isotopes in zircon and baddeleyite: Chinese Science Bulletin, v. 53, p. 1565–1573, http://dx.doi.org/10.1007/s11434-008-0086-y

Xu, X., O'Reilly, S. Y., Griffin, W. L., Wang, X., Pearson, N. J., and He, Z., 2007, The crust of Cathaysia: Age, assembly and reworking of two terranes: Precambrian Research, v. 158, p. 51–78, http://dx.doi.org/10.1016/j.precamres.2007.04.010

Yang, Z., Sun, Z., Yang, T., and Pei, J., 2004, A long connection (750–380 Ma) between South China and Australia: paleomagnetic constraints: Earth and Planetary Science Letters, v. 220, p. 423–434, http://dx.doi.org/10.1016/S0012-821X(04)00053-6

Yao, J., Shu, L., and Santosh, M., 2011, Detrital zircon U–Pb geochronology, Hf–isotopes and geochemistry – new clues for the Precambrian crustal evolution of Cathaysia Block, South China: Gondwana Research, v. 20, p. 553–567, http://dx.doi.org/10.1016/j.gr.2011.01.005

Yao J., Shu, L., Santosh, M., and Li, J., 2012, Precambrian crustal evolution of the South China Block and its relation to supercontinent history: Constraints from U–Pb ages, Lu–Hf isotopes and REE geochemistry of zircons from sandstones and granodiorite: Precambrian Research, v. 208–211, p. 19–48, http://dx.doi.org/10.1016/j.precamres.2012.03.009

Ye, M. F., Li, X. H., Li, W. X., Liu, Y., and Li, Z. X., 2007, SHRIMP zircon U–Pb geochronological and whole-rock geochemical evidence for an early Neoproterozoic Sibaoan magmatic arc along the southeastern margin of the Yangtze Block: Gondwana Research, v. 12, p. 144–156, http://dx.doi.org/10.1016/j.gr.2006.09.001

Yin, A., Nie, S., Craig, P., Harrison, T. M., Ryerson, F. J., Qian, X., and Yang, G., 1998, Late Cenozoic tectonic evolution of the southern Chinese Tian Shan: Tectonics, v. 17, no. 1, p. 1–27, http://dx.doi.org/10.1029/97TC03140

Yin, A., Dubey, C. S., Kelty, T. K., Webb, A. A. G., Harrison, T. M., Chou, C. Y., and Célérier, J., 2010a, Geologic correlation of the Himalayan orogen and Indian craton: Part 2, Structural geology, U–Pb zircon geochronology, and tectonic

evolution of the south flank of the eastern Himalayan orogen: Geological Society of America Bulletin, v. 12, p. 360–395, http://dx.doi.org/10.1130/B26461.1

Yin, A., Dubey, C. S., Webb, A. A. G., Kelty, T. K., Grove, M., Gehrels, G. E., and Burgess, W. P., 2010b, Geologic correlation of the Himalayan orogen and Indian craton: Part 1, Structural geology, U–Pb zircon geochronology, and tectonic evolution of the Shillong Plateau and its neighboring regions in NE India: Geological Society of America Bulletin, v. 122, p. 336–359, http://dx.doi.org/10.1130/B26460.1

Yu, J. H., O'Reilly, S. Y., Wang, L., Griffin, W. L., Zhang, M., Wang, R., Jiang, S., and Shu, L., 2008, Where was South China in the Rodinia supercontinent? Evidence from U–Pb geochronology and Hf isotopes of detrital zircons: Precambrian Research, v. 164, p. 1–15, http://dx.doi.org/10.1016/j.precamres.2008.03.002

Yu, J. H., Wang, L., O'Reilly, S. Y., Griffin, W. L., Zhang, M., Li, C., and Shu, L., 2009, A Paleoproterozoic orogeny recorded in a long-lived cratonic remnant (Wuyishan terrane), eastern Cathaysia Block, China: Precambrian Research, v. 174, p. 347–363, http://dx.doi.org/10.1016/j.precamres.2009.08.009

Yu, J. H., O'Reilly, S. Y., Wang, L., Griffin, W. L., Zhou, M. F., Zhang, M., and Shu, L., 2010, Components and episodic growth of Precambrian crust in the Cathaysia Block, South China: evidence from U–Pb ages and Hf isotopes of zircons in Newproterozoic sediments: Precambrian Research, v. 181, p. 97–114, http://dx.doi.org/10.1016/j.precamres.2010.05.016

Yu, J. H., O'Reilly, S. Y., Zhou, M. F., Griffin, W. L., and Wang, L., 2011, U–Pb geochronology and Hf–Nd isotopic geochemistry of the Badu Complex, Southeastern China: implications for the Precambrian crustal evolution and paleogeography of the Cathaysia Block: Precambrian Research, v. 222–223, p. 424–449, http://dx.doi.org/10.1016/j.precamres.2011.07.014

Zeng, W., Zhang, L., Zhou, H. W., Zhong, Z. Q., Xiang, H., Liu, R., Jin, S., Lu, X. Q., and Li C. Z., 2008, Caledonian reworking of Paleoproterozoic basement in the Cathaysia Block: constraints from zircon U–Pb dating, Hf isotopes and trace elements: Chinese Science Bulletin, v. 53, p. 895–904, http://dx.doi.org/10.1007/s11434-008-0076-0

Zhang, L., and He, Q., 1993, On the revision of Bacun Group and the establishment

of Xiazhai, Oujiadong and Laoshuzhai Formations in northern Guangdong Province: Guangdong Geology, v. 8, p. 1–14 (in Chinese with English abstract).

Zhang, Q. R., and Piper, J. D. A., 1997, Palaeomagnetic study of Neoproterozoic glacial rocks of the Yangtze Block: palaeolatitude and configuration of South China in the late Proterozoic Supercontinent: Precambrian Research, v. 85, p. 173–199, http://dx.doi.org/10.1016/S0301-9268(97)00031-4

Zhang, S., 2004, South China's Gondwana connection in the Paleozoic: Paleomagnetic evidence: Progress in Natural Science, v. 14, p. 85–90.

Zhang, S. B., Zheng, Y. F., Wu, Y. B., Zhao, Z. F., Gao, S., and Wu, F. Y., 2006, Zircon U–Pb age and Hf–O isotope evidence for Paleoproterozoic metamorphic event in South China: Precambrian Research, v. 151, p. 265–288, http://dx.doi.org/10.1016/j.precamres.2006.08.009

Zhang, J. Y., Yin, A., Liu, W. C., Wu, F. Y., Lin, D., Grove, M., 2012, Coupled U–Pb dating and Hf isotopic analysis of detrital zircon of modern river sand from the Yalu River (Yalung Tsangpo) drainage system in southern Tibet: Constraints on the transport processes and evolution of Himalayan river: Geological Society of America Bulletin, v. 124, p. 1449–1473, http://dx.doi.org/10.1130/B30592.1

Zhang S., Evans, D. A. D., Li, H., Wu, H., Jiang, G., Dong, J., Zhao, Q., Raub, T., Yang, T., 2013, Paleomagnetism of the late Cryogenian Nantuo Formation and paleogeographic implications for the South China Block: Journal of Asian Earth Sciences, v. 72, p. 164–177, http://dx.doi.org/10.1016/j.jseaes.2012.11.022

Zhao, X. F., Zhou, M. F., Li, J. W., Sun, M., Gao, J. F., Sun, W. H., and Yang, J. H., 2010, Late Paleoproterozoic to early Mesoproterozoic Dongchuan Group in Yunnan, SW China: Implications for tectonic evolution of the Yangtze Block: Precambrian Research, v. 182, p. 57–69, http://dx.doi.org/10.1016/j.precamres.2010.06.021

Zheng, J. P., Griffin, W. L., Li, L. S., O'Reilly, S. Y., Pearson, N. J., Tang, H. Y., Liu, G. L., Zhao, J. H., Yu, C. M., and Su, Y. P., 2011, Highly evolved Archean basement beneath the western Cathaysia Block, South China: Geochimica et Cosmochimica Acta, v. 75, p. 242–255, http://dx.doi.org/10.1016/j.gca.2010.09.035

Zheng, J., Griffin, W. L., O'Reilly, S. Y., Zhang, M., Pearson, N., and Pan, Y., 2006, Widespread Archean basement beneath the Yangtze craton: Geology, v. 34, p. 417–420, http://dx.doi.org/10.1130/G22282.1

Zhou, M. F., Yan, D. P., Kennedy, A. K., Li, Y., and Ding, J., 2002, SHRIMP U–Pb zircon geochronological and geochemical evidence for Neoproterozoic arc-magmatism along the western margin of the Yangtze Block, South China: Earth and Planetary Science Letters, v. 196, p. 51–67, http://dx.doi.org/10.1016/S0012-821X(01)00595-7

Zhou, M. F., Ma, Y., Yan, D. P., Xia, X., Zhao, J. H., and Sun, M., 2006, The Yanbian Terrane (Southern Sichuan Province, SW China): A Neoproterozoic arc assemblage in the western margin of the Yangtze Block: Precambrian Research, v. 144, p. 19–38, http://dx.doi.org/10.1016/j.precamres.2005.11.002

Zhu, M., Strauss, H., and Shields, G. A., 2007, From snowball earth to the Cambrian bioradiation: Calibration of Ediacaran–Cambrian earth history in South China: Palaeogeography, Palaeoclimatology, Palaeoecology, v. 254, p. 1–6, http://dx.doi.org/10.1016/j.palaeo.2007.03.026

Zhu, D. C., Zhao, Z. D., Niu, Y., Dilek, Y., and Mo, X. X., 2011, Lhasa terrane in southern Tibet came from Australia: Geology, v. 39, p. 727–730, http://dx.doi.org/10.1130/G31895.1

Zhu, D. C., Zhao, Z. D., Niu, Y., Dilek, Y., Wang, Q., Ji, W. H., Dong, G.C ., Sui, Q. L., Liu, Y. S., Yuan, H. L., and Mo, X. X., 2012, Cambrian bimodal volcanism in the Lhasa Terrane, southern Tibet: Record of an early Paleozoic Andean-type magmatic arc in the Australian proto-Tethyan margin: Chemical Geology, v. 328, p. 290–308, http://dx.doi.org/10.1016/j.chemgeo.2011.12.024

CHAPTER 4 STRATIGRAPHIC HISTORY OF THE LOWER PALAEOZOIC NANHUA FORELAND BASIN IN SOUTH CHINA: RESPONSE TO TWO SUCCESSIVE OROGENIES

Wei-Hua Yao*, Zheng-Xiang Li

ARC Centre of Excellence for Core to Crust Fluid Systems (CCFS) and The Institute for Geoscience Research (TIGeR), Department of Applied Geology, Curtin University, Perth, WA 6845, Australia

* Corresponding author: weihua.yao@curtin.edu.au

Abstract

We present here the stratigraphic history of the lower Palaeozoic Nanhua Basin in the South China Block (SCB) and explore the relationship between clastic sedimentation of the basin and advance of the adjacent orogens. The sedimentary facies comprise marine turbiditic, shallow marine and fluvial-dominated deltaic facies in an ascending order in the basin, and feature a lateral migration from southeast to northwest. We interpret that the Nanhua Basin was a peripheral foreland basin which started to receive foreland deposits as early as the Ediacaran. The evolution of the foreland basin can be divided into two stages: (1) The Cambrian (and possibly Ediacaran) to earliest-Ordovician underfilled to filled stage with marine clastic deposits, fed by an exotic orogen outboard the SCB; and (2) the early-Ordovician to Silurian overfilled stage with dominant deltaic clastic deposits, fed by the northwestward advancing Wuyi–Yunkai orogen. The first stage was likely related to collision between the SCB and northern India during the assembly of Gondwanaland, whereas the second stage was related to the intraplate Wuyi–Yunkai orogeny caused by far-field stress of the aforementioned collision.

Key Words: South China, the Nanhua foreland basin, the Wuyi–Yunkai Orogen, stratigraphy, sedimentary facies

4.1 Introduction

The South China Block (SCB), including the Yangtze Block in the northwest and the Cathaysia Block in the southeast (Figure 4.1A inset), is one of the major continental blocks in East Asia and experienced important tectonic events that shaped the current Asian configuration. The early Palaeozoic Wuyi–Yunkai orogeny was a regional-scale event responsible for deformation and metamorphism over much of the Cathaysia Block [e.g., *Ren,* 1964, 1991; *Huang et al.,* 1980; *Yang et al.,* 1986; *Charvet et al.,* 1996, 2010; *Wang Y.J. et al.,* 2007; *Faure et al.,* 2009; *Li Z.X. et al.,* 2010], and the inversion of the lower Palaeozoic Nanhua Basin (Figure 4.1A). However, the nature and stratigraphic evolution of the Nanhua Basin have not been systematically documented yet. This basin history is relevant to a more widely debated issue of when and how the Cathaysia and Yangtze blocks joined together to form the SCB.

There are two main opposing opinions regarding the formation of the SCB. One considers that the amalgamation of the Cathaysia and Yangtze blocks occurred in the Phanerozoic [e.g., *Hsü et al.,* 1988, 1990; *Shui,* 1988; *Liu and Xu,* 1994], and the "Huanan Ocean" existed between the two blocks from the late Neoproterozoic to early Palaeozoic [*Shui,* 1988; *Liu and Xu,* 1994] or even to the middle Mesozoic [*Hsü et al.,* 1988, 1990]. *Shui* [1988] suggested that the Yangtze and Cathaysia blocks first amalgamated at their eastern ends during the early- to middle-Neoproterozoic, with a remnant ocean to the west until the Cambrian. Further amalgamation eventually closed the ocean during the late-Ordovician to Silurian, resulting in intense regional deformation and metamorphism, an event generally referred to as the "Caledonian Orogeny" [e.g., *Huang et al.,* 1980; *Yang et al.,* 1986; *Ren,* 1991]. The boundary between the Yangtze and Cathaysia blocks was therefore considered by those researchers as a lower Palaeozoic suture [*Liu and Xu,* 1994, *Chen et al.,* 2006], although there appears to be little geological or geophysical evidence for such an ocean closure [*Li Z.X.,* 1998]. The model of *Hsü et al.*'s [1988, 1990, 1994], on the other hand, requires the ocean to have been closed by an Alpine-style collision during the Jurassic. Again, there is a lack of evidence for such a young suture, and the so-called "Mesozoic Banxi mélange" was later shown to consist of Neoproterozoic rocks with different tectonic affinities [e.g., *Zhou,* 1989; *Li*

X.H. et al., 1994; *Li Z.X. et al.,* 2003]. The alternative opinion considers that the Yangtze–Cathaysia amalgamation occurred in the Precambrian, at either 1100–900 Ma [*Li Z.X. et al.,* 2002, 2008; *Li X.H. et al.,* 2009] or 820–750 Ma [*Zhou M.F. et al.,* 2002a, 2002b; *Wang X.L. et al.,* 2004]. However, Neoproterozoic intracontinental rifting in the SCB has long been recognized [e.g., *Wang,* 1985; *Dong and Liu,* 1991; *Li J.L.,* 1991], and the Neoproterozoic Nanhua Basin was further shown to be a failed rift basin during *ca.* 850–700 Ma [*Li Z.X.,* 1998; *Wang and Li,* 2003; *Li W.X. et al.,* 2010].

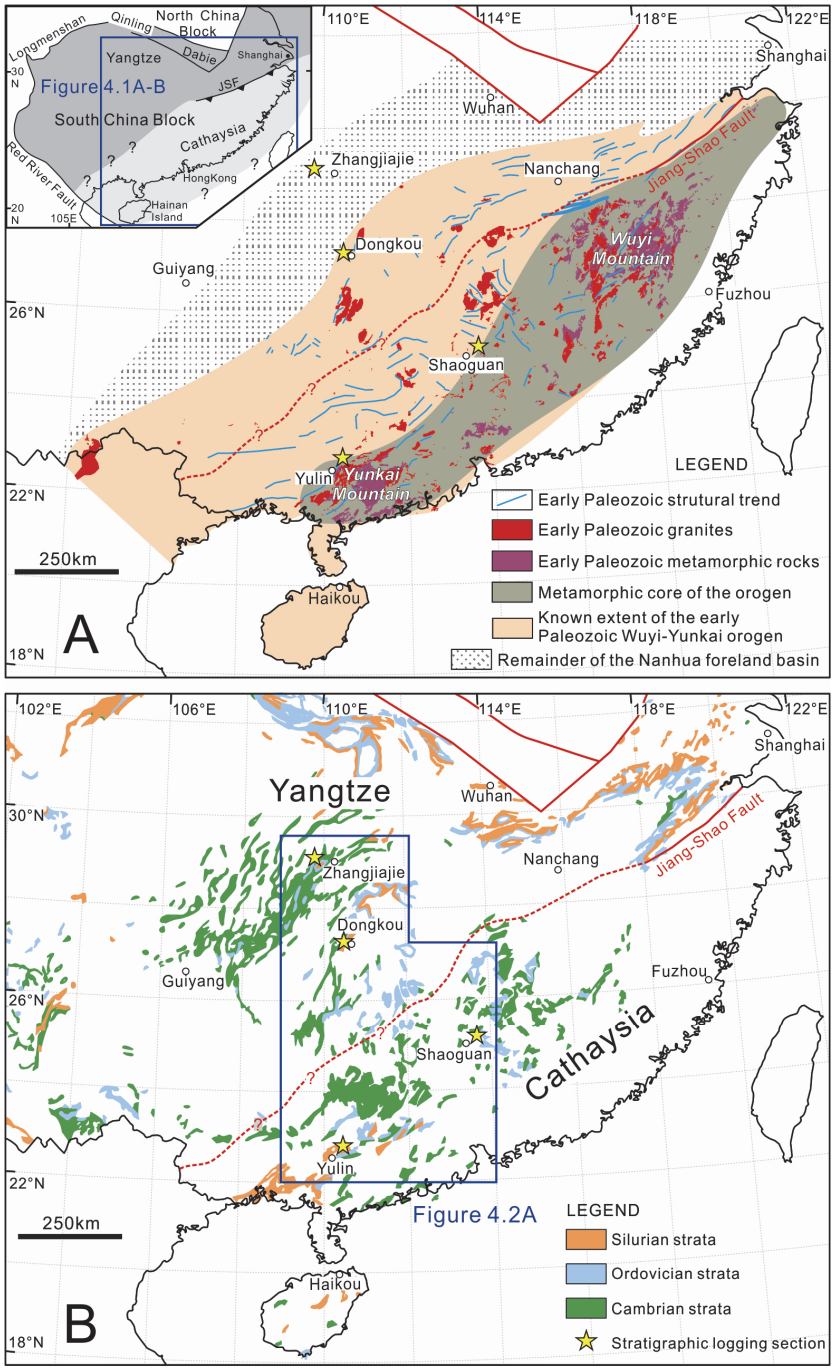

Figure 4.1. (A) A simplified regional map of the South China Block (SCB), highlighting the regional extent of the lower Palaeozoic Wuyi–Yunkai orogen including the distribution of metamorphic rocks and granites, interpreted early Palaeozoic structural trends and extent of the remnant Nanhua Basin. The inset shows the Cathaysia and Yangtze blocks as parts of the SCB. (B) Distribution of Palaeozoic sedimentary outcrops in the SCB, highlighting the Cambrian, Ordovician and Silurian rocks. Localities of the four logged stratigraphic sections are marked by yellow stars.

The failed Neoproterozoic Nanhua rift basin was succeeded by a lower Palaeozoic basin of apparently the same age as the Wuyi–Yunkai orogeny (i.e., mid-Ordovician to Silurian) [*Li Z.X. et al.,* 2010], although orogenesis-related clastic deposition could have started as early as the Ediacaran [*Yao et al.,* 2014]. As no systematic basin research has been conducted on the lower Palaeozoic strata, the precise nature and evolution of this long-lived basin is still under debate. It has been variously interpreted to be a back-arc/marginal basin [*Pan,* 1984; *Guo et al.,* 1989], a retro-arc foreland basin [*Jiang et al.,* 2014], or an intraplate foreland basin [*Li Z.X.,* 1998; *Wang Y.J. et al.,* 2010; *Li Z.X. et al.,* 2010; *Yao et al.,* 2014], but neither an arc terrane nor arc-related magmatism has been identified from the early Palaeozoic SCB.

In this paper we explore the stratigraphic history of the lower Palaeozoic Nanhua Basin, and discuss its time and space relationship with the Wuyi–Yunkai orogen. By documenting the stratigraphic record from four sections across the basin, we attempt to address the following scientific questions: (1) what type of sedimentary basin it was, (2) when it began to receive sediments from the Wuyi–Yunkai orogen, and (3) whether there was a relationship between basin infilling and orogenic uplift.

4.2 Geological Setting

The boundary between the Yangtze and Cathaysia blocks, which constitute the SCB [e.g., *Li Z.X. et al.,* 2002, 2008; *Li X.H. et al.,* 2009; *Zhou M.F. et al.,* 2002a, 2002b; *Wang X.L. et al.,* 2004], approximately follows the Jiangshan–Shaoxing Fault in the east, but its western extension is unclear due to younger tectonic modifications (Figure 4.1A-B). The first Phanerozoic tectonic event in the region was the early Palaeozoic Wuyi–Yunkai orogeny, recorded as an angular unconformity between upper Palaeozoic terrestrial deposits (Devonian and younger) and lower Palaeozoic meta-sedimentary/sedimentary rocks (Silurian and older) in the southeast part of the

SCB [*Huang et al.,* 1980; *BGMRJX,* 1984; *BGMRGX,* 1985; *BGMRGD,* 1988; *BGMRHN,* 1988; *Ren,* 1991; *Li Z.X. et al.,* 2010; *Wang Y.J. et al.,* 2007, 2011]. This angular unconformity, together with the widespread Silurian granitic intrusions, defines the regional extent of the Wuyi–Yunkai orogen (Figure 4.1A) [e.g., *Li Z.X. et al.,* 2010; Yao *et al.* 2012]. This tectonic event was traditionally referred as the Caledonian orogeny in the Chinese literature [e.g., *Huang et al.,* 1980; *Yang et al.,* 1986; *Ren,* 1991], but was re-named the Wuyi–Yunkai orogeny after the outcropped metamorphic orogenic core along the Wuyi and Yunkai mountains (Figure 4.1A), and is now known to have lasted from >460 Ma to 420–415 Ma [*Li Z.X. et al.,* 2010].

The lower Palaeozoic Nanhua Basin once covered a large area of the Cathaysia Block and part of the southeastern Yangtze Block (Figure 4.1A). With the advancing of the Wuyi–Yunkai orogen towards the Yangtze Block, a part of the basin on the Cathaysia side was assimilated into the fold-and-thrust belt of the orogen, leaving only a remnant basin in the northwest (Figure 4.1A) [*Li Z.X.,* 1998; *Li Z.X. et al,* 2010; *Chen et al.,* 2012]. Both the orogenic core and the fold-and-thrust belt have wide distribution of syn- to post-kinematic granites (Figure 4.1A) [*Li Z.X. et al.,* 2010; *Yao et al.,* 2012]. Cambrian strata are widespread in South China, including the orogenic core and the fold-and-thrust belt of the Wuyi–Yunkai orogen, whereas outcropping of Ordovician–Silurian sedimentary rocks is much more restricted (Figure 4.1B).

4.3 Methodology

Figure 4.2A shows locations of the four sections in the Nanhua Basin, which were documented for variations in stratigraphy, lithology and sedimentary structures [*BGMRGX,* 1985; *BGMRGD,* 1988; *BGMRHN,* 1988]. The four sections are: (1) the Yulin section in the southern part of the early basin, preserving lower- to mid-Cambrian rocks [*RGMRGX-b,* 1968] and a upper-Cambrian to Silurian succession (Figures 4.2B-D); (2) the Shaoguan section in the southeastern part of the early basin, preserving a Cambro-Ordovician sedimentary succession (Figure 4.2E); (3) the Dongkou section in the central part of the basin, preserving a Cambro-Silurian succession (Figure 4.2F), and (4) the Zhangjiajie section in the northwestern part of the basin, preserving a Cambro-Silurian succession (Figure

4.2G). The detailed Cambro-Silurian stratigraphy of the four sections is present in Figure 4.3, along with their geological contacts with underlying Ediacaran and overlying Devonian strata, respectively.

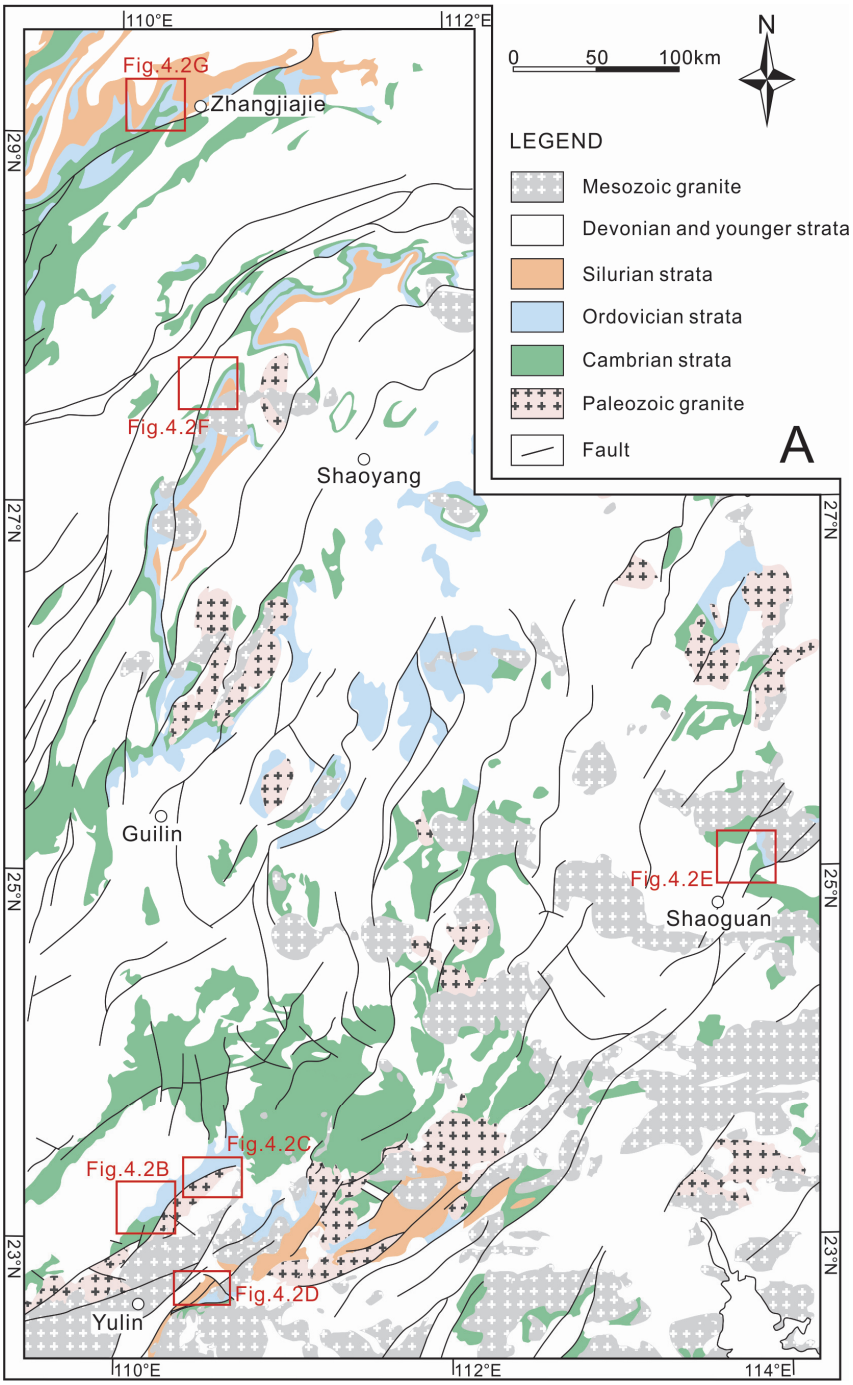

Figure 4.2. (A) Regional geological map of central South China highlighting the early Palaeozoic sedimentary outcrops and granitic intrusions. (B) Geological map of the Rongxian county, showing a part of the Yulin Section; (C) Geological map of the Cenxi county, showing a part of the Yulin Section; (D) Geological map of the Beiliu county, showing a part of the Yulin Section; (E) Geological map of the Shaoguan Section; (F) Geological map of the Dongkou Section; (G) Geological map of the Zhangjiajie Section (revised after *RGMRGD,* 1962; *RGMRGX-a,* 1966; *RGMRGX-b,* 1968; *RGMRHN-a,* 1965; *RGMRHN-b,* 1968).

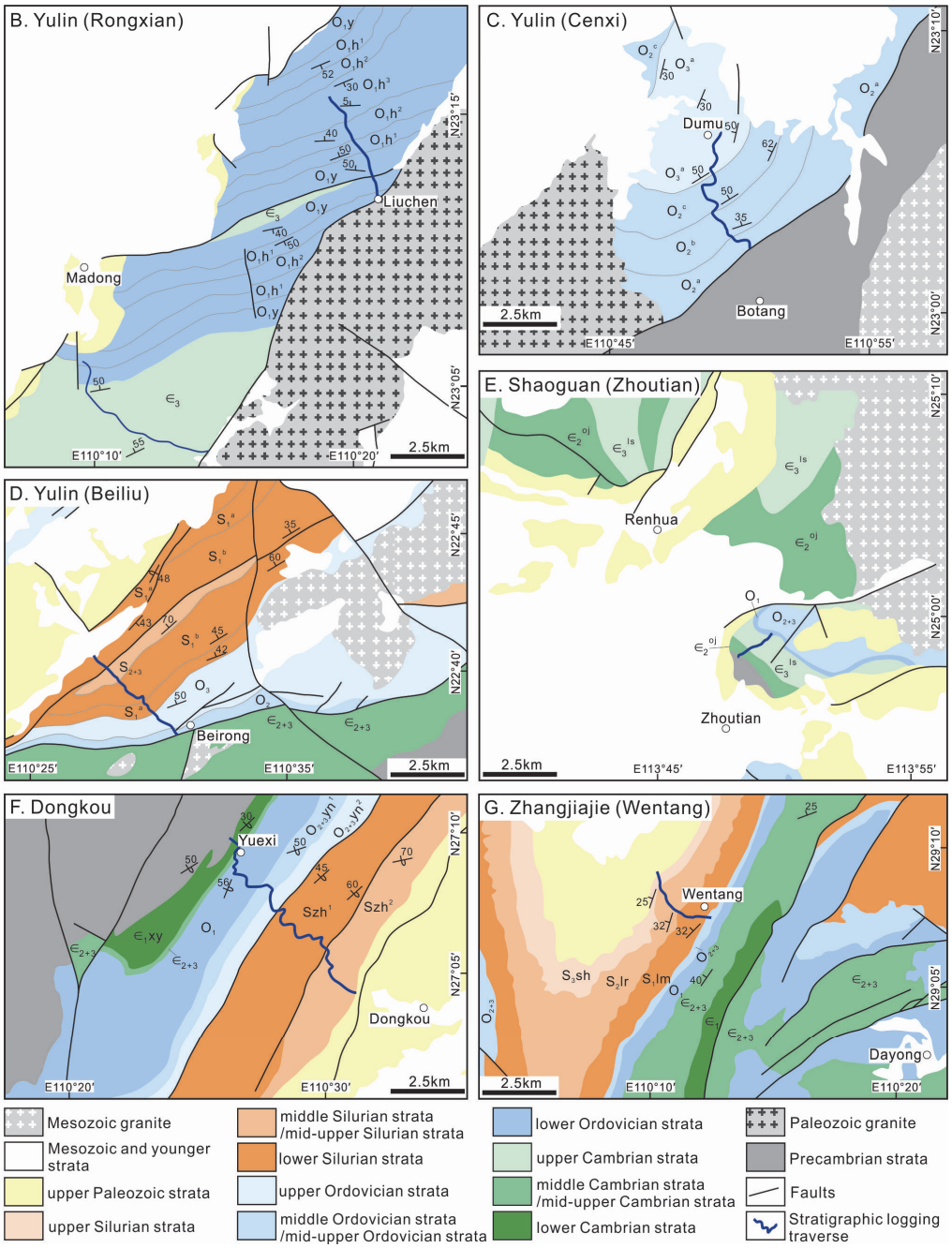

Figure 4.2. (continued)

Strata were measured in the field using a 20-m-long tape measure and a compass. Grain size and colour of the clastic strata were documented following the Udden-Wentworth grain-size scale [*Udden,* 1914; *Wentworth,* 1922]. Sedimentary structures and fossils from the strata were recorded where present. Stratification is not always well exposed due to weathering and vegetation cover, which can obliterate some of the stratifications and conceal the originial sedimentology and stratigraphy (Figures 4.4–4.7). A ~9000 m upper-Cambrian to Silurian siliciclastic sedimentary succession were measured in the Yulin section (Figures 4.2B-D and 4.4),

and the lower- to mid-Cambrian metamorphosed strata were correlated from a published nearby section [*RGMRGX-b,* 1968]. *Ca.* 2500 m of siliciclastic sedimentary rocks were measured for the mid- to upper-Cambrian strata in the Shaoguan section (Figures 4.2E and 4.5). Because of the missing lower-Cambrian strata and dense vegetation cover on Ordovician strata in the measured section, a published lower-Cambrian section located ~50 km to the east [*Zhang and He,* 1993], and previously published Ordovician strata in the measured section [*RGMRGD,* 1962], were used to establish the Shaoguan Section. The Dongkou section comprises *ca.* 4000 m of siliciclastic Cambro-Silurian strata, which were measured along a country road (Figures 4.2F and 4.6). A total of 2400 m of siliciclastic Silurian strata were measured at the Zhangjiajie section (Figures 4.2G and 4.7), and Cambro-Ordovician carbonate strata for that section were adopted from published work [*RGMRHN-b,* 1968].

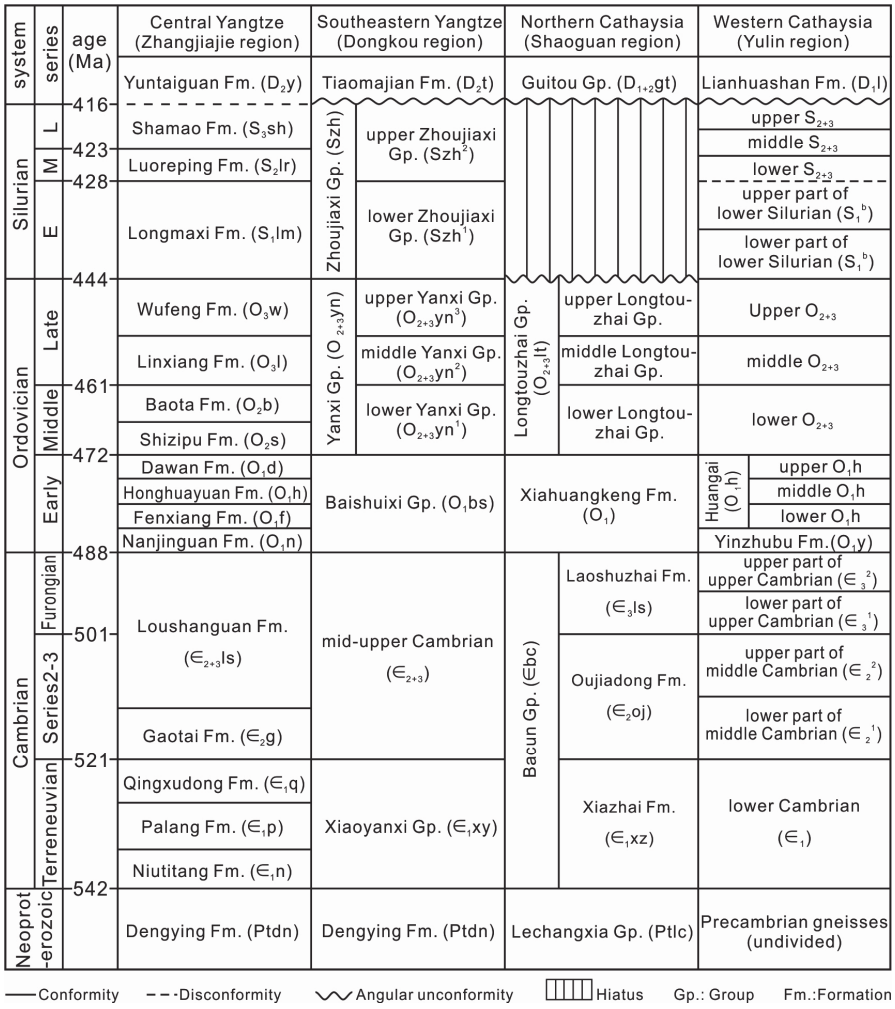

Figure 4.3. Synthesized early Palaeozoic stratigraphic chart of the Yulin, Shaoguan, Dongkou and Zhangjiajie sections in the South China Block (revised after *RGMRGD,* 1962; *RGMRGX-a,* 1966; *RGMRHN-a,* 1965, *RGMRHN-b,* 1968).

Preliminary interpretations of sedimentary facies were given for each individual section based on lithological packges, sedimentary structures and fossils. A time and space diagram showing Cambrian–Silurian rocks across the Nanhua Basin was then established according to the rock ages and facies similarities among these four sections. Utilizing the sedimentary facies and regional tectono-magmatic records, we reconstruct a spatial–temporal tectonosedimentary evolution model for the lower Palaeozoic Nanhua Basin.

4.4 Stratigraphy and Sedimentology

4.4.1 The Yulin section

The Yulin section comprises metamorphosed lower- to mid-Cambrian strata and non-metamorphosed upper-Cambrian to Silurian strata which are cut by a series of NE-trending faults and intruded by granites (Figure 4.2B–D) [*BGMRGX,* 1985; *RGMRGX-a,* 1966; *RGMRGX-b,* 1968]. The Cambro-Silurian strata are grouped into four lithological packages.

Package 1: lower- to mid-Cambrian. This package was metamorphosed during the Wuyi–Yunkai orogeny, represented by mica schist, mica quartzite, gneiss and migmatite that overlay on Ediacaran schists (Figures 4.3 and 4.4). The protolith of the metamorphic rocks is of siliciclastic nature, but the original sedimentary structures and grain characteristics were destroyed by metamorphism [*RGMRGX-b,* 1968; *BGMRGX,* 1985]. Whereas it was not possible to work out likely sedimentary settings for the protolith, a marine shelf environment is inferred based on lateral correlation with the Shaoguan section (see section 4.4.2).

Package 2: upper-Cambrian to lowest-Ordovician. This package is generally upwards-coarsening, comprising inter-bedded, horizontally laminated mudstone and sandstone (Figure 4.4). Thin beds of medium-grained sandstone are found in the upper part of this package, with occasional coarse-grained quartz sandstone (Figure 4.4 photo A). A 1.5 m pebbly conglomeratic unit is present in the top part of the package. Cambrian-aged fossils of brachiopod, sponge spicule and trilobite and Ordovician-aged graptolite were reported in the upper-Cambrian and

lowest-Ordovician strata, respectively [*RGMRGX-a,* 1966]. The upwards-coarsening package indicates an increasing supply of clastics from the source region, which could also imply the approaching of source at that time. The topmost conglomerate units in the lowest-Ordovician strata may indicate the uplift of the Wuyi–Yunkai orogen in the earliest-Ordovician. Marine fossils and light-coloured, oxidized mudstone and sandstone suggest a possible shallow water setting. Overall, the upper-Cambrian to lowest-Ordovician package is preliminarily interpreted as shallow marine nearshore deposits.

Package 3: lower- to upper-Ordovician. This package exhibits another upwards-coarsening cycle (Figure 4.4). It comprises rhythmical interlayers of thick, rippled sandstone and thin mudstone in the lower part (Figure 4.4 photo B), sandstone with planar and trough cross-beds in the middle, and dominantly horizontal beds of thick sandstone with a few mudstone layers in the upper part (Figure 4.4). Ordovician graptolites (e.g., *Didymograpeus* cf.) were reported from the lower part of the package [*RGMRGX-a,* 1966]. This package recorded an upwards transition from marine to subaerial sedimentation, possibly representing a delta prograding into a shallow marine setting. Rippled sandstones likely represented a coastal marine setting, whereas rhythmic beds of sandstone and mudstone were more likely deposited in the prodelta area. The mid-package, comprising massive sandstone cross beds, probably represents a delta-front fed by distributary channels. The upper-package, featuring horizontally-laminated fine-grained sandstone beds, was probably flooding deposits in the delta plain.

Package 4: lower part of lower-Silurian. This package mainly comprises medium- to coarse-grained sandstones and paraconglomerates, with a very thin layer of mudstone in between (Figure 4.4). Paraconglomerates are matrix-supported, poorly sorted, and well-rounded (Figure 4.4 photo C). The pebbles are of micaceous and quartzofeldspathic composition, and commonly imbricated, with the clast orientation indicating a palaeo-flow toward the northwest. The poor-sorted, well-rounded pebbles in the paraconglomerates possibly indicate a rapid mass flow into the delta. Packages 3 and 4 were both deposited in a fluvial-dominated delta setting, with a general trend of upwards-shallowing in water depth and gradually filling in clastics.

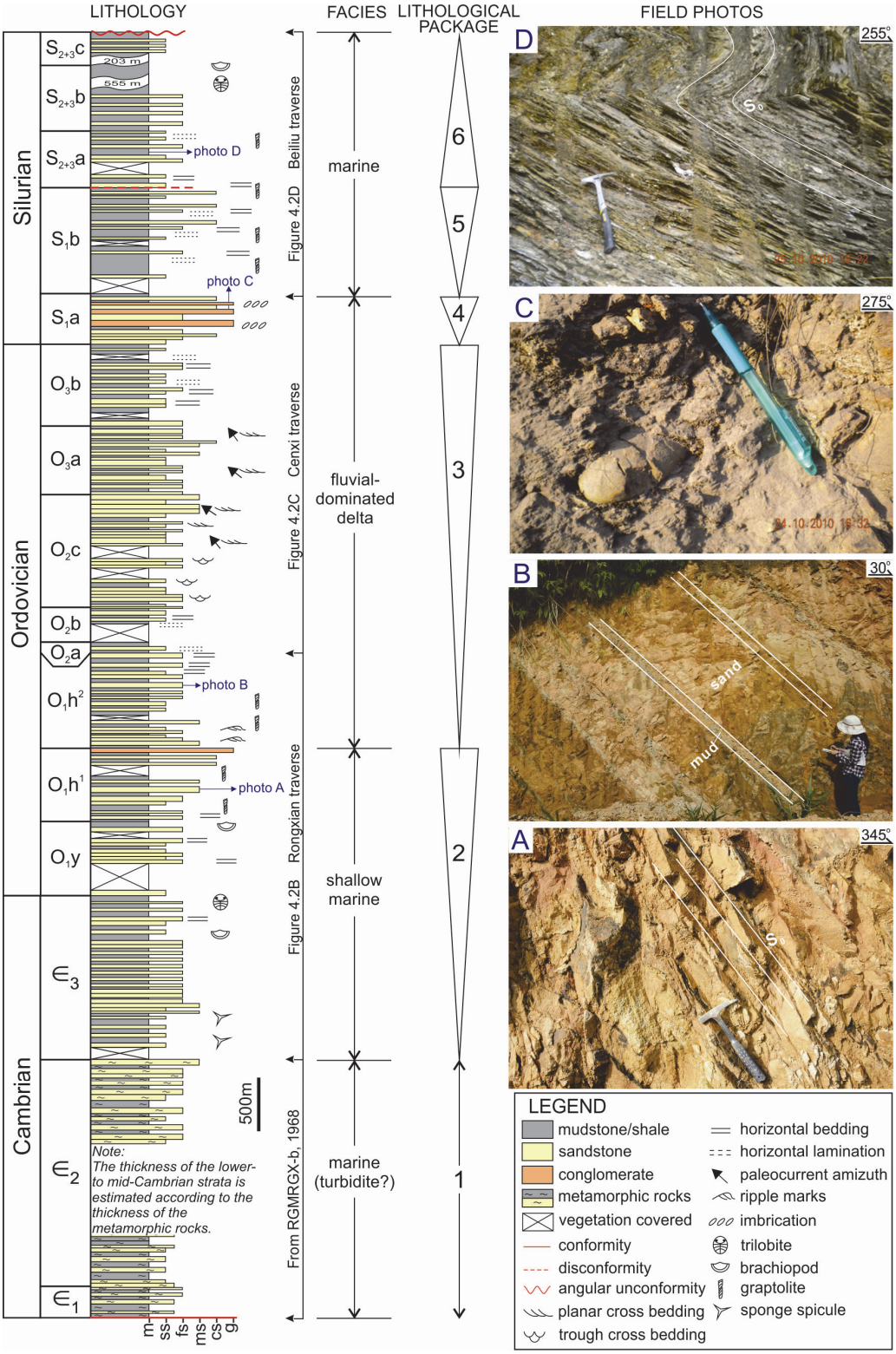

Figure 4.4. Cambro-Silurian lithostratigraphic column of the Yulin Section. Lithologic scale: m = mudstone/shale, ss = siltstone, fs = fine-grained sandstone, ms = medium-grained sandstone, cs = coarse-grained sandstone, g = gravel/conglomerate. Field photos: (A) medium-grained sandstone beds in lower Ordovician strata, with a hammer (30 cm long) for scale; (B) rhythmical intercalations of thick-bedded fine sandstone and thin-bedded shale in the lower Ordovician strata; (C) muddy conglomerates with oriented pebbles in the lowest Silurian strata with a pen (15 cm long) for scale; (D) folded, thin-layered shales in the mid- to upper-Silurian strata, with a hammer (30 cm long) for scale.

Package 5: upper part of lower-Silurian. This is an upwards-coarsening package, dominated by thick mudstone beds (900 m mudstone out of a total of 1000 m package). Dark-grey mudstones are found in the package with sporadic horizontal sand beds, which coarsen upwards from fine- to coarse-grained (Figure 4.4). Graptolite fossils in the mudstone give a Silurian age [*RGMRGX-a,* 1966; *BGMRGX,* 1985].

Package 6: mid- to upper-Silurian. This package disconformably overlies the lower-Silurian strata (Figure 4.4). It is an upwards-fining package, comprising dominant mudstone with minor sandstone. Thin layers of mudstone and siltstone are tightly folded in some outcrops (Figure 4.4 photo D). In the Yulin region, Silurian strata are overlain by lower-Devonian quartz-rich sandstones with an angular unconformity (Figure 4.3). Packages 5 and 6 are considered as marine deposits based on the presence of dominant dark-grey graptolitic mudstones and sporadic fine sandstones. Dominant mudstone beds through package 5 indicate a low-energetic setting. The angular unconformity above the Silurian strata was possibly related to a regional uplift during the Wuyi–Yunkai orogeny [*BGMRGX,* 1985].

4.4.2 The Shaoguan section

The Shaoguan section, near the town of Zhoutian on the northwestern margin of the Wuyi–Yunkai orogenic core (Figure 4.1A-B), comprises mid-Cambrian to Ordovician strata that are unconformably overlain by Devonian quartz-rich sandstones (Figures 4.2E and 4.3). The lower-Cambrian strata only crop out in a parallel section ~50 km to the east [*Zhang and He,* 1993]. The Cambro-Ordovician strata in the Shaoguan section are divided into three lithological packages.

Package 1: lower-Cambrian to lower part of mid-Cambrian. This package comprises rhythmical interlayers of thick, horizontally-laminated sandstone and thin, dark-grey mudstone. Sandstone beds are of felspathic quartz sandstone and siltstone, and mudstone beds are carbonaceous shales containing nodular pyrite [*Zhang and He,* 1993]. Such interlayers of sandstone, siltstone and mudstone have been interpreted as turbiditic deposits in a hemipelagic to shallow marine setting [*Zhang and He,* 1993]. The lower part of mid-Cambrian strata, with horizontally-laminated sandstone, is

possibly indicative of T_b division in the Bouma Sequence [*Bouma,* 1962].

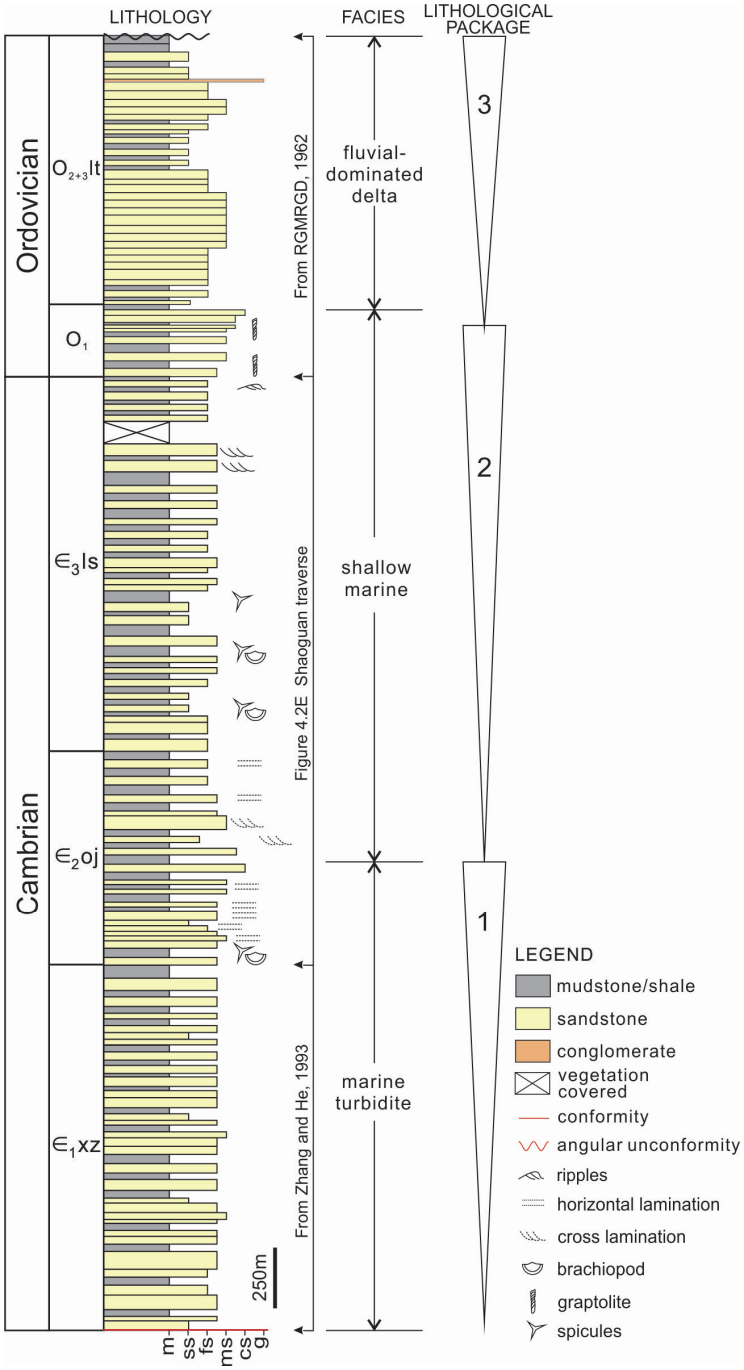

Figure 4.5. Cambro-Ordovician lithostratigraphic column of the Shaoguan Section. Lithologic scale and information are the same as in Figure 4.4.

Package 2: upper part of mid-Cambrian to lower-Ordovician. The package is an upwards-coarsening assemblage of fine- to medium-grained quartz feldspathic sandstone intercalated with calcareous mudstone. Sandy units are commonly horizontally laminated or low-angle cross-laminated [*Yao et al.,* 2014], with ripple-marked sandstone layers found in the upper-Cambrian (Figure 4.5). The upper

part of the package features thicker and coarser sandstone than the lower part. Cambrian-aged brachiopod and sponge spicules are found in the Cambrian strata [*Zhang and He,* 1993], whereas lower-Ordovician strata are graptolitic [*RGMRGD,* 1962]. The low-angle cross-laminated sandstone along with grey-purple mudstone imply deposition in an oxidised, low energy environment. Marine fossils throughout the package imply normal marine salinities. Hence, package 2 is interpreted to have been deposited in a shallow marine setting.

Package 3: mid- to upper-Ordovician. This package, named the Longtouzhai Group (Figure 4.3), comprises intercalations of thick-bedded, fine- to medium-grained feldspathic sandstones and thin-bedded mudstones [*RGMRGD,* 1962, *BGMRGD,* 1988]. A thin conglomeratic layer crops out at the top part of the package, followed by upward-increasing mud-rich layers (Figure 4.5). No sedimentary structures or fossils were found in this package due to poor outcropping. Silurian sedimentary strata are missing in the Shaoguan section and adjacent regions. The entire package was regarded as deltaic deposits with sufficient supply of terrestrial detritus [*BGMRGD,* 1988], as shown by the dominant thick sandstone beds likely deposited in a delta front with fluvial distributary channels.

4.4.3 The Dongkou section

The Dongkou section is located near the town of Yuexi in Dongkou county (Figure 4.2F). The section comprises Cambro-Silurian strata, with two NE-trending faults cutting off Silurian strata [*RGMRHN-a,* 1965; *BGMRHN,* 1988]. All beds are overturned and dip toward southeast, possibly reflecting Mesozoic deformation. Three lithological packages are identified in this section.

Package 1: Cambrian. The package mainly consists of siliceous and carbonaceous shale (Figure 4.6). The lower-Cambrian strata comprises dark-grey siliceous and carbonaceous shales (Figure 4.6 photo A) that contain sponge spicules (*Protospongia* sp.) [*RGMRHN-a,* 1965]. The mid- to upper-Cambrian strata comprises dark-grey limestones intercalated with green shales [*RGMRHN-a,* 1965]. Dark-grey siliceous shales in the lower-Cambrian were likely deposited in an anoxic deep-water environment. The upwards transition to carbonates probably recorded shallowing.

Overall, this package was likely deposited on a carbonate ramp.

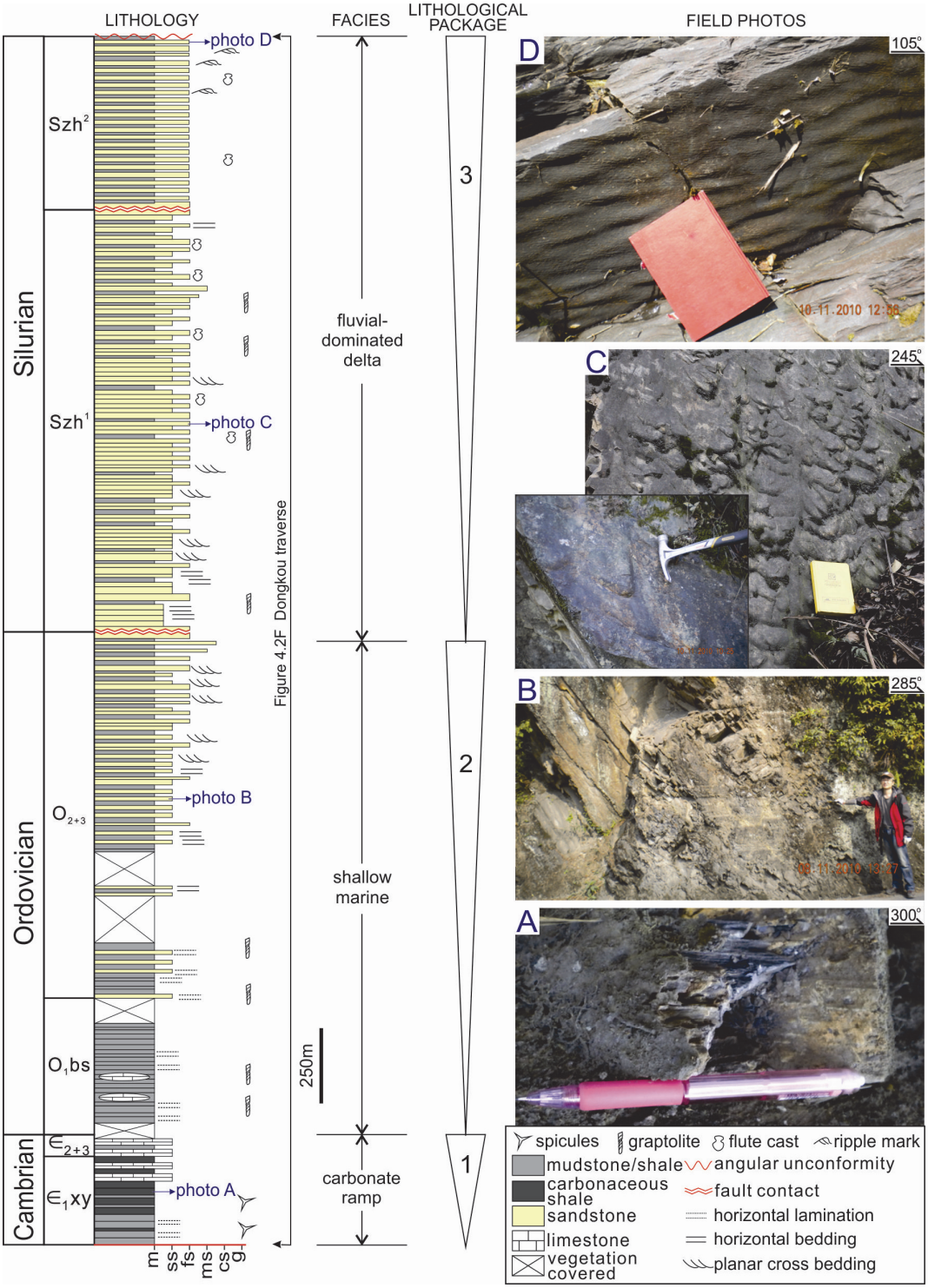

Figure 4.6. Cambro-Silurian lithostratigraphic column of the Dongkou Section. Lithologic scale and information are the same as in Figure 4.4. Field photos: (A) lower Cambrian horizontal-laminated black carbonaceous shale, with a pen (15 cm long) for scale; (B) thick-bedded fine sandstone intercalated with thin-bedded yellowish shale packages in mid-Ordovician strata; (C) a series of flute casts on sandstone surface with a notebook (18 cm in length) for scale, and (c) an enlarged flute cast, with a hammer (30 cm long); (D) Asymmetrical ripple marks on the topmost Silurian sandstones with a notebook (18 cm long) for scale.

Package 2: Ordovician. This package consists of the lower-Ordovician part and mid- to upper-Ordovician part. The lower-Ordovician part comprises grey graptolitic carbonaceous shales intercalated with limestone lenses [*RGMRHN-a,* 1965]. The mid- to upper-Ordovician part comprises grey graptolitic shale and minor horizontal-laminated siltstone in the lower part, and horizontal-bedded fine-grained sandstone with minor graptolitic shale in the upper part (Figure 4.6 photo B). Siliceous shales in the top part of Ordovician are separated from the overlying Silurian strata by a thrust fault (Figure 4.2F) [*RGMRHN-a,* 1965]. The abundant shale in the lower part are indicative of a low energy setting, and the upward transition to cross-bedded sandstones implies an increased detrital supply and water energy in a possible shallow marine setting. The overall package is interpreted as shallow marine deposition.

Package 3: Silurian. The package comprises a lower part of siltstone–mudstone and an upper part of sandstone–siltstone–mudstone, separated by a thrust fault (Figure 4.2F) [*RGMRHN-a,* 1965; *BGMRHN,* 1988]. Flute casts throughout Silurian sandstone surfaces imply northwest-directed palaeoflows (Figure 4.6 photo C). Planar cross beddings are preserved in the lower part of the package, and ripple marks are present in the upper part (Figure 4.6 photo D). Graptolites (*Glyptograptus* sp. and *Pristiograptus* sp.) preserved in the dark-grey mudstone are indicative of Silurian ages [*RGMRHN-a,* 1965]. Silurian strata are overlain by mid-Devonian quartz sandstone on an angular unconformity (Figure 4.3). The Silurian package is interpreted as possible deltaic deposits in a marine-subaerial transitional setting. The lower part of the package was likely deposited in a delta front with dominant arenaceous deposition. The upper part was possibly in a lower energitic delta plain with rhythmical intercalations of fine-grained sandstone and shale.

4.4.4 The Zhangjiajie section

The Zhangjiajie section is located near the Wentang town to the northwest of Zhangjiajie city (Figures 4.1A and 4.2G). It comprises Cambro-Ordovician carbonates and Silurian siliciclastic rocks, and is disconformably overlain by mid-Devonian quartz sandstone [*RGMRHN-b,* 1968; *BGMRHN,* 1988]. The section is divided into three lithological packages.

Package 1: Cambrian to Ordovician. The package consists of the lower part (lower-Cambrian) and the upper part (mid-Cambrian to upper-Ordovician). The lower part comprises dominant black carbonaceous shales with minor carbonates at the top (Figure 4.7). The upper part comprises carbonate, grey grainstone, wackestone, anhydritic dolomite and nodular muddy limestone (Figure 4.7 photo A) [*RGMRHN-b,* 1968]. A carbonate to clastic transition was observed in the top part of the package (Figure 4.7). Abundant trilobites, brachiopod and graptolites are preserved throughout the package [*RGMRHN-b,* 1968]. Black shales in the lower part were possible anoxic deep-water deposits, and shale–carbonate interbeds are considered to be deposits in transitional settings from deep-water to carbonate ramp. The dominant carbonates in the upper part probably recorded a carbonate ramp setting (Figure 4.7).

Package 2: lower part of lower-Silurian. This package comprises abundant green and purple mudstone (Figure 4.7 photo B), intercalated with minor siltstones and sandstones. Silurian-aged graptolites are preserved throughout the package [*RGMRHN-b,* 1968; *BGMRHN,* 1988]. Horizontal-laminated, graptolitic siltstone and mudstone beds are interpreted as marine deposits in a low energitic and saline water setting. The finest grain size and lowest content of sandstones in the Zhangjiajie section compared to the other sections indicate that the detritus probably travelled a long way to a distal part of the basin.

Package 3: upper part of lower-Silurian to upper-Silurian. This package comprises thick-bedded quartz sandstone and minor shale in the lower part, and ripple-marked, bioturbated, and/or cross-bedded sandstone with purple shale in the upper part (Figure 4.7 photo C). It is in disconformable contact with the mid-Devonian quartz sandstone (Figure 4.7 photo D). Graptolite fossils in the lower part and brachiopod–cephalopod fossils in the middle part of the package are of Silurian ages [*RGMRHN-b,* 1968]. The overall package is interpreted to have been formed in a deltaic setting, with the lower part as prodelta facies, and the upper part as delta front facies with high energy features such as ripple marks and cross laminations.

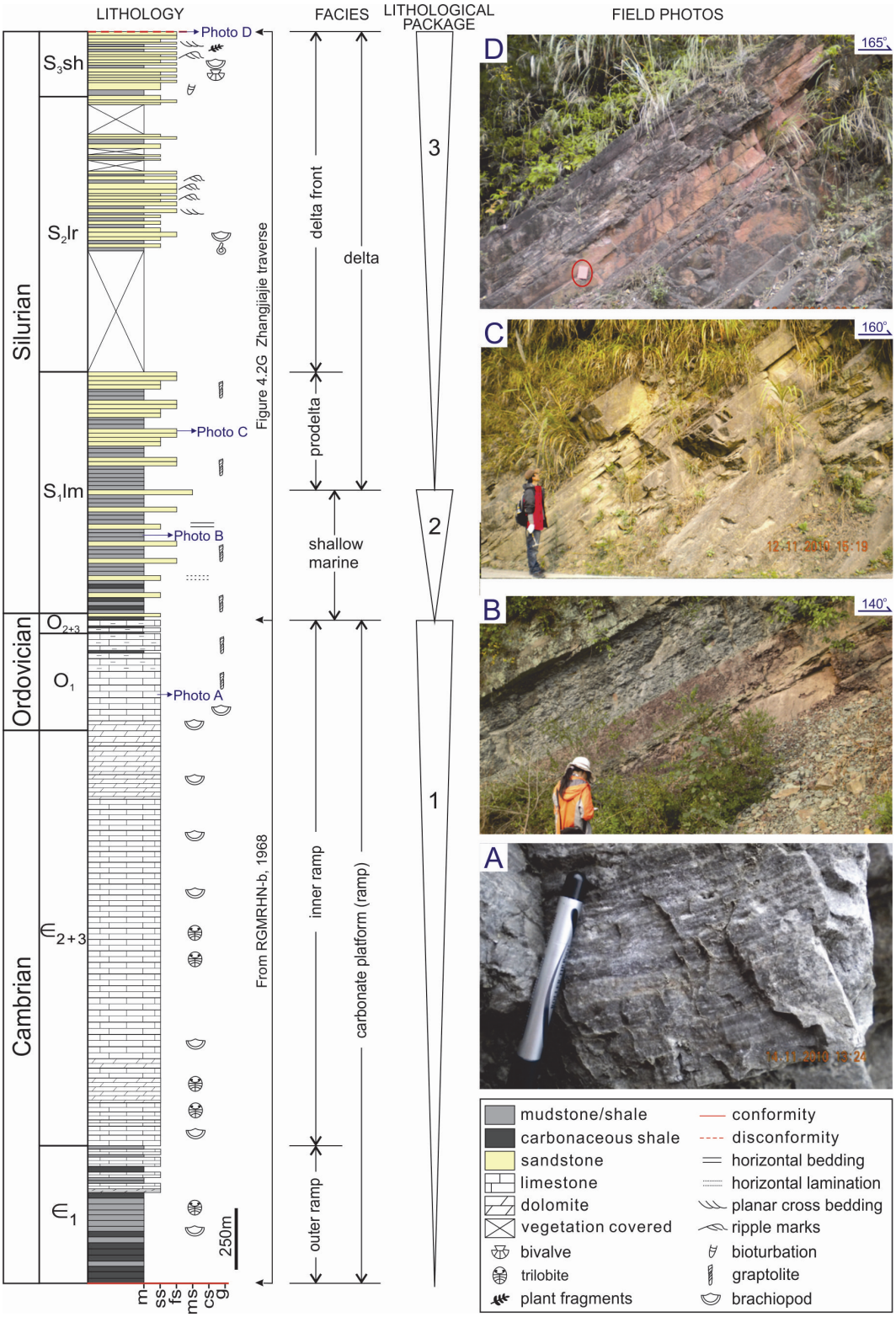

Figure 4.7. Cambro-Silurian lithostratigraphic column of the Zhangjiajie Section. Lithologic scale and information are the same as Figure 4.4. Field photos: (A) lower-Ordovician crystalline limestone, with a pen (15 cm long) for scale; (B) lower-Silurian green and purple shale interlayers; (C) thick- to medium-bedded fine sandstones intercalated with thin-layered shales; (D) mid-Devonian brick-red fine-grained quartz sandstone disconformably overlying Silurian sandstones. The notebook is 18 cm in length for scale.

4.4.5 Palaeocurrent analysis

Sedimentary structures indicative of palaeocurrent directions include trough cross-beds, planar cross-beds, flute casts and ripple marks [*Nichols,* 2009]. After restoring the tilted beds, two groups of measurements from Ordovician cross-bedded sandstones in the Yulin section show a northwestward palaeoflow (Figure 4.8B). Silurian flute casts from the Dongkou section also indicate a northwestward transport of detritus (Figure 4.6 photo C). Furthermore, Cambro-Ordovician cross-beds and asymmetrical ripple marks, to the northeast of the Shaoguan section, and cross beds in Silurian strata at Zhangjiajie indicate palaeoflow to the northwest [*Wang Y.J. et al.,* 2010]. Therefore, all palaeocurrent measurements across the basin indicate a dominantly northwest-directed transport direction (Figure 4.8A-C). This northwest-directed clastic transport direction also agrees with lower Palaeozoic palaeography in the SCB [*Liu and Xu,* 1994], which suggests that the southeastern Cathaysian margin was probably uplifted during the Ordovician and the uplifting continued into the Silurian and expanded to almost the entire Cathaysia Block (Figure 4.8B-C). The uplift also resulted in lithofacies variation from lower-Ordovician graptolitic shale to upper-Ordovician nearshore sandstone in the regions close to the Shaoguan section [*Chen et al.,* 2012], and a northwestward decrease of bentonite thickness in the basin [*Su et al.,* 2009].

4.5 Basin Evolution

4.5.1 The early Palaeozoic palaeogeography of the SCB

Based on the lithostratigraphic and palaeocurrent analyses in section 4.4, it appears that a lower Palaeozoic sedimentary basin covered the entire SCB. The depositional architecture of the basin and sediment dispersal was grossly progradational to the northwest, and sediment composition was mostly of siliciclastic nature (Figure 4.8A-C). During the Cambrian, the Yangtze Block mostly developed a carbonate depositional system, although minor siliciclastic intercalations are recorded in lower-Cambrian strata of western Yangtze [*BGMRGX,* 1985; *BGMRGZ,* 1988; *BGMRHN,* 1988]. In contrast, sedimentation on the Cathysia Block was overwhelmingly siliciclastic [*BGMRGD,* 1988; *BGMRGX,* 1985; *BGMRHN,* 1988;

BGMRJX, 1984]. Although the margin of western Yangtze (blank areas with question marks in Figure 4.8A) was locally uplifted during the early Cambrian as indicated by an early Cambrian hiatus there [*Liu and Xu,* 1994; *Liu et al.,* 1995], the regionally dominant carbonate lithofacies in northwestern Yangtze, and the consistant northwest-ward paleoflow directions in the studied clastic strata along the southeastern margin of the Yangtze Block, do not support the existence of a high topography at the western Yangtze Block at that time (Figure 4.8A). The contrast between the carbonate-dominated deposition over Yangtze and the siliciclastic deposition over Cathaysia, and the lack of known elevated land area on Cathaysia lead to the conclusion that the clastic source was outboard of the current southeastern Cathaysia margin [*Chen et al.,* 1995, 1997], which is supported by detrital provenance analyses [*Yao et al.,* 2014] and paleocurrent measurements (Figure 4.8).

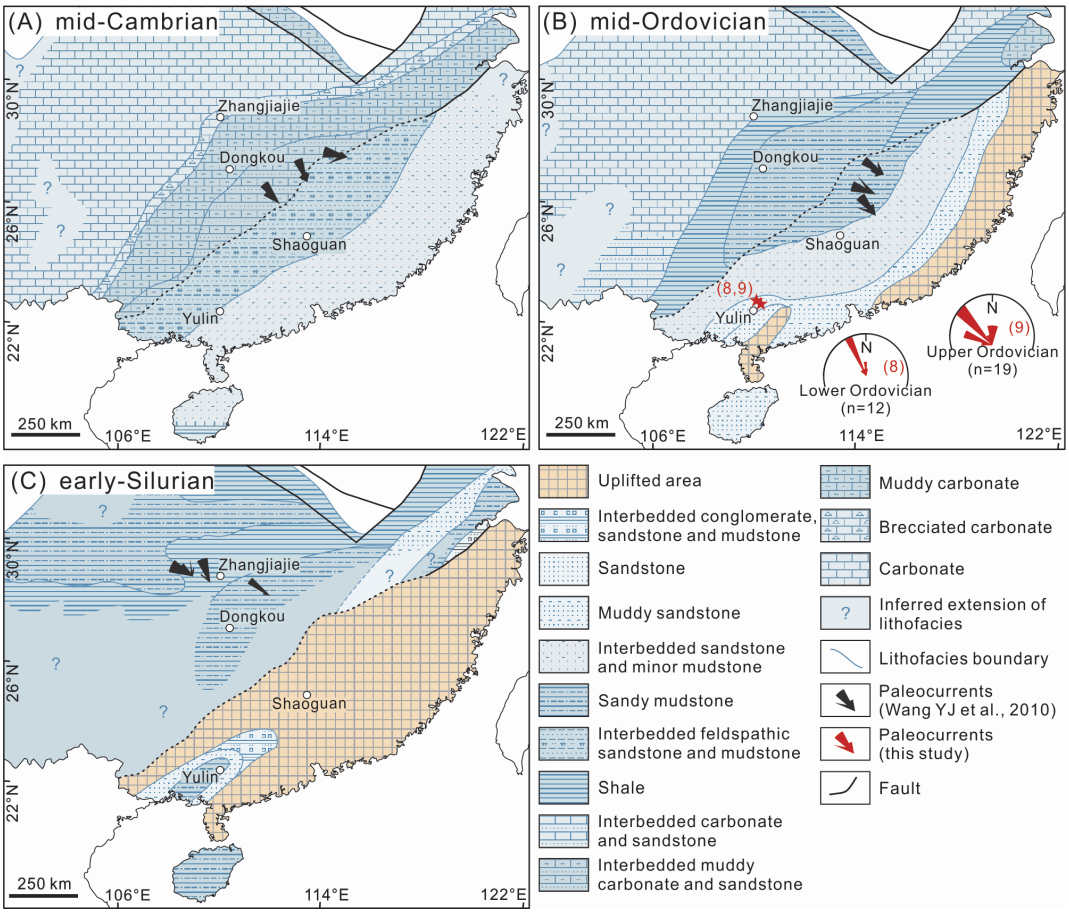

Figure 4.8. Palaeogeographic maps of the South China Block showing the evolution of the Nanhua foreland basin and the Wuyi–Yunkai orogen through the (A) mid-Cambrian, (B) mid-Ordovician and (C) early-Silurian (revised after *Liu and Xu,* 1994).

The northwestward progradation of clastic sedimentation continued from the Cambrian into the Ordovician, resulting in an expanding clastic depositional area.

The southeastern Cathaysia Block started to elevate in the early-Ordovician [*Liu and Xu,* 1994], and the uplifted area expanded during the mid-Ordovician, continuing to shed detritus to the northwest (Figure 4.8B). The presence of the uplift is supported by both the palaeogeography of South China and the absence of Ordovician strata in southeastern Cathaysia (Figure 4.1B). The local uplift starting in the earliest-Ordovician (Figure 4.1A) and expanding to the northwestward, along with the northwestward migration of clastic depostional centres, indicate that the Wuyi–Yunkai orogeny may have started from the earliest-Ordovician (*ca.* 480 Ma), older than the oldest retrograde metamorphic age of *ca.* 460 Ma (mid-Ordovician) [*Li Z.X. et al.,* 2010]. The siliciclastic progradation led to changes of lithology and facies in the southeastern Yangtze (i.e. the Dongkou section), from shale–carbonate (Cambrian) to sand–shale (mid-Ordovician) (Figure 4.6).

By the early-Silurian, carbonate deposition had effectively been terminated in the SCB (Figure 4.8C). The Yangtze Block was covered by fine-grained sandstone and shale, with coarse-grained sediments deposited along the Jiangshan–Shaoxing Fault. Much of the Cathaysia Block was uplifted by then. The Yulin–Hainan region in southern Cathaysia was the only region in Cathaysia that received Silurian clastic sedimentation (Figure 4.8C), consisting of thousand metres of sandstone–mudstone (Figure 4.4). This Silurian clastic package was named the "Qinfang Trough" in the Chinese literature, and has long been an enigma regarding its sedimentary and tectonic regime [*BGMRGX,* 1985; *Liu and Xu,* 1994; *Liu,* 1998; *Xu et al.,* 2001] (see 4.5.3 for further discussion).

4.5.2 The lower Palaeozoic Nanhua Basin: a peripheral foreland basin

The palaeogeographic evolution of the SCB indicates that the uplift and erosion along the southeastern Cathaysian margin progressively migrated to the northwest during the early Palaeozoic. The stratigraphic correlation through the four sections indicates that the lower Palaeozoic Nanhua Basin is northeasterly-oriented (Figure 4.9), with the main, elongated depocentre of the clastic deposition typically laying along the northern boundary of the Wuyi–Yunkai orogenic belt [*Liu and Xu,* 1994; *Li Z.X. et al.,* 2010]. These features suggest that the Nanhua Basin is of compressional origin – either a retro-arc foreland basin or a peripheral foreland basin.

The major difference between the two aforementioned foreland basins is that a magmatic arc is presented in front of a retro-arc foreland basin, but not for a peripheral foreland basin [*Dickinson,* 1974; *Busby and Ingersoll,* 1995]. To test whether there was an early Palaeozoic arc in southern SCB, we examined all Cambro-Silurian magmatic rocks in the region. A few volcanic rocks have been found, mainly within the Wuyi–Yunkai orogenic core and with Silurian ages (*ca.* 435 Ma) [*Yao et al.,* 2012], whereas dominant plutonic rocks are distributed in both the orogenic core and fold-and-thrust areas and in a slightly younger age range (*ca.* 440–400 Ma) [*Li Z.X. et al.,* 2010 and references therein; *Wang Y.J. et al.,* 2011]. The Silurian volcanic rocks carried no arc signature, but were interpreted as products of lithospheric delamination during the late Wuyi–Yunkai orogeny [*Yao et al.,* 2012; *Wang Y.J. et al.,* 2013], whereas the *ca.* 440–400 Ma plutonic rocks were remelted from old crustal rocks with little input of juvenile mantle [e.g., *Chen and Jahn,* 1998; *Zeng et al.,* 2008; *Zhou,* 2003; *Li Z.X. et al.,* 2010; *Wang Y.J. et al.,* 2011]. No Cambrian–Ordovician magmatic rock has yet been found in the region.

Therefore, the lower Palaeozoic Nanhua Basin has preserved no convincing evidence for the presence of a magmatic arc, and is thus interpreted as a peripheral foreland basin [e.g, *Li Z.X.,* 1998]. Five lines of supporting geological evidence are presented as follows. First, the Nanhua Basin has an asymmetrical wedge-shaped basin-fill, thickening southeastward, bounded by the Wuyi–Yunkai orogen to its southeast (Figures 4.1A). Second, the sedimentation across the basin generally shows a trend of upwards-coarsening clastics and coupled upwards-shallowing water depth. Third, the palaeocurrents to the northwest indicate that detritus were transported from the southeast: regions outboard of the current Cathaysia Block during the Cambrian and the Wuyi–Yunkai orogen during the Ordovician–Silurian, respectively (Figure 4.8). Fourth, the Wuyi–Yunkai fold-and-thrust belt advanced towards the basin, as recorded by the northwestward migration of clastic depocentres. Fifth, the evolution of foreland fills is recorded by the lateral propagation of sedimentary facies from southeast to northwest. The time-space correlation indicates that the basin was gradually filled, from an underfilled to filled basin dominated by marine facies to an overfilled basin dominated by subaerial facies (Figure 4.9).

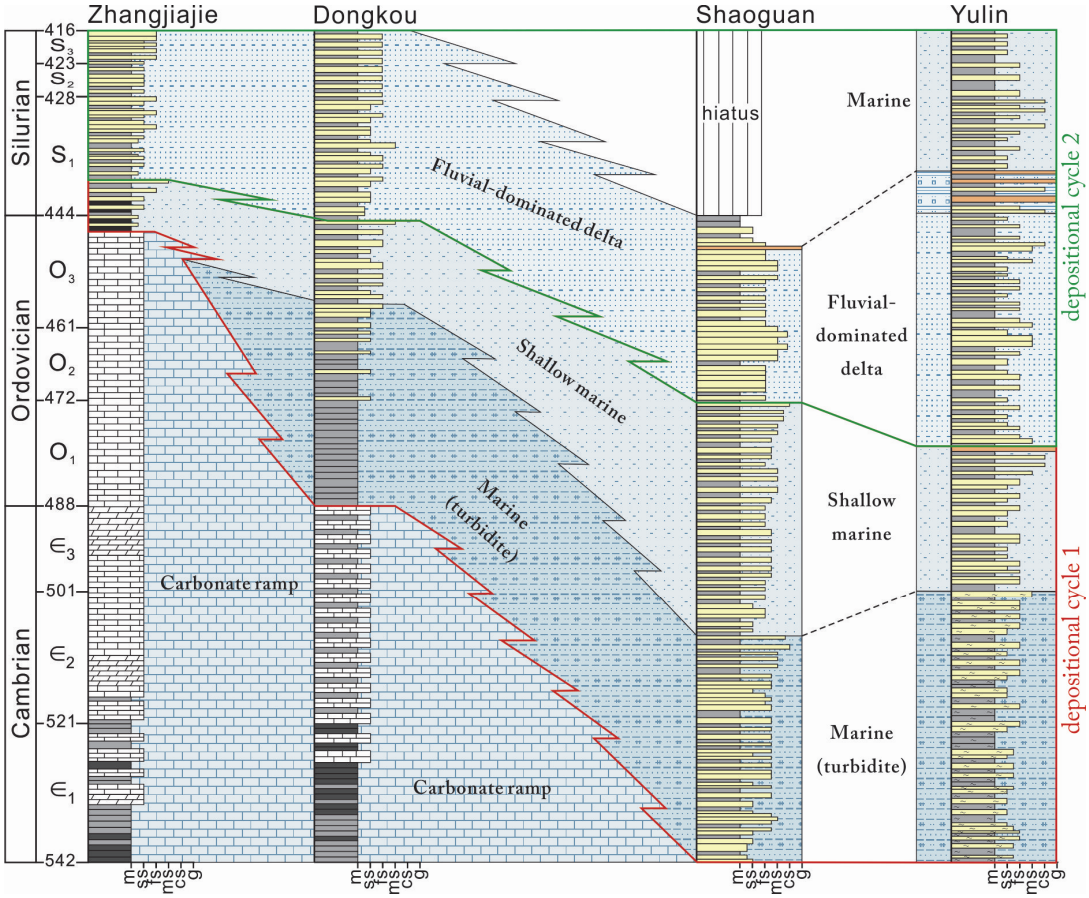

Figure 4.9. Time-space diagram of the Cambro–Silurian South China Block, covering the Zhangjiajie, Dongkou, Yulin and Shaoguan sections across the Nanhua Basin.

4.5.3 Sedimentary response to two successive orogenies which affected the SCB

According to the sedimentary facies and stratigraphy analysis, the lower Palaeozoic Nanhua foreland basin is made up of two depositional cycles (Figure 4.9).

The first depositional cycle exhibits an underfilled to filled basin-fill during the Cambrian to earliest-Ordovician, with diachronous turbiditic facies and shallow marine facies across the basin (Figure 4.9). The marine turbiditic facies was limited to the Yulin and Shaoguan sections during the early- to mid-Cambrian, and pinched off before reaching the Dongkou section (Figure 4.9). The foredeep of the Nanhua foreland basin during the first depositional cycle was in the Shaoguan–Yulin area (Figure 4.10A-B), as suggested by the much thicker clastic strata (2300m in Shaoguan and 3000m in Yulin) than that in the Dongkou region (450m of clastic strata) (Figures 4.4–4.6). We notice that the conformably underlying Ediacaran strata share same lithological associations and clastic provenance with the Cambrian strata

in the Cathaysia Block [*BGMRGD,* 1988; *BGMRGX,* 1985; *BGMRHN,* 1988; BGMRJX, 1984; *Yao et al.,* 2014], which leads to a speculation that the Nanhua Basin probably started to receive foreland deposits as early as the Ediacaran [*Yao et al.,* 2014].

Because of the northwest-deepening water depth, the northwest-directed palaeoflows, and the lack of exposed land area within the Cathaysia Block during the Cambrian to earliest-Ordovician (Figure 4.8A) [*Liu and Xu*, 1994], it is speculated that the source region of foreland deposits was outboard the current southeastern Cathaysia [e.g., *Wang Y.J. et al.,* 2010; *Jiang et al.,* 2014; *Yao et al.,* 2014]. *Yao et al.* [2014] proposed that the SCB probably started to collide with the northern Indian margin of Gondwanaland since the Ediacaran. This collisional orogen, along with direct or recycled detritus from the East African orogen, probably provided foreland deposits to the Nanhua Basin during the Ediacaran to earliest-Ordovician.

The second depositional cycle records an overfilled stage during the early-Ordovician to Silurian, and comprises a diachronous fluvial-dominated deltaic facies across the basin (Figure 4.9). The deltaic clastic facies covered the Yulin–Shaoguan area during the early-Ordovician to earliest-Silurian, migrated to the Dongkou section in the early-Silurian, and reached the Zhangjiajie section slightly later. The lowest-Silurian clastic sediments at Zhangjiajie are taken as the lateral equivalent of shallow marine facies that migrated from the southeast, whereas the mid- to upper-Silurian clastics may represent a lateral migration of fluvial-dominated deltaic facies from the southeast. The dominant fluvial-deltaic facies in the Shaoguan–Yulin sections and lateral migration suggests that the lower Palaeozoic Nanhua foreland basin was in a filled-overfilled stage during the early-Ordovician to Silurian (Figure 4.10C-D).

The dominant subaerial sedimentary facies over the Nanhua Basin during the early-Ordovician to Silurian was related to the local Wuyi–Yunkai orogen uplifting in the Cathaysia Block, which activated during >460–415 Ma [*Li Z.X. et al.,* 2010]. The Wuyi–Yunkai orogen provided more proximal and coarser detritus to the second stage of foreland sedimentation in the Nanhua Basin, forming the shallow marine to deltaic depositional strata. This local orogeny was also recorded by the widespread

ca. 460–415 Ma magmatism, metamorphism and deformation along the Wuyi and Yunkai Mountains (Figure 4.1A). Our stratigraphic analysis of the Yulin section, however, shows that the conglomeratic units started to deposit along the Wuyi-Yunkai Mountains in the early-Ordovician (Figure 4.4). It thus implies that the Wuyi–Yunkai orogeny may have been activated, and the southeastern Cathaysia Block started to elevate as early as the early-Ordovician [*Liu and Xu*, 1994]. The absence of Silurian sedimentary strata in the Shaoguan section suggests that the Yulin–Shaoguan region had already been uplifted by the early-Silurian (Figure 4.1A). The fact is that the region was likely a part of the orogenic core as suggested by the metamorphism of lower- to mid-Cambrian strata in the Yulin section (Figure 4.4). The dominance of Silurian silt- to fine- sandstones in the Zhangjiajie section indicates that it is on the distal edge of the Nanhua Basin, receiving finest sediments in the late stage of foreland deposition (Figure 4.10D). The disconformity between the Silurian and Devonian strata in the Zhangjiajie section instead of Silurian–Devonian and/or Ordovician–Devonian angular unconformities in the Yulin, Shaoguan and Dongkou sections also indicates that the fold-and-thrust deformation did not reach the Zhangjiajie region (Figure 4.3). It is noteworthy that the Yulin section, despite being located within the orogenic core, deposited thick marine strata during the Silurian (Figures 4.4 and 4.9). This abnormal Silurian package (the "Qinfang Trough") was likely deposited either in a piggy-back basin, and/or a graben formed during orogenic collapse (Figure 4.10D). The Wuyi–Yunkai orogeny is thus expected to have started as early as the early-Ordovician, marked by the first conglomeratic unit in the Yulin section [the early stage of the lower-Ordovician Huang'ai Formation (O_1h^1) in Figure 4.4].

4.6 Conclusions

According to the stratigraphic and sedimentary analyses of the four lower Palaeozoic sections in South China, we interpret the Nanhua Basin as a peripheral foreland basin activated from the Ediacaran to the Silurian. Our main findings are listed as following:

(1) The stratigraphic history show that the Nanhua foreland basin involved two stages of sedimentation: the first underfilled to filled stage (Cambrian to

earliest-Ordovician), with siliciclastic marine facies covering the entire Cathaysia and part of the southeastern Yangtze blocks; and the second overfilled stage (early-Ordovician to Silurian), with dominant deltaic facies covering the majority of Yangtze and part of the northern and southwestern Cathaysia blocks.

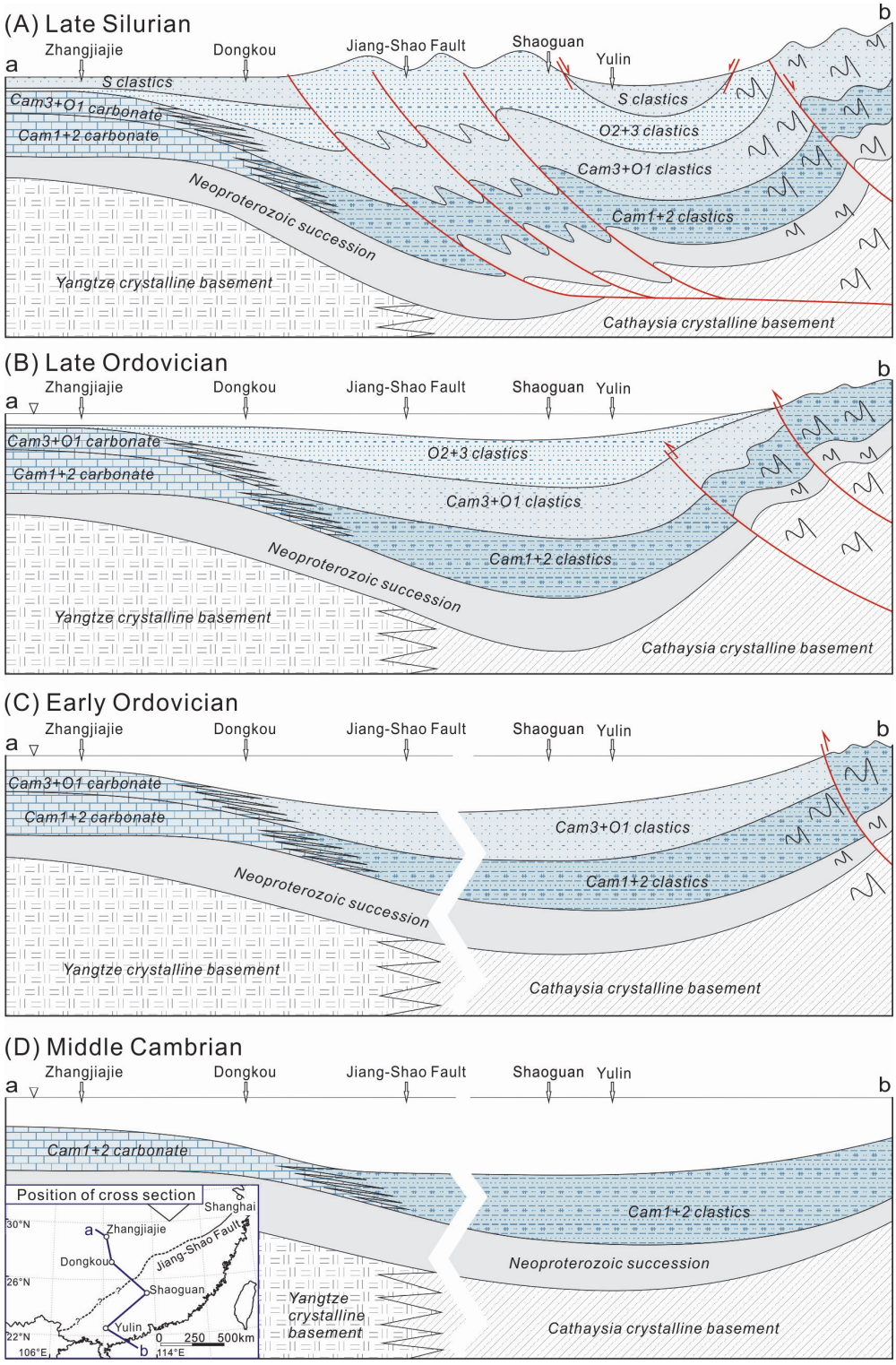

Figure 4.10. Cross-sections of the lower Palaeozoic Nanhua foreland basin showing its sedimentary and tectonic evolution in different time intervals.

(2) The two stages of foreland sedimentation were likely linked to two orogenic events that affected the SCB. The first stage (Cambrian to earliest-Ordovician) was likely related to an orogeny outboard the SCB, generated from the collision between the SCB and northern India of eastern Gondwanaland. The second stage (early-Ordovician to Silurian) was likely related to the local intraplate Wuyi–Yunkai orogeny within the SCB, which was resulted from far-field stress of the aforementioned collision.

(3) The thick Silurian marine clastic package in the southwestern Cathaysia Block was probably piggy-back basin deposits and/or possible graben deposits formed during the collapse of the Wuyi–Yunkai orogen.

4.7 Acknowledgement

We thank Lifeng Meng and Xinglei Feng for indispensable assistance with the stratigraphic section logging, Wuxian Li for assistance with geological field maps, and Bryan Krapež, Galen Halverson, Milo Barham and Chris Elders for commenting on the manuscript. This study was supported by the Australian Research Council (DP110104799), Chinese Academy of Science SAFEA International Partnership Program for Creative Research Teams grant (KZCX2-YW-Q04-06), and National Natural Sciences Foundation of China (41173039). This is TIGeR (The Institute for Geoscience Research) publication *#xxx*, and contribution *xxx* from the ARC Centre of Excellence for Core to Crust Fluid Systems (http://www.ccfs.mq.edu.au/).

4.8 References

BGMRGD (Bureau of Geology and Mineral Resources of Guangdong Province) (1988), *Regional Geology of the Guangdong Province,* report, 971 pp., Geological Publishing House, Beijing (in Chinese with English abstract).

BGMRGX (Bureau of Geology and Mineral Resources of Guangxi Province) (1985), *Regional Geology of the Guangxi Province,* report, 853 pp., Geological Publishing House, Beijing (in Chinese with English abstract).

BGMRGZ (Bureau of Geology and Mineral Resources of Guizhou Province) (1988), *Regional Geology of the Guangxi Province,* report, 698 pp., Geological

Publishing House, Beijing (in Chinese with English abstract).

BGMRHN (Bureau of Geology and Mineral Resources of Hunan Province) (1988), *Regional Geology of the Hunan Province,* report, 719 pp., Geological Publishing House, Beijing (in Chinese with English abstract).

BGMRJX (Bureau of Geology and Mineral Resources of Jiangxi Province) (1984), *Regional Geology of the Jiangxi Province,* report, 921 pp., Geological Publishing House, Beijing (in Chinese with English abstract).

Bouma, A.H. (1962), Sedimentology of some flysch deposits: a graphic approach to facies interpretation. Elsevier, Amsterdam, 168 pp.

Busby, C.J., and R.V. Ingersoll (1995), Tectonics of sedimentary basins, Blackwell Scientific, Oxford, 579 pp.

Charvet, J., L. Shu, Y. Shi, L. Guo, and M. Faure (1996), The building of south China: collision of Yangzi and Cathaysia blocks, problems and tentative answers, *J. Southeast Asian Earth Sci.*, *13(3),* 223–235, doi:10.1016/0743-9547(96)00029-3

Charvet, J., L. Shu, M. Faure, F. Choulet, B. Wang, H. Lu, and N. Le Breton (2010), Structural development of the Lower Paleozoic belt of South China: Genesis of an intracontinental orogen, *J. Asian Earth Sci., 39,* 309–330, doi:10.1016/j.jseaes.2010.03.006.

Chen, H., M. Hou, X. Xu, and J. Tian (2006), Tectonic evolution and sequence stratigraphic framework in South China during Caledonian, *J. Chengdu Uni. Technol.*, *33(1),* 1–8 (in Chinese with English Abstract).

Chen, J. F., and B. M. Jahn (1998), Crustal evolution of southeastern China: Nd and Sr isotopic evidence, *Tectonophysics, 284,* 101–133, doi:10.1016/S0040-1951(97)00186-8.

Chen X., J.Y. Rong, D.B. Rowley, J. Zhang, Y.D. Zhang, and R.B. Zhan (1995), Is the early Paleozoic Banxi Ocean in South China necessary?, *Geol. Rev., 41(5),* 389–400.

Chen, X., D.B. Rowley, J.Y. Rong, J. Zhang, Y.D. Zhang, and R.B. Zhan (1997), Late Precambrian through early Paleozoic stratigraphic and tectonic evolution of the Nanling region, Hunan province, South China, *Int. Geol. Rev., 39(5),* 469–478, doi:10.1080/00206819709465285.

Chen, X., Y.D. Zhang, J.X. Fan, L. Tang, and H.Q. Sun (2012), Onset of the Kwangsian Orogeny as evidenced by biofacies and lithofacies, *Sci. Chin.*

Earth Sci., *55,* 1592–1600, doi:10.1007/s11430-012-4490-4.

Dickinson, W.R. (1974), Plate tectonics and sedimentation, in *Tectonics and sedimentation,* edited by W. R. Dickinson, *Soc. Econ. Paleontol. Mineral. Spec. Publ., 22,* 1–27.

Dong, R., and H. Liu (1991), Regional stratigraphy (in Chinese), in *The Sinian system in China*, edited by H. Liu, Beijing, Science Press, 11–114.

Faure, M., L. Shu, B. Wang, J. Charvet, F. Choulet, and P. Monie (2009), Intracontinental subduction: a possible mechanism for the Early Paleozoic Orogen of SE China, *Terra Nova, 21(5),* 360–368, doi:10.1111/j.1365-3121.2009.00888.x.

Guo, L.Z., Y.S. Shi, H.F. Lu, R.S. Ma, H.G. Dong, and S.F. Yang (1989), The pre-Devonian tectonic patterns and evolution of South China, *J. Southeast Asian Earth Sci.*, *3(1–4),* 87–93, doi:10.1016/0743-9547(89) 90012-3.

Hsü, K.J., (1994), Tectonic facies in an archipelago model of intra-plate orogenesis, *GSA Today, 4,* 289–293.

Hsü, K.J., S. Sun, J. Li, H. Chen, H. Pen, and A.M.C. Sengör (1988), Mesozoic overthrust tectonics in south China, *Geology*, *16,* 418–421, doi:10.1130/0091-7613(1988)016.

Hsü, K.J., J.L. Li, H.H. Chen, Q.C. Wang, S. Sun, and A.M.C. Sengör (1990), Tectonics of South China: Key to understanding West Pacific geology, *Tectonophysics*, *193,* 9–39, doi:10.1016/0040-1951(90)90186-C.

Huang, J., J. Ren, C. Jiang, Z. Zhang, and D. Qin (1980), *The Geotectonic Evolution of China,* 124 pp., Science, Beijing.

Jiang, B., H.D. Sinclair, Y. Niu, and J. Yu (2014), Late Neoproterozoic-Early Paleozoic evolution of the South China Block as a retroarc thrust wedge/foreland basin system, *Int. J. Earth Sci., 103,* 23–40.

Li, J.L. (1991), Characteristics of Jinning-Chengjiang magmatic rocks and plate tectonic movements, in *the Sinian System in China* (in Chinese), pp. 220–300, Science Press, Beijing.

Li, W.X., X.H. Li and Z.X. Li (2010), *Ca.* 850 Ma bimodal volcanic rocks in northeastern Jiangxi Province, South China: Initial extension during the breakup of Rodinia? *Am. J. Sci., 310,* 951–980, doi:10.2475/09.2010.08.

Li, X.H., G. Zhou, J. Zhao, C.M. Fanning, and W. Compston (1994), SHRIMP ion microprobe zircon U-Pb age of the NE Jiangxi ophiolite and its tectonic

implications, *Geochimica, 23,* 125–131 (in Chinese with English abstract).

Li, X.H., W.X. Li, Z.X. Li, C.H. Lo, J. Wang, M.F. Ye, and Y.H. Yang (2009), Amalgamation between the Yangtze and Cathaysia blocks in South China: Constraints from SHRIMP U-Pb zircon ages, geochemistry and Nd-Hf isotopes of the Shuangxiwu volcanic rocks, *Precambrian Res., 174,* 117–128, doi:10.1016/j.precamres.2009.07.004.

Li, Z.X. (1998), Tectonic history of the major East Asian lithospheric blocks since the mid-Proterozoic: A synthesis, in *Mantle Dynamics and Plate Interactions in East Asia,* edited by M.F.J. Flower et al., *Geo dyn. Ser.*, *27,* pp. 221–243, AGU, Washington, D.C.

Li, Z.X., X.H. Li, H.W. Zhou, and P.D. Kinny (2002), Grenvillian continental collision in south China: New SHRIMP U-Pb zircon results and implications for the configuration of Rodinia, *Geology*, *30,* 163–166, doi:10.1130/0091-7613(2002)030.

Li, Z.X., X.H. Li, P.D. Kinny, J. Wang, S. Zhang, and H. Zhou (2003), Geochronology of Neoproterozoic syn-rift magmatism in the Yangtze Craton, South China and correlations with other continents: evidence for a mantle superplume that broke up Rodinia, *Precambrian Res., 122,* 85–109, doi:10.1016/S0301-9268(02)00208-5.

Li, Z.X., S.V. Bogdanova, A.S. Collins, A. Davidson, B. De Waele, R.E. Ernst, I.C.W. Fitzsimons, R.A. Fuck, D.P. Gladkochub, J. Jacobs, K.E. Karlstrom, S. Lu, L.M. Natapov, V. Pease, S.A. Pisarevsky, K. Thrane, and V. Vernikosky (2008), Assembly, configuration, and break-up history of Rodinia: a synthesis, *Precambrian Res.*, *160,* 179–210, doi:10.1016/j.precamres.2007.04.021.

Li, Z.X., X.H. Li, J.A. Wartho, C. Clark, W.X. Li, C.L. Zhang, and C.M. Bao (2010), Magmatic and metamorphic events during the Early Paleozoic Wuyi-Yunkai orogeny, southeastern south China: New age constraints and P-T conditions, *Geol. Soc. Am. Bull.,122(5–6),* 772–793, doi:10.1130/B30021.1.

Liu, B.J., and X.S. Xu (2004), Atlas of Lithofacies and Paleogeography of South China, 188 pp., Science Press, Beijing.

Liu, B.J., X.S. Xu, and Q. Xu (1995) Sequence stratigraphy and basin geodynamic of the southeastern margin of the Yangtze plate during the late proterozoic to early Paleozoic, *Lithofacies Paleogeography, 5,* 1–16.

Liu, W.J. (1998), Evolution of sedimentation of South China plate in the

Hercynian-Indosinian stage, *J. Chengdu Univ. Technol., 25,* 328–336 (in Chinese with English abstract).

Nichols, G. (2009), Sedimentology and stratigraphy, 2nd ed., 419 pp., Blackwell Scientific, Oxford, U.K.

Pan, G. (1984), The late Precambrian and early Paleozoic marginal basin of South China, in *Marginal Basin Geology,* edited by B.P. Kokelaor, and M.F. Howell, Blackwell Scientific, Oxford, pp. 279–283.

Ren, J.S. (1964), A preliminary study on pre-Devonian geotectonic problems of southeastern China, *Acta Geologica Sinica, 44(4),* 418–431.

Ren, J.S. (1991), On the geotectonics of Southern China, *Acta Geologica Sinica, 4(2),* 111–136.

RGMRGD (1962), *Regional Geological Mapping and Report of Guangdong Province – scale 1:200,000 Shaoguan Sheet,* Beijing, Institute of Geoscience, Ministry of Geology (in Chinese).

RGMRGX-a (1966), *Regional Geological Mapping and Report of Guangxi Province – scale 1:200,000 Rongxian Sheet,* Beijing, Institute of Geoscience, Ministry of Geology (in Chinese).

RGMRGX-b (1968), *Regional Geological Mapping and Report of Guangxi Province – scale 1:200,000 Yulin Sheet,* Beijing, Institute of Geoscience, Ministry of Geology (in Chinese).

RGMRHN-a (1965), *Regional Geological Mapping and Report of Hunan Province – scale 1:200,000 Dongkou Sheet,* Beijing, Institute of Geoscience, Ministry of Geology (in Chinese).

RGMRHN-b (1968), *Regional Geological Mapping and Report of Hunan Province – scale 1:200,000 Dayong Sheet,* Beijing, Institute of Geoscience, Ministry of Geology (in Chinese).

Shui, T. (1988), Tectonic framework of the southeastern China continental basement, *Scientia Sinica (Series B), 31,* 885–896 (in Chinese with English abstract).

Su, W., W.D. Huff, F.R. Ettensohn, X. Liu, J. Zhang, and Z. Li (2009), K-bentonite, black-shale and flysch successions at the Ordovician-Silurian transition, South China: possible sedimentary responses to the accretion of Cathaysia to the Yangtze Block and its implications for the evolution of Gondwana, *Gondwana Res., 15,* 111–130, doi:10.1016/j.gr.2008.06.004.

Udden, J.A. (1914), Mechanical composition of clastic sediments, *Geol. Soc. Am.*

Bull., 25, 655–744.

Wang, H.Z. (1985), *Atlas of the Paleogeography of China,* 281 pp., Beijing, Cartographic Publishing House.

Wang, J., and Z.X. Li (2003), History of Neoproterozoic rift basins in South China: implications for Rodinia break-up, *Precambrian Res.*, *122,* 141–158, doi:10.1016/S0301-9268(02)00209-7.

Wang, X., S.F. Yang , J.N. Shi, L.Z. Guo, Y.S. Shi, H.F. Lu, H.G. Dong, J.K. Xu, H.N. Kong, and X.J. Hu, (1988), Discovery of collision mélange in Longquan, Zhejiang province and its significance for studying collision orogenic belt in southeastern China, *J. Nanjing Uni. (Natural Sci.), 24,* 367–378 (in Chinese with English abstract).

Wang, X.L., J.C. Zhou, J.S. Qiu, and J.F. Gao (2004), Geochemistry of the Meso- to Neoproterozoic basic-acid rocks from Hunan Province, South China: implications for the evolution of the western Jiangnan orogen, *Precambrian Res., 135,* 79–103, doi:10.1016/j.precamres.2004.07.006.

Wang, Y., W. Fan, G. Zhao, S. Ji, and T. Peng (2007), Zircon U-Pb geochronology of gneissic rocks in the Yunkai massif and its implications on the Caledonian event in the South China Block, *Gondwana Res., 12(4),* 404–416, doi:10.1016/j.gr.2006.10.003.

Wang, Y., F. Zhang, W. Zhang, G. Zhang, S. Chen, P.A. Cawood, and A. Zhang (2010), Tectonic setting of the South China Block in the early Paleozoic: Resolving intracontinental and ocean closure models from detrital zircon U-Pb geochronology, *Tectonics, 29,* doi:10.1029/2010TC002750.

Wang, Y., A. Zhang, W. Fan, G. Zhao, G. Zhang, Y. Zhang, F. Zhang, and S. Li (2011), Kwangsian crustal anatexis within the eastern South China Block: Geochemical, zircon U-Pb geochronological and Hf isotopic fingerprints from the gneissoid granites of Wugong and Wuyi-Yunkai Domains, *Lithos, 127,* 239–260, doi:10.1016/j.lithos.2011.07.027.

Wang, Y., A. Zhang, W. Fan, Y. Zhang, and Y. Zhang (2013), Origin of paleosubduction-modified mantle for Silurian gabbro in the Cathaysia Block: Geochronological and geochemical evidence, *Lithos, 160-161,* 37–54. doi:10.1016/j.lithos.2012.11.004

Wentworth, C.K. (1922), A scale of grade and class terms for clastic sediments, *J. Geol, 30,* 377–392.

Xu, X., F. Yin, F. Wan, Z. Liang, B. Wei, and J. Zhang (2001), The migration of the Qinzhou-Fangcheng trough in Guangxi and associated sedimentary-tectonic transform surfaces, *Sedimentary Geology and Tethyan Geology, 21,* 1–10 (in Chinese with English abstract).

Yang, Z., Y.Q. Cheng, and H.C. Wang (1986), The geology of China, Clarendon Press, Oxford, 276 p.

Yao, W.H., Z.X. Li, W.X. Li, X.C. Wang, X.H. Li, and J.H. Yang (2012), Post-kinematic lithospheric delamination of the Wuyi-Yunkai orogen in South China: Evidence from *ca.* 435 Ma high-Mg basalts, *Lithos, 154,* 115–129, doi:10.1016/j.lithos.2012.06.033.

Yao, W.H., Z.X. Li, W.X. Li, X.H. Li, and J.H. Yang (2014), From Rodinia to Gondwanaland: a tale from detrital provenance analyses of the Cathaysia Block, South China, *Am. J. Sci., 314,* 278–313, doi:10.2475/01.2014.08.

Zeng, W., L. Zhang, H. Zhou, Z. Zhong, H. Xiang, R. Liu, S. Jin, X. Lu, and C. Li (2008), Caledonian reworking of Paleoproterozoic basement in the Cathaysia Block: Constraints from zircon U-Pb dating, Hf isotopes and trace elements, *Chin. Sci. Bull., 53(6),* 895–904, doi:10.1007/s11434-008-0076-0.

Zhang, L., and Q.Y. He (1993), On the revision of Bacun Group and the establishment of Xiazhai, Oujiadong and Laoshuzhai Formations in northern Guangdong Province, *Guangdong Geology, 8,* 1–14 (in Chinese with English abstract).

Zhou, G. (1989), The discovery and significance of the northeastern Jiangxi Province ophiolite (NEJXO), its metamorphic peridotite and associated high temperature-high pressure metamorphic rocks, *J. SE Asian Earth Sci., 3,* 237–247, doi:10.1016/0743-9547(89)90028-7.

Zhou, M.F., A.K. Kennedy, M. Sun, J. Malpas, and C.M. Lesher (2002a), Neoproterozoic arc-related mafic intrusions along the northern margin of South China: implications for the accretion of Rodinia, *J. Geol., 110,* 611–618, doi:10.1086/341762.

Zhou, M.F., D.P. Yan, A.K. Kennedy, Y.Q. Li, and J. Ding (2002b), SHRIMP U-Pb zircon geochronological and geochemical evidence for Neoproterozoic arc-magmatism along the western margin of the Yangtze Block, South China, *Earth Planet. Sci. Lett., 196,* 51–67, doi:10.1016/S0012-821X(01)00595-7.

Zhou, X.M. (2003), My thinking about granite geneses of south China, *Geol. J. Chin.*

Univ., 9(4), 556–565 (in Chinese with English abstract).

CHAPTER 5 DETRITAL PROVENANCE EVOLUTION OF THE LOWER PALAEOZOIC NANHUA FORELAND BASIN, SOUTH CHINA

Wei-Hua Yao[a*], Zheng-Xiang Li[a], Wu-Xian Li[b], Li Su[c], Jin-Hui Yang[d]

[a]ARC Center of Excellence for Core to Crust Fluid Systems (CCFS) and The Institute for Geoscience Research (TIGeR), Department of Applied Geology, Curtin University, Perth 6845, Australia

[b]Key Laboratory of Isotope Geochronology and Geochemistry, Guangzhou Institute of Geochemistry, Chinese Academy of Sciences, Guangzhou 510640, China

[c]The Institute of Earth Science, Chinese University of Geosciences, Beijing 100083, China

[d]State Key Laboratory of Lithospheric Evolution, Institute of Geology and Geophysics, Chinese Academy of Sciences, Beijing 100029, China

* Corresponding author: weihua.yao@curtin.edu.au

Abstract

We report here *in-situ* U–Pb and Hf isotopic results of detrital zircons from sixteen Cambrian–Silurian clastic samples across the Nanhua foreland basin, South China. Together with published data from Ediacaran–Silurian sandstones in the region, we establish the temporal and spatial provenance evolution across the basin. Except for samples from northeast Yangtze, all other Ediacaran–Silurian samples exhibit a prominent population of 1100–900 Ma, moderate populations of 850–700 Ma and 650–490 Ma, and minor populations of *ca.* 2500 Ma and 2000–1300 Ma, grossly matching that of crystalline and sedimentary rocks in northern India. Zircon Hf isotopes further reveal four episodes of juvenile crustal growth at 2.5 Ga, 1.8 Ga, 1.4 Ga and 1.0 Ga in the source regions. Utilizing the basin history and early Palaeozoic palaeogeography of South China, we conclude that the Ediacaran–Cambrian sediments in the Nanhua foreland basin were mainly sourced from northern India and adjacent

orogens, and the Ordovician–Silurian sediments were derived from both locally recycled Ediacaran–Cambrian rocks and eroded Cathaysian basement. The Wuyi–Yunkai late-orogenic magmatic rocks also contributed to the Silurian sediments in the basin. The upper-Ordovician to Silurian samples in northeast Yangtze received higher proportions of local Cryogenian (850–700 Ma) rift-related magmatic rocks which were uplifted during late-Ordovician to Silurian time. We speculate that there was an Ediacaran–Cambrian collisional orogeny between South China and northern India, shedding sediments to the early Nanhua foreland basin. Far-field stress during the late stage of this collisional orogeny triggered the Ordovician–Silurian intraplate Wuyi–Yunkai orogeny in South China, and erosion of this local orogen provided detritus to the late Nanhua foreland basin.

Key Words: South China, Nanhua foreland basin, Detrital provenance, Ediacaran–Cambrian, Ordovician–Silurian

5.1 Introduction

Sedimentary provenance analysis of peripheral foreland deposits can provide important insights into nature of the adjacent orogen which may have lost much of its record due to syn- to post-orogenic erosion (e.g., Cawood et al., 2007; Myrow et al., 2010). Zircon U–Pb age patterns can indicate provenance, patterns of sediment dispersal and timing of orogenic uplift (e.g., Condie et al., 2009; Squire et al., 2006). Age spectra of detrital zircons can act as a census of ages of (1) crystalline rocks exposed along an orogen at the time of erosion and transport of detritus, and (2) detritus recycled from older sedimentary rocks. The proportion of different zircon age peaks reflect the input of various sources, as controlled by the extent of exposed bedrocks, erosional rates, and degrees of recycling of older sedimentary rocks along transport paths (e.g., Amidon et al., 2005; Dickson, 2008). Zircon Hf isotopes can reveal the nature of source rocks, and/or proportion of mantle input to the source (e.g., Hawkesworth and Kemp, 2006; Kemp et al., 2006; Belousva et al., 2010). Integrated analyses of detrital zircon U–Pb and Hf isotopes have thus become a powerful tool for deciphering provenance evolution of a sedimentary basin and denudation history of source regions (e.g., Myrow et al., 2010; Zhang et al., 2012).

The South China Block (SCB), one of the largest continental blocks in East Asia, underwent its first Phanerozoic tectonic event during the early Palaeozoic – the Wuyi–Yunkai orogeny (e.g., Li et al., 2010a). This orogeny not only produced a series of metamorphic complexes along the Wuyi–Baiyun–Yunkai Mountains (e.g., Wang et al., 2007b; Yu et al., 2008, 2010; Li et al., 2010a; Wan et al., 2010), but also generated a peripheral foreland basin – the Nanhua basin (Figure 5.1), with thousands of metres of sedimentary strata accumulated (e.g., Li, 1998; Yao et al., 2014b and references therein). However, due to Mesozoic tectonic modifications in the region, neither nature of this early Palaeozoic orogeny nor provenance changes throughout the history of this foreland basin have been well constrained.

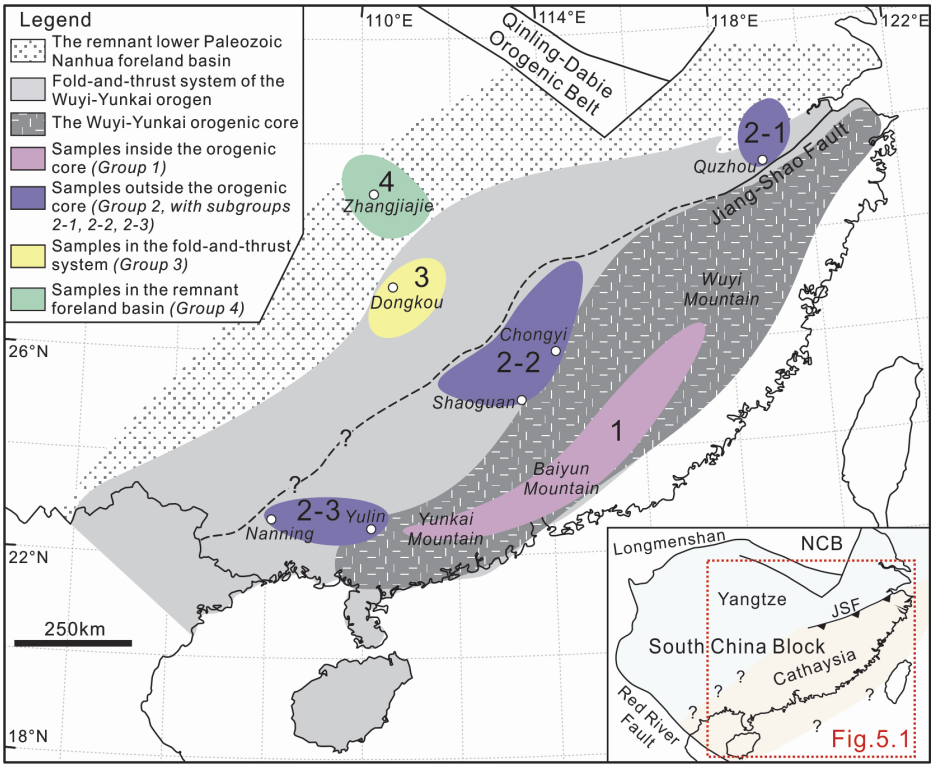

Figure 5.1. A simplified regional map highlights the lower Palaeozoic Wuyi–Yunkai orogen and the Nanhua foreland basin in the South China Block. The Ediacaran–Silurian sandstone samples for detrital zircon analyses are divided into four groups according to their positions in the orogen–basin system.

In this paper, we present detrital zircon U–Pb ages and Hf isotopes from sixteen Cambrian–Silurian sedimentary samples across the Nanhua foreland basin. Together with published detrital zircon data, we establish a temporal and spatial framework of sediment dispersals across the basin, to better address provenance evolution of the Nanhua foreland basin and denudation history of the Wuyi–Yunkai orogen.

5.2 Geological Background and Sampling

5.2.1 Geological setting of the SCB

The SCB consists of the Yangtze Block in the northwest and the Cathaysia Block in the southeast (Figure 5.1 inset), which joined together in the early Neoproterozoic (e.g., Li et al., 2002, 2008a, 2009; Zhou et al., 2002a, 2002b; Wang et al., 2004). The boundary between these two blocks is approximately along the Jiangshan–Shaoxing Fault at the eastern end, whereas its western extension is unclear due to poor exposure and tectonic modifications (Figure 5.1) (e.g., Ren, 1991; Li et al., 2010a).

The Yangtze and Cathaysia blocks have different crystalline basement compositions. The Yangtze basement consists of Archean outcrops (3.3–3.2 Ga and 2.95–2.90 Ga) in the Kongling Complex of northern Yangtze (Qiu et al., 2000; Zheng et al., 2006; Jiao et al., 2009; Gao et al., 2011) and more widespread Proterozoic rocks, include: (1) Mesoproterozoic metasediments (≤1.53 Ga) (Li et al., 2007) and magmatic rocks (1.16–0.88 Ga) (Ye et al., 2007; Li et al., 2008b, 2009, 2013a) on the southeastern Yangtze margin; (2) volcanoclastic rocks (1.7–0.9 Ga) and metamorphosed equivalents on the southwestern Yangtze margin (Li et al., 2002; Greentree et al., 2006; Greentree and Li, 2008; Sun et al., 2009; Zhao et al., 2010). The Cathaysia basement rocks are poorly-exposed and scattered, with the oldest known crystalline rocks being granites and amphibolites (1.89–1.77 Ga) in northeastern Cathaysia (Li, 1997; Li and Li, 2007; Xiang et al., 2008; Zeng et al., 2008; Yu et al., 2011) and gneissic granitoids (1.43 Ga) in southern Cathaysia (Ma et al., 1998; Li et al., 2002, 2008c). Mid- to late-Neoproterozoic magmatic rocks (860–750 Ma) and volcanoclastic successions are well preserved in the mid-Neoproterozoic Nanhua rift basin between the Yangtze and Cathaysia blocks as well as in the Kangdian rift basin on the western Yangtze margin (e.g., Zhou et al., 2002a, 2006; Li et al., 2003a, 2003b, 2005, 2010b; Wang et al., 2006; Shu et al., 2011).

The early Palaeozoic Wuyi–Yunkai orogeny in the SCB is represented by an angular unconformity between upper Palaeozoic terrestrial deposits (Devonian and younger) and lower Palaeozoic clastic successions, granites and Precambrian rocks in the southeastern SCB (e.g., Huang et al., 1980; BGMRJX, 1984; BGMRGX, 1985;

BGMRGD, 1988; BGMRHN, 1988; Ren, 1991; Wang et al., 2007b; Li et al., 2010a). This tectonic event was traditionally referred as "the Caledonian orogeny" (430–400 Ma) in Chinese literature (e.g., Huang et al., 1980; Yang et al., 1986; Ren, 1991), but has been re-named the Wuyi–Yunkai orogeny after the metamorphic complexes exposed along the Wuyi–Baiyun–Yunkai Mountains (Figure 5.1) (Li et al., 2010a). The Wuyi–Yunkai orogeny, active from >460 Ma to 415 Ma, resulted in uplift of the Wuyi–Yunkai orogen and subsidence of the Nanhua foreland basin to its northwest (Figure 5.1) (Li et al., 2010a).

Based on basin geometry and stratigraphic analyses of the Nanhua foreland basin, Yao et al. (2014b) proposed that the foreland deposition probably started from the Ediacaran (late-Neoproterozoic), much earlier than the starting time of the Wuyi–Yunkai orogeny at the Ordovician. The early Nanhua foreland basin covered much of the Cathaysia as well as southeastern Yangtze during the Ediacaran–Cambrian. As the Wuyi–Yunkai orogen activated and propagated towards the northwest, the early basin was partly assimilated into the orogenic core and the fold-and-thrust belt, and left a remnant basin to its northwest by the late Silurian (Figure 5.1) (e.g., Li, 1998; Li et al, 2010a; Chen et al., 2012; Yao et al., 2014b).

5.2.2 Stratigraphic sections and detrital sample groups

Clastic samples were systematically collected from Ediacaran to Silurian strata across the entire width of the Nanhua foreland basin (Figure 5.1). Sixteen new samples from this study and fifty-four samples from previous studies are put into four groups according to their geological locations in relation to the Wuyi–Yunkai orogen. Group 1 samples were from the orogenic core, group 2 from the northwestern margin of the orogen (subgroup 2-1 from the northeastern end, subgroup 2-2 from the central section, and subgroup 2-3 from the southwestern end), group 3 from the fold-and-thrust belt, and group 4 from the remnant Nanhua foreland basin (Figure 5.1). A summary of all detrital samples employed in this study is given in Table 5.1.

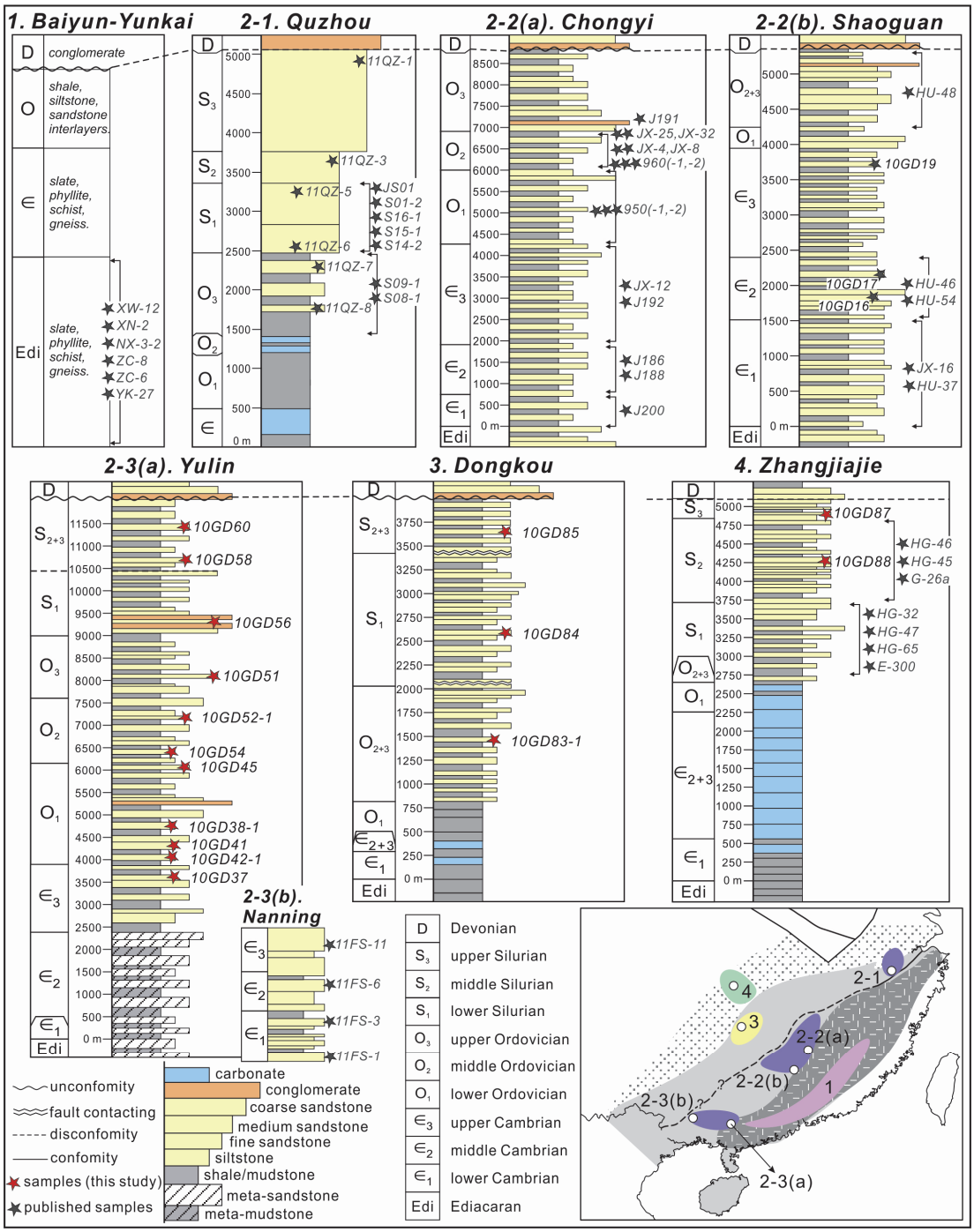

Figure 5.2. Late Neoproterozoic (Ediacaran) to Silurian stratigraphic sections and positions of detrital samples across the Nanhua foreland basin, South China. Detrital samples from this study are marked as red stars, and those from previous studies are marked as grey stars. Data source for stratigraphic sections: 1 – BGMRFJ, 1985; BGMRGX, 1985; BGMRGD, 1988; 2-1 – Xu et al. (2012); 2-2(a) – Wu et al. (2010); 2-2(b) – Yao et al. (2014b); 2-3(a) – Yao et al. (2014b); 2-3(b) – Xu et al. (2014); 3 – Yao et al. (2014b); 4 – Yao et al. (2014b). Data source for detrital samples can be found in Table 5.1. Inset map shows positions of the stratigraphic sections in the orogen–basin system.

Sample subgroup 2-3 includes eleven new clastic samples from the Yulin section and four published samples from the Nanning section (Xu et al., 2014), both locating in

the southern part of the early Nanhua foreland basin (Figure 5.2, Table 5.1). The Yulin section consists of Ediacaran–Silurian clastic strata, comprising intercalations of shale, siltstone and sandstone (RGMRGX-a, 1966; RGMRGX-b, 1968; BGMRGX, 1985). The Ediacaran–Silurian strata generally include a metamorphosed Ediacaran to mid-Cambrian package, an upward-coarsening upper-Cambrian to lower-Ordovician package and an upward-coarsening mid-Ordovician to lowest-Silurian package, followed by an upward-fining Silurian package (Figure 5.2) (Yao et al., 2014b). Shallow water sedimentary structures such as planar cross bedding, ripple marks and clast imbrication are preserved in the succession (RGMRGX-a, 1966; BGMRGX, 1985; Yao et al., 2014b). The mid- to upper-Silurian strata overlie the lower Silurian coarse-grained sandstones above a disconformity, and are overlain by Devonian quartz sandstones with an angular unconformity (RGMRGX-a, 1966; RGMRGX-b, 1968; BGMRGX, 1985).

Sample group 3 includes three new clastic samples from the Dongkou section and two published samples from adjacent areas (Wang et al., 2010), located in the fold-and-thrust zone (Figure 5.2, Table 5.1). The Dongkou section consists of Ediacaran to lower-Ordovician interstratifies of shale and carbonaceous shale, and mid-Ordovician to Silurian interstratifies of shale, siltstone, and variable-grained sandstone (RGMRHN-a, 1965; BGMRHN, 1988). The mid-Ordovician to Silurian clastic succession exhibits an upward-coarsening trend, with three packages of mid- to upper-Ordovician, lower-Silurian and mid- to upper-Silurian (Yao et al., 2014b).

Sample group 4 includes two new clastic samples from the Zhangjiajie section, and seven published samples from adjacent areas (Wang et al., 2010), locating in the remnant foreland basin (Figure 5.2, Table 5.1). The Zhangjiajie section comprises Ediacaran–Ordovician shales and carbonates, and uppermost-Ordovician to Silurian interstratifies of shale, siltstone and sandstone (RGMRHN-b, 1968; BGMRHN, 1988) in two upward-coarsening packages (Yao et al., 2014b).

Details of regional stratigraphy and sampling lithology for the other sections can be found in published literature: the Baiyun–Yunkai section, group 1 (Yu et al., 2008, 2010); the Quzhou section, subgroup 2-1 (Xu et al., 2012; Li et al., 2013b); the Chongyi–Shaoguan sections, subgroup 2-2 (Wang et al., 2010; Wu et al., 2010; Yao

et al., 2011, 2014a). Some of the samples (Yu et al., 2008, 2010; Wang et al., 2010; Yao et al., 2011) were collected from areas adjacent to the published stratigraphic columns with correlatable lithostratigraphic sections.

5.3 Analytical Methods

5.3.1 Sample preparation

Mineral separation was conducted at the Institute of Hebei Regional Geology and Mineral Survey in Langfang, China. Zircon crystals were extracted from bulk-rocks using standard density and magnetic separation techniques. Zircon grains were hand-picked under a binocular microscope, and cast in epoxy mounts together with zircon U–Pb standards 91500 and Plešovice, followed by polishing to section the crystals in half. All zircon grains were imaged in transmitted and reflected light as well as cathodoluminescence (CL) to better reveal their internal structures.

5.3.2 Zircon U–Pb geochronology

5.3.2.1 LA-ICP-MS U–Pb dating

Detrital zircon U–Pb analyses on all samples (except 10GD83-1) were carried out using LA-ICP-MS facilities at the Institute of Geology and Geophysics (IGG), Chinese Academy of Sciences (CAS), and the Institute of Earth Science in China University of Geosciences (CUG-Beijing). When using the IGG LA-ICP-MS facility, external zircon standards 91500 with $^{207}U/^{206}Pb$ age of 1065.4 ± 0.6 Ma (Wiedenbeck et al., 1995, 2004) and GJ-1 with $^{206}U/^{238}Pb$ age of 608.5 ± 0.4 Ma (Jackson et al., 2004) were employed to calibrate U–Th–Pb ratios of unknown zircon grains. Glass NIST 610 was used for U/Th ratio determination. The detailed analytical procedure followed that in Xie et al. (2008). When using the CUG-Beijing LA-ICP-MS facility, we used zircon 91500 as an external standard for measuring U–Th–Pb concentrations. Zircons TEMORA with $^{206}U/^{238}Pb$ age of 416.8 ± 1.1 Ma (Black et al., 2003) and Plešovice with $^{206}U/^{238}Pb$ age of 337.1 ± 0.4 Ma (Sláma et al., 2008) were used as additional standards for monitoring the element measurements and age calculations.

Table 5.1. Summary of provenance analysis samples reported in this study and from previous work, including sample names, locations, lithologies and stratigraphic ages

Samples	Location	Latitude (N), Longitude (E)	Lithology	Stratigraphic age	Data source
Sample Group 1: Uppermost Neoproterozoic strata inside the Wuyi–Yunkai orogenic core (Baiyun-Yunkai area)					
XW-12	Xunwu	24°11′44″, 115°28′27″	fine-grained biotite gneiss	Ediacaran	Yu et al. (2010)
XN-2	Longchuan	25°02′15″, 115°15′44″	biotite-plagioclase gneiss	Ediacaran	Yu et al. (2010)
NX-3-2	Tanxi, Heyuan	25°14′11″, 114°11′17″	fine-grained biotite gneiss	Ediacaran	Yu et al. (2008)
ZC-8	Zengcheng	23°16′24″, 113°48′23″	banded migmatite	Ediacaran	Yu et al. (2008)
ZC-6	Zengcheng	23°21′32″, 113°51′25″	biotite gneiss	Ediacaran	Yu et al. (2008)
YK-27	Luoding	22°43′52″, 111°14′18″	biotite-plagioclase gneiss	Ediacaran	Yu et al. (2010)
Sample Group 2: Lower Paleozoic strata outside the Wuyi–Yunkai orogenic core					
Subgroup 2-1: Quzhou area					
11QZ-1	Quzhou		coarse-grained sandstone	Upper Silurian	Xu et al. (2012)
11QZ-3	Quzhou		fine-grained sandstone	Middle Silurian	Xu et al. (2012)
11QZ-5	Quzhou		fine-grained sandstone	Lower Silurian	Xu et al. (2012)
11QZ-6	Quzhou		fine-grained sandstone	Lower Silurian	Xu et al. (2012)
JS01	Danyang, Jiangsu	31°47'01.0", 119°18'35.3"	sandstone	Lower Silurian	Li et al. (2013)
S01-2	Danyang, Jiangsu	31°44'23.8", 119°18'55.4"	sandstone	Lower Silurian	Li et al. (2013)
S16-1	Nanjing, Jiangsu	32°03'21.5", 118°59'36.3"	sandstone	Lower Silurian	Li et al. (2013)
S15-1	Anji, Zhejiang	30°36'42.5", 119°31'51.9"	sandstone	Lower Silurian	Li et al. (2013)
S14-2	Anji, Zhejiang	30°36'00.6", 119°32'01.2"	sandstone	Lower Silurian	Li et al. (2013)
S09-1	Fuyang, Zhejiang	29°56'02.2", 119°49'42.3"	sandstone	Upper Ordovician	Li et al. (2013)
S08-1	Fuyang, Zhejiang	29 55'53.6", 119°49'49.0"	sandstone	Upper Ordovician	Li et al. (2013)
11QZ-7	Quzhou		siltstone	Upper Ordovician	Xu et al. (2012)
11QZ-8	Quzhou		siltstone	Upper Ordovician	Xu et al. (2012)
Subgroup 2-2: Chongyi and Shaoguan areas					
J191	Jinggangshan	26°30′54″, 114°12′31″	fine-medium meta-sandstone	Middle Ordovician	Wu et al. (2010)

JX-25	Guopu, Chongyi	25°43′36″, 114°13′43″	grey fine sandstone	Middle Ordovician	Wang et al. (2010)
JX-32	Guanting, Chongyi	25°36′15″, 114°05′04″	grey fine sandstone	Middle Ordovician	Wang et al. (2010)
JX-4	Shikou, Yongxin	26°48′37″, 114°00′22″	quartz sandstone	Middle Ordovician	Wang et al. (2010)
JX-8	Shikou, Yongxin	26°48′37″, 114°00′22″	grey fine sandstone	Middle Ordovician	Wang et al. (2010)
960	Tianluoniu, Chongyi	25°45′03″, 114°07′29″	coarse quartz sandstone	Middle Ordovician	Yao et al. (2011)
960-1	Tianluoniu, Chongyi	25°45′03″, 114°07′29″	coarse quartz sandstone	Middle Ordovician	Yao et al. (2011)
960-2	Tianluoniu, Chongyi	25°45′03″, 114°07′29″	coarse quartz sandstone	Middle Ordovician	Yao et al. (2011)
950	Guopu, Chongyi	25°45′20″, 114°11′51″	coarse-grained arkose	Lower Ordovician	Yao et al. (2011)
950-1	Guopu, Chongyi	25°45′20″, 114°11′51″	coarse-grained arkose	Lower Ordovician	Yao et al. (2011)
950-2	Guopu, Chongyi	25°45′20″, 114°11′51″	coarse-grained arkose	Lower Ordovician	Yao et al. (2011)
JX-12	Xiache, Jinggangshan	26°25′15″, 114°13′48″	grey fine sandstone	Upper Cambrian	Wang et al. (2010)
J192	Jinggangshan	26°27′16″, 114°12′49″	fine-medium meta-sandstone	Upper Cambrian	Wu et al. (2010)
J186	Yongxin	26°49′37″, 114°37′16″	fine-medium meta-sandstone	Middle Cambrian	Wu et al. (2010)
J188	Yongxin	26°48′50″, 114°26′16″	fine-medium meta-sandstone	Middle Cambrian	Wu et al. (2010)
J200	Dayu	25°24′27″, 114°18′36″	fine-medium meta-sandstone	Lower Cambrian	Wu et al. (2010)
HU-48	Shuishi, Ningyuan	25°24′59″, 111°54′53″	grey fine sandstone	Middle Ordovician	Wang et al. (2010)
10GD19	Zhoutian, Renhua	25°01′46″, 113°48′45″	grey-black fine sandstone	Upper Cambrian	Yao et al. (2014)
10GD17	Zhoutian, Renhua	25°01′28″, 113°48′12″	grey-white fine sandstone	Middle Cambrian	Yao et al. (2014)
10GD16	Zhoutian, Renhua	25°01′20″, 113°47′56″	grey siltstone	Middle Cambrian	Yao et al. (2014)
HU-46	Shuishi, Ningyuan	25°24′01″, 111°54′06″	grey fine sandstone	Middle Cambrian	Wang et al. (2010)
HU-54	Baishui, Guiyang	26°05′53″, 112°21′43″	grey fine sandstone	Middle Cambrian	Wang et al. (2010)
JX-16	Penzhu, Suichuan	26°21′43″, 114°27′09″	grey fine sandstone	Lower Cambrian	Wang et al. (2010)
HU-37	Reshui, Rucheng	25°32′47″, 113°51′50″	grey fine sandstone	Lower Cambrian	Wang et al. (2010)
Subgroup 2-3: Yulin and Nanning areas					
10GD60	Xinrong, Beiliu	22°46′14″, 110°26′43″	fine sandstone	Mid-Upper Silurian	This study
10GD58	Xinrong, Beiliu	22°40′18″, 110°28′24″	grey-yellow fine sandstone	Mid-Upper Silurian	This study
10GD56	Xinrong, Beiliu	22°39′03″, 110°29′45″	grey-white sandstone	Lower Silurian	This study
10GD51	Botang, Cenxi	23°06′16″, 110°49′21″	grey-white sandstone	Upper Ordovician	This study

10GD52-1	Botang, Cenxi	23°04′58″, 110°48′42″	grey quartz fine sandstone	Middle Ordovician	This study
10GD54	Botang, Cenxi	23°02′53″, 110°50′36″	purple mica siltstone	Middle Ordovician	This study
10GD45	Liuchen, Pingnan	23°15′25″, 110°19′45″	purple quartz fine sandstone	Lower Ordovician	This study
10GD38-1	Madong, Guiping	23°06′00″, 110°09′43″	grey-white siltstone	Lower Ordovician	This study
10GD41	Madong, Guiping	23°05′28″, 110°10′02″	grey-white siltstone	Lower Ordovician	This study
10GD42-1	Madong, Guiping	23°05′05″, 110°10′00″	grey-white siltstone	Lower Ordovician	This study
10GD37	Madong, Guiping	23°02′57″, 110°13′23″	grey-white siltstone	Upper Cambrian	This study
11FS-11	Nanning		pale-green sandstone	Upper Cambrian	Xu et al. (2014)
11FS-6	Nanning		pale-green sandstone	Middle Cambrian	Xu et al. (2014)
11FS-3	Nanning		pale-green sandstone	Lower Cambrian	Xu et al. (2014)
11FS-1	Nanning		pale-green sandstone	Lower Cambrian	Xu et al. (2014)
Sample Group 3: Lower Paleozoic strata in the Wuyi–Yunkai fold-and-thrust system (Dongkou area)					
10GD85	Yuexi, Dongkou	27°05′01″, 110°30′37″	grey-green fine sandstone	Upper Silurian	This study
10GD84	Yuexi, Dongkou	27°06′34″, 110°29′01″	grey-green fine sandstone	Lower Silurian	This study
10GD83-1	Yuexi, Dongkou	27°07′27″, 110°28′02″	grey-green siltstone	Mid-Upper Ordovician	This study
Sample Group 4: Lower Paleozoic strata in the remnant lower Paleozoic foreland Basin (Zhangjiajie area)					
10GD87	Wentang, Zhangjiajie	29°11′27″, 110°10′14″	grey-green quartz sandstone	Upper Silurian	This study
10GD88	Wentang, Zhangjiajie	29°10′47″, 110°10′27″	grey quartz sandstone	Middle Silurian	This study
HG-46	Xiangyang, Longshan	29°15′13″, 109°34′31″	purple fine sandstone	Middle Silurian	Wang et al. (2010)
HG-45	Xiangyang, Longshan	29°15′14″, 109°34′28″	purple fine sandstone	Middle Silurian	Wang et al. (2010)
G-26a	Wentang, Zhangjiajie	29°11′27″, 110°10′13″	grey sandstone	Middle Silurian	Wang et al. (2010)
HG-32	Xiaoxi, Sangzhi	29°22′15″, 110°14′18″	grey fine sandstone	Lower Silurian	Wang et al. (2010)
HG47	Xiangyang, Longshan	29°14′55″, 109°34′44″	grey pelitic siltstone	Lower Silurian	Wang et al. (2010)
HG-65	Pingpo, Xupu	27°54′57″, 110°51′05″	grey siltstone	Lower Silurian	Wang et al. (2010)
E-300	Muzi, Anhua	28°06′53″, 111°20′53″	grey siltstone	Lower Silurian	Wang et al. (2010)

The detailed analytical procedure follows that in Song et al. (2010). The ablation pits on zircon grains in both labs were generally ~36 μm in diameter and 20–30 μm in depth. Data reduction was carried out using Glitter v4.0 (Van Achterbergh et al., 2001), ComPbCorr#3_151 (Anderson, 2002) and Isoplot/Ex v2.49 (Ludwig, 2001a) packages. The U–Pb age data of zircon LA-ICP-MS analyses are presented in Appendix C1.

5.3.2.2 SHRIMP U–Pb dating

Detrital zircon U–Pb analyses on sample 10GD83-1 were carried out in John de Laeter Centre at Curtin University, Australia, using the Sensitive High Resolution Ion MicroProbe (SHRIMP) facility. Standard operation conditions of 2 nA O_2^- primary beam, 20 μm spot size and *ca.* 5000 mass resolution were followed, and five scans were made for each age determination. U abundance was calibrated using zircon standard BR266 (Stern, 2001), and $^{206}Pb/^{238}U$ ratio was constrained by zircon standard Plešovice (Sláma et al., 2008). The detailed analytical procedure follows that of Williams (1998). Data reduction was carried out using Squid v2.50 (Ludwig, 2001b) and Isoplot/Ex v2.49 (Ludwig, 2001a) packages. The U–Pb age data of SHRIMP analyses on sample 10GD83-1 can also be found in Appendix C1.

5.3.3 Zircon Hf isotopic analyses

Laser ablation zircon Hf isotopic analyses for selected samples in the Yulin section (Figure 5.2) were carried out at IGG–CAS, using a ThermoFinnigan Neptune MC-ICP-MS equipped with a 193 nm laser. Zircon 91500 and GJ-1 were used as reference standards, with a recommended $^{176}Hf/^{177}Hf$ ratio of 0.282307 ± 0.000031 (2σ) (e.g., Wu et al., 2006) and 0.282000 ± 0.000005 (2σ) (Morel et al., 2008), respectively. Laser ablation Hf sites were centered as close as possible to the spot for U–Pb dating, with spot sizes of 60 μm in diameter and 45 μm in depth. More details on analytical and calibration procedures can be found in Wu et al. (2006). A decay constant for ^{176}Lu of $1.865 \pm 0.015 \times 10^{-11}$/year (Scherer et al., 2001), the present-day chondritic ratios of $^{176}Hf/^{177}Hf = 0.282772$ and $^{176}Lu/^{177}Hf = 0.0332$ (Blichert-Toft and Albarède, 1997) were accepted for calculating $\varepsilon_{Hf}(t)$ values. One-stage model ages (T_{DM}) were calculated relative to depleted mantle with a present-day

$(^{176}Hf/^{177}Hf)_{DM}$ = 0.28325 and $(^{176}Lu/^{177}Hf)_{DM}$ = 0.0384 (Griffin, et al., 2000). Two-stage model ages (T_{DM}^{2}) were calculated by forcing a growth-curve through the zircon initial ratio with an assumed $(^{176}Lu/^{177}Hf)_{C}$ value of 0.0093 corresponding to the upper continental crust (Amelin et al., 1999). The Hf isotopic data of samples from the Yulin section are listed in Appendix C2.

5.4 Analytical Results

Zircon U–Pb ages of individual zircon grains are plotted in Figures 5.3–5.5, zircon $\varepsilon_{Hf}(t)$ results are plotted in Figure 5.6, and relatively probability plots of detrital zircon U–Pb ages are plotted in Figure 5.7.

5.4.1 Zircon U–Pb ages

5.4.1.1 Cambrian–Silurian samples in sungroup 2-3

Upper-Cambrian sample 10GD37 is a pale-white siltstone from the Yulin section (Figure 5.2). One hundred and twenty U–Pb spots were analyzed on 120 zircon grains, of which 119 analyses are concordant (Figure 5.3a). The concordant U–Pb ages range from 480 Ma to 3050 Ma, with a majority falling in clusters of 610–490 Ma and 1100–800 Ma (Figure 5.7). The five youngest grains give a weighted mean $^{206}Pb/^{238}U$ age of 496 ± 8 Ma (Figure 5.3a).

Four lower-Ordovician samples are from the Yulin section, with three pale-white siltstones (10GD42-1, 10GD41 and 10GD38-1) and a brick-red quartz fine-grained sandstone (10GD45) (Figure 5.2). Four hundred and fifty-nine U–Pb spots were analyzed on 459 zircon grains, of which 453 analyses are concordant (Figure 5.3b-e). The concordant ages range from 480 Ma to 3450 Ma, but the majority fall in clusters of 610–490 Ma and 1100–800 Ma (Figure 5.7). The 19 youngest grains give a weighted mean $^{206}Pb/^{238}U$ age of 515 ± 7 Ma for sample 10GD42-1 (Figure 5.3b), and five youngest grains in sample 10GD41 give a weighted mean age of 503 ± 7 Ma (Figure 5.3c). While five youngest grains give a weighted mean age of 501 ± 7 Ma for sample 10GD38-1 (Figure 5.3d), and one youngest grain gives a $^{206}Pb/^{238}U$ age of 499 ± 7 Ma for sample 10GD45 (Figure 5.3e).

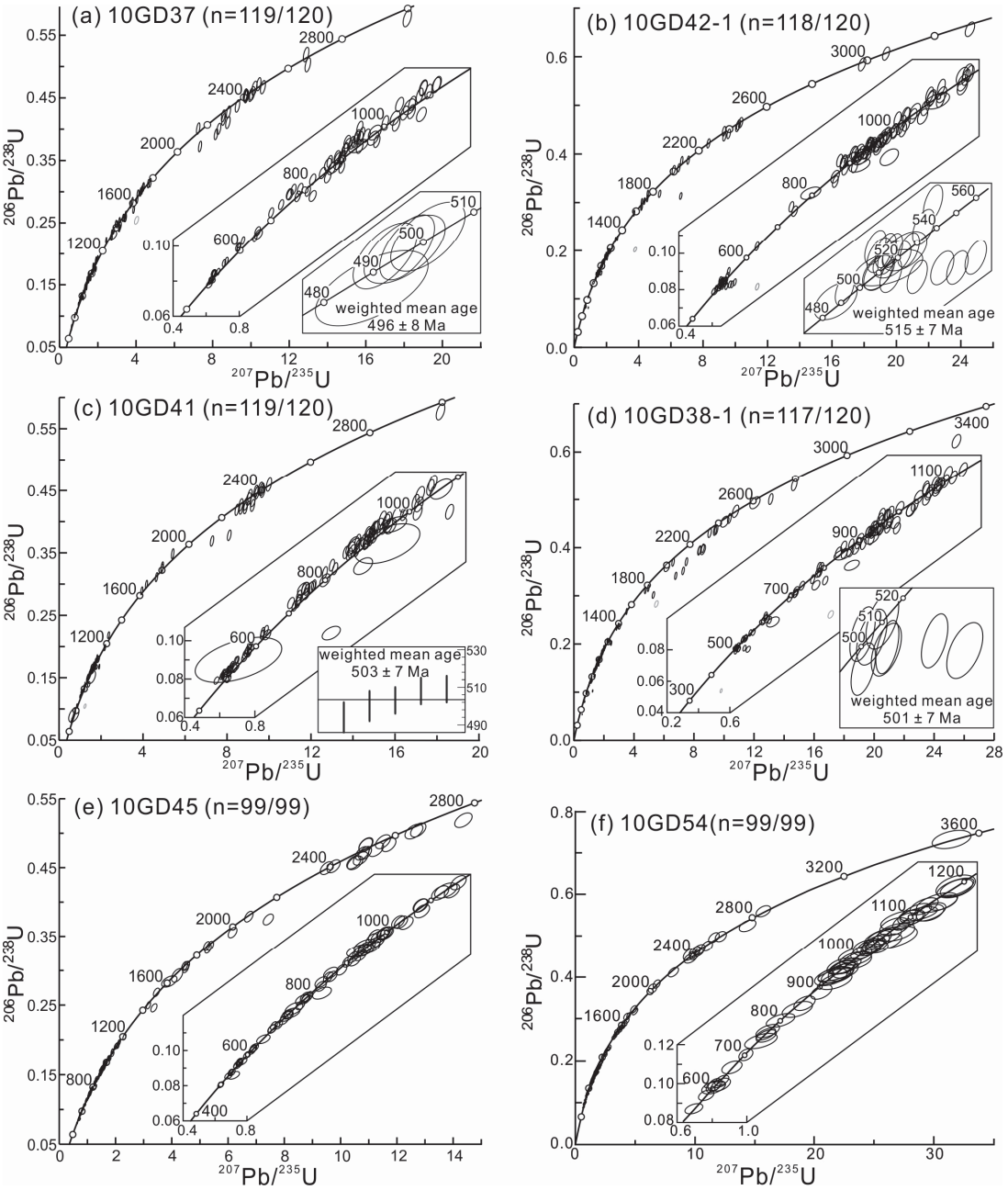

Figure 5.3. LA-ICP-MS zircon U–Pb Concordia age plots of Cambrian to Ordovician clastic samples from the Yulin section. "n = 119/120" indicates the number of concordant ages and number of total analyses, with concordance cut-off level is et at 90% – 110%. Ages are shown with 1σ uncertainties. The same applied to Figures 5.4 and 5.5.

Two mid-Ordovician samples 10GD54 (a purple mica–quartz siltstone) and 10GD52-1 (a grey fine-grained quartz sandstone) are from the Yulin section (Figure 5.2). One hundred and ninety-nine U–Pb spots were analyzed on 199 zircon grains for these two samples, of which 197 analyses are concordant (Figures 5.3f and 5.4a). The concordant ages range from 525 Ma to 3520 Ma, but the majority fall in clusters of 700–490 Ma and 1100–800 Ma (Figure 5.7). The youngest grain gives a $^{206}Pb/^{238}U$

age of 539 ± 10 Ma for sample 10GD54, and two youngest grains in sample 10GD52-1 give a weighted mean $^{206}Pb/^{238}U$ age of 527 ± 7 Ma.

Upper-Ordovician sample 10GD51 is a grey-white, coarse-grained sandstone from the Yulin section (Figure 5.2). One hundred U–Pb spots were analyzed on 100 zircon grains, of which 99 analyses are concordant (Figure 5.4b). The concordant ages range from 510 Ma to 3170 Ma, but the majority fall in clusters of 700–500 Ma and 1100–900 Ma (Figure 5.7). The three youngest grains give a weighted mean $^{206}Pb/^{238}U$ age of 512 ± 8 Ma (Figure 5.4b).

Lower-Silurian sample 10GD56 is a coarse-grained sandstone from the Yulin section (Figure 5.2). One hundred U–Pb concordant ages were obtained from 100 zircon grains. A small group of 25 analyses gives an age range of 490 Ma to 2800 Ma (Figure 5.7), whereas the dominant 75 concordant analyses yield a weighted mean $^{206}Pb/^{238}U$ age of 437 ± 6 Ma (MSWD = 0.66) and a concordia age of 436 ± 6 Ma (MSWD of concordance = 0.66) (Figure 5.4c). All the 75 analyses gave Th/U ratios of 0.1–1.1 (Appendix C1), suggesting a likely magmatic origin. The hand specimen is grey-white in colour, fine-grained and high in plagioclase. Thin-section of the sample exhibits abundant euheral quartz and plagioclase. Therefore, sample 10GD56 is taken as tuffaceous sandstone with a crystallization age of *ca.* 435 Ma, probably corresponding to a Silurian magmatic event (Yao et al., 2012).

Mid- to upper-Silurian samples 10GD58 and 10GD60 are two pale-yellow, fine-grained sandstones from the Yulin section (Figure 5.2). Two hundred U–Pb spots were analyzed on 200 zircon grains, all of which are concordant (Figure 5.4d-e). The concordant ages range from 440 Ma to 3730 Ma, but the majority fall in clusters of 610–430 Ma and 1100–800 Ma (Figure 5.7). The three youngest grains in sample 10GD58 give a weighted mean $^{206}Pb/^{238}U$ age of 512 ± 8 Ma, and the youngest grain in sample 10GD60 gives a $^{206}Pb/^{238}U$ age of 446 ± 7 Ma.

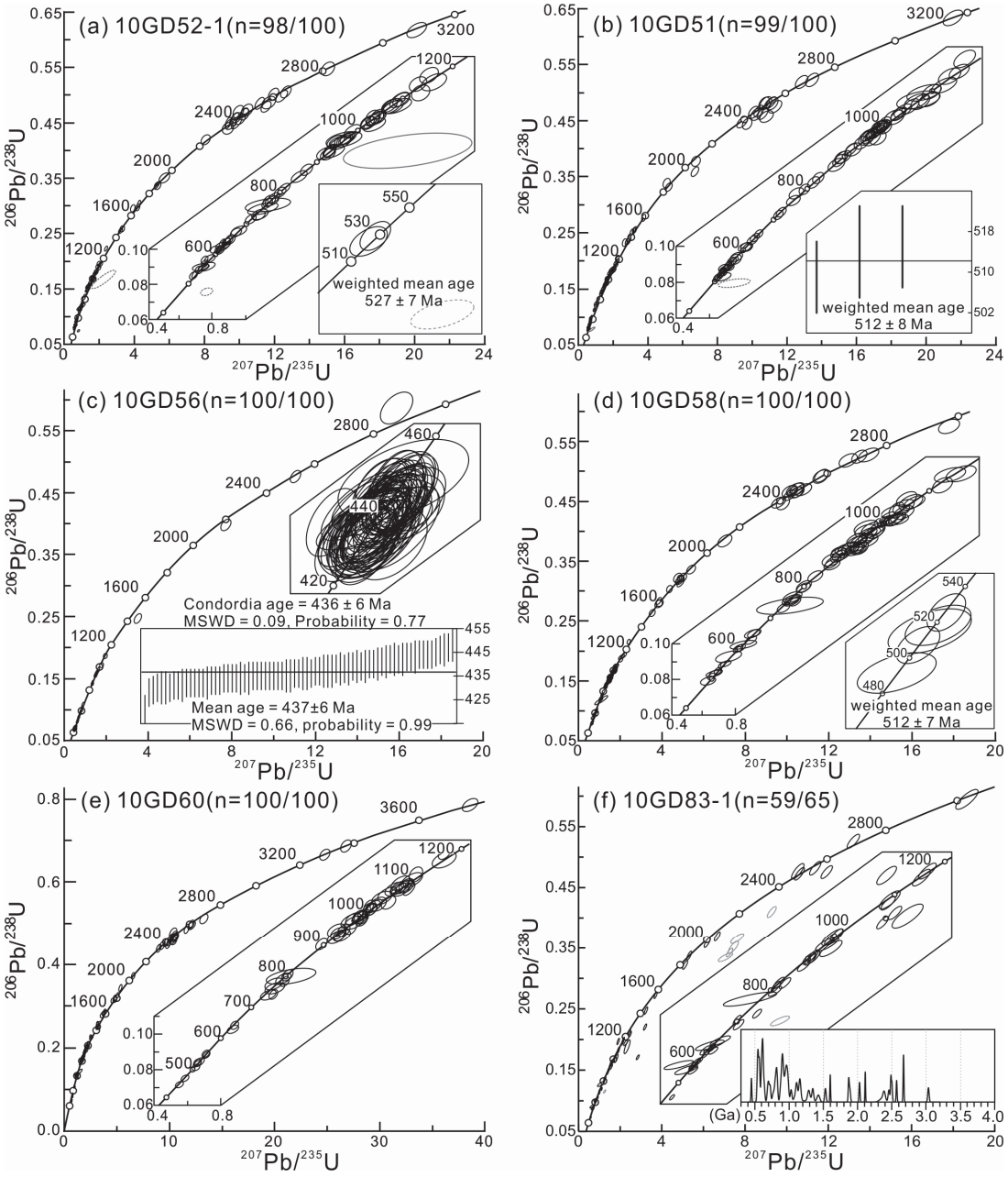

Figure 5.4. LA-ICP-MS zircon U–Pb Concordia age diagrams of Ordovician–Silurian clastic samples from the Yulin section (a-e), and SHRIMP zircon U–Pb Concordia age diagram of an Ordovician clastic sample from the Dongkou section (f).

5.4.1.2 Ordovician–Silurian samples in group 3

Mid- to upper-Ordovician sample 10GD83-1 is a pale-green siltstone from the Dongkou section (Figure 5.2). Sixty-five U–Pb spots were analyzed on 65 zircon grains, of which 59 analyses are concordant. The concordant ages range from 450 Ma to 3035 Ma, and form two clusters of 650–500 Ma and 1000–850 Ma in similar probabilities (Figure 5.4f). The youngest grain gives a $^{206}Pb/^{238}U$ age of 446 ± 7 Ma,

and the oldest grain yields an age of 3.0 Ga.

Lower-Silurian sample 10GD84 is a pale-green sandstone from the Dongkou section (Figure 5.2). One hundred U–Pb spots were analyzed on 100 zircon grains, of which 99 analyses are concordant. The concordant ages range from 430 Ma to 3560 Ma, and form two clusters of 850–750 Ma and 1100–960 Ma in similar probabilities (Figure 5.5a). The two youngest grains give a weighted mean $^{206}Pb/^{238}U$ age of 436 ± 6 Ma, and two oldest grains yield an average age of 3.5 Ga (Figure 5.5a).

Mid- to upper-Silurian sample 10GD85 is a pale-green sandstone from the Dongkou section (Figure 5.2). One hundred U–Pb spots were analyzed on 100 zircon grains, all of which are concordant. The concordant ages range from 430 Ma to 3180 Ma, and form a broad population of 1200–850 Ma (Figure 5.5b). The youngest grain gives a $^{206}Pb/^{238}U$ age of 431 ± 6 Ma, and two oldest grains yield an average age of 3.0 Ga (Figure 5.5b).

5.4.1.3 Silurian samples in group 4

Mid-Silurian sample 10GD88 is a grey quartz sandstone from the Zhangjiajie section (Figure 5.2). One hundred U–Pb spots were analysed on 100 zircon grains, of which 98 analyses are concordant. The concordant ages range from 520 Ma to 2840 Ma, with a large population of 1100–900 Ma (Figure 5.5c). The youngest grain gives a $^{206}Pb/^{238}U$ age of 517 ± 8 Ma, and two oldest concordant grains yield an average age of 2.8 Ga.

Upper-Silurian sample 10GD87 is a pale-green quartz sandstone from the Zhangjiajie section (Figure 5.2). One hundred U–Pb spots were analyzed on 100 zircon grains, of which 96 analyses are concordant. The concordant ages range from 515 Ma to 3200 Ma, and form clusters of 700–500 Ma, 850–720 Ma, 1100–900 Ma, 1850–1600 Ma and 2600–2450 Ma (Figure 5.5d). The two youngest grains give a weighted mean $^{206}Pb/^{238}U$ age of 520 ± 7 Ma, and four oldest grains yield an average age of 3.1–3.0 Ga (Figure 5.5d).

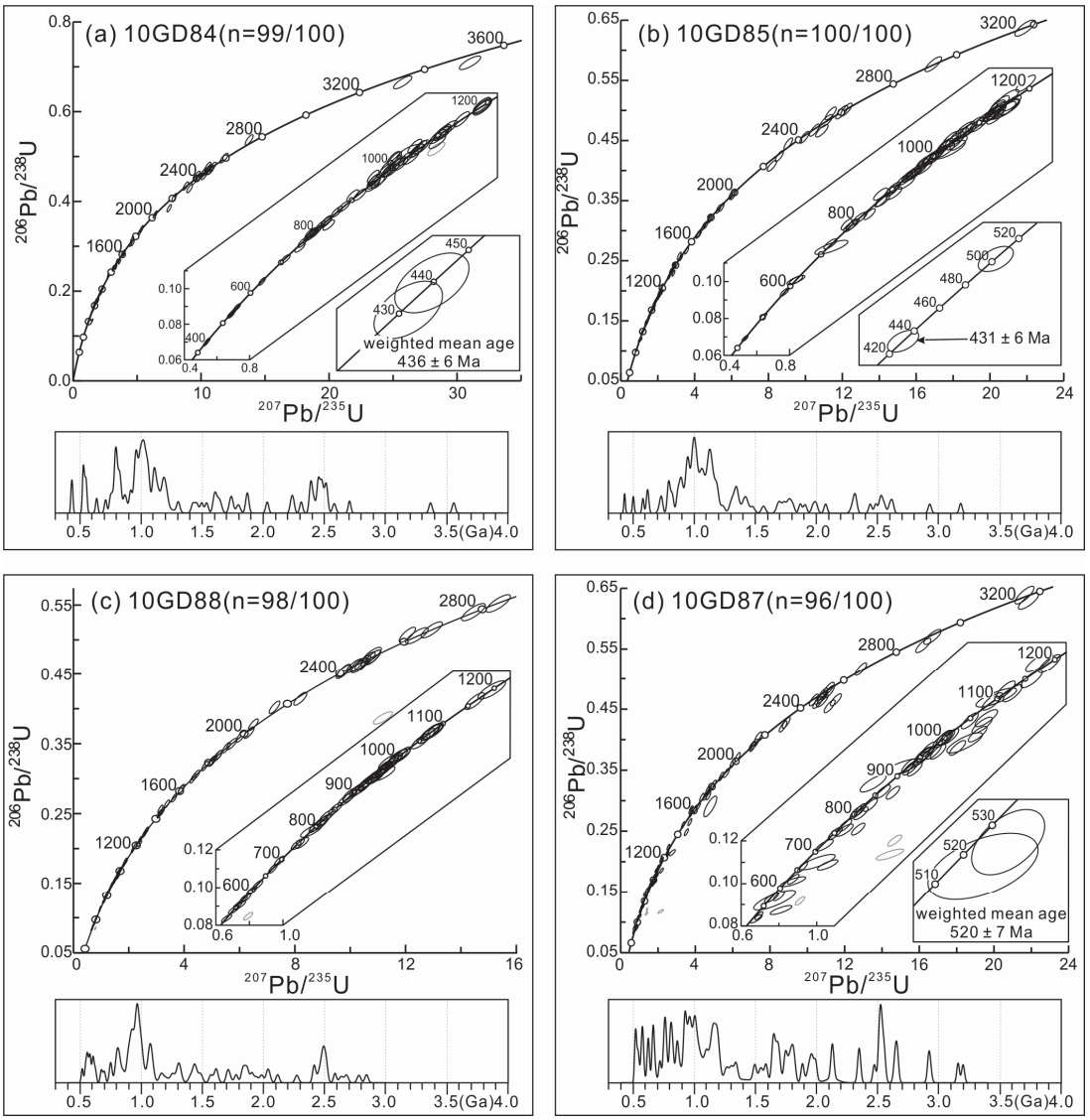

Figure 5.5. LA-ICP-MS zircon U–Pb Concordia age diagrams and relative probability plots of Silurian clastic samples from the Dongkou and Zhangjiajie sections.

5.4.2 Zircon Lu–Hf isotopes

5.4.2.1 Cambrian sample in subgroup 2-3

In situ Hf isotopic analyses were conducted on a total of 119 dated detrital zircons from the upper-Cambrian sample (10GD37) of the Yulin section. The zircons yielded variable $^{176}Hf/^{177}Hf$ ratios (0.280763–0.282476) and $\varepsilon_{Hf}(t)$ values (–40 to +22). Apart from two zircons with ages of 2.27 Ga and 2.45 Ga, all others plot below the new continental crust line (Figure 5.6a).

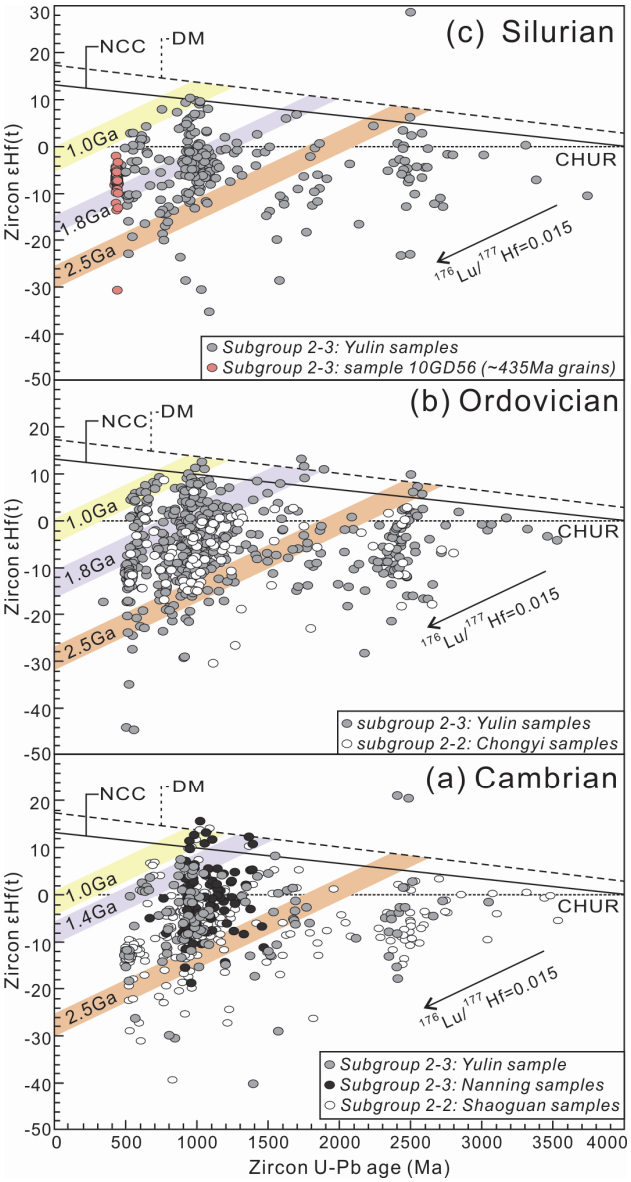

Figure 5.6. Plots of zircon $\varepsilon_{Hf}(t)$ values versus U–Pb ages from (a) Cambrian, (b) Ordovician and (c) Silurian sandstone samples in the Nanhua foreland basin. Data sources for published Hf isotopic data: (a) Xu et al. (2014); Yao et al. (2014a); (b) Yao et al. (2011). The depleted mantle (DM) and new continental crust (NCC) evolution lines were extrapolated after Griffin et al. (2000) and Dhuime et al. (2011), respectively.

5.4.2.2 Ordovician samples in subgroup 2-3

Five Ordovician samples (10GD42-1, 10GD41, 10GD38-1, 10GD54 and 10GD51) from the Yulin section were selected for Hf isotopic analyses, and a total of 516 detrital zircons with concordant U–Pb ages were analysed. The zircons yielded variable $^{176}Hf/^{177}Hf$ ratios (0.280433–0.282607) and $\varepsilon_{Hf}(t)$ values (–45 to +21) (Figure 6b). Five zircons with ages of 2.9–1.7 Ga plot above the depleted mantle line, and eight zircons with ages of 2.9–1.0 Ga plot between the depleted mantle and new

continental crust lines. The remaining 503 zircons plot below the new continental crust line, with 74% of them yielding negative $\varepsilon_{Hf}(t)$ values (Figure 6b).

5.4.2.3 Silurian samples in subgroup 2-3

Hf isotopic analyses were carried out on a total of 300 detrital zircons in three Silurian samples (10GD56, 10GD58 and 10GD60) from the Yulin section. Zircons giving the predominant Silurian ages (~435 Ma) in sample 10GD56 exhibit negative $\varepsilon_{Hf}(t)$ values (–31 to –2) and Hf model ages of 1.14–2.26 Ga with a dominant model age of 1.33 Ga (Figure 6c). Zircons with pre-Silurian ages in this sample, together with 200 analyses of the other two samples, yielded variable $^{176}Hf/^{177}Hf$ ratios (0.280153 – 0.282542) and $\varepsilon_{Hf}(t)$ values (–35 to +29). All analyses are plotted below the depleted mantle line, except for one with an age of 2.5 Ga (Figure 6c).

5.5 Discussions

5.5.1 Sources of Cambrian–Silurian sediments in the southern part of the early Nanhua foreland basin

Samples from the Nanning–Yulin region (subgroup 2-3) cover the entire Cambrian–Silurian strata in the southern part of the early Nanhua foreland basin (Figure 5.2). Except for the tuffaceous sample (10GD56), all other 14 samples share similar zircon age spectra, ranging from Archean to Palaeozoic (Figure 5.7). These samples commonly consist of a prominent 1100–900 Ma population, a subordinate 650–490 Ma population, a moderate 850–700 Ma population, and minor 2500 Ma and 2000–1300 Ma populations. The major populations of 1100–900 Ma and 650–490 Ma indicate that the source region probably underwent Grenvillian and Pan-African orogenesis, and the moderate 850–700 Ma population implies that it possibly experienced Cryogenian magmatism during the Rodinia break-up. The minor age peaks of 2500 Ma and 2000–1300 Ma are indicative of possible Archean basement and Palaeo- to Mesoproterozoic magmatism in the source area(s) (Figure 5.7). We performed the Kolmogorov–Smirnov (K–S) test to determine whether these 14 samples shared a same provenance. A probabilities (p values) > 0.05 indicate the provenance of paired samples cannot be distinguished at a 95% confidence level

(Press et al., 1986; Berry et al., 2001). The results show that a majority of *p* values are greater than 0.05, with an average value of 0.468 (Table 5.2), indicating that most Cambrian–Silurian samples likely had a common provenance. The lower Ordovician sample 10GD41 yields only two out of fourteen *p* values larger than 0.05 when pairing with others, probably due to its larger percentage of younger grains (Figure 5.7).

Common provenance for the Cambrian–Silurian samples indicates that these detritus were likely transported continuously from a same source region. Alternatively, younger sediments may have involved recycled detritus from local older sediments. The following evidence suggest that Ordovician–Silurian sediments were probably at least partly derived from recycled detritus of local Ediacaran–Cambrian strata. (1) The early Palaeozoic palaeogeography suggests that the southeastern South China started to uplift from the early Ordovician (Figure 5.8d), and the uplift spread to much of the Cathaysia Block by the Silurian (Figure 5.8e-f) (Liu and Xu, 1994, Liu et al., 1995); (2) Conglomeratic units in both the lower Ordovician and Silurian strata in the Yulin section (Figure 5.2) indicate a proximal detrital source within the Cathaysia Block (Yao et al., 2014b); (3) Northwest-directed palaeocurrent directions in the Yulin Ordovician strata indicate that detritus were probably transported from the southeast (BGMRGX, 1985; Liu and Xu, 1994; Yao et al., 2014b); (4) zircon U–Pb age patterns of Ordovician–Silurian samples mimic that of the Ediacaran–Cambrian samples (Figures 5.7 and 5.8).

According to the provenance, tectono-magmatic and metamorphism analysis, detritus for the Ediacaran–Cambrian sandstones in western Cathaysia likely derived from northern Indian margin and possible East African orogen – an external source outside the SCB (Yao et al., 2014a). Such a speculated external source is also supported by (1) mismatches between zircon age patterns of the Ediacaran–Cambrian samples and zircon age constitutes of Cathaysian basement rocks (Figure 5.8a-c) (e.g., Li, 1997; Wan et al., 2007; Yu et al., 2009; Li et al., 2002, 2008a, 2010a), and (2) South China in a marine setting during the Cambrian (Liu and Xu, 1994; Liu et al., 1995) which prohibits local detrital denudation but demands external clastic sources (Yao et al., 2014a).

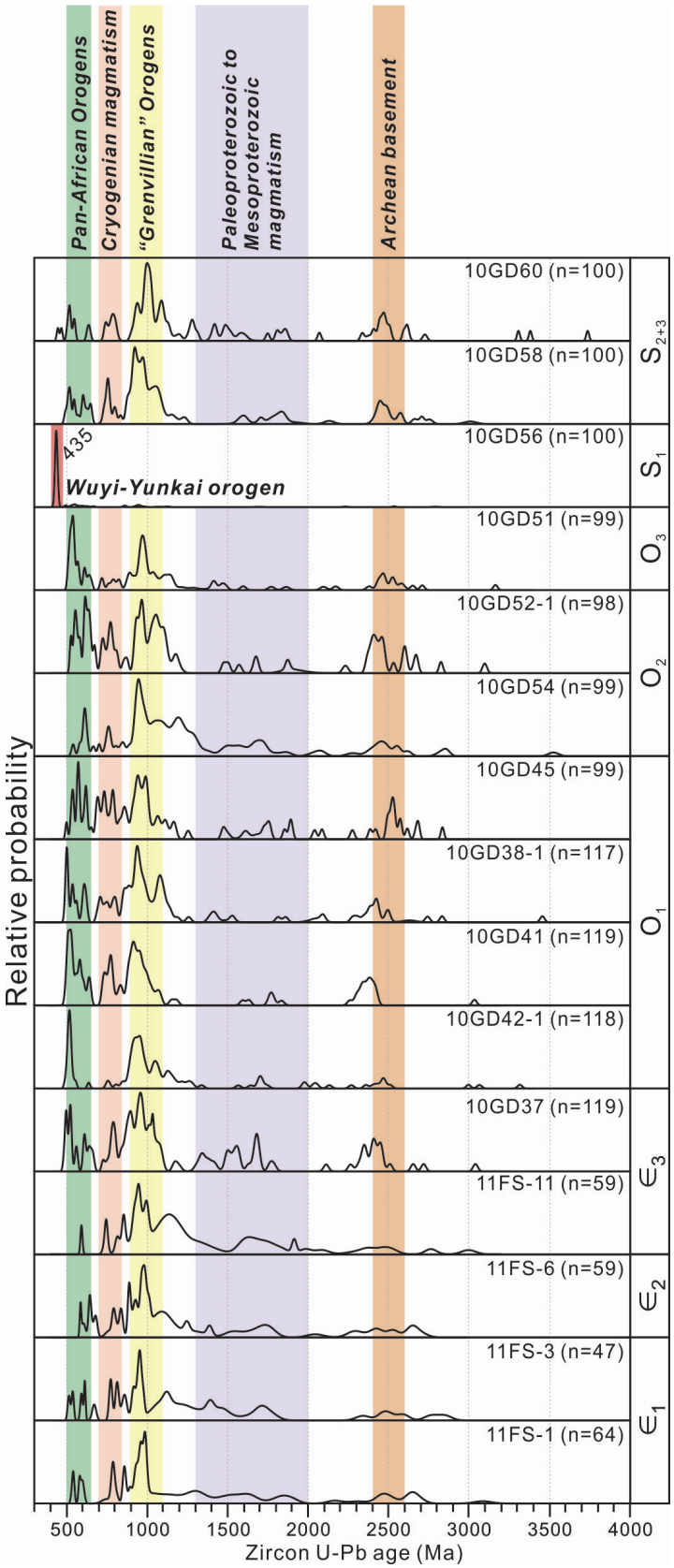

Figure 5.7. Relative probability plots of detrital zircon U–Pb ages (with concordance of 90–110%) for sample subgroup 2-3 from the Nanning–Yulin area. Samples 11FS-1, -3, -6 and -11 are from Xu et al. (2014).

Table 5.2. *P* and *D* values of two-sample Kolmogorov–Smirnov (K-S) test on the Cambrian–Silurian samples of subgroup 2-3 from the southern part of the Nanhua foreland basin

	11FS-1	11FS-3	11FS-6	11FS-11	10GD 37	10GD 42-1	10GD 41	10GD 38-1	10GD 45	10GD 54	10GD 52-1	10GD 51	10GD 58	10GD 60	
11FS-1		0.064	0.088	0.128	0.115	0.210	0.321	0.222	0.193	0.093	0.183	0.209	0.188	0.099	
11FS-3	**1.000**		0.088	0.121	0.152	0.212	0.332	0.241	0.198	0.076	0.170	0.203	0.227	0.105	
11FS-6	**0.973**	**0.987**		0.130	0.102	0.169	0.315	0.180	0.192	0.097	0.176	0.212	0.138	0.097	
11FS-11	**0.696**	**0.840**	**0.701**		0.199	0.256	0.400	0.276	0.271	0.081	0.257	0.268	0.267	0.113	
10GD37	**0.636**	**0.417**	**0.803**	**0.088**		0.162	0.212	0.137	0.107	0.163	0.098	0.124	0.109	0.183	
10GD42-1	**0.051**	**0.096**	**0.210**	0.012	**0.090**		0.231	0.107	0.159	0.212	0.132	0.133	0.101	0.219	
10GD41	0.000	0.001	0.001	0.000	0.009	0.004		0.149	0.142	0.363	0.224	0.189	0.211	0.392	
10GD38-1	0.034	0.041	**0.159**	0.005	**0.217**	**0.507**	**0.144**		0.087	0.236	0.091	0.100	0.080	0.258	
10GD45	**0.109**	**0.165**	**0.132**	0.009	**0.561**	**0.130**	**0.227**	**0.811**		0.234	0.096	0.116	0.130	0.251	
10GD54	**0.889**	**0.993**	**0.877**	**0.970**	**0.114**	0.016	0.000	0.005	0.009		0.180	0.218	0.224	0.072	
10GD52-1	**0.149**	**0.314**	**0.207**	0.015	**0.675**	**0.309**	0.009	**0.772**	**0.755**	**0.082**		0.124	0.092	0.175	
10GD51	**0.068**	**0.146**	**0.073**	0.010	**0.374**	**0.298**	0.042	**0.651**	**0.520**	0.018	**0.439**		0.143	0.232	
10GD58	**0.128**	**0.075**	**0.476**	0.010	**0.541**	**0.641**	0.016	**0.879**	**0.370**	0.014	**0.795**	**0.264**		0.218	
10GD60	**0.839**	**0.872**	**0.879**	**0.735**	**0.053**	0.011	0.000	0.002	0.004	**0.957**	**0.095**	0.009	0.018		
															D value

Zircon Hf isotopes from Cambrian samples of the Nanning–Yulin region indicate that the source region(s) likely underwent two major episodes of crustal reworking at 850–700 Ma and 650–490 Ma and three episodes of juvenile crustal growth at 2.5 Ga, 1.4 Ga and 1.0 Ga (Figure 5.6a). *Ca.* 2.5 Ga tectono-magmatic events are reported in northwestern India (Wiedenbeck et al., 1996), 1.6–1.4 Ga events in the Eastern Ghats Belt of eastern India (e.g., Mezger and Cosca, 1999; Simmat and Raith, 2008), 1.1–1.0 Ga, 880–820 Ma and 550–470 Ma in northern India (e.g., Schärer et al.,1986; Brookfield, 1993; Miller et al., 2001; Singh et al., 2002; Cawood et al., 2007; Liu et al., 2007; Cottle et al., 2009), and 680–500 Ma in the East African Orogen that was connect to northwestern India and supplied detritus during the assembly of Gondwanaland (e.g., Stern, 1994; Myrow et al., 2010 and references therein). All these regions likely contributed to the Cambrian sediments in the SCB. Although *ca.* 1.4 Ga magmatic rocks have been documented in Cathaysia (Li et al., 2002, 2008c), it is unlikely that Cathaysia was a detrital source for the Cambrian sediments since almost the entire Cathaysia Block was under seawater with no sure exposure at this time (Liu and Xu, 1994; Liu et al., 1995; Yao et al., 2014a). Hf isotopic data from the Yulin Ordovician samples suggest an additional episode of crustal growth at 1.8 Ga in the source region(s) (Figure 5.6b), indicating locally uplifted *ca.* 1.89–1.77 Ga Cathaysian basement rocks since the Ordovician (Figure 5.8d–g) (Li, 1997; Wan et al., 2007; Yu et al., 2009; Li et al., 2010a). Hf isotopic data for the Yulin Silurian samples show three episodes of juvenile crustal input at 2.5 Ga, 1.8 Ga (a small peak) and 1.0 Ga (Figure 5.6c). It indicates that Silurian sediments contained both recycled Cambrian–Ordovician rocks and old basement rocks during the Wuyi–Yunkai orogeny. The tuffaceous sandstone (10GD56), with an age (*ca.* 435 Ma) consistent with the Silurian basalts (Yao et al., 2012), likely represents a late-orogenic volcanic event during the Wuyi–Yunkai orogeny.

In summary, Cambrian sandstones in the southern part of the early Nanhua foreland basin were likely transported from northern India and adjacent continents during the assembly of Gondwanaland (Yao et al., 2014a). Ordovician sandstones probably contain both detritus recycled from local Cambrian strata and Cathaysian basement rocks uplifted during the early Wuyi-Yunkai orogeny. Silurian sandstones were mixed products of recycled Cambrian–Ordovician sediments, Cathaysian basement rocks and syn- to late-orogenic magmatic rocks.

5.5.2 Source variations of Ediacaran–Silurian sediments across the Nanhua foreland basin in time and space

The four sample groups cover seven time intervals from Ediacaran to Silurian and four different geological locations in the Nanhua foreland basin (Figure 5.8a–g). For each time interval, K–S test was conducted on pairs of samples within the same group, and the results indicate that samples within each group were homogeneous in provenance (tables not shown). Further K–S tests applied on pairs of sample groups suggest that, regardless time intervals and locations, most sample groups likely shared a common provenance (Appendix C3).

The Ediacaran–Cambrian sample groups, from both inside and outside of the Wuyi–Yunkai orogenic core, generally have a prominent population of 1100–900 Ma, subordinate populations of 850–700 Ma and 650–500 Ma, and minor populations of *ca.* 2500 Ma and 2000–1300 Ma in detrital zircon age patterns (Figure 5.8a-c). They share similar zircon U–Pb age populations and Hf isotopes with the Cambrian samples of subgroup 2-3 (section 5.5.1; Figures 5.6a and 5.7), indicating a common source supplying sediments across the southern side of the Nanhua Basin during the Ediacaran–Cambrian (e.g., Yao et al., 2014a). Because no area was subaerially exposed for the entire South China during the Ediacaran–Cambrian (Figure 5.8a–c; Wang, 1985; Liu and Xu, 1994), and the age spectra of Ediacaran–Cambrian samples do not match that of the Cathaysian crystalline basement (see section 5.5.1), an external detrital source is therefore demanded for clastic deposition over the Cathaysia Block. On the other hand, the age spectra grossly match that of similar-aged rocks in northern India (e.g., Schärer et al.,1986; Brookfield, 1993; Stern, 1994; Wiedenbeck et al., 1996; Mezger and Cosca, 1999; Miller et al., 2001; Singh et al., 2002; Cawood et al., 2007; Liu et al., 2007; Simmat and Raith, 2008; Cottle et al., 2009). We therefore interpret that the Cathaysia side of the Nanhua Basin probably shared a similar clastic source region with basins in northern India, including input from elevated northern Indian crystalline rocks (Yu et al., 2008; Xu et al., 2014; Yao et al., 2014a).

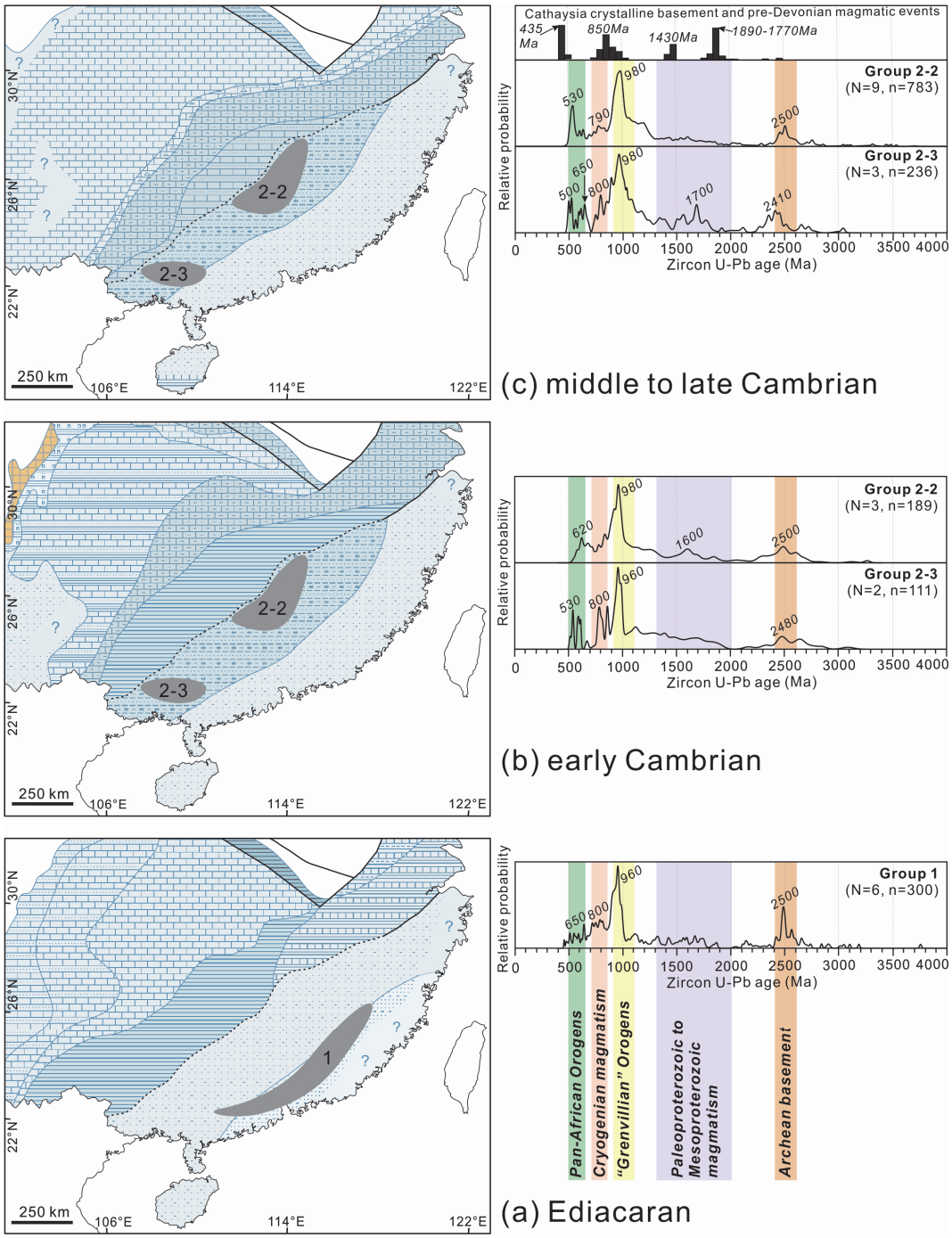

Figure 5.8. Palaeogeographic maps of South China in seven time intervals (revised after Wang, 1985; Liu and Xu, 1994) and relative probability plots of detrital zircon U–Pb ages from corresponding strata from the four sample groups: (a) – latest Neoproterozoic (Ediacaran); (b) – early Cambrian; (c) – middle to late Cambrian; (d) – early Ordovician; (e) – middle to late Ordovician; (f) – early Silurian; (g) – middle to late Silurian. U–Pb ages are within 90–110% concordance, and N = number of samples, n = numbers of concordant analyses. A compilation plot of age constitutes from Cathaysia basement rocks and pre-Devonian magmatic events is presented for provenance comparison, and the data are referred from Li, 1997, Wan et al. (2007), Li et al. (2002, 2003b, 2008a, 2008b, 2008c, 2010a), Liu et al. (2009), Yu et al., (2009), Wang et al. (2006, 2007a, 2007b; 2011), and Yao et al. (2012).

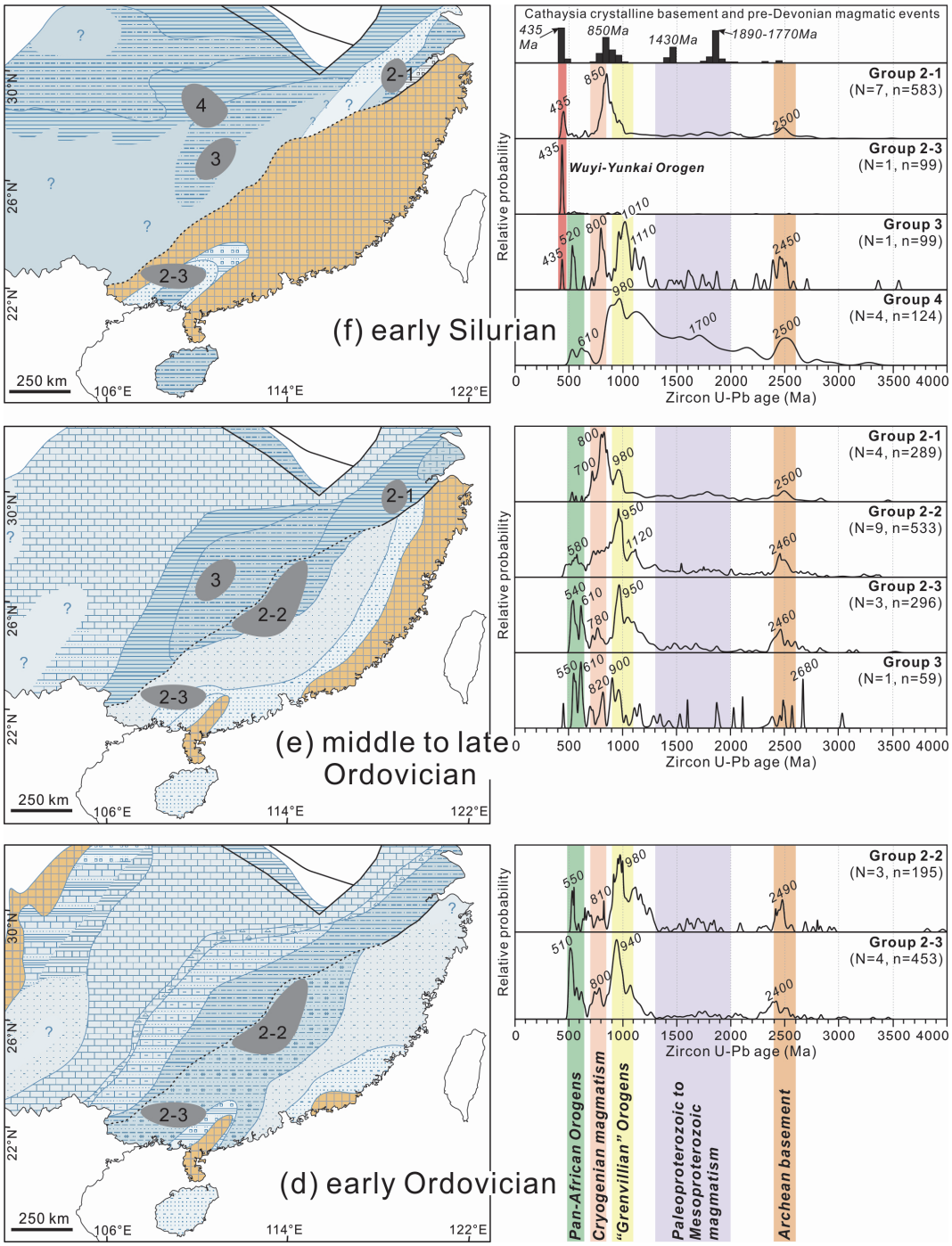

Figure 5.8. (continued-1)

Most of the Ordovician–Silurian sample groups across the Nanhua basin generally mimic zircon age patterns of the Ediacaran–Cambrian groups, showing a prominent population of 1100–900 Ma (Figure 5.8d–g). This indicates that the overall detrital composition did not change too much throughout the basin history from the Ediacaran to Silurian, which could be interpreted as either a continued sedimentary transport from northern India to the Nanhua Basin, or extensive local sedimentary reworking and redeposition within South China. As the Wuyi–Yunkai orogeny

started since the early Ordovician, uplift initially occurred along the southeast coastal region (present-day coordinates; Figure 5.8d) and gradually expanded to the northwest to cover almost the entire Cathaysia Block by the Silurian (Figure 5.8f) (e.g., Wang, 1985; Liu and Xu, 1994; Liu et al., 1995; Li et al., 2010a; Wang et al., 2010). Therefore, we infer that the Ordovician–Silurian sediments across the basin were probably mostly recycled from uplifted Ediacaran–Cambrian strata in the Wuyi–Yunkai orogen, with some input from uplifted Cathaysian basement as indicated by provenance analysis above (section 5.5.1). This interpretation is supported by (1) similar zircon Hf isotope signatures of Cambrian–Silurian samples across the basin (Figure 5.6); and (2) the addition of minor age populations of 1700 Ma and 1400 Ma in the Silurian samples, interpreted as possible contributions from exposed Cathaysian basement and/or recycled Indian basement (Figure 5.8f–g). Silurian samples also commonly have a new 435 Ma population (Figure 5.8f–g), which is likely contributed from *ca.* 435 Ma volcanic activities (Yao et al., 2012) and/or exposed *ca.* 440–400 Ma granitic rocks in the region (e.g., Wang et al., 1998, 2007b; Xu et al., 2005; Chen et al., 2008; Li et al., 2010a; Yao et al., 2012). The *ca.* 435 Ma volcanic activities are also recorded by the Yulin tuffaceous sandstone (Figure 5.8f).

Different from the main 1100–900 Ma population in most samples, the upper-Ordovician to Silurian samples from northeastern Yangtze (subgroup 2-1) show a distinct ~800 Ma dominant peak (Figure 5.8e–g) (Xu et al., 2012; Li et al., 2013b), which may indicate a local variation in detrital source. We speculate that sediments in this region were mainly contributed from local middle-Neoproterozoic rift-related magmatism (860–750 Ma), which were uplifted during the Wuyi–Yunkai orogeny (e.g., Li, 1998; Wang and Li, 2003; Li et al., 2008a, 2008b). Such an interpretation is consistent with the observation that (1) alluvial conglomeratic lithofacies along the Jiangshan–Shaoxing Fault (Figure 5.8f–g), impling a proximal source region (e.g., BGMRZJ, 1989; Liu and Xu, 1994; Liu et al., 1995); and (2) widespread middle-Neoproterozoic volcanic and volcanoclastic rocks in northeastern Yangtze (e.g., Li et al., 2003, 2008b, 2008d, 2010c). There is also a possibility that the Ediacaran–Cambrian clastic strata became thinner toward northeastern Cathaysia, thus providing less clastic cover rocks for recycling during the orogenic advance, but this could not be easily verified due to more intense deformation and metamorphism

of Ediacaran–Cambrian strata toward northeastern Cathaysia.

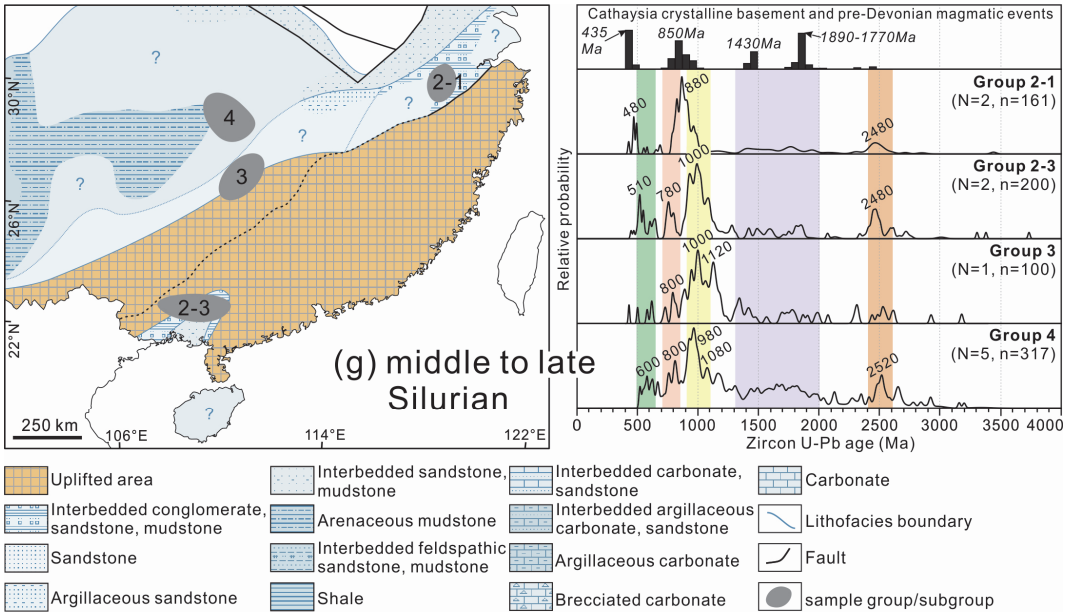

Figure 5.8. (continued-2)

5.5.3. An Ediacaran–Cambrian collisional orogeny and an Ordovician–Silurian intraplate orogeny (Wuyi–Yunkai) that affected the SCB

The Nanhua foreland basin was active during the Ediacaran–Silurian, recording a general northwestward migration of depocentres (Yao et al., 2014b) and changes in sedimentary environment, from a marine setting in the Ediacaran–Cambrian to a largely subaerial, deltaic-fluvial setting in the Ordovician–Silurian (Figure 5.8a–g) (Liu and Xu, 1994; Liu et al., 1995; Li et al., 2010a; Wang et al., 2010; Yao et al., 2014b). By the late Silurian, the southeastern South China was largely uplifted with only a limited area left as depositional accommodation in the southwest (Figure 5.8g).

The Wuyi–Yunkai orogeny resulted in an angular unconformity in South China, and the unconformity surface overlies progressively younger strata from south to north across the SCB (Xu et al., 2012 and reference therein). Unconformably underlying the Devonian basal conglomerates are Ediacanran–Cambrian strata in southern Cathaysia, Ordovician strata in central Cathaysia and southeastern Yangtze, and Silurian strata in central and northeastern Yangtze (BGMRJX, 1984; BGMRGX, 1985; BGMRGD, 1988; BGMRHN, 1988; BGMRHN, 1989). Infilling of the Nanhua foreland basin was previously considered to correspond with the timing of

the Wuyi–Yunkai orogeny, which started since at least the middle Ordovician (>460 Ma, Li et al., 2010a). However, tectonostratigraphic and provenance analyses across the basin suggest that it started to receive sediments shed off young orogen outboard the SCB as early as the Ediacaran (Yao et al., 2014b). Provenance analyses further reveal that Ordovician–Silurian sediments in the basin share a similar detrital provenance with the Ediacaran–Cambrian sediments, but with additional input from crystalline rocks in the emerging local Wuyi–Yunkai orogen. Therefore, provenance history of the Nanhua Basin after its pre-600 Ma failed rift stage can be divided into two stages: the Ediacaran–Cambrian foreland sedimentation sourced from distal orogens outside the SCB (Yao et al., 2014a), and the Ordovician–Silurian foreland sedimentation sourced from the emerging Wuyi–Yunkai orogen from the Cathaysia Block, involving extensive recycling of older sediments as well as eroded local crystalline rocks. Yao et al. (2014a) interpreted the first stage of foreland deposition with sediments shed from northern India and adjacent orogens during the Gondwana assembly, and deposited on the Cathaysia side of the Nanhua Basin when South China started its diachronous collision with northern India. This convergence between India (as a part of just assembled Gondwanaland) and the SCB was probably close to completion by early Ordovician time, when the far-field stress from this collisional event was transmitted to the SCB interior, causing the intraplate Wuyi–Yunkai orogeny, the second stage of foreland deposition in the Nanhua Basin, and the gradual closure of the basin during the Ordovician–Silurian.

5.6 Conclusions

We reported here new detrital zircon U–Pb ages and Hf isotopes from Cambrian–Silurian sandstone samples across the Nanhua foreland basin, South China. Combined with previously results, we established a temporal–spatial framework of provenance evolution for the Nanhua foreland basin. We further discussed the relationships between orogenic events in and adjacent the SCB during the assembly of Gondwanaland, and two stages of foreland deposition in the Nanhua Basin. Our main findings are the followings:

(1) Detrital zircon U–Pb patterns of Ediacaran–Silurian sandstones in the Nanhua Basin consist of a prominent population of 1100–900 Ma, subordinate populations of

850–700 Ma and 650–500 Ma, and minor populations at 2500 Ma and 2000–1300 Ma. Zircon Hf isotopes reveal four episodes of juvenile crustal growth at 2.5 Ga, 1.8 Ga, 1.4 Ga and 1.0 Ga for the source regions.

(2) Sedimentary provenance data of the Ediacaran–Cambrian strata in the Nanhua Basin does not match that of basement rocks for the Cathaysia Block; instead, they show close affinities to same-aged sedimentary rocks in northern India and basement rocks there. The Ordovician–Silurian sediments were likely sourced from both locally recycled Ediacaran–Cambrian sedimentary rocks and uplifted Cathaysia basement during the intraplate Wuyi–Yunkai orogeny. Silurian magmatic rocks during the late Wuyi–Yunkai orogeny also provided detritus to the Silurian strata.

(3) Upper-Ordovician to Silurian sandstones in northeastern Yagntze had more contributions from local rift-related magmatic materials rather than recycled Ediacaran–Cambrian sediments.

(4) The Nanhua Basin changed from a middle-Neoproterozoic rift basin to a failed rift in the late-Neoproterozoic. It started to receive foreland deposition from the Ediacaran. The provenance history of this foreland basin can be divided into two stages. During the first stage (Ediacaran–Cambrian), the clastic sediments shed off from northern India and surrounded young orogens to primarily the Cathaysia side of the Nanhua Basin. This stage was linked to a speculated diachronous collision between the SCB and northern India during the Gondwana assembly. The second stage (Ordovician–Silurian) involved deposition of recycled sedimentary cover, as well as eroded basement rocks, from the expanding Wuyi–Yunkai orogen in the Cathaysia Block towards the Yangtze Block. This latter orogeny is interpreted to be an intraplate event due to far-field stress from the aforementioned collision.

5.7 Acknowledgement

We thank L.F. Meng, J.H. Tao and X.L. Feng for help in sample collection and stratigraphic work during the fieldtrip, H.X. Ma for help in making zircon mounts, Y.F. Wang and Y.H. Yang for assistance in LA (MC)-ICP-MS U–Pb age/Hf-isotope analyses. Prof. Chris Elders is appreciated for polishing the manuscript. This study

was supported by the Australian Research Council (DP110104799), Chinese Academy of Sciences SAFEA International Partnership Program for Creative Research Teams grant (KZCX2-YW-Q04-06) and the National Natural Sciences Foundation of China (41173039). This is TIGeR (The Institute for Geoscience Research) publication #xxx, and contribution xxx from the ARC Centre of Excellence for Core to Crust Fluid Systems (http://www.ccfs.mq.edu.au/).

5.8 References

Amelin, Y., Lee, D.C., Halliday, A.N., Pidgeon, R.T., 1999. Nature of the Earth's earliest crust from hafnium isotopes in single detrital zircons. Nature 399, 252–255.

Amidon, W.H., Burbank, D.W., Gehrels, G.E., 2005. Construction of detrital mineral populations: Insights from mixing of U-Pb zircon ages in Himalayan rivers. Basin Research 17, 463–485.

Anderson, T., 2002. Correction of common lead in U-Pb analyses that do not report ^{204}Pb. Chemical Geology 192, 59–79.

Belousova, E.A., Kostitsyn, Y.A., Griffin, W.L., Begg, G.C., O'Reilly, S.Y., Pearson, N.J., 2010. The growth of the continental crust: constraints from zircon Hf-isotope data. Lithos 119, 457–466.

Berry, R.F., Jenner, G.A., Meffre, S., Tubrett, M.N., 2001. A North American provenance for Neoproterozoic to Cambrian sandstones in Tasmania? Earth and Planetary Science Letters 192, 207–222.

BGMRFJ (Bureau of Geology and Mineral Resources of Guangdong Province), 1988. Regional Geology of the Guangdong Province. Geological Publishing House, Beijing, 671 p. (in Chinese with English abstract).

BGMRGD (Bureau of Geology and Mineral Resources of Guangdong Province), 1988. Regional Geology of the Guangdong Province. Geological Publishing House, Beijing, 971 p. (in Chinese with English abstract).

BGMRGX (Bureau of Geology and Mineral Resources of Guangxi Province), 1985. Regional Geology of the Guangxi Province. Geological Publishing House, Beijing, 853 p. (in Chinese with English abstract).

BGMRHN (Bureau of Geology and Mineral Resources of Hunan Province), 1988.

Regional Geology of the Hunan Province. Geological Publishing House, Beijing, 719 p. (in Chinese with English abstract).

BGMRJX (Bureau of Geology and Mineral Resources of Jiangxi Province), 1984. Regional Geology of the Jiangxi Province. Geological Publishing House, Beijing, 921 p. (in Chinese with English abstract).

BGMRZJ (Bureau of Geology and Mineral Resources of Guangdong Province), 1988. Regional Geology of the Guangdong Province. Geological Publishing House, Beijing, 688 p. (in Chinese with English abstract).

Black L.P., Kamo, S.L., Allen, C.M., Aleinikoff, J.N., Davis, D.W., Korsch, R.J., Foudoulis, C., 2003. TEMORA1: a new zircon standard for Phanerozoic U-Pb geochronology. Chemical Geology 200, 155–170.

Blichert-Toft, J., Albarède, F., 1997. The Lu-Hf isotope geochemistry of chondrites and the evolution of the mantle-crust system. Earth and Planetary Science Letters 148, 243–258.

Brookfield, M.E., 1993. The Himalayan passive margin from Precambrian to Cretaceous. Sedimentary Geology 84, 1–35.

Cawood, P.A., Johnson, M.R.W., Nemchin, A.A., 2007. Early Palaeozoic orogenesis along the Indian margin of Gondwana: Tectonic response to Gondwana assembly. Earth and Planetary Science Letters 255, 70–84.

Chen, C.H., Lee, C.Y., Hsieh, P.S., Zeng, W., Zhou, H.W., 2008. Approaching the age problem for some metamorphosed Precambrian basement rocks and Phanerozoic granitic bodies in the Wuyi area: the application of EMP monazite age dating. Geological Journal of China University 14, 1–15 (in Chinese with English abstract).

Chen, X., Zhang, Y.D., Fan, J.X., Tang, L., Sun, H.Q., 2012. Onset of the Kwangsian Orogeny as evidenced by biofacies and lithofacies. Science China: Earth Sciences 55, 1592–1600.

Condie, K.C., Belousova, E., Griffin, W.L., Sircombe, K.N., 2009. Granitoid events in space and time: Constraints from igneous and detrital zircon age spectra. Gondwana Research 15, 228–242.

Cottle, J.M., Jessup, M.J., Newell, D.L., Horstwood, M.S.A., Noble, S.R., Parrish, R.R., Waters, D.J., Searle, M.P., 2009. Geochronology of granulitized eclogite from the Ama Drime Massif: Implications for the tectonic evolution of the South Tibetan Himalaya. Tectonics 28, doi: 10.1029/2008TC002256.

Dhuime, B., Hawkesworth, C., Cawood, P., 2011. When continents formed? Science 331, 154–155.

Dickinson, W.R., 2008. Impact of differential zircon fertility of granitoid basement rocks in North America on age populations of detrital zircons and implications for granite petrogenesis. Earth and Planetary Science Letters 275, 80–92.

Gao, S., Yang, J., Zhou, L., Li, M., Hu, Z., Guo, J., Yuan, H., Gong, H., Xiao, G., Wei, J., 2011. Age and growth of the Archean Kongling terrain, South China, with emphasis on 3.3 Ga granitoid gneisses. American Journal of Science 311, 153–182.

Greentree, M.R., Li, Z.X., Li, X.H., Wu, H.C., 2006. Late Mesoproterozoic to earliest Neoproterozoic basin record of the Sibao orogenesis in western South China and relationship to the assembly of Rodinia. Precambrian Research 151, 79–100.

Greentree, M.R., Li, Z.X., 2008. The oldest known rocks in south-western China: SHRIMP U-Pb magmatic crystallisation age and detrital provenance analysis of the Paleoproterozoic Dahongshan Group. Journal of Asian Earth Sciences 33, 289–302.

Griffin, W.L., Pearson, N.J., Belousova, E., Jackson, S.E., Achterbergh, E.V., O'Reilly, S.Y., Shee, S.R., 2000. The Hf isotope composition of cratonic mantle: LAM-MC-ICPMS analysis of zircon megacrysts in kimberlites. Geochimica et Cosmochimica Acta 64, 133–147.

Hawkesworth, C.J., Kemp, A.I.S., 2006. Using hafnium and oxygen isotopes in zircons to unravel the record of crustal evolution. Chemical Geology 226, 144–162.

Huang, J., Ren, J., Jiang, C., Zhang, Z., Qin, D., 1980. The geotectonic evolution of China. Science Press, Beijing, 124 p. (in Chinese with English abstract).

Jackson, S.E., Pearson, N.J., Griffin, W.L, Belousova, E.A., 2004. The application of laser ablation-inductively coupled plasma-mass spectrometry to in situ U-Pb zircon geochronology. Chemical Geology 211, 47–69.

Jiao, W.F., Wu, Y.B., Yang, S.H., Peng, M., Yang, J., 2009. The oldest basement rock in the Yangtze Craton revealed by zircon U-Pb age and Hf isotope composition. Science in China Series D: Earth Sciences 52, 1393–1399.

Kemp, A.I.S., Hawkerworth, C.J., Paterson, B.A., Kinny, P.D., 2006. Episodic growth of the Gondwana supercontinent from hafnium and oxygen isotopes in

zircon. Nature 439, 580–583.

Li, X.H., 1997. Timing of the Cathaysia block formation: constraints from SHRIMP U-Pb zircon geochronology. Episodes 20, 188–192.

Li, Z.X., 1998. Tectonic history of the major East Asian lithospheric blocks since the mid-Proterozoic — a synthesis. In: Flower, M.J., Chung, S.L., Lo, C.H., Lee, T.Y. (Eds.), Mantle Dynamics and Plate Interactions in East Asia. American Geophysical Union, Washington DC, pp. 221–243.

Li, Z.X., Li, X.H., Zhou, H., Kinny, P.D., 2002. Grenvillian continental collision in south China: New SHRIMP U-Pb zircon results and implications for the configuration of Rodinia. Geology 30, 163–166.

Li, X.H., Li, Z.X., Ge, W.C., Zhou, H.W., Li, W.X., Liu, Y., Wingate, M.T.D., 2003a. Neoproterozoic granitoids in South China: crustal melting above a mantle plume at ca. 825 Ma? Precambrian Research 122, 45–83.

Li, Z.X., Li, X.H., Kinny, P.D., Wang, J., Zhang, S., Zhou, H., 2003b. Geochronology of Neoproterozoic syn-rift magmatism in the Yangtze Craton, South China and correlations with other continents: evidence for a mantle superplume that broke up Rodinia. Precambrian Research 122, 85–109.

Li, W.X., Li, X.H., Li, Z.X., 2005. Neoproterozoic bimodal magmatism in the Cathaysia Block of South China and its tectonic significance. Precambrian Research 136, 51–66.

Li, Z.X., Li, X.H., 2007. Formation of the 1300 km-wide intracontinental orogen and postorogenic magmatic province in Mesozoic South China: a flat-slab subduction model. Geology 35, 179–182.

Li, Z.X., Wartho, J.A., Occhipinti, S., Zhang, C.L., Li, X.H., Wang, J., Bao, C.M., 2007. Early history of the eastern Sibao Orogen (South China) during the assembly of Rodinia: New mica $^{40}Ar/^{39}Ar$ dating and SHRIMP U-Pb detrital zircon provenance constraints. Precambrian Research 159, 79–94.

Li, Z.X., Bogdanova, S.V., Collins, A.S., Davidson, A., De Waele, B., Ernst, R.E., Fitzsimons, I.C.W., Fuck, R.A., Gladkochub, D.P., Jacobs, J., Karlstrom, K.E., Lu, S., Natapov, L.M., Pease, V., Pisarevsky, S.A., Thrane, K., Vernikovsky, V., 2008a. Assembly, configuration, and break-up history of Rodina: A synthesis. Precambrian Research 160, 179–210.

Li, W.X., Li, X.H., Li, Z.X., 2008b. Middle Neoproterozoic syn-rifting volcanic rocks in Guangfeng, South China: petrogenesis and tectonic significance.

Geological Magazine 145, 475–489.

Li, Z.X., Li, X.H., Li, W.X., Ding, S., 2008c. Was Cathaysia part of Proterozoic Larentia? – new data from Hainan Island, south China. Terran Nova 20, 154–164.

Li, X.H., Li, W.X., Li, Z.X., Liu, Y., 2008d. 850-790 Ma bimodal volcanic and intrusive rocks in northern Zhejiang, South China: A major episode of continental rift magmatism during the breakup of Rodinia. Lithos 102, 341–357.

Li, X.H., Li, W.X., Li, Z.X., Lo, C.H., Wang, J., Ye, M.F., Yang, Y.H., 2009. Amalgamation between the Yangtze and Cathaysia Blocks in South China: Constraints from SHRIMP U–Pb zircon ages, geochemistry and Nd–Hf isotopes of the Shuangxiwu volcanic rocks. Precambrian Research 174, 117–128.

Li, Z.X., Li, X.H., Wartho, J.A., Clark, C., Li, W.X., Zhang, C.L., Bao, C.M., 2010a. Magmatic and metamorphic events during the early Paleozoic Wuyi–Yunkai orogeny, southeastern South China: new age constraints and pressure–temperature conditions. Geological Society of America Bulletin 122, 772–793.

Li, W.X., Li, X.H., Li, Z.X., 2010b. Ca. 850 Ma bimodal volcanic rocks in northeastern Jiangxi Province, South China: Initial extension during the breakup of Rodinia? American Journal of Science 310, 951–980.

Li, X.H., Li, W.X., Li, Q.L., Wang, X.C., Liu, Y., Yang, Y.H., 2010c. Petrogenesis and tectonic significance of the ~850 Ma Gangbian alkaline complex in South China: Evidence from in situ zircon U-Pb dating, Hf-O isotopes and whole-rock geochemistry. Lithos 114, 1–15.

Li, L., Lin, S., Xing, G., Davis, D.W., Davis, W.J., Xiao, W., Yin, C., 2013a. Geochemistry and tectonic implications of late Mesoproterozoic alkaline bimodal volcanic rocks from the Tieshajie Group in the southeastern Yangtze Block, South China. Precambrian Research 230, 179–192.

Li, H.B., Jia, D., Wu, L., Zhang, Y., Yin, H.W., Wei, G.Q., Li, B.L., 2013b. Detrital zircon provenance of the Lower Yangtze foreland basin deposits: constraints on the evolution of the early Palaeozoic Wuyi-Yunkai orogenic belt in South China. Geological Magazine 150, 959–974.

Liu, B., Xu, X., 1994. Atlas of Lithofacies and Paleogeography of South China. Science Press, Beijing, 188 p. (in Chinese with English abstract).

Liu, B.J., Xu, X.S., Xu, Q., 1995. Sequence stratigraphy and basin geodynamic of the

southeastern margin of the Yangtze plate during the late Proterozoic to early Paleozoic. Lithofacies Paleogeography 5, 1–16.

Liu, Y., Siebel, W., Massonne, H., Xiao, X., 2007. Geochronological and petrological constraints for tectonic evolution of the central Greater Himalayan sequence in the Kharta area, southern Tibet. The Journal of Geology 115, 215–230.

Liu, R., Zhou, H.W., Zhang, L., Zhong, Z.Q., Zeng, W., Xiang, H., Jin, S., Lu, X.Q., Li, C.Z., 2009. Paleoproterozoic reworking of ancient crust in the Cathaysia Block, South China: Evidence from zircon trace elements, U–Pb and Lu–Hf isotopes. Chinese Science Bulletin 54, 1543–1554.

Ludwig, K.R., 2001a. ISOPLOT/EX version 2.49 – A geochronological toolkit for Microsoft excel. Berkley Geochronological Centre Special Publication No. 1, 56 p.

Ludwig, K. R., 2001b. SQUID version 1.02 – A geochronological toolkit for Microsoft excel. Berkley Geochronological Centre Special Publication No. 2, 19 p.

Ma, D., Huang, X., Xiao, Z., Chen, Z., Zhang, W., Zhong, S., 1998. The crystalline basement of the Hainan Island – stratigraphy and geochronology of the Baoban group. China University of Geosciences Press, Wuhan, 60 p. (in Chinese with English abstract).

Mezger, K., Cosca, M., 1999. The thermal history of the Eastern Ghats Belt (India), as revealed by U-Pb and $^{40}Ar/^{39}Ar$ dating of metamorphic and magmatic minerals: implications for the SWEAT correlation. Precambrian Research 94, 251–271.

Miller, C., Thoni, M., Frank, W., Grasemann, B., Klotzli, U., Guntli, P., Draganits, E., 2001. The early Palaeozoic magmatic event in the Northwest Himalaya, India: source, tectonic setting and age of emplacement. Geological Magazine 138, 237–251.

Morel, M.L.A., Nebel, O., Nebel-Jacobsen, Y.J., Miller, J.S., Vroon, P.Z., 2008. Hafnium isotope characterization of the GJ-1 zircon reference material by solution and laser-ablation MC-ICPMS. Chemical Geology 255, 231–235.

Myrow, P.M., Hughes, N.C., Goodge, J.W., Fanning, C.M., Williams, I.S., Peng, S.C., Bhargava, O.N., Parcha, S.K., Pogue, K.R., 2010. Extraordinary transport and mixing of sediment across Himalayan central Gondwana during the

Cambrian-Ordovician. Geological Society of America Bulletin 122, 1660–1670.

Press, W.H., Flannery, B.P., Teukolsky, S.A., Vetterling, W.T., 1986. Numerical Recipes: The Art of Scientific Computing. Cambridge University Press, Cambridge, UK, 186 p.

Qiu, Y.M., Gao, S., McNaughton, N.J., Groves, D.I., Ling, W., 2000. First evidence of >3.2 Ga continental crust in the Yangtze craton of south China and its implications for Archean crustal evolution and Phanerozoic tectonics. Geology 28, 11–14.

Ren, J., 1991. On the geotectonics of southern China. Acta Geologica Sinica 4, 111–130.

RGMRGX-a, 1966. Regional Geological Mapping and Report of Guangxi Province – 1:200,000 Rongxian Sheet. Institute of Geoscience, Ministry of Geology, Beijing, (in Chinese with English abstract).

RGMRGX-b, 1968. Regional Geological Mapping and Report of Guangxi Province – 1:200,000 Yulin Sheet. Institute of Geoscience, Ministry of Geology, Beijing, (in Chinese with English abstract).

RGMRHN-a, 1965. Regional Geological Mapping and Report of Hunan Province – 1:200,000 Dongkou Sheet. Institute of Geoscience, Ministry of Geology, Beijing, (in Chinese with English abstract).

RGMRHN-b, 1968. Regional Geological Mapping and Report of Hunan Province – 1:200,000 Dayong Sheet. Institute of Geoscience, Ministry of Geology, Beijing, (in Chinese with English abstract).

Schärer, U., Xu, R.H., Allègre1, C.J., 1986. U-(Th)-Pb systematics and ages of Himalayan leucogranites, South Tibet: Earth and Planetary Science Letters 77, 35–48.

Scherer, E.M., 2001. Calibration of the lutetium–hafnium clock. Science 293, 683–687.

Shu, L.S., Faure, M., Yu, J.H., Jahn, B.M., 2011. Geochronological and geochemical features of the Cathaysia block (South China): New evidence for the Neoproterozoic breakup of Rodinia. Precambrian Research 187, 263–276.

Simmat, R., Raith, M.M., 2008. U-Th-Pb monazite geochronometry of the Eastern Ghats Belt, India: Timing and spatial disposition of poly-metamorphism. Precambrian Research 162, 16–39.

Singh, S., Barley, M.E., Brown, S.J., Jain, A.K., Manickavasagam, R.M., 2002.

SHRIMP U-Pb in zircon geochronology of the Chor granitoid: evidence for Neoproterozoic magmatism in the Lesser Himalayan granite belt of NW India. Precambrian Research 118, 285–292.

Sláma, J., Košler, J., Condon, D.J., Crowley, J.L., Gerdes, A., Hanchar, J.M., Horstwood, M.S.A., Morris, G.A., Nasdala, L., Norberg, N., Schaltegger, U., Schoene, B., Tubrett, M.N., Whitehouse, M.J., 2008. Plesovice zircon – A new natural reference material for U-Pb and Hf isotopic microanalysis. Chemical Geology 249, 1–35.

Song, S., Niu, Y., Wei, C., Ji, J., Su, L., 2010. Metamorphis, anatexis, zircon ages and tectonic evolution of the Gongshan block in the northern Indochina continent – an eastern extension of the Lhasa Block. Lithos 120, 327–346.

Squire, R.J., Campbell, I.H., Allen, C.M., Wilson, C.L., 2006. Did the Transgondwanan Supermountain trigger the explosive radiation of animals on Earth? Earth and Planetary Science Letters 250, 116–133.

Stern, R.J., 1994. Arc assembly and continental collision in the Neoproterozoic East African Orogen: Implications for the Consolidation of Gondwanaland. Annual Review of Earth and Planetary Sciences 22, 319–351.

Stern, R.A., 2001. A new isotopic and trace-element standard for the ion microprobe: preliminary thermal ionization mass spectrometry (TIMS) U-Pb and electron-microprobe data. Radiogenic Age and Isotopic Studies Report 14, Geological Survey of Canada, Current Research 2001-F1, 11p.

Sun, W.H., Zhou, M.F., Gao, J.F., Yang, Y.H., Zhao, X.F., Zhao, J.H., 2009. Detrital zircon U-Pb geochronological and Lu-Hf isotopic constraints on the Precambrian magmatic and crustal evolution of the western Yangtze Block, SW China. Precambrian Research 172, 99–126.

Van Achterbergh, E., Ryan, C.G., Jackson, S.E., Griffin,W.L., 2001. Data reduction software for LA-ICP-MS: appendix. In: Sylvester, P.J. (Eds.), Laser Ablation-ICP-Mass Spectrometry in the Earth Sciences: Principles and Applications. Mineralogist Association Canada (MAC) Short Course Series 29, Ottawa, Canada, pp. 239–243.

Wan, Y., Liu, D., Xu, M., Zhuang, J., Song, B., Shi, Y., Du, L., 2007. SHRIMP U-Pb zircon geochronology and geochemistry of metavolcanic and metasedimentary rocks in Northwestern Fujian, Cathaysia block, China: Tectonic implications and the need to redefine lithostratigraphic units. Gondwana Research 12,

166–183.

Wan, Y., Liu, D., Wilde, S.A., Cao, J., Chen, B., Dong, C., Song, B., Du, L., 2010. Evolution of the Yunkai Terrane, South China: Evidence from SHRIMP zircon U-Pb dating, geochemistry and Nd isotope. Journal of Asian Earth Sciences 37, 140–153.

Wang, H., 1985, Atlas of the Palaeogeography of China. Cartographic Publishing House, Beijing, 281 p. (in Chinese with English abstract).

Wang, J., Sun, D., Chang, X., Deng, S., Zhang, H., Zhou, H., 1998. U-Pb dating of the Napeng granite at the NW margin of the Yunkai block, Guangdong, South China. Acta Mineralogica Sinica 18, 130–133 (in Chinese with English abstract).

Wang, J., Li, Z.X., 2003. History of Neoproterozoic rift basins in South China: implications for Rodinia break-up. Precambrian Research 122, 141–158.

Wang, X., Zhou, J., Qiu, J., Gao, J., 2004. Geochemistry of the Meso- to Neoproterozoic basic–acid rocks from Hunan Province, South China: implications for the evolution of the western Jiangnan orogen. Precambrian Research 135, 79–103.

Wang, X.L., Zhou, J.C., Qiu, J.S., Zhang, W.L., Liu, X.M., Zhang, G.L., 2006. LA-ICP-MS U-Pb zircon geochronology of the Neoproterozoic igneous rocks from Northern Guangxi, South China: implications for tectonic evolution. Precambrian Research 145, 111–130.

Wang, X.C., Li, X.H., Li, W.X., Li, Z.X., 2007a. Ca. 825 Ma komatiitic basalts in South China: First evidence for >1500 °C mantle melts by a Rodinian mantle plume. Geology 35, 1103–1106.

Wang, Y., Fan, W., Zhao, G., Ji, S., Peng, T., 2007b. Zircon U-Pb geochronology of gneissic rocks in the Yunkai massif and its implications on the Caledonian event in the South China Block. Gondwana Research 12, 404–416.

Wang, Y., Zhang, F., Fan, W., Zhang, G., Chen, S., Cawood, P.A., Zhang, A., 2010. Tectonic setting of the South China Block in the early Paleozoic: Resolving intracontinental and ocean closure models from detrital zircon U-Pb geochronology. Tectonics 29, doi:10.1029/2010TC002750.

Wang, Y., Zhang, A., Fan, W., Zhao, G., Zhang, G., Zhang, Y., Zhang, F., Li, S., 2011. Kwangsian crustal anatexis within the eastern South China Block: Geochemical, zircon U-Pb geochronological and Hf isotopic fingerprints from

the gneissoid granites of Wugong and Wuyi-Yunkai Domains. Lithos 127, 239–260.

Wiedenbeck, M., Alle, P., Corfu, F., Griffin, W.L., Meer, M., Oberli, F., Vonquadt, A., Roddick., J.C., Spegel, W., 1995. Three natural zircon standards for U-Th-Pb, Lu-Hf, trace element and REE analysis. Geostandards and Geoanalytical Research 19, 1–23.

Wiedenbeck, M., Goswami, J.N., Roy, A.B., 1996. Stabilization of the Aravalli Craton of northwestern India at 2.5 Ga: An iro microprobe zircon study. Chemical Geology 129, 325–340.

Wiedenbeck, M., Hanchar, J.M., Peck, W.H., Sylvester, P., Valley, J., Whitehouse, M., Kronz, A., Morishita, Y., Nasdala, L., Fiebig, J., Franchi, I., Girard, J.P., Greenwood, R.C., Hinton, R., Kita, N., Mason, P.R.D., Norman, M., Ogasawara, M., Piccoli, P.M., Rhede, D., Satoh, H., Schulz-Dobrick, B., Spicuzza, M.J., Terada, K., Tindle, A., Togashi, S., Vennemann, T., Xie, Q., Zheng, Y.F., 2004. Further characterisation of the 91500 zircon crystal. Geostandards Newsletter 28, 9–39.

Williams, I.S., 1998. U-Th-Pb geochronology by ion microprobe. In: McKibben, M. A., Shanks III, W. C., Ridley, W. I. (Eds.), Applications of microanalytical techniques to understanding mineralizing processes. Reviews in Economic Geology 7, pp. 1–35.

Wu, F.Y., Yang, Y.H., Xie, L.W., Yang, J.H., Xu, P., 2006. Hf isotopic compositions of the standard zircons and baddeleyites used in U-Pb geochronology. Chemical Geology 234, 105–126.

Wu, L., Jia, D., Li, H., Deng, F., Li, Y., 2010. Provenance of detrital zircons from the late Neoproterozoic to Ordovician sandstones of South China: implications for its continental affinity. Geological Magazine 147, 974–980.

Xiang, H., Zhang, L., Zhou, H., Zhong, Z., Zeng, W., Liu, R., Jin, S., 2008. U-Pb zircon geochronology and Hf isotope study of metamorphosed basic-ultrabasic rocks from metamorphic basement in southwestern Zhejiang: The response of the Cathaysia Block to Indosinian orogenic event. Science in China Series D: Earth Sciences 51, 788–800.

Xie, L.W., Zhang, Y.B., Zhang, H.H., Sun, J.F., Wu, F.W., 2008. In situ simultaneous determination of trace elements, U-Pb and Lu-Hf isotopes in zircon and baddeleyite. Chinese Science Bulletin 53, 1565–1573.

Xu, X.S., O'Reilly, S.Y., Griffin, W.L., Deng, P., Pearson, N.J., 2005. Relict Proterozoic basement in the Nanling Mountains (SE China) and its tectonothermal overprinting. Tectonics 24, 1–16.

Xu, Y., Du, Y., Cawood, P.A., Zhu, Y., Li, W., Yu, W., 2012. Detrital zircon provenance of Upper Ordovician and Silurian strata in the northeastern Yangtze Block: Response to orogenesis in South China. Sedimentary Geology 267-268, 63–72.

Xu, Y., Cawood, P.A., Du, Y., Hu, L., Yu, W., Zhu, Y., Li, W., 2014. Linking South China to northern Australia and India on the margin of Gondwana: Constraints from detrital zircon U-Pb and Hf isotopes in Cambrian strata. Tectonics, doi: 10.1002/tect.20099

Yang, Tsun-i, 1986. The geology of China. Clarendon Press, Oxford, England, 363p.

Yao, J., Shu, L., Santosh, M., 2011. Detrital zircon U-Pb geochronology, Hf-isotopes and geochemistry – new clues for the Precambrian crustal evolution of Cathaysia Block, South China. Gondwana Research 20, 553–567.

Yao, W.H., Li, Z.X., Li, W.X., Wang, X.C., Li, X.H., Yang, J.H., 2012. Post-kinematic lithospheric delamination of the Wuyi–Yunkai orogen in South China: evidence from ca. 435 Ma high-Mg basalts. Lithos 154, 115–129.

Yao, W.H., Li, Z.X., Li, W.X., Li, X.H., Yang, J.H., 2014a. From Rodinia to Gondwanaland: a tale of detrital zircon provenance analyses from the southern Nanhua Basin, South China. American Journal of Science 314, 278–313.

Yao, W.H., Li, Z.X., 2014b. Stratigraphic history of the Cambrian-Silurian Nanhua foreland basin in South China: Response to the Wuyi-Yunkai Orogen. Tectonics (under review).

Ye, M.F., Li, X.H., Li, W.X., Liu, Y., Li, Z.X., 2007. SHRIMP zircon U-Pb geochronological and whole-rock geochemical evidence for an early Neoproterozoic Sibaoan magmatic arc along the southeastern margin of the Yangtze Block. Gondwana Research 12, 144–156.

Yu, J.H., O'Reilly, S.Y., Wang, L., Griffin, W.L., Zhang, M., Wang, R., Jiang, S., Shu, L., 2008. Where was South China in the Rodinia supercontinent? Evidence from U-Pb geochronology and Hf isotopes of detrital zircons. Precambrian Research 164, 1–15.

Yu, J.H., Wang, L., O'Reilly, S.Y., Griffin, W.L., Zhang, M., Li, C., Shu, L., 2009. A Paleoproterozoic orogeny recorded in a long-lived cratonic remnant

(Wuyishan terrane), eastern Cathaysia Block, China. Precambrian Research 174, 347–363.

Yu, J.H., O'Reilly, S.Y., Wang, L., Griffin, W.L., Zhou, M.F., Zhang, M., Shu, L., 2010. Components and episodic growth of Precambrian crust in the Cathaysia Block, South China: evidence from U-Pb ages and Hf isotopes of zircons in Newproterozoic sediments. Precambrian Research 181, 97–114.

Yu, J.H., O'Reilly, S.Y., Zhou, M.F., Griffin, W.L., Wang, L., 2011. U-Pb geochronology and Hf-Nd isotopic geochemistry of the Badu Complex, Southeastern China: implications for the Precambrian crustal evolution and paleogeography of the Cathaysia Block. Precambrian Research 222–223, 424–449.

Zeng, W., Zhang, L., Zhou, H., Zhong, Z., Xiang, H., Liu, R., Jin, S., Lu, X.Q., Li C.Z., 2008. Caledonian reworking of Paleoproterozoic basement in the Cathaysia Block: constraints from zircon U-Pb dating, Hf isotopes and trace elements. Chinese Science Bulletin 53, 895–904.

Zhang, J.Y., Yin, A., Liu, W.C., Wu, F.Y., Lin, D., Grove, M., 2012. Coupled U-Pb dating and Hf isotopic analysis of detrital zircon of modern river sand from the Yalu River (Yarlung Tsangpo) drainage system in southern Tibet: Constraints on the transport processes and evolution of Himalayan rivers. Geological Society of America Bulletin 124, 1449–1473.

Zhao, X.F., Zhou, M.F., Li, J.W., Sun, M., Gao, J.F., Sun, W.H., Yang, J.H., 2010. Late Paleoproterozoic to early Mesoproterozoic Dongchuan Group in Yunnan, SW China: Implications for tectonic evolution of the Yangtze Block. Precambrian Research 182, 57–69.

Zheng, J., Griffin, W.L., O'Reilly, S.Y., Zhang, M., Pearson, N., Pan, Y., 2006. Widespread Archean basement beneath the Yangtze craton. Geology 34, 417–420.

Zhou, M.F., Yan, D.P., Kennedy, A.K., Li, Y., Ding, J., 2002a. SHRIMP U-Pb zircon geochronological and geochemical evidence for Neoproterozoic arc-magmatism along the western margin of the Yangtze Block, South China. Earth and Planetary Science Letters 196, 51–67.

Zhou, M.F., Kennedy, A.K., Sun, M., Malpas, J., Lesher, C.M., 2002b. Neoproterozoic arc-related mafic intrusions along the northern margin of South China: Implications for the accretion of Rodinia. The Journal of Geology 110,

611–618.

Zhou, M.F., Ma, Y., Yan, D.P., Xia, X., Zhao, J.H., Sun, M., 2006. The Yanbian Terrane (Southern Sichuan Province, SW China): A Neoproterozoic arc assemblage in the western margin of the Yangtze Block. Precambrian Research 144, 19–38.

CHAPTER 6 WAS THERE A CAMBRIAN OCEAN IN SOUTH CHINA? – INSIGHTS FROM DETRITAL PROVENANCE ANALYSES

WEI-HUA YAO*†, ZHENG-XIANG LI* & WU-XIAN LI**

*ARC Center of Excellence for Core to Crust Fluid Systems (CCFS) and The Institute for Geoscience Research (TIGeR), Department of Applied Geology, Curtin University, Perth, WA 6845, Australia

**Key Laboratory of Isotope Geochronology and Geochemistry, Guangzhou Institute of Geochemistry, Chinese Academy of Sciences, Guangzhou 510640, China

†Author for correspondence: weihua.yao@curtin.edu.au

Abstract

We use detrital provenance data from Cambrian sandstones to examine whether the Yangtze and Cathaysia blocks in South China were separated by an ocean during the Cambrian period. Zircons from Cambrian sandstones exhibit a dominant ~800 Ma age peak in central Yangtze, being sourced from western Yangtze; whereas a ~980 Ma peak dominates in the northwestern Cathaysia Block, being sourced from an exotic continent once connected to Cathaysia. A mixed provenance with both age peaks is found in Cambrian sandstones from southeastern Yangtze Blcok, indicating that detritus can travel from the Cathaysia Block to the Yangtze Block, and therefore arguing against the existence of a broad Cambrian ocean.

Keywords: South China, Cambrian ocean, detrital provenance, U–Pb geochronology

6.1 Introduction

The South China Block comprises the Yangtze Block in the northwest and the Cathaysia Block in the southeast (Figure 6.1a). The Ordovician–Silurian Wuyi–Yunkai orogeny caused deformation and metamorphism over much of the southeastern South China, and the development of a foreland basin in northwestern

Cathaysia Block and southern Yangtze Block (Li *et al.* 2010). However, the pre-Wuyi–Yunkai configuration of South China and the nature of the orogeny remain controversial. Some suggested that an ocean existed between the Yangtze and Cathaysia blocks for at least the latest Neoproterozoic to Cambrian period (Shui, 1988; Liu & Xu, 1994) or even until the Jurassic (Hsü *et al.* 1988, 1990) before the two blocks joined together. The Mesozoic ocean model did not receive much support because the key evidence for the so-called 'Mesozoic Banxi mélange' was later proven to be Neoproterozoic in age and with different tectonic affinities (e.g. Zhou, 1989; Li *et al.* 1994; Li, Z.X. *et al.* 2003). The Cambrian ocean model (Shui, 1988; Liu & Xu, 1994) suggests that the Yangtze and Cathaysia blocks first docked at their eastern ends during the early to middle Neoproterozoic period, with a V-shaped ocean widening to the west (as wide as ~2000 km) until the Cambrian period. This residual ocean closed during the Ordovician–Silurian period, leading to the formation of a coherent South China Block. Such a collision was taken as the cause for the Ordovician–Silurian 'Caledonian orogeny' in South China (Huang *et al.* 1980; Yang *et al.* 1986; Ren, 1991), which was renamed the Wuyi–Yunkai orogeny with a redefined age range of >460 – 415 Ma (Li *et al.* 2010). The boundary between the two blocks was consequently considered as a suture zone due to the closure of the Cambrian ocean (e.g. Xu & Qiao, 1989; Liu & Xu, 1994; Xu, Xu & Pan, 1996; Chen *et al.* 2006).

Alternatively, it has been argued that the complete amalgamation between the Yangtze and Cathaysia blocks had already finished by the Neoproterozoic period (e.g. Li, Zhang & Powell, 1995; Charvet *et al.* 1996; Zhao *et al.* 1999; Zhou *et al.* 2002; Li *et al.* 2008, 2009), and the Wuyi–Yunkai orogeny was an intraplate orogeny related to South China's collision with Gondwanaland which closed a Neoproterozoic failed continental rift (Li, 1998; Li & Powell, 2001). In such a model, no ocean floor is required for the basin (the Nanhua Basin) between the Yangtze and Cathaysia blocks. The intraplate model was also supported by other researchers, based on magmatic and metamorphic analyses of lower Palaeozoic rocks (Li *et al.* 2010), provenance analyses of Cambrian–Silurian sandstones (Wang *et al.* 2010), and structural analyses of lower Palaeozoic strata in the region (e.g. Faure *et al.* 2009; Charvet *et al.* 2010; Shu *et al.* 2014). However, the provenance analyses by Wang *et al.* (2010) combined data from Cambrian–Silurian sandstones together, thus mixing

the Cambrian provenance data with that of the Ordovician–Silurian sandstones formed during the Yangtze-ward propagation of the intraplate Wuyi–Yunkai orogeny from the Cathaysia Block. As syn-orogenic foreland basin sedimentary rocks on the Yangtze Block would naturally contain detritus shed off the growing orogen on the Cathaysia Block, we do not regard the Wang *et al.* (2010)'s provenance analyses as a vigorous-enough test for the Cambrian ocean model.

Here we use a provenance study of Cambrian sedimentary rocks to test whether or not a Cambrian ocean was present. If the ocean existed, the provenances of Cambrian sandstones from the Yangtze and Cathaysia sides of the Nanhua Basin will likely be different. Otherwise, detrital exchanges between the two blocks are expected. We report new detrital zircon U–Pb geochronological data for four Cambrian sandstone samples from the Yangtze side (two from central Yangtze and two from southeastern Yangtze) of the Nanhua Basin, and compare them with published U–Pb results from both northwestern Cathaysia and southeastern Yangtze to argue against the Cambrian ocean model in South China.

6.2 Geological Setting and Sampling

The boundary between the Yangtze and Cathaysia blocks lies approximately along the Jiangshan–Shaoxing Fault in the NE South China Block (Figure 6.1a). The southwestern extension of the boundary is unclear due to poor exposure and tectonic modifications (Ren, 1991; Li *et al.* 2010), but has been defined using the mostly disconnected lithofacies boundaries between Cathaysia clastics facies and Yangtze clastic–carbonate facies (Figure 6.2a, b) (Liu & Xu, 1994). This boundary was also taken as a suture zone of the Cambrian ocean by Liu & Xu (1994) and Chen *et al.* (2006). During the Cambrian period, sedimentation over the Yangtze Block was dominated by carbonate, muddy carbonate and sandy carbonate, with some clastic–carbonate intercalations in the lower Cambrian (Figure 6.2a) (e.g. RGMRHN-a, 1975; RGMRHN-b, 1972; BGMRHN, 1988; Liu & Xu, 1994). In contrast, the Cathaysia Block received massive clastic sedimentation, consisting of shale, siltstone, arkosic sandstone, quartz sandstone and pebbly sandstone (Figure 6.2a, b) (e.g. BGMRJX, 1984; BGMRGD, 1988; Zhang & He, 1993; Liu & Xu, 1994; Yao *et al.* 2014).

Three sampling localities across the Yangtze–Cathaysia boundary were selected, including central Yangtze (Xinhuang), southeastern Yangtze (Xinning) and northwestern Cathaysia (Shaoguan) (Figure 6.1b). The Xinhuang section consists of ~ 1400 m of Cambrian strata, with massive carbonate–shale units and minor fine-grained sandstone layers in the lower-Cambrian strata (Figure 6.2c) (RGMRHN-b, 1972). The Xinning section has ~ 1800 m of Cambrian strata, including 680 m of clastic strata. It consists of shale, siliceous shale and minor carbonate in the lower-Cambrian strata, shale and sandstone intercalations in the middle Cambrian strata, and carbonate with minor shale in the upper Cambrian strata (Figure 6.2d) (RGMRHN-a, 1975). The Shaoguan section has ~ 3800 m of Cambrian strata, with thick siltstone, feldspathic quartz sandstone, pebbly sandstone, and thin grey-purple mudstone beds (Figure 6.2e) (Zhang & He, 1993).

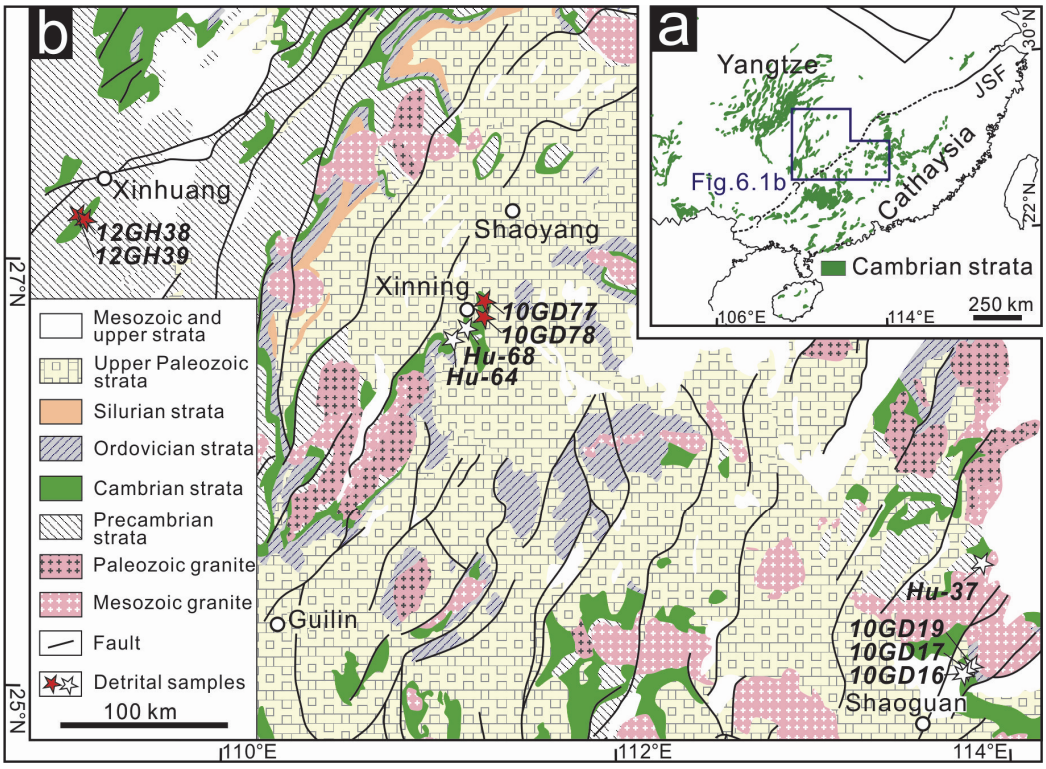

Figure 6.1. (a) Distribution of Cambrian strata in the South China Block, highlighting the inferred boundary between the Yangtze and Cathaysia blocks. JSF = the Jiaoshan–Shaoxing Fault. (b) Geological map of central South China, highlighting three Cambrian sampling regions from central Yangtze, southeastern Yangtze and northern Cathaysia. Red stars are samples from this study, and white stars are samples reported in previous studies.

A grey medium-grained quartz sandstone sample (12GH38) and a grey-white fine-grained sandstone sample (12GH39) were collected from the lower Cambrian strata at the Xinhuang section (Figure 6.2c), whereas a dark green medium-grained

sandstone sample (10GD77) and a grey fine-grained sandstone sample (10GD78) were collected from the middle Cambrian strata at the Xinning section (Figure 6.2d). Results of two sandstone samples (Hu-64, Hu-68) from the middle- to upper-Cambrian strata of the Xinning region (Figure 6.2d), three sandstone samples (10GD16, 10GD17, 10GD19) from the middle to upper Cambrian strata and one sandstone sample (Hu-37) from the lower Cambrian strata of the Shaoguan region (Figure 6.2e), were reported in previous studies (Wang *et al.* 2010; Yao *et al.* 2014) and used here for comparison.

6.3 Analytical Methods

Mineral separation of sandstone samples was conducted at the Institute of Hebei Regional Geology and Mineral Survey in Langfang, China. Conventional magnetic and density techniques were adopted to concentrate non-magnetic and heavy fractions. Zircon grains, together with zircon standards, were cast in epoxy mounts and polished to reveal half sections for analysis. All zircons were documented with transmitted and reflected light microphotos as well as cathodoluminescence (CL) images to reveal their internal structures. Zircon U–Pb analyses were carried out in the John de Laeter Centre at Curtin University, Australia, using the Sensitive High Resolution Ion MicroProbe (SHRIMP) facility. Standard operation conditions of 2 nA O_2^- primary beam and spot size of ~25 μm in diameter and ~2 μm in depth were followed and each U–Th–Pb measurement consisted of six cycles. U abundance was calibrated using zircon standard BR266 (Stern, 2001), and $^{206}Pb/^{238}U$ ratio was constrained by the Plešovice zircon (Sláma *et al.* 2008). The detailed analytical procedure follows that of Williams (1998). Data reduction was carried out using Squid v2.50 (Ludwig, 2001a) and Isoplot/Ex v2.49 (Ludwig, 2001b) packages. Zircon U–Pb data and Concordia plots are shown in Appendix D1.

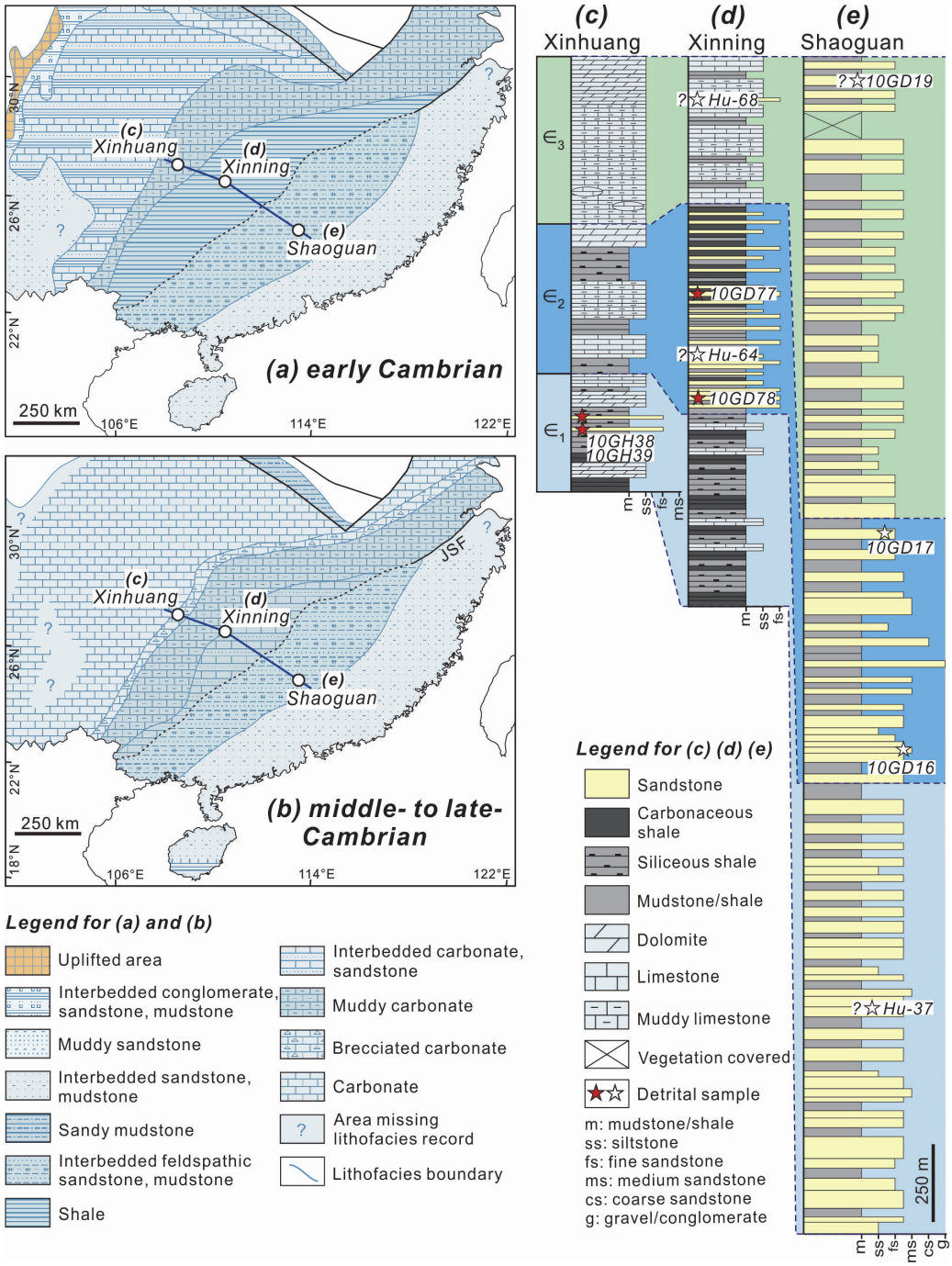

Figure 6.2. (a)–(b) Palaeogeographic maps of the South China Block (revised after Liu & Xu, 1994): (a) early Cambrian, (b) middle to late Cambrian. (c)–(e) Stratigraphic columns of Cambrian strata and sandstone samples from (c) the Xinhuang section of central Yangtze (RGMRHN-b, 1972), (d) the Xinning section of southeastern Yangtze (RGMRHN-a, 1975), and (e) the Shaoguan section of northern Cathaysia (Yao *et al.* 2014; W.H. Yao & Z.X. Li, unpub. data, 2014). Red stars are samples from this study, and white stars are samples reported in previous studies.

6.4 Analytical Results

Samples 12GH38 and 12GH39 from central Yangtze (the Xinhuang section) are

similar in U–Pb age patterns. Of the total 161 analyses, 145 are concordant (with concordance of 90–110%), ranging in age from 3050 ± 12 to 480 ± 10 Ma. Both samples yield a prominent age peak at 850–750 Ma and a moderate age peak at 530–500 Ma, with a few scattered Proterozoic ages (Figure 6.3a). Samples 10GD77 and 10GD78 from southeastern Yangtze (the Xinning section) are quite consistent in their U–Pb age patterns. Of the total 133 analyses, 132 are concordant, ranging from 3576 ± 11 to 509 ± 6 Ma. Both samples yield prominent age peaks at 1100–900 Ma and 530–500 Ma, and present a moderate age peak at 2500 Ma with a few scattered Proterozoic ages (Figure 6.3b). The detrital zircons of all four samples exhibit large compositional variations of Th and U, and most zircons (84 %) have Th/U > 0.3; only 8 grains (3%) have Th/U < 0.1 (Appendix D1). Th/U ratios and zoning structures of zircons suggest that most detrital zircons are probably of magmatic origin.

6.5 Discussion

6.5.1 Cambrian sediment dispersal across South China

Geochronological results show that lower Cambrian sandstones from central Yangtze (Xinhuang) have a prominent age peak at ~790 Ma and a subordinate peak at ~530 Ma (Figure 6.3a), whereas Cambrian sandstones from northwestern Cathaysia (Shaoguan) have a different prominent peak at ~960–910 Ma and a subordinate peak at ~530 Ma, with minor peaks at ~800 Ma and ~2500 Ma (Figure 6.3d–e) (Wang *et al.* 2010; Yao *et al.* 2014). This indicates that the Yangtze and Cathaysia blocks likely had different provenances during the Cambrian period. Statistical analysis (K–S test) (Kolmogorov, 1933; Smirnov, 1944) was conducted on samples from central Yangtze and northwestern Cathaysia, and the results (Appendix D2) also indicate that these two groups of samples had different provenances.

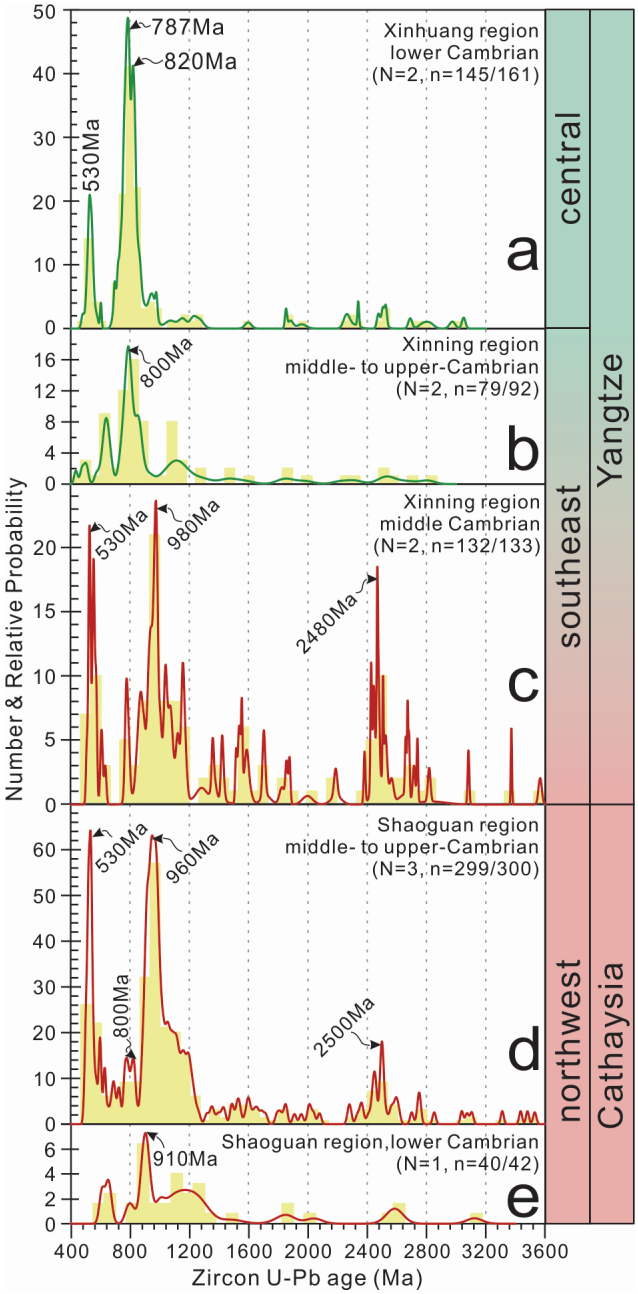

Figure 6.3. Plots of zircon U–Pb age histogram and relative probability of Cambrian sandstone samples from (a) Xinhuang (this study), (b) Xinning (this study), (c) Xinning (Wang *et al.* 2010), (d) Shaoguan (Yao *et al.* 2014), and (e) Shaoguan (Wang *et al.* 2010). Plotted ages are within concordance of 90–110% for analysed zircons. N = number of samples, n = number of concordant analyses/number of total analyses.

The palaeogeography of South China shows that, during the early Cambrian period, the Yangtze Block was dominantly a marine carbonate platform, consisting of intercalated clastic and carbonate sediments, with water deepening to the southeast (Figure 6.2a). During the middle to late Cambrian period, it received carbonate and muddy carbonate deposition (Figure 6.2b) (Liu & Xu, 1994). Since Cryogenian volcanic, volcanoclastic and intrusive rocks (860–750 Ma) are widespread in western

Yangtze Neoproterozoic rift basins (e.g. Zhou *et al.* 2002, 2006; Li, X.H. *et al.* 2003; Li, Z.X. *et al.* 2003; Li, X. *et al.* 2003; Wang & Li, 2003), we speculate that these *c.* 860–750 Ma rocks in western Yangtze were probably uplifted during the early Cambrian period and provided detritus to the Cambrian sandstones of central Yangtze Block (Figure 6.4a, b). The Cathaysia Block, on the other hand, received deposits of intercalated marine sandstones and mudstones, possibly with no exposed land in the region during the Cambrian period (Figure 6.2a, b). Both the NW-directed palaeocurrents and northwestward-fining sediments in the Cambrian strata of Cathaysia and southeastern Yangtze indicate an external provenance outboard to southeastern Cathaysia (Wang *et al.* 2010; W.H. Yao & Z.X. Li, unpub. data, 2014). Yao *et al.* (2014) proposed that South China was probably once connected to the northern Indian part of Gondwanaland, along the southeastern margin of Cathaysia. The Grenvillian magmatic rocks (1100–950 Ma) (e.g. Liu *et al.* 2007; Cottle *et al.* 2009), minor *c.* 880–820 Ma magmatic rocks and recycled 2500 Ma zircons in sedimentary rocks (e.g. Myrow *et al.* 2010) of northern India probably provided detritus to Cathaysia during the Cambrian (Figures 6.4b, 6.5).

The common age peak at ~530 Ma in both central Yangtze and northwestern Cathaysia (Figure 6.3a, d, e) suggests that both source areas (western Yangtze and northern India?) were affected by an early Palaeozoic orogeny and produced ~530 Ma magmatic rocks in the source region. The 530 Ma magmatic detritus was recorded in Cambrian sandstones not only from central Yangtze and northwestern Cathaysia, but also from southeastern Yangtze (Xinning) (Figure 6.3c). However, Cambrian sandstones in southeastern Yangtze exhibit mixed age patterns, with a major ~800 Ma peak in the middle to upper Cambrian sandstones (Figure 6.3b) and a major ~980 Ma peak in the middle Cambrian sandstones (Figure 6.3c). The ~800 Ma age peak is probably of the same origin as those in the lower Cambrian sandstones from central Yangtze (Figure 6.3a), i.e., from western Yangtze. However, the ~980 Ma peak in southeastern Yangtze (Figure 6.3c) indicates that detritus was probably sourced from northern India, and transported across Cathaysia to southeastern Yangtze (Figure 6.4b; Figure 6.5). This interpretation is supported by the NW-directed palaeocurrents in the Xinning Cambrian strata (Wang *et al.* 2010).

Sediment dispersal in South China can thus be summarized as the following. During

the early-Cambrian period, Cryogenian magmatic rocks in western Yangtze provided detritus to central Yangtze (Xinhuang). Northwestern Cathaysia (Shaoguan) received detritus from the southeast – an external source, possibly northern India, which likely hosted a Grenvillian-aged orogen (Figure 6.4b). In southeastern Yangtze (Xinning), on the lower slope of Yangtze platform compared to the Xinhuang region, mainly deep-water shale and siliceous shale were deposited during the early Cambrian period. During the middle to late Cambrian period, southeastern Yangtze probably received a major flux of detritus from a Grenvillian-aged orogen to the southeast, with a smaller portion of detritus from local western Yangtze sources (Figure 6.4b).

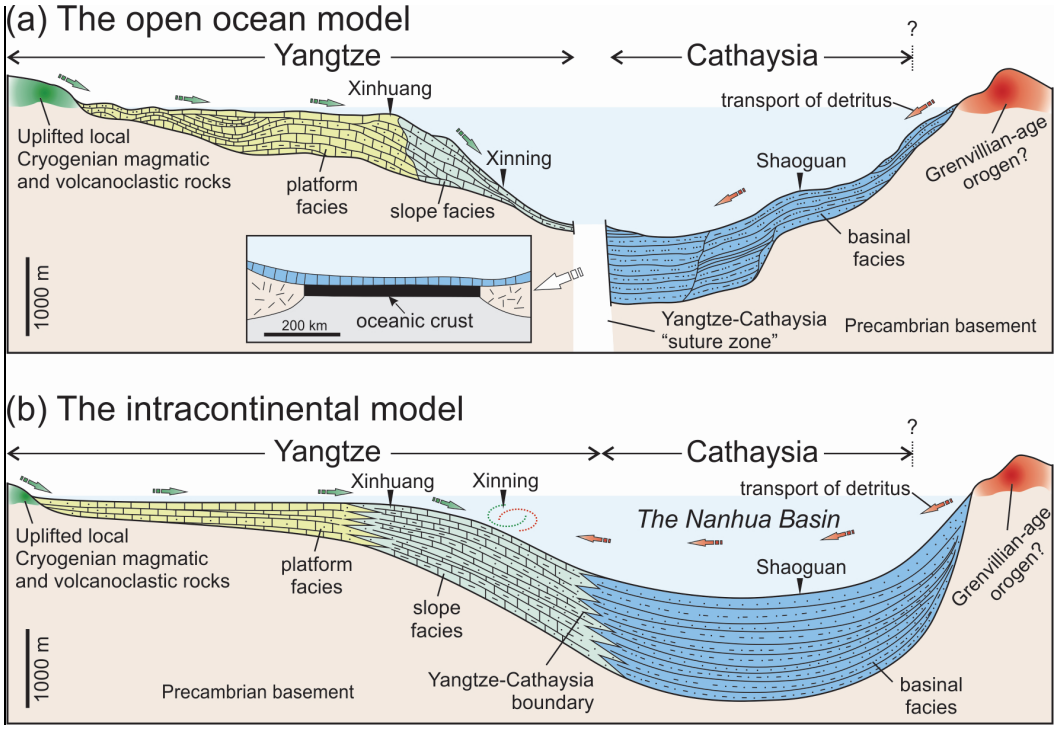

Figure 6.4. Cartoons illustrating possible paths of sediment transport during the Cambrian period for (a) the open ocean model and (b) the intracontinental model (revised after Liu & Xu, 1994). Detrital provenance analyses of Cambrian sandstones support the intracontinental model.

6.5.2 Was there a Cambrian ocean in South China?

In the Cambrian ocean model as proposed by Shui (1988) and Liu & Xu (1994), the Yangtze Block (central and southeastern Yangtze) should only have recorded detrital grains from western Yangtze (e.g. with a ~ 800 Ma peak) (Figure 6.3a, b) rather than showing a ~ 980 Ma age peak (Figure 6.3a). The fact that the southeastern Yangtze recorded a dominant Cathaysia-like provenance argues against the Cambrian ocean model. There are additional lines of evidence arguing against the ocean model,

including: (1) the absence of early Palaeozoic ophiolites or arc-like magmatic rocks related to ocean closure in the region (Chen *et al.* 1995; Li, 1998); (2) early Palaeozoic granites in South China that are largely sourced from remelting of old basement rocks with little input of juvenile mantle (e.g. Chen & Jahn, 1998; Zeng *et al.* 2008; Zhou, 2003; Li *et al.* 2010; Wang *et al.* 2011); (3) lower Palaeozoic sedimentary rocks in South China exhibit strongly negative $\varepsilon_{Nd}(t)$ values (e.g. Li & McCulloch, 1996; Chen & Jahn, 1998), which is inconsistent with being originated from a juvenile crust generated during an ocean closure in the early Palaeozoic period; and (4) sedimentary facies across the Cambrian Nanhua Basin are laterally coherent and vertically continuous and conformable (e.g. Liu & Xu, 1994), with no sign of convergent tectonics.

Based on the palaeogeography of South China and mixed provenance of Cambrian sandstones in southeastern Yangtze, we therefore favour the intracontinental model (e.g. Li, 1998; Faure *et al.* 2009; Charvet *et al.* 2010; Li *et al.* 2010; Wang *et al.* 2010; Shu *et al.* 2014). In this model, the Yangtze and Cathaysia blocks had become a coherent block before the Cambrian period. Detritus from uplifted western Yangtze was transported along the Yangtze platform and deposited in central Yangtze (Xinhuang) (Figure 6.3a) as well as southeastern Yangtze (Xinning) (Figure 6.3b). Detritus shed from northern India or even eastern Africa (a Grenvillian-age orogen? see Yao *et al.* 2014 for detailed discussion) travelled to northern Cathaysia (Shaoguan) (Figure 6.3d, e) and all the way to southeastern Yangtze (Xinning) (Figure 6.3c). Since central Yangtze (Xinhuang) is located on the upper opposite slope of the Nanhua Basin, it was difficult for Indian detritus to reach that region.

Provenance analyses of Cambrian sandstones across the Yangtze–Cathaysia boundary therefore provide evidence that argues against the existence of a broad Cambrian ocean, but is consistent with the intracontinental model which is also supported by sedimentary facies analyses across South China (Chen *et al.* 1995; Shu *et al.* 2014; W.H. Yao & Z.X. Li, unpub. data, 2014). Since southeastern Yangtze received shale and siliceous shale without clastic deposits in the lower Cambrian strata, it failed to record provenance mixing from the Cathaysia side. This may lead to the speculation that an ocean could have existed during the early Cambrian period. However, as mentioned before, such a speculation can be ruled out because there is

neither any record of an arc system nor any sign of convergent tectonics within the Nanhua Basin during the entire Cambrian period.

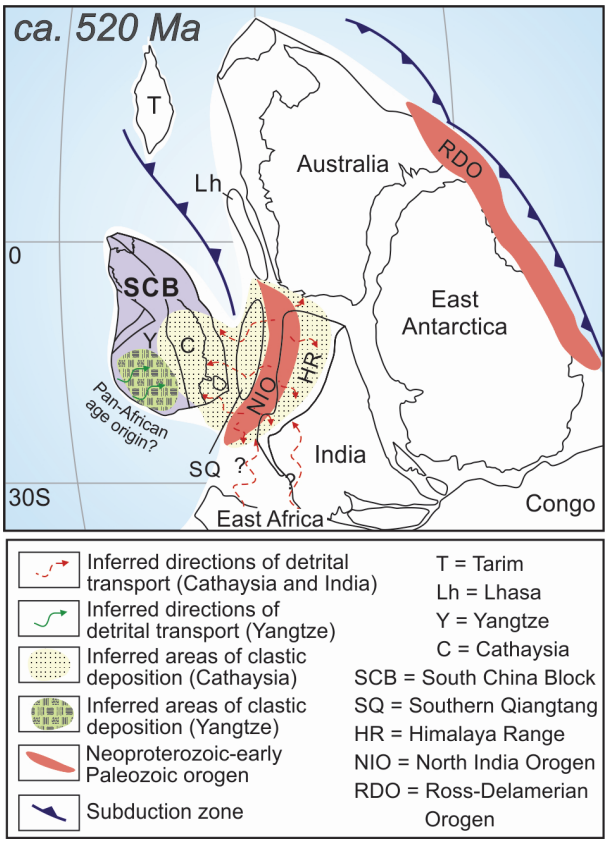

Figure 6.5. A paleogeographic reconstruction of South China on the margin of eastern Gondwanaland at ca. 520 Ma (modified after Yao et al. 2014), showing mixing of two different detrital provenances at the Yangtze–Cathaysia boundary.

6.6 Acknowledgements

The authors thank Hao Gao for assistances in SHRIMP U–Pb dating, Hongxia Ma for making zircon mounts, and Chris Elders for commenting on the manuscript. Comments from chief editor Mark Allen, reviewer Jacques Charvet and an anonymous reviewer improved this manuscript greatly. This study was supported by the Australian Research Council (DP110104799), Chinese Academy of Science SAFEA International Partnership Program for Creative Research Teams grant (KZCX2-YW-Q04-06) and National Natural Sciences Foundation of China (41173039). This is TIGeR (The Institute for Geoscience Research) publication #569, and contribution 469 from the ARC Centre of Excellence for Core to Crust Fluid Systems (http://www.ccfs.mq.edu.au/).

6.7 References

BGMRGD (Bureau of Geology and Mineral Resources of Guangdong Province) 1988. *Regional Geology of the Guangdong Province.* Beijing: Geological Publishing House, 971 p. (in Chinese with English abstract).

BGMRHN (Bureau of Geology and Mineral Resources of Hunan Province) 1988. *Regional Geology of the Hunan Province.* Beijing: Geological Publishing House, 719 p. (in Chinese with English abstract).

BGMRJX (Bureau of Geology and Mineral Resources of Jiangxi Province) 1984. *Regional Geology of the Jiangxi Province.* Beijing: Geological Publishing House, 921 p. (in Chinese with English abstract).

CHARVET, J., SHU, L., FAURE, M., CHOULET, F., WANG, B., LU, H. & LE BRETON, N. 2010. Structural development of the Lower Paleozoic belt of South China: Genesis of an intracontinental orogen. *Journal of Asian Earth Sciences* **39**, 309–330.

CHARVET, J., SHU, L., SHI, Y., GUO, L. & FAURE, M. 1996. The building of south China: collision of Yangzi and Cathaysia blocks, problems and tentative answers. *Journal of Southeast Asian Earth Sciences* **13**, 223–235.

CHEN, H., HOU, M., XU, X. & TIAN, J. 2006. Tectonic evolution and sequence stratigraphic framework in South China during Caledonian. *Journal of Chengdu University of Technology* **33**, 1–8 (in Chinese with English abstract).

CHEN, J. & JAHN, B.M. 1998. Crustal evolution of southeastern China: Nd and Sr isotopic evidence. *Tectonophysics* **284**, 101–133.

CHEN, X., RONG, J., ROWLEY, D.E., ZHANG, J., ZHANG, Y. & ZHAN, R. 1995. Is the early Paleozoic Banxi ocean in South China necessary? *Geological Review* **41**, 389–400.

COTTLE, J.M., JESSUP, M.J., NEWELL, D.L., HORSTWOOD, M.S.A., NOBLE, S.R., PARRISH, R.R., WATERS, D.J. & SEARLE, M.P. 2009. Geochronology of granulitized eclogite from the Ama Drime Massif: Implications for the tectonic evolution of the South Tibetan Himalaya. *Tectonics* **28**, doi:10.1029/2008TC002256

FAURE, M., SHU, L., WANG, B., CHARVET, J., CHOULET, F. & MONIE, P. 2009. Intracontinental subduction: a possible mechanism for the Early Palaeozoic Orogen of SE China. *Terra Nova* **21**, 360–368.

HSU, K.J., LI, J., CHEN, H., WANG, Q., SUN, S. & SENGOR, A.M.C. 1990. Tectonics of South China: Key to understanding West Pacific geology. *Tectonophysics* **183**, 9–39.

HSU, K.J., SUN, S., LI, J., CHEN, H., PEN, H. & SENGOR, A.M.C. 1988. Mesozoic overthrust tectonics in South China. *Geology* **16**, 418–421.

HUANG, J., REN, J., JIANG, C., ZHANG, Z. & QIN, D. 1980. *The Geotectonic Evolution of China.* Beijing: Science Press, 124 pp.

KOLMOGOROV, A.N. 1933. Sulla determinazione empirica di una legge di distribuzione. *Giornale dell'Istituto Italiano degli Attuari* **4**, 83–91.

LI, Z.X. 1998. Tectonic history of the major East Asian lithospheric blocks since the mid-Proterozoic: A synthesis. In *Mantle Dynamics and Plate Interactions in East Asia* (eds. M.F.J. Flower), pp. 221–243. *Geodynamics Series* **27**.

LI, Z.X., BOGDANOVA, S.V., COLLISONS, A.S., DAVIDSON, A., DE WAELE, B., ERNST, R.E., FITZSIMONS, I.C.W., FUCK, R.A., GLADKOCHUB, D.P., JACOBS, J., KARLSTROM, K.E., LU, S., NATAPOV, L.M., PEASE, V., PISAREVSKY, S.A., THRANE, K. & VERNIKOSKY, V. 2008. Assembly, configuration, and break-up history of Rodinia: a synthesis. *Precambrian Research* **160**, 179–210.

LI, X.H., LI, Z.X., GE, W.C., ZHOU, H.W., LI, W.X., LIU, Y. & WINGATE, M.T.D. 2003. Neoproterozoic granitoids in South China: crustal melting above a mantle plume at *ca.* 825 Ma? *Precambrian Research* **122**, 45–83.

LI, Z.X., LI, X.H., KINNY, P.D., WANG, J., Zhang, S. & Zhou, H. 2003. Geochronology of Neoproterozoic syn-rift magmatism in the Yangtze Craton, South China and correlations with other continents: evidence for a mantle superplume that broke up Rodinia. *Precambrian Research* **122**, 85–109.

LI, X.H., LI, W.X., LI, Z.X., LO, C.H., WANG, J., YE, M.F. & YANG, Y.H. 2009. Amalgamation between the Yangtze and Cathaysia blocks in South China: Constraints from SHRIMP U–Pb zircon ages, geochemistry and Nd–Hf isotopes of the Shuangxiwu volcanic rocks. *Precambrian Research* **174,** 117–128.

LI, Z.X., LI, X.H., WARTHO, J.A., CLARK, C., LI, W.X., ZHANG, C.L. & Bao, C.M. 2010. Magmatic and metamorphic events during the early Paleozoic Wuyi–Yunkai orogeny, southeastern South China: New age constraints and pressure–temperature conditions. *Geological Society of America Bulletin* **122**, 772–793.

LI, X., LI, Z., ZHOU, H., LIU, Y., LIANG, X. & LI, W. 2003. SHRIMP U–Pb zircon age, geochemistry and Nd isotope of the Guandaoshan pluton in SW Sichuan: petrogenesis and tectonic significance. *Science in China (Series D)* **46**, 73–83.

LI, X.H. & MCCULLOCH, M.T. 1996. Secular variation in the Nd isotopic composition of Neoproterozoic sediments from the southern margin of the Yangtze Block: evidence for a Proterozoic continental collision in southeast China. *Precambrian Research* **76**, 67–76.

LI, Z.X. & POWELL, C.M. 2001. An outline of the Palaeogeographic evolution of the Australasian region since the beginning of the Neoproterozoic. *Earth-Science Reviews* **53**, 237–277.

LI, Z.X., ZHANG, L.H. & POWELL, C.M. 1995. South China in Rodinia — part of the missing link between Australia-East Antarctica and Laurentia? *Geology* **23**, 407–410.

LI, X.H., ZHOU, G., ZHAO, J., FANNING, C.M. & COMPSTON, W. 1994. SHRIMP ion microprobe zircon U–Pb age of the NE Jiangxi ophiolite and its tectonic implications. *Geochimica* **23**, 125–131.

LIU, Y., SIEBEL, W., MASSONNE, H. & XIAO, X. 2007. Geochronological and petrological constraints for tectonic evolution of the central Greater Himalayan sequence in the Kharta area, southern Tibet. *The Journal of Geology* **115**, 215–230.

LIU, B. & Xu, X. 1994. *Atlas of Lithofacies and Paleogeography of South China.* Beijing: Science Press, 188 pp.

LUDWIG, K.R. 2001*a*. *SQUID version 1.02 – A geochronological toolkit for Microsoft excel.* Berkley Geochronological Centre, Special Publication no. 2.

LUDWIG, K.R. 2001*b*. *ISOPLOT/EX version 2.49 – A geochronological toolkit for Microsoft excel*. Berkley Geochronological Centre, Special Publication no. 1.

MYROW, P.M., HUGHES, N.C., GOODGE, J.W., FANNING, C.M., WILLIAMS, I.S., PENG, S.C., BHARGAVA, O.N., PARCHA, S.K. & POGUE, K.R. 2010. Extraordinary transport and mixing of sediment across Himalayan central Gondwana during the Cambrian–Ordovician. *Geological Society of America Bulletin* **122**, 1660–1670.

REN, J. 1991. On the geotectonics of southern China. *Acta Geologica Sinica* **4**, 111–130.

RGMRHN-a, 1975. *Regional Geological Mapping and Report of Hunan Province – 1:200,000 Lingling Sheet*. Beijing: Institute of Geoscience, Ministry of Geology (in Chinese with English abstract).

RGMRHN-b, 1972. *Regional Geological Mapping and Report of Hunan Province – 1:200,000 Huitong Sheet*. Beijing: Institute of Geoscience, Ministry of Geology (in Chinese with English abstract).

SHU, L.S., JAHN, B.M., CHARVET. J., SANTOSH, M., WANG, B., XU, X.S. & JIANG, S.Y. 2014. Early Paleozoic depositional environment and intraplate tectono-magmatism in the Cathaysia Block (South China): Evidence from stratigraphic, structural, geochemical and geochronological investigations. *American Journal of Science* **314**, 154–186.

SHUI, T. 1988. Tectonic framework of the southeastern China continental basement. *Scientia Sinica (Series B)* **31**, 885–896.

SLAMA, J., KOSLER, J., CONDON, D.J., CROWLEY, J.L., GERDES, A., HANCHAR, J.M., HORSTWOOD, M.S.A., MORRIS, G.A., NASDALA, L., NORBERG, N., SCHALTEGGER, U., SCHOENE, B., TUBRETT, M.N. & WHITEHOURSE, M.J. 2008. Plesovice zircon – A new natural reference material for U–Pb and Hf isotopic microanalysis. *Chemical Geology* **249**, 1–35.

SMIRNOV, N.V. 1944. Approximate laws of distribution of random variables from empirical data. *Uspekhi Matematicheskikh Nauk* **10**, 179–206 (in Russian).

STERN, R.A. 2001. A new isotopic and trace-element standard for the ion microprobe: preliminary thermal ionization mass spectrometry (TIMS) U–Pb and electron-microprobe data. *Radiogenic Age and Isotopic Studies Report* **14**, *Geological Survey of Canada, Current Research 2001-F1*.

WANG, J. & LI, Z.X. 2003. History of Neoproterozoic rift basins in South China: implications for Rodinia break-up. *Precambrian Research* **122**, 141–158.

WANG, Y., ZHANG, F., FAN, W., ZHANG, G., CHEN, S., CAWOOD, P.A. & ZHANG, A. 2010. Tectonic setting of the South China Block in the early Paleozoic: Resolving intracontinental and ocean closure models from detrital zircon U–Pb geochronology. *Tectonics* **29**, doi:10.1029/2010TC002750.

WANG, Y., ZHANG, A., FAN, W., ZHAO, G., ZHANG, G., ZHANG, Y., ZHANG, F. & LI, S. 2011. Kwangsian crustal anatexis within the eastern South China Block: Geochemical, zircon U–Pb geochronological and Hf isotopic fingerprints from the gneissoid granites of Wugong and Wuyi–Yunkai Domains. *Lithos* **127**,

239–260.

WILLIAMS, I.S. 1998. U–Th–Pb geochronology by ion microprobe. In *Applications of Microanalytical Techniques to Understanding Mineralizing Processes, Reviews in Economic Geology vol. 7* (eds M.A. MCKIBBEN, W.C. SHANKS, III & W.I. RIDLEY), pp. 1–35. Littleton, CO: Society of Economic Geologists.

XU, B. & QIAO, G.S. 1989. Sm–Nd isotopic age and tectonic setting of the Late Proterozoic ophiolites in northeastern Jiangxi province. *Journal of Nanjing University (Science and Technology)* **3**, 108–114.

XU, X., XU, Q. & PAN, G. 1996. The continental evolution of southern China and its global comparison. Beijing: Geological, 161pp.

YANG, Z., CHENG, Y.Q. & Wang, H.C. 1986. *The geology of China.* Oxford: Clarendon Press, 276 pp.

YAO, W.H., LI, Z.X., LI, W.X., LI, X.H. & YANG, J.H. 2014. From Rodinia to Gondwanaland: a tale of detrital zircon provenance analyses from the southern Nanhua Basin, South China. *American Journal of Science* **314**, 278–313.

ZENG, W., ZHANG, L., ZHOU, H., ZHONG, Z., XIANG, H., LIU, R., JIN, S., LU, X.Q. & LI, C.Z. 2008. Caledonian reworking of Paleoproterozoic basement in the Cathaysia Block: constraints from zircon U–Pb dating, Hf isotopes and trace elements. *Chinese Science Bulletin* **53**, 895–904.

ZHANG, L. & HE, Q. 1993. On the revision of Bacun Group and the establishment of Xiazhai, Oujiadong and Laoshuzhai Formations in northern Guangdong Province. *Guangdong Geology* **8**, 1–14 (in Chinese with English abstract).

ZHAO, G. & CAWOOD, P.A. 1999. Tectonothermal evolution of the Mayuan assemblage in the Cathaysia Block: implications for Neoproterozoic collision-related assembly of the South China Craton. *American Journal of Science* **299**, 309–339.

ZHOU, G. 1989. The discovery and significance of the northeastern Jiangxi Province ophiolite (NEJXO), its metamorphic peridotite and associated high temperature–high pressure metamorphic rocks. *Journal of Southeast Asian Earth Science* **3**, 237–247.

ZHOU, X. M. 2003. My thinking about granite geneses of south China. *Geological Journal of China Universities* **9**, 556–565 (in Chinese with English abstract).

ZHOU, M.F., MA, Y., YAN, D.P., XIA, X., ZHAO, J.H. & SUN, M. 2006. The

Yanbian Terrane (Southern Sichuan Province, SW China): A Neoproterozoic arc assemblage in the western margin of the Yangtze Block. *Precambrian Research* **144**, 19–38.

ZHOU, M.F., YAN, D.P., KENNEDY, A.K., LI, Y. & DING, J. 2002. SHRIMP U–Pb zircon geochronological and geochemical evidence for Neoproterozoic arc-magmatism along the western margin of the Yangtze Block, South China. *Earth and Planetary Science Letters* **196**, 51–67.

CHAPTER 7 SUMMARIES AND CONCLUSIONS

7.1 Orogenic Collapse as a Mechanism for Widespread Syn- to Late-Orogenic Magmatism during the Wuyi–Yunkai Orogeny?

The early Palaeozoic South China features a wide occurrence of syn-orogenic high-grade metamorphism (*ca.* 460–440 Ma) in the core of the Wuyi–Yunkai orogen, and syn- to late-orogenic granites (*ca.* 440–415 Ma) in both the orogenic core and fold-and-thrust belt (Chapter 2, Figure 2.1a). However, neither syn- to late-orogenic volcanic rocks, nor mafic rocks of any type, have previously been reported, although such mafic rocks can shed clues on understanding any mantle–crust interaction during the Wuyi–Yunkai orogeny, and thus the geodynamic process involved.

The Silurian mafic–intermediate volcanic succession reported in Chapter 2 from northern Guangdong, near the edge of the metamorphic orogenic core (Figure 2.1a), is the first reported mafic rock suite in the region. The volcanic succession unconformably overlies the strongly-deformed Cambro-Ordovician strata (deformed by the Wuyi–Yunkai orogeny before the eruption of the Silurian volcanic rocks), but are overlain, with a low-angle angular unconformity, by the post-orogenic middle-Devonian strata (Figure 2.1b). Geochronological and geochemical analyses show that the volcanic succession consists of basalts, andesites and dacites with a crystallization age of *ca.* 435 Ma. The basalts, characterised by high Mg content (MgO = 12.3–19.2 wt.%), low $\varepsilon_{Nd}(t)$ values (–8.0 to –8.4) and low Nb/La ratios (0.4–0.8), were likely derived from partial melting of an ancient hydrated and metasomatized sub-continental lithospheric mantle with a potential melting temperature of ~1300 °C. The andesites and dacites were likely generated from the same basaltic magma by AFC processes.

The orogenic root delamination model (Figure 2.9), as proposed by Li et al. (2010), can best explain the generation of the Silurian volcanic rocks. Crustal shortening during the early stage of the Wuyi–Yunkai orogeny would have led to a thickened crust and high topography at the orogenic core, and the crustal root could have experienced eclogite facies metamorphism, causing the delamination of both the

eclogitic lower crust and the attached lithospheric mantle late during the orogenic cycle. The delamination likely caused partial melting near the edge of the remaining sub-continental lithospheric mantle by upwelling asthenosphere, producing the Silurian mafic–intermediate volcanic rocks. The widespread post-kinematic granites were likely caused by either the heat from the underplated basaltic magma, or decompressional melting of the lithosphere, or both (Figure 2.9), which is consistent with the observation that the age of the mafic–intermediate volcanism (*ca.* 435 Ma) post-dates that of the high-grade metamorphism (*ca.* 460–440 Ma), but synchronous with the widespread, dominant post-kinematic granites (*ca.* 440–415 Ma) (Li et al., 2010). The model is subsequently supported by the reporting of *ca.* 425–435 Ma gabbroic rocks on the opposite edge of the Wuyi–Yunkai orogenic core (Wang et al., 2013).

7.2 Evolution of the Lower Palaeozoic Nanhua Foreland Basin: Record of Two Orogenic Events

The Nanhua Basin in South China started as a failed rift basin during middle-Neoproterozoic (*ca.* 860–600 Ma), which covered the southeastern Yangtze and northwesten Cathaysia blocks (Wang and Li, 2003; Li et al., 2014). However, the post-600 Ma sedimentation of the Nanhua Basin was poorly understood and has been a topic of debate regarding its basin type, sedimentary history and tectonic relationship with the Wuyi–Yunkai orogen (e.g., Pan et al., 1984; Guo et al., 1989; Li, 1998; Li et al., 2010; Wang et al., 2010; Jiang et al., 2014; Yao et al., 2014a). In this study we discussed the stratigraphic and provenance evolution of the early Palaeozoic Nanhua Basin in order to address its tectono-sedimentary relationship with relevant orogens (e.g., the Wuyi–Yunkai orogen).

The stratigraphic study of four sections across the lower Palaeozoic Nanhua Basin (Chapter 4) shows that it is a northeasterly-oriented basin with thick clastic rocks developed on the southeastern side of the basin (Figure 4.9), which is bounded by, and partly got involved into, the Wuyi–Yunkai orogenic belt to the southeast (Li et al., 2010). Investigations on magmatic rocks show no early Palaeozoic arc or arc-related magmatism in the southeastern SCB (e.g., Chen and Jahn, 1998; Zeng et al., 2008; Li et al., 2010; Wang et al., 2011; Yao et al., 2012). The general trend of

upwards-coarsening clastics, coupled upwards-shallowing water level across the basin, is indicative of a foreland basin infilling, which terminated in subaerial sedimentation in the distal basin. Based on the analysis of basin geometry and stratigraphy features, the lower Palaeozoic Nanhua Basin is interpreted as a peripheral foreland basin.

The foreland basin evolution of the Nanhua Basin can be divided into two stages (see Chapter 4 for detailed discussion): (1) a Cambrian (and possibly Ediacaran) to earliest-Ordovician underfilled to filled stage with marine to shallow marine clastic facies covering the Cathaysia Block and part of the southeastern Yangtze Block; and (2) an early-Ordovician to Silurian overfilled stage with fluvial-dominated deltaic facies and possible alluvial facies covering majority of the Yangtze Block and part of the northern and southwestern Cathaysia block. Ediacaran–Cambrian provenance (Yao et al., 2014a) and lithostratigraphic (Yao et al., 2014b) analyses in the region indicate that the first stage of the Nanhua foreland basin may have started as early as the Ediacaran. The two stages of the foreland basin evolution were probably linked to two orogenic processes which affected South China: (1) the first stage was linked to an orogeny outboard the Cathaysia Block, resulted from the possible collision between the SCB and northern India during the assembly of Gondwanaland (Yao et al., 2014a). The second stage was linked to the local intraplate Wuyi–Yunkai orogeny in South China, which was caused by far-field stress from the aforementioned collision. An extremely thick package of Silurian marine sedimentary strata was deposited in the southwestern Cathaysia Block, inside the Wuyi–Yunkai orogenic core (the so-called "Qinfang Tough" in Chinese literature, Liu and Xu, 1994; Liu, 1998; Xu et al., 2001). This abnormal Silurian package is considered to have started as a piggy-back basin among the fold-and-thrust belt of the orogen, which may have later become a graben during the orogenic collapse of the Wuyi–Yunkai orogen (Figure 4.10D).

The provenance evolution of the Nanhua foreland basin was also studied in this thesis (Chapter 5). Ediacaran–Silurian sandstone/metasandstone samples from the basin were analysed to establish the tempo-spatial variations of provenance across the Nanhua foreland basin. Except for clastic samples from northeast Yangtze and a tuffaceous sample, all other samples exhibit a prominent population of 1100–900 Ma,

moderate populations of 850–700 Ma and 650–490 Ma, a minor population of 2500 Ma, and scattering ages of 2000–1300 Ma (Figures 5.7–5.8) (Yao et al., 2014c), grossly matching that of crystalline and sedimentary rocks in northern India (see Chapter 5 for detailed discussion). Zircon Hf isotopes further reveal four episodes of juvenile crustal growth at 2.5 Ga, 1.8 Ga, 1.4 Ga and 1.0 Ga in the source region(s), all of which are consistent with crystalline basement compostions of northern Inda and surrounding orogens/cratons (see Chapter 3 and referecences therein).

Utilizing the sedimentary evolution of the Nanhua foreland basin (Chapter 4) (Yao et al., 2014b) and the early Palaeozoic palaeogeography of South China (Figure 5.8) (Liu and Xu, 1994), we conclude that the Ediacaran–Cambrian sediments in the Nanhua foreland basin were probably sourced from northern India and adjacent orogens, and the Ordovician–Silurian sediments were derived from both locally recycled Ediacaran–Cambrian rocks and eroded Cathaysian basement rocks. The Wuyi–Yunkai late-orogenic magmatic rocks also contributed to the Silurian sediments in the basin (Yao et al., 2014c). The upper-Ordovician to Silurian samples in northeast Yangtze received higher proportions of detritus from local Cryogenian (850–700 Ma) rift-related magmatic rocks which were uplifted during late-Ordovician to Silurian time. We speculate that there was probably an Ediacaran–Cambrian collisional orogeny between South China and northern India, shedding sediments to the first stage of the Nanhua foreland basin. Far-field stress during this collisional orogeny triggered the Ordovician–Silurian intraplate Wuyi–Yunkai orogeny in South China, and erosion of the local Wuyi–Yunkai orogen provided detritus to the second stage of the Nanhua foreland basin (Yao et al., 2014c).

A spin-off of the provenance analyses across the Nanhua foreland basin was to examine whether there was a broad ocean between the Yangtze and Cathaysia blocks during the Cambrian (Chapter 6). The results reveal that detrital zircons of Cambrian sandstones from central Yangtze exhibit a major ~800 Ma age peak, being sourced from western Yangtze, whereas those from northwestern Cathaysia exhibit a major ~980 Ma peak, being sourced from an exotic continent connecting to the Cathaysia Block at the time (i.e., northern India). However, mixed provenances are detected in Cambrian sandstones from southeastern Yangtze, indicating that detritus can travel

across the proposed oceanic suture, from Cathaysia to Yangtze. It therefore argues against the existence of a broad Cambrian ocean between the two blocks, but supports an intraplate regime for the region (Figure 6.4) (Yao et al., 2014d).

7.3 Implications for Global Palaeogeography

Last but not least, it is important to understand regional geotectonic events in a global context. Chapter 3 presents an integrated *in-situ* U–Pb age and Hf–O isotope analyses of detrital zircons from Cambrian sedimentary rocks in the southwestern South China. The results indicate that the source provenance of these Cambrian sandstones is distinctly different from the known tectonomagmatic record of South China (Figure 3.7), but matches well with that of the Ediacaran–Cambrian clastic sedimentary rocks and granitic intrusions in the NW Indian Himalaya (Figure 3.8). The SCB–NW India provenance linkage appears to have started from the Ediacaran. We propose that after breaking away from central Rodinia (e.g., Li et al., 2002, 2008), the SCB collided with NW India during the Ediacaran–Ordovician, causing the "Pan-African" orogeny at the northern margin of India as well as the intraplate Wuyi–Yunkai orogeny in South China, and the formation of foreland basins on both the northern Indian and South China sides of the orogen (Figure 3.9) (Yao et al., 2014a).

7.4 Conclusions

This study, including the nature of the early Palaeozoic Wuyi–Yunkai orogeny and the evolution of the Nanhua Basin in South China, provides new insights on the geodynamics and palaeopositions of South China during the transition from the break-up the supercontinent Rodinia to the assembly of Gondwanaland.

Provenance results from Ediacaran–Cambrian sandstone/metasandstone samples in the Cathaysia Block (part of South China) revealed that these sediments were mainly derived from the northern Indian margin and the adjacent East African orogen. Similarities between South China and northern India are not only found in their detrital provenances, but also in stratigraphy, magmatism, tectonic unconformity and palaeontology. It thus led to a self-consistent tectonic interpretation that after

breaking away from central Rodinia, South China probably collided with northern India during the Ediacaran–Ordovician, generating an orogen at the collision zone and foreland basins on both the Indian and South China sides of the orogen. The foreland basin on the South China side was the first stage (Ediacaran? to earliest-Ordovician) of the Nanhua foreland basin. The sedimentary evolution during this time interval shows that the Nanhua foreland basin was an underfilled to filled basin with marine turbidites and shallow marine deposits.

During the early-Ordovician to Silurian, far-field stress from the SCB–northern India collision probably produced the intraplate Wuyi–Yunkai orogeny in South China. Provenance analysis suggests that most of the early-Ordovician to Silurian sandstones across the Nanhua foreland basin were likely derived from locally recycled Ediacaran to Cambrian rocks and eroded Cathaysian basement rocks. The Wuyi–Yunkai late-orogenic magmatic rocks (~435 Ma) also contributed to the Silurian sediments in the basin. Stratigraphic study shows that the Nanhua foreland basin was by then an overfilled basin with fluvial-dominated deltaic sediments, which covered much of the Yangtze Block and a part of the southwestern Cathaysia Block.

Overall, the sedimentary process of the Nanhua foreland basin was linked to (1) the Ediacaran–Cambrian collisional orogeny between South China and northern India and (2) the Ordovician–Silurian intraplate Wuyi–Yunkai orogeny. The sedimentation of the basin featured upward-coarsening clastic deposition, upward-shallowing water, northwestward-migrating depocentres and northwest-directed transportation of detritus. The Wuyi–Yunkai orogen featured (1) an intraplate regime, which argues against the proposed broad Cambrian ocean between the Yangtze and Cathaysia blocks, and (2) a post-kinematic lithospheric delamination, which caused the orogenic collapse and widespread late-orogenic magmatism.

7.5 Future Work

This study interprets that South China likely collided with northern India to become part of Gondwanaland during the Ediacaran–Cambrian time. However, questions remain regarding exactly how the collision occurred and what other geological

evidence are there for such a collision (Li, 1998; Li and Powell, 2001; Yao et al., 2014a).

To advance our understanding on palaeopositions of South China in Gondwanaland and their geodynamic interactions, the following aspects of future research are crucial. (1) There are lower-Cambrian siliciclastic basin fills in the western and southwestern Yangtze Block that need to be better documented in both sedimentary stratigraphy and detrital provenance, so to understand whether these sediments had any connection with the proposed collision. (2) Early Palaeozoic volcanic and volcanoclastic rocks in the Nanhua foreland basin, if any, need to be analysed for geochronology, geochemistry and Hf–O and Sr–Nd isotopes to reveal their tectonic affinities. (3) The Hainan Island, located in southern Cathaysia Block, needs to be targeted for its lower Palaeozoic sedimentary rocks and magmatic rocks (if any), to better constrain the interaction between South China and other continents(s) during the Gondwana assembly. (4) The ca. 435 Ma basalts in Chapter 2 need to be further investigated in petrology (both in field and under microscope), to further explore its petrological and petrogenesis features. A systematic investigation of geochronology, petrology, geochemistry and isotopes on all early Palaeozoic granites in South China needs to be conducted. Granites need to be further compared with the basalts and mafic rocks (if any) in the region, to explore their relationship in petrogenesis and primary melts. Such work will thus help to establish the tempo-spatial magmatic evolution during the Ordovician–Silurian intraplate Wuyi–Yunkai orogeny. By answering these questions, it will help to better understand the geodynamic evolution of the South China Block from the late Neoproterozoic to early Palaeozoic and its global significance.

7.6 References

Chen, J., Jahn, B.M., 1998. Crustal evolution of southeastern China: Nd and Sr isotopic evidence. Tectonophysics 284, 101–133.

Guo, L.Z., Shi, Y.S., Lu, H.F., Ma, R.S., Dong, H.G., Yang, S.F., 1989. The pre-Devonian tectonic patterns and evolution of South China. Journal of Southeast Asian Earth Sciences 3, 87–93.

Jiang, B., Sinclair, H.D., Niu, Y., Yu, J., 2014. Late Neoproterozoic–Early Paleozoic

evolution of the South China Block as a retroarc thrust wedge/foreland basin system. International Journal of Earth Sciences 103, 23–40.

Li, Z.X., 1998. Tectonic history of the major East Asian lithospheric blocks since the mid-Proterozoic – a synthesis, In: Flower, M.J., Chung, S.L., Lo, C.H., Lee, T.Y. (Eds.), Mantle dynamics and plate interactions in East Asia. American Geophysical Union, Washington, DC, pp. 221–243.

Li, Z.X., Bogdanova, S.V., Collins, A.S., Davidson, A., De Waele, B., Ernst, R.E., Fitzsimons, I.C.W., Fuck, R.A., Gladkochub, D.P., Jacobs, J., Karlstrom, K.E., Lu, S., Natapov, L.M., Pease, V., Pisarevsky, S.A., Thrane, K., Vernikosky, V., 2008. Assembly, configuration, and break-up history of Rodinia: a synthesis. Precambrian Research 160, 179–210.

Li, Z.X., Chen, H., Li, X.H., Zhang, F.Q., 2014. Tectonics of the South China Block — An overview and a field guide of eastern South China. Chinese Science Press, Beijing (in-press).

Li, Z.X., Li, X.H., Wartho, J.A., Clark, C., Li, W.X., Zhang, C.L., Bao, C.M., 2010. Magmatic and metamorphic events during the early Paleozoic Wuyi–Yunkai orogeny, southeastern South China: New age constraints and pressure–temperature conditions. Geological Society of America Bulletin 122, 772–793.

Li, Z.X., Li, X.H., Zhou, H.W., Kinny, P.D., 2002. Grenvillian continental collision in south China: new SHRIMP U–Pb zircon results and implications for the configuration of Rodinia. Geology 30, 163–166.

Li, Z.X., Powell, C.M., 2001. An outline of the Palaeogeographic evolution of the Australasian region since the beginning of the Neoproterozoic. Earth-Science Reviews 53, 237–277.

Liu, B., Xu, X., 1994. Atlas of Lithofacies and Paleogeography of South China. Beijing: Science Press, 188 p.

Liu, W.J., 1998. Evolution of sedimentation of South China plate in the Hercynian-Indosinian stage. Journal of Chengdu University of Technology 25, 328–336 (in Chinese with English abstract).

Pan, G., 1984. The late Precambrian and early Paleozoic marginal basin of South China. In: Kokelaor, B.P., Howell, M.F. (Eds.), Marginal Basin Geology. Blackwell Scientific, Oxford, pp. 279–283.

Wang, Y., Zhang, A., Fan, W., Zhang, Y., Zhang, Y., 2013. Origin of

paleosubduction-modified mantle for Silurian gabbro in the Cathaysia Block: Geochronological and geochemical evidence. Lithos 160–161, 37–54.

Wang, Y., Zhang, A., Fan, W., Zhao, G., Zhang, G., Zhang, Y., Zhang, F., Li, S., 2011. Kwangsian crustal anatexis within the eastern South China Block: Geochemical, zircon U–Pb geochronological and Hf isotopic fingerprints from the gneissoid granites of Wugong and Wuyi–Yunkai Domains. Lithos 127, 239–260.

Wang, Y., Zhang, F., Fan, W., Zhang, G., Chen, S., Cawood, P.A., Zhang, A., 2010. Tectonic setting of the South China Block in the early Paleozoic: Resolving intracontinental and ocean closure models from detrital zircon U–Pb geochronology. Tectonics 29, doi:10.1029/2010TC002750.

Xu, X., Yin, F., Wan, F., Liang, Z., Wei, B., Zhang, J., 2001. The migration of the Qinzhou-Fangcheng trough in Guangxi and associated sedimentary-tectonic transform surfaces. Sedimentary Geology and Tethyan Geology 21, 1–10 (in Chinese with English abstract).

Yao, W.H., Li, Z.X., Li, W.X., Wang, X.C., Li, X.H., Yang, J.H., 2012. Post-kinematic lithospheric delamination of the Wuyi–Yunkai orogen in South China: evidence from *ca.* 435 Ma high-Mg basalts. Lithos 154, 115–129.

Yao, W.H., Li, Z.X., Li, W.X., Li, X.H., Yang, J.H., 2014a. From Rodinia to Gondwanaland: a tale of detrital zircon provenance analyses from the southern Nanhua Basin, South China. American Journal of Science 314, 278–313.

Yao, W.H., Li, Z.X., 2014b. Stratigraphic history of the lower Palaeozoic Nanhua foreland basin in South China: Response to two successive orogenies. Tectonics (to be submitted).

Yao, W.H., Li, Z.X., Li, W.X., Su, L., Yang, J.H., 2014c. Detrital provenance evolution of the lower Paleozoic Nanhua foreland basin, South China. Gondwana Research (to be submitted).

Yao, W.H., Li, Z.X., Li, W.X., 2014d. Was there a Cambrian ocean in South China? – Insight from detrital provenance analyses. Geological Magazine (in press).

Zeng, W., Zhang, L., Zhou, H., Zhong, Z., Xiang, H., Liu, R., Jin, S., Lü, X., Li, C., 2008. Caledonian reworking of Paleoproterozoic basement in the Cathaysia Block: Constraints from zircon U–Pb dating, Hf isotopes and trace elements.

Chinese Science Bulletin 53, 895–904.

CHAPTER 8 REFERENCES

Ameen, S.M.M., Wilde, S.A., Kabir, Z., Akon, E., Chowdhury, K.R., Khan, S.H., 2007. Paleoproterozoic granitoids in the basement of Bangladesh: A piece of the Indian shield or an exotic fragment of the Gondwana jigsaw? Gondwana Research 12, 380–387.

Amelin, Y., Lee, D.C., Halliday, A.N., Pidgeon, R.T., 1999. Nature of the Earth's earliest crust from hafnium isotopes in single detrital zircons. Nature 399, 252–255.

Amidon, W.H., Burbank, D.W., Gehrels, G.E., 2005. Construction of detrital mineral populations: Insights from mixing of U-Pb zircon ages in Himalayan rivers. Basin Research 17, 463–485.

Anderson, T., 2002. Correction of common lead in U–Pb analyses that do not report 204Pb. Chemical Geology 192, 59–79.

Bagati, T.N., Kumar, R., Ghosh, S.K., 1991. Regressive–transgressive sedimentation in the Ordovician sequence of the Spiti (Tethys) basin, Himachal Pradesh, India. Sedimentary Geology 73, 171–184.

Barth, A.P., Wooden, J.L., Coleman, D.S., Fanning, C.M., 2000. Geochronology of the Proterozoic basement of southwesternmost North America, and the orogin and evolution of the Mojave crustal province. Tectonics 19, 616–629.

Belousova, E.A., Kostitsyn, Y.A., Griffin, W.L., Begg, G.C., O'Reilly, S.Y., Pearson, N.J., 2010. The growth of the continental crust: constraints from zircon Hf-isotope data. Lithos 119, 457–466.

Berry, R.F., Jenner, G.A., Meffre, S., Tubrett, M.N., 2001. A North American provenance for Neoproterozoic to Cambrian sandstones in Tasmania? Earth and Planetary Science Letters 192, 207–222.

BGMRFJ (Bureau of Geology and Mineral Resources of Fujian Province), 1985. Regional Geology of the Fujian Province. Beijing: Geological Publishing House, 671 p. (in Chinese with English abstract).

BGMRGD (Bureau of Geology and Mineral Resources of Guangdong Province), 1988. Regional Geology of the Guangdong Province. Beijing: Geological Publishing House, 971 p. (in Chinese with English abstract).

BGMRGX (Bureau of Geology and Mineral Resources of Guangxi Province), 1985.

Regional Geology of the Guangxi Province. Beijing: Geological Publishing House, 853 p. (in Chinese with English abstract).

BGMRGZ (Bureau of Geology and Mineral Resources of Guizhou Province), 1988. Regional Geology of the Guizhou Province. Beijing: Geological Publishing House, 698 p. (in Chinese with English abstract).

BGMRHN (Bureau of Geology and Mineral Resources of Hunan Province), 1988. Regional Geology of the Hunan Province. Beijing: Geological Publishing House, 719 p. (in Chinese with English abstract).

BGMRJX (Bureau of Geology and Mineral Resources of Jiangxi Province), 1984. Regional Geology of the Jiangxi Province. Beijing: Geological Publishing House, 921 p. (in Chinese with English abstract).

BGMRZJ (Bureau of Geology and Mineral Resources of Zhejiang Province), 1989. Regional Geology of the Zhejiang Province. Beijing: Geological Publishing House, 688 p. (in Chinese with English abstract).

Bhargava, O.N., Frank, W., Bertle, R., 2011. Late Cambrian deformation in the Lesser Himalaya. Journal of Asian Earth Sciences 40, 201–212.

Black L.P., Kamo, S.L., Allen, C.M., Aleinikoff, J.N., Davis, D.W., Korsch, R.J., Foudoulis, C., 2003. TEMORA1: a new zircon standard for Phanerozoic U–Pb geochronology. Chemical Geology 200, 155–170.

Blichert Toft, J., Albarède, F., 1997. The Lu-Hf isotope geochemistry of chondrites and the evolution of the mantle-crust system. Earth and Planetary Science Letters 148, 243–258.

Bouma, A.H., 1962. Sedimentology of some flysch deposits: a graphic approach to facies interpretation. Elsevier, Amsterdam, 168 pp.

Brookfield, M.E., 1993. The Himalayan passive margin from Precambrian to Cretaceous. Sedimentary Geology 84, 1–35.

Busby, C.J., Ingersoll, R.V., 1995. Tectonics of sedimentary basins. Blackwell Scientific, Oxford, 579 pp.

Cawood, P.A., Johnson, M.R.W., Nemchin, A.A., 2007. Early Palaeozoic orogenesis along the Indian margin of Gondwana: Tectonic response to Gondwana assembly. Earth and Planetary Science Letters 255, 70–84.

Cawood, P.A., Nemchin, A.A., 2000. Provenance record of a rift basin: U/Pb ages of detrital zircons from the Perth Basin, Western Australia. Sedimentary Geology 134, 209–234.

Cawood, P.A., Wang, Y., Xu, Y., Zhao, G., 2013. Locating South China in Rodinia and Gondwana: A fragment of greater India lithosphere? Geology 41, 903–906.

Charvet, J., Shu, L., Shi, Y., Guo, L., & Faure, M., 1996. The building of south China: collision of Yangzi and Cathaysia blocks, problems and tentative answers. Journal of Southeast Asian Earth Sciences 13, 223–235.

Charvet, J., Shu, L., Faure, M., Choulet, F., Wang, B., Lu, H., Le Breton, N., 2010. Structural development of the Lower Paleozoic belt of South China: Genesis of an intracontinental orogen. Journal of Asian Earth Sciences 39, 309–330.

Chen, C.H., Lee, C.Y., Hsieh, P.S., Zeng, W., Zhou, H.W., 2008. Approaching the age problem for some metamorphosed Precambrian basement rocks and Phanerozoic granitic bodies in the Wuyi area: the application of EMP monazite age dating. Geological Journal of China University 14, 1–15 (in Chinese with English abstract).

Chen, H., Hou, M., Xu, X., Tian, J., 2006. Tectonic evolution and sequence stratigraphic framework in South China during Caledonian. Journal of Chengdu University of Technology 33, 1–8 (in Chinese with English abstract).

Chen, J., Jahn, B.M., 1998. Crustal evolution of southeastern China: Nd and Sr isotopic evidence. Tectonophysics 284, 101–133.

Chen, X., Rong, J., Rowley, D.B., Zhang, J., Zhang, Y.D., Zhan, R.B., 1995. Is the early Paleozoic Banxi Ocean in South China necessary? Geological Review 41, 389–400 (in Chinese with English abstract).

Chen, X., Rong, J.Y., Li, Y., Boucot, A.J., 2004. Facies patterns and geography of the Yangtze region, South China, through the Ordovician and Silurian transition. Palaeogeography Palaeoclimatology Palaeontology 204, 353–372.

Chen, X., Rowley, D.B., Rong, J., Zhang, J., Zhang, Y.D., Zhan, R.B., 1997. Late Precambrian through Early Paleozoic stratigraphic and tectonic evolution of the Nanling region, Hunan Province, South China. International Geology Review 39, 469–478.

Chen, X., Zhang, Y.D., Fan, J.X., Tang, L., Sun, H.Q., 2012. Onset of the Kwangsian Orogeny as evidenced by biofacies and lithofacies. Science China: Earth Sciences 55, 1592–1600.

Chen, Z.H., Xing, G.F., Guo, K.Y., Dong, Y.G., Chen, R., Zeng, Y., Li, L.M., He, Z.Y.,

Zhao, L., 2009. Petrogenesis of keratophyes in the Pingshui Group, Zhejiang: Constraints from zircon U–Pb ages and Hf isotopes. Chinese Science Bulletin 54, 1570–1578.

Cocks, L.R.M., Torsvik, T.H., 2013. The dynamic evolution of the Palaeozoic geography of eastern Asia. Earth-Science Reviews 117, 40–79.

Condie, K.C., Belousova, E., Griffin, W.L., Sircombe, K.N., 2009. Granitoid events in space and time: Constraints from igneous and detrital zircon age spectra. Gondwana Research 15, 228–242.

Corfu, F., Hanchar, J.M., Hoskin, P.W.O., Kinny, P., 2003. Altas of zircon textures. Reviews in Mineralogy and Geochemistry 53, 469–500.

Cottle, J.M., Jessup, M.J., Newell, D.L., Horstwood, M.S.A., Noble, S.R., Parrish, R.R., Waters, D.J., Searle, M.P., 2009. Geochronology of granulitized eclogite from the Ama Drime Massif: Implications for the tectonic evolution of the South Tibetan Himalaya. Tectonics 28, doi:10.1029/2008TC002256.

DeCelles, P.G., Gehrels, G.E., Quade, J., Lareau, B., Spurlin, M., 2000. Tectonic implications of U–Pb zircon ages of the Himalayan orogenic belt in Nepal: Science 288, 497–499.

DeCelles, P.G., Giles, K.A., 1996. Foreland basin systems. Basin Research 8, 105–123.

Dhuime, B., Hawkesworth, C., Cawood, P., 2011. When continents formed. Science 331, 154–155.

Dickinson, W.R., 1970, Interpreting detrital modes of greywacke and arkose. Journal of Sedimentary Research 40, 695–707.

Dickinson, W.R., 1985. Interpreting provenance relations from detrital modes of sandstones. In: Zuffa, G.G. (Eds.), Provenance of arenites: NATO ASI series C 148, Dordrecht/Boston/Lancaster, D. Reidel Publishing Company, pp. 333–361.

Dickinson, W.R., 2008. Impact of differential zircon fertility of granitoid basement rocks in North America on age populations of detrital zircons and implications for granite petrogenesis. Earth and Planetary Science Letters 275, 80–92.

Dickinson, W.R., Beard, L.S., Brakenridge, G.R., Erjavec, J.L., Ferguson, R.C., Inman, K.F., Knepp, R.A., Lindberg, F.A., Ryberg, P.T., 1983. Provenance of North American Phanerozoic sandstones in relation to tectonic setting.

Geological Society of America Bulletin 94, 222–235.

Ding, S.J., Xu, C.H., Long, W.G., Zhou, Z.Y., Liao, Z.T., 2002. Tectonic attribute and geochronology of metavolcanic rocks, Tunchang, Hainan Island. Acta Petrologica Sinica 18, 83–90 (in Chinese with English abstract).

Dong, C.Y., Li, C., Wan, Y.S., Wang, W., Wu, Y.W., Xie, H.Q., Liu, D.Y., 2011. Detrital zircon age model of Ordovician Wenquan quartzite south of Lungmuco–Shuanghu suture in the Qiangtang area, Tibet: Constraint on tectonic affinity and source regions. Science China Earth Sciences 54, 1034–1042.

Dong, R., Liu, H., 1991. Regional stratigraphy. In: Liu, H. (Eds.), The Sinian System in China. Science Press, Beijing, pp. 11–114 (in Chinese).

Draganits, E., 2000. The Muth Formation in the Pin Valley (Spiti, N-India): Depositional environment and Ichnofauna of a Lower Devonian barrier island system. Ph.D. thesis, University of Viena, Viena, 144 p.

Faure, M., Shu, L., Wang, B., Charvet, J., Choulet, F., Monie, P., 2009. Intracontinental subduction: a possible mechanism for the Early Palaeozoic Orogen of SE China. Terra Nova 21, 360–368.

Gan, X.C., Li, H.M., Sun, D.Z., 1995. A geochronological study on early Proterozoic granitic rocks, Southwestern Zhejiang. Acta Petrologica et Mineralogica 14, 1–8 (in Chinese with English abstract).

Gao, S., Yang, J., Zhou, L., Li, M., Hu, Z., Guo, J., Yuan, H., Gong, H., Xiao, G., Wei, J., 2011. Age and growth of the Archean Kongling terrain, South China, with emphasis on 3.3 Ga granitoid gneisses. American Journal of Science 311, 153–182.

Garzanti, E., Casnedi, R., Jadoul, F., 1986. Sedimentary evidence of a Cambro-Ordovician orogenic event in the northwestern Himalaya. Sedimentary Geology 48, 237–265.

Gazzi, P., 1966. Le arenarie del flysch sopracretaceo dell'Appennino modenese; correlazioni con il flysch di Monghidoro. Acta Mineralogica-Peteographica 12, 69–97.

Gehrels, G.E., DeCelles, P.G., Matin, A., Ojha, T.P., Pinhassi, G., 2003. Initiation of the Himalayan orogen as an early Paleozoic thin-skinned thrust belt. GSA today 13, 4–9.

Gehrels, G.E., DeCelles, P.G., Ojha, T.P., Upreti, B.N., 2006a. Geologic and

U–Th–Pb geochronologic evidence for early Paleozoic tectonism in the Kathmandu thrust sheet, central Nepal Himalaya. Geological Society of America Bulletin 118, 185–198.

Gehrels, G.E., DeCelles, P.G., Ojha, T.P., Upreti, B.N., 2006b. Geologic and U–Pb geochronologic evidence for early Paleozoic tectonism in the Dadeldhura thrust sheet, far-west Nepar Himalaya. Journal of Asian Earth Sciences 28, 386–408.

Gehrels, G.E., Kapp, P., DeCelles, P., Pullen, A., Blakey, R., Weislogel, A., Ding, L., Guynn, J., Martin, A., McQuarrie, N., Yin, A., 2011. Detrital zircon geochronology of pre-Tertiary strata in the Tibetan–Himalayan orogen. Tectonics 30, 1–27.

Greentree, M.R., Li, Z.X., 2008. The oldest known rocks in south-western China: SHRIMP U–Pb magmatic crystallisation age and detrital provenance analysis of the Paleoproterozoic Dahongshan Group. Journal of Asian Earth Sciences 33, 289–302.

Greentree, M.R., Li, Z.X., Li, X.H., Wu, H.C., 2006. Late Mesoproterozoic to earliest Neoproterozoic basin record of the Sibao orogenesis in western South China and relationship to the assembly of Rodinia. Precambrian Research 151, 79–100.

Griffin, W.L., Belousova, E.A., Shee, S.R., Pearson, N.J., O'Reilly, S.Y., 2004. Archean crustal evolution in the northern Yilgarn Craton: U–Pb and Hf–isotope evidence from detrital zircons. Precambrian Research 131, 231–282.

Griffin, W.L., Pearson, N.J., Belousova, E., Jackson, S.E., Achterbergh, E.V., O'Reilly, S.Y., Shee, S.R., 2000. The Hf isotope composition of cratonic mantle: LAM-MC-ICPMS analysis of zircon megacrysts in kimberlites. Geochimica et Cosmochimica Acta 64, 133–147.

Guo, L.Z., Shi, Y.S., Lu, H.F., Ma, R.S., Dong, H.G., Yang, S.F., 1989. The pre-Devonian tectonic patterns and evolution of South China. Journal of Southeast Asian Earth Sciences 3, 87–93.

Guo, L.Z., Shi, Y.S., Ma, R.S., 1980. The geotectonic framework and crustal evolution of South China. In: Guo, L.Z. (Eds.), The plate tectonics of South China. Geological Publishing House, Beijing, pp. 1–264 (in Chinese).

Hawkesworth, C.J., Kemp, A.I.S., 2006. Using hafnium and oxygen isotopes in

zircons to unravel the record of crustal evolution. Chemical Geology 226, 144–162.

Hoffman, P.F., 1991. Did the breakout of Laurentia turn Gondwanaland inside-out? Science 252, 1409–1412.

Hsü, K.J., 1994. Tectonic facies in an archipelago model of intraplate orogenesis. GSA today 4, 289–293.

Hsü, K.J., Li, J., Chen, H., Wang, Q., Sun, S., Sengr, A.M.C., 1990. Tectonics of South China: Key to understanding West Pacific geology. Tectonophysics 183, 9–39.

Hsü, K.J., Shu, S., Jiliang, L., Haihong, C., Haipo, P., Sengor, A.M.C., 1988. Mesozoic overthrust tectonics in south China. Geology 16, 418–421.

Huang, J., Ren, J., Jiang, C., Zhang, Z., Qin, D., 1980. The geotectonic evolution of China. Beijing: Science Press, 124 p. (in Chinese with English abstract).

Huang, J.Q., Ren, J.S., Jiang, C.F., Zhang, Z.K., Qin, D.Y., 1987. Geotectonic evolution of China. Berlin: Springer-Verlag, pp. 1–203.

Hughes, N.C., Myrow, P.M., Mckenzie, N.R., Harper, D.A.T., Bhargava, O.N., Tangri, S.K., Ghalley, K.S., Fanning, C.M., 2011. Cambrian rocks and faunas of the Wachi La, Black Mountains, Bhutan. Geological Magazine 148,351–379.

Ingersoll, R.V., Bullard, T.P., Ford, R.L., Grimm, P., Pickle, L.D., Sares, S.W., 1984. The effect of grain size on detrital modes: A test of the Gazzi–Dickinson point-counting method. Sedimentary Petrology 54, 103–116.

Jackson, S.E., Pearson, N.J., Griffin, W.L., Belousova, E.A., 2004. The application of laser ablation-inductively coupled plasma-mass spectrometry to *in-situ* U–Pb zircon geochronology. Chemical Geology 211, 47–69.

Jell, P.A., Hughes, N.C., 1997. Himalayan Cambrian trilobites. Special Papers in Palaeontology 58, 1–113.

Jiang, B., Sinclair, H.D., Niu, Y., Yu, J., 2014. Late Neoproterozoic-Early Paleozoic evolution of the South China Block as a retroarc thrust wedge/foreland basin system. International Journal of Earth Sciences 103, 23–40.

Jiang, G., Sohl, L.E., Christie-Blick, N., 2003. Neoproterozoic stratigraphic comparison of the Lesser Himalaya (India) and Yangtze block (south China): Paleogeographic implications. Geology 31, 917–920.

Jiao, W., Wu, Y., Yang, S., Peng, M., Wang, J., 2009. The oldest basement rock in the

Yangtze Craton revealed by zircon U–Pb age and Hf isotope composition. Science in China Series D: Earth Sciences 52, 1393–1399.

Johnson, H.D., Baldwin, C.T., 1996. Shallow clastic seas. In: Reading, H.G. (Eds.), Sedimentary environments: Processes, facies and stratigraphy. Blackwell Science, Oxford, pp. 232–280.

Kemp, A.I.S., Hawkerworth, C.J., Paterson, B.A., Kinny, P.D., 2006. Episodic growth of the Gondwana supercontinent from hafnium and oxygen isotopes in zircon. Nature 439, 580–583.

Kim, S.W., Oh, C.W., Williams, I.S., Rubatto, D., Ryu, I.C., Rajesh, V.J., Kim, C.B., Guo, J., Zhai, M., 2006. Phanerozoic high-pressure eclogite and intermediate-pressure granulite facies metamorphism in the Gyeonggi Massif, South Korea: Implications for the eastward extension of the Dabie–Sulu continental collision zone. Lithos 92, 357–377.

Kohn, M.J., Pau, S.K., Corrie, S.L., 2010. The lower Lesser Himalayan sequence: a Paleoproterozoic arc on the northern margin of the Indian plate. Geological Society of America Bulletin 122, 323–335.

Kolmogorov, A. N., 1933. Sulla determinazione empirica di una legge di distribuzione. Giornale dell'Istituto Italiano degli Attuari 4, 83–91.

Kumar, G., 1984. The Precambrian–Cambrian boundary beds, northwest Himalaya, India, and boundary problems, In: Proceedings of the Fifth Indian Geophytological Conference, Lucknow, November 1983. Palaeobotanical Society of India, Special Publications, Lucknow, pp. 98–111.

Le Fort, P., 1975. Himalayas: collided range. Present knowledge of continental arc. American Journal of Science 275, 1–44.

Leier, A.L., Kapp, P., Gehrels, G.E., DeCelles, P.G., 2007. Detrital zircon geochronology of Carboniferous–Cretaceous strata in the Lhasa terrane, Southern Tibet. Basin Research 19, 361–378.

Li, H.B., Jia, D., Wu, L., Zhang, Y., Yin, H.W., Wei, G.Q., Li, B.L., 2013b. Detrital zircon provenance of the Lower Yangtze foreland basin deposits: constraints on the evolution of the early Palaeozoic Wuyi-Yunkai orogenic belt in South China. Geological Magazine 150, 959–974.

Li, J.L., 1991. Characteristics of Jinning-Chengjiang magmatic rocks and plate tectonic movements. In: the Sinian System in China. Science Press, Beijing, pp. 220–300 (in Chinese).

Li, L., Lin, S., Xing, G., Davis, D.W., Davis, W.J., Xiao, W., Yin, C., 2013. Geochemistry and tectonic implications of late Mesoproterozoic alkaline bimodal volcanic rocks from the Tieshajie Group in the southeastern Yangtze Block, South China. Precambrian Research 230, 179–192.

Li, W.X., Li, X.H., Li, Z.X., 2005. Neoproterozoic bimodal magmatism in the Cathaysia Block of South China and its tectonic significance. Precambrian Research 136, 51–66.

Li, W.X., Li, X.H., Li, Z.X., 2008. Middle Neoproterozoic syn-rifting volcanic rocks in Guangfeng, South China: petrogenesis and tectonic significance. Geological Magazine 145, 475–489.

Li, W.X., Li, X.H., Li, Z.X., 2010. *Ca.* 850 Ma bimodal volcanic rocks in northeastern Jiangxi Province, South China: Initial extension during the breakup of Rodinia? American Journal of Science 310, 951–980.

Li, X.H., Zhou, G., Zhao, J., Fanning, C.M., Compston, W., 1994. SHRIMP ion microprobe zircon U-Pb age of the NE Jiangxi ophiolite and its tectonic implications. Geochimica 23, 125–131.

Li, X.H., McCulloch, M.T. 1996. Secular variation in the Nd isotopic composition of Neoproterozoic sediments from the southern margin of the Yangtze Block: evidence for a Proterozoic continental collision in southeast China. Precambrian Research 76, 67–76.

Li, X.H., 1997. Timing of the Cathaysia block formation: constraints from SHRIMP U–Pb zircon geochronology. Episodes 20, 188–192.

Li, X.H., Li, Z.X., Ge, W.C., Zhou, H.W., Li, W.X., Liu, Y., Wingate, M.T.D., 2003. Neoproterozoic granitoids in South China: crustal melting above a mantle plume at *ca.* 825 Ma? Precambrian Research 122, 45–83.

Li, X.H., Li, W.X., Li, Z.X., Liu, Y., 2008. 850-790 Ma bimodal volcanic and intrusive rocks in northern Zhejiang, South China: A major episode of continental rift magmatism during the breakup of Rodinia. Lithos 102, 341–357.

Li, X.H., Li, W.X., Li, Z.X., Lo, C.H., Wang, J., Ye, M.F., Yang, Y.H., 2009. Amalgamation between the Yangtze and Cathaysia blocks in South China: Constraints from SHRIMP U–Pb zircon ages, geochemistry and Nd–Hf isotopes of the Shuangxiwu volcanic rocks. Precambrian Research 174, 117–128.

Li, X.H., Long, W.G., Li, Q.L., Liu, Y., Zheng, Y.F., Yang, Y.H., Chamberlain, K.R., Wan, D.F., Guo, C.H., Wang, X.C., Tao, H., 2010a. Penglai zircon megacrysts: a potential new working reference material for microbeam determination of Hf–O isotopes and U–Pb age. Geostandards and Geoanalytical Research 34, 117–134.

Li, X.H., Li, W.X., Li, Q.L., Wang, X.C., Liu, Y., Yang, Y.H., 2010b. Petrogenesis and tectonic significance of the ~850 Ma Gangbian alkaline complex in South China: Evidence from *in-situ* zircon U-Pb dating, Hf-O isotopes and whole-rock geochemistry. Lithos 114, 1–15.

Li, X.H., Li, Z.X., He, B., Li, W.X., Li, Q.L., Gao, Y.Y., Wang, X.C., 2012. The Early Permian active continental margin and crustal growth of the Cathaysia Block: *in-situ* U–Pb, Lu–Hf and O isotope analyses of detrital zircons. Chemical Geology 328, 195–207.

Li, Z.X., Zhang, L.H., Powell, C.M., 1996. Positions of the East Asian cratons in the Neoproterozoic supercontinent Rodinia. Australian Journal of Earth Science 43, 593–604.

Li, Z.X., 1998. Tectonic history of the major East Asian lithospheric blocks since the mid-Proterozoic – a synthesis. In: Flower, M.J., Chung, S.L., Lo, C.H., Lee, T.Y. (Eds.), Mantle dynamics and plate interactions in East Asia. American Geophysical Union, Washington, DC, pp. 221–243.

Li, Z.X., 1999. 830–820 Ma Mafic to felsic igneous activity in South China and the breakup of Rodinia. Gondwana Research 2, 591–591.

Li, Z.X., Powell, C.M., 2001. An outline of the Palaeogeographic evolution of the Australasian region since the beginning of the Neoproterozoic. Earth-Science Reviews 53, 237–277.

Li, Z.X., Li, X.H., Zhou, H.W., Kinny, P.D., 2002. Grenvillian continental collision in south China: new SHRIMP U–Pb zircon results and implications for the configuration of Rodinia. Geology 30, 163–166.

Li, Z.X., Li, X.H., Kinny, P.D., Wang, J., Zhang, S., Zhou, H.W., 2003a. Geochronology of Neoproterozoic syn-rift magmatism in the Yangtze Craton, South China and correlations with other continents: evidence for a mantle superplume that broke up Rodinia. Precambrian Research 122, 85–109.

Li, Z.X., Li, X.H., Wang, J., Zhang, S., 2003b. A tectonic overview of the South China Block. In: Li, Z.X., Wang, J., Li, X.H., Zhang, S. (Eds.), From Sibao

Orogenesis to Nanhua Rifting: Late Precambrian Tectonic History of Eastern South China. Geological Publishing House, Beijing, pp.1–13.

Li, Z.X., Evans, D.A.D., Zhang, S.H., 2004. A 90º Spin on Rodinia: Possible causal links between the Neoproterozoic supercontinent, superplume, true polar wander and low-latitude glaciation. Earth and Planetary Science Letters 220, 409–421.

Li, Z.X., Li, X.H., 2007a. Formation of the 1300 km-wide intracontinental orogen and postorogenic magmatic province in Mesozoic South China: a flat-slab subduction model. Geology 35, 179–182.

Li, Z.X., Wartho, J.A., Occhipinti, S., Zhang, C.L., Li, X.H., Wang, J., Bao, C.M., 2007b. Early history of the eastern Sibao Orogen (South China) during the assembly of Rodinia: New mica 40Ar/39Ar dating and SHRIMP U–Pb detrital zircon provenance constraints. Precambrian Research 159, 79–94.

Li, Z.X., Li, X.H., Li, W.X., Ding, S., 2008a. Was Cathaysia part of Proterozoic Larentia? – new data from Hainan Island, south China. Terran Nova 20, 154–164.

Li, Z.X., Bogdanova, S.V., Collins, A.S., Davidson, A., De Waele, B., Ernst, R.E., Fitzsimons, I.C.W., Fuck, R.A., Gladkochub, D.P., Jacobs, J., Karlstrom, K.E., Lu, S., Natapov, L.M., Pease, V., Pisarevsky, S.A., Thrane, K., Vernikosky, V., 2008b. Assembly, configuration, and break-up history of Rodinia: a synthesis. Precambrian Research 160, 179–210.

Li, Z.X., Li, X.H., Wartho, J.A., Clark, C., Li, W.X., Zhang, C.L., Bao, C.M., 2010. Magmatic and metamorphic events during the early Paleozoic Wuyi–Yunkai orogeny, southeastern South China: New age constraints and pressure–temperature conditions. Geological Society of America Bulletin 122, 772–793.

Li, Z.X., Evans, D.A.D., 2011. Late Neoproterozoic 40° intraplate rotation within Australia allows for a tighter-fitting and longer-lasting Rodinia. Geology 39, 39–42.

Li, Z.X., Evans, D.A.D., Halverson, G.P., 2013. Neoproterozoic glaciations in a revised global paleogeography from the breakup of Rodinia to the assembly of Gondwanaland. Sedimentary Geology 294, 219–232.

Li, Z.X., Chen, H., Li, X.H., Zhang, F.Q., 2014. Tectonics of the South China Block — An overview and a field guide of eastern South China. Chinese Science

Press, Beijing (in-press).

Ling, W., Gao, S., Zhang, B., Li, H., Liu, Y., 2003. Neoproterozoic tectonic evolution of Yangtze craton, South China: implications for amalgamation and break-up of Rodinia Supercontinent. Precambrian Research 122, 111–140.

Liu, B., Xu, X., 1994. Atlas of Lithofacies and Paleogeography of South China. Beijing: Science Press, 188 p.

Liu, B., Xu, X., Xu, Q., 1995. Sequence stratigraphy and basin geodynamic of the southeastern margin of the Yangtze plate during the late Proterozoic to early Paleozoic. Lithofacies Paleogeography 5, 1–16.

Liu, R., Zhou, H.W., Zhang, L., Zhong, Z.Q., Zeng, W., Xiang, H., Jin, S., Lu, X.Q., Li, C.Z., 2009. Paleoproterozoic reworking of ancient crust in the Cathaysia Block, South China: Evidence from zircon trace elements, U–Pb and Lu–Hf isotopes. Chinese Science Bulletin 54, 1543–1554.

Liu, X., Hsü, K.J., Ju, Y., Li, G., Liu, X., Wei, L., Zhou, X., Zhang, X., 2012. New interpretation of tectonic model in south Tibet. Journal of Asian Earth Sciences 56, 147–159.

Liu, Y., Siebel, W., Massonne, H., Xiao, X., 2007. Geochronological and petrological constraints for tectonic evolution of the central Greater Himalayan sequence in the Kharta area, southern Tibet. The Journal of Geology 115, 215–230.

Lu, H.F., Jia, D., Guo, L.Z., 1993. Formation and collisional history of the Min-Tai microcontinent. In: Li, J.L. (Eds.) Continental lithosphere structures and geological evolution of southeast China. Metallurgy Industry Publishing House, Beijing, pp 12–25 (in Chinese).

Liu, W.J., 1998. Evolution of sedimentation of South China plate in the Hercynian-Indosinian stage. Journal of Chengdu University of Technology 25, 328–336 (in Chinese with English abstract).

Ludwig, K. R., 2001a. ISOPLOT/EX version 2.49 – A geochronological toolkit for Microsoft excel. Berkley Geochronological Centre Special Publication No. 1, 56 p.

Ludwig, K. R., 2001b. SQUID version 1.02 – A geochronological toolkit for Microsoft excel. Berkley Geochronological Centre Special Publication No. 2, 19 p.

Ma, D., Huang, X., Xiao, Z., Chen, Z., Zhang, W., Zhong, S., 1998. The crystalline basement of the Hainan Island – stratigraphy and geochronology of the

Baoban group. Wuhan: China University of Geosciences Press, 60p. (in Chinese).

Martin, A.J., DeCelles, P.G., Gehrels, G.E., Patchett, P.J., Isachsen, C., 2005. Isotopic and structural constraints on the location of the main Central thrust in the Annapurna Range, central Nepal Himalaya. Geological Society of America Bulletin 117, 926–944.

McKenzie, N.R., Hughes, N.C., Myrow, P.M., Choi, D.K., Park, T.-y., 2011. Trilobites and zircons link north China with the eastern Himalaya during the Cambrian: Geology 39, 591–594.

McQuarrie, N., Long, S.P., Tobgay, T., Nesbit, J.N., Gehrels, G., Ducea, M.N., 2013. Documenting basin scale, geometry and provenance through detrital geochemical data: Lessons from the Neoproterozoic to Ordovician Lesser, Greater, and Tethyan Himalayan strata of Bhutan. Gondwana Research 23, 1491–1510.

McQuarrie, N., Robinson, D., Long, S., Tobgay, T., Grujic, D., Gehrels, G., Duce, M., 2008. Preliminary stratigraphic and structural architecture of Bhutan: Implications for the alongstrike architecture of the Himalayan system. Earth and Planetary Science Letters 272, 105–117.

Metcalfe, I., 1996. Gondwanaland dispersion, Asian accretion and evolution of eastern Tethys. Australian Journal of Earth Sciences 43, 605–623.

Mezger, K., Cosca, M., 1999. The thermal history of the Eastern Ghats Belt (India), as revealed by U-Pb and 40Ar/39Ar dating of metamorphic and magmatic minerals: implications for the SWEAT correlation. Precambrian Research 94, 251–271.

Miller, C., Klotzli, U., Frank, W., Thoni, M., Grasemann, B., 2000. Proterozoic crustal evolution in the NW Himalaya (India) as recorded by circa 1.80 Ga mafic and 1.84 Ga granitic magmatism. Precambrian Research 103, 191–206.

Miller, C., Thoni, M., Frank, W., Grasemann, B., Klotzli, U., Guntli, P., Draganits, E., 2001. The early Palaeozoic magmatic event in the Northwest Himalaya, India: source, tectonic setting and age of emplacement. Geological Magazine 138, 237–251.

Morel, M.L.A., Nebel, O., Nebel-Jacobsen, Y.J., Miller, J.S., Vroon, P.Z., 2008. Hafnium isotope characterization of the GJ-1 zircon reference material by solution and laser-ablation MC-ICPMS. Chemical Geology 255, 231–235.

Myrow, P.M., Hughes, N.C., Goodge, J.W., Fanning, C.M., Williams, I.S., Peng, S.C., Bhargava, O.N., Parcha, S.K., Pogue, K.R., 2010. Extraordinary transport and mixing of sediment across Himalayan central Gondwana during the Cambrian–Ordovician. Geological Society of America Bulletin 122, 1660–1670.

Myrow, P.M., Hughes, N.C., Paulsen, T.S., Williams, I.S., Parcha, S.K., Thompson, K.R., Bowring, S.A., Peng, S.C., Ahluwalia, A.D., 2003. Intergrated tectonostratigraphic analysis of the Himalaya and implications for its tectonic reconstruction. Earth and Planetary Science Letters 212, 433–441.

Myrow, P.M., Hughes, N.C., Searle, M.P., Fanning, C.M., Peng, S.C., Parcha, S.K., 2009. Stratigraphic correlation of Cambrian–Ordovician deposits along the Himalaya: Implications for the age and nature of rocks in the Mount Everest region. Geological Society of America Bulletin 120, 323–332.

Myrow, P.M., Snell, K.E., Hughes, N.C., Paulsen, T.S., Heim, N.A., Parcha, S.K., 2006a. Cambrian depositional history of the Zanskar Valley region of the Indian Himalaya: tectonic implications. Journal of Sedimentary Research 76, 364–381.

Myrow, P.M., Thompson, K.R., Hughes, N.C., Paulsen, T.S., Sell, B.K., Parcha, S.K., 2006b. Cambrian stratigraphy and depositional history of the northern Indian Himalaya, Spiti Valley, north-central India. Geological Society of America Bulletin 118, 491–510.

Nesheim, T.O., Vervoort, J.D., McClelland, W.C., Gilotti, J.A., Lang, H.M., 2012. Mesoproterozoic syntectonic garnet within Belt Supergroup metamorphic tectonites: Evidence of Grenville-age metamorphism and deformation along northwest Laurentia. Lithos 134 – 135, 91–107.

Neves, S.P., 2003. Proterozoic history of the Borborema province (NE Brazil): Correlations with neighboring cratons and Pan-African belts and implications for the evolution of western Gondwana. Tectonics 22, doi:10.1029/2001TC001352.

Nichols, G., 2009. Sedimentology and Stratigraphy (second edition). London: Blackwell Science Publishing, 419 p.

Pan, G., 1984. The late Precambrian and early Paleozoic marginal basin of South China. In: Kokelaor, B.P., Howell, M.F. (Eds.), Marginal Basin Geology. Blackwell Scientific, Oxford, pp. 279–283.

Peng, S., Hughes, N.C., Heim, N.A., Sell, B.K., Zhu, X.J, Myrow, P.M., Parcha, S.K., 2009. Cambrian trilobites from the Parahio and Zanskar Valleys, Indian Himalaya. Paleontological Society Memoirs (Journal of Paleontology Supplement) 71, 1–95.

Pogue, K.R., Hylland, M.D., Yeats, R.S., Khattak, W.U., Hussain, A., 1999. Stratigraphic and structural framework of Himalayan foothills, northern Pakistan, in Macfarlane, A., Sorkhabi, R.B., and Quade, J., editors, Himalaya and Tibet: Mountain Roots to Mountain Tops. Geological Society of America Special Papers 328, 257–274.

Press, W.H., Flannery, B.P., Teukolsky, S.A., Vetterling, W.T., 1986. Numerical Recipes: The Art of Scientific Computing. Cambridge: Cambridge University Press, 186 p.

Pullen, A., Kapp, P., Gehrels, G.E., Ding, L., Zhang, Q., 2011. Metamorphic rocks in central Tibet: Lateral variations and implications for crustal structure. Geological Society of America Bulletin 123, 585–600.

Qiu, Y., Gao, S., McNaughton, N.J., Groves, D.I., Ling, W., 2000. First evidence of >3.2 Ga continental crust in the Yangtze craton of south China and its implications for Archean crustal evolution and Phanerozoic tectonic. Geology 28, 11–14.

Reading, H. G., 1996. Sedimentary Environments: Processes, Facies and Stratigraphy. London: Blackwell Science Publishing, 687 p.

Ren, J., 1964. A preliminary study on pre-Devonian geotectonic problems of southeastern China. Acta Geologica Sinica 44, 418–431.

Ren, J., 1991. On the geotectonics of southern China. Acta Geologica Sinica 4, 111–130.

Ren, J., Wang, Z., Chen, B., Jiang, C., Niu, B., 1997. Tectonic map of China and adjacent regions. Beijing: Geological Publishing House, scale 1:5,000,000.

RGMRGD-a, 1962. Regional Geological Mapping and Report of Guangdong Province – 1:200,000 Shaoguan Sheet. Institute of Geoscience, Ministry of Geology, Beijing (in Chinese).

RGMRGD-b, 1964. Regional Geological Mapping and Report of Guangdong Province – 1:200,000 Yangjiang Sheet. Institute of Geoscience, Ministry of Geology, Beijing (in Chinese with English abstract).

RGMRGX-a, 1966. Regional Geological Mapping and Report of Guangxi Province

– 1:200,000 Rongxian Sheet. Institute of Geoscience, Ministry of Geology, Beijing (in Chinese with English abstract).

RGMRGX-b, 1968. Regional Geological Mapping and Report of Guangxi Province – 1:200,000 Yulin Sheet. Institute of Geoscience, Ministry of Geology, Beijing (in Chinese with English abstract).

RGMRHN-a, 1965. Regional Geological Mapping and Report of Hunan Province – 1:200,000 Dongkou Sheet. Institute of Geoscience, Ministry of Geology, Beijing (in Chinese with English abstract).

RGMRHN-b, 1968. Regional Geological Mapping and Report of Hunan Province – 1:200,000 Dayong Sheet. Institute of Geoscience, Ministry of Geology, Beijing (in Chinese with English abstract).

RGMRHN-c, 1972. Regional Geological Mapping and Report of Hunan Province – 1:200,000 Huitong Sheet. Institute of Geoscience, Ministry of Geology, Beijing (in Chinese with English abstract).

RGMRHN-d, 1975. Regional Geological Mapping and Report of Hunan Province – 1:200,000 Lingling Sheet. Institute of Geoscience, Ministry of Geology, Beijing (in Chinese with English abstract).

Roger, F., Maluski, H., Leyreloup, A., Lepvrier, C., Troung Thi, P., 2007. U–Pb dating of high temperature metamorphic episodes in the Kon Tum Massif (Vietnam). Journal of Asian Earth Sciences 30, 565–572.

Rong, J.Y., Fan, J.X., Miller, A.I., Li, G.X., 2007. Dynamic patterns of latest Proterozoic–Paleozoic–early Mesozoic marine biodiversity in South China. Geological Journal 42, 431–454.

Schärer, U., Xu, R.H., Allègre1, C.J., 1986. U-(Th)-Pb systematics and ages of Himalayan leucogranites, South Tibet: Earth and Planetary Science Letters 77, 35–48.

Scherer, E.M., 2001. Calibration of the lutetium–hafnium clock. Science 293, 683–687.

Schervish, M.J., 1996. P values: what they are and what they are not. The American Statistician 50, 203–206.

Shu, L.S., Deng, P., Yu, J.H., Wang, Y.B., Jiang, S.Y., 2008. The age and tectonic environment of the rhyolitic rocks on the western side of Wuyi Mountain, South China. Science in China Series D: Earth Sciences 51, 1053–1063.

Shu, L.S., Faure, M., Yu, J.H., Jahn, B.M., 2011. Geochronological and geochemical

features of the Cathaysia block (South China): New evidence for the Neoproterozoic breakup of Rodinia. Precambrian Research 187, 263–276.

Shui, T., 1988. Tectonic framework of the continental basement of southeast China. Science in China (series B) 31, 885–896.

Simmat, R., Raith, M.M., 2008. U-Th-Pb monazite geochronometry of the Eastern Ghats Belt, India: Timing and spatial disposition of poly-metamorphism. Precambrian Research 162, 16–39.

Singh, S., Barley, M.E., Brown, S.J., Jain, A.K., Manickavasagam, R.M., 2002. SHRIMP U-Pb in zircon geochronology of the Chor granitoid: evidence for Neoproterozoic magmatism in the Lesser Himalayan granite belt of NW India. Precambrian Research 118, 285–292.

Singh, S., Claesson, S., Jain, A.K., Gee, D.G., Andreasson, P.G., Manickavasagam, R.M., 2006. 2.0 Ga granite of the lower package of the Higher Himalayan crystallines, Maglad Khad, Sutlej Valley, Himachal Pradesh. Journal of the Geological Society of India 67, 295–300.

Sláma, J., Košler, J., Condon, D.J., Crowley, J.L., Gerdes, A., Hanchar, J.M., Horstwood, M.S.A., Morris, G.A., Nasdala, L., Norberg, N., Schaltegger, U., Schoene, B., Tubrett, M.N., Whitehouse, M.J., 2008. Plesovice zircon – A new natural reference material for U-Pb and Hf isotopic microanalysis. Chemical Geology 249, 1–35.

Smirnov, N.V., 1944. Approximate laws of distribution of random variables from empirical data. Uspekhi Matematicheskikh Nauk 10, 179–206 (In Russian).

Smith, M., Gehrels, G., 1994. Detrital zircon geochronology and the provenance of the Harmony and Valmy Formations, Roberts Mountains allochthon, Nevada. Geological Society of America Bulletin 106, 968–979.

Song, S., Niu, Y., Wei, C., Ji, J., Su, L., 2010. Metamorphis, anatexis, zircon ages and tectonic evolution of the Gongshan block in the northern Indochina continent – an eastern extension of the Lhasa Block. Lithos 120, 327–346.

Squire, R.J., Campbell, I.H., Allen, C.M., Wilson, C.L., 2006. Did the Transgondwanan Supermountain trigger the explosive radiation of animals on Earth? Earth and Planetary Science Letters 250, 116–133.

Srikantia, S. V., 1977. Sedimentary cycles in the Himalaya and their significance on the Orogenic evolution of the mountain belt. International Colloquium Centre National de la Recherche Scientiques 268, 395–407.

Stern, R.A., 2001. A new isotopic and trace-element standard for the ion microprobe: preliminary thermal ionization mass spectrometry (TIMS) U-Pb and electron-microprobe data. Radiogenic Age and Isotopic Studies Report 14, Geological Survey of Canada, Current Research 2001-F1, 11p.

Stern, R.J., 1994. Arc assembly and continental collision in the Neoproterozoic East African Orogen: Implications for the Consolidation of Gondwanaland. Annual Review of Earth and Planetary Sciences 22, 319–351.

Stewart, J.H., Gehrels, G.E., Barth, A.P., Link, P.K., Christie-Blick, N., Wrucke, C.T., 2001. Detrital zircon provenance of Mesoproterozoic to Cambrian arenites in the western United States and northwestern Mexico: Geological Society of America Bulletin 113, 1343–1356.

Su, W., Huff, W.D., Ettensohn, F.R., Liu, X., Zhang, J., Li, Z., 2009. K-bentonite, black-shale and flysch successions at the Ordovician-Silurian transition, South China: possible sedimentary responses to the accretion of Cathaysia to the Yangtze Block and its implications for the evolution of Gondwana. Gondwana Research 15, 111–130.

Sun, W.H., Zhou, M.F., Gao, J.F., Yang, Y.H., Zhao, X.F., Zhao, J.H., 2009. Detrital zircon U-Pb geochronological and Lu-Hf isotopic constraints on the Precambrian magmatic and crustal evolution of the western Yangtze Block, SW China. Precambrian Research 172, 99–126.

Torsvik, T.H., Paulsen, N.C., Hughes, P.M., Myrow, M., Ganerod, 2009. The Tethyan Himalaya: palaeogeographical and tectonic constraints from Ordovician palaeomagnetic data. Journal of the Geological Society 166, 679–687.

Udden, J.A., 1914. Mechanical composition of clastic sediments. Geological Society of America Bulletin 25, 655–744.

Valdiya, K.S., 1970. Simla slate: the Precambrian flysch of the Lesser Himalaya, its turbidites, sedimentary structures and paleocurrents. Geological Society of America Bulletin 81, 451–468.

Valley, J.W., Kinny, P.D., Schulze, D.J., Spicuzza, M.J., 1998. Zircon megacrysts from kimberlite: oxygen isotope variability among mantle melts. Contribution to Mineralogy and Petrology 133, 1–11.

Valley, J.W., Lackey, J.S., Cavosie, A.J., Clechenko, C.C., Spicuzza, M.J., Basei, M.A.S., Bindeman, I.N., Ferreira, V.P., Sial, A.N., King, E.M., Peck, W.H., Sinha, A.K., Wei, C.S., 2005. 4.4 billion years of crustal maturation; oxygen

isotope ratios of magmatic zircon. Contributions to Mineralogy and Petrology 150, 561–580.

Van Achterbergh, E., Ryan, C.G., Jackson, S.E., Griffin,W.L., 2001. Data reduction software for LA-ICP-MS: appendix. In: Sylvester, P.J. (Eds.), Laser Ablation-ICP-Mass Spectrometry in the Earth Sciences: Principles and Applications. Mineralogist Association Canada (MAC) Short Course Series 29, Ottawa, Canada, pp. 239–243.

Veevers, J.J., Belousova, E.A., Saeed, A., Sircombe, K., Cooper, A.F., Read, S.E., 2006. Pan-Gondwanaland detrital zircons from Australia analysed for Hf–isotopes and trace elements reflect an ice-covered Antarctic provenance of 700–500 Ma age, TDM of 2.0–1.0 Ga, and alkaline affinity. Earth-Science Reviews 76, 135–174.

Veevers, J.J., Saeed, A., Belousova, E.A., Griffin, W.L., 2005. U–Pb ages and source composition by Hf–isotope and trace–element analysis of detrital zircons in Permian sandstone and modern sand from southwestern Australia and a review of the paleogeographical and denudational history of the Yilgarn Craton. Earth-Science Reviews 68, 245–279.

Vega-Granillo, R., Salgado-Souto, S., Herrera-Urbina, S., Valencia, V., Ruiz, J., Meza-Figueroa, D., Talavera-Mendoza, O., 2008. U–Pb detrital zircon data of the Rio Fuerte Formation (NW Mexico): Its peri-Gondwanan provenance and exotic nature in relation to southwestern North America. Journal of South American Earth Sciences 26, 343–354.

Wan, Y., Liu, D., Wilde, S.A., Cao, J., Chen, B., Dong, C., Song, B., Du, L., 2010. Evolution of the Yunkai Terrane, South China: Evidence from SHRIMP zircon U-Pb dating, geochemistry and Nd isotope. Journal of Asian Earth Sciences 37, 140–153.

Wan, Y., Liu, D., Xu, M., Zhuang, J., Song, B., Shi, Y., Du, L., 2007. SHRIMP U-Pb zircon geochronology and geochemistry of metavolcanic and metasedimentary rocks in Northwestern Fujian, Cathaysia block, China: Tectonic implications and the need to redefine lithostratigraphic units. Gondwana Research 12, 166–183.

Wang, H., 1985, Atlas of the Palaeogeography of China. Beijing: Cartographic Publishing House, 281 p. (in Chinese with English abstract).

Wang, J., Li, Z.X., 2003. History of Neoproterozoic rift basins in South China:

implications for Rodinia break-up. Precambrian Research 122, 141–158.

Wang, J., Sun, D., Chang, X., Deng, S., Zhang, H., Zhou, H., 1998. U-Pb dating of the Napeng granite at the NW margin of the Yunkai block, Guangdong, South China. Acta Mineralogica Sinica 18, 130–133 (in Chinese with English abstract).

Wang, K.L., O'Reilly, S.Y., Griffin, W.L., Pearson, N.J., Zhang, M., 2009. Sulfides in mantle peridotites from Penghu Islands, Taiwan: Melt percolation, PGE fractionation, and the lithospheric evolution of the South China block. Geochimica et Cosmochimica Acta 73, 4531–4557.

Wang, L.J., Griffin, W.L., Yu, J.H., O'Reilly, S.Y., 2010. Precambrian crustal evolution of the Yangtze Block tracked by detrital zircons from Neoproterozoic sedimentary rocks. Precambrian Research 177, 131–144.

Wang, W., Kirby, E., Zhang, P., Zhang, D., Zhang, G., Zhang, H., Zheng, W., Chai, C., 2013a. Tertiary basin evolution along the northeastern margin of the Tibetan Plateau: Evidence for basin formation during Oligocene transtension. Geological Society of America Bulletin 125, 377–400.

Wang, X., Yang, S.F., Shi, J.N., Guo, L.Z., Shi, Y.S., Lu, H.F., Dong, H.G., Xu, J.K., Kong, H.N., Hu, X.J., 1988. Discovery of collision mélange in Longquan, Zhejiang province and its significance for studying collision orogenic belt in southeastern China. Journal of Nanjing University (Natural Science) 24, 367–378 (in Chinese with English abstract).

Wang, X., Zhang, J., Santosh, M., Liu, J., Yan, S., Guo, L., 2012. Andean-type orogeny in the Himalayas of south Tibet: Implications for early Paleozoic tectonics along the Indian margin of Gondwana. Lithos 154, 248–262.

Wang, X., Zhou, J., Qiu, J., Gao, J., 2004. Geochemistry of the Meso- to Neoproterozoic basic–acid rocks from Hunan Province, South China: implications for the evolution of the western Jiangnan orogen. Precambrian Research 135, 79–103.

Wang, X.C., Li, X.H., Li, W.X., Li, Z.X., 2007. *Ca.* 825 Ma komatiitic basalts in South China: First evidence for >1500 °C mantle melts by a Rodinian mantle plume. Geology 35, 1103–1106.

Wang, X.C., Li, X.H., Li, Z.X., Li, Q.L., Tang, G.Q., Gao, Y.Y., Zhang, Q.R., Liu, Y., 2012. Episodic Precambrian crust growth: evidence from U–Pb ages and Hf–O isotopes of zircon in the Nanhua Basin, central South China.

Precambrian Research 222–223, 386–403.

Wang, X.L., Zhou, J.C., Qiu, J.S., Zhang, W.L., Liu, X.M., Zhang, G.L., 2006. LA-ICP-MS U–Pb zircon geochronology of the Neoproterozoic igneous rocks from Northern Guangxi, South China: implications for tectonic evolution. Precambrian Research 145, 111–130.

Wang, Y., Fan, W., Zhang, G., Zhang, Y., 2013b. Phanerozoic tectonics of the South China Block: Key observations and controversies. Gondwana Research 23, 1273–1305.

Wang, Y., Zhang, A., Fan, W., Zhang, Y., Zhang, Y., 2013c. Origin of paleosubduction-modified mantle for Silurian gabbro in the Cathaysia Block: Geochronological and geochemical evidence. Lithos 160-161, 37–54.

Wang, Y., Fan, W., Zhao, G., Ji, S., Peng, T., 2007. Zircon U-Pb geochronology of gneissic rocks in the Yunkai massif and its implications on the Caledonian event in the South China Block. Gondwana Research 12, 404–416.

Wang, Y., Zhang, A., Fan, W., Zhao, G., Zhang, G., Zhang, Y., Zhang, F., Li, S., 2011. Kwangsian crustal anatexis within the eastern South China Block: Geochemical, zircon U-Pb geochronological and Hf isotopic fingerprints from the gneissoid granites of Wugong and Wuyi-Yunkai Domains. Lithos 127, 239–260.

Wang, Y., Zhang, F., Fan, W., Zhang, G., Chen, S., Cawood, P.A., Zhang, A., 2010. Tectonic setting of the South China Block in the early Paleozoic: Resolving intracontinental and ocean closure models from detrital zircon U-Pb geochronology. Tectonics 29, doi:10.1029/2010TC002750.

Wang, Y., Zhang, Y., Fan, W., Peng, T., 2005. Structural signatures and $^{40}Ar/^{39}Ar$ geochronology of the Indosinian Xuefengshan tectonic belt, South China Block. Journal of Structural Geology 27, 985–998.

Wang, Y., Fan,W., Cawood, P.A., Ji, S., Peng, T., Chen, X., 2007. Indosinian high-strain deformation for the Yunkaidashan tectonic belt, South China: Kinematics and $^{40}Ar/^{39}Ar$ geochronological constraints. Tectonics 26, doi:10.1029/2007TC002099.

Webb, A.A.G., Yin, A., Harrison, T.M., Celerier, J., Gehrels, G.E., Manning, C.E., Grove, M., 2011. Cenozoic tectonic history of the Himachal Himalaya (northwestern India) and its constraints on the formation mechanism of the Himalayan orogen. Geosphere 7, 1013–1061.

Wentworth, C.K., 1922. A scale of grade and class terms for clastic sediments. The Journal of Geology 30, 377–392.

Wiedenbeck, M., Alle, P., Corfu, F., Griffin, W.L., Meier, M., Oberli, F., Von Quadt, A., Roddick, J.C., Spiegel, W., 1995. Three natural zircon standards for U–Th–Pb, Lu–Hf, trace element and REE analyses. Geostandards newsletter 19, 1–23.

Wiedenbeck, M., Goswami, J.N., Roy, A.B., 1996. Stabilization of the Aravalli Craton of northwestern India at 2.5 Ga: An iro microprobe zircon study. Chemical Geology 129, 325–340.

Wiedenbeck, M., Hanchar, J.M., Peck, W.H., Sylvester, P., Valley, J., Whitehouse, M., Kronz, A., Morishita, Y., Nasdala, L., Fiebig, J., Franchi, I., Girard, J.P., Greenwood, R.C., Hinton, R., Kita, N., Mason, P.R.D., Norman, M., Ogasawara, M., Piccoli, P.M., Rhede, D., Satoh, H., Schulz-Dobrick, B., Skar, O., Spicuzza, M.J., Terada, K., Tindle, A., Togashi, S., Vennemann, T., Xie, Q., Zheng, Y.F., 2004, Further characterization of the 91500 zircon crystal. Geostandards newsletter 28, 9–39.

Williams, I.S., 1998. U-Th-Pb geochronology by ion microprobe. In: McKibben, M.A., Shanks III, W.C., Ridley, W.I. (Eds.), Applications of microanalytical techniques to understanding mineralizing processes. Reviews in Economic Geology 7, pp. 1–35.

Wu, F.Y., Yang, Y.H., Xie, L.W., Yang, J.H., Xu, P., 2006. Hf isotopic compositions of the standard zircons and baddeleyites used in U-Pb geochronology. Chemical Geology 234, 105–126.

Wu, L., Jia, D., Li, H., Deng, F., Li, Y., 2010. Provenance of detrital zircons from the late Neoproterozoic to Ordovician sandstones of South China: implications for its continental affinity. Geological Magazine 147, 974–980.

Xiang, H., Zhang, L., Zhou, H., Zhong, Z., Zeng, W., Liu, R., Jin, S., 2008. U–Pb zircon geochronology and Hf isotope study of metamorphosed basic-ultrabasic rocks from metamorphic basement in southwestern Zhejiang: The response of the Cathaysia Block to Indosinian orogenic event. Science in China Series D: Earth Sciences 51, 788–800.

Xie, L.W., Zhang, Y.B., Zhang, H.H., Sun, J.F., Wu, F.W., 2008. *In-situ* simultaneous determination of trace elements, U-Pb and Lu-Hf isotopes in zircon and baddeleyite. Chinese Science Bulletin 53, 1565–1573.

Xu, B., Qiao, G.S., 1989. Sm–Nd isotopic age and tectonic setting of the Late Proterozoic ophiolites in northeastern Jiangxi province. Journal of Nanjing University (Science and Technology) 3, 108–114.

Xu, X., O'Reilly, S.Y., Griffin, W.L., Wang, X., Pearson, N.J., He, Z., 2007. The crust of Cathaysia: Age, assembly and reworking of two terranes. Precambrian Research 158, 51–78.

Xu, X., Yin, F., Wan, F., Liang, Z., Wei, B., Zhang, J., 2001. The migration of the Qinzhou-Fangcheng trough in Guangxi and associated sedimentary-tectonic transform surfaces. Sedimentary Geology and Tethyan Geology 21, 1–10.

Xu, X.S., O'Reilly, S.Y., Griffin, W.L., Deng, P., Pearson, N.J., 2005. Relict Proterozoic basement in the Nanling Mountains (SE China) and its tectonothermal overprinting. Tectonics 24, 1–16.

Xu, X.S., Xu, Q., Pan, G.T., 1996a. The continental evolution of southern China and its global comparison. Beijing: Geological.

Xu, X.S., Xu, Q., Pan, G.T., Liu, Q.H., Fan, Y.N., He, Y.X., 1996b. Paleogeography of the south China continent SCC and its contrast with Pangea. Geological Publishing House, Beijing, pp. 1–161 (in Chinese with English abstract).

Xu, Y., Cawood, P.A., Du, Y., Hu, L., Yu, W., Zhu, Y., Li, W., 2014. Linking South China to northern Australia and India on the margin of Gondwana: Constraints from detrital zircon U-Pb and Hf isotopes in Cambrian strata. Tectonics, doi: 10.1002/tect.20099

Xu, Y., Du, Y., Cawood, P.A., Zhu, Y., Li, W., Yu, W., 2012. Detrital zircon provenance of Upper Ordovician and Silurian strata in the northeastern Yangtze Block: Response to orogenesis in South China. Sedimentary Geology 267-268, 63–72.

Yang, D.S., Li, X.H., Li, W.X., Liang, X.Q., Long, W.G., Xiong, X.L., 2010. U–Pb and 40Ar–39Ar geochronology of the Baiyunshan gneiss (central Guangdong, south China): constraints on the timing of early Paleozoic and Mesozoic tectonothermal events in the Wuyun (Wuyi-Yunkai) Orogen. Geological Magazine 147, 481–496.

Yang, Z., Cheng, Y.Q., Wang, H.C., 1986. The geology of China. Oxford: Clarendon Press, 276 p.

Yang, Z., Sun, Z., Yang, T., Pei, J., 2004. A long connection (750–380 Ma) between South China and Australia: paleomagnetic constraints. Earth and Planetary

Science Letters 220, 423–434.

Yao J., Shu, L., Santosh, M., Li, J., 2012. Precambrian crustal evolution of the South China Block and its relation to supercontinent history: Constraints from U–Pb ages, Lu–Hf isotopes and REE geochemistry of zircons from sandstones and granodiorite. Precambrian Research 208–211, 19–48.

Yao, J., Shu, L., Santosh, M., 2011. Detrital zircon U-Pb geochronology, Hf-isotopes and geochemistry – new clues for the Precambrian crustal evolution of Cathaysia Block, South China. Gondwana Research 20, 553–567.

Yao, W.H., Li, Z.X., Li, W.X., Wang, X.C., Li, X.H., Yang, J.H., 2012. Post-kinematic lithospheric delamination of the Wuyi–Yunkai orogen in South China: evidence from *ca.* 435 Ma high-Mg basalts. Lithos 154, 115–129.

Yao, W.H., Li, Z.X., Li, W.X., Li, X.H., Yang, J.H., 2014a. From Rodinia to Gondwanaland: a tale of detrital zircon provenance analyses from the southern Nanhua Basin, South China. American Journal of Science 314, 278–313.

Yao, W.H., Li, Z.X., 2014b. Stratigraphic history of the lower Palaeozoic Nanhua foreland basin in South China: Response to two successive orogenies. Tectonics (to be submitted).

Yao, W.H., Li, Z.X., Li, W.X., Su, L., Yang, J.H., 2014c. Detrital provenance evolution of the lower Palaeozoic Nanhua foreland basin, South China. Gondwana Research (to be submitted).

Yao, W.H., Li, Z.X., Li, W.X., 2014d. Was there a Cambrian ocean in South China? – Insight from detrital provenance analyses. Geological Magazine (in press).

Ye, M.F., Li, X.H., Li, W.X., Liu, Y., Li, Z.X., 2007. SHRIMP zircon U–Pb geochronological and whole-rock geochemical evidence for an early Neoproterozoic Sibaoan magmatic arc along the southeastern margin of the Yangtze Block. Gondwana Research 12, 144–156.

Yin, A., Dubey, C.S., Kelty, T.K., Webb, A.A.G., Harrison, T.M., Chou, C.Y., Célérier, J., 2010a. Geologic correlation of the Himalayan orogen and Indian craton: Part 2, Structural geology, U–Pb zircon geochronology, and tectonic evolution of the south flank of the eastern Himalayan orogen. Geological Society of America Bulletin 12, 360–395.

Yin, A., Dubey, C.S., Webb, A.A.G., Kelty, T.K., Grove, M., Gehrels, G.E., Burgess,

W.P., 2010b. Geologic correlation of the Himalayan orogen and Indian craton: Part 1, Structural geology, U–Pb zircon geochronology, and tectonic evolution of the Shillong Plateau and its neighboring regions in NE India. Geological Society of America Bulletin 122, 336–359.

Yin, A., Nie, S., Craig, P., Harrison, T.M., Ryerson, F.J., Qian, X., Yang, G., 1998. Late Cenozoic tectonic evolution of the southern Chinese Tian Shan. Tectonics 17, 1–27.

Yu, J.H., Wang, L.J., Wei, Z.Y., Sun, T., Shu, L.S., 2007. Phanerozoic metamorphic episodes and characteristics of Cathaysia Block. Geological Journal of China Universities 1, 474–483.

Yu, J.H., O'Reilly, S.Y., Wang, L., Griffin, W.L., Zhang, M., Wang, R., Jiang, S., Shu, L., 2008. Where was South China in the Rodinia supercontinent? Evidence from U-Pb geochronology and Hf isotopes of detrital zircons. Precambrian Research 164, 1–15.

Yu, J.H., Wang, L., O'Reilly, S.Y., Griffin, W.L., Zhang, M., Li, C., Shu, L., 2009. A Paleoproterozoic orogeny recorded in a long-lived cratonic remnant (Wuyishan terrane), eastern Cathaysia Block, China. Precambrian Research 174, 347–363.

Yu, J.H., O'Reilly, S.Y., Wang, L., Griffin, W.L., Zhou, M.F., Zhang, M., Shu, L., 2010. Components and episodic growth of Precambrian crust in the Cathaysia Block, South China: evidence from U-Pb ages and Hf isotopes of zircons in Newproterozoic sediments. Precambrian Research 181, 97–114.

Yu, J.H., O'Reilly, S.Y., Zhou, M.F., Griffin, W., Wang, L., 2011. U–Pb geochronology and Hf–Nd isotopic geochemistry of the Badu Complex, Southeastern China: Implications for the Precambrian crustal evolution and paleogeography of the Cathaysia Block. Precambrian Research 222–223, 424–449.

Zeng, W., Zhang, L., Zhou, H., Zhong, Z., Xiang, H., Liu, R., Jin, S., Lü, X., Li, C., 2008. Caledonian reworking of Paleoproterozoic basement in the Cathaysia Block: Constraints from zircon U–Pb dating, Hf isotopes and trace elements. Chinese Science Bulletin 53, 895–904.

Zeng, Y., Liao, Q.A., 2000. Caledonian granite in the western Wuyi area and inversion of the orogenic process. Regional Geology of China 19, 344–349 (in Chinese with English abstract).

Zhang, A., Wang, Y., Fan, W., Zhang, F., Zhang, Y., 2010. LA-ICPMS zircon U–Pb geochronology and Hf isotopic compositions of Caledonian granites from the Qingliu area, southwest Fujian. Geotectonica et Metallogenia 34, 08–418.

Zhang S., Evans, D.A.D., Li, H., Wu, H., Jiang, G., Dong, J., Zhao, Q., Raub, T., Yang, T., 2013. Paleomagnetism of the late Cryogenian Nantuo Formation and paleogeographic implications for the South China Block. Journal of Asian Earth Sciences 72, 164–177.

Zhang, J.Y., Yin, A., Liu, W.C., Wu, F.Y., Lin, D., Grove, M., 2012. Coupled U-Pb dating and Hf isotopic analysis of detrital zircon of modern river sand from the Yalu River (Yarlung Tsangpo) drainage system in southern Tibet: Constraints on the transport processes and evolution of Himalayan rivers. Geological Society of America Bulletin 124, 1449–1473.

Zhang, L., He, Q., 1993. On the revision of Bacun Group and the establishment of Xiazhai, Oujiadong and Laoshuzhai Formations in northern Guangdong Province. Guangdong Geology 8, 1–14 (in Chinese with English abstract).

Zhang, Q.R., Piper, J.D.A., 1997. Palaeomagnetic study of Neoproterozoic glacial rocks of the Yangtze Block: palaeolatitude and configuration of South China in the late Proterozoic Supercontinent. Precambrian Research 85, 173–199.

Zhang, S., 2004. South China's Gondwana connection in the Paleozoic: Paleomagnetic evidence. Progress in Natural Science 14, 85–90.

Zhang, S.B., Zheng, Y.F., Wu, Y.B., Zhao, Z.F., Gao, S., Wu, F.Y., 2006. Zircon U–Pb age and Hf–O isotope evidence for Paleoproterozoic metamorphic event in South China. Precambrian Research 151, 265–288.

Zhao, G., Cawood, P.A. 1999. Tectonothermal evolution of the Mayuan assemblage in the Cathaysia Block: implications for Neoproterozoic collision-related assembly of the South China Craton. American Journal of Science 299, 309–339.

Zhao, X.F., Zhou, M.F., Li, J.W., Sun, M., Gao, J.F., Sun, W.H., Yang, J.H., 2010. Late Paleoproterozoic to early Mesoproterozoic Dongchuan Group in Yunnan, SW China: Implications for tectonic evolution of the Yangtze Block. Precambrian Research 182, 57–69.

Zheng, J., Griffin, W., O'Reilly, S.Y., Zhang, M., Pearson, N., Pan, Y., 2006. Widespread Archean basement beneath the Yangtze craton. Geology 34, 417–420.

Zheng, J.P., Griffin, W.L., Li, L.S., O'Reilly, S.Y., Pearson, N.J., Tang, H.Y., Liu, G.L., Zhao, J.H., Yu, C.M., Su, Y.P., 2011. Highly evolved Archean basement beneath the western Cathaysia Block, South China. Geochimica et Cosmochimica Acta 75, 242–255.

Zhou, G. 1989. The discovery and significance of the northeastern Jiangxi Province ophiolite (NEJXO), its metamorphic peridotite and associated high temperature-high pressure metamorphic rocks. Journal of Southeast Asian Earth Science 3, 237–247.

Zhou, M.F., Yan, D.P., Kennedy, A.K., Li, Y., Ding, J., 2002a. SHRIMP U-Pb zircon geochronological and geochemical evidence for Neoproterozoic arc-magmatism along the western margin of the Yangtze Block, South China. Earth and Planetary Science Letters 196, 51–67.

Zhou, M.F., Kennedy, A.K., Sun, M., Malpas, J., Lesher, C.M., 2002b. Neoproterozoic Arc-related mafic intrusions along the northern margin of South China: Implications for the Accretion of Rodinia. The Journal of Geology 110, 611–618.

Zhou, M.F., Ma, Y., Yan, D.P., Xia, X., Zhao, J.H., Sun, M., 2006. The Yanbian Terrane (Southern Sichuan Province, SW China): A Neoproterozoic arc assemblage in the western margin of the Yangtze Block. Precambrian Research 144, 19–38.

Zhou, X.M. 2003. My thinking about granite geneses of south China. Geological Journal of China Universities 9, 556–565 (in Chinese with English abstract).

Zhu, D.C., Zhao, Z.D., Niu, Y., Dilek, Y., Mo, X.X., 2011. Lhasa terrane in southern Tibet came from Australia. Geology 39, 727–730.

Zhu, D.C., Zhao, Z.D., Niu, Y., Dilek, Y., Wang, Q., Ji, W.H., Dong, G.C ., Sui, Q.L., Liu, Y.S., Yuan, H.L., Mo, X.X., 2012. Cambrian bimodal volcanism in the Lhasa Terrane, southern Tibet: Record of an early Paleozoic Andean-type magmatic arc in the Australian proto-Tethyan margin. Chemical Geology 328, 290–308.

Zhu, M., Strauss, H., Shields, G.A., 2007. From snowball earth to the Cambrian bioradiation: Calibration of Ediacaran–Cambrian earth history in South China. Palaeogeography Palaeoclimatology Palaeoecology 254, 1–6.

material. I would be pleased to hear from any copyright owner who has been omitted or incorrectly acknowledged.

Appendix A1 LA-ICP-MS zircon U–Pb data for samples 10GD23-1 (andesite) and 10GD25 (dacite) in the Chayuanshan volcanic succession, Guangdong Province

spot	Th (ppm)	U (ppm)	Th/U	Ratio						Age (Ma)					
				$^{207}Pb/^{206}Pb$	1σ	$^{207}Pb/^{235}U$	1σ	$^{206}Pb/^{238}U$	1σ	$^{207}Pb/^{206}Pb$	1σ	$^{207}Pb/^{235}U$	1σ	$^{206}Pb/^{238}U$	1σ
Sample 10GD23–1 andesite															
01	65	100	0.66	0.0550	0.0011	0.5328	0.0093	0.0703	0.0012	413	18	434	6	438	7
02	171	270	0.63	0.0564	0.0012	0.5436	0.0101	0.0699	0.0012	468	18	441	7	436	7
03	87	95	0.92	0.0743	0.0011	1.7302	0.0217	0.1689	0.0028	1050	16	1020	8	1006	15
04	94	139	0.68	0.0558	0.0009	0.5435	0.0078	0.0707	0.0012	443	16	441	5	440	7
05	144	183	0.79	0.0555	0.0009	0.5390	0.0073	0.0704	0.0012	434	16	438	5	439	7
06	95	120	0.79	0.1030	0.0011	4.2741	0.0389	0.3010	0.0048	1679	16	1688	7	1696	24
07	146	161	0.91	0.0566	0.0009	0.5319	0.0076	0.0682	0.0011	476	16	433	5	425	7
08	158	255	0.62	0.0554	0.0008	0.5323	0.0067	0.0698	0.0011	427	17	433	4	435	7
09	176	205	0.86	0.0565	0.0008	0.5509	0.0070	0.0707	0.0012	472	17	446	5	441	7
10	95	145	0.65	0.0548	0.0009	0.5328	0.0075	0.0705	0.0012	404	16	434	5	439	7
11	59	88	0.67	0.0563	0.0014	0.5356	0.0119	0.0690	0.0013	464	22	435	8	430	8
12	22	30	0.73	0.0627	0.0017	1.0349	0.0254	0.1197	0.0024	698	24	721	13	729	14
13	62	99	0.63	0.1554	0.0018	9.6163	0.0949	0.4489	0.0073	2406	15	2399	9	2390	33
14	112	143	0.78	0.0565	0.0015	0.5116	0.0125	0.0657	0.0013	472	25	420	8	410	8
15	25	61	0.41	0.0659	0.0015	1.0861	0.0223	0.1196	0.0022	803	19	747	11	728	13
16	90	137	0.65	0.0554	0.0009	0.5333	0.0077	0.0698	0.0012	429	16	434	5	435	7
17	89	126	0.71	0.0553	0.0010	0.5410	0.0086	0.0709	0.0012	426	17	439	6	442	7
18	99	169	0.59	0.0558	0.0008	0.5391	0.0071	0.0701	0.0011	444	16	438	5	437	7
19	108	165	0.65	0.0550	0.0009	0.5325	0.0075	0.0702	0.0012	413	16	433	5	437	7
20	78	97	0.80	0.0870	0.0011	2.6185	0.0289	0.2184	0.0035	1360	16	1306	8	1274	19
21	85	130	0.66	0.0552	0.0010	0.5474	0.0084	0.0720	0.0012	420	17	443	5	448	7
22	101	170	0.60	0.0563	0.0010	0.5421	0.0083	0.0698	0.0012	465	17	440	5	435	7
23	102	163	0.62	0.0551	0.0011	0.5024	0.0089	0.0662	0.0011	417	18	413	6	413	7

24	72	130	0.55	0.0734	0.0011	1.7128	0.0215	0.1693	0.0028	1025	16	1013	8	1008	15
25	74	123	0.60	0.0566	0.0012	0.5284	0.0095	0.0677	0.0012	476	18	431	6	422	7
26	79	148	0.54	0.0554	0.0009	0.5439	0.0078	0.0712	0.0012	428	16	441	5	444	7
27	134	170	0.79	0.0612	0.0013	0.5568	0.0108	0.0660	0.0012	647	19	449	7	412	7
28	98	142	0.69	0.0559	0.0010	0.5494	0.0091	0.0714	0.0012	447	17	445	6	444	7
29	148	176	0.84	0.0561	0.0008	0.5431	0.0070	0.0703	0.0011	456	17	440	5	438	7
30	221	427	0.52	0.0549	0.0007	0.5305	0.0060	0.0701	0.0011	408	17	432	4	437	7
31	92	156	0.59	0.0559	0.0009	0.5410	0.0076	0.0703	0.0012	446	16	439	5	438	7
32	117	161	0.73	0.0554	0.0009	0.5270	0.0072	0.0691	0.0011	427	16	430	5	431	7
33	38	104	0.37	0.0716	0.0010	1.6522	0.0193	0.1674	0.0027	975	16	990	7	998	15
34	77	108	0.71	0.0569	0.0016	0.5306	0.0132	0.0676	0.0013	489	25	432	9	422	8
35	113	142	0.80	0.0558	0.0012	0.5482	0.0107	0.0713	0.0013	445	19	444	7	444	8
36	488	492	0.99	0.0543	0.0007	0.5172	0.0054	0.0691	0.0011	383	18	423	4	431	7
37	185	267	0.69	0.0559	0.0008	0.5359	0.0065	0.0696	0.0011	448	17	436	4	434	7
38	97	171	0.57	0.0562	0.0010	0.5237	0.0082	0.0677	0.0011	459	17	428	5	422	7
39	79	68	1.17	0.0723	0.0012	1.6562	0.0238	0.1663	0.0028	994	15	992	9	992	16
40	93	134	0.69	0.0560	0.0010	0.5443	0.0089	0.0706	0.0012	452	17	441	6	440	7
41	113	166	0.68	0.0566	0.0011	0.5251	0.0087	0.0674	0.0011	475	17	429	6	420	7
42	326	337	0.97	0.0559	0.0010	0.5381	0.0083	0.0698	0.0012	450	16	437	5	435	7
Sample 10GD25 dacite															
01	92	207	0.44	0.0603	0.0016	0.5532	0.0130	0.0665	0.0013	616	23	447	9	415	8
02	516	457	1.13	0.0562	0.0012	0.5468	0.0104	0.0706	0.0012	460	19	443	7	440	7
03	89	138	0.64	0.0504	0.0011	0.4698	0.0095	0.0676	0.0011	213	21	391	7	422	7
04	115	229	0.50	0.2963	0.0028	28.4937	0.2153	0.6975	0.0105	3451	14	3436	7	3411	40
05	135	296	0.46	0.0553	0.0008	0.5283	0.0064	0.0693	0.0011	425	16	431	4	432	7
06	184	332	0.55	0.0536	0.0008	0.5143	0.0064	0.0696	0.0011	354	16	421	4	434	7
07	99	199	0.50	0.0531	0.0009	0.5124	0.0073	0.0700	0.0011	333	16	420	5	436	7
08	103	223	0.46	0.0587	0.0009	0.5583	0.0070	0.0690	0.0011	555	16	450	5	430	7
09	140	286	0.49	0.0552	0.0008	0.5239	0.0065	0.0689	0.0011	420	16	428	4	429	7
10	170	293	0.58	0.0542	0.0008	0.5172	0.0064	0.0692	0.0011	380	16	423	4	431	7
11	217	531	0.41	0.0535	0.0007	0.5014	0.0052	0.0679	0.0010	352	17	413	3	424	6

12	127	250	0.51	0.0542	0.0008	0.5213	0.0066	0.0697	0.0011	380	16	426	4	435	7
13	167	337	0.49	0.0556	0.0007	0.5295	0.0058	0.0691	0.0011	434	17	431	4	431	6
14	145	279	0.52	0.0544	0.0009	0.5037	0.0075	0.0672	0.0011	387	16	414	5	419	7
15	168	283	0.59	0.0933	0.0010	2.5927	0.0220	0.2015	0.0031	1495	16	1299	6	1183	16
16	95	205	0.46	0.0580	0.0012	0.5694	0.0100	0.0712	0.0012	531	17	458	6	443	7
17	72	159	0.45	0.0552	0.0009	0.5303	0.0078	0.0697	0.0011	420	16	432	5	434	7
18	97	199	0.49	0.0551	0.0008	0.5376	0.0072	0.0708	0.0011	415	16	437	5	441	7
19	107	223	0.48	0.0545	0.0008	0.5230	0.0067	0.0696	0.0011	391	16	427	4	434	7
20	222	375	0.59	0.0754	0.0010	1.9190	0.0229	0.1846	0.0030	1080	15	1088	8	1092	16
21	114	431	0.26	0.0543	0.0007	0.5231	0.0053	0.0699	0.0011	383	18	427	4	436	7
22	149	297	0.50	0.0724	0.0008	1.6958	0.0147	0.1699	0.0026	997	17	1007	6	1012	14
23	211	300	0.70	0.0546	0.0008	0.5281	0.0062	0.0701	0.0011	397	17	431	4	437	7
24	176	276	0.64	0.0545	0.0008	0.5197	0.0063	0.0691	0.0011	393	16	425	4	431	7
25	115	151	0.76	0.0572	0.0009	0.5560	0.0080	0.0705	0.0012	499	16	449	5	439	7
26	107	242	0.44	0.0559	0.0008	0.5338	0.0070	0.0692	0.0011	450	16	434	5	432	7
27	140	281	0.50	0.0553	0.0008	0.5404	0.0066	0.0709	0.0011	426	16	439	4	441	7
28	250	440	0.57	0.1324	0.0013	5.2019	0.0401	0.2852	0.0043	2129	16	1853	7	1617	22
29	268	320	0.84	0.0551	0.0008	0.5340	0.0065	0.0704	0.0011	415	16	434	4	438	7
30	47	110	0.43	0.0686	0.0014	1.3121	0.0242	0.1387	0.0025	887	17	851	11	838	14
31	148	314	0.47	0.0558	0.0008	0.5288	0.0062	0.0688	0.0011	442	17	431	4	429	7
32	115	244	0.47	0.0577	0.0009	0.5448	0.0076	0.0685	0.0011	519	16	442	5	427	7
33	139	316	0.44	0.0575	0.0010	0.5485	0.0080	0.0692	0.0011	510	16	444	5	432	7
34	126	262	0.48	0.0552	0.0008	0.5243	0.0065	0.0689	0.0011	420	17	428	4	430	7
35	58	90	0.65	0.1653	0.0017	10.8047	0.0944	0.4743	0.0075	2510	15	2506	8	2502	33
36	137	292	0.47	0.0557	0.0009	0.5484	0.0077	0.0714	0.0012	440	16	444	5	445	7
37	226	61	3.71	0.1600	0.0018	10.1934	0.0980	0.4622	0.0075	2455	15	2452	9	2449	33
38	170	269	0.63	0.0558	0.0008	0.5481	0.0066	0.0712	0.0011	446	17	444	4	443	7
39	226	303	0.74	0.0556	0.0008	0.5419	0.0064	0.0707	0.0011	437	17	440	4	440	7
40	74	189	0.39	0.0667	0.0008	1.2433	0.0135	0.1351	0.0021	829	16	820	6	817	12
41	104	219	0.47	0.0558	0.0010	0.5400	0.0084	0.0702	0.0012	444	17	438	6	437	7
42	104	211	0.49	0.0577	0.0012	0.5415	0.0104	0.0681	0.0012	519	19	439	7	424	7

Appendix A2 SHRIMP zircon U–Pb data for samples 10GD23-1 (andesite) and 10GD25 (dacite) in the Chayuanshan volcanic succession

spot	Th (ppm)	U (ppm)	Th/U	f_{206}(%)	Ratio						Age (Ma)			
					$^{207}Pb/^{206}Pb$	1σ	$^{207}Pb/^{235}U$	1σ	$^{206}Pb/^{238}U$	1σ	$^{206}Pb/^{238}U$	1σ	$^{207}Pb/^{235}U$	1σ
Sample 10GD23−1 andesite														
s1	151	175	0.89	0.29	0.0570	0.0017	0.5360	0.0176	0.0682	0.0008	425	5	436	5
s2	234	244	0.99	-0.08	0.0587	0.0012	0.5649	0.0129	0.0698	0.0008	435	5	455	5
s3	157	281	0.58	4.44	0.0775	0.0195	0.7935	0.2040	0.0742	0.0038	462	23	593	29
s4	145	235	0.64	0.00	0.0579	0.0009	0.5569	0.0111	0.0698	0.0008	435	5	450	5
s5	69	113	0.63	0.47	0.0541	0.0026	0.5040	0.0252	0.0676	0.0010	421	6	414	6
s6	137	237	0.60	1.49	0.0536	0.0031	0.5273	0.0309	0.0714	0.0009	445	5	430	5
s7	122	182	0.69	0.47	0.0569	0.0020	0.5267	0.0201	0.0671	0.0008	419	5	430	5
s8	80	163	0.50	-0.34	0.0618	0.0020	0.5904	0.0204	0.0693	0.0009	432	5	471	6
s9	87	154	0.58	0.57	0.0547	0.0024	0.5076	0.0236	0.0673	0.0010	420	6	417	6
s10	140	218	0.66	-0.25	0.0580	0.0016	0.5703	0.0167	0.0714	0.0008	444	5	458	5
s11	151	214	0.73	0.00	0.0568	0.0010	0.4864	0.0101	0.0621	0.0007	388	4	402	5
s12	93	127	0.76	0.86	0.0448	0.0031	0.4213	0.0294	0.0683	0.0010	426	6	357	5
s13	132	156	0.87	0.00	0.0574	0.0012	0.5487	0.0133	0.0694	0.0009	432	5	444	6
s14	103	166	0.64	1.33	0.0494	0.0098	0.3695	0.0732	0.0542	0.0008	340	5	319	5
s15	111	163	0.70	0.58	0.0581	0.0025	0.5574	0.0247	0.0696	0.0009	434	5	450	6
s16	108	133	0.84	0.24	0.0547	0.0018	0.5073	0.0184	0.0672	0.0009	419	6	417	6
s17	76	109	0.72	0.86	0.0522	0.0032	0.4658	0.0291	0.0648	0.0010	405	6	388	6
s18	233	251	0.96	0.38	0.0560	0.0016	0.5359	0.0376	0.0694	0.0045	432	27	436	27
s19	183	231	0.82	0.09	0.0575	0.0013	0.5576	0.0138	0.0704	0.0008	438	5	450	5
s20	145	257	0.58	-0.07	0.0582	0.0011	0.5817	0.0131	0.0725	0.0008	451	5	466	5
s21	99	150	0.68	-0.26	0.0637	0.0020	0.6032	0.0207	0.0687	0.0009	428	6	479	6
s22	172	246	0.72	-0.24	0.0569	0.0015	0.5570	0.0157	0.0710	0.0008	442	5	450	5
s23	277	266	1.07	0.18	0.0549	0.0012	0.5377	0.0134	0.0711	0.0008	443	5	437	5

s24	144	198	0.75	0.30	0.0572	0.0018	0.5623	0.0190	0.0713	0.0009	444	5	453	5
s25	251	157	1.66	-0.09	0.0595	0.0013	0.7025	0.0182	0.0856	0.0011	529	7	540	7
s26	136	197	0.71	0.67	0.0556	0.0023	0.5356	0.0235	0.0699	0.0009	435	5	436	5
Sample 10GD25 dacite														
s1	206	308	0.69	0.93	0.0545	0.0024	0.5080	0.0232	0.0677	0.0008	422	5	417	5
s2	147	382	0.40	0.00	0.0575	0.0008	0.5583	0.0096	0.0704	0.0007	439	4	450	5
s3	165	832	0.20	0.09	0.0566	0.0006	0.5521	0.0081	0.0708	0.0007	441	4	446	4
s4	179	395	0.47	0.05	0.0550	0.0009	0.5401	0.0107	0.0712	0.0007	444	4	439	4
s5	99	497	0.21	-0.18	0.0581	0.0009	0.5656	0.0108	0.0706	0.0007	440	4	455	4
s6	135	295	0.47	0.18	0.0550	0.0012	0.5299	0.0130	0.0699	0.0008	435	5	432	5
s7	204	458	0.46	0.19	0.0546	0.0010	0.5321	0.0111	0.0707	0.0007	441	4	433	4
s8	123	286	0.44	0.22	0.0531	0.0012	0.4982	0.0216	0.0680	0.0025	424	15	411	15
s9	135	301	0.46	-0.17	0.0575	0.0011	0.5430	0.0354	0.0685	0.0043	427	26	440	26
s10	138	318	0.45	0.00	0.0585	0.0009	0.5629	0.0106	0.0698	0.0008	435	5	453	5
s11	137	327	0.43	0.06	0.0560	0.0046	0.5368	0.0539	0.0696	0.0040	434	24	436	24
s12	122	284	0.44	-0.16	0.0603	0.0015	0.5715	0.0158	0.0687	0.0008	429	5	459	5
s13	160	338	0.49	0.17	0.0544	0.0012	0.5244	0.0125	0.0699	0.0008	436	5	428	4
s14	128	312	0.42	0.23	0.0562	0.0014	0.5518	0.0153	0.0712	0.0008	443	5	446	5
s15	220	393	0.58	0.11	0.0580	0.0011	0.5532	0.0118	0.0692	0.0007	431	4	447	5
s16	119	258	0.48	0.07	0.0560	0.0011	0.5317	0.0121	0.0689	0.0008	429	5	433	5
s17	229	397	0.60	0.05	0.0553	0.0008	0.5103	0.0094	0.0669	0.0007	417	4	419	4
s18	136	325	0.43	0.27	0.0562	0.0014	0.5365	0.0148	0.0693	0.0008	432	5	436	5
s19	217	463	0.48	0.07	0.0555	0.0008	0.5449	0.0094	0.0712	0.0007	443	4	442	4
s20	173	287	0.62	0.45	0.0534	0.0042	0.4694	0.0479	0.0638	0.0042	398	25	391	25

f_{206}(%) means the percentage of common ^{206}Pb in total Pb.

Appendix A3 LA-MC-ICP-MS zircon Lu–Hf isotope data and SIMS zircon oxygen isotope data for the Chayuanshan volcanic samples 10GD23-1 (andesite) and 10GD25 (dacite)

spot	age	1σ	$^{176}Lu/^{177}Hf$	2σ	$^{176}Hf/^{177}Hf$	2σ	$\varepsilon_{Hf}(t)$	2σ	T_{DM} (Ma)	T_{DM}^{C} (Ma)	$f_{Lu/Hf}$	δO18(‰)	2σ
Sample 10GD23−1 andesite													
01	438	7	0.000572	0.000003	0.282210	0.000024	-10.4	1.4	1453	1756	-0.98	8.99	0.22
02	436	7	0.001512	0.000033	0.282224	0.000033	-10.3	1.6	1470	1746	-0.95	8.39	0.24
03	1050	16	0.000838	0.000009	0.282124	0.000027	-0.27	1.6	1582	1736	-0.97	4.74	0.33
04	440	7	0.000782	0.000004	0.282204	0.000026	-10.6	1.4	1469	1769	-0.98	8.42	0.23
05	439	7	0.000937	0.000010	0.282252	0.000029	-9.0	1.5	1409	1686	-0.97	8.19	0.29
06	1679	16	0.000617	0.000011	0.281860	0.000024	4.5	1.5	1935	2011	-0.98	6.35	0.24
07	425	7	0.000742	0.000014	0.282226	0.000023	-10.2	1.3	1437	1733	-0.98	8.38	0.23
08	435	7	0.000960	0.000007	0.282257	0.000026	-8.9	1.4	1403	1679	-0.97	8.48	0.26
09	441	7	0.001235	0.000009	0.282255	0.000027	-8.9	1.4	1414	1683	-0.96	8.77	0.27
10	439	7	0.000723	0.000002	0.282266	0.000027	-8.5	1.4	1381	1658	-0.98	8.00	0.21
11	430	8	0.000942	0.000007	0.282285	0.000025	-8.0	1.4	1363	1629	-0.97	8.05	0.24
12	729	14	0.000385	0.000006	0.282349	0.000029	1.0	1.6	1254	1415	-0.99	7.25	0.16
13	2406	15	0.000275	0.000002	0.281283	0.000026	0.83	1.6	2695	2784	-0.99	5.01	0.15
14	410	8	0.001130	0.000006	0.282210	0.000027	-11.2	1.5	1473	1771	-0.97	8.85	0.23
15	728	13	0.000384	0.000002	0.281598	0.000029	-25.7	1.6	2279	2751	-0.99	6.64	0.27
16	435	7	0.000764	0.000004	0.282241	0.000029	-9.4	1.5	1416	1703	-0.98	8.85	0.22
17	442	7	0.001152	0.000003	0.282199	0.000030	-10.9	1.5	1491	1783	-0.97	8.30	0.32
18	437	7	0.000821	0.000001	0.282234	0.000028	-9.7	1.5	1429	1717	-0.98	7.98	0.27
19	437	7	0.000727	0.000002	0.282328	0.000029	-6.3	1.5	1296	1547	-0.98	8.39	0.24
20	1360	16	0.000776	0.000005	0.281989	0.000030	1.8	1.7	1765	1884	-0.98	7.99	0.24
21	448	7	0.000702	0.000003	0.282214	0.000030	-10.1	1.5	1453	1748	-0.98	8.53	0.18
22	435	7	0.000793	0.000003	0.282245	0.000027	-9.3	1.4	1412	1697	-0.98	7.80	0.28
23	413	7	0.000586	0.000001	0.282211	0.000026	-10.9	1.4	1452	1762	-0.98	7.29	0.32

24	1025	16	0.000664	0.000011	0.282176	0.000029	1.2	1.6	1503	1644	-0.98	6.08	0.20
25	422	7	0.001004	0.000013	0.282255	0.000030	-9.3	1.5	1406	1686	-0.97	8.05	0.28
26	444	7	0.000774	0.000004	0.282253	0.000027	-8.8	1.4	1400	1679	-0.98	8.74	0.18
27	412	7	0.000933	0.000012	0.282092	0.000028	-15.3	1.5	1631	1980	-0.97	8.48	0.20
28	444	7	0.000633	0.000005	0.282242	0.000027	-9.2	1.4	1411	1698	-0.98	8.01	0.33
29	438	7	0.001010	0.000006	0.282264	0.000029	-8.6	1.5	1395	1666	-0.97	8.64	0.36
30	437	7	0.001033	0.000012	0.282260	0.000029	-8.8	1.5	1400	1672	-0.97	8.34	0.23
31	438	7	0.000646	0.000004	0.282217	0.000024	-10.2	1.4	1446	1744	-0.98	7.98	0.30
32	431	7	0.000810	0.000004	0.282260	0.000026	-8.9	1.4	1393	1672	-0.98	8.22	0.29
33	998	15	0.000895	0.000002	0.282455	0.000024	10.3	1.5	1124	1160	-0.97	6.94	0.26
34	422	8	0.000754	0.000005	0.282049	0.000028	-16.5	1.5	1682	2051	-0.98	8.41	0.20
35	444	8	0.001267	0.000037	0.282230	0.000026	-9.8	1.4	1452	1729	-0.96	8.91	0.35
36	431	7	0.001069	0.000002	0.282173	0.000026	-12.0	1.4	1524	1831	-0.97	8.46	0.16
37	434	7	0.001102	0.000019	0.282257	0.000029	-9.0	1.5	1407	1680	-0.97	8.61	0.22
38	422	7	0.000736	0.000003	0.282200	0.000029	-11.2	1.5	1473	1781	-0.98	7.80	0.22
39	992	16	0.002043	0.000048	0.282116	0.000030	-2.6	1.6	1645	1807	-0.94	5.12	0.28
40	440	7	0.000806	0.000003	0.282215	0.000026	-10.3	1.4	1455	1750	-0.98	7.99	0.21
41	420	7	0.001196	0.000024	0.282271	0.000027	-8.8	1.4	1392	1661	-0.96	7.94	0.32
42	435	7	0.000977	0.000005	0.282188	0.000027	-11.4	1.4	1499	1802	-0.97	8.33	0.19
Sample 10GD25 dacite													
01	415	8	0.001098	0.000006	0.282251	0.000028	-9.6	1.5	1416	1696	-0.97	7.73	0.30
02	440	7	0.000271	0.000002	0.281889	0.000024	-21.7	1.4	1879	2323	-0.99	7.59	0.26
03	422	7	0.001168	0.000008	0.282293	0.000030	-8.0	1.5	1359	1620	-0.96	7.62	0.31
04	3451	14	0.001019	0.000009	0.280481	0.000029	-5.3	1.7	3827	3934	-0.97	5.91	0.19
05	432	7	0.001138	0.000006	0.282262	0.000026	-8.9	1.4	1401	1672	-0.97	7.90	0.23
06	434	7	0.001084	0.000007	0.282256	0.000026	-9.0	1.4	1408	1682	-0.97	8.79	0.27
07	436	7	0.000933	0.000007	0.282239	0.000028	-9.6	1.5	1427	1710	-0.97	7.72	0.27
08	430	7	0.000956	0.000009	0.282248	0.000028	-9.3	1.5	1414	1695	-0.97	8.31	0.31
09	429	7	0.000957	0.000003	0.282276	0.000026	-8.4	1.4	1375	1645	-0.97	7.57	0.11
10	431	7	0.001070	0.000005	0.282316	0.000027	-7.0	1.5	1324	1575	-0.97	7.95	0.33
11	424	6	0.001312	0.000011	0.282272	0.000027	-8.7	1.4	1394	1659	-0.96	8.03	0.24

12	435	7	0.001116	0.000005	0.282236	0.000029	-9.7	1.5	1438	1718	-0.97	7.86	0.16
13	431	6	0.001203	0.000006	0.282207	0.000028	-10.9	1.5	1481	1772	-0.96	8.10	0.22
14	419	7	0.001061	0.000005	0.282312	0.000031	-7.4	1.5	1329	1585	-0.97	8.35	0.37
15	1495	16	0.000887	0.000006	0.281882	0.000029	0.87	1.6	1919	2041	-0.97	5.53	0.21
16	443	7	0.000947	0.000002	0.282255	0.000027	-8.8	1.4	1404	1678	-0.97	8.34	0.25
17	434	7	0.000946	0.000006	0.282243	0.000029	-9.4	1.5	1421	1703	-0.97	8.17	0.21
18	441	7	0.000957	0.000006	0.282237	0.000029	-9.5	1.5	1429	1711	-0.97	8.16	0.21
19	434	7	0.001028	0.000014	0.282270	0.000030	-8.5	1.5	1386	1655	-0.97	8.73	0.26
20	1080	15	0.000708	0.000001	0.282086	0.000029	-0.85	1.6	1629	1790	-0.98	7.88	0.18
21	436	7	0.000450	0.000005	0.282216	0.000029	-10.2	1.5	1440	1745	-0.99	8.21	0.26
22	997	17	0.000767	0.000005	0.282242	0.000025	2.8	1.6	1415	1537	-0.98	8.23	0.29
23	437	7	0.001274	0.000005	0.282246	0.000029	-9.4	1.5	1429	1702	-0.96	8.04	0.31
24	431	7	0.001177	0.000019	0.282257	0.000030	-9.1	1.5	1410	1682	-0.96	7.87	0.23
25	439	7	0.001057	0.000004	0.282277	0.000028	-8.2	1.5	1378	1642	-0.97	7.97	0.22
26	432	7	0.001053	0.000004	0.282217	0.000023	-10.4	1.3	1461	1751	-0.97	8.89	0.25
27	441	7	0.001172	0.000003	0.282291	0.000030	-7.7	1.5	1362	1618	-0.96	8.34	0.19
28	2129	16	0.000158	0.000005	0.281231	0.000020	-7.2	1.5	2756	2952	-1.00	4.82	0.30
29	438	7	0.001411	0.000010	0.282319	0.000030	-6.8	1.5	1332	1573	-0.96	8.96	0.35
30	838	14	0.000638	0.000004	0.282326	0.000032	2.4	1.7	1295	1430	-0.98	7.18	0.26
31	429	7	0.001292	0.000011	0.282274	0.000029	-8.5	1.5	1390	1654	-0.96	7.94	0.34
32	427	7	0.001085	0.000007	0.282213	0.000036	-10.7	1.7	1468	1761	-0.97	7.99	0.32
33	432	7	0.001145	0.000008	0.282219	0.000030	-10.4	1.5	1462	1749	-0.97	8.32	0.17
34	430	7	0.001069	0.000002	0.282261	0.000026	-8.9	1.4	1400	1674	-0.97	8.61	0.23
35	2510	15	0.000294	0.000007	0.281357	0.000028	5.8	1.6	2596	2623	-0.99	7.57	0.20
36	445	7	0.001193	0.000009	0.282269	0.000028	-8.4	1.5	1394	1658	-0.96	7.79	0.22
37	2455	15	0.000283	0.000001	0.280934	0.000027	-10.5	1.6	3159	3376	-0.99	6.50	0.30
38	443	7	0.001280	0.000009	0.282196	0.000027	-11.0	1.4	1499	1789	-0.96	7.93	0.21
39	440	7	0.001225	0.000011	0.282286	0.000030	-7.9	1.5	1371	1628	-0.96	8.70	0.27
40	817	12	0.001116	0.000008	0.282208	0.000029	-2.5	1.6	1477	1661	-0.97	8.41	0.29
41	437	7	0.000780	0.000013	0.282185	0.000029	-11.4	1.5	1495	1803	-0.98	8.56	0.42
42	424	7	0.000932	0.000003	0.282110	0.000027	-14.4	1.4	1606	1944	-0.97	7.95	0.22

$\varepsilon_{Hf}(t)=10{,}000\times\{[(^{176}Hf/^{177}Hf)_S-(^{176}Lu/^{177}Hf)_S\times(e^{\lambda t}-1)] / [(^{176}Hf/^{177}Hf)_{CHUR,0}-(^{176}Lu/^{177}Hf)_{CHUR}\times(e^{\lambda t}-1)]-1\}$.

$T_{DM}=1/\lambda\times\ln\{1+[(^{176}Hf/^{177}Hf)_S-(^{176}Hf/^{177}Hf)_{DM}] /[(^{176}Lu/^{177}Hf)_S-(^{176}Lu/^{177}Hf)_{DM}]\}$.

$T_{DM}^{C}=T_{DM}-(T_{DM}-t)\times[(f_{cc}-f_s)/(f_{cc}-f_{DM})]$. $f_{Lu/Hf}=(^{176}Lu/^{177}Hf)_S/(^{176}Lu/^{177}Hf)_{CHUR}-1$.

where, $\lambda=1.865\times10^{-11}$ year^{-1} (Scherer et al., 2001); $(^{176}Lu/^{177}Hf)_S$ and $(^{176}Hf/^{177}Hf)_S$ are the measured values of the samples; $(^{176}Lu/^{177}Hf)_{CHUR}=0.0332$ and $(^{176}Hf/^{177}Hf)_{CHUR,0}=0.28277$ (Blichert-Toft and Albarède, 1997); $(^{176}Lu/^{177}Hf)_{DM}=0.0384$ and $(^{176}Hf/^{177}Hf)_{DM}=0.28325$ (Griffin et al., 2000); $(^{176}Lu/^{177}Hf)_{upper\ crust}=0.0093$; $f_{cc}=[(^{176}Lu/^{177}Hf)_{upper\ crust}/(^{176}Lu/^{177}Hf)_{CHUR}]-1$; $f_s=f_{Lu/Hf}$; $f_{DM}=[(^{176}Lu/^{177}Hf)_{DM}/(^{176}Lu/^{177}Hf)_{CHUR}]-1$; t=crystallization age of zircon.

Appendix B1 LA-ICP-MS detrital zircon U–Pb data for Cambrian clastic samples from southwestern and northern Guangdong

Spot#	Th (ppm)	U (ppm)	Th/U	Corrected Ratios						Corrected Ages (Ma)					
				$^{207}Pb/^{206}Pb$	1σ	$^{207}Pb/^{235}U$	1σ	$^{206}Pb/^{238}U$	1σ	$^{207}Pb/^{206}Pb$	1σ	$^{207}Pb/^{235}U$	1σ	$^{206}Pb/^{238}U$	1σ
Sample 10GD48 (N22°04'28.2", E111°26'44.9")															
1	77	208	0.37	0.0706	0.0008	1.5994	0.0153	0.1644	0.0025	945	16	970	6	981	14
2	179	217	0.82	0.0742	0.0009	1.6564	0.0166	0.1619	0.0025	1048	16	992	6	967	14
3	203	575	0.35	0.0707	0.0007	1.5971	0.0130	0.1640	0.0024	948	17	969	5	979	14
4	136	141	0.96	0.0746	0.0009	1.8106	0.0184	0.1761	0.0027	1057	16	1049	7	1046	15
5	114	191	0.60	0.0725	0.0009	1.5964	0.0174	0.1597	0.0025	1001	15	969	7	955	14
6	247	262	0.94	0.1598	0.0016	9.9683	0.0809	0.4526	0.0068	2454	15	2432	7	2407	30
7	69	274	0.25	0.0599	0.0009	0.7251	0.0095	0.0878	0.0014	600	16	554	6	543	8
8	75	405	0.19	0.0733	0.0008	1.7214	0.0145	0.1705	0.0026	1021	17	1017	5	1015	14
9	113	241	0.47	0.0740	0.0008	1.8140	0.0163	0.1778	0.0027	1042	17	1051	6	1055	15
10	109	134	0.81	0.0757	0.0010	1.9617	0.0217	0.1879	0.0029	1088	15	1102	7	1110	16
11	98	125	0.78	0.0765	0.0009	2.0681	0.0212	0.1962	0.0030	1108	16	1138	7	1155	16
12	192	415	0.46	0.0598	0.0007	0.8008	0.0075	0.0972	0.0015	596	17	597	4	598	9
13	53	130	0.41	0.0756	0.0009	1.8201	0.0187	0.1748	0.0027	1083	16	1053	7	1038	15
14	174	309	0.56	0.0601	0.0007	0.8183	0.0082	0.0989	0.0015	605	17	607	5	608	9
15	242	268	0.90	0.0743	0.0008	1.8472	0.0162	0.1804	0.0027	1049	17	1062	6	1069	15
16	129	254	0.51	0.0766	0.0008	2.0301	0.0181	0.1923	0.0029	1110	16	1126	6	1134	16
17	185	177	1.05	0.0836	0.0009	2.4181	0.0220	0.2099	0.0032	1283	16	1248	7	1228	17
18	155	361	0.43	0.0740	0.0018	1.8005	0.0348	0.1765	0.0027	1041	51	1046	13	1048	15
19	96	329	0.29	0.0842	0.0009	2.5783	0.0216	0.2221	0.0033	1297	16	1295	6	1293	18
20	120	208	0.58	0.0596	0.0008	0.8063	0.0091	0.0981	0.0015	589	16	600	5	603	9
21	56	99	0.57	0.1986	0.0021	14.8027	0.1345	0.5410	0.0085	2814	14	2803	9	2787	35
22	243	484	0.50	0.0991	0.0010	3.6387	0.0278	0.2664	0.0039	1608	16	1558	6	1522	20

23	83	297	0.28	0.0601	0.0009	0.6445	0.0083	0.0779	0.0012	606	15	505	5	483	7
24	93	257	0.36	0.0737	0.0008	1.6978	0.0152	0.1671	0.0025	1034	17	1008	6	996	14
25	334	604	0.55	0.0614	0.0007	0.8117	0.0073	0.0959	0.0014	655	17	603	4	590	8
26	135	273	0.50	0.0737	0.0008	1.7746	0.0158	0.1747	0.0026	1034	17	1036	6	1038	14
27	103	249	0.41	0.0759	0.0008	1.7978	0.0160	0.1719	0.0026	1091	16	1045	6	1023	14
28	44	111	0.40	0.0731	0.0010	1.5886	0.0189	0.1576	0.0025	1018	15	966	7	944	14
29	56	102	0.56	0.0738	0.0010	1.7736	0.0212	0.1744	0.0027	1036	15	1036	8	1036	15
30	54	203	0.26	0.1551	0.0015	9.3882	0.0727	0.4391	0.0065	2403	15	2377	7	2347	29
31	92	143	0.64	0.0709	0.0009	1.5370	0.0162	0.1573	0.0024	955	16	945	6	942	13
32	17	63	0.26	0.0764	0.0011	1.9097	0.0244	0.1815	0.0029	1105	15	1084	9	1075	16
33	105	128	0.82	0.0818	0.0010	2.3612	0.0229	0.2096	0.0032	1240	16	1231	7	1227	17
34	83	95	0.88	0.1568	0.0016	9.4413	0.0791	0.4369	0.0066	2422	15	2382	8	2337	30
35	23	31	0.73	0.0784	0.0019	1.9827	0.0442	0.1835	0.0036	1157	20	1110	15	1086	20
36	63	102	0.62	0.0830	0.0011	2.5516	0.0298	0.2230	0.0035	1270	15	1287	9	1298	19
37	92	150	0.61	0.1076	0.0030	3.7152	0.0817	0.2503	0.0041	1760	51	1575	18	1440	21
38	98	178	0.55	0.0618	0.0008	0.9239	0.0104	0.1085	0.0017	667	16	664	5	664	10
39	191	213	0.90	0.0849	0.0009	2.6003	0.0224	0.2223	0.0033	1313	16	1301	6	1294	18
40	88	425	0.21	0.0695	0.0007	1.3069	0.0110	0.1364	0.0020	914	17	849	5	824	11
41	90	187	0.48	0.1581	0.0016	9.7434	0.0772	0.4472	0.0067	2435	15	2411	7	2383	30
42	90	202	0.44	0.0725	0.0008	1.6771	0.0158	0.1680	0.0025	999	16	1000	6	1001	14
43	161	272	0.59	0.0734	0.0008	1.8273	0.0158	0.1805	0.0027	1026	17	1055	6	1070	15
44	139	279	0.50	0.0848	0.0021	2.4804	0.0480	0.2122	0.0033	1311	49	1266	14	1240	17
45	246	384	0.64	0.0670	0.0009	1.0903	0.0119	0.1181	0.0018	838	16	749	6	719	10
46	321	329	0.97	0.0749	0.0008	1.8071	0.0164	0.1750	0.0026	1067	16	1048	6	1040	14
47	111	82	1.35	0.0664	0.0011	1.2172	0.0173	0.1330	0.0021	819	15	808	8	805	12
48	328	666	0.49	0.0616	0.0006	0.9038	0.0076	0.1065	0.0016	659	18	654	4	653	9
49	151	134	1.13	0.0709	0.0009	1.5439	0.0165	0.1579	0.0024	955	15	948	7	945	13
50	129	261	0.50	0.0613	0.0008	0.8544	0.0090	0.1012	0.0015	648	16	627	5	622	9
51	150	322	0.46	0.0727	0.0008	1.7070	0.0150	0.1704	0.0025	1006	17	1011	6	1014	14
52	181	644	0.28	0.0615	0.0007	0.9215	0.0078	0.1087	0.0016	657	18	663	4	665	9
53	46	176	0.26	0.1410	0.0031	4.0991	0.0611	0.2109	0.0033	2239	38	1654	12	1233	18
54	224	118	1.89	0.0629	0.0010	0.9461	0.0123	0.1091	0.0017	706	15	676	6	668	10

55	26	60	0.43	0.0750	0.0012	1.8109	0.0240	0.1753	0.0028	1068	15	1049	9	1041	15
56	98	194	0.50	0.0709	0.0009	1.5023	0.0163	0.1538	0.0024	954	15	931	7	922	13
57	144	202	0.71	0.0720	0.0011	1.4018	0.0192	0.1413	0.0023	985	15	890	8	852	13
58	285	563	0.51	0.0790	0.0020	2.0031	0.0409	0.1840	0.0028	1171	52	1117	14	1089	15
59	95	141	0.67	0.0721	0.0009	1.5270	0.0165	0.1536	0.0024	990	15	941	7	921	13
60	156	260	0.60	0.0714	0.0008	1.5430	0.0139	0.1568	0.0023	969	16	948	6	939	13
61	261	471	0.55	0.0760	0.0008	1.8108	0.0152	0.1729	0.0026	1095	17	1049	5	1028	14
62	74	150	0.49	0.0694	0.0011	1.3293	0.0182	0.1389	0.0022	912	15	859	8	839	13
63	116	398	0.29	0.0749	0.0008	1.8233	0.0153	0.1767	0.0026	1065	17	1054	5	1049	14
64	93	120	0.77	0.2312	0.0025	18.2677	0.1692	0.5735	0.0090	3060	14	3004	9	2922	37
65	91	134	0.68	0.0782	0.0010	1.9175	0.0202	0.1780	0.0027	1151	15	1087	7	1056	15
66	355	386	0.92	0.0738	0.0008	1.6406	0.0148	0.1614	0.0024	1035	16	986	6	964	13
67	261	296	0.88	0.0706	0.0008	1.3882	0.0128	0.1427	0.0021	945	16	884	5	860	12
68	70	193	0.36	0.0733	0.0009	1.7360	0.0170	0.1719	0.0026	1022	16	1022	6	1022	14
69	55	39	1.40	0.1614	0.0019	10.0607	0.1032	0.4522	0.0072	2471	14	2440	9	2405	32
70	148	538	0.28	0.0656	0.0015	1.1152	0.0184	0.1233	0.0018	794	48	761	9	749	11
71	206	1128	0.18	0.0670	0.0007	1.2184	0.0097	0.1319	0.0019	839	18	809	4	799	11
72	284	749	0.38	0.0640	0.0017	1.0896	0.0234	0.1236	0.0019	740	57	748	11	751	11
73	231	593	0.39	0.0682	0.0017	1.3529	0.0271	0.1438	0.0022	875	53	869	12	866	12
74	105	111	0.94	0.0745	0.0010	1.7741	0.0199	0.1729	0.0027	1054	15	1036	7	1028	15
75	92	208	0.44	0.0837	0.0009	2.4104	0.0212	0.2091	0.0031	1284	16	1246	6	1224	17
76	28	218	0.13	0.0620	0.0014	0.8566	0.0141	0.1002	0.0015	674	49	628	8	616	9
77	485	339	1.43	0.1477	0.0015	8.0632	0.0640	0.3961	0.0059	2320	15	2238	7	2151	27
78	83	302	0.27	0.0729	0.0008	1.7118	0.0148	0.1704	0.0025	1011	17	1013	6	1014	14
79	87	305	0.29	0.0716	0.0008	1.2548	0.0118	0.1272	0.0019	974	16	826	5	772	11
80	345	518	0.67	0.0610	0.0007	0.8811	0.0077	0.1049	0.0015	638	17	642	4	643	9
81	110	129	0.85	0.1194	0.0013	5.5468	0.0499	0.3372	0.0051	1947	15	1908	8	1873	25
82	234	259	0.90	0.0757	0.0008	1.9469	0.0169	0.1867	0.0028	1086	16	1097	6	1104	15
83	169	346	0.49	0.0737	0.0008	1.5902	0.0145	0.1565	0.0023	1034	16	966	6	938	13
84	18	27	0.65	0.0791	0.0017	2.1775	0.0407	0.1998	0.0036	1175	17	1174	13	1174	19
85	16	41	0.38	0.2308	0.0033	18.8234	0.2480	0.5919	0.0108	3057	14	3033	13	2997	44
86	161	288	0.56	0.0750	0.0008	1.8133	0.0161	0.1754	0.0026	1069	16	1050	6	1042	14

87	121	275	0.44	0.1149	0.0011	5.4279	0.0416	0.3429	0.0050	1878	16	1889	7	1901	24
88	497	1028	0.48	0.0839	0.0020	2.0080	0.0373	0.1736	0.0026	1290	48	1118	13	1032	15
89	230	369	0.62	0.1179	0.0012	5.2882	0.0403	0.3256	0.0048	1924	15	1867	6	1817	23
90	93	264	0.35	0.2010	0.0019	13.3740	0.0997	0.4829	0.0071	2834	14	2706	7	2540	31
91	225	519	0.43	0.1515	0.0014	8.7961	0.0650	0.4213	0.0062	2363	15	2317	7	2266	28
92	190	171	1.11	0.0755	0.0009	1.8867	0.0185	0.1814	0.0027	1081	15	1076	7	1075	15
93	67	180	0.37	0.0702	0.0019	1.3826	0.0294	0.1428	0.0022	935	55	882	13	860	12
94	111	392	0.28	0.0680	0.0007	1.3696	0.0121	0.1461	0.0022	870	17	876	5	879	12
95	660	505	1.31	0.0867	0.0009	2.1660	0.0173	0.1812	0.0027	1355	16	1170	6	1074	14
96	225	314	0.72	0.0697	0.0008	1.4979	0.0131	0.1559	0.0023	920	17	930	5	934	13
97	138	192	0.72	0.0708	0.0010	1.2728	0.0146	0.1305	0.0020	951	15	834	7	791	11
98	69	163	0.42	0.0725	0.0009	1.6988	0.0175	0.1700	0.0026	1001	15	1008	7	1012	14
99	117	216	0.54	0.0713	0.0008	1.6382	0.0158	0.1667	0.0025	967	16	985	6	994	14
100	49	70	0.70	0.1713	0.0020	11.3440	0.1113	0.4807	0.0076	2570	14	2552	9	2530	33
101	63	303	0.21	0.1435	0.0025	6.8529	0.0669	0.3463	0.0051	2270	31	2093	9	1917	24
102	26	29	0.90	0.0681	0.0018	1.2217	0.0288	0.1301	0.0025	873	22	811	13	789	14
103	215	508	0.42	0.0605	0.0007	0.6651	0.0064	0.0797	0.0012	623	16	518	4	495	7
104	90	85	1.06	0.0683	0.0011	1.2288	0.0179	0.1305	0.0021	878	15	814	8	791	12
105	545	953	0.57	0.0601	0.0006	0.7881	0.0064	0.0951	0.0014	608	18	590	4	586	8
106	385	304	1.27	0.0684	0.0008	1.2685	0.0119	0.1346	0.0020	881	16	832	5	814	11
107	283	628	0.45	0.0811	0.0008	2.2441	0.0175	0.2009	0.0029	1223	17	1195	5	1180	16
108	80	343	0.23	0.1443	0.0014	7.7905	0.0579	0.3919	0.0057	2279	15	2207	7	2132	26
109	72	276	0.26	0.0628	0.0008	0.9430	0.0094	0.1091	0.0016	700	16	674	5	667	9
110	65	200	0.32	0.0681	0.0009	1.1965	0.0134	0.1275	0.0019	871	15	799	6	774	11
111	196	468	0.42	0.0698	0.0007	1.5432	0.0126	0.1604	0.0023	923	17	948	5	959	13
112	532	538	0.99	0.0733	0.0008	1.5705	0.0135	0.1554	0.0023	1023	16	959	5	931	13
113	190	664	0.29	0.0623	0.0006	1.0116	0.0083	0.1178	0.0017	685	17	710	4	718	10
114	176	374	0.47	0.1284	0.0013	6.2789	0.0478	0.3548	0.0052	2077	15	2016	7	1957	25
115	59	53	1.11	0.1225	0.0015	5.9628	0.0629	0.3533	0.0055	1993	14	1970	9	1950	26
116	28	71	0.40	0.0706	0.0022	1.4970	0.0396	0.1538	0.0025	946	65	929	16	922	14
117	56	340	0.17	0.0930	0.0017	2.8148	0.0306	0.2195	0.0032	1488	35	1359	8	1279	17
118	189	380	0.50	0.0703	0.0008	1.4378	0.0126	0.1485	0.0022	936	16	905	5	893	12

119	124	360	0.34	0.0701	0.0007	1.4811	0.0125	0.1533	0.0022	932	17	923	5	919	13
120	100	175	0.57	0.0703	0.0008	1.5780	0.0155	0.1630	0.0024	936	16	962	6	973	13
Sample 10GD49-1 (N21°52'53.0", E111°49'35.1")															
1	141	315	0.45	0.0756	0.0009	1.8859	0.0188	0.1810	0.0027	1085	15	1076	7	1072	15
2	118	236	0.50	0.0706	0.0009	1.5378	0.0155	0.1580	0.0024	947	16	946	6	946	13
3	161	335	0.48	0.0754	0.0009	1.8733	0.0182	0.1803	0.0027	1080	16	1072	6	1068	15
4	18	26	0.68	0.0581	0.0035	0.6458	0.0358	0.0806	0.0025	535	69	506	22	500	15
5	46	207	0.22	0.0603	0.0009	0.9222	0.0114	0.1110	0.0017	614	15	664	6	679	10
6	340	481	0.71	0.0698	0.0008	1.3285	0.0122	0.1381	0.0021	922	16	858	5	834	12
7	428	346	1.24	0.0906	0.0009	2.8863	0.0240	0.2313	0.0034	1437	16	1378	6	1341	18
8	141	141	1.00	0.0716	0.0010	1.6064	0.0193	0.1627	0.0025	976	15	973	8	972	14
9	147	292	0.50	0.0761	0.0009	1.8078	0.0175	0.1724	0.0026	1098	16	1048	6	1025	14
10	140	199	0.71	0.0674	0.0026	1.3768	0.0478	0.1482	0.0025	850	82	879	20	891	14
11	95	248	0.38	0.0719	0.0009	1.6664	0.0166	0.1683	0.0025	982	16	996	6	1003	14
12	99	160	0.62	0.0849	0.0027	2.5173	0.0673	0.2151	0.0036	1312	62	1277	19	1256	19
13	182	516	0.35	0.1419	0.0027	5.8586	0.0683	0.2996	0.0045	2250	34	1955	10	1689	22
14	116	129	0.90	0.0695	0.0010	1.5882	0.0189	0.1657	0.0026	915	15	966	7	989	14
15	50	104	0.49	0.1748	0.0018	12.0185	0.1028	0.4990	0.0076	2604	14	2606	8	2609	33
16	215	191	1.13	0.0733	0.0009	1.8174	0.0184	0.1799	0.0027	1023	16	1052	7	1066	15
17	316	287	1.10	0.0714	0.0009	1.5326	0.0168	0.1558	0.0024	969	15	944	7	933	13
18	44	114	0.38	0.0724	0.0011	1.6154	0.0219	0.1620	0.0026	996	15	976	9	968	14
19	315	476	0.66	0.0590	0.0007	0.8069	0.0079	0.0993	0.0015	566	17	601	4	610	9
20	154	262	0.59	0.0723	0.0009	1.5361	0.0152	0.1542	0.0023	994	16	945	6	924	13
21	27	208	0.13	0.0702	0.0009	1.5931	0.0161	0.1648	0.0025	933	16	968	6	983	14
22	75	266	0.28	0.0750	0.0009	1.7780	0.0165	0.1721	0.0026	1068	16	1037	6	1024	14
23	23	53	0.44	0.0696	0.0013	1.5450	0.0256	0.1612	0.0027	915	16	949	10	963	15
24	74	516	0.14	0.0685	0.0007	1.3527	0.0119	0.1433	0.0021	884	17	869	5	863	12
25	100	503	0.20	0.0718	0.0008	1.6515	0.0142	0.1669	0.0025	980	17	990	5	995	14
26	63	138	0.46	0.1945	0.0020	14.2629	0.1193	0.5323	0.0081	2780	14	2767	8	2751	34
27	75	166	0.45	0.1275	0.0014	6.3630	0.0567	0.3621	0.0055	2064	15	2027	8	1992	26
28	215	529	0.41	0.0689	0.0007	1.2786	0.0111	0.1348	0.0020	894	17	836	5	815	11

29	67	492	0.14	0.0748	0.0008	1.8426	0.0152	0.1788	0.0026	1062	17	1061	5	1061	14
30	335	288	1.16	0.0916	0.0010	3.1019	0.0265	0.2457	0.0037	1460	16	1433	7	1416	19
31	51	158	0.32	0.0736	0.0010	1.7393	0.0190	0.1715	0.0026	1031	15	1023	7	1020	14
32	86	146	0.59	0.1040	0.0012	4.1418	0.0375	0.2889	0.0044	1697	15	1663	7	1636	22
33	79	99	0.80	0.0753	0.0010	2.0627	0.0242	0.1987	0.0031	1077	15	1137	8	1168	17
34	31	61	0.51	0.0639	0.0014	1.0051	0.0193	0.1142	0.0020	737	18	706	10	697	11
35	38	250	0.15	0.0759	0.0009	1.8421	0.0171	0.1761	0.0026	1093	16	1061	6	1046	14
36	49	93	0.53	0.0721	0.0011	1.6376	0.0220	0.1649	0.0026	988	15	985	8	984	15
37	169	118	1.43	0.0749	0.0010	1.7940	0.0204	0.1737	0.0027	1067	15	1043	7	1033	15
38	91	126	0.72	0.0806	0.0027	2.3476	0.0675	0.2113	0.0035	1211	67	1227	20	1236	18
39	120	141	0.85	0.0703	0.0009	1.5086	0.0170	0.1558	0.0024	936	15	934	7	934	13
40	79	112	0.70	0.0749	0.0010	1.8204	0.0210	0.1763	0.0027	1067	15	1053	8	1047	15
41	211	612	0.34	0.0691	0.0007	1.4430	0.0120	0.1516	0.0022	900	17	907	5	910	12
42	58	70	0.83	0.0748	0.0012	1.8602	0.0269	0.1805	0.0030	1063	15	1067	10	1069	16
43	23	30	0.77	0.0731	0.0021	1.7537	0.0453	0.1740	0.0036	1018	24	1029	17	1034	19
44	66	406	0.16	0.1025	0.0010	3.9324	0.0311	0.2785	0.0041	1669	16	1620	6	1584	21
45	300	245	1.22	0.0721	0.0009	1.5245	0.0152	0.1534	0.0023	988	16	940	6	920	13
46	119	215	0.55	0.0714	0.0009	1.6151	0.0167	0.1641	0.0025	969	15	976	6	980	14
47	25	534	0.05	0.0764	0.0014	1.8050	0.0188	0.1714	0.0025	1105	37	1047	7	1020	14
48	150	187	0.80	0.0658	0.0009	1.2371	0.0139	0.1364	0.0021	800	15	818	6	824	12
49	78	97	0.81	0.1014	0.0012	3.8829	0.0383	0.2778	0.0043	1650	15	1610	8	1580	21
50	497	482	1.03	0.0591	0.0007	0.7880	0.0076	0.0967	0.0014	572	17	590	4	595	8
51	12	23	0.53	0.1910	0.0028	12.6396	0.1693	0.4801	0.0086	2751	14	2653	13	2528	38
52	109	240	0.45	0.1010	0.0011	3.9812	0.0335	0.2860	0.0043	1643	15	1630	7	1622	21
53	173	290	0.59	0.0600	0.0008	0.8433	0.0100	0.1019	0.0016	604	15	621	6	626	9
54	55	294	0.19	0.0701	0.0015	1.4821	0.0218	0.1533	0.0023	932	44	923	9	919	13
55	299	572	0.52	0.0734	0.0008	1.7619	0.0144	0.1743	0.0026	1024	17	1032	5	1036	14
56	16	7	2.13	0.0709	0.0031	1.7386	0.0698	0.1780	0.0045	954	43	1023	26	1056	25
57	346	672	0.52	0.0606	0.0007	0.8581	0.0078	0.1028	0.0015	625	17	629	4	631	9
58	79	184	0.43	0.0727	0.0009	1.6877	0.0172	0.1684	0.0026	1006	15	1004	7	1003	14
59	125	616	0.20	0.0690	0.0007	1.3752	0.0112	0.1446	0.0021	899	17	878	5	870	12
60	99	131	0.75	0.0733	0.0010	1.7014	0.0205	0.1685	0.0026	1022	15	1009	8	1004	15

61	60	112	0.53	0.0773	0.0010	2.1664	0.0231	0.2033	0.0031	1129	15	1170	7	1193	17
62	315	240	1.31	0.0739	0.0008	1.7993	0.0166	0.1766	0.0026	1039	16	1045	6	1048	14
63	82	64	1.28	0.0748	0.0012	1.8461	0.0259	0.1790	0.0029	1064	15	1062	9	1061	16
64	87	240	0.36	0.0613	0.0008	0.9337	0.0099	0.1106	0.0017	649	16	670	5	676	10
65	95	406	0.23	0.0699	0.0015	1.3967	0.0209	0.1450	0.0022	924	44	888	9	873	12
66	317	188	1.68	0.0767	0.0009	1.8258	0.0178	0.1728	0.0026	1112	16	1055	6	1028	14
67	214	366	0.59	0.2293	0.0045	18.6984	0.2180	0.5914	0.0092	3047	32	3026	11	2995	37
68	176	308	0.57	0.0743	0.0008	1.7732	0.0157	0.1732	0.0026	1049	16	1036	6	1030	14
69	4	32	0.13	0.1068	0.0035	1.9995	0.0535	0.1358	0.0025	1745	61	1115	18	821	14
70	78	187	0.42	0.0750	0.0009	1.8214	0.0176	0.1762	0.0027	1069	16	1053	6	1046	15
71	30	288	0.10	0.0759	0.0009	1.8935	0.0174	0.1810	0.0027	1093	16	1079	6	1072	15
72	51	104	0.49	0.0704	0.0011	1.4973	0.0205	0.1543	0.0025	941	15	929	8	925	14
73	126	267	0.47	0.0631	0.0008	1.0055	0.0106	0.1156	0.0017	713	16	707	5	705	10
74	75	612	0.12	0.0607	0.0007	0.8861	0.0080	0.1059	0.0016	629	17	644	4	649	9
75	170	215	0.79	0.0824	0.0009	2.4069	0.0219	0.2119	0.0032	1256	16	1245	7	1239	17
76	88	184	0.48	0.0818	0.0010	2.3653	0.0226	0.2098	0.0032	1241	15	1232	7	1228	17
77	275	182	1.51	0.0614	0.0010	0.8905	0.0123	0.1052	0.0017	654	15	647	7	645	10
78	111	182	0.61	0.2438	0.0024	21.0414	0.1637	0.6263	0.0093	3145	14	3141	8	3135	37
79	55	114	0.48	0.0733	0.0010	1.7607	0.0210	0.1742	0.0027	1023	15	1031	8	1035	15
80	27	54	0.50	0.0945	0.0014	3.3786	0.0427	0.2595	0.0042	1518	14	1499	10	1487	21
81	113	214	0.53	0.0715	0.0009	1.5779	0.0159	0.1602	0.0024	971	16	962	6	958	13
82	100	557	0.18	0.1536	0.0015	9.2039	0.0690	0.4348	0.0064	2386	15	2359	7	2327	29
83	248	210	1.18	0.0728	0.0010	1.6904	0.0192	0.1686	0.0026	1007	15	1005	7	1004	14
84	595	708	0.84	0.0741	0.0007	1.7926	0.0142	0.1756	0.0026	1044	17	1043	5	1043	14
85	232	465	0.50	0.1284	0.0013	6.6919	0.0506	0.3782	0.0055	2076	15	2072	7	2068	26
86	85	418	0.20	0.0747	0.0008	1.7925	0.0155	0.1742	0.0026	1059	16	1043	6	1035	14
87	23	260	0.09	0.0827	0.0015	2.2745	0.0238	0.1996	0.0029	1261	36	1204	7	1173	16
88	69	331	0.21	0.0615	0.0014	0.9719	0.0164	0.1146	0.0017	657	50	689	8	699	10
89	32	103	0.31	0.0744	0.0011	1.7783	0.0219	0.1734	0.0027	1053	15	1038	8	1031	15
90	113	167	0.67	0.0602	0.0010	0.8469	0.0116	0.1020	0.0016	612	15	623	6	626	9
91	76	51	1.49	0.0756	0.0013	1.8920	0.0296	0.1816	0.0030	1085	15	1078	10	1075	17
92	119	136	0.88	0.0753	0.0010	1.8606	0.0200	0.1794	0.0027	1075	15	1067	7	1064	15

93	39	167	0.24	0.2518	0.0046	20.9739	0.2067	0.6041	0.0093	3196	30	3137	10	3046	37
94	166	110	1.51	0.0919	0.0012	2.8643	0.0322	0.2262	0.0035	1465	14	1373	8	1315	19
95	77	25	3.01	0.1083	0.0018	4.6471	0.0692	0.3113	0.0054	1772	14	1758	12	1747	27
96	108	441	0.24	0.0761	0.0008	1.8708	0.0162	0.1784	0.0026	1097	16	1071	6	1058	14
97	109	269	0.41	0.0732	0.0009	1.3950	0.0134	0.1382	0.0021	1021	16	887	6	834	12
98	103	198	0.52	0.0753	0.0010	1.8047	0.0190	0.1740	0.0027	1075	15	1047	7	1034	15
99	428	501	0.85	0.0649	0.0007	1.0175	0.0093	0.1138	0.0017	771	16	713	5	695	10
100	187	117	1.60	0.0777	0.0011	2.1026	0.0243	0.1963	0.0031	1140	15	1150	8	1155	16
101	224	458	0.49	0.0722	0.0008	1.5715	0.0136	0.1580	0.0023	991	16	959	5	946	13
102	23	90	0.25	0.0735	0.0012	1.5976	0.0216	0.1576	0.0025	1029	15	969	8	944	14
103	14	29	0.48	0.0675	0.0018	1.2834	0.0311	0.1379	0.0026	854	23	838	14	833	15
104	10	16	0.64	0.0833	0.0022	2.5054	0.0611	0.2183	0.0044	1275	21	1274	18	1273	23
105	128	325	0.40	0.0760	0.0008	1.8830	0.0168	0.1797	0.0027	1096	16	1075	6	1065	15
106	94	649	0.14	0.0612	0.0007	0.9124	0.0079	0.1081	0.0016	647	17	658	4	662	9
107	131	142	0.92	0.0747	0.0010	1.8437	0.0201	0.1790	0.0027	1061	15	1061	7	1062	15
108	166	258	0.64	0.0765	0.0009	1.8504	0.0172	0.1754	0.0026	1109	16	1064	6	1042	14
109	54	53	1.02	0.0740	0.0013	1.7647	0.0281	0.1731	0.0029	1041	15	1033	10	1029	16
110	98	403	0.24	0.0708	0.0008	1.4620	0.0132	0.1499	0.0022	950	16	915	5	900	12
111	177	394	0.45	0.0721	0.0008	1.6619	0.0143	0.1672	0.0025	989	16	994	5	997	14
112	60	97	0.61	0.0750	0.0011	1.6286	0.0202	0.1576	0.0025	1068	14	981	8	943	14
113	31	103	0.30	0.0627	0.0011	0.9504	0.0150	0.1100	0.0018	697	16	678	8	673	10
114	71	111	0.64	0.0735	0.0010	1.7188	0.0204	0.1697	0.0026	1027	15	1016	8	1011	15
115	116	124	0.93	0.0748	0.0011	1.6540	0.0201	0.1604	0.0025	1064	15	991	8	959	14
116	118	396	0.30	0.0702	0.0008	1.5902	0.0139	0.1643	0.0024	935	17	966	5	981	13
117	85	110	0.77	0.2334	0.0027	19.0242	0.1917	0.5914	0.0095	3075	14	3043	10	2995	39
118	130	520	0.25	0.0896	0.0017	2.8464	0.0360	0.2303	0.0034	1418	38	1368	9	1336	18
119	87	125	0.70	0.1481	0.0016	8.4748	0.0759	0.4153	0.0063	2324	14	2283	8	2239	29
120	315	611	0.51	0.2418	0.0023	19.8962	0.1494	0.5970	0.0087	3132	14	3086	7	3018	35
Sample 10GD16 (N25°01'19.9", E113°47'55.5")															
1	99	232	0.43	0.0705	0.0009	1.4909	0.0229	0.1533	0.0021	943	14	927	9	920	12
2	105	142	0.74	0.3019	0.0037	29.039	0.4231	0.6974	0.0094	3480	10	3455	14	3411	36

3	73	240	0.30	0.0724	0.0009	1.6570	0.0252	0.1660	0.0022	996	14	992	10	990	12
4	197	162	1.21	0.0703	0.0010	1.4667	0.0232	0.1513	0.0021	936	15	917	10	908	12
5	141	168	0.84	0.0705	0.0010	1.5293	0.0240	0.1572	0.0021	944	14	942	10	941	12
6	210	507	0.41	0.0700	0.0009	1.4756	0.0219	0.1529	0.0021	927	14	920	9	917	11
7	214	194	1.10	0.0587	0.0009	0.6756	0.0119	0.0835	0.0012	554	18	524	7	517	7
8	68	72	0.94	0.0698	0.0016	1.5077	0.0347	0.1566	0.0024	923	24	933	14	938	13
9	24	150	0.16	0.1447	0.0019	8.4173	0.1293	0.4219	0.0059	2284	12	2277	14	2269	27
10	324	352	0.92	0.0580	0.0008	0.7126	0.0115	0.0890	0.0012	531	16	546	7	550	7
11	250	177	1.42	0.0720	0.0010	1.5209	0.0241	0.1532	0.0021	986	14	939	10	919	12
12	330	399	0.83	0.0755	0.0010	1.8399	0.0275	0.1767	0.0024	1082	13	1060	10	1049	13
13	42	676	0.06	0.0702	0.0009	1.4680	0.0226	0.1516	0.0021	935	14	917	9	910	11
14	388	452	0.86	0.0658	0.0009	1.1406	0.0173	0.1257	0.0017	800	14	773	8	763	10
15	170	120	1.41	0.0574	0.0011	0.6643	0.0138	0.0839	0.0012	507	23	517	8	519	7
16	235	487	0.48	0.0755	0.0010	1.8656	0.0279	0.1793	0.0024	1081	13	1069	10	1063	13
17	208	147	1.41	0.0744	0.0011	1.8193	0.0293	0.1774	0.0024	1052	15	1052	11	1053	13
18	508	433	1.17	0.0703	0.0009	1.4879	0.0226	0.1534	0.0021	937	14	925	9	920	12
19	165	208	0.79	0.1643	0.0020	10.3130	0.1526	0.4553	0.0061	2500	11	2463	14	2419	27
20	393	1012	0.39	0.0639	0.0008	1.0436	0.0156	0.1183	0.0016	740	14	726	8	721	9
21	452	1066	0.42	0.1851	0.0023	12.721	0.1869	0.4982	0.0067	2699	11	2659	14	2606	29
22	131	244	0.53	0.0770	0.0010	1.9782	0.0304	0.1863	0.0025	1121	14	1108	10	1101	14
23	180	128	1.41	0.0706	0.0011	1.4786	0.0262	0.1519	0.0021	946	17	922	11	911	12
24	37	64	0.58	0.1049	0.0015	4.1302	0.0666	0.2855	0.0040	1713	13	1660	13	1619	20
25	86	393	0.22	0.0700	0.0009	1.4471	0.0221	0.1500	0.0020	927	14	909	9	901	11
26	108	1404	0.08	0.0650	0.0008	1.1849	0.0176	0.1322	0.0018	773	14	794	8	801	10
27	68	168	0.41	0.0703	0.0010	1.5247	0.0248	0.1572	0.0022	938	15	940	10	941	12
28	69	121	0.57	0.1649	0.0021	10.698	0.1616	0.4705	0.0064	2506	11	2497	14	2486	28
29	133	144	0.92	0.0706	0.0010	1.5031	0.0249	0.1545	0.0021	944	15	932	10	926	12
30	268	416	0.64	0.0986	0.0012	3.8305	0.0573	0.2817	0.0038	1598	12	1599	12	1600	19
31	422	511	0.83	0.0598	0.0013	0.7361	0.0168	0.0893	0.0014	595	25	560	10	551	8
32	149	144	1.04	0.0599	0.0011	0.6930	0.0135	0.0840	0.0012	599	20	535	8	520	7
33	195	162	1.20	0.0950	0.0015	3.4609	0.0615	0.2642	0.0038	1528	15	1518	14	1511	19
34	389	179	2.18	0.0572	0.0010	0.6383	0.0120	0.0809	0.0011	498	20	501	7	502	7

35	105	662	0.16	0.1256	0.0016	6.5025	0.0979	0.3754	0.0051	2037	12	2046	13	2055	24
36	179	323	0.55	0.0598	0.0009	0.6792	0.0113	0.0823	0.0011	597	16	526	7	510	7
37	157	273	0.57	0.0742	0.0010	1.7420	0.0272	0.1702	0.0023	1048	14	1024	10	1013	13
38	395	992	0.40	0.0696	0.0009	1.4668	0.0222	0.1529	0.0021	915	14	917	9	917	12
39	90	682	0.13	0.0719	0.0009	1.5978	0.0244	0.1611	0.0022	984	14	969	10	963	12
40	235	308	0.76	0.0707	0.0010	1.5602	0.0246	0.1601	0.0022	948	14	955	10	957	12
41	101	105	0.96	0.0583	0.0013	0.6712	0.0152	0.0835	0.0012	542	26	521	9	517	7
42	90	255	0.35	0.1716	0.0022	11.356	0.1725	0.4800	0.0065	2573	11	2553	14	2527	28
43	57	217	0.26	0.0755	0.0011	1.8095	0.0289	0.1739	0.0024	1081	14	1049	10	1033	13
44	94	122	0.77	0.0700	0.0011	1.4743	0.0260	0.1527	0.0021	929	17	920	11	916	12
45	80	403	0.20	0.0719	0.0010	1.6538	0.0257	0.1668	0.0023	983	14	991	10	995	13
46	173	105	1.65	0.0724	0.0012	1.5612	0.0277	0.1564	0.0022	997	17	955	11	937	12
47	301	680	0.44	0.0584	0.0008	0.7479	0.0119	0.0929	0.0013	545	16	567	7	572	7
48	81	193	0.42	0.0733	0.0011	1.6244	0.0267	0.1607	0.0022	1022	15	980	10	961	12
49	106	79	1.34	0.0584	0.0015	0.6894	0.0183	0.0857	0.0013	543	33	532	11	530	7
50	257	940	0.27	0.0688	0.0009	1.4193	0.0220	0.1495	0.0020	894	14	897	9	898	11
51	156	115	1.36	0.0669	0.0011	1.2655	0.0229	0.1371	0.0019	836	17	830	10	828	11
52	74	68	1.09	0.0799	0.0013	2.1991	0.0396	0.1997	0.0028	1194	16	1181	13	1173	15
53	673	811	0.83	0.0608	0.0009	0.7609	0.0130	0.0908	0.0013	632	17	575	8	560	7
54	29	107	0.27	0.0762	0.0012	1.9153	0.0323	0.1822	0.0026	1101	15	1086	11	1079	14
55	83	461	0.18	0.0594	0.0009	0.7875	0.0129	0.0962	0.0013	581	16	590	7	592	8
56	206	386	0.53	0.0767	0.0011	2.0178	0.0322	0.1907	0.0026	1114	14	1122	11	1125	14
57	78	181	0.43	0.0751	0.0011	1.8606	0.0310	0.1797	0.0025	1070	15	1067	11	1065	14
58	178	123	1.44	0.0580	0.0011	0.6925	0.0140	0.0865	0.0012	531	21	534	8	535	7
59	97	185	0.52	0.0652	0.0010	1.1395	0.0199	0.1268	0.0018	780	17	772	9	769	10
60	128	215	0.60	0.0672	0.0010	1.3001	0.0220	0.1403	0.0020	843	16	846	10	847	11
61	101	393	0.26	0.0718	0.0010	1.6132	0.0262	0.1629	0.0023	981	15	975	10	973	12
62	36	156	0.23	0.1198	0.0017	5.7988	0.0931	0.3509	0.0049	1954	13	1946	14	1939	23
63	265	255	1.04	0.0700	0.0010	1.5285	0.0253	0.1583	0.0022	928	15	942	10	948	12
64	46	84	0.54	0.1232	0.0019	6.3012	0.1089	0.3708	0.0054	2004	14	2019	15	2033	25
65	236	350	0.67	0.0702	0.0010	1.4655	0.0242	0.1515	0.0021	933	15	916	10	909	12
66	666	479	1.39	0.0655	0.0010	1.1604	0.0191	0.1284	0.0018	791	16	782	9	779	10

67	166	112	1.49	0.0574	0.0013	0.6387	0.0148	0.0807	0.0012	508	27	501	9	500	7
68	119	1017	0.12	0.0955	0.0013	3.5617	0.0570	0.2705	0.0037	1537	13	1541	13	1543	19
69	16	43	0.37	0.0812	0.0016	2.3983	0.0491	0.2143	0.0032	1225	19	1242	15	1252	17
70	78	39	1.97	0.0805	0.0018	2.2502	0.0526	0.2028	0.0032	1208	23	1197	16	1190	17
71	189	136	1.39	0.0717	0.0012	1.5857	0.0283	0.1604	0.0023	977	17	965	11	959	13
72	78	192	0.40	0.0702	0.0011	1.5135	0.0259	0.1562	0.0022	935	16	936	10	936	12
73	142	116	1.22	0.0577	0.0012	0.6679	0.0141	0.0839	0.0012	519	23	519	9	519	7
74	195	241	0.81	0.0685	0.0011	1.4029	0.0241	0.1486	0.0021	883	16	890	10	893	12
75	102	214	0.47	0.0630	0.0010	1.0022	0.0178	0.1153	0.0016	710	17	705	9	703	9
76	43	101	0.42	0.0698	0.0012	1.5734	0.0293	0.1634	0.0024	923	18	960	12	976	13
77	64	338	0.19	0.0885	0.0013	3.0002	0.0499	0.2459	0.0034	1392	14	1408	13	1417	18
78	394	337	1.17	0.0723	0.0011	1.6646	0.0282	0.1670	0.0023	994	16	995	11	996	13
79	327	137	2.39	0.0574	0.0011	0.6460	0.0134	0.0816	0.0012	507	22	506	8	506	7
80	188	145	1.29	0.0750	0.0012	1.8964	0.0332	0.1833	0.0026	1069	16	1080	12	1085	14
81	331	319	1.04	0.0688	0.0011	1.4416	0.0248	0.1520	0.0021	892	16	906	10	912	12
82	189	517	0.37	0.0800	0.0012	2.1484	0.0362	0.1949	0.0027	1196	15	1165	12	1148	15
83	107	671	0.16	0.0930	0.0014	3.1971	0.0536	0.2492	0.0035	1488	14	1456	13	1434	18
84	445	390	1.14	0.0640	0.0010	1.1452	0.0198	0.1297	0.0018	742	17	775	9	786	10
85	172	707	0.24	0.0724	0.0011	1.6928	0.0286	0.1695	0.0024	998	16	1006	11	1009	13
86	42	117	0.36	0.0788	0.0013	2.1865	0.0395	0.2013	0.0029	1166	16	1177	13	1182	15
87	49	117	0.41	0.0612	0.0011	0.9229	0.0183	0.1094	0.0016	645	20	664	10	669	9
88	460	969	0.47	0.1518	0.0023	8.8799	0.1505	0.4241	0.0059	2367	13	2326	15	2279	27
89	114	382	0.30	0.0714	0.0011	1.5519	0.0269	0.1575	0.0022	970	16	951	11	943	12
90	296	148	2.00	0.0576	0.0011	0.6681	0.0135	0.0842	0.0012	513	21	520	8	521	7
91	132	178	0.74	0.1556	0.0024	9.4943	0.1632	0.4426	0.0062	2408	13	2387	16	2362	28
92	23	60	0.39	0.1902	0.0030	13.950	0.2433	0.5318	0.0076	2744	13	2746	17	2749	32
93	845	629	1.34	0.0630	0.0011	0.8893	0.0172	0.1023	0.0015	710	19	646	9	628	9
94	223	328	0.68	0.0710	0.0011	1.5473	0.0273	0.1581	0.0022	957	17	949	11	946	12
95	108	238	0.45	0.0719	0.0012	1.6066	0.0289	0.1621	0.0023	983	17	973	11	968	13
96	293	551	0.53	0.1128	0.0018	4.9233	0.0856	0.3165	0.0045	1845	14	1806	15	1773	22
97	160	298	0.54	0.0664	0.0011	1.2491	0.0226	0.1365	0.0019	818	17	823	10	825	11
98	822	1104	0.74	0.0576	0.0009	0.6259	0.0111	0.0788	0.0011	513	18	494	7	489	7

99	149	227	0.66	0.0709	0.0012	1.5301	0.0279	0.1565	0.0022	954	17	943	11	938	12
100	334	240	1.39	0.0720	0.0012	1.6348	0.0298	0.1646	0.0024	987	17	984	11	982	13
Sample 10GD17 (N25°01'27.6", E113°48'12.1")															
1	98	255	0.39	0.0760	0.0010	1.9648	0.0297	0.1875	0.0026	1095	14	1104	10	1108	14
2	58	317	0.18	0.0785	0.0009	2.1298	0.0313	0.1967	0.0027	1160	13	1159	10	1158	14
3	258	182	1.42	0.0590	0.0009	0.6587	0.0110	0.0810	0.0011	566	16	514	7	502	7
4	110	74	1.49	0.0572	0.0016	0.6324	0.0177	0.0802	0.0012	498	36	498	11	497	7
5	116	354	0.33	0.0715	0.0009	1.5513	0.0230	0.1574	0.0022	971	14	951	9	942	12
6	269	195	1.38	0.0579	0.0010	0.6649	0.0121	0.0832	0.0012	527	19	518	7	515	7
7	158	135	1.17	0.0580	0.0012	0.6773	0.0148	0.0847	0.0012	528	24	525	9	524	7
8	109	100	1.09	0.0581	0.0011	0.6931	0.0143	0.0865	0.0013	534	22	535	9	535	7
9	120	213	0.57	0.0723	0.0010	1.6199	0.0253	0.1626	0.0023	993	14	978	10	971	12
10	570	234	2.44	0.0698	0.0009	1.4417	0.0224	0.1498	0.0021	922	14	906	9	900	12
11	31	30	1.03	0.0714	0.0024	1.6076	0.0550	0.1633	0.0026	969	44	973	21	975	14
12	152	356	0.43	0.0799	0.0010	2.2052	0.0327	0.2001	0.0027	1195	13	1183	10	1176	15
13	131	105	1.25	0.0581	0.0013	0.6691	0.0160	0.0836	0.0012	532	28	520	10	517	7
14	297	402	0.74	0.0579	0.0008	0.6881	0.0110	0.0862	0.0012	524	16	532	7	533	7
15	274	346	0.79	0.0715	0.0009	1.5843	0.0240	0.1606	0.0022	972	14	964	9	960	12
16	274	192	1.43	0.1595	0.0019	10.115	0.1483	0.4598	0.0063	2451	11	2445	14	2439	28
17	103	107	0.96	0.0787	0.0012	2.0801	0.0350	0.1917	0.0027	1164	15	1142	12	1131	15
18	239	307	0.78	0.0656	0.0009	1.1989	0.0186	0.1326	0.0018	792	15	800	9	803	10
19	173	109	1.58	0.0584	0.0013	0.7091	0.0170	0.0881	0.0013	543	28	544	10	544	8
20	210	162	1.29	0.0850	0.0011	2.5727	0.0396	0.2195	0.0030	1316	13	1293	11	1279	16
21	319	557	0.57	0.0692	0.0009	1.4458	0.0216	0.1515	0.0021	905	14	908	9	909	12
22	95	181	0.53	0.0869	0.0012	2.8516	0.0452	0.2380	0.0033	1358	14	1369	12	1376	17
23	32	57	0.56	0.0653	0.0016	1.0865	0.0273	0.1207	0.0018	784	29	747	13	734	10
24	265	295	0.90	0.1109	0.0015	4.7787	0.0772	0.3124	0.0045	1814	13	1781	14	1753	22
25	197	251	0.78	0.0576	0.0009	0.6811	0.0119	0.0858	0.0012	513	17	527	7	531	7
26	252	364	0.69	0.0575	0.0008	0.6849	0.0110	0.0864	0.0012	511	16	530	7	534	7
27	10	629	0.02	0.0589	0.0008	0.7776	0.0118	0.0957	0.0013	564	15	584	7	589	8
28	181	189	0.96	0.0777	0.0010	2.1572	0.0336	0.2012	0.0028	1140	14	1167	11	1182	15

29	194	374	0.52	0.0697	0.0009	1.4739	0.0224	0.1534	0.0021	918	14	920	9	920	12
30	42	23	1.82	0.0719	0.0021	1.6133	0.0469	0.1627	0.0026	983	34	975	18	972	14
31	171	369	0.46	0.0731	0.0009	1.6966	0.0257	0.1683	0.0023	1017	14	1007	10	1003	13
32	21	35	0.59	0.0755	0.0016	1.8851	0.0415	0.1810	0.0027	1083	22	1076	15	1072	15
33	151	370	0.41	0.0694	0.0009	1.4372	0.0221	0.1501	0.0021	911	14	905	9	902	12
34	84	533	0.16	0.0668	0.0008	1.2602	0.0191	0.1369	0.0019	831	14	828	9	827	11
35	129	144	0.90	0.0741	0.0011	1.7635	0.0290	0.1727	0.0024	1043	15	1032	11	1027	13
36	48	290	0.17	0.2707	0.0033	23.531	0.3483	0.6304	0.0087	3310	10	3249	14	3151	34
37	274	407	0.67	0.1590	0.0019	9.9566	0.1479	0.4541	0.0062	2445	11	2431	14	2413	28
38	508	468	1.09	0.0706	0.0009	1.5694	0.0240	0.1611	0.0022	946	14	958	9	963	12
39	109	95	1.14	0.0736	0.0011	1.8775	0.0320	0.1851	0.0026	1029	16	1073	11	1095	14
40	509	511	1.00	0.0747	0.0010	1.7607	0.0268	0.1710	0.0024	1060	14	1031	10	1017	13
41	101	56	1.80	0.0690	0.0014	1.3943	0.0296	0.1465	0.0021	899	22	887	13	882	12
42	44	55	0.80	0.0793	0.0015	2.1190	0.0419	0.1937	0.0028	1180	19	1155	14	1142	15
43	494	491	1.00	0.0660	0.0009	1.1818	0.0185	0.1299	0.0018	806	15	792	9	787	10
44	73	108	0.68	0.0710	0.0011	1.6006	0.0282	0.1636	0.0023	956	16	970	11	977	13
45	126	598	0.21	0.0584	0.0008	0.7098	0.0113	0.0882	0.0012	543	16	545	7	545	7
46	159	230	0.69	0.1603	0.0020	10.172	0.1548	0.4600	0.0064	2459	11	2451	14	2440	28
47	87	408	0.21	0.0681	0.0009	1.3747	0.0215	0.1465	0.0020	870	14	878	9	881	11
48	120	216	0.56	0.0735	0.0010	1.7412	0.0281	0.1718	0.0024	1027	15	1024	10	1022	13
49	139	217	0.64	0.0585	0.0011	0.7279	0.0144	0.0902	0.0013	549	21	555	8	557	8
50	83	143	0.58	0.0743	0.0011	1.7582	0.0304	0.1716	0.0024	1049	16	1030	11	1021	13
51	141	124	1.14	0.0714	0.0011	1.5295	0.0272	0.1553	0.0022	969	17	942	11	931	12
52	355	681	0.52	0.0581	0.0008	0.6927	0.0111	0.0865	0.0012	533	16	534	7	535	7
53	52	308	0.17	0.0904	0.0012	3.1011	0.0484	0.2489	0.0035	1433	13	1433	12	1433	18
54	52	88	0.59	0.2031	0.0027	15.443	0.2401	0.5515	0.0077	2851	11	2843	15	2831	32
55	29	423	0.07	0.0864	0.0011	2.7671	0.0432	0.2323	0.0032	1346	13	1347	12	1347	17
56	144	290	0.50	0.1914	0.0025	13.866	0.2132	0.5254	0.0073	2754	11	2741	15	2722	31
57	75	474	0.16	0.0743	0.0010	1.7931	0.0282	0.1751	0.0024	1049	14	1043	10	1040	13
58	176	442	0.40	0.0720	0.0010	1.5686	0.0249	0.1581	0.0022	985	14	958	10	946	12
59	213	132	1.61	0.1642	0.0022	10.757	0.1679	0.4752	0.0066	2499	12	2502	14	2506	29
60	223	125	1.79	0.0581	0.0012	0.6814	0.0149	0.0851	0.0012	532	24	528	9	526	7

61	126	395	0.32	0.0732	0.0010	1.7115	0.0274	0.1697	0.0024	1018	14	1013	10	1010	13
62	114	212	0.54	0.0616	0.0010	0.9556	0.0177	0.1125	0.0016	660	18	681	9	687	9
63	300	234	1.28	0.0590	0.0010	0.6955	0.0125	0.0855	0.0012	566	18	536	8	529	7
64	508	748	0.68	0.1640	0.0021	10.709	0.1667	0.4735	0.0066	2497	12	2498	14	2499	29
65	77	70	1.09	0.0715	0.0013	1.6190	0.0313	0.1643	0.0024	970	19	978	12	981	13
66	154	440	0.35	0.0695	0.0010	1.4512	0.0234	0.1515	0.0021	913	15	910	10	909	12
67	171	117	1.47	0.0732	0.0011	1.7590	0.0304	0.1742	0.0025	1020	16	1030	11	1035	14
68	173	236	0.73	0.0705	0.0010	1.5450	0.0256	0.1590	0.0022	942	15	949	10	951	12
69	112	186	0.60	0.1631	0.0022	10.5577	0.1677	0.4693	0.0066	2488	12	2485	15	2481	29
70	273	177	1.54	0.0600	0.0011	0.8044	0.0155	0.0972	0.0014	603	20	599	9	598	8
71	59	136	0.43	0.0729	0.0012	1.6382	0.0296	0.1631	0.0023	1010	17	985	11	974	13
72	667	490	1.36	0.0573	0.0009	0.6561	0.0113	0.0830	0.0012	503	17	512	7	514	7
73	172	350	0.49	0.0693	0.0010	1.5087	0.0250	0.1580	0.0022	906	15	934	10	945	12
74	137	192	0.71	0.1635	0.0023	10.3250	0.1665	0.4581	0.0064	2492	12	2464	15	2431	28
75	232	171	1.35	0.0714	0.0011	1.6239	0.0280	0.1649	0.0024	970	16	979	11	984	13
76	253	299	0.85	0.0774	0.0011	2.0008	0.0333	0.1875	0.0026	1131	15	1116	11	1108	14
77	24	62	0.39	0.0684	0.0015	1.4943	0.0345	0.1584	0.0024	881	25	928	14	948	13
78	80	52	1.52	0.1669	0.0025	10.764	0.1818	0.4677	0.0068	2527	13	2503	16	2473	30
79	221	274	0.81	0.0816	0.0012	2.3660	0.0395	0.2103	0.0030	1235	15	1232	12	1230	16
80	217	284	0.76	0.0764	0.0011	1.9036	0.0320	0.1807	0.0026	1105	15	1082	11	1071	14
81	204	182	1.12	0.0786	0.0012	2.1538	0.0368	0.1987	0.0028	1162	15	1166	12	1168	15
82	114	64	1.79	0.0577	0.0017	0.6530	0.0197	0.0821	0.0013	517	40	510	12	509	8
83	154	496	0.31	0.1168	0.0017	5.3547	0.0879	0.3324	0.0047	1908	13	1878	14	1850	23
84	17	335	0.05	0.0606	0.0009	0.8523	0.0149	0.1019	0.0015	626	17	626	8	626	8
85	213	321	0.67	0.0764	0.0011	1.9889	0.0334	0.1888	0.0027	1106	15	1112	11	1115	14
86	244	270	0.90	0.0721	0.0011	1.5849	0.0273	0.1594	0.0023	988	16	964	11	954	13
87	70	254	0.27	0.0780	0.0012	1.9788	0.0341	0.1839	0.0026	1147	15	1108	12	1088	14
88	176	502	0.35	0.0759	0.0011	2.0468	0.0344	0.1955	0.0028	1092	15	1131	11	1151	15
89	164	427	0.38	0.0728	0.0011	1.6921	0.0287	0.1686	0.0024	1008	16	1006	11	1004	13
90	106	299	0.35	0.0651	0.0010	1.1262	0.0199	0.1255	0.0018	777	17	766	10	762	10
91	127	116	1.09	0.0581	0.0012	0.7022	0.0152	0.0877	0.0013	533	23	540	9	542	8
92	403	640	0.63	0.0793	0.0012	2.1835	0.0369	0.1996	0.0028	1181	15	1176	12	1173	15

93	40	61	0.65	0.0593	0.0030	0.8290	0.0407	0.1014	0.0020	576	72	613	23	623	12
94	26	26	1.02	0.0621	0.0029	0.9611	0.0444	0.1123	0.0019	676	69	684	23	686	11
95	94	152	0.62	0.1740	0.0026	11.740	0.1998	0.4893	0.0070	2596	13	2584	16	2567	30
96	260	303	0.86	0.0578	0.0010	0.6948	0.0129	0.0872	0.0013	521	19	536	8	539	7
97	358	520	0.69	0.0778	0.0012	1.9965	0.0345	0.1860	0.0026	1143	16	1114	12	1100	14
98	231	591	0.39	0.0718	0.0011	1.6810	0.0290	0.1697	0.0024	981	16	1001	11	1010	13
99	393	292	1.34	0.0732	0.0012	1.6662	0.0296	0.1652	0.0024	1018	16	996	11	985	13
100	132	146	0.91	0.0722	0.0012	1.7572	0.0326	0.1765	0.0026	991	17	1030	12	1048	14
Sample 10GD19 (N25°01'45.6", E113°48'45.2")															
1	1233	1989	0.62	0.0796	0.0010	1.9760	0.0300	0.1801	0.0024	1186	13	1107	10	1067	13
2	254	250	1.02	0.0726	0.0030	1.7168	0.0673	0.1716	0.0026	1002	87	1015	25	1021	14
3	191	213	0.90	0.0928	0.0011	3.2379	0.0476	0.2529	0.0034	1485	12	1466	11	1453	17
4	25	41	0.61	0.0714	0.0018	1.4273	0.0378	0.1450	0.0021	969	31	900	16	873	12
5	344	766	0.45	0.0702	0.0009	1.5454	0.0224	0.1596	0.0021	935	13	949	9	954	12
6	207	254	0.81	0.1131	0.0014	5.1456	0.0755	0.3299	0.0044	1850	12	1844	12	1838	21
7	82	147	0.56	0.2278	0.0027	18.434	0.2660	0.5867	0.0079	3037	10	3013	14	2976	32
8	524	643	0.82	0.0744	0.0010	1.7883	0.0269	0.1743	0.0024	1052	14	1041	10	1036	13
9	332	238	1.39	0.1035	0.0013	4.1079	0.0612	0.2879	0.0039	1687	12	1656	12	1631	19
10	260	395	0.66	0.0725	0.0009	1.5984	0.0238	0.1598	0.0021	1000	13	970	9	956	12
11	34	44	0.78	0.1490	0.0022	8.5234	0.1411	0.4148	0.0060	2334	13	2288	15	2237	27
12	359	511	0.70	0.1699	0.0020	10.793	0.1567	0.4605	0.0062	2557	11	2505	13	2442	27
13	279	498	0.56	0.0724	0.0009	1.4820	0.0220	0.1484	0.0020	997	13	923	9	892	11
14	171	417	0.41	0.0768	0.0010	1.9037	0.0281	0.1797	0.0024	1117	13	1082	10	1065	13
15	99	102	0.97	0.0783	0.0012	2.0285	0.0344	0.1878	0.0026	1155	15	1125	12	1109	14
16	140	517	0.27	0.0729	0.0009	1.5572	0.0231	0.1550	0.0021	1010	13	953	9	929	12
17	264	291	0.91	0.1640	0.0020	10.697	0.1555	0.4731	0.0064	2497	11	2497	13	2497	28
18	119	516	0.23	0.0725	0.0009	1.6380	0.0243	0.1639	0.0022	999	13	985	9	979	12
19	228	311	0.73	0.1237	0.0015	6.2928	0.0924	0.3688	0.0050	2011	12	2017	13	2024	23
20	183	235	0.78	0.1511	0.0019	9.2116	0.1362	0.4421	0.0060	2358	11	2359	14	2360	27
21	309	308	1.00	0.0719	0.0009	1.5791	0.0240	0.1593	0.0022	982	14	962	9	953	12
22	27	237	0.11	0.0947	0.0012	3.4125	0.0516	0.2613	0.0036	1522	13	1507	12	1496	18

23	171	195	0.87	0.1284	0.0017	6.5662	0.1024	0.3707	0.0052	2077	12	2055	14	2033	25
24	173	577	0.30	0.0635	0.0008	1.0386	0.0158	0.1187	0.0016	724	14	723	8	723	9
25	188	340	0.55	0.0723	0.0010	1.3599	0.0209	0.1364	0.0019	994	14	872	9	824	10
26	45	117	0.38	0.0749	0.0011	1.7456	0.0288	0.1689	0.0023	1067	15	1026	11	1006	13
27	26	49	0.54	0.0772	0.0027	2.0106	0.0631	0.1889	0.0028	1127	71	1119	21	1115	15
28	157	303	0.52	0.0700	0.0009	1.4031	0.0217	0.1454	0.0020	928	14	890	9	875	11
29	40	89	0.44	0.0747	0.0012	1.7292	0.0308	0.1679	0.0024	1059	16	1019	11	1001	13
30	166	401	0.41	0.1735	0.0021	11.704	0.1719	0.4892	0.0066	2592	11	2581	14	2567	29
31	92	370	0.25	0.0694	0.0009	1.4196	0.0218	0.1484	0.0020	909	14	897	9	892	11
32	4	21	0.20	0.0642	0.0031	0.9954	0.0485	0.1125	0.0019	747	74	701	25	687	11
33	98	566	0.17	0.1906	0.0023	13.970	0.2059	0.5314	0.0072	2748	11	2748	14	2747	30
34	52	138	0.37	0.0711	0.0011	1.5206	0.0254	0.1552	0.0021	959	15	939	10	930	12
35	40	67	0.60	0.2931	0.0037	28.156	0.4219	0.6967	0.0096	3434	10	3425	15	3408	36
36	332	659	0.50	0.0807	0.0010	2.2672	0.0339	0.2037	0.0028	1214	13	1202	11	1195	15
37	116	176	0.66	0.0708	0.0010	1.5270	0.0249	0.1565	0.0022	950	15	941	10	937	12
38	114	87	1.31	0.1095	0.0015	4.7614	0.0745	0.3153	0.0044	1791	13	1778	13	1766	21
39	350	1029	0.34	0.0627	0.0009	0.9171	0.0145	0.1061	0.0015	698	15	661	8	650	9
40	142	275	0.52	0.0707	0.0010	1.5279	0.0239	0.1567	0.0022	949	14	942	10	938	12
41	274	381	0.72	0.0724	0.0010	1.6669	0.0257	0.1669	0.0023	997	14	996	10	995	13
42	362	762	0.48	0.0595	0.0008	0.7950	0.0124	0.0969	0.0013	585	15	594	7	596	8
43	123	199	0.62	0.0588	0.0009	0.7027	0.0124	0.0866	0.0012	561	18	540	7	535	7
44	190	282	0.67	0.1021	0.0013	3.9714	0.0607	0.2821	0.0039	1662	13	1628	12	1602	19
45	226	115	1.96	0.0579	0.0011	0.6893	0.0142	0.0863	0.0012	527	22	532	9	533	7
46	157	310	0.51	0.0602	0.0009	0.8062	0.0131	0.0971	0.0013	610	16	600	7	598	8
47	407	253	1.61	0.0662	0.0009	1.2288	0.0198	0.1347	0.0019	811	15	814	9	814	11
48	124	268	0.46	0.1578	0.0020	10.146	0.1541	0.4661	0.0064	2432	11	2448	14	2467	28
49	323	1047	0.31	0.0647	0.0008	1.1473	0.0176	0.1286	0.0018	765	14	776	8	780	10
50	22	22	1.01	0.0712	0.0025	1.5756	0.0556	0.1606	0.0025	962	46	961	22	960	14
51	117	304	0.38	0.0721	0.0010	1.6308	0.0257	0.1641	0.0023	988	14	982	10	979	13
52	249	162	1.54	0.0582	0.0010	0.6790	0.0129	0.0846	0.0012	537	20	526	8	523	7
53	159	293	0.54	0.0704	0.0010	1.5078	0.0239	0.1553	0.0021	939	15	934	10	931	12
54	126	335	0.38	0.0717	0.0010	1.6474	0.0260	0.1667	0.0023	976	14	989	10	994	13

55	176	463	0.38	0.1439	0.0019	8.2053	0.1260	0.4135	0.0057	2274	12	2254	14	2231	26
56	132	535	0.25	0.0732	0.0010	1.7945	0.0281	0.1779	0.0025	1018	14	1043	10	1055	13
57	231	287	0.81	0.0826	0.0011	2.3200	0.0367	0.2036	0.0028	1261	14	1218	11	1194	15
58	17	31	0.55	0.0971	0.0028	3.0510	0.0892	0.2279	0.0046	1568	27	1420	22	1324	24
59	35	69	0.51	0.0763	0.0013	1.9477	0.0362	0.1850	0.0026	1104	17	1098	12	1094	14
60	74	319	0.23	0.0615	0.0009	0.8715	0.0145	0.1027	0.0014	658	16	636	8	630	8
61	92	748	0.12	0.1586	0.0021	10.202	0.1597	0.4665	0.0065	2440	12	2453	14	2468	28
62	156	191	0.82	0.0986	0.0014	3.8169	0.0610	0.2806	0.0039	1598	13	1596	13	1595	20
63	162	354	0.46	0.3117	0.0041	30.674	0.4791	0.7136	0.0099	3529	11	3509	15	3472	37
64	203	301	0.67	0.0718	0.0010	1.6520	0.0269	0.1668	0.0023	980	15	990	10	995	13
65	44	66	0.66	0.2376	0.0033	20.244	0.3261	0.6179	0.0088	3104	11	3103	16	3102	35
66	344	358	0.96	0.0738	0.0010	1.7524	0.0284	0.1723	0.0024	1035	15	1028	10	1025	13
67	60	53	1.14	0.1598	0.0023	10.201	0.1675	0.4629	0.0066	2453	12	2453	15	2452	29
68	52	585	0.09	0.0724	0.0010	1.6391	0.0263	0.1642	0.0023	996	15	985	10	980	13
69	374	326	1.15	0.0598	0.0010	0.7029	0.0125	0.0852	0.0012	598	18	541	7	527	7
70	126	109	1.15	0.0695	0.0011	1.4648	0.0266	0.1528	0.0022	915	17	916	11	916	12
71	758	1290	0.59	0.0811	0.0012	2.3774	0.0403	0.2126	0.0030	1223	15	1236	12	1243	16
72	278	956	0.29	0.0583	0.0008	0.7870	0.0129	0.0979	0.0014	540	16	589	7	602	8
73	154	355	0.43	0.1011	0.0014	3.9010	0.0631	0.2798	0.0039	1645	13	1614	13	1590	20
74	44	102	0.43	0.0698	0.0012	1.5632	0.0293	0.1624	0.0023	923	18	956	12	970	13
75	149	696	0.21	0.0718	0.0010	1.6185	0.0263	0.1634	0.0023	981	15	977	10	976	13
76	186	285	0.65	0.0678	0.0010	1.2565	0.0213	0.1343	0.0019	863	16	826	10	813	11
77	108	179	0.60	0.0702	0.0011	1.7207	0.0297	0.1777	0.0025	935	16	1016	11	1055	14
78	1188	1544	0.77	0.0600	0.0009	0.7217	0.0119	0.0873	0.0012	602	16	552	7	539	7
79	137	136	1.00	0.1642	0.0024	10.477	0.1725	0.4627	0.0065	2500	12	2478	15	2451	29
80	124	379	0.33	0.0723	0.0011	1.5187	0.0254	0.1523	0.0022	994	15	938	10	914	12
81	228	268	0.85	0.1000	0.0015	3.9464	0.0656	0.2861	0.0040	1624	14	1623	13	1622	20
82	139	219	0.63	0.0697	0.0011	1.5475	0.0269	0.1611	0.0023	918	16	950	11	963	13
83	411	782	0.52	0.0796	0.0011	2.2436	0.0372	0.2043	0.0029	1188	15	1195	12	1198	15
84	163	1166	0.14	0.1757	0.0025	11.947	0.1968	0.4932	0.0069	2612	12	2600	15	2585	30
85	46	483	0.10	0.0702	0.0010	1.5724	0.0265	0.1624	0.0023	935	16	959	10	970	13
86	38	1031	0.04	0.0775	0.0011	2.1606	0.0361	0.2023	0.0029	1133	15	1168	12	1188	15

87	83	1373	0.06	0.0704	0.0010	1.6224	0.0272	0.1673	0.0024	939	15	979	11	997	13
88	13	34	0.38	0.0700	0.0021	1.5299	0.0454	0.1585	0.0025	929	36	942	18	948	14
89	1603	1239	1.29	0.0689	0.0011	1.4848	0.0267	0.1562	0.0023	897	17	924	11	936	13
90	69	447	0.15	0.0711	0.0011	1.6068	0.0275	0.1640	0.0023	959	16	973	11	979	13
91	140	750	0.19	0.0580	0.0009	0.6983	0.0122	0.0873	0.0013	529	17	538	7	540	7
92	118	182	0.65	0.0977	0.0015	3.4963	0.0606	0.2597	0.0037	1580	15	1526	14	1488	19
93	169	407	0.41	0.0711	0.0011	1.5902	0.0276	0.1622	0.0023	961	16	966	11	969	13
94	394	896	0.44	0.0568	0.0009	0.7280	0.0127	0.0929	0.0013	485	17	555	7	573	8
95	96	81	1.18	0.2328	0.0035	19.387	0.3343	0.6039	0.0087	3072	12	3061	17	3046	35
96	38	453	0.08	0.0799	0.0012	2.1562	0.0379	0.1957	0.0028	1195	16	1167	12	1152	15
97	150	533	0.28	0.0711	0.0011	1.6451	0.0288	0.1678	0.0024	961	16	988	11	1000	13
98	84	130	0.64	0.0898	0.0015	3.0828	0.0558	0.2490	0.0036	1421	16	1428	14	1433	19
99	201	79	2.56	0.0651	0.0016	1.1264	0.0281	0.1254	0.0019	779	28	766	13	762	11
100	205	187	1.10	0.0766	0.0013	1.9923	0.0365	0.1887	0.0028	1111	17	1113	12	1114	15

Appendix B2 SHRIMP detrital zircon U–Pb data for Cambrian clastic samples from southwestern Guangdong

Spot#	Th (ppm)	U (ppm)	Th/U	f_{206}(%)	Corrected Ratios						Corrected Ages (Ma)			
					$^{207}Pb/^{206}Pb$	1σ	$^{207}Pb/^{235}U$	1σ	$^{206}Pb/^{238}U$	1σ	$^{207}Pb/^{206}Pb$	1σ	$^{206}Pb/^{238}U$	1σ
Sample 10GD48 (N22°04'28.2", E111°26'44.9")														
s01	128	773	0.17	-0.06	0.0783	0.0005	2.0514	0.0222	0.1901	0.0016	1154	13	1122	9
s02	659	941	0.70	0.10	0.0708	0.0008	1.6865	0.0262	0.1728	0.0019	951	22	1028	11
s03	169	623	0.27	-0.04	0.1074	0.0009	4.8190	0.0616	0.3255	0.0032	1755	15	1817	16
s04	585	937	0.62	0.09	0.0745	0.0007	1.9237	0.0256	0.1872	0.0017	1056	20	1106	9
s05	95	88	1.07	0.19	0.0766	0.0019	2.2492	0.0656	0.2131	0.0033	1110	49	1245	18
s06	184	247	0.75	0.06	0.1813	0.0012	13.5295	0.1885	0.5414	0.0066	2664	11	2789	27
s07	26	555	0.05	0.11	0.0739	0.0023	1.5334	0.0488	0.1504	0.0014	1040	62	903	8
s08	173	521	0.33	0.00	0.0735	0.0008	1.9783	0.0299	0.1952	0.0020	1028	23	1149	11
s09	56	42	1.34	0.00	0.0800	0.0022	1.8507	0.0634	0.1678	0.0033	1197	55	1000	18
s10	377	2085	0.18	0.26	0.0725	0.0006	1.2849	0.0148	0.1285	0.0010	1001	17	779	6
s11	111	141	0.79	0.00	0.0763	0.0011	1.9441	0.0370	0.1848	0.0023	1102	29	1093	12
s12	25	105	0.24	0.45	0.0701	0.0018	1.6173	0.0480	0.1673	0.0023	932	54	997	13
s13	94	136	0.69	-0.04	0.0815	0.0011	2.2885	0.0422	0.2037	0.0025	1233	27	1195	13
s14	36	739	0.05	0.19	0.0567	0.0010	0.4225	0.0083	0.0541	0.0005	479	39	339	3
s15	98	295	0.33	0.01	0.1598	0.0008	9.6113	0.1086	0.4363	0.0044	2453	8	2334	20
s16	176	330	0.53	0.24	0.0787	0.0010	2.0551	0.0326	0.1894	0.0019	1165	24	1118	10
s17	168	228	0.74	0.03	0.0815	0.0010	2.2434	0.0362	0.1997	0.0022	1233	23	1174	12
s18	115	227	0.51	0.22	0.0702	0.0012	1.4822	0.0292	0.1531	0.0017	935	34	918	9
s19	3	986	0.00	0.12	0.0512	0.0009	0.2722	0.0054	0.0386	0.0004	248	40	244	2
s20	79	215	0.37	0.14	0.0701	0.0011	1.5461	0.0293	0.1599	0.0018	932	32	956	10
s21	108	139	0.78	-0.08	0.0981	0.0012	3.7060	0.0654	0.2739	0.0035	1589	23	1561	18
s22	292	625	0.47	0.00	0.0841	0.0005	2.5243	0.0318	0.2177	0.0024	1294	12	1270	13
s23	3	851	0.00	0.00	0.0535	0.0010	0.2743	0.0064	0.0372	0.0005	349	42	236	3
s24	202	350	0.58	0.04	0.0742	0.0008	1.7369	0.0246	0.1697	0.0016	1047	21	1011	9

s25	58	294	0.20	0.21	0.0598	0.0012	0.8630	0.0191	0.1046	0.0011	597	43	642	6
s26	178	596	0.30	-0.05	0.0760	0.0007	1.7513	0.0219	0.1671	0.0015	1096	18	996	8
s27	153	309	0.49	0.07	0.0770	0.0009	1.8933	0.0288	0.1784	0.0018	1121	23	1058	10
s28	49	565	0.09	0.00	0.0695	0.0011	1.3281	0.0450	0.1386	0.0042	913	32	837	24
s29	87	605	0.14	0.03	0.0725	0.0017	1.6393	0.0530	0.1640	0.0036	1000	48	979	20
s30	110	891	0.12	0.13	0.0632	0.0009	0.5616	0.0104	0.0645	0.0008	714	29	403	5
s31	278	605	0.46	0.00	0.1617	0.0005	10.1906	0.0953	0.4571	0.0040	2473	6	2427	18
s32	54	432	0.12	-0.02	0.0761	0.0007	1.8421	0.0237	0.1757	0.0016	1097	18	1043	9
s33	112	234	0.48	0.07	0.0925	0.0009	3.0722	0.0456	0.2410	0.0026	1477	19	1392	13
s34	126	926	0.14	0.04	0.0758	0.0005	1.7702	0.0188	0.1693	0.0014	1091	13	1008	8
s35	59	288	0.20	0.18	0.0715	0.0010	1.6451	0.0279	0.1670	0.0017	970	28	995	9
s36	168	468	0.36	-0.02	0.1031	0.0006	4.1114	0.0451	0.2893	0.0027	1680	11	1638	13
s37	54	362	0.15	0.16	0.0653	0.0018	1.0911	0.0324	0.1212	0.0012	783	59	738	7
s38	43	204	0.21	0.03	0.0725	0.0009	1.9359	0.0323	0.1936	0.0021	1001	25	1141	12
s39	99	168	0.59	0.05	0.1667	0.0079	9.4346	0.5121	0.4104	0.0110	2525	79	2217	50
s40	118	456	0.26	0.10	0.0748	0.0007	1.9538	0.0259	0.1894	0.0018	1063	19	1118	10
s41	226	892	0.25	0.04	0.0829	0.0005	2.5985	0.0280	0.2273	0.0019	1267	13	1320	10
s42	173	564	0.31	0.02	0.0716	0.0006	1.4377	0.0181	0.1457	0.0013	974	18	877	7
s43	120	933	0.13	0.14	0.0655	0.0007	0.6656	0.0093	0.0738	0.0006	789	24	459	4
s44	162	1166	0.14	0.18	0.0639	0.0007	0.6182	0.0094	0.0701	0.0007	739	24	437	4
s45	204	613	0.33	0.06	0.1442	0.0008	4.4115	0.0457	0.2219	0.0020	2278	9	1292	10
s46	48	580	0.08	0.00	0.0709	0.0006	1.5519	0.0193	0.1587	0.0014	956	18	949	8
s47	239	428	0.56	0.04	0.0759	0.0010	2.1565	0.0369	0.2062	0.0022	1091	27	1208	12
s48	52	125	0.42	0.00	0.0706	0.0018	1.4154	0.0410	0.1455	0.0021	945	52	876	12
s49	18	51	0.35	0.56	0.0792	0.0043	2.3326	0.1348	0.2137	0.0041	1176	108	1249	22
s50	294	615	0.48	0.21	0.0730	0.0009	1.7522	0.0279	0.1740	0.0016	1015	26	1034	9
Sample 10GD49-1 (N21°52'53.0", E111°49'35.1")														
s01	107	1732	0.00	0.01	0.1051	0.0006	3.8988	0.0413	0.2689	0.0024	1717	10	1535	12
s02	296	1033	0.05	0.00	0.0772	0.0006	2.0791	0.0307	0.1952	0.0024	1128	16	1150	13
s03	339	1354	0.10	0.01	0.0798	0.0006	2.1996	0.0288	0.2000	0.0022	1192	14	1175	12
s04	57	294	0.12	0.18	0.0766	0.0015	2.1807	0.0502	0.2066	0.0025	1110	39	1211	13
s05	46	149	0.14	0.00	0.2085	0.0017	17.1311	0.2865	0.5960	0.0086	2894	14	3014	35

s06	338	668	0.13	0.01	0.1073	0.0011	4.6115	0.0635	0.3118	0.0027	1754	19	1749	13
s07	222	289	0.81	-0.08	0.0761	0.0009	1.8509	0.0293	0.1763	0.0018	1099	24	1047	10
s08	183	1106	0.20	0.01	0.0700	0.0004	1.4879	0.0149	0.1541	0.0012	929	12	924	7
s09	122	1346	0.10	0.09	0.0722	0.0004	1.3266	0.0133	0.1332	0.0010	993	13	806	6
s10	666	454	0.78	-0.04	0.0800	0.0010	2.2321	0.0368	0.2024	0.0021	1196	25	1188	11
s11	445	770	0.15	0.05	0.0744	0.0005	1.7864	0.0217	0.1741	0.0018	1053	14	1035	10
s12	40	91	0.68	0.00	0.1124	0.0013	5.0605	0.0916	0.3264	0.0046	1839	21	1821	22
s13	294	553	0.18	0.07	0.0720	0.0008	1.6902	0.0251	0.1703	0.0016	985	24	1014	9
s14	138	585	0.31	0.00	0.0926	0.0006	2.0943	0.0234	0.1640	0.0014	1480	13	979	8
s15	77	169	0.09	-0.09	0.0780	0.0030	2.5167	0.1573	0.2339	0.0115	1148	77	1355	60
s16	498	1244	0.04	0.03	0.0724	0.0004	1.6656	0.0189	0.1668	0.0017	998	11	995	9
s17	154	1595	0.09	0.29	0.0756	0.0006	1.1255	0.0163	0.1080	0.0013	1085	16	661	8
s18	33	39	0.11	0.37	0.1001	0.0023	4.1416	0.1264	0.3002	0.0059	1625	43	1692	29
s19	4	39	0.27	0.00	0.0603	0.0036	0.4646	0.0316	0.0559	0.0019	615	127	350	11
s20	95	578	0.42	-0.01	0.0735	0.0006	1.7519	0.0206	0.1728	0.0015	1028	16	1028	8
s21	128	324	0.31	-0.02	0.0732	0.0008	1.6941	0.0245	0.1679	0.0016	1019	22	1000	9
s22	131	212	0.69	0.15	0.1462	0.0015	7.8583	0.1729	0.3899	0.0075	2302	18	2122	35
s23	278	721	0.44	-0.13	0.0717	0.0009	1.7137	0.0265	0.1732	0.0016	979	25	1030	9
s24	84	510	0.05	0.07	0.1021	0.0007	3.3166	0.0384	0.2357	0.0021	1662	13	1364	11
s25	391	1773	0.51	0.00	0.0746	0.0009	2.0089	0.0288	0.1952	0.0016	1059	24	1150	9
s26	102	2549	0.17	1.95	0.1043	0.0057	1.9368	0.1083	0.1347	0.0015	1702	101	815	8
s27	463	1005	0.97	0.34	0.0742	0.0011	2.1377	0.0432	0.2090	0.0029	1047	30	1223	15
s28	314	406	0.08	0.08	0.0655	0.0008	1.0551	0.0165	0.1168	0.0011	790	26	712	6
s29	146	951	0.37	0.12	0.1122	0.0011	2.7799	0.0369	0.1797	0.0016	1835	18	1066	9
s30	44	1441	0.54	-0.01	0.0725	0.0004	1.7086	0.0234	0.1709	0.0021	1000	11	1017	12
s31	490	1514	0.70	0.00	0.0791	0.0005	2.2211	0.0230	0.2037	0.0017	1174	13	1195	9
s32	651	1490	0.58	0.09	0.0685	0.0007	1.4110	0.0182	0.1495	0.0012	882	20	898	7
s33	62	78	0.14	-1.08	0.0872	0.0049	2.2356	0.1345	0.1859	0.0039	1365	109	1099	21
s34	75	433	0.24	0.06	0.0763	0.0007	1.9031	0.0240	0.1809	0.0016	1103	17	1072	9
s35	129	223	0.16	0.18	0.0715	0.0011	1.5840	0.0301	0.1606	0.0017	973	32	960	9
s36	128	333	0.40	-0.02	0.1012	0.0008	4.1028	0.0527	0.2939	0.0030	1647	14	1661	15

s37	35	152	0.20	0.10	0.1619	0.0012	9.4700	0.1335	0.4243	0.0051	2475	12	2280	23
s38	904	1110	0.30	0.00	0.0615	0.0005	0.8821	0.0101	0.1040	0.0009	657	17	638	5
s39	163	1124	0.24	-0.01	0.2381	0.0008	22.1754	0.2094	0.6754	0.0060	3107	5	3327	23
s40	59	375	1.34	-0.02	0.0729	0.0007	1.6546	0.0330	0.1646	0.0028	1011	21	982	16
s41	398	521	0.39	-0.07	0.1378	0.0009	6.6732	0.1183	0.3511	0.0058	2200	11	1940	28
s42	82	170	0.80	0.05	0.1095	0.0011	4.6478	0.0697	0.3078	0.0035	1792	18	1730	17
s43	110	262	0.14	-0.08	0.1911	0.0013	10.6101	0.1367	0.4027	0.0045	2751	11	2182	21
s44	75	108	0.58	0.42	0.0743	0.0019	1.6423	0.0479	0.1602	0.0021	1050	52	958	12
s45	284	553	0.53	-0.04	0.0779	0.0007	2.0124	0.0266	0.1873	0.0017	1145	19	1107	9
s46	541	711	0.58	0.01	0.0752	0.0005	1.8384	0.0194	0.1774	0.0015	1073	13	1053	8
s47	82	261	0.03	0.00	0.0671	0.0010	1.2248	0.0311	0.1323	0.0027	842	32	801	15
s48	60	590	0.70	0.05	0.0768	0.0008	2.1404	0.0366	0.2022	0.0027	1116	21	1187	15
s49	83	121	0.16	0.55	0.0670	0.0021	1.3605	0.0470	0.1473	0.0019	837	67	886	11
s50	71	131	0.39	0.28	0.0686	0.0015	1.5158	0.0385	0.1602	0.0020	887	46	958	11
s51	27	251	0.48	-0.07	0.0683	0.0010	1.3401	0.0240	0.1423	0.0015	877	30	858	8
s52	187	192	0.58	0.24	0.0683	0.0015	1.4928	0.0469	0.1584	0.0035	879	46	948	20
s53	79	32	0.12	0.91	0.0734	0.0039	2.0678	0.1198	0.2043	0.0045	1026	108	1198	24
s54	212	311	0.77	-0.04	0.0639	0.0009	1.0947	0.0216	0.1243	0.0017	738	30	755	10
s55	419	579	0.13	-0.03	0.0767	0.0008	2.0353	0.0292	0.1925	0.0018	1113	22	1135	10
s56	505	538	0.49	0.04	0.0786	0.0006	2.2395	0.0259	0.2067	0.0018	1161	15	1211	10
s57	296	414	0.15	-0.07	0.0785	0.0008	2.1606	0.0290	0.1996	0.0019	1160	19	1173	10
s58	510	640	0.17	0.02	0.0753	0.0005	1.7493	0.0195	0.1685	0.0014	1077	14	1004	8
s59	842	1081	0.79	0.03	0.0869	0.0007	3.0525	0.0370	0.2547	0.0023	1359	16	1463	12
s60	112	896	0.36	0.10	0.0749	0.0007	1.8393	0.0239	0.1781	0.0016	1066	19	1056	9
s61	102	116	0.79	0.43	0.0733	0.0024	1.9313	0.0689	0.1910	0.0030	1023	65	1127	16
s62	94	815	0.62	0.13	0.0722	0.0015	1.9965	0.0771	0.2005	0.0066	992	41	1178	36
s63	504	630	0.51	0.00	0.0780	0.0008	2.1863	0.0348	0.2033	0.0025	1147	20	1193	13
s64	339	1270	0.53	13.58	0.0810	0.0277	1.6143	0.5554	0.1445	0.0055	1222	672	870	31
s65	170	291	0.26	0.03	0.0731	0.0009	1.7178	0.0276	0.1704	0.0017	1017	25	1014	10

f_{206}(%) means the percentage of common ^{206}Pb in total Pb.

Appendix B3 MC-ICP-MS zircon Lu–Hf isotope data and SIMS zircon oxygen isotope data for Cambrian samples from Guangdong

Spot#	age	1σ	$^{176}Lu/^{177}Hf$	2σ	$^{176}Hf/^{177}Hf$	2σ	$\varepsilon_{Hf}(t)^{*}$	2σ	T_{DM} (Ma)†	T_{DM}^{C} (Ma)§	$f_{Lu/Hf}$	δO^{18}(‰)	2σ
sample 10GD48 (N22°04'28.2'', E111°26'44.9'')													
1	981	14	0.000839	0.000005	0.282372	0.000023	7.0	1.5	1238	1313	-0.97	6.34	0.23
2	967	14	0.000962	0.000026	0.281919	0.000028	-9.3	1.6	1872	2130	-0.97	7.49	0.31
3	979	14	0.001050	0.000002	0.282290	0.000018	3.9	1.4	1359	1466	-0.97	7.79	0.17
4	1057	16	0.000760	0.000012	0.282017	0.000020	-3.8	1.5	1726	1922	-0.98	7.26	0.12
5	955	14	0.000602	0.000003	0.281778	0.000016	-14.4	1.3	2046	2371	-0.98	8.30	0.27
6	2454	15	0.001267	0.000008	0.281443	0.000020	6.0	1.5	2546	2571	-0.96	5.94	0.34
7	543	8	0.000829	0.000011	0.282385	0.000025	-2.0	1.4	1220	1416	-0.98	11.94	0.13
8	1021	17	0.000530	0.000008	0.282112	0.000018	-1.1	1.4	1586	1755	-0.98	9.34	0.24
9	1042	17	0.000482	0.000004	0.282050	0.000018	-2.8	1.4	1668	1857	-0.99	6.80	0.20
10	1088	15	0.000903	0.000017	0.282090	0.000021	-0.69	1.4	1632	1789	-0.97	8.59	0.28
11	1108	16	0.000500	0.000003	0.281885	0.000020	-7.2	1.4	1896	2133	-0.98	5.38	0.25
12	598	9	0.000337	0.000003	0.282376	0.000019	-0.95	1.3	1216	1405	-0.99	11.86	0.21
13	1083	16	0.000672	0.000009	0.282013	0.000022	-3.4	1.5	1728	1918	-0.98	7.14	0.29
14	608	9	0.000390	0.000003	0.282400	0.000019	0.09	1.3	1185	1360	-0.99	6.60	0.33
15	1049	17	0.000672	0.000004	0.282107	0.000019	-0.79	1.5	1599	1762	-0.98	7.28	0.21
16	1110	16	0.000231	0.000003	0.281802	0.000015	-9.9	1.4	1995	2269	-0.99	8.62	0.21
17	1283	16	0.000881	0.000004	0.281817	0.000021	-6.1	1.5	2007	2215	-0.97	6.62	0.26
18	1041	51	0.000100	0.000002	0.281914	0.000017	-7.4	2.6	1836	2086	-1.00	9.88	0.33
19	1297	16	0.000272	0.000010	0.281830	0.000019	-4.8	1.4	1959	2163	-0.99	8.67	0.19
20	603	9	0.000849	0.000004	0.282205	0.000024	-7.1	1.4	1470	1721	-0.97	8.94	0.15
21	2814	14	0.001016	0.000027	0.280979	0.000021	-2.0	1.5	3158	3256	-0.97	6.46	0.19
22	1608	16	0.000564	0.000003	0.281577	0.000020	-7.1	1.5	2318	2530	-0.98	7.82	0.27
23	483	7	0.001130	0.000015	0.282342	0.000023	-4.9	1.3	1289	1514	-0.97	9.23	0.24

24	996	14	0.000628	0.000002	0.281998	0.000016	-5.0	1.3	1747	1959	-0.98	5.35	0.28
25	590	8	0.000812	0.000007	0.282533	0.000020	4.2	1.3	1012	1134	-0.98	5.83	0.26
26	1034	17	0.000823	0.000016	0.282194	0.000024	1.9	1.6	1485	1616	-0.98	11.04	0.24
27	1091	16	0.000655	0.000006	0.281638	0.000020	-16.5	1.5	2240	2580	-0.98	9.55	0.28
28	944	14	0.001171	0.000011	0.282510	0.000025	10.9	1.5	1054	1085	-0.96	9.67	0.15
29	1036	15	0.001109	0.000002	0.282142	0.000022	-0.12	1.5	1568	1718	-0.97	5.52	0.18
30	2403	15	0.000754	0.000004	0.281306	0.000021	0.82	1.5	2696	2782	-0.98	7.19	0.23
31	942	13	0.000785	0.000019	0.281933	0.000021	-9.4	1.4	1843	2106	-0.98	6.89	0.22
32	1105	15	0.001058	0.000008	0.282416	0.000019	11.1	1.4	1183	1205	-0.97	5.07	0.25
33	1240	16	0.000819	0.000019	0.282072	0.000023	2.1	1.5	1653	1773	-0.98	6.25	0.20
34	2422	15	0.001033	0.000009	0.281396	0.000024	4.0	1.6	2594	2642	-0.97	5.62	0.26
35	1157	20	0.000541	0.000026	0.282421	0.000022	12.8	1.6	1160	1161	-0.98	5.06	0.27
36	1270	15	0.000726	0.000006	0.281977	0.000020	-0.57	1.4	1780	1930	-0.98	7.76	0.36
37	1760	51	0.000615	0.000007	0.281329	0.000022	-12.6	2.7	2657	2923	-0.98	4.54	0.22
38	664	10	0.000471	0.000002	0.282080	0.000020	-10.1	1.3	1627	1918	-0.99	7.66	0.29
39	1313	16	0.000437	0.000005	0.282077	0.000019	4.2	1.4	1630	1726	-0.99	6.45	0.28
40	824	11	0.000792	0.000003	0.282204	0.000024	-2.3	1.4	1470	1658	-0.98	8.39	0.28
41	2435	15	0.000560	0.000005	0.281405	0.000026	5.4	1.6	2550	2584	-0.98	4.67	0.27
42	999	16	0.001014	0.000017	0.282450	0.000025	10.1	1.6	1134	1171	-0.97	5.23	0.24
43	1026	17	0.000666	0.000006	0.281806	0.000019	-11.9	1.5	2011	2302	-0.98	5.99	0.37
44	1311	49	0.001031	0.000014	0.282101	0.000018	4.5	2.5	1622	1709	-0.97	4.63	0.22
45	719	10	0.000814	0.000016	0.282266	0.000020	-2.4	1.3	1384	1577	-0.98	10.47	0.19
46	1067	16	0.000862	0.000005	0.282031	0.000024	-3.2	1.5	1712	1898	-0.97	6.42	0.21
47	805	12	0.001040	0.000017	0.282320	0.000028	1.2	1.5	1317	1461	-0.97	5.82	0.26
48	653	9	0.000841	0.000004	0.282508	0.000024	4.7	1.4	1047	1162	-0.97	6.46	0.30
49	945	13	0.001202	0.000009	0.282215	0.000022	0.45	1.4	1470	1615	-0.96	7.98	0.25
50	622	9	0.000746	0.000006	0.282597	0.000021	7.2	1.3	921	1009	-0.98	6.49	0.15
51	1006	17	0.000809	0.000027	0.282059	0.000021	-3.5	1.5	1670	1863	-0.98	7.38	0.17
52	665	9	0.001095	0.000009	0.282515	0.000021	5.1	1.3	1045	1151	-0.97	5.10	0.18
53	2239	38	0.000909	0.000020	0.281637	0.000026	8.7	2.3	2256	2260	-0.97	4.57	0.32
54	668	10	0.000526	0.000003	0.282249	0.000023	-4.0	1.4	1398	1616	-0.98	9.49	0.32
55	1068	15	0.000447	0.000010	0.282171	0.000020	2.1	1.4	1502	1633	-0.99	5.14	0.17

56	922	13	0.000557	0.000003	0.282065	0.000026	-5.0	1.5	1651	1869	-0.98	7.00	0.26
57	852	13	0.001488	0.000063	0.282215	0.000042	-1.7	1.9	1481	1649	-0.96	9.01	0.15
58	1171	52	0.000695	0.000005	0.281892	0.000020	-5.7	2.7	1895	2108	-0.98	7.95	0.17
59	921	13	0.000968	0.000003	0.282371	0.000026	5.6	1.5	1244	1336	-0.97	6.73	0.27
60	939	13	0.000955	0.000007	0.282185	0.000019	-0.60	1.4	1502	1663	-0.97	5.97	0.23
61	1095	17	0.000775	0.000003	0.282013	0.000021	-3.2	1.5	1733	1919	-0.98	5.69	0.28
62	839	13	0.000804	0.000005	0.282381	0.000023	5.9	1.4	1224	1314	-0.98	5.98	0.26
63	1065	17	0.001168	0.000011	0.281997	0.000020	-4.7	1.5	1773	1971	-0.96	8.74	0.30
64	3060	14	0.000515	0.000001	0.280955	0.000020	3.7	1.5	3150	3177	-0.98	7.09	0.34
65	1151	15	0.000952	0.000016	0.281896	0.000021	-6.2	1.5	1902	2116	-0.97	8.10	0.25
66	1035	16	0.001817	0.000070	0.282086	0.000029	-4.1	1.6	1678	1861	-0.95	7.85	0.22
67	860	12	0.001414	0.000029	0.281786	0.000022	-16.7	1.4	2079	2408	-0.96	6.34	0.29
68	1022	16	0.000464	0.000002	0.282197	0.000021	2.0	1.5	1466	1600	-0.99	8.29	0.30
69	2471	14	0.000806	0.000008	0.281029	0.000022	-7.6	1.5	3074	3249	-0.98	6.33	0.18
70	749	11	0.000955	0.000003	0.282319	0.000019	0.04	1.3	1315	1477	-0.97	6.97	0.25
71	799	11	0.001988	0.000012	0.282491	0.000027	6.7	1.5	1105	1182	-0.94	7.29	0.30
72	751	11	0.001057	0.000021	0.281899	0.000024	-14.9	1.4	1904	2229	-0.97	7.15	0.36
73	866	12	0.000988	0.000003	0.282060	0.000019	-6.6	1.3	1677	1907	-0.97	7.77	0.25
74	1054	15	0.000454	0.000004	0.281987	0.000027	-4.8	1.6	1753	1965	-0.99	6.80	0.24
75	1284	16	0.001139	0.000007	0.281959	0.000021	-1.3	1.5	1825	1976	-0.97	6.19	0.25
76	616	9	0.000728	0.000006	0.282447	0.000024	1.8	1.4	1130	1281	-0.98	9.14	0.26
77	2320	15	0.000992	0.000033	0.281395	0.000021	1.7	1.5	2593	2670	-0.97	4.74	0.21
78	1011	17	0.001023	0.000031	0.282107	0.000020	-1.8	1.5	1613	1783	-0.97	10.55	0.31
79	772	11	0.000675	0.000003	0.282036	0.000025	-9.3	1.5	1696	1969	-0.98	8.95	0.27
80	643	9	0.000818	0.000007	0.282492	0.000018	3.9	1.3	1070	1194	-0.98	6.49	0.23
81	1947	15	0.000830	0.000004	0.281465	0.000019	-3.9	1.4	2486	2642	-0.97	8.64	0.29
82	1086	16	0.000569	0.000002	0.281792	0.000021	-11.1	1.5	2026	2307	-0.98	7.14	0.24
83	938	13	0.001406	0.000046	0.282271	0.000021	2.2	1.4	1399	1523	-0.96	7.06	0.16
84	1175	17	0.000352	0.000001	0.281739	0.000028	-10.8	1.6	2086	2365	-0.99	7.93	0.27
85	3057	14	0.001216	0.000009	0.281070	0.000028	6.3	1.6	3051	3050	-0.96	5.03	0.20
86	1069	16	0.000695	0.000006	0.281931	0.000019	-6.6	1.4	1842	2069	-0.98	6.33	0.24
87	1878	16	0.000814	0.000006	0.281492	0.000018	-4.4	1.4	2448	2613	-0.98	4.51	0.33

88	1032	15	0.000746	0.000007	0.281744	0.000020	-8.4	1.4	2100	2338	-0.98	6.32	0.24
89	1924	15	0.001550	0.000016	0.281504	0.000022	-3.9	1.5	2480	2627	-0.95	8.57	0.19
90	2834	14	0.000609	0.000007	0.280975	0.000018	-0.93	1.4	3131	3219	-0.98	7.17	0.20
91	2363	15	0.000945	0.000012	0.281357	0.000020	1.4	1.5	2641	2721	-0.97	4.84	0.14
92	1081	15	0.000515	0.000010	0.282037	0.000019	-2.5	1.4	1689	1871	-0.98	7.99	0.22
93	860	12	0.000843	0.000002	0.282379	0.000021	4.6	1.4	1228	1334	-0.97	6.96	0.30
94	879	12	0.001384	0.000002	0.282401	0.000021	5.5	1.4	1215	1306	-0.96	6.27	0.28
95	1074	14	0.000665	0.000004	0.282082	0.000018	5.1	1.4	1633	1716	-0.98	5.88	0.23
96	934	13	0.000603	0.000007	0.282071	0.000017	-4.5	1.3	1646	1857	-0.98	8.12	0.23
97	791	11	0.000593	0.000015	0.282325	0.000027	1.4	1.5	1294	1444	-0.98	9.84	0.25
98	1001	15	0.000558	0.000002	0.282172	0.000018	0.55	1.4	1505	1656	-0.98	7.62	0.10
99	994	14	0.000792	0.000003	0.282147	0.000022	-0.62	1.4	1548	1709	-0.98	7.90	0.21
100	2570	14	0.000535	0.000001	0.281426	0.000018	9.2	1.4	2520	2505	-0.98	7.0	0.21
101	2270	31	0.000772	0.000010	0.281459	0.000021	3.2	1.9	2491	2556	-0.98	7.30	0.19
102	789	14	0.000717	0.000012	0.282289	0.000023	-0.02	1.5	1348	1513	-0.98	7.05	0.33
103	495	7	0.000627	0.000004	0.282444	0.000020	-0.92	1.3	1131	1320	-0.98	7.92	0.26
104	791	12	0.001089	0.000012	0.282426	0.000023	4.7	1.4	1170	1277	-0.97	7.58	0.26
105	586	8	0.001480	0.000026	0.282489	0.000029	2.3	1.5	1092	1228	-0.96	9.43	0.26
106	814	11	0.000921	0.000008	0.282280	0.000020	0.07	1.3	1369	1528	-0.97	5.89	0.38
107	1223	17	0.001343	0.000004	0.281829	0.000022	-7.3	1.5	2015	2230	-0.96	5.60	0.29
108	2279	15	0.000900	0.000001	0.281185	0.000017	-6.5	1.4	2871	3042	-0.97	6.83	0.22
109	667	9	0.000779	0.000003	0.282059	0.000021	-10.9	1.3	1669	1962	-0.98	6.53	0.29
110	774	11	0.000836	0.000004	0.281886	0.000021	-14.7	1.4	1911	2240	-0.97	6.79	0.26
111	959	13	0.000917	0.000002	0.282363	0.000017	6.2	1.3	1252	1336	-0.97	6.05	0.19
112	1023	16	0.001999	0.000022	0.282070	0.000024	-5.5	1.5	1709	1904	-0.94	5.08	0.31
113	718	10	0.000959	0.000005	0.281992	0.000018	-12.2	1.3	1770	2071	-0.97	6.47	0.24
114	2077	15	0.000846	0.000009	0.281325	0.000018	-6.0	1.4	2677	2851	-0.97	6.55	0.35
115	1993	14	0.000369	0.000002	0.281092	0.000018	-15.5	1.4	2956	3251	-0.99	5.92	0.35
116	922	14	0.000983	0.000009	0.282365	0.000020	5.4	1.4	1253	1347	-0.97	7.87	0.19
117	1488	35	0.000187	0.000004	0.281265	0.000020	-20.5	2.0	2713	3095	-0.99	10.12	0.27
118	893	12	0.000729	0.000003	0.282287	0.000020	2.2	1.4	1352	1487	-0.98	5.01	0.22
119	919	13	0.001186	0.000007	0.282154	0.000016	-2.3	1.3	1555	1732	-0.96	7.83	0.28

120	973	13	0.000662	0.000003	0.282137	0.000018	-1.4	1.4	1556	1729	-0.98	8.89	0.23
sample 10GD49-1 (N21°52'53.0", E111°49'35.1")													
1	1085	15	0.000816	0.000016	0.282142	0.000023	1.2	1.5	1556	1692	-0.98	4.80	0.25
2	946	13	0.000394	0.000001	0.282151	0.000025	-1.3	1.5	1527	1704	-0.99	6.84	0.24
3	1080	16	0.000256	0.000009	0.281960	0.000021	-5.0	1.5	1781	1998	-0.99	11.21	0.19
4	500	15	0.000272	0.000002	0.282223	0.000027	-8.5	1.6	1423	1709	-0.99	5.88	0.34
5	679	10	0.000254	0.000001	0.282414	0.000026	2.2	1.5	1161	1310	-0.99	6.43	0.40
6	834	12	0.001910	0.000064	0.282150	0.000022	-4.6	1.4	1591	1782	-0.94	7.93	0.23
7	1437	16	0.001062	0.000022	0.281925	0.000023	0.97	1.5	1867	1988	-0.97	5.49	0.26
8	972	14	0.000936	0.000016	0.282334	0.000026	5.4	1.5	1295	1387	-0.97	5.06	0.28
9	1098	16	0.000723	0.000004	0.282146	0.000028	1.7	1.6	1546	1678	-0.98	7.69	0.32
10	891	14	0.000621	0.000018	0.282104	0.000028	-4.3	1.6	1601	1811	-0.98	11.88	0.28
11	1003	14	0.000592	0.000007	0.282183	0.000029	0.98	1.6	1490	1635	-0.98	5.91	0.20
12	1312	62	0.001457	0.000020	0.282007	0.000027	0.78	3.1	1773	1896	-0.96	5.66	0.24
13	2250	34	0.000559	0.000003	0.281236	0.000028	-4.8	2.2	2778	2935	-0.98	6.54	0.22
14	989	14	0.000855	0.000011	0.282095	0.000023	-2.6	1.5	1623	1806	-0.97	9.55	0.31
15	2604	14	0.000936	0.000003	0.281064	0.000026	-3.6	1.6	3038	3162	-0.97	7.09	0.26
16	1023	16	0.001346	0.000017	0.282021	0.000030	-4.9	1.6	1748	1945	-0.96	5.97	0.14
17	933	13	0.001213	0.000049	0.282331	0.000028	4.3	1.6	1308	1411	-0.96	11.90	0.21
18	968	14	0.000810	0.000004	0.282451	0.000025	9.6	1.5	1127	1173	-0.98	7.56	0.28
19	610	9	0.000529	0.000005	0.282394	0.000029	-0.12	1.5	1197	1373	-0.98	8.61	0.27
20	924	13	0.000961	0.000005	0.281892	0.000029	-11.3	1.6	1908	2189	-0.97	7.53	0.27
21	983	14	0.000689	0.000007	0.282477	0.000029	10.9	1.6	1086	1117	-0.98	5.75	0.28
22	1068	16	0.000092	0.000004	0.281950	0.000030	-5.5	1.7	1787	2014	-1.00	9.64	0.29
23	963	15	0.000779	0.000025	0.282328	0.000028	5.1	1.6	1296	1393	-0.98	4.66	0.26
24	863	12	0.000133	0.000001	0.281998	0.000023	-8.4	1.4	1724	1995	-1.00	8.59	0.25
25	995	14	0.000553	0.000005	0.282022	0.000022	-4.9	1.5	1711	1925	-0.98	7.65	0.33
26	2780	14	0.000526	0.000002	0.281062	0.000027	1.1	1.6	3008	3077	-0.98	0.06	0.26
27	2064	15	0.000424	0.000001	0.281300	0.000029	-6.6	1.6	2682	2870	-0.99	4.97	0.21
28	815	11	0.001108	0.000003	0.282609	0.000030	11.7	1.6	913	940	-0.97	7.70	0.36
29	1062	17	0.000469	0.000013	0.282045	0.000024	-2.5	1.5	1675	1860	-0.99	7.33	0.18

30	1460	16	0.000623	0.000010	0.281710	0.000028	-5.8	1.6	2141	2343	-0.98	6.60	0.22
31	1031	15	0.001102	0.000017	0.282419	0.000029	9.6	1.6	1180	1222	-0.97	4.94	0.32
32	1697	15	0.000597	0.000001	0.281785	0.000026	2.2	1.6	2036	2137	-0.98	5.60	0.29
33	1077	15	0.001052	0.000039	0.282337	0.000029	7.7	1.6	1293	1355	-0.97	5.29	0.29
34	697	11	0.000409	0.000003	0.282476	0.000030	4.7	1.6	1080	1196	-0.99	7.86	0.34
35	1093	16	0.000958	0.000011	0.281946	0.000019	-5.7	1.4	1834	2045	-0.97	8.05	0.34
36	984	15	0.000430	0.000001	0.282303	0.000026	4.9	1.5	1319	1421	-0.99	6.59	0.28
37	1067	15	0.000953	0.000003	0.282153	0.000024	1.1	1.5	1547	1684	-0.97	5.77	0.23
38	1211	67	0.000497	0.000036	0.281887	0.000025	-4.9	3.3	1893	2098	-0.99	7.39	0.23
39	934	13	0.000585	0.000002	0.282172	0.000024	-0.95	1.5	1506	1677	-0.98	9.66	0.24
40	1067	15	0.000514	0.000007	0.281889	0.000027	-8.0	1.6	1890	2138	-0.98	7.25	0.24
41	910	12	0.000227	0.000001	0.281893	0.000021	-11.1	1.4	1871	2169	-0.99	9.17	0.33
42	1063	15	0.000591	0.000007	0.282105	0.000030	-0.47	1.6	1598	1757	-0.98	6.12	0.24
43	1018	24	0.000684	0.000003	0.282305	0.000024	5.6	1.7	1325	1416	-0.98	6.00	0.42
44	1669	16	0.000287	0.000006	0.281581	0.000022	-5.3	1.5	2296	2489	-0.99	7.58	0.26
45	920	13	0.000613	0.000016	0.281940	0.000024	-9.5	1.5	1825	2094	-0.98	9.82	0.15
46	980	14	0.000024	0.000001	0.281887	0.000023	-9.7	1.5	1869	2151	-1.00	11.14	0.24
47	1105	37	0.000581	0.000009	0.281899	0.000023	-6.9	2.1	1881	2112	-0.98	11.39	0.24
48	824	12	0.000583	0.000005	0.282170	0.000019	-3.4	1.3	1508	1712	-0.98	6.18	0.17
49	1650	15	0.000403	0.000002	0.281568	0.000025	-6.3	1.5	2320	2524	-0.99	7.59	0.34
50	595	8	0.000695	0.000011	0.282223	0.000021	-6.6	1.3	1440	1688	-0.98	6.81	0.30
51	2751	14	0.000303	0.000001	0.280835	0.000020	-7.2	1.5	3292	3459	-0.99	6.59	0.25
52	1643	15	0.000367	0.000001	0.281486	0.000021	-9.3	1.5	2428	2668	-0.99	6.82	0.15
53	626	9	0.000344	0.000013	0.282402	0.000019	0.57	1.3	1180	1350	-0.99	11.48	0.28
54	919	13	0.000139	0.000007	0.281861	0.000018	-12.0	1.4	1910	2220	-1.00	5.22	0.20
55	1024	17	0.000348	0.000003	0.281794	0.000023	-12.2	1.5	2012	2314	-0.99	7.53	0.30
56	954	43	0.000178	0.000001	0.281339	0.000019	-29.8	2.3	2613	3131	-0.99	6.01	0.23
57	631	9	0.000632	0.000003	0.282549	0.000018	5.8	1.3	985	1090	-0.98	6.69	0.32
58	1006	15	0.000895	0.000002	0.282368	0.000026	7.4	1.5	1245	1314	-0.97	7.06	0.18
59	870	12	0.000347	0.000001	0.282162	0.000017	-2.6	1.3	1510	1706	-0.99	9.02	0.16
61	1129	15	0.000210	0.000000	0.281762	0.000019	-10.9	1.4	2047	2333	-0.99	8.31	0.20
62	1039	16	0.000537	0.000003	0.281968	0.000024	-5.8	1.5	1784	2007	-0.98	7.28	0.30

63	1064	15	0.000478	0.000002	0.281378	0.000018	-26.1	1.4	2580	3038	-0.99	5.87	0.30
64	676	10	0.001206	0.000007	0.282542	0.000026	5.7	1.5	1009	1109	-0.96	6.25	0.20
65	873	12	0.000348	0.000011	0.282024	0.000020	-6.3	1.4	1698	1936	-0.99	7.92	0.22
66	1112	16	0.001056	0.000024	0.281669	0.000024	-17.0	1.5	2221	2557	-0.97	6.90	0.35
67	3047	32	0.002107	0.000073	0.280869	0.000027	-4.1	2.1	3404	3504	-0.94	5.87	0.37
68	1049	16	0.001636	0.000028	0.282248	0.000028	3.2	1.6	1440	1547	-0.95	8.80	0.25
69	821	14	0.000060	0.000003	0.282135	0.000018	-4.4	1.4	1536	1762	-1.00	11.64	0.31
70	1069	16	0.000549	0.000009	0.281879	0.000022	-8.8	1.5	1906	2163	-0.98	6.55	0.26
71	1093	16	0.000225	0.000004	0.282088	0.000020	-0.63	1.5	1606	1772	-0.99	9.84	0.24
72	925	14	0.000562	0.000009	0.282344	0.000023	5.3	1.5	1268	1365	-0.98	11.60	0.34
73	705	10	0.000628	0.000004	0.282399	0.000023	2.2	1.4	1194	1336	-0.98	7.00	0.22
74	649	9	0.000044	0.000000	0.281919	0.000020	-15.9	1.3	1828	2201	-1.00	5.92	0.22
75	1256	16	0.000445	0.000005	0.281832	0.000020	-6.2	1.5	1965	2184	-0.99	6.32	0.28
76	1241	15	0.000666	0.000007	0.282062	0.000022	1.6	1.5	1661	1789	-0.98	6.42	0.47
77	645	10	0.000346	0.000015	0.282190	0.000019	-6.3	1.3	1472	1723	-0.99	11.72	0.22
78	3145	14	0.000786	0.000003	0.280834	0.000023	0.57	1.5	3334	3392	-0.98	6.25	0.15
79	1023	15	0.000298	0.000002	0.282272	0.000022	5.0	1.5	1358	1457	-0.99	7.56	0.18
80	1518	14	0.000426	0.000002	0.281890	0.000022	1.5	1.5	1884	2005	-0.99	5.81	0.21
81	958	13	0.000736	0.000020	0.282057	0.000020	-4.3	1.4	1671	1876	-0.98	8.84	0.23
82	2386	15	0.000387	0.000005	0.281239	0.000023	-1.4	1.5	2762	2876	-0.99	7.17	0.30
83	1007	15	0.000808	0.000049	0.282153	0.000024	-0.14	1.5	1540	1695	-0.98	6.16	0.31
84	1044	17	0.001133	0.000001	0.282131	0.000020	-0.34	1.5	1584	1735	-0.97	6.24	0.20
85	2076	15	0.001230	0.000007	0.281452	0.000025	-2.0	1.6	2531	2656	-0.96	5.18	0.22
86	1059	16	0.000907	0.000013	0.281946	0.000024	-6.4	1.5	1832	2054	-0.97	7.88	0.28
87	1261	36	0.000169	0.000003	0.281903	0.000024	-2.9	2.1	1855	2041	-0.99	10.74	0.25
88	699	10	0.000614	0.000004	0.282487	0.000023	5.1	1.4	1071	1182	-0.98	7.51	0.33
89	1053	15	0.000382	0.000004	0.282053	0.000026	-2.4	1.5	1661	1846	-0.99	6.95	0.26
90	626	9	0.000801	0.000004	0.282492	0.000030	3.6	1.5	1069	1197	-0.98	7.35	0.25
91	1085	15	0.000692	0.000011	0.282042	0.000025	-2.3	1.5	1689	1866	-0.98	7.08	0.19
92	1075	15	0.000609	0.000011	0.282202	0.000028	3.2	1.6	1465	1582	-0.98	7.89	0.26
93	3196	30	0.000770	0.000024	0.280759	0.000028	-4.1	2.1	3434	3547	-0.98	6.70	0.19
94	1465	14	0.000476	0.000012	0.281996	0.000026	1.3	1.5	1742	1871	-0.99	11.92	0.40

95	1772	14	0.000654	0.000012	0.281542	0.000027	-5.4	1.6	2371	2555	-0.98	8.00	0.25
96	1097	16	0.000056	0.000002	0.282049	0.000022	-2.2	1.5	1652	1840	-1.00	7.90	0.27
97	834	12	0.001695	0.000035	0.282336	0.000024	2.1	1.4	1318	1444	-0.95	7.78	0.22
98	1075	15	0.001230	0.000020	0.281868	0.000028	-9.1	1.6	1955	2199	-0.96	8.63	0.21
99	695	10	0.001141	0.000008	0.282523	0.000023	6.0	1.4	1035	1130	-0.97	5.77	0.22
100	1140	15	0.000674	0.000002	0.282109	0.000027	1.3	1.6	1596	1730	-0.98	5.72	0.21
101	946	13	0.001233	0.000008	0.282136	0.000022	-2.4	1.4	1582	1757	-0.96	9.33	0.36
102	944	14	0.001067	0.000010	0.282459	0.000029	9.1	1.6	1124	1174	-0.97	5.39	0.32
103	833	15	0.000442	0.000002	0.281847	0.000025	-14.6	1.5	1944	2280	-0.99	6.52	0.27
104	1275	21	0.000219	0.000001	0.281623	0.000027	-12.6	1.7	2234	2533	-0.99	7.67	0.28
105	1096	16	0.000672	0.000031	0.282001	0.000022	-3.5	1.5	1744	1935	-0.98	8.26	0.15
106	662	9	0.001247	0.000006	0.282184	0.000018	-6.8	1.3	1515	1750	-0.96	6.68	0.22
107	1061	15	0.000716	0.000002	0.281751	0.000022	-13.2	1.5	2090	2392	-0.98	6.59	0.31
108	1109	16	0.000935	0.000025	0.282031	0.000023	-2.3	1.5	1715	1888	-0.97	8.66	0.21
109	1041	15	0.000421	0.000003	0.281556	0.000022	-20.3	1.5	2338	2732	-0.99	5.41	0.29
110	900	12	0.001588	0.000007	0.282137	0.000020	-3.5	1.4	1595	1779	-0.95	8.03	0.28
111	997	14	0.000952	0.000010	0.282097	0.000022	-2.5	1.4	1625	1804	-0.97	7.61	0.30
112	943	14	0.000945	0.000015	0.282399	0.000023	7.1	1.5	1203	1277	-0.97	5.31	0.22
113	673	10	0.000409	0.000005	0.282527	0.000029	6.0	1.5	1010	1112	-0.99	7.07	0.31
114	1027	15	0.000832	0.000007	0.282220	0.000020	2.7	1.4	1448	1570	-0.97	6.94	0.31
115	959	14	0.000909	0.000004	0.282126	0.000022	-2.2	1.4	1583	1762	-0.97	5.59	0.27
116	981	13	0.001585	0.000009	0.282122	0.000021	-2.3	1.4	1617	1785	-0.95	8.80	0.33
117	3075	14	0.000408	0.000006	0.280839	0.000022	0.16	1.5	3296	3363	-0.99	7.19	0.34
118	1418	38	0.000262	0.000005	0.281588	0.000022	-10.6	2.2	2284	2552	-0.99	9.36	0.17
119	2324	14	0.000795	0.000017	0.281151	0.000025	-6.6	1.5	2910	3080	-0.98	6.00	0.18
120	3132	14	0.000982	0.000005	0.280779	0.000019	-1.9	1.5	3425	3509	-0.97	7.60	0.23
Sample 10GD16 (N25°01'19.9", E113°47'55.5")													
1	920	12	0.000051	0.000010	0.281867	0.000020	-11.7	1.4	1897	2206	-1.00	N.A.	N.A.
2	3480	10	0.002411	0.000107	0.280705	0.000026	0.01	1.6	3660	3702	-0.93	N.A.	N.A.
3	990	12	0.000345	0.000002	0.282494	0.000021	11.9	1.4	1054	1074	-0.99	N.A.	N.A.
4	908	12	0.000566	0.000008	0.281753	0.000022	-16.3	1.4	2078	2428	-0.98	N.A.	N.A.

5	941	12	0.000832	0.000006	0.282143	0.000022	-2.0	1.4	1556	1734	-0.97	N.A.	N.A.
6	917	11	0.000418	0.000009	0.281830	0.000021	-13.3	1.4	1966	2284	-0.99	N.A.	N.A.
7	517	7	0.000418	0.000009	0.281830	0.000021	-22.1	1.3	1966	2406	-0.99	N.A.	N.A.
8	938	13	0.000418	0.000009	0.281830	0.000021	-12.9	1.4	1966	2278	-0.99	N.A.	N.A.
9	2284	12	0.000693	0.000019	0.281111	0.000020	-8.7	1.4	2955	3153	-0.98	N.A.	N.A.
10	550	7	0.001081	0.000020	0.282132	0.000020	-10.9	1.3	1582	1872	-0.97	N.A.	N.A.
11	919	12	0.001081	0.000020	0.282132	0.000020	-3.0	1.4	1582	1768	-0.97	N.A.	N.A.
12	1082	13	0.000046	0.000001	0.282500	0.000016	14.4	1.3	1037	1022	-1.00	N.A.	N.A.
13	910	11	0.000513	0.000026	0.281512	0.000030	-24.8	1.6	2403	2851	-0.98	N.A.	N.A.
14	763	10	0.000702	0.000003	0.282073	0.000018	-8.3	1.3	1647	1907	-0.98	N.A.	N.A.
15	519	7	0.000306	0.000002	0.282083	0.000021	-13.1	1.3	1617	1955	-0.99	N.A.	N.A.
16	1081	13	0.001374	0.000037	0.282272	0.000021	5.3	1.4	1396	1481	-0.96	N.A.	N.A.
17	1052	15	0.001252	0.000018	0.282082	0.000022	-2.0	1.5	1658	1825	-0.96	N.A.	N.A.
18	920	12	0.000278	0.000003	0.281965	0.000021	-8.4	1.4	1776	2041	-0.99	N.A.	N.A.
19	2500	11	0.000728	0.000003	0.281119	0.000019	-3.6	1.4	2947	3078	-0.98	N.A.	N.A.
20	721	9	0.001322	0.000002	0.282211	0.000018	-4.6	1.3	1480	1687	-0.96	N.A.	N.A.
21	2699	11	0.001345	0.000009	0.281222	0.000025	3.4	1.5	2854	2896	-0.96	N.A.	N.A.
22	1121	14	0.000853	0.000002	0.282213	0.000018	4.4	1.4	1459	1556	-0.97	N.A.	N.A.
23	911	12	0.001304	0.000009	0.282121	0.000019	-3.7	1.3	1607	1797	-0.96	N.A.	N.A.
24	1713	13	0.001031	0.000046	0.281884	0.000019	5.6	1.4	1923	1982	-0.97	N.A.	N.A.
25	901	11	0.000696	0.000008	0.282128	0.000018	-3.3	1.3	1571	1768	-0.98	N.A.	N.A.
26	801	10	0.000172	0.000000	0.282086	0.000015	-6.7	1.3	1606	1857	-0.99	N.A.	N.A.
27	941	12	0.000737	0.000002	0.282329	0.000018	4.7	1.3	1294	1398	-0.98	N.A.	N.A.
28	2506	11	0.000451	0.000002	0.280949	0.000017	-9.0	1.3	3153	3348	-0.99	N.A.	N.A.
29	926	12	0.000548	0.000007	0.281975	0.000016	-8.1	1.3	1774	2028	-0.98	N.A.	N.A.
30	1598	12	0.000931	0.000002	0.281631	0.000019	-5.8	1.4	2265	2456	-0.97	N.A.	N.A.
31	551	8	0.001018	0.000038	0.281945	0.000019	-17.5	1.3	1837	2202	-0.97	N.A.	N.A.
32	520	7	0.000244	0.000001	0.282101	0.000015	-12.4	1.2	1589	1921	-0.99	N.A.	N.A.
33	1528	15	0.001851	0.000009	0.281882	0.000017	0.60	1.4	1968	2081	-0.94	N.A.	N.A.
34	502	7	0.000573	0.000008	0.282160	0.000017	-10.8	1.2	1521	1826	-0.98	N.A.	N.A.
35	2037	12	0.000181	0.000003	0.281331	0.000016	-5.7	1.3	2623	2806	-0.99	N.A.	N.A.
36	510	7	0.000427	0.000016	0.282164	0.000016	-10.4	1.2	1511	1814	-0.99	N.A.	N.A.

37	1048	14	0.000641	0.000003	0.282005	0.000016	-4.4	1.4	1738	1942	-0.98	N.A.	N.A.
38	917	12	0.001084	0.000006	0.282143	0.000019	-2.6	1.3	1566	1748	-0.97	N.A.	N.A.
39	963	12	0.000113	0.000005	0.282074	0.000014	-3.5	1.3	1620	1827	-1.00	N.A.	N.A.
40	957	12	0.001174	0.000030	0.282100	0.000017	-3.4	1.3	1630	1817	-0.96	N.A.	N.A.
41	517	7	0.000461	0.000005	0.281917	0.000017	-19.0	1.2	1850	2253	-0.99	N.A.	N.A.
42	2573	11	0.001196	0.000005	0.281005	0.000018	-6.8	1.4	3139	3296	-0.96	N.A.	N.A.
43	1081	14	0.000283	0.000009	0.282023	0.000016	-2.8	1.3	1697	1887	-0.99	N.A.	N.A.
44	916	12	0.000799	0.000004	0.282195	0.000019	-0.63	1.4	1481	1646	-0.98	N.A.	N.A.
45	995	13	0.000953	0.000005	0.282220	0.000018	1.9	1.3	1453	1583	-0.97	N.A.	N.A.
46	937	12	0.001113	0.000002	0.282168	0.000019	-1.3	1.4	1532	1699	-0.97	N.A.	N.A.
47	572	7	0.000484	0.000004	0.282108	0.000015	-11.1	1.2	1589	1896	-0.99	N.A.	N.A.
48	1022	15	0.001991	0.000009	0.282554	0.000020	13.6	1.4	1014	1013	-0.94	N.A.	N.A.
49	530	7	0.000185	0.000001	0.282073	0.000018	-13.1	1.3	1625	1967	-0.99	N.A.	N.A.
50	898	11	0.000036	0.000000	0.282030	0.000014	-6.4	1.3	1677	1923	-1.00	N.A.	N.A.
51	828	11	0.000592	0.000008	0.282134	0.000014	-4.6	1.3	1558	1775	-0.98	N.A.	N.A.
52	1194	16	0.000581	0.000004	0.282063	0.000015	0.94	1.4	1655	1793	-0.98	N.A.	N.A.
53	560	7	0.002131	0.000049	0.282141	0.000017	-10.8	1.2	1614	1872	-0.94	N.A.	N.A.
54	1101	15	0.000953	0.000005	0.282246	0.000020	5.1	1.4	1417	1507	-0.97	N.A.	N.A.
55	592	8	0.000240	0.000002	0.282064	0.000015	-12.1	1.2	1639	1963	-0.99	N.A.	N.A.
56	1114	14	0.000800	0.000005	0.281977	0.000016	-4.0	1.3	1783	1978	-0.98	N.A.	N.A.
57	1070	15	0.000597	0.000005	0.281938	0.000022	-6.2	1.5	1827	2052	-0.98	N.A.	N.A.
58	535	7	0.000318	0.000005	0.282093	0.000017	-12.3	1.2	1602	1930	-0.99	N.A.	N.A.
59	769	10	0.000298	0.000001	0.281851	0.000019	-15.8	1.3	1932	2290	-0.99	N.A.	N.A.
61	847	11	0.000342	0.000002	0.281878	0.000016	-13.1	1.3	1897	2219	-0.99	N.A.	N.A.
62	1954	13	0.000984	0.000020	0.281614	0.000016	1.4	1.3	2292	2388	-0.97	N.A.	N.A.
63	948	12	0.001105	0.000049	0.282057	0.000026	-5.0	1.5	1687	1894	-0.97	N.A.	N.A.
64	2004	14	0.001008	0.000036	0.282300	0.000126	12.4	4.7	1344	1156	-0.97	N.A.	N.A.
65	909	12	0.000441	0.000004	0.282086	0.000017	-4.4	1.3	1617	1832	-0.99	N.A.	N.A.
66	779	10	0.000330	0.000000	0.282173	0.000015	-4.2	1.3	1494	1714	-0.99	N.A.	N.A.
67	500	7	0.000171	0.000000	0.282084	0.000016	-13.4	1.2	1610	1956	-0.99	N.A.	N.A.
68	1537	13	0.001032	0.000004	0.281988	0.000020	5.4	1.4	1779	1847	-0.97	N.A.	N.A.
69	1225	19	0.000655	0.000012	0.281911	0.000019	-3.8	1.5	1868	2058	-0.98	N.A.	N.A.

70	1208	23	0.000717	0.000006	0.281276	0.000018	-26.8	1.6	2735	3183	-0.98	N.A.	N.A.
71	959	13	0.000545	0.000006	0.281634	0.000018	-19.4	1.4	2239	2623	-0.98	N.A.	N.A.
72	936	12	0.000999	0.000004	0.282488	0.000015	10.0	1.3	1080	1121	-0.97	N.A.	N.A.
73	519	7	0.000251	0.000001	0.282109	0.000017	-12.1	1.2	1578	1906	-0.99	N.A.	N.A.
74	893	12	0.001041	0.000007	0.282155	0.000015	-2.7	1.3	1547	1732	-0.97	N.A.	N.A.
75	703	9	0.000173	0.000002	0.282080	0.000014	-9.1	1.2	1615	1900	-0.99	N.A.	N.A.
76	976	13	0.000496	0.000009	0.281962	0.000015	-7.4	1.3	1790	2035	-0.99	N.A.	N.A.
77	1392	14	0.001002	0.000009	0.281995	0.000014	2.5	1.3	1769	1876	-0.97	N.A.	N.A.
78	996	13	0.000770	0.000042	0.281965	0.000016	-7.0	1.3	1798	2032	-0.98	N.A.	N.A.
79	506	7	0.000532	0.000004	0.282137	0.000016	-11.5	1.2	1552	1866	-0.98	N.A.	N.A.
80	1069	16	0.000921	0.000013	0.281901	0.000016	-7.8	1.4	1893	2130	-0.97	N.A.	N.A.
81	912	12	0.000529	0.000007	0.281856	0.000016	-12.6	1.3	1936	2243	-0.98	N.A.	N.A.
82	1196	15	0.000642	0.000006	0.281940	0.000015	-3.4	1.4	1826	2013	-0.98	N.A.	N.A.
83	1488	14	0.001166	0.000015	0.281533	0.000023	-11.9	1.5	2415	2673	-0.96	N.A.	N.A.
84	786	10	0.000328	0.000002	0.282040	0.000014	-8.7	1.2	1676	1949	-0.99	N.A.	N.A.
85	1009	13	0.001357	0.000009	0.282106	0.000015	-2.2	1.3	1630	1798	-0.96	N.A.	N.A.
86	1166	16	0.000724	0.000009	0.281898	0.000020	-5.6	1.4	1888	2099	-0.98	N.A.	N.A.
87	669	9	0.000697	0.000006	0.282555	0.000017	6.8	1.3	978	1069	-0.98	N.A.	N.A.
88	2367	13	0.001153	0.000025	0.280994	0.000016	-11.7	1.4	3150	3368	-0.97	N.A.	N.A.
89	943	12	0.000380	0.000006	0.282028	0.000015	-5.7	1.3	1694	1924	-0.99	N.A.	N.A.
90	521	7	0.000352	0.000002	0.282182	0.000013	-9.5	1.2	1482	1777	-0.99	N.A.	N.A.
91	2408	13	0.000675	0.000012	0.281342	0.000016	2.3	1.4	2642	2711	-0.98	N.A.	N.A.
92	2744	13	0.000647	0.000006	0.281033	0.000015	-1.0	1.4	3057	3149	-0.98	N.A.	N.A.
93	628	9	0.000613	0.000006	0.281997	0.000014	-13.8	1.2	1748	2080	-0.98	N.A.	N.A.
94	946	12	0.001147	0.000009	0.282143	0.000015	-2.0	1.3	1568	1742	-0.97	N.A.	N.A.
95	968	13	0.001121	0.000010	0.282134	0.000016	-1.9	1.3	1580	1752	-0.97	N.A.	N.A.
96	1845	14	0.000499	0.000004	0.281348	0.000016	-9.9	1.4	2623	2857	-0.98	N.A.	N.A.
97	825	11	0.000137	0.000007	0.282134	0.000018	-4.4	1.3	1540	1764	-1.00	N.A.	N.A.
98	489	7	0.001030	0.000003	0.282067	0.000014	-14.5	1.2	1669	2003	-0.97	N.A.	N.A.
99	938	12	0.001244	0.000019	0.282136	0.000015	-2.5	1.3	1582	1760	-0.96	N.A.	N.A.
100	982	13	0.000757	0.000013	0.282089	0.000015	-2.9	1.3	1626	1815	-0.98	N.A.	N.A.

Sample 10GD17 (N25°01'27.6", E113°48'12.1")

1	1095	14	0.000637	0.000004	0.282043	0.000017	-2.0	1.4	1686	1861	-0.98	N.A.	N.A.
2	1160	13	0.000308	0.000001	0.281908	0.000017	-5.1	1.3	1855	2069	-0.99	N.A.	N.A.
3	502	7	0.000274	0.000002	0.282088	0.000018	-13.2	1.2	1608	1950	-0.99	N.A.	N.A.
4	497	7	0.000290	0.000002	0.282129	0.000016	-11.9	1.2	1553	1878	-0.99	N.A.	N.A.
5	942	12	0.000482	0.000001	0.282068	0.000016	-4.4	1.3	1644	1855	-0.99	N.A.	N.A.
6	515	7	0.000449	0.000003	0.282126	0.000020	-11.7	1.3	1563	1880	-0.99	N.A.	N.A.
7	524	7	0.000330	0.000004	0.282097	0.000019	-12.4	1.3	1597	1927	-0.99	N.A.	N.A.
8	535	7	0.000215	0.000001	0.282072	0.000020	-13.1	1.3	1627	1967	-0.99	N.A.	N.A.
9	971	12	0.000679	0.000002	0.282153	0.000015	-0.86	1.3	1536	1702	-0.98	N.A.	N.A.
10	900	12	0.000432	0.000000	0.281915	0.000018	-10.7	1.3	1851	2140	-0.99	N.A.	N.A.
11	975	14	0.000505	0.000003	0.282107	0.000020	-2.3	1.4	1592	1777	-0.98	N.A.	N.A.
12	1195	13	0.000710	0.000005	0.282081	0.000018	1.5	1.4	1637	1766	-0.98	N.A.	N.A.
13	517	7	0.000215	0.000003	0.282082	0.000018	-13.1	1.3	1614	1955	-0.99	N.A.	N.A.
14	533	7	0.000463	0.000004	0.282071	0.000015	-13.2	1.2	1640	1974	-0.99	N.A.	N.A.
15	960	12	0.000945	0.000014	0.282163	0.000016	-0.91	1.3	1532	1696	-0.97	N.A.	N.A.
16	2451	11	0.000317	0.000001	0.281029	0.000015	-7.2	1.3	3036	3216	-0.99	N.A.	N.A.
17	1164	15	0.000345	0.000003	0.281816	0.000016	-8.3	1.4	1981	2232	-0.99	N.A.	N.A.
18	803	10	0.000295	0.000000	0.282192	0.000016	-2.9	1.3	1467	1671	-0.99	N.A.	N.A.
19	544	8	0.000305	0.000008	0.282096	0.000017	-12.0	1.2	1598	1923	-0.99	N.A.	N.A.
20	1316	13	0.002183	0.000039	0.282011	0.000020	0.37	1.4	1802	1920	-0.93	N.A.	N.A.
21	909	12	0.000970	0.000007	0.282160	0.000018	-2.1	1.3	1537	1716	-0.97	N.A.	N.A.
22	1358	14	0.000769	0.000004	0.282239	0.000016	10.6	1.4	1420	1437	-0.98	N.A.	N.A.
23	734	10	0.001623	0.000008	0.282458	0.000022	4.3	1.4	1141	1248	-0.95	N.A.	N.A.
24	1814	13	0.000489	0.000001	0.280919	0.000015	-25.8	1.3	3196	3612	-0.99	N.A.	N.A.
25	531	7	0.000258	0.000003	0.282163	0.000017	-9.9	1.2	1505	1806	-0.99	N.A.	N.A.
26	534	7	0.000359	0.000000	0.282176	0.000016	-9.4	1.2	1491	1784	-0.99	N.A.	N.A.
27	589	8	0.000012	0.000000	0.281645	0.000014	-26.9	1.2	2194	2704	-1.00	N.A.	N.A.
28	1140	14	0.000651	0.000005	0.282054	0.000017	-0.65	1.4	1671	1828	-0.98	N.A.	N.A.
29	920	12	0.000041	0.000000	0.282097	0.000016	-3.5	1.3	1586	1797	-1.00	N.A.	N.A.
30	972	14	0.000268	0.000001	0.282085	0.000019	-3.0	1.4	1612	1809	-0.99	N.A.	N.A.

31	1017	14	0.000407	0.000002	0.282045	0.000016	-3.5	1.3	1672	1871	-0.99	N.A.	N.A.
32	1083	22	0.000424	0.000002	0.282206	0.000022	3.7	1.6	1453	1565	-0.99	N.A.	N.A.
33	902	12	0.000070	0.000000	0.281995	0.000015	-7.6	1.3	1726	1986	-1.00	N.A.	N.A.
34	827	11	0.000270	0.000003	0.281125	0.000017	-40.2	1.3	2905	3547	-0.99	N.A.	N.A.
35	1043	15	0.000661	0.000004	0.282058	0.000020	-2.6	1.4	1666	1850	-0.98	N.A.	N.A.
36	3310	10	0.001107	0.000010	0.280745	0.000019	0.67	1.4	3482	3530	-0.97	N.A.	N.A.
37	2445	11	0.000547	0.000002	0.281011	0.000015	-8.4	1.3	3078	3268	-0.98	N.A.	N.A.
38	963	12	0.001223	0.000009	0.282083	0.000015	-3.9	1.3	1656	1847	-0.96	N.A.	N.A.
39	1029	16	0.000936	0.000029	0.282105	0.000021	-1.4	1.5	1612	1779	-0.97	N.A.	N.A.
40	1060	14	0.001717	0.000015	0.281997	0.000019	-5.2	1.4	1799	1990	-0.95	N.A.	N.A.
41	882	12	0.000112	0.000001	0.282124	0.000017	-3.5	1.3	1553	1764	-1.00	N.A.	N.A.
42	1180	19	0.001369	0.000001	0.282036	0.000024	-1.0	1.6	1728	1877	-0.96	N.A.	N.A.
43	787	10	0.000369	0.000002	0.282169	0.000015	-4.1	1.3	1501	1719	-0.99	N.A.	N.A.
44	977	13	0.000762	0.000016	0.282159	0.000017	-0.55	1.3	1530	1692	-0.98	N.A.	N.A.
45	545	7	0.000162	0.000002	0.282122	0.000015	-11.0	1.2	1557	1873	-1.00	N.A.	N.A.
46	2459	11	0.000550	0.000002	0.280980	0.000017	-9.2	1.3	3120	3317	-0.98	N.A.	N.A.
47	881	11	0.000045	0.000000	0.282130	0.000014	-3.3	1.2	1542	1751	-1.00	N.A.	N.A.
48	1027	15	0.001573	0.000009	0.281985	0.000020	-6.2	1.4	1809	2016	-0.95	N.A.	N.A.
49	557	8	0.000254	0.000001	0.282142	0.000016	-10.1	1.2	1534	1837	-0.99	N.A.	N.A.
50	1049	16	0.000805	0.000010	0.282071	0.000016	-2.1	1.4	1654	1830	-0.98	N.A.	N.A.
51	931	12	0.001059	0.000015	0.282264	0.000023	2.0	1.4	1396	1527	-0.97	N.A.	N.A.
52	535	7	0.000502	0.000002	0.282133	0.000016	-11.0	1.2	1556	1863	-0.98	N.A.	N.A.
53	1433	13	0.001552	0.000026	0.282042	0.000018	4.6	1.4	1727	1806	-0.95	N.A.	N.A.
54	2851	11	0.000667	0.000004	0.280998	0.000020	0.16	1.4	3105	3180	-0.98	N.A.	N.A.
55	1346	13	0.000306	0.000027	0.282001	0.000016	2.3	1.3	1728	1846	-0.99	N.A.	N.A.
56	2754	11	0.000745	0.000007	0.280961	0.000018	-3.5	1.4	3161	3280	-0.98	N.A.	N.A.
57	1049	14	0.000310	0.000003	0.282141	0.000016	0.70	1.3	1537	1687	-0.99	N.A.	N.A.
58	946	12	0.000223	0.000004	0.281873	0.000017	-11.0	1.3	1898	2193	-0.99	N.A.	N.A.
59	2499	12	0.000911	0.000013	0.281052	0.000019	-6.3	1.4	3052	3211	-0.97	N.A.	N.A.
61	526	7	0.000385	0.000005	0.282061	0.000018	-13.7	1.3	1650	1992	-0.99	N.A.	N.A.
62	1018	14	0.000410	0.000006	0.281892	0.000015	-8.9	1.3	1882	2145	-0.99	N.A.	N.A.
63	687	9	0.000715	0.000004	0.282474	0.000021	4.3	1.3	1092	1210	-0.98	N.A.	N.A.

64	529	7	0.000394	0.000012	0.282120	0.000017	-11.6	1.2	1570	1887	-0.99	N.A.	N.A.
65	2497	12	0.000887	0.000008	0.280936	0.000016	-10.5	1.4	3207	3411	-0.97	N.A.	N.A.
66	981	13	0.001036	0.000037	0.282137	0.000019	-1.4	1.4	1573	1740	-0.97	N.A.	N.A.
67	909	12	0.000346	0.000007	0.282080	0.000020	-4.6	1.4	1622	1841	-0.99	N.A.	N.A.
68	1020	16	0.001382	0.000027	0.282079	0.000019	-2.9	1.4	1668	1843	-0.96	N.A.	N.A.
69	951	12	0.000464	0.000003	0.282143	0.000016	-1.5	1.3	1540	1718	-0.99	N.A.	N.A.
70	2488	12	0.000317	0.000004	0.280995	0.000019	-7.6	1.4	3081	3263	-0.99	N.A.	N.A.
71	598	8	0.000459	0.000003	0.282127	0.000016	-9.8	1.2	1563	1854	-0.99	N.A.	N.A.
72	974	13	0.001614	0.000041	0.282159	0.000016	-1.2	1.3	1566	1722	-0.95	N.A.	N.A.
73	514	7	0.000286	0.000001	0.282099	0.000015	-12.6	1.2	1593	1926	-0.99	N.A.	N.A.
74	945	12	0.000277	0.000009	0.281735	0.000016	-16.0	1.3	2088	2440	-0.99	N.A.	N.A.
75	2492	12	0.000492	0.000002	0.281064	0.000016	-5.3	1.3	3003	3157	-0.99	N.A.	N.A.
76	984	13	0.000737	0.000002	0.282134	0.000019	-1.3	1.4	1564	1734	-0.98	N.A.	N.A.
77	1131	15	0.001378	0.000007	0.282152	0.000019	2.1	1.4	1565	1683	-0.96	N.A.	N.A.
78	948	13	0.000724	0.000005	0.282489	0.000018	10.5	1.4	1072	1108	-0.98	N.A.	N.A.
79	2527	13	0.000577	0.000003	0.281281	0.000019	3.0	1.4	2718	2775	-0.98	N.A.	N.A.
80	1235	15	0.000388	0.000009	0.281876	0.000016	-4.6	1.4	1902	2106	-0.99	N.A.	N.A.
81	1105	15	0.000739	0.000005	0.282033	0.000018	-2.2	1.4	1703	1879	-0.98	N.A.	N.A.
82	1162	15	0.000330	0.000002	0.281778	0.000016	-9.7	1.4	2032	2299	-0.99	N.A.	N.A.
83	509	8	0.000356	0.000003	0.282158	0.000015	-10.6	1.2	1515	1823	-0.99	N.A.	N.A.
84	1908	13	0.000715	0.000007	0.281386	0.000018	-7.4	1.4	2586	2785	-0.98	N.A.	N.A.
85	626	8	0.000080	0.000002	0.282025	0.000018	-12.7	1.3	1686	2020	-1.00	N.A.	N.A.
86	1106	15	0.000906	0.000007	0.282159	0.000015	2.1	1.4	1537	1661	-0.97	N.A.	N.A.
87	954	13	0.000445	0.000005	0.281983	0.000016	-7.1	1.3	1759	2003	-0.99	N.A.	N.A.
88	1147	15	0.000547	0.000005	0.281803	0.000017	-9.3	1.4	2009	2267	-0.98	N.A.	N.A.
89	1092	15	0.000405	0.000005	0.281858	0.000015	-8.5	1.4	1928	2182	-0.99	N.A.	N.A.
90	1008	16	0.000423	0.000003	0.282362	0.000016	7.5	1.4	1238	1308	-0.99	N.A.	N.A.
91	762	10	0.000056	0.000000	0.281935	0.000016	-12.8	1.3	1807	2137	-1.00	N.A.	N.A.
92	542	8	0.000328	0.000004	0.282107	0.000015	-11.7	1.2	1584	1904	-0.99	N.A.	N.A.
93	1181	15	0.000486	0.000001	0.281892	0.000017	-5.3	1.4	1885	2097	-0.99	N.A.	N.A.
94	623	12	0.000441	0.000001	0.281912	0.000017	-16.9	1.3	1855	2229	-0.99	N.A.	N.A.
95	686	11	0.000677	0.000004	0.282536	0.000022	6.5	1.4	1004	1098	-0.98	N.A.	N.A.

96	2596	13	0.000225	0.000003	0.281039	0.000015	-3.4	1.4	3016	3147	-0.99	N.A.	N.A.
97	539	7	0.000218	0.000003	0.282084	0.000018	-12.5	1.3	1611	1943	-0.99	N.A.	N.A.
98	1143	16	0.000696	0.000002	0.282080	0.000016	0.33	1.4	1637	1782	-0.98	N.A.	N.A.
99	981	16	0.000570	0.000013	0.282108	0.000015	-2.2	1.4	1593	1776	-0.98	N.A.	N.A.
100	1018	16	0.001116	0.000018	0.282126	0.000018	-1.1	1.4	1591	1751	-0.97	N.A.	N.A.
Sample 10GD19 (N25°01'45.6", E113°48'45.2")													
1	1186	13	0.002426	0.000032	0.282106	0.000017	0.83	1.3	1676	1792	-0.93	N.A.	N.A.
2	1002	87	0.000799	0.000067	0.281900	0.000016	-9.2	4.1	1889	2147	-0.98	N.A.	N.A.
3	1485	12	0.000473	0.000006	0.281455	0.000017	-14.1	1.3	2477	2776	-0.99	N.A.	N.A.
4	873	12	0.000195	0.000001	0.281661	0.000017	-20.2	1.3	2183	2591	-0.99	N.A.	N.A.
5	954	12	0.000229	0.000001	0.281936	0.000016	-8.6	1.3	1813	2080	-0.99	N.A.	N.A.
6	1850	12	0.000669	0.000003	0.281274	0.000016	-12.6	1.3	2735	2996	-0.98	N.A.	N.A.
7	3037	10	0.000384	0.000002	0.280599	0.000019	-9.2	1.4	3611	3786	-0.99	N.A.	N.A.
8	1052	14	0.001241	0.000013	0.282003	0.000014	-4.8	1.3	1768	1965	-0.96	N.A.	N.A.
9	1687	12	0.000547	0.000013	0.281772	0.000017	1.6	1.3	2052	2161	-0.98	N.A.	N.A.
10	956	12	0.001265	0.000022	0.282149	0.000017	-1.7	1.3	1564	1732	-0.96	N.A.	N.A.
11	2334	13	0.000368	0.000002	0.281210	0.000014	-3.6	1.3	2799	2941	-0.99	N.A.	N.A.
12	2557	11	0.000822	0.000011	0.280906	0.000016	-10.0	1.3	3240	3439	-0.98	N.A.	N.A.
13	892	11	0.000574	0.000018	0.282004	0.000016	-7.8	1.3	1736	1988	-0.98	N.A.	N.A.
14	1117	13	0.000821	0.000008	0.282028	0.000015	-2.2	1.3	1714	1888	-0.98	N.A.	N.A.
15	1155	15	0.000393	0.000003	0.281895	0.000014	-5.7	1.3	1876	2096	-0.99	N.A.	N.A.
16	929	12	0.000721	0.000014	0.282009	0.000015	-6.9	1.3	1736	1972	-0.98	N.A.	N.A.
17	2497	11	0.001072	0.000011	0.281093	0.000018	-5.2	1.4	3010	3154	-0.97	N.A.	N.A.
18	979	12	0.000383	0.000011	0.281886	0.000014	-10.0	1.3	1889	2166	-0.99	N.A.	N.A.
19	2011	12	0.000438	0.000011	0.281407	0.000015	-4.0	1.3	2539	2700	-0.99	N.A.	N.A.
20	2358	11	0.000546	0.000005	0.281036	0.000018	-9.5	1.4	3044	3250	-0.98	N.A.	N.A.
21	953	12	0.000636	0.000004	0.282011	0.000013	-6.3	1.3	1730	1960	-0.98	N.A.	N.A.
22	1522	13	0.001302	0.000071	0.281491	0.000014	-12.8	1.3	2481	2743	-0.96	N.A.	N.A.
23	2077	12	0.000589	0.000003	0.281241	0.000017	-8.6	1.3	2773	2981	-0.98	N.A.	N.A.
24	723	9	0.000635	0.000041	0.281728	0.000014	-21.3	1.2	2116	2528	-0.98	N.A.	N.A.
25	824	10	0.001035	0.000006	0.282087	0.000016	-6.6	1.3	1642	1873	-0.97	N.A.	N.A.

26	1067	15	0.000660	0.000008	0.282241	0.000018	4.4	1.4	1413	1516	-0.98	N.A.	N.A.
27	1127	71	0.000680	0.000001	0.281961	0.000021	-4.2	3.4	1800	1998	-0.98	N.A.	N.A.
28	875	11	0.000051	0.000000	0.281992	0.000014	-8.3	1.2	1729	2000	-1.00	N.A.	N.A.
29	1059	16	0.000562	0.000003	0.282135	0.000016	0.51	1.4	1556	1705	-0.98	N.A.	N.A.
30	2592	11	0.000585	0.000004	0.280983	0.000016	-6.1	1.3	3119	3276	-0.98	N.A.	N.A.
31	892	11	0.000010	0.000000	0.281699	0.000014	-18.3	1.3	2121	2512	-1.00	N.A.	N.A.
32	687	11	0.000373	0.000010	0.282543	0.000022	6.9	1.4	987	1079	-0.99	N.A.	N.A.
33	2748	11	0.000789	0.000005	0.280974	0.000015	-3.3	1.3	3147	3263	-0.98	N.A.	N.A.
34	930	12	0.000503	0.000029	0.281983	0.000015	-7.7	1.3	1761	2011	-0.98	N.A.	N.A.
35	3434	10	0.000519	0.000002	0.280592	0.000017	-0.57	1.4	3632	3692	-0.98	N.A.	N.A.
36	1214	13	0.000777	0.000011	0.281890	0.000016	-4.9	1.3	1902	2103	-0.98	N.A.	N.A.
37	937	12	0.001322	0.000005	0.282208	0.000018	-0.04	1.3	1484	1634	-0.96	N.A.	N.A.
38	1791	13	0.000457	0.000004	0.281436	0.000016	-7.9	1.3	2502	2716	-0.99	N.A.	N.A.
39	650	9	0.001019	0.000009	0.282332	0.000014	-1.7	1.2	1300	1484	-0.97	N.A.	N.A.
40	938	12	0.000102	0.000005	0.281704	0.000013	-17.1	1.3	2119	2491	-1.00	N.A.	N.A.
41	995	13	0.000623	0.000003	0.282142	0.000015	-0.67	1.3	1548	1712	-0.98	N.A.	N.A.
42	596	8	0.000298	0.000005	0.282085	0.000015	-11.3	1.2	1613	1926	-0.99	N.A.	N.A.
43	535	7	0.000135	0.000000	0.281827	0.000015	-21.7	1.2	1956	2402	-1.00	N.A.	N.A.
44	1662	13	0.002305	0.000041	0.281849	0.000018	1.8	1.4	2039	2130	-0.93	N.A.	N.A.
45	533	7	0.000450	0.000003	0.282086	0.000013	-12.7	1.2	1618	1946	-0.99	N.A.	N.A.
46	598	8	0.000279	0.000001	0.282436	0.000018	1.2	1.3	1132	1297	-0.99	N.A.	N.A.
47	814	11	0.001218	0.000033	0.282085	0.000019	-7.0	1.3	1653	1885	-0.96	N.A.	N.A.
48	2432	11	0.000951	0.000034	0.281026	0.000021	-8.8	1.4	3090	3278	-0.97	N.A.	N.A.
49	780	10	0.000480	0.000001	0.281758	0.000016	-18.9	1.3	2068	2456	-0.99	N.A.	N.A.
50	960	14	0.000426	0.000003	0.281836	0.000020	-12.2	1.4	1958	2261	-0.99	N.A.	N.A.
51	979	13	0.001424	0.000018	0.282150	0.000017	-1.3	1.3	1570	1729	-0.96	N.A.	N.A.
52	523	7	0.000585	0.000006	0.281651	0.000019	-28.4	1.3	2219	2724	-0.98	N.A.	N.A.
53	931	12	0.000665	0.000005	0.282251	0.000019	1.7	1.4	1400	1538	-0.98	N.A.	N.A.
54	994	13	0.001704	0.000015	0.282169	0.000016	-0.45	1.3	1555	1700	-0.95	N.A.	N.A.
55	2274	12	0.000557	0.000002	0.281163	0.000017	-6.9	1.4	2875	3055	-0.98	N.A.	N.A.
56	1018	14	0.001035	0.000073	0.282073	0.000018	-2.9	1.4	1662	1844	-0.97	N.A.	N.A.
57	1261	14	0.001645	0.000017	0.281938	0.000018	-2.9	1.4	1878	2040	-0.95	N.A.	N.A.

58	1568	27	0.000716	0.000014	0.282543	0.000016	12.1	1.7	995	827	-0.98	N.A.	N.A.
59	1104	17	0.000734	0.000012	0.282117	0.000018	0.74	1.4	1588	1730	-0.98	N.A.	N.A.
61	630	8	0.000317	0.000002	0.280950	0.000018	-30.8	1.3	3141	3913	-0.99	N.A.	N.A.
62	2440	12	0.000348	0.000008	0.280835	0.000015	-14.4	1.3	3296	3559	-0.99	N.A.	N.A.
63	1598	13	0.000558	0.000002	0.281428	0.000016	-12.6	1.3	2519	2795	-0.98	N.A.	N.A.
64	3529	11	0.000548	0.000011	0.280398	0.000019	-5.3	1.4	3891	3999	-0.98	N.A.	N.A.
65	995	13	0.000631	0.000009	0.281804	0.000017	-12.7	1.3	2012	2314	-0.98	N.A.	N.A.
66	3104	11	0.001022	0.000021	0.280747	0.000018	-3.8	1.4	3472	3577	-0.97	N.A.	N.A.
67	1035	15	0.000868	0.000014	0.282127	0.000016	-0.49	1.4	1579	1735	-0.97	N.A.	N.A.
68	2453	12	0.000424	0.000007	0.280862	0.000018	-13.3	1.4	3267	3514	-0.99	N.A.	N.A.
69	980	13	0.000363	0.000003	0.281895	0.000017	-9.6	1.3	1875	2149	-0.99	N.A.	N.A.
70	527	7	0.000478	0.000004	0.282113	0.000016	-11.9	1.2	1582	1901	-0.99	N.A.	N.A.
71	916	12	0.000802	0.000053	0.282107	0.000022	-3.8	1.4	1604	1804	-0.98	N.A.	N.A.
72	1223	15	0.000999	0.000041	0.281356	0.000022	-23.8	1.5	2645	3049	-0.97	N.A.	N.A.
73	602	8	0.000684	0.000012	0.281541	0.000016	-30.6	1.2	2373	2895	-0.98	N.A.	N.A.
74	1645	13	0.000583	0.000006	0.281518	0.000023	-8.4	1.5	2398	2623	-0.98	N.A.	N.A.
75	970	13	0.000606	0.000011	0.282355	0.000020	6.3	1.4	1254	1338	-0.98	N.A.	N.A.
76	976	13	0.000744	0.000016	0.282052	0.000015	-4.4	1.3	1677	1883	-0.98	N.A.	N.A.
77	813	11	0.000523	0.000012	0.282274	0.000019	0.05	1.3	1363	1529	-0.98	N.A.	N.A.
78	1055	14	0.001368	0.000012	0.281978	0.000015	-5.7	1.3	1809	2013	-0.96	N.A.	N.A.
79	539	7	0.000551	0.000003	0.282108	0.000016	-11.8	1.2	1592	1907	-0.98	N.A.	N.A.
80	2500	12	0.000383	0.000007	0.281239	0.000018	1.3	1.4	2761	2840	-0.99	N.A.	N.A.
81	914	12	0.000705	0.000018	0.281989	0.000015	-7.9	1.3	1762	2012	-0.98	N.A.	N.A.
82	1624	14	0.000227	0.000001	0.281521	0.000016	-8.4	1.4	2373	2606	-0.99	N.A.	N.A.
83	963	13	0.000750	0.000023	0.282078	0.000016	-3.7	1.3	1642	1840	-0.98	N.A.	N.A.
84	1188	15	0.000729	0.000006	0.281721	0.000015	-11.5	1.4	2132	2408	-0.98	N.A.	N.A.
85	2612	12	0.001489	0.000008	0.281081	0.000017	-3.8	1.4	3059	3178	-0.96	N.A.	N.A.
86	970	13	0.000103	0.000002	0.282046	0.000018	-4.3	1.3	1659	1875	-1.00	N.A.	N.A.
87	1133	15	0.000148	0.000002	0.281857	0.000014	-7.4	1.3	1916	2161	-1.00	N.A.	N.A.
88	997	13	0.000097	0.000001	0.281942	0.000013	-7.4	1.3	1798	2050	-1.00	N.A.	N.A.
89	948	14	0.000994	0.000010	0.282469	0.000016	9.6	1.3	1107	1152	-0.97	N.A.	N.A.
90	936	13	0.001592	0.000020	0.281913	0.000017	-10.7	1.3	1911	2168	-0.95	N.A.	N.A.

91	979	13	0.000112	0.000001	0.282040	0.000014	-4.3	1.3	1666	1882	-1.00	N.A.	N.A.
92	540	7	0.000313	0.000008	0.282134	0.000015	-10.8	1.2	1547	1857	-0.99	N.A.	N.A.
93	1580	15	0.000562	0.000008	0.281327	0.000017	-16.6	1.4	2655	2976	-0.98	N.A.	N.A.
94	969	13	0.001057	0.000019	0.282097	0.000016	-3.1	1.3	1629	1816	-0.97	N.A.	N.A.
95	573	8	0.000607	0.000007	0.282119	0.000015	-10.7	1.2	1579	1878	-0.98	N.A.	N.A.
96	3072	12	0.000843	0.000012	0.280874	0.000016	0.42	1.4	3286	3348	-0.97	N.A.	N.A.
97	1195	16	0.001110	0.000009	0.281596	0.000018	-16.0	1.4	2325	2641	-0.97	N.A.	N.A.
98	1000	13	0.000697	0.000007	0.282000	0.000015	-5.7	1.3	1747	1967	-0.98	N.A.	N.A.
99	1421	16	0.000568	0.000001	0.281736	0.000017	-5.6	1.4	2101	2305	-0.98	N.A.	N.A.
100	762	11	0.001265	0.000022	0.281678	0.000020	-22.5	1.4	2220	2621	-0.96	N.A.	N.A.

Note: N.A. = not applicable

*$\varepsilon_{Hf}(t) = 10{,}000\times\{[(^{176}Hf/^{177}Hf)_S-(^{176}Lu/^{177}Hf)_S\times(e^{\lambda t}-1)] / [(^{176}Hf/^{177}Hf)_{CHUR,0}-(^{176}Lu/^{177}Hf)_{CHUR}\times(e^{\lambda t}-1)]-1\}$.

†$T_{DM} = 1/\lambda\times\ln\{1+[(^{176}Hf/^{177}Hf)_S-(^{176}Hf/^{177}Hf)_{DM}] /[(^{176}Lu/^{177}Hf)_S-(^{176}Lu/^{177}Hf)_{DM}]\}$.

§$T_{DM}^C = T_{DM}-(T_{DM}-t)\times[(f_{cc}-f_s)/(f_{cc}-f_{DM})]$. $f_{Lu/Hf} = (^{176}Lu/^{177}Hf)_S/(^{176}Lu/^{177}Hf)_{CHUR}-1$.

where, $\lambda = 1.867\times10^{-11}$ $year^{-1}$ (Soderlund et al., 2004); $(^{176}Lu/^{177}Hf)_S$ and $(^{176}Hf/^{177}Hf)_S$ are the measured values of the samples; $(^{176}Lu/^{177}Hf)_{CHUR} = 0.0332$ and $(^{176}Hf/^{177}Hf)_{CHUR,0} = 0.28277$ (Blichert-Toft and Albarède, 1997); $(^{176}Lu/^{177}Hf)_{DM} = 0.0384$ and $(^{176}Hf/^{177}Hf)_{DM} = 0.28325$ (Griffin et al., 2000); $(^{176}Lu/^{177}Hf)_{upper\ crust}=0.0093$ (Amelin et al., 1999); $f_{cc} = [(^{176}Lu/^{177}Hf)_{upper\ crust}/(^{176}Lu/^{177}Hf)_{CHUR}]-1$; $f_s = f_{Lu/Hf}$; $f_{DM} = [(^{176}Lu/^{177}Hf)_{DM}/(^{176}Lu/^{177}Hf)_{CHUR}]-1$; t = zircon crystallization age.

Appendix C1 Detrital zircon U–Pb data for Cambrian–Silurian clastic samples across the lower Palaeozoic Nanhua foreland basin, South China

Spot#	Th (ppm)	U (ppm)	Th/U	Corrected Ratios						Corrected Ages (Ma)					
				$^{207}Pb/^{206}Pb$	1σ	$^{207}Pb/^{235}U$	1σ	$^{206}Pb/^{238}U$	1σ	$^{207}Pb/^{206}Pb$	1σ	$^{207}Pb/^{235}U$	1σ	$^{206}Pb/^{238}U$	1σ
Sample 10GD37, Upper Cambrian, Yulin															
1	338	492	0.69	0.0953	0.0009	3.4585	0.0266	0.2631	0.0040	1534	17	1518	6	1506	20
2	313	558	0.56	0.0848	0.0008	2.7365	0.0212	0.2341	0.0035	1311	18	1338	6	1356	18
3	136	98	1.38	0.0575	0.0012	0.6196	0.0119	0.0781	0.0014	512	19	490	7	485	8
4	187	238	0.78	0.0651	0.0008	1.1546	0.0112	0.1285	0.0020	779	17	779	5	779	11
5	464	583	0.80	0.1474	0.0014	8.5587	0.0632	0.4212	0.0064	2316	16	2292	7	2266	29
6	320	309	1.03	0.0555	0.0007	0.6473	0.0068	0.0845	0.0013	434	17	507	4	523	8
7	93	194	0.48	0.0615	0.0007	1.1025	0.0113	0.1299	0.0020	658	17	755	5	787	12
8	70	103	0.68	0.2284	0.0022	18.1645	0.1440	0.5768	0.0089	3041	15	2998	8	2936	36
9	257	684	0.38	0.0686	0.0007	1.4245	0.0113	0.1507	0.0023	886	18	899	5	905	13
10	113	97	1.17	0.0890	0.0038	2.8258	0.1093	0.2303	0.0042	1404	84	1362	29	1336	22
11	141	272	0.52	0.1431	0.0014	7.3441	0.0558	0.3723	0.0056	2265	16	2154	7	2040	26
12	89	140	0.64	0.1499	0.0015	8.8313	0.0699	0.4273	0.0065	2345	15	2321	7	2293	29
13	60	85	0.70	0.0970	0.0011	3.4524	0.0341	0.2582	0.0041	1567	15	1516	8	1480	21
14	90	111	0.81	0.0702	0.0009	1.2450	0.0143	0.1287	0.0020	933	16	821	6	781	12
15	64	48	1.32	0.0934	0.0017	3.1551	0.0509	0.2451	0.0044	1495	15	1446	12	1413	23
16	86	129	0.67	0.0620	0.0008	1.1074	0.0126	0.1296	0.0020	673	16	757	6	785	12
17	207	277	0.75	0.0750	0.0008	1.7502	0.0149	0.1694	0.0026	1067	17	1027	5	1009	14
18	30	46	0.66	0.1587	0.0017	10.1805	0.0940	0.4654	0.0074	2441	15	2451	9	2463	32
19	110	300	0.37	0.1093	0.0011	4.7381	0.0364	0.3144	0.0048	1788	17	1774	6	1762	23
20	47	64	0.74	0.0740	0.0011	1.8305	0.0243	0.1793	0.0029	1043	15	1056	9	1063	16
21	75	123	0.61	0.1311	0.0013	7.2465	0.0587	0.4009	0.0061	2113	16	2142	7	2173	28
22	35	108	0.33	0.0609	0.0009	0.9122	0.0115	0.1087	0.0017	635	16	658	6	665	10

23	111	368	0.30	0.0572	0.0007	0.6730	0.0065	0.0853	0.0013	501	18	523	4	528	8
24	163	101	1.62	0.0557	0.0009	0.6473	0.0097	0.0844	0.0014	439	16	507	6	522	8
25	95	88	1.08	0.0941	0.0011	3.1372	0.0306	0.2418	0.0038	1510	16	1442	7	1396	20
26	164	439	0.37	0.0970	0.0009	3.8060	0.0286	0.2845	0.0043	1568	17	1594	6	1614	21
27	41	90	0.46	0.0623	0.0011	0.9177	0.0150	0.1069	0.0018	683	16	661	8	655	10
28	241	365	0.66	0.0935	0.0009	3.3309	0.0256	0.2584	0.0039	1498	17	1488	6	1481	20
29	229	199	1.15	0.0731	0.0010	1.7429	0.0196	0.1730	0.0027	1016	16	1025	7	1029	15
30	162	495	0.33	0.0584	0.0006	0.7988	0.0070	0.0992	0.0015	544	18	596	4	610	9
31	196	196	1.00	0.0571	0.0008	0.6376	0.0079	0.0810	0.0013	497	16	501	5	502	8
32	50	124	0.40	0.1597	0.0016	10.0021	0.0821	0.4545	0.0070	2452	15	2435	8	2415	31
33	207	431	0.48	0.0883	0.0008	3.0164	0.0230	0.2477	0.0037	1390	17	1412	6	1427	19
34	142	251	0.57	0.0702	0.0021	1.5204	0.0378	0.1571	0.0025	934	62	939	15	941	14
35	55	74	0.74	0.0724	0.0012	1.6108	0.0225	0.1615	0.0027	996	15	974	9	965	15
36	112	282	0.40	0.0700	0.0008	1.5715	0.0143	0.1630	0.0025	927	17	959	6	973	14
37	266	324	0.82	0.0863	0.0011	2.8281	0.0294	0.2378	0.0037	1344	15	1363	8	1375	19
38	56	50	1.11	0.0714	0.0013	1.6209	0.0259	0.1647	0.0028	969	16	978	10	983	16
39	111	238	0.47	0.0662	0.0007	1.4537	0.0134	0.1594	0.0024	811	17	911	6	954	14
40	229	466	0.49	0.0659	0.0007	1.3481	0.0109	0.1484	0.0022	804	18	867	5	892	12
41	147	171	0.86	0.1498	0.0015	8.5764	0.0678	0.4154	0.0063	2343	15	2294	7	2240	29
42	67	951	0.07	0.0688	0.0007	1.4220	0.0107	0.1500	0.0022	891	18	898	4	901	13
43	95	385	0.25	0.0732	0.0007	1.9153	0.0153	0.1898	0.0029	1020	18	1086	5	1120	15
44	262	668	0.39	0.0579	0.0006	0.8233	0.0067	0.1032	0.0016	524	19	610	4	633	9
45	147	356	0.41	0.0964	0.0009	3.7243	0.0284	0.2803	0.0042	1556	17	1577	6	1593	21
46	151	208	0.73	0.0754	0.0008	1.9928	0.0172	0.1917	0.0029	1080	17	1113	6	1130	16
47	157	480	0.33	0.0682	0.0007	1.5418	0.0122	0.1640	0.0025	875	18	947	5	979	14
48	84	166	0.51	0.0690	0.0010	1.4011	0.0183	0.1474	0.0024	898	15	889	8	886	13
49	114	586	0.19	0.0676	0.0007	1.5157	0.0118	0.1627	0.0024	856	18	937	5	972	13
50	74	241	0.31	0.0730	0.0008	1.9139	0.0162	0.1903	0.0029	1013	17	1086	6	1123	16
51	315	465	0.68	0.0800	0.0008	2.4459	0.0187	0.2219	0.0033	1196	18	1256	6	1292	17
52	1588	365	4.35	0.0695	0.0008	1.3356	0.0131	0.1394	0.0021	914	16	861	6	841	12
53	174	685	0.25	0.0682	0.0007	1.5010	0.0116	0.1598	0.0024	873	18	931	5	955	13
54	50	132	0.38	0.1032	0.0011	4.3044	0.0374	0.3026	0.0046	1683	16	1694	7	1704	23

55	43	157	0.27	0.1032	0.0010	4.3752	0.0358	0.3075	0.0046	1683	16	1708	7	1728	23
56	254	341	0.74	0.0559	0.0007	0.6486	0.0068	0.0842	0.0013	449	17	508	4	521	8
57	18	45	0.40	0.0686	0.0012	1.3751	0.0210	0.1454	0.0024	888	15	878	9	875	14
58	212	649	0.33	0.0709	0.0008	1.5294	0.0134	0.1564	0.0024	955	17	942	5	937	13
59	63	281	0.22	0.0674	0.0007	1.4388	0.0125	0.1548	0.0023	851	17	905	5	928	13
~~*60*~~	~~*18*~~	~~*48*~~	~~*0.39*~~	~~*0.1148*~~	~~*0.0028*~~	~~*4.0244*~~	~~*0.0706*~~	~~*0.2542*~~	~~*0.0042*~~	~~*1877*~~	~~*44*~~	~~*1639*~~	~~*14*~~	~~*1460*~~	~~*21*~~
61	421	306	1.38	0.0687	0.0007	1.5310	0.0129	0.1616	0.0024	890	17	943	5	966	13
62	211	208	1.01	0.0638	0.0007	1.1690	0.0112	0.1329	0.0020	736	17	786	5	804	11
63	70	113	0.62	0.0860	0.0010	2.9467	0.0270	0.2487	0.0038	1337	16	1394	7	1432	20
64	159	43	3.70	0.1599	0.0018	10.0697	0.0933	0.4570	0.0072	2454	15	2441	9	2426	32
65	181	191	0.95	0.0552	0.0008	0.6426	0.0078	0.0844	0.0013	422	16	504	5	522	8
66	14	88	0.15	0.1555	0.0017	8.7983	0.0782	0.4106	0.0064	2407	15	2317	8	2217	29
67	46	496	0.09	0.0897	0.0009	3.1315	0.0241	0.2532	0.0038	1420	17	1440	6	1455	19
68	224	429	0.52	0.0582	0.0006	0.7986	0.0070	0.0996	0.0015	537	18	596	4	612	9
69	48	110	0.44	0.0661	0.0009	1.3372	0.0146	0.1467	0.0023	811	16	862	6	882	13
70	2295	2951	0.78	0.1025	0.0009	4.0600	0.0284	0.2874	0.0042	1670	17	1646	6	1628	21
71	59	147	0.40	0.0579	0.0008	0.7926	0.0093	0.0993	0.0015	526	16	593	5	610	9
72	92	245	0.37	0.1601	0.0015	10.4126	0.0761	0.4718	0.0070	2457	15	2472	7	2491	31
73	211	117	1.81	0.0671	0.0008	1.4585	0.0151	0.1578	0.0024	840	16	913	6	944	13
74	194	270	0.72	0.0677	0.0007	1.4838	0.0125	0.1589	0.0024	861	17	924	5	951	13
75	68	155	0.44	0.0711	0.0008	1.7706	0.0161	0.1806	0.0027	961	17	1035	6	1070	15
76	155	509	0.31	0.1034	0.0010	4.3741	0.0316	0.3070	0.0045	1686	17	1707	6	1726	22
77	529	861	0.61	0.0739	0.0007	1.8927	0.0139	0.1858	0.0027	1039	18	1079	5	1099	15
78	219	240	0.91	0.0873	0.0009	2.7262	0.0223	0.2265	0.0034	1368	16	1336	6	1316	18
79	81	160	0.51	0.1551	0.0015	9.7105	0.0734	0.4542	0.0068	2403	15	2408	7	2414	30
80	168	288	0.58	0.1560	0.0015	9.7450	0.0728	0.4532	0.0067	2413	15	2411	7	2409	30
81	260	580	0.45	0.0621	0.0007	0.8965	0.0079	0.1048	0.0016	677	18	650	4	642	9
82	187	376	0.50	0.1027	0.0010	4.2392	0.0316	0.2995	0.0044	1674	16	1682	6	1689	22
83	98	169	0.58	0.1567	0.0015	9.7637	0.0733	0.4520	0.0067	2421	15	2413	7	2404	30
84	370	380	0.97	0.0574	0.0006	0.7239	0.0065	0.0915	0.0014	508	18	553	4	564	8
85	168	189	0.89	0.0754	0.0008	1.9977	0.0172	0.1923	0.0029	1079	17	1115	6	1134	16
86	128	254	0.50	0.0669	0.0007	1.3931	0.0120	0.1511	0.0023	835	17	886	5	907	13

87	580	415	1.40	0.0739	0.0007	1.8475	0.0143	0.1813	0.0027	1040	18	1063	5	1074	15
88	190	246	0.77	0.0618	0.0007	1.0540	0.0102	0.1238	0.0019	666	17	731	5	753	11
89	142	233	0.61	0.0605	0.0007	0.9941	0.0097	0.1193	0.0018	620	17	701	5	727	10
90	155	296	0.52	0.0674	0.0007	1.4439	0.0121	0.1554	0.0023	850	17	907	5	931	13
91	67	144	0.46	0.0682	0.0008	1.4208	0.0139	0.1511	0.0023	876	16	898	6	907	13
92	86	173	0.50	0.0744	0.0008	1.8014	0.0160	0.1758	0.0026	1051	16	1046	6	1044	14
93	486	460	1.06	0.0717	0.0007	1.6845	0.0132	0.1705	0.0025	977	18	1003	5	1015	14
94	55	151	0.37	0.0655	0.0008	1.2453	0.0124	0.1381	0.0021	789	16	821	6	834	12
95	118	291	0.41	0.1515	0.0014	8.1795	0.0608	0.3919	0.0058	2362	15	2251	7	2131	27
96	333	614	0.54	0.0679	0.0007	1.5130	0.0118	0.1618	0.0024	864	18	936	5	967	13
97	1439	1436	1.00	0.1079	0.0010	4.6519	0.0331	0.3129	0.0046	1764	16	1759	6	1755	22
98	78	138	0.56	0.1037	0.0011	3.8783	0.0321	0.2715	0.0041	1690	16	1609	7	1549	21
99	301	554	0.54	0.0751	0.0007	1.9461	0.0145	0.1879	0.0028	1072	18	1097	5	1110	15
100	70	96	0.73	0.0789	0.0010	1.9027	0.0197	0.1750	0.0027	1170	15	1082	7	1039	15
101	721	403	1.79	0.0712	0.0007	1.4211	0.0115	0.1449	0.0021	962	17	898	5	872	12
102	227	453	0.50	0.1003	0.0009	4.1005	0.0301	0.2966	0.0044	1630	16	1654	6	1674	22
103	858	404	2.12	0.0570	0.0006	0.6309	0.0058	0.0804	0.0012	490	18	497	4	498	7
104	1116	1600	0.70	0.0958	0.0009	3.4006	0.0236	0.2576	0.0038	1544	17	1505	5	1477	19
105	130	161	0.80	0.0676	0.0008	1.3964	0.0134	0.1498	0.0023	857	16	887	6	900	13
106	132	311	0.42	0.0618	0.0007	1.1286	0.0101	0.1325	0.0020	668	17	767	5	802	11
107	49	275	0.18	0.0757	0.0008	1.8427	0.0153	0.1766	0.0026	1088	17	1061	5	1048	14
108	28	83	0.34	0.0684	0.0010	1.3600	0.0164	0.1443	0.0023	881	15	872	7	869	13
109	215	372	0.58	0.0663	0.0007	1.5303	0.0124	0.1675	0.0025	816	18	943	5	998	14
110	31	70	0.44	0.1652	0.0017	10.6317	0.0865	0.4669	0.0070	2510	15	2491	8	2470	31
111	132	267	0.49	0.0567	0.0007	0.6239	0.0067	0.0799	0.0012	479	16	492	4	495	7
112	192	406	0.47	0.0742	0.0007	1.6329	0.0128	0.1598	0.0024	1046	17	983	5	955	13
113	95	154	0.62	0.1873	0.0018	12.9752	0.0959	0.5027	0.0074	2719	15	2678	7	2625	32
114	98	127	0.77	0.0570	0.0009	0.6301	0.0086	0.0803	0.0013	491	15	496	5	498	8
115	71	76	0.95	0.1509	0.0016	8.3238	0.0698	0.4004	0.0061	2356	15	2267	8	2171	28
116	73	348	0.21	0.0570	0.0007	0.7085	0.0067	0.0902	0.0013	491	17	544	4	557	8
117	580	732	0.79	0.0671	0.0007	1.2156	0.0105	0.1315	0.0019	841	17	808	5	796	11
118	72	75	0.97	0.1545	0.0016	9.3006	0.0776	0.4369	0.0066	2396	15	2368	8	2337	30

119	112	150	0.75	0.1801	0.0017	12.8805	0.0959	0.5191	0.0077	2654	15	2671	7	2695	32
120	234	166	1.41	0.0668	0.0008	1.3046	0.0130	0.1418	0.0021	831	16	848	6	855	12
Sample 10GD42-1, Lower Ordovician, Yulin															
1	108	56	1.93	0.0564	0.0012	0.6155	0.0121	0.0792	0.0014	468	19	487	8	491	8
2	71	48	1.46	0.2219	0.0022	17.8722	0.1494	0.5842	0.0090	2995	14	2983	8	2966	37
3	36	44	0.82	0.0788	0.0019	1.6619	0.0363	0.1530	0.0030	1167	19	994	14	918	17
4	326	565	0.58	0.0562	0.0006	0.6233	0.0054	0.0805	0.0012	459	18	492	3	499	7
5	154	610	0.25	0.1551	0.0014	9.3246	0.0651	0.4361	0.0064	2403	16	2370	6	2333	29
6	277	343	0.81	0.0607	0.0007	0.8691	0.0078	0.1039	0.0016	628	18	635	4	637	9
7	90	149	0.61	0.1510	0.0014	9.2942	0.0703	0.4464	0.0067	2358	15	2367	7	2379	30
8	72	146	0.49	0.0748	0.0009	1.9147	0.0182	0.1857	0.0028	1063	16	1086	6	1098	15
9	289	463	0.62	0.0806	0.0008	2.0428	0.0155	0.1839	0.0027	1211	17	1130	5	1088	15
10	316	369	0.86	0.0553	0.0006	0.6496	0.0060	0.0852	0.0013	426	18	508	4	527	8
11	134	287	0.47	0.0713	0.0007	1.4537	0.0123	0.1479	0.0022	966	17	911	5	889	12
12	73	123	0.59	0.1268	0.0013	6.4895	0.0527	0.3714	0.0056	2053	16	2044	7	2036	26
13	141	633	0.22	0.0569	0.0006	0.6599	0.0055	0.0841	0.0013	489	19	515	3	520	7
14	35	102	0.34	0.0731	0.0009	1.6514	0.0175	0.1640	0.0025	1016	16	990	7	979	14
15	93	121	0.77	0.0698	0.0008	1.4961	0.0152	0.1555	0.0024	922	16	929	6	932	13
16	46	59	0.79	0.0739	0.0010	1.8159	0.0218	0.1782	0.0028	1039	15	1051	8	1057	15
17	238	897	0.26	0.1040	0.0009	4.5636	0.0322	0.3185	0.0047	1696	17	1743	6	1782	23
18	90	334	0.27	0.1325	0.0012	7.0714	0.0512	0.3872	0.0057	2131	16	2120	6	2110	27
19	51	261	0.19	0.0775	0.0009	2.1315	0.0200	0.1995	0.0031	1134	16	1159	6	1173	16
20	200	300	0.67	0.0681	0.0010	1.3371	0.0170	0.1424	0.0023	873	15	862	7	858	13
21	38	106	0.36	0.0671	0.0009	1.3897	0.0149	0.1502	0.0023	841	16	885	6	902	13
22	186	372	0.50	0.0673	0.0007	1.3834	0.0112	0.1492	0.0022	847	18	882	5	896	13
23	102	333	0.31	0.1046	0.0010	4.1819	0.0310	0.2902	0.0043	1706	17	1670	6	1642	22
24	124	419	0.30	0.0782	0.0008	2.1216	0.0163	0.1968	0.0029	1152	18	1156	5	1158	16
25	25	30	0.83	0.1219	0.0015	6.1716	0.0651	0.3673	0.0059	1984	15	2000	9	2017	28
26	81	97	0.83	0.0676	0.0009	1.4489	0.0155	0.1555	0.0024	856	16	909	6	932	13
27	66	46	1.42	0.1614	0.0017	10.3264	0.0923	0.4642	0.0072	2470	15	2464	8	2458	32
28	129	318	0.41	0.0728	0.0007	1.7669	0.0142	0.1761	0.0026	1008	18	1033	5	1046	14

29	92	259	0.35	0.0655	0.0007	1.3639	0.0117	0.1512	0.0023	789	18	874	5	908	13
30	300	204	1.47	0.0680	0.0007	1.4547	0.0131	0.1552	0.0023	869	17	912	5	930	13
31	158	291	0.54	0.0709	0.0007	1.5659	0.0130	0.1602	0.0024	955	17	957	5	958	13
32	122	233	0.52	0.0835	0.0008	2.5634	0.0205	0.2227	0.0033	1281	17	1290	6	1296	18
33	124	371	0.33	0.0695	0.0007	1.3382	0.0114	0.1396	0.0021	915	17	862	5	843	12
34	37	158	0.23	0.0713	0.0008	1.5641	0.0147	0.1593	0.0024	965	17	956	6	953	14
35	420	305	1.38	0.0620	0.0007	1.0749	0.0094	0.1259	0.0019	673	18	741	5	764	11
36	54	228	0.24	0.0724	0.0008	1.7604	0.0161	0.1763	0.0027	998	17	1031	6	1047	15
37	234	567	0.41	0.0753	0.0008	1.7431	0.0144	0.1680	0.0025	1076	17	1025	5	1001	14
38	393	262	1.50	0.0774	0.0008	1.9687	0.0162	0.1845	0.0028	1132	17	1105	6	1092	15
39	60	376	0.16	0.0732	0.0008	1.6923	0.0141	0.1676	0.0025	1021	17	1006	5	999	14
40	409	997	0.41	0.0630	0.0007	0.7199	0.0061	0.0829	0.0012	708	18	551	4	513	7
41	134	744	0.18	0.0810	0.0008	2.1921	0.0170	0.1964	0.0029	1221	17	1179	5	1156	16
42	102	335	0.30	0.0748	0.0007	1.9735	0.0157	0.1915	0.0029	1063	18	1107	5	1129	15
43	158	428	0.37	0.0701	0.0007	1.5466	0.0124	0.1602	0.0024	930	18	949	5	958	13
44	188	349	0.54	0.0738	0.0007	1.9035	0.0152	0.1873	0.0028	1035	18	1082	5	1107	15
45	329	429	0.77	0.0563	0.0006	0.6585	0.0059	0.0848	0.0013	465	18	514	4	525	8
46	72	164	0.44	0.1254	0.0012	6.6714	0.0519	0.3860	0.0058	2034	16	2069	7	2104	27
47	267	658	0.41	0.0635	0.0007	0.7356	0.0061	0.0841	0.0013	725	18	560	4	520	7
48	394	631	0.62	0.0619	0.0007	0.7069	0.0065	0.0829	0.0013	670	17	543	4	513	7
49	96	162	0.59	0.0750	0.0008	1.9112	0.0173	0.1850	0.0028	1067	17	1085	6	1094	15
50	433	1143	0.38	0.0563	0.0006	0.6990	0.0055	0.0902	0.0013	462	19	538	3	556	8
51	267	627	0.43	0.0568	0.0006	0.6644	0.0057	0.0848	0.0013	485	19	517	3	525	8
52	275	347	0.79	0.0701	0.0007	1.5350	0.0129	0.1590	0.0024	930	17	944	5	951	13
53	709	822	0.86	0.1010	0.0009	4.1971	0.0306	0.3015	0.0045	1643	17	1673	6	1699	22
54	98	170	0.58	0.0745	0.0008	1.8027	0.0168	0.1756	0.0027	1055	16	1046	6	1043	15
55	135	98	1.37	0.0689	0.0010	1.4839	0.0188	0.1564	0.0025	894	15	924	8	937	14
56	592	850	0.70	0.0769	0.0023	1.9487	0.0492	0.1839	0.0029	1118	61	1098	17	1088	16
57	208	247	0.84	0.0562	0.0007	0.6530	0.0070	0.0843	0.0013	460	17	510	4	522	8
58	84	261	0.32	0.1044	0.0010	4.1863	0.0333	0.2909	0.0044	1704	16	1671	7	1646	22
59	71	62	1.13	0.0577	0.0012	0.6746	0.0126	0.0848	0.0015	520	18	523	8	524	9
60	160	378	0.42	0.0709	0.0007	1.5223	0.0125	0.1558	0.0023	954	18	939	5	933	13

61	172	401	0.43	0.0739	0.0008	1.7245	0.0142	0.1692	0.0025	1040	17	1018	5	1008	14
~~*62*~~	~~*381*~~	~~*721*~~	~~*0.53*~~	~~*0.1358*~~	~~*0.0031*~~	~~*3.7806*~~	~~*0.0607*~~	~~*0.2019*~~	~~*0.0032*~~	~~*2175*~~	~~*40*~~	~~*1589*~~	~~*13*~~	~~*1185*~~	~~*17*~~
63	459	594	0.77	0.0969	0.0009	3.7155	0.0277	0.2781	0.0041	1566	17	1575	6	1582	21
64	931	1719	0.54	0.0607	0.0006	0.6854	0.0057	0.0819	0.0012	630	18	530	3	507	7
65	163	303	0.54	0.0643	0.0008	1.0943	0.0116	0.1235	0.0019	752	16	751	6	750	11
66	70	887	0.08	0.1068	0.0010	4.5373	0.0332	0.3083	0.0046	1745	17	1738	6	1733	23
67	386	531	0.73	0.0580	0.0006	0.6780	0.0061	0.0849	0.0013	528	18	526	4	525	8
68	183	361	0.51	0.0696	0.0007	1.5402	0.0127	0.1605	0.0024	918	18	947	5	959	13
69	76	179	0.43	0.2316	0.0022	19.3610	0.1456	0.6064	0.0091	3063	15	3060	7	3055	37
70	225	146	1.55	0.0575	0.0008	0.6521	0.0082	0.0823	0.0013	510	16	510	5	510	8
71	57	64	0.88	0.0686	0.0010	1.4374	0.0186	0.1520	0.0024	886	15	905	8	912	14
72	189	375	0.50	0.0578	0.0019	0.6609	0.0193	0.0829	0.0013	523	75	515	12	513	8
73	128	283	0.45	0.1209	0.0014	5.2990	0.0501	0.3179	0.0050	1970	15	1869	8	1780	24
74	81	703	0.12	0.0734	0.0007	1.7415	0.0135	0.1721	0.0026	1025	18	1024	5	1024	14
75	291	1146	0.25	0.1651	0.0015	6.9801	0.0508	0.3067	0.0046	2509	15	2109	6	1724	22
76	119	221	0.54	0.0709	0.0008	1.5403	0.0139	0.1576	0.0024	955	17	947	6	943	13
77	296	448	0.66	0.0586	0.0007	0.6628	0.0062	0.0820	0.0012	553	18	516	4	508	7
78	67	69	0.98	0.0771	0.0010	2.0990	0.0237	0.1976	0.0031	1122	15	1148	8	1162	17
79	425	475	0.89	0.0573	0.0006	0.6909	0.0062	0.0875	0.0013	503	18	533	4	541	8
80	280	569	0.49	0.0828	0.0008	2.3666	0.0188	0.2072	0.0031	1265	17	1233	6	1214	17
81	90	155	0.58	0.0724	0.0023	1.4833	0.0412	0.1485	0.0024	998	67	924	17	893	14
82	165	351	0.47	0.1434	0.0014	8.3329	0.0626	0.4216	0.0063	2268	16	2268	7	2268	29
83	123	265	0.46	0.0697	0.0008	1.4752	0.0131	0.1534	0.0023	921	17	920	5	920	13
84	124	408	0.30	0.0714	0.0007	1.7113	0.0140	0.1739	0.0026	968	18	1013	5	1034	14
85	202	126	1.60	0.1612	0.0016	10.1382	0.0822	0.4562	0.0069	2468	15	2447	7	2423	31
86	61	106	0.58	0.0765	0.0009	1.9760	0.0200	0.1873	0.0029	1109	16	1107	7	1107	16
87	319	250	1.28	0.0691	0.0008	1.3972	0.0127	0.1466	0.0022	903	17	888	5	882	13
88	96	53	1.82	0.0724	0.0011	1.6244	0.0220	0.1627	0.0027	997	15	980	9	972	15
89	221	394	0.56	0.2714	0.0026	24.5632	0.1942	0.6564	0.0100	3314	14	3291	8	3253	39
90	229	427	0.54	0.1576	0.0015	9.5894	0.0720	0.4413	0.0066	2430	15	2396	7	2357	30
91	158	216	0.73	0.0786	0.0009	2.1009	0.0202	0.1938	0.0030	1163	16	1149	7	1142	16
92	94	368	0.26	0.0770	0.0010	1.8613	0.0202	0.1753	0.0028	1121	15	1067	7	1041	15

93	126	74	1.71	0.0574	0.0011	0.6639	0.0108	0.0838	0.0014	508	17	517	7	519	8
94	85	185	0.46	0.0860	0.0009	2.6679	0.0230	0.2251	0.0034	1338	16	1320	6	1309	18
95	94	204	0.46	0.0717	0.0008	1.6035	0.0148	0.1622	0.0025	978	17	972	6	969	14
96	176	410	0.43	0.0703	0.0007	1.5517	0.0129	0.1602	0.0024	936	18	951	5	958	13
97	167	273	0.61	0.1042	0.0010	4.3517	0.0345	0.3029	0.0046	1701	16	1703	7	1705	23
98	100	282	0.35	0.0757	0.0008	1.8774	0.0163	0.1800	0.0027	1086	17	1073	6	1067	15
99	28	63	0.44	0.0698	0.0010	1.4794	0.0192	0.1538	0.0025	922	15	922	8	922	14
100	289	320	0.90	0.0822	0.0010	2.2563	0.0225	0.1991	0.0031	1250	16	1199	7	1170	17
101	171	297	0.58	0.0735	0.0008	1.6926	0.0150	0.1670	0.0025	1027	17	1006	6	996	14
102	56	187	0.30	0.0668	0.0008	1.3893	0.0139	0.1509	0.0023	831	17	884	6	906	13
103	250	496	0.50	0.0748	0.0008	1.7638	0.0144	0.1711	0.0026	1062	17	1032	5	1018	14
104	66	177	0.37	0.0685	0.0018	1.4376	0.0299	0.1522	0.0024	884	55	905	12	913	13
105	412	517	0.80	0.0723	0.0007	1.6280	0.0134	0.1634	0.0025	994	18	981	5	975	14
106	192	293	0.65	0.0648	0.0024	1.1914	0.0396	0.1333	0.0022	768	80	797	18	807	13
107	90	133	0.68	0.0731	0.0009	1.5928	0.0162	0.1580	0.0024	1017	16	967	6	945	14
108	112	1021	0.11	0.0724	0.0008	1.5902	0.0135	0.1593	0.0024	997	17	966	5	953	13
109	328	355	0.92	0.0794	0.0009	2.0997	0.0206	0.1917	0.0030	1183	16	1149	7	1130	16
110	96	297	0.32	0.0728	0.0008	1.6251	0.0142	0.1619	0.0025	1008	17	980	5	967	14
111	229	114	2.02	0.0574	0.0009	0.6522	0.0090	0.0824	0.0013	507	16	510	6	511	8
~~*112*~~	~~*652*~~	~~*2619*~~	~~*0.25*~~	~~*0.0774*~~	~~*0.0008*~~	~~*0.8704*~~	~~*0.0069*~~	~~*0.0816*~~	~~*0.0012*~~	~~*1131*~~	~~*17*~~	~~*636*~~	~~*4*~~	~~*505*~~	~~*7*~~
113	211	626	0.34	0.0721	0.0007	1.6484	0.0132	0.1658	0.0025	988	18	989	5	989	14
114	184	310	0.59	0.0709	0.0021	1.4930	0.0379	0.1528	0.0024	954	63	928	15	916	14
115	40	134	0.30	0.0709	0.0017	1.4901	0.0279	0.1524	0.0024	955	51	926	11	914	13
116	294	425	0.69	0.0782	0.0008	2.1436	0.0174	0.1988	0.0030	1151	17	1163	6	1169	16
117	192	170	1.13	0.1607	0.0016	10.1950	0.0817	0.4600	0.0070	2463	15	2453	7	2440	31
118	524	362	1.45	0.0706	0.0008	1.5150	0.0133	0.1556	0.0024	946	17	936	5	932	13
119	223	350	0.64	0.0719	0.0008	1.5887	0.0137	0.1601	0.0024	984	17	966	5	957	14
120	47	59	0.80	0.0720	0.0011	1.6361	0.0224	0.1647	0.0027	987	15	984	9	983	15
Sample 10GD42, Lower Ordovician, Yulin															
1	193	383	0.50	0.0683	0.0007	1.4378	0.0116	0.1526	0.0022	878	17	905	5	916	12
2	178	303	0.59	0.0716	0.0007	1.6477	0.0136	0.1669	0.0024	974	17	989	5	995	13

3	106	107	0.99	0.0561	0.0009	0.6527	0.0093	0.0843	0.0013	458	16	510	6	522	8
4	148	180	0.83	0.0984	0.0010	3.9274	0.0308	0.2893	0.0042	1594	16	1619	6	1638	21
5	37	29	1.26	0.0750	0.0019	1.8591	0.0415	0.1797	0.0035	1069	20	1067	15	1065	19
6	61	105	0.58	0.1005	0.0011	4.1509	0.0353	0.2994	0.0044	1634	15	1664	7	1688	22
7	79	95	0.83	0.1502	0.0015	8.8662	0.0703	0.4281	0.0063	2348	15	2324	7	2297	29
8	224	421	0.53	0.0651	0.0007	1.3164	0.0104	0.1465	0.0021	779	18	853	5	882	12
9	67	96	0.70	0.1486	0.0015	9.0598	0.0713	0.4420	0.0065	2330	15	2344	7	2360	29
10	51	79	0.65	0.0585	0.0010	0.7397	0.0110	0.0917	0.0015	548	16	562	6	566	9
11	249	383	0.65	0.0547	0.0006	0.6195	0.0058	0.0821	0.0012	401	17	490	4	509	7
12	324	330	0.98	0.0539	0.0006	0.6148	0.0059	0.0827	0.0012	366	17	487	4	512	7
13	252	481	0.52	0.1461	0.0013	8.4455	0.0582	0.4191	0.0060	2301	15	2280	6	2256	27
14	110	174	0.63	0.0586	0.0008	0.7658	0.0086	0.0948	0.0014	553	16	577	5	584	8
15	140	128	1.10	0.1546	0.0015	9.6287	0.0728	0.4518	0.0066	2397	15	2400	7	2403	29
16	93	155	0.60	0.0625	0.0008	1.0469	0.0111	0.1215	0.0018	691	16	727	6	739	11
17	85	138	0.62	0.0688	0.0008	1.5544	0.0152	0.1639	0.0025	892	16	952	6	978	14
18	175	310	0.57	0.0665	0.0007	1.3360	0.0111	0.1457	0.0021	821	17	862	5	877	12
~~*19*~~	~~*26*~~	~~*43*~~	~~*0.60*~~	~~*0.0856*~~	~~*0.0027*~~	~~*1.2335*~~	~~*0.0343*~~	~~*0.1045*~~	~~*0.0024*~~	~~*1330*~~	~~*25*~~	~~*816*~~	~~*16*~~	~~*640*~~	~~*14*~~
20	259	271	0.96	0.0539	0.0007	0.6100	0.0063	0.0820	0.0012	368	17	484	4	508	7
21	361	581	0.62	0.0573	0.0006	0.7541	0.0062	0.0955	0.0014	501	18	571	4	588	8
22	272	235	1.16	0.1563	0.0014	9.6692	0.0691	0.4487	0.0065	2416	15	2404	7	2389	29
23	73	28	2.59	0.0612	0.0014	1.0762	0.0229	0.1276	0.0023	646	21	742	11	774	13
24	513	387	1.32	0.0553	0.0006	0.6691	0.0061	0.0878	0.0013	424	17	520	4	542	8
25	319	446	0.71	0.0549	0.0006	0.6472	0.0057	0.0854	0.0013	409	18	507	4	528	7
26	54	239	0.23	0.0674	0.0007	1.4206	0.0122	0.1529	0.0023	850	17	898	5	917	13
27	51	415	0.12	0.0718	0.0007	1.7131	0.0131	0.1730	0.0025	980	18	1013	5	1029	14
28	195	178	1.10	0.0625	0.0007	1.0955	0.0108	0.1271	0.0019	692	16	751	5	771	11
29	100	162	0.62	0.0561	0.0008	0.6275	0.0076	0.0811	0.0013	457	16	495	5	503	7
30	55	35	1.58	0.0782	0.0012	2.3518	0.0320	0.2181	0.0036	1152	15	1228	10	1272	19
31	172	489	0.35	0.0568	0.0006	0.7822	0.0066	0.1000	0.0015	482	18	587	4	614	9
32	519	397	1.31	0.0675	0.0007	1.4652	0.0117	0.1574	0.0023	854	18	916	5	942	13
33	79	111	0.72	0.2276	0.0021	18.1160	0.1359	0.5773	0.0086	3035	14	2996	7	2938	35
34	435	242	1.80	0.1520	0.0014	8.8480	0.0639	0.4221	0.0062	2369	15	2322	7	2270	28

35	59	30	1.94	0.0570	0.0017	0.6802	0.0188	0.0866	0.0017	491	30	527	11	535	10
36	130	248	0.52	0.1090	0.0010	4.8852	0.0363	0.3251	0.0048	1783	16	1800	6	1814	23
37	81	169	0.48	0.0732	0.0008	1.7319	0.0163	0.1716	0.0026	1020	16	1020	6	1021	14
38	124	215	0.58	0.0691	0.0008	1.4758	0.0131	0.1549	0.0023	902	17	921	5	928	13
39	144	64	2.25	0.0680	0.0010	1.5040	0.0192	0.1605	0.0025	867	15	932	8	960	14
40	27	89	0.30	0.0633	0.0009	1.0901	0.0136	0.1248	0.0020	719	15	749	7	758	11
41	0	3	0.06	0.0566	0.0137	0.7060	0.1627	0.0905	0.0078	474	353	542	97	559	46
42	23	68	0.34	0.1532	0.0016	9.5686	0.0801	0.4531	0.0069	2382	15	2394	8	2409	31
43	49	194	0.25	0.0590	0.0007	0.8620	0.0088	0.1061	0.0016	565	16	631	5	650	9
44	148	256	0.58	0.0614	0.0007	1.0506	0.0097	0.1240	0.0019	654	17	729	5	754	11
45	167	431	0.39	0.0641	0.0006	1.2372	0.0098	0.1399	0.0021	746	18	818	4	844	12
46	154	93	1.67	0.0528	0.0009	0.5805	0.0091	0.0797	0.0013	321	16	465	6	494	8
47	85	290	0.29	0.0561	0.0007	0.6987	0.0067	0.0904	0.0014	455	17	538	4	558	8
48	181	256	0.71	0.0557	0.0007	0.6918	0.0072	0.0902	0.0014	438	17	534	4	556	8
49	122	257	0.47	0.0589	0.0007	0.8422	0.0081	0.1037	0.0016	565	17	620	4	636	9
50	77	48	1.63	0.0654	0.0011	1.3612	0.0204	0.1510	0.0025	787	15	872	9	906	14
51	310	255	1.21	0.0674	0.0007	1.4788	0.0128	0.1593	0.0024	849	17	922	5	953	13
52	29	51	0.57	0.0658	0.0012	1.1974	0.0191	0.1320	0.0022	800	16	799	9	799	13
53	292	262	1.11	0.0624	0.0007	1.0480	0.0098	0.1219	0.0018	686	17	728	5	742	11
54	181	3	71.60	0.0745	0.0064	1.5524	0.1222	0.1511	0.0069	1055	88	951	49	907	38
55	130	210	0.62	0.1428	0.0013	7.2653	0.0540	0.3690	0.0055	2261	16	2145	7	2025	26
56	74	50	1.48	0.0795	0.0012	2.1722	0.0286	0.1982	0.0032	1184	15	1172	9	1166	17
57	466	467	1.00	0.0658	0.0007	1.3842	0.0109	0.1526	0.0023	800	18	882	5	916	13
58	200	414	0.48	0.0689	0.0007	1.4566	0.0116	0.1534	0.0023	895	18	913	5	920	13
59	113	93	1.21	0.1526	0.0015	9.3979	0.0757	0.4466	0.0068	2376	15	2378	7	2380	30
60	273	718	0.38	0.0613	0.0006	1.0774	0.0084	0.1275	0.0019	650	19	742	4	773	11
61	148	238	0.62	0.0538	0.0007	0.6211	0.0066	0.0837	0.0013	364	17	491	4	518	8
62	246	320	0.77	0.0673	0.0007	1.5258	0.0131	0.1644	0.0025	848	17	941	5	981	14
63	161	154	1.04	0.1466	0.0014	8.6343	0.0667	0.4272	0.0064	2307	15	2300	7	2293	29
64	56	470	0.12	0.0583	0.0006	0.8440	0.0072	0.1051	0.0016	540	18	621	4	644	9
65	105	204	0.51	0.1488	0.0014	8.6466	0.0645	0.4214	0.0063	2333	15	2301	7	2267	29
66	245	432	0.57	0.0668	0.0007	1.4417	0.0116	0.1565	0.0023	832	18	906	5	937	13

67	81	167	0.49	0.0697	0.0008	1.6473	0.0155	0.1714	0.0026	920	17	989	6	1020	14
68	81	166	0.49	0.0686	0.0008	1.4383	0.0142	0.1521	0.0023	887	16	905	6	913	13
69	17	43	0.39	0.0736	0.0021	1.4147	0.0355	0.1394	0.0029	1031	23	895	15	841	16
70	220	256	0.86	0.0696	0.0008	1.5318	0.0148	0.1597	0.0024	916	16	943	6	955	14
71	680	1085	0.63	0.1550	0.0014	8.0808	0.0579	0.3783	0.0056	2401	16	2240	6	2068	26
72	95	500	0.19	0.0676	0.0007	1.3777	0.0110	0.1477	0.0022	858	18	879	5	888	12
73	52	147	0.36	0.0578	0.0008	0.7434	0.0090	0.0934	0.0015	520	16	564	5	575	9
74	132	248	0.53	0.1511	0.0014	9.3460	0.0684	0.4487	0.0067	2359	16	2373	7	2389	30
75	459	228	2.01	0.0569	0.0008	0.6532	0.0075	0.0833	0.0013	488	16	510	5	515	8
76	137	560	0.25	0.0685	0.0007	1.4298	0.0112	0.1513	0.0023	885	18	901	5	908	13
77	50	83	0.60	0.0547	0.0010	0.6316	0.0103	0.0837	0.0014	401	17	497	6	518	8
78	115	230	0.50	0.0689	0.0007	1.5462	0.0137	0.1627	0.0025	897	17	949	5	972	14
79	187	195	0.96	0.0627	0.0007	1.0255	0.0102	0.1187	0.0018	698	17	717	5	723	10
80	25	60	0.42	0.1497	0.0016	9.0014	0.0792	0.4361	0.0068	2343	15	2338	8	2333	30
81	255	123	2.07	0.0704	0.0009	1.5578	0.0166	0.1604	0.0025	941	16	954	7	959	14
82	24	89	0.27	0.0668	0.0009	1.3549	0.0163	0.1472	0.0023	831	15	870	7	885	13
83	141	75	1.88	0.0656	0.0010	1.3426	0.0173	0.1485	0.0024	793	15	864	7	893	13
84	248	541	0.46	0.0659	0.0007	1.2549	0.0100	0.1381	0.0021	804	18	826	5	834	12
85	106	95	1.11	0.0633	0.0009	1.1219	0.0137	0.1285	0.0020	720	16	764	7	779	12
86	249	659	0.38	0.0638	0.0006	1.1973	0.0094	0.1361	0.0020	736	19	799	4	822	12
87	158	172	0.92	0.0556	0.0008	0.6550	0.0079	0.0855	0.0013	435	16	512	5	529	8
88	55	99	0.56	0.0607	0.0009	1.0045	0.0126	0.1202	0.0019	627	16	706	6	731	11
89	65	152	0.43	0.0675	0.0008	1.4489	0.0145	0.1557	0.0024	853	17	909	6	933	13
90	72	112	0.64	0.0616	0.0008	1.0853	0.0128	0.1278	0.0020	661	16	746	6	775	11
91	105	403	0.26	0.0722	0.0007	1.7974	0.0142	0.1805	0.0027	992	18	1045	5	1070	15
92	21	53	0.39	0.0608	0.0011	0.8679	0.0144	0.1036	0.0018	632	17	634	8	635	10
93	22	167	0.13	0.0578	0.0008	0.6848	0.0081	0.0860	0.0014	521	16	530	5	532	8
94	64	153	0.42	0.0589	0.0008	0.7652	0.0086	0.0942	0.0015	565	16	577	5	580	9
95	501	833	0.60	0.0636	0.0006	1.1340	0.0086	0.1294	0.0019	728	19	770	4	784	11
96	18	35	0.50	0.0660	0.0012	1.3642	0.0221	0.1500	0.0026	806	16	874	10	901	14
97	297	274	1.09	0.0683	0.0007	1.4647	0.0124	0.1557	0.0024	876	18	916	5	933	13
98	18	45	0.41	0.0711	0.0011	1.5704	0.0215	0.1602	0.0026	961	15	959	8	958	15

99	207	417	0.50	0.1564	0.0014	9.1891	0.0661	0.4261	0.0064	2418	16	2357	7	2288	29
100	71	344	0.21	0.0574	0.0006	0.7741	0.0071	0.0979	0.0015	505	18	582	4	602	9
101	72	147	0.49	0.0576	0.0008	0.7519	0.0089	0.0947	0.0015	515	16	569	5	583	9
102	69	147	0.47	0.0713	0.0008	1.7384	0.0166	0.1768	0.0027	966	17	1023	6	1050	15
103	35	229	0.15	0.0568	0.0007	0.7672	0.0079	0.0980	0.0015	484	17	578	5	603	9
104	120	479	0.25	0.0824	0.0008	1.9067	0.0150	0.1678	0.0025	1256	18	1083	5	1000	14
105	279	663	0.42	0.0553	0.0006	0.6635	0.0056	0.0870	0.0013	424	19	517	3	538	8
106	251	277	0.91	0.1083	0.0010	4.8998	0.0375	0.3282	0.0050	1771	17	1802	6	1829	24
107	202	287	0.70	0.0718	0.0024	1.5941	0.0452	0.1611	0.0027	979	68	968	18	963	15
108	145	244	0.59	0.0677	0.0007	1.4859	0.0132	0.1593	0.0024	858	18	925	5	953	14
109	226	162	1.39	0.0748	0.0009	1.7251	0.0168	0.1674	0.0026	1062	17	1018	6	998	14
110	146	125	1.17	0.0582	0.0011	0.6469	0.0105	0.0807	0.0014	535	17	507	6	500	8
111	16	50	0.33	0.1537	0.0016	9.2036	0.0820	0.4345	0.0069	2387	15	2358	8	2326	31
112	100	212	0.47	0.0719	0.0008	1.8107	0.0160	0.1828	0.0028	982	17	1049	6	1082	15
113	210	224	0.94	0.0632	0.0007	1.1163	0.0107	0.1281	0.0020	715	17	761	5	777	11
114	110	99	1.12	0.0553	0.0009	0.6505	0.0097	0.0853	0.0014	424	16	509	6	528	8
115	194	244	0.79	0.0629	0.0007	1.0432	0.0100	0.1204	0.0019	704	17	725	5	733	11
116	176	256	0.69	0.1123	0.0011	5.3949	0.0415	0.3486	0.0053	1836	17	1884	7	1928	25
117	22	65	0.34	0.0702	0.0011	1.6149	0.0215	0.1669	0.0028	934	15	976	8	995	15
118	78	82	0.95	0.0673	0.0010	1.3965	0.0174	0.1505	0.0024	848	16	887	7	904	14
119	63	83	0.75	0.1572	0.0016	9.9649	0.0837	0.4597	0.0072	2426	15	2432	8	2438	32
120	79	180	0.44	0.1079	0.0011	4.6279	0.0381	0.3111	0.0048	1764	16	1754	7	1746	24
Sample 10GD38-1, Lower Ordovician, Yulin															
1	46	205	0.22	0.0630	0.0008	0.9816	0.0103	0.1130	0.0017	708	16	694	5	690	10
2	406	384	1.06	0.1296	0.0013	6.6057	0.0547	0.3697	0.0056	2093	15	2060	7	2028	26
3	103	137	0.75	0.0893	0.0011	2.4822	0.0260	0.2016	0.0032	1411	15	1267	8	1184	17
4	387	404	0.96	0.0738	0.0008	1.8506	0.0150	0.1818	0.0027	1037	17	1064	5	1077	15
5	59	136	0.43	0.0752	0.0009	1.8763	0.0180	0.1810	0.0028	1074	16	1073	6	1072	15
6	157	179	0.88	0.0763	0.0009	1.8527	0.0169	0.1760	0.0027	1104	16	1064	6	1045	15
~~*7*~~	~~*226*~~	~~*388*~~	~~*0.58*~~	~~*0.1407*~~	~~*0.0031*~~	~~*5.4908*~~	~~*0.0826*~~	~~*0.2831*~~	~~*0.0045*~~	~~*2236*~~	~~*39*~~	~~*1899*~~	~~*13*~~	~~*1607*~~	~~*22*~~
8	94	951	0.10	0.0697	0.0013	1.3672	0.0143	0.1423	0.0021	919	38	875	6	858	12

9	81	232	0.35	0.0601	0.0008	0.8127	0.0086	0.0981	0.0015	608	16	604	5	603	9
10	167	297	0.56	0.2970	0.0028	25.4879	0.1902	0.6225	0.0093	3455	14	3327	7	3120	37
11	138	300	0.46	0.0755	0.0008	1.8681	0.0159	0.1794	0.0027	1082	17	1070	6	1064	15
12	70	124	0.56	0.1632	0.0016	10.3580	0.0830	0.4604	0.0070	2489	15	2467	7	2442	31
13	337	682	0.49	0.0700	0.0007	1.4982	0.0118	0.1553	0.0023	928	18	930	5	930	13
14	636	1256	0.51	0.0747	0.0021	1.3771	0.0312	0.1338	0.0021	1059	57	879	13	809	12
15	106	141	0.75	0.1251	0.0032	6.1939	0.1231	0.3590	0.0059	2031	47	2004	17	1977	28
16	385	781	0.49	0.1567	0.0015	9.3999	0.0693	0.4350	0.0065	2421	15	2378	7	2328	29
17	153	172	0.89	0.1606	0.0040	10.0477	0.1860	0.4537	0.0076	2462	43	2439	17	2412	34
18	79	351	0.23	0.0637	0.0008	1.0192	0.0110	0.1160	0.0018	733	16	713	6	707	10
19	300	209	1.43	0.0721	0.0008	1.5625	0.0140	0.1572	0.0024	989	17	955	6	941	13
20	25	750	0.03	0.0695	0.0007	1.4816	0.0115	0.1547	0.0023	913	18	923	5	927	13
21	269	187	1.44	0.0647	0.0010	0.7167	0.0092	0.0804	0.0013	764	15	549	5	498	8
22	93	113	0.83	0.0759	0.0009	1.9231	0.0189	0.1838	0.0028	1092	16	1089	7	1088	15
23	181	336	0.54	0.0590	0.0007	0.8270	0.0076	0.1018	0.0015	565	18	612	4	625	9
24	64	795	0.08	0.0631	0.0012	1.0221	0.0119	0.1176	0.0017	710	41	715	6	716	10
25	207	1182	0.18	0.0732	0.0007	1.8481	0.0139	0.1833	0.0027	1018	18	1063	5	1085	15
26	266	363	0.73	0.1500	0.0015	7.2749	0.0564	0.3517	0.0053	2346	15	2146	7	1943	25
27	125	62	2.03	0.0649	0.0022	0.8742	0.0265	0.0977	0.0021	771	31	638	14	601	13
28	190	148	1.28	0.0653	0.0008	1.1625	0.0118	0.1291	0.0020	785	16	783	6	783	11
29	112	223	0.50	0.0596	0.0007	0.7495	0.0077	0.0913	0.0014	588	17	568	4	563	8
30	463	557	0.83	0.0584	0.0006	0.7303	0.0064	0.0907	0.0014	544	18	557	4	560	8
31	470	318	1.48	0.0585	0.0007	0.6379	0.0063	0.0791	0.0012	549	17	501	4	491	7
32	61	108	0.56	0.0716	0.0009	1.6825	0.0172	0.1704	0.0026	975	16	1002	7	1014	14
33	160	283	0.57	0.0725	0.0008	1.6057	0.0153	0.1607	0.0025	999	16	972	6	961	14
34	10	367	0.03	0.0591	0.0011	0.6558	0.0077	0.0804	0.0012	572	43	512	5	499	7
35	162	172	0.94	0.0579	0.0008	0.6996	0.0081	0.0877	0.0014	526	16	539	5	542	8
36	370	367	1.01	0.0750	0.0008	1.7774	0.0145	0.1720	0.0026	1068	17	1037	5	1023	14
37	36	60	0.59	0.2008	0.0021	14.6838	0.1251	0.5305	0.0082	2832	14	2795	8	2744	35
38	265	511	0.52	0.0599	0.0006	0.8302	0.0071	0.1006	0.0015	599	18	614	4	618	9
39	354	651	0.54	0.1441	0.0014	6.7815	0.0504	0.3413	0.0051	2277	16	2083	7	1893	24
40	207	306	0.68	0.1540	0.0016	8.3755	0.0682	0.3946	0.0060	2390	15	2273	7	2144	28

41	206	278	0.74	0.0657	0.0007	1.1714	0.0105	0.1293	0.0020	798	17	787	5	784	11
42	18	34	0.53	0.0604	0.0014	0.8274	0.0170	0.0994	0.0018	617	20	612	9	611	10
43	224	378	0.59	0.0637	0.0007	1.0172	0.0090	0.1159	0.0018	731	18	713	5	707	10
44	233	299	0.78	0.0647	0.0007	1.1818	0.0106	0.1325	0.0020	765	17	792	5	802	11
45	457	702	0.65	0.0699	0.0007	1.5977	0.0125	0.1657	0.0025	927	18	969	5	988	14
46	73	862	0.08	0.1468	0.0014	7.5007	0.0553	0.3707	0.0055	2308	16	2173	7	2033	26
47	164	276	0.59	0.0882	0.0009	2.8444	0.0230	0.2338	0.0035	1388	17	1367	6	1354	18
48	302	497	0.61	0.0627	0.0007	0.8542	0.0074	0.0989	0.0015	697	18	627	4	608	9
49	202	244	0.83	0.0573	0.0007	0.6850	0.0073	0.0868	0.0013	501	17	530	4	537	8
50	268	259	1.04	0.1775	0.0045	12.0643	0.2263	0.4930	0.0083	2629	43	2609	18	2584	36
51	90	204	0.44	0.0659	0.0008	1.3253	0.0126	0.1458	0.0022	804	17	857	5	877	13
52	511	629	0.81	0.0591	0.0006	0.6566	0.0059	0.0806	0.0012	570	18	513	4	500	7
53	215	216	1.00	0.0746	0.0010	1.6548	0.0186	0.1609	0.0025	1057	15	991	7	962	14
54	44	113	0.39	0.0738	0.0009	1.8023	0.0183	0.1772	0.0027	1035	16	1046	7	1052	15
55	153	278	0.55	0.0702	0.0008	1.5006	0.0131	0.1552	0.0024	933	17	931	5	930	13
56	144	648	0.22	0.0703	0.0007	1.6061	0.0127	0.1657	0.0025	938	18	973	5	988	14
57	92	88	1.05	0.1523	0.0016	9.0429	0.0760	0.4308	0.0066	2372	15	2342	8	2309	30
58	137	218	0.63	0.0701	0.0008	1.5666	0.0144	0.1621	0.0025	932	17	957	6	968	14
59	108	74	1.46	0.0709	0.0012	1.5273	0.0224	0.1564	0.0026	953	15	941	9	937	15
60	116	117	0.99	0.0951	0.0011	3.5056	0.0324	0.2674	0.0041	1530	16	1528	7	1528	21
61	75	137	0.55	0.0680	0.0022	1.3181	0.0363	0.1406	0.0023	868	68	854	16	848	13
62	251	619	0.40	0.0767	0.0008	1.6641	0.0146	0.1573	0.0024	1114	17	995	6	942	13
63	120	372	0.32	0.1109	0.0011	4.7573	0.0374	0.3113	0.0047	1813	16	1777	7	1747	23
64	211	313	0.68	0.0760	0.0008	1.9408	0.0162	0.1854	0.0028	1094	17	1095	6	1096	15
65	202	294	0.69	0.0567	0.0007	0.6374	0.0065	0.0815	0.0013	481	17	501	4	505	7
66	205	338	0.61	0.0776	0.0008	2.0862	0.0171	0.1951	0.0029	1136	17	1144	6	1149	16
67	16	34	0.48	0.1577	0.0023	8.6023	0.1104	0.3958	0.0069	2431	14	2297	12	2150	32
68	122	494	0.25	0.0763	0.0008	1.9728	0.0157	0.1876	0.0028	1103	18	1106	5	1108	15
69	347	353	0.98	0.0636	0.0008	1.0595	0.0110	0.1208	0.0019	729	17	734	5	735	11
70	33	38	0.86	0.0711	0.0013	1.5350	0.0238	0.1565	0.0027	961	15	945	10	937	15
71	156	711	0.22	0.1900	0.0018	13.1159	0.0979	0.5007	0.0075	2742	15	2688	7	2617	32
72	151	361	0.42	0.0722	0.0008	1.5570	0.0132	0.1563	0.0024	993	17	953	5	936	13

73	337	482	0.70	0.0825	0.0009	2.3567	0.0225	0.2071	0.0032	1258	16	1230	7	1213	17
74	99	224	0.44	0.0703	0.0008	1.6230	0.0146	0.1675	0.0026	937	17	979	6	998	14
75	205	365	0.56	0.0696	0.0007	1.4165	0.0120	0.1476	0.0022	916	18	896	5	888	13
76	64	321	0.20	0.1273	0.0024	5.2958	0.0556	0.3016	0.0046	2062	33	1868	9	1699	23
77	357	315	1.13	0.0621	0.0007	0.6933	0.0068	0.0810	0.0012	676	17	535	4	502	7
78	251	596	0.42	0.0723	0.0007	1.6217	0.0128	0.1627	0.0025	994	18	979	5	972	14
79	146	237	0.61	0.0682	0.0008	1.3287	0.0122	0.1414	0.0022	873	17	858	5	853	12
80	211	244	0.86	0.0574	0.0009	0.6527	0.0084	0.0825	0.0013	508	16	510	5	511	8
81	73	247	0.30	0.0709	0.0008	1.5097	0.0134	0.1545	0.0024	954	17	934	5	926	13
82	118	450	0.26	0.0692	0.0007	1.5582	0.0127	0.1632	0.0025	906	18	954	5	975	14
83	177	554	0.32	0.0738	0.0007	1.6060	0.0128	0.1579	0.0024	1035	18	973	5	945	13
84	129	345	0.37	0.1538	0.0015	8.3409	0.0640	0.3934	0.0059	2389	15	2269	7	2138	27
85	172	352	0.49	0.0902	0.0009	2.9597	0.0243	0.2381	0.0036	1429	17	1397	6	1377	19
86	489	634	0.77	0.0574	0.0006	0.6799	0.0059	0.0859	0.0013	507	18	527	4	531	8
87	305	433	0.70	0.0773	0.0008	2.0231	0.0161	0.1899	0.0029	1128	18	1123	5	1121	15
88	201	98	2.05	0.0583	0.0009	0.6984	0.0099	0.0870	0.0014	540	16	538	6	537	8
89	156	576	0.27	0.0639	0.0006	1.1685	0.0095	0.1326	0.0020	740	18	786	4	802	11
90	181	255	0.71	0.1564	0.0015	8.5892	0.0658	0.3985	0.0060	2417	15	2295	7	2162	28
91	149	385	0.39	0.0745	0.0008	1.9092	0.0155	0.1860	0.0028	1054	18	1084	5	1099	15
92	83	120	0.69	0.0780	0.0009	2.2287	0.0212	0.2073	0.0032	1147	16	1190	7	1214	17
93	574	1107	0.52	0.0655	0.0006	1.1275	0.0087	0.1249	0.0019	789	19	767	4	759	11
94	93	174	0.54	0.0749	0.0008	1.9898	0.0179	0.1926	0.0030	1067	17	1112	6	1135	16
95	148	311	0.47	0.1137	0.0011	4.9540	0.0382	0.3160	0.0048	1860	16	1812	7	1770	23
96	138	352	0.39	0.0705	0.0009	1.4015	0.0155	0.1443	0.0023	942	16	890	7	869	13
~~*97*~~	~~*996*~~	~~*1660*~~	~~*0.60*~~	~~*0.0732*~~	~~*0.0007*~~	~~*0.5445*~~	~~*0.0045*~~	~~*0.0539*~~	~~*0.0008*~~	~~*1020*~~	~~*18*~~	~~*441*~~	~~*3*~~	~~*339*~~	~~*5*~~
98	97	270	0.36	0.0754	0.0008	1.9256	0.0163	0.1852	0.0028	1080	17	1090	6	1095	15
99	128	151	0.85	0.0764	0.0009	1.9183	0.0178	0.1821	0.0028	1106	17	1087	6	1078	15
100	114	304	0.37	0.0722	0.0018	1.5024	0.0294	0.1509	0.0024	992	52	931	12	906	13
101	109	180	0.60	0.1574	0.0015	9.4840	0.0737	0.4370	0.0066	2428	15	2386	7	2337	30
102	270	434	0.62	0.0698	0.0007	1.5257	0.0124	0.1585	0.0024	922	18	941	5	949	13
103	22	101	0.22	0.0689	0.0009	1.4297	0.0158	0.1504	0.0024	897	16	901	7	903	13
104	112	117	0.95	0.0660	0.0008	1.2926	0.0139	0.1421	0.0022	806	16	842	6	856	13

105	102	445	0.23	0.0677	0.0007	1.3734	0.0113	0.1472	0.0022	859	18	878	5	885	13
106	108	169	0.64	0.0753	0.0010	1.7523	0.0192	0.1688	0.0027	1076	16	1028	7	1006	15
107	274	151	1.81	0.0575	0.0008	0.6446	0.0078	0.0813	0.0013	511	16	505	5	504	8
~~*108*~~	~~*1268*~~	~~*1792*~~	~~*0.71*~~	~~*0.0879*~~	~~*0.0010*~~	~~*1.2421*~~	~~*0.0114*~~	~~*0.1025*~~	~~*0.0016*~~	~~*1381*~~	~~*16*~~	~~*820*~~	~~*5*~~	~~*629*~~	~~*9*~~
109	55	266	0.21	0.0694	0.0007	1.5146	0.0132	0.1583	0.0024	911	18	936	5	947	13
110	218	431	0.51	0.0796	0.0008	2.2494	0.0191	0.2049	0.0031	1188	17	1197	6	1202	17
111	69	939	0.07	0.0706	0.0012	1.2075	0.0112	0.1241	0.0018	946	37	804	5	754	10
112	144	312	0.46	0.0685	0.0007	1.5688	0.0135	0.1662	0.0025	883	18	958	5	991	14
113	74	219	0.34	0.0932	0.0020	3.0335	0.0447	0.2360	0.0037	1493	41	1416	11	1366	19
114	105	115	0.91	0.0751	0.0009	1.7499	0.0174	0.1691	0.0026	1070	16	1027	6	1007	15
115	140	270	0.52	0.0724	0.0008	1.5003	0.0129	0.1502	0.0023	998	17	931	5	902	13
116	60	268	0.22	0.0728	0.0008	1.6179	0.0138	0.1613	0.0025	1008	17	977	5	964	14
117	133	171	0.77	0.1643	0.0024	10.7651	0.1445	0.4753	0.0086	2500	14	2503	12	2507	38
118	243	335	0.73	0.0694	0.0007	1.4838	0.0126	0.1550	0.0024	912	18	924	5	929	13
119	197	654	0.30	0.0715	0.0007	1.4502	0.0117	0.1472	0.0022	971	18	910	5	885	13
120	165	262	0.63	0.0688	0.0011	1.1480	0.0166	0.1211	0.0020	892	15	776	8	737	12
Sample 10GD45, Lower Ordovician, Yulin															
1	121	309	0.39	0.1834	0.0021	12.7600	0.1794	0.5047	0.0068	2684	10	2662	13	2634	29
2	60	127	0.48	0.0738	0.0010	1.7663	0.0275	0.1735	0.0024	1037	14	1033	10	1031	13
3	53	103	0.51	0.0672	0.0011	1.2646	0.0222	0.1365	0.0019	844	17	830	10	825	11
4	85	421	0.20	0.0617	0.0008	0.9697	0.0143	0.1140	0.0015	663	14	688	7	696	9
5	87	167	0.52	0.1759	0.0020	11.7166	0.1659	0.4831	0.0065	2615	11	2582	13	2541	28
6	132	166	0.79	0.1157	0.0014	5.2892	0.0761	0.3316	0.0045	1891	12	1867	12	1846	22
7	19	35	0.54	0.0699	0.0020	1.5397	0.0446	0.1597	0.0025	926	34	946	18	955	14
8	20	58	0.34	0.0709	0.0012	1.5356	0.0289	0.1570	0.0022	955	18	945	12	940	12
9	17	323	0.05	0.1673	0.0019	10.8692	0.1535	0.4712	0.0063	2531	11	2512	13	2489	28
10	263	194	1.36	0.0691	0.0009	1.4331	0.0217	0.1505	0.0020	901	14	903	9	904	11
11	103	49	2.11	0.1057	0.0015	4.4599	0.0710	0.3061	0.0043	1726	13	1724	13	1721	21
12	104	47	2.21	0.0720	0.0016	1.5814	0.0356	0.1592	0.0023	987	24	963	14	952	13
13	81	94	0.86	0.0922	0.0012	3.1741	0.0483	0.2497	0.0034	1471	13	1451	12	1437	18
14	157	255	0.62	0.0719	0.0009	1.6555	0.0245	0.1669	0.0023	984	13	992	9	995	12

15	21	22	0.94	0.0699	0.0026	1.5128	0.0575	0.1571	0.0025	924	52	936	23	940	14
16	45	159	0.28	0.0730	0.0010	1.7487	0.0270	0.1737	0.0024	1014	14	1027	10	1033	13
17	90	321	0.28	0.0603	0.0008	0.8415	0.0131	0.1012	0.0014	616	15	620	7	621	8
18	68	67	1.02	0.1077	0.0014	4.4974	0.0697	0.3028	0.0042	1761	13	1730	13	1705	21
19	73	102	0.72	0.0656	0.0011	1.1767	0.0216	0.1301	0.0018	794	18	790	10	788	10
20	112	165	0.68	0.0724	0.0010	1.6724	0.0258	0.1675	0.0023	998	14	998	10	998	13
21	294	335	0.88	0.2008	0.0023	14.3654	0.2050	0.5188	0.0070	2833	10	2774	14	2694	30
22	78	61	1.28	0.0580	0.0013	0.6849	0.0157	0.0856	0.0013	530	26	530	9	530	7
23	75	139	0.54	0.0638	0.0010	1.0608	0.0186	0.1205	0.0017	736	17	734	9	734	10
24	83	86	0.97	0.1290	0.0016	6.7383	0.0998	0.3788	0.0052	2085	12	2078	13	2071	24
25	140	310	0.45	0.0656	0.0008	1.1699	0.0177	0.1293	0.0018	795	14	787	8	784	10
26	249	595	0.42	0.0592	0.0008	0.7580	0.0114	0.0929	0.0013	574	15	573	7	572	7
27	96	82	1.17	0.0718	0.0011	1.5966	0.0277	0.1612	0.0022	981	16	969	11	963	12
28	155	243	0.64	0.1133	0.0014	5.2428	0.0763	0.3355	0.0045	1853	12	1860	12	1865	22
29	84	109	0.77	0.0698	0.0010	1.5000	0.0248	0.1558	0.0022	923	15	930	10	933	12
30	403	853	0.47	0.0719	0.0011	1.6579	0.0277	0.1672	0.0024	983	15	993	11	997	13
31	424	691	0.61	0.0578	0.0007	0.6975	0.0104	0.0876	0.0012	521	15	537	6	541	7
32	197	87	2.26	0.1070	0.0015	4.5232	0.0728	0.3065	0.0043	1750	13	1735	13	1723	21
33	8	24	0.34	0.0644	0.0022	1.0774	0.0362	0.1213	0.0019	756	45	742	18	738	11
34	324	216	1.50	0.1637	0.0020	10.8927	0.1585	0.4827	0.0065	2494	11	2514	14	2539	28
35	78	506	0.15	0.0670	0.0008	1.3096	0.0194	0.1417	0.0019	838	14	850	9	854	11
36	21	58	0.36	0.1659	0.0021	10.7701	0.1614	0.4708	0.0065	2517	11	2503	14	2487	28
37	43	167	0.26	0.0603	0.0009	0.8387	0.0141	0.1008	0.0014	616	17	618	8	619	8
38	118	128	0.93	0.0680	0.0010	1.3320	0.0223	0.1421	0.0020	868	16	860	10	857	11
39	101	180	0.56	0.0587	0.0009	0.7523	0.0130	0.0930	0.0013	556	17	570	8	573	8
40	244	376	0.65	0.0725	0.0009	1.6260	0.0244	0.1628	0.0022	999	14	980	9	972	12
41	162	302	0.54	0.1158	0.0015	5.3641	0.0803	0.3360	0.0046	1892	12	1879	13	1867	22
42	26	938	0.03	0.0694	0.0009	1.4658	0.0218	0.1532	0.0021	910	14	916	9	919	12
43	331	365	0.91	0.0786	0.0010	2.1261	0.0326	0.1962	0.0027	1161	14	1157	11	1155	14
44	274	241	1.14	0.0655	0.0009	1.1362	0.0180	0.1258	0.0017	791	15	771	9	764	10
45	277	319	0.87	0.0747	0.0010	1.8865	0.0294	0.1832	0.0025	1060	14	1076	10	1085	14
46	106	279	0.38	0.0632	0.0009	0.9990	0.0160	0.1146	0.0016	715	15	703	8	700	9

47	108	56	1.94	0.0645	0.0015	1.1467	0.0278	0.1289	0.0019	759	28	776	13	781	11
48	104	383	0.27	0.0582	0.0008	0.7515	0.0121	0.0936	0.0013	538	16	569	7	577	8
49	83	221	0.37	0.0749	0.0010	1.8917	0.0295	0.1831	0.0025	1066	14	1078	10	1084	14
50	252	148	1.70	0.0573	0.0011	0.6362	0.0125	0.0805	0.0011	503	21	500	8	499	7
51	46	118	0.39	0.0638	0.0011	1.0310	0.0194	0.1172	0.0017	735	19	719	10	714	10
52	283	396	0.71	0.0790	0.0010	2.0861	0.0319	0.1915	0.0026	1172	14	1144	10	1129	14
53	188	259	0.73	0.0765	0.0011	1.8984	0.0313	0.1799	0.0025	1109	15	1081	11	1067	14
54	78	490	0.16	0.0698	0.0009	1.5092	0.0232	0.1569	0.0021	921	14	934	9	940	12
55	276	534	0.52	0.0580	0.0008	0.7343	0.0115	0.0917	0.0013	531	15	559	7	566	7
56	99	64	1.55	0.0993	0.0020	3.3668	0.0731	0.2460	0.0039	1610	19	1497	17	1418	20
57	11	72	0.15	0.0695	0.0021	1.2712	0.0390	0.1326	0.0023	914	36	833	17	803	13
58	138	385	0.36	0.1635	0.0021	10.9012	0.1658	0.4834	0.0066	2492	11	2515	14	2542	29
59	183	334	0.55	0.0703	0.0010	1.5847	0.0250	0.1636	0.0022	936	14	964	10	977	12
60	124	271	0.46	0.1711	0.0022	11.5058	0.1760	0.4876	0.0067	2569	11	2565	14	2560	29
61	67	104	0.65	0.0642	0.0022	1.0950	0.0368	0.1238	0.0023	747	40	751	18	752	13
62	134	177	0.75	0.0701	0.0010	1.6014	0.0263	0.1657	0.0023	931	15	971	10	988	13
63	33	634	0.05	0.0595	0.0008	0.7981	0.0128	0.0973	0.0013	585	16	596	7	599	8
64	226	285	0.79	0.0693	0.0010	1.3935	0.0222	0.1459	0.0020	906	15	886	9	878	11
65	119	153	0.78	0.0619	0.0010	0.9593	0.0168	0.1124	0.0016	671	17	683	9	686	9
66	205	141	1.45	0.1715	0.0023	11.2597	0.1766	0.4762	0.0066	2572	12	2545	15	2510	29
67	42	65	0.64	0.0766	0.0012	2.0121	0.0356	0.1904	0.0027	1112	16	1120	12	1124	15
68	328	339	0.97	0.1564	0.0021	9.7507	0.1528	0.4519	0.0062	2418	12	2412	14	2404	28
69	45	142	0.32	0.0587	0.0012	0.7410	0.0154	0.0916	0.0013	555	22	563	9	565	8
70	100	197	0.51	0.0754	0.0011	1.7978	0.0295	0.1730	0.0024	1078	15	1045	11	1029	13
71	302	275	1.10	0.1534	0.0021	9.5052	0.1502	0.4493	0.0062	2384	12	2388	15	2392	28
72	94	270	0.35	0.0824	0.0012	2.3188	0.0375	0.2041	0.0028	1254	14	1218	11	1197	15
73	190	202	0.94	0.1676	0.0023	10.7077	0.1697	0.4632	0.0064	2534	12	2498	15	2454	28
74	104	155	0.67	0.0667	0.0014	1.3258	0.0296	0.1441	0.0021	829	24	857	13	868	12
75	437	1010	0.43	0.1659	0.0023	10.4695	0.1655	0.4577	0.0063	2516	12	2477	15	2429	28
76	275	780	0.35	0.1438	0.0020	7.4318	0.1210	0.3746	0.0053	2274	13	2165	15	2051	25
77	4	6	0.55	0.0999	0.0047	3.9131	0.1795	0.2839	0.0054	1623	57	1616	37	1611	27
78	19	48	0.40	0.0638	0.0016	1.0510	0.0263	0.1194	0.0019	735	28	729	13	727	11

79	85	299	0.28	0.0637	0.0010	1.0577	0.0181	0.1204	0.0017	732	16	733	9	733	10
80	116	324	0.36	0.0710	0.0010	1.5118	0.0251	0.1543	0.0022	959	15	935	10	925	12
81	8	32	0.26	0.0606	0.0021	0.7174	0.0242	0.0859	0.0014	624	44	549	14	531	9
82	31	102	0.30	0.1820	0.0027	12.6059	0.2099	0.5023	0.0071	2671	12	2651	16	2624	31
83	73	205	0.36	0.0649	0.0010	1.1670	0.0208	0.1304	0.0018	771	17	785	10	790	10
85	41	51	0.80	0.0717	0.0015	1.6340	0.0359	0.1653	0.0024	976	23	983	14	986	13
86	90	113	0.80	0.0705	0.0012	1.5410	0.0283	0.1586	0.0023	941	17	947	11	949	13
87	107	61	1.76	0.0662	0.0013	1.2680	0.0270	0.1389	0.0020	812	22	831	12	838	12
88	73	183	0.40	0.0619	0.0011	0.9582	0.0181	0.1122	0.0016	672	19	682	9	685	9
89	42	94	0.45	0.0933	0.0018	3.4541	0.0714	0.2683	0.0041	1495	19	1517	16	1532	21
90	108	220	0.49	0.1257	0.0019	6.1641	0.1029	0.3555	0.0050	2039	13	1999	15	1961	24
91	222	272	0.81	0.0586	0.0010	0.7067	0.0132	0.0875	0.0012	550	19	543	8	541	7
92	98	384	0.25	0.0604	0.0010	0.8333	0.0146	0.1000	0.0014	619	17	615	8	614	8
93	58	108	0.53	0.0723	0.0014	1.6659	0.0351	0.1670	0.0024	995	21	996	13	995	13
94	67	107	0.63	0.0604	0.0012	0.8457	0.0179	0.1016	0.0015	616	22	622	10	624	9
95	16	44	0.37	0.0774	0.0017	2.0477	0.0467	0.1918	0.0029	1132	23	1132	16	1131	16
96	60	69	0.87	0.1038	0.0032	4.1906	0.1323	0.2927	0.0064	1693	29	1672	26	1655	32
97	84	100	0.84	0.1669	0.0026	10.5160	0.1809	0.4569	0.0065	2527	13	2481	16	2426	29
98	325	414	0.78	0.0706	0.0011	1.4737	0.0258	0.1513	0.0021	946	16	920	11	908	12
99	46	46	1.01	0.0616	0.0019	0.9035	0.0280	0.1064	0.0017	659	40	654	15	652	10
100	83	102	0.82	0.0594	0.0016	0.7679	0.0212	0.0937	0.0014	581	34	579	12	578	8
Sample 10GD54, Middle Ordovician, Yulin															
1	129	150	0.86	0.0656	0.0030	1.1997	0.0544	0.1326	0.0023	794	66	800	25	803	13
2	234	626	0.37	0.1700	0.0042	11.5876	0.2817	0.4943	0.0075	2558	21	2572	23	2589	32
3	59	56	1.04	0.0982	0.0038	3.6806	0.1402	0.2719	0.0049	1589	44	1567	30	1550	25
4	445	406	1.10	0.1060	0.0027	4.3183	0.1072	0.2954	0.0045	1731	24	1697	20	1669	23
5	306	834	0.37	0.1633	0.0041	10.3534	0.2522	0.4598	0.0070	2490	22	2467	23	2439	31
6	58	1158	0.05	0.0800	0.0021	2.1391	0.0534	0.1939	0.0030	1197	26	1162	17	1142	16
7	495	677	0.73	0.1049	0.0027	4.4493	0.1102	0.3077	0.0047	1712	24	1722	21	1729	23
8	61	983	0.06	0.0756	0.0019	1.9176	0.0479	0.1839	0.0028	1085	27	1087	17	1088	15
9	351	408	0.86	0.0768	0.0021	2.0293	0.0539	0.1917	0.0030	1115	29	1125	18	1130	16

10	98	269	0.36	0.0644	0.0023	1.1136	0.0382	0.1254	0.0020	755	45	760	18	761	12
11	561	1133	0.50	0.0630	0.0017	0.9982	0.0266	0.1150	0.0018	707	31	703	14	701	10
12	104	124	0.83	0.1032	0.0031	4.0921	0.1200	0.2876	0.0047	1682	31	1653	24	1629	23
13	218	1250	0.17	0.0836	0.0022	2.5599	0.0647	0.2220	0.0034	1284	26	1289	18	1292	18
14	248	474	0.52	0.0735	0.0020	1.7704	0.0472	0.1747	0.0027	1028	30	1035	17	1038	15
15	498	983	0.51	0.0845	0.0022	2.5878	0.0656	0.2222	0.0034	1303	26	1297	19	1293	18
16	2427	702	3.45	0.1600	0.0044	9.9516	0.2662	0.4511	0.0077	2456	24	2430	25	2400	34
17	580	1488	0.39	0.0734	0.0019	1.7395	0.0444	0.1718	0.0026	1025	28	1023	16	1022	15
18	544	324	1.68	0.0740	0.0022	1.7614	0.0496	0.1726	0.0028	1042	32	1031	18	1026	15
19	100	192	0.52	0.0932	0.0027	3.3441	0.0947	0.2602	0.0043	1492	30	1491	22	1491	22
20	111	139	0.80	0.0976	0.0035	3.7417	0.1296	0.2779	0.0052	1580	37	1580	28	1581	26
21	697	2192	0.32	0.0717	0.0019	1.5611	0.0402	0.1579	0.0024	978	29	955	16	945	13
22	460	515	0.89	0.2041	0.0054	15.7051	0.4018	0.5582	0.0086	2859	23	2859	24	2859	35
23	61	736	0.08	0.1025	0.0028	4.0549	0.1057	0.2868	0.0044	1670	26	1645	21	1626	22
24	253	411	0.62	0.0761	0.0023	1.8190	0.0526	0.1734	0.0028	1097	33	1052	19	1031	15
25	132	922	0.14	0.0712	0.0020	1.5388	0.0417	0.1567	0.0024	964	31	946	17	938	14
26	264	339	0.78	0.1684	0.0046	11.0000	0.2928	0.4737	0.0075	2542	24	2523	25	2500	33
27	876	1847	0.47	0.1763	0.0048	12.1067	0.3167	0.4982	0.0077	2618	24	2613	25	2606	33
28	50	151	0.33	0.0761	0.0025	1.9435	0.0611	0.1853	0.0031	1097	37	1096	21	1096	17
29	276	1544	0.18	0.0597	0.0017	0.8154	0.0226	0.0990	0.0016	594	34	605	13	608	9
30	83	675	0.12	0.0834	0.0025	2.5405	0.0738	0.2210	0.0036	1278	32	1284	21	1287	19
31	640	1217	0.53	0.0601	0.0018	0.8265	0.0236	0.0998	0.0016	606	35	612	13	613	9
32	624	871	0.72	0.0794	0.0023	2.0694	0.0572	0.1890	0.0030	1182	31	1139	19	1116	16
33	453	288	1.58	0.0651	0.0023	1.1175	0.0387	0.1245	0.0021	778	45	762	19	756	12
35	58	133	0.44	0.0709	0.0027	1.5578	0.0579	0.1594	0.0028	954	48	954	23	953	15
36	123	1088	0.11	0.0706	0.0021	1.4340	0.0409	0.1473	0.0023	946	33	903	17	886	13
37	96	1011	0.10	0.0817	0.0024	2.3089	0.0654	0.2049	0.0033	1239	31	1215	20	1201	17
38	290	499	0.58	0.0725	0.0022	1.6795	0.0498	0.1679	0.0027	1001	35	1001	19	1001	15
39	211	1703	0.12	0.0790	0.0023	2.0536	0.0580	0.1884	0.0030	1173	32	1133	19	1113	16
40	195	378	0.52	0.0876	0.0027	2.7937	0.0826	0.2313	0.0037	1374	33	1354	22	1341	19
41	176	439	0.40	0.0829	0.0026	2.4559	0.0740	0.2150	0.0035	1266	34	1259	22	1255	19
42	318	439	0.72	0.0804	0.0025	2.2887	0.0692	0.2065	0.0034	1206	34	1209	21	1210	18

43	184	609	0.30	0.0744	0.0023	1.8596	0.0557	0.1812	0.0029	1053	35	1067	20	1074	16
44	102	126	0.81	0.0761	0.0029	1.8696	0.0694	0.1783	0.0031	1097	46	1070	25	1058	17
45	384	714	0.54	0.0748	0.0023	1.8169	0.0545	0.1763	0.0028	1062	35	1052	20	1047	16
46	235	838	0.28	0.1289	0.0039	6.7864	0.2001	0.3818	0.0061	2083	30	2084	26	2085	28
47	67	75	0.89	0.1531	0.0055	9.5481	0.3377	0.4522	0.0096	2381	33	2392	33	2405	43
48	354	442	0.80	0.0799	0.0025	2.2246	0.0682	0.2019	0.0033	1195	35	1189	21	1185	18
49	69	1330	0.05	0.0685	0.0022	1.3369	0.0408	0.1415	0.0023	885	37	862	18	853	13
50	499	1818	0.27	0.0730	0.0023	1.7195	0.0520	0.1708	0.0027	1015	36	1016	19	1016	15
51	85	693	0.12	0.0797	0.0026	2.2069	0.0683	0.2009	0.0033	1189	36	1183	22	1180	17
52	352	1421	0.25	0.0765	0.0024	1.9842	0.0609	0.1881	0.0030	1108	36	1110	21	1111	16
53	579	1016	0.57	0.0724	0.0024	1.5764	0.0493	0.1580	0.0026	996	38	961	19	946	14
54	37	1876	0.02	0.1142	0.0037	4.9838	0.1534	0.3165	0.0051	1867	33	1817	26	1773	25
55	94	188	0.50	0.0714	0.0029	1.5262	0.0604	0.1550	0.0027	969	53	941	24	929	15
56	138	888	0.16	0.0962	0.0033	3.5798	0.1172	0.2700	0.0046	1551	37	1545	26	1541	23
57	1431	1606	0.89	0.0611	0.0020	0.8587	0.0276	0.1019	0.0017	643	41	629	15	626	10
58	15	854	0.02	0.0701	0.0024	1.5521	0.0505	0.1605	0.0026	932	40	951	20	960	15
59	181	1570	0.12	0.1997	0.0066	14.3759	0.4583	0.5222	0.0085	2824	31	2775	30	2708	36
60	494	620	0.80	0.0804	0.0028	2.3716	0.0789	0.2140	0.0036	1206	40	1234	24	1250	19
61	1006	1426	0.71	0.0793	0.0027	2.2077	0.0728	0.2018	0.0033	1181	39	1183	23	1185	18
62	111	116	0.96	0.1566	0.0056	9.5902	0.3303	0.4442	0.0078	2419	35	2396	32	2369	35
63	79	1053	0.08	0.0828	0.0029	2.2404	0.0747	0.1963	0.0033	1264	39	1194	23	1155	18
64	355	309	1.15	0.0803	0.0030	2.2807	0.0804	0.2059	0.0035	1205	43	1206	25	1207	19
65	233	723	0.32	0.1581	0.0055	10.0185	0.3346	0.4596	0.0077	2435	34	2436	31	2438	34
66	107	158	0.68	0.0720	0.0031	1.5169	0.0633	0.1529	0.0028	985	55	937	26	917	16
67	433	557	0.78	0.0857	0.0031	2.6789	0.0937	0.2267	0.0039	1331	42	1323	26	1317	20
68	120	169	0.71	0.3106	0.0111	31.3850	1.0785	0.7327	0.0126	3524	32	3531	34	3544	47
69	136	583	0.23	0.0740	0.0027	1.7280	0.0615	0.1694	0.0029	1041	44	1019	23	1009	16
70	317	217	1.46	0.0608	0.0037	0.8367	0.0491	0.0998	0.0019	632	93	617	27	613	11
71	56	502	0.11	0.1255	0.0046	6.4266	0.2255	0.3715	0.0063	2035	38	2036	31	2036	30
72	193	361	0.53	0.0789	0.0031	2.1049	0.0794	0.1935	0.0034	1169	47	1150	26	1140	18
73	67	865	0.08	0.1604	0.0059	10.2924	0.3633	0.4654	0.0079	2460	37	2461	33	2463	35
74	52	995	0.05	0.0926	0.0035	3.2565	0.1164	0.2551	0.0044	1480	42	1471	28	1464	22

75	164	377	0.43	0.1093	0.0041	4.8597	0.1759	0.3224	0.0056	1788	41	1795	30	1801	27
76	176	482	0.37	0.0804	0.0031	2.2921	0.0852	0.2067	0.0036	1207	46	1210	26	1211	19
77	626	1263	0.50	0.1440	0.0055	8.1567	0.2962	0.4108	0.0071	2276	39	2249	33	2219	32
78	352	1081	0.33	0.0593	0.0024	0.7702	0.0294	0.0941	0.0016	580	53	580	17	580	10
79	1541	1419	1.09	0.0730	0.0029	1.7171	0.0644	0.1707	0.0030	1013	48	1015	24	1016	16
80	444	730	0.61	0.0719	0.0029	1.6337	0.0627	0.1647	0.0029	984	50	983	24	983	16
81	91	821	0.11	0.0772	0.0031	1.9909	0.0760	0.1871	0.0033	1126	48	1112	26	1106	18
82	187	2358	0.08	0.0715	0.0028	1.5711	0.0598	0.1594	0.0028	971	49	959	24	954	16
83	439	345	1.27	0.0704	0.0031	1.5131	0.0631	0.1558	0.0028	940	56	936	25	934	16
84	143	754	0.19	0.1031	0.0041	4.3182	0.1650	0.3037	0.0053	1680	45	1697	32	1710	26
85	639	447	1.43	0.0643	0.0029	1.1244	0.0480	0.1268	0.0023	752	60	765	23	770	13
86	80	1108	0.07	0.0701	0.0029	1.5061	0.0594	0.1559	0.0028	930	52	933	24	934	15
87	399	1047	0.38	0.0724	0.0030	1.6279	0.0646	0.1630	0.0029	998	52	981	25	973	16
88	2675	858	3.12	0.0713	0.0030	1.6337	0.0654	0.1661	0.0030	967	53	983	25	991	16
89	567	358	1.58	0.0678	0.0031	1.2940	0.0568	0.1383	0.0026	863	60	843	25	835	15
90	394	344	1.14	0.1009	0.0043	3.9048	0.1573	0.2805	0.0051	1641	48	1615	33	1594	26
91	276	1070	0.26	0.0937	0.0039	3.4594	0.1384	0.2676	0.0048	1503	49	1518	32	1529	24
92	160	160	1.00	0.0598	0.0035	0.8113	0.0459	0.0983	0.0020	598	88	603	26	604	12
93	357	101	3.53	0.0646	0.0038	1.0865	0.0620	0.1219	0.0026	762	84	747	30	742	15
94	3179	1588	2.00	0.0614	0.0027	0.9191	0.0387	0.1085	0.0020	654	59	662	20	664	12
95	581	380	1.53	0.0582	0.0029	0.6991	0.0336	0.0872	0.0017	535	71	538	20	539	10
96	144	982	0.15	0.0748	0.0033	1.9037	0.0797	0.1846	0.0034	1063	55	1082	28	1092	19
97	48	69	0.69	0.0758	0.0044	1.8355	0.1017	0.1756	0.0039	1089	75	1058	36	1043	21
98	980	752	1.30	0.0723	0.0032	1.6264	0.0688	0.1632	0.0030	993	56	980	27	974	17
99	1596	1691	0.94	0.0708	0.0031	1.5670	0.0658	0.1605	0.0029	951	56	957	26	959	16
100	250	1267	0.20	0.0698	0.0031	1.4886	0.0631	0.1547	0.0029	922	57	926	26	927	16
Sample 10GD52-1, Middle Ordovician, Yulin															
1	102	147	0.70	0.0700	0.0012	1.5095	0.0280	0.1563	0.0022	929	18	934	11	936	12
2	27	520	0.05	0.0746	0.0011	1.8011	0.0302	0.1750	0.0024	1059	15	1046	11	1040	13
3	308	734	0.42	0.0924	0.0013	3.2480	0.0536	0.2550	0.0036	1475	14	1469	13	1464	18
4	183	346	0.53	0.1149	0.0032	5.3233	0.1273	0.3359	0.0049	1879	52	1873	20	1867	24

5	163	244	0.67	0.0703	0.0011	1.5148	0.0267	0.1563	0.0022	937	17	936	11	936	12
6	1058	1555	0.68	0.0577	0.0009	0.6800	0.0115	0.0855	0.0012	517	17	527	7	529	7
7	343	1185	0.29	0.1749	0.0025	11.5485	0.1895	0.4788	0.0066	2605	12	2569	15	2522	29
8	238	411	0.58	0.0733	0.0011	1.7719	0.0306	0.1754	0.0025	1021	16	1035	11	1042	14
9	408	508	0.80	0.0939	0.0014	3.3439	0.0557	0.2584	0.0036	1505	14	1491	13	1481	18
10	99	161	0.61	0.1521	0.0023	9.4235	0.1619	0.4494	0.0064	2369	13	2380	16	2392	29
11	51	181	0.28	0.0735	0.0012	1.7473	0.0320	0.1724	0.0025	1028	17	1026	12	1025	13
12	51	85	0.60	0.0761	0.0015	1.9419	0.0416	0.1851	0.0027	1097	21	1096	14	1095	15
13	100	78	1.29	0.1674	0.0026	11.1807	0.1925	0.4844	0.0069	2532	13	2538	16	2546	30
14	56	136	0.42	0.0657	0.0015	1.0791	0.0253	0.1191	0.0018	797	26	743	12	725	10
15	39	116	0.34	0.2001	0.0030	15.0781	0.2551	0.5465	0.0077	2827	12	2820	16	2810	32
16	156	178	0.88	0.0647	0.0013	1.1424	0.0243	0.1281	0.0019	764	22	774	12	777	11
17	170	266	0.64	0.1824	0.0027	12.7054	0.2127	0.5050	0.0071	2675	13	2658	16	2635	30
18	130	214	0.61	0.1737	0.0026	11.9879	0.2015	0.5005	0.0070	2594	13	2603	16	2616	30
19	147	320	0.46	0.0792	0.0012	2.0691	0.0363	0.1894	0.0027	1178	16	1139	12	1118	14
20	71	667	0.11	0.0766	0.0012	2.0549	0.0356	0.1947	0.0027	1109	16	1134	12	1147	15
21	287	315	0.91	0.0593	0.0039	0.7375	0.0467	0.0903	0.0015	576	146	561	27	557	9
22	98	334	0.29	0.0761	0.0012	1.9508	0.0343	0.1858	0.0026	1099	16	1099	12	1099	14
23	415	1312	0.32	0.0732	0.0011	1.7407	0.0295	0.1723	0.0024	1021	16	1024	11	1025	13
24	373	376	0.99	0.0580	0.0011	0.7076	0.0142	0.0884	0.0013	531	21	543	8	546	7
25	40	360	0.11	0.0744	0.0012	1.8070	0.0320	0.1761	0.0025	1053	16	1048	12	1046	14
26	333	330	1.01	0.0575	0.0011	0.6723	0.0141	0.0848	0.0012	509	23	522	9	525	7
27	172	701	0.24	0.0588	0.0010	0.7446	0.0134	0.0918	0.0013	561	18	565	8	566	8
28	127	274	0.46	0.1147	0.0018	5.3022	0.0917	0.3354	0.0047	1874	14	1869	15	1864	23
29	106	206	0.52	0.0646	0.0012	1.1265	0.0217	0.1264	0.0018	762	19	766	10	767	10
30	222	327	0.68	0.0739	0.0012	1.7743	0.0317	0.1742	0.0025	1038	17	1036	12	1035	13
31	87	496	0.18	0.0682	0.0011	1.3694	0.0242	0.1456	0.0020	874	17	876	10	876	11
32	57	509	0.11	0.1031	0.0016	4.2273	0.0746	0.2972	0.0042	1681	15	1679	14	1678	21
33	102	166	0.62	0.0659	0.0013	1.2062	0.0249	0.1328	0.0019	803	21	803	11	804	11
34	26	163	0.16	0.0661	0.0013	1.2291	0.0259	0.1348	0.0019	810	22	814	12	815	11
35	251	569	0.44	0.0718	0.0011	1.6200	0.0288	0.1637	0.0023	980	17	978	11	977	13
36	165	350	0.47	0.0609	0.0011	0.8351	0.0167	0.0995	0.0014	635	21	616	9	611	8

37	88	430	0.21	0.0769	0.0013	2.1195	0.0388	0.1998	0.0028	1119	17	1155	13	1174	15
38	267	916	0.29	0.0748	0.0012	1.8775	0.0333	0.1820	0.0026	1063	16	1073	12	1078	14
39	6	21	0.27	0.0654	0.0054	1.1304	0.0917	0.1253	0.0025	787	138	768	44	761	14
40	64	128	0.50	0.0655	0.0014	1.1669	0.0258	0.1293	0.0019	789	23	785	12	784	11
41	101	122	0.83	0.0678	0.0016	1.3258	0.0324	0.1418	0.0021	863	27	857	14	855	12
42	14	271	0.05	0.0973	0.0016	3.9562	0.0719	0.2949	0.0042	1572	16	1625	15	1666	21
43	67	189	0.36	0.0593	0.0015	0.7753	0.0207	0.0948	0.0014	579	33	583	12	584	8
44	53	110	0.49	0.0607	0.0021	0.8559	0.0296	0.1022	0.0016	630	48	628	16	627	9
45	599	700	0.86	0.0695	0.0012	1.5378	0.0283	0.1605	0.0023	913	18	946	11	959	13
46	70	347	0.20	0.0610	0.0012	0.8775	0.0182	0.1043	0.0015	640	22	640	10	640	9
47	50	1715	0.03	0.0581	0.0010	0.8024	0.0148	0.1001	0.0014	534	19	598	8	615	8
48	291	786	0.37	0.0573	0.0010	0.7439	0.0142	0.0941	0.0013	503	20	565	8	580	8
49	201	379	0.53	0.1564	0.0026	9.8720	0.1796	0.4576	0.0064	2418	14	2423	17	2429	28
50	63	290	0.22	0.0616	0.0013	0.8996	0.0195	0.1059	0.0015	660	23	652	10	649	9
51	222	441	0.50	0.1026	0.0017	4.2885	0.0794	0.3030	0.0043	1672	16	1691	15	1706	21
52	191	348	0.55	0.1549	0.0026	9.7798	0.1806	0.4577	0.0065	2401	15	2414	17	2429	29
53	88	149	0.59	0.1609	0.0028	10.1045	0.1894	0.4554	0.0065	2465	15	2444	17	2419	29
54	84	94	0.89	0.1613	0.0028	10.3217	0.1958	0.4641	0.0067	2469	15	2464	18	2457	29
55	459	220	2.08	0.0714	0.0014	1.5894	0.0323	0.1614	0.0023	969	20	966	13	964	13
56	203	394	0.51	0.0602	0.0011	0.8287	0.0167	0.0998	0.0014	612	21	613	9	613	8
57	78	110	0.71	0.2368	0.0041	20.1536	0.3817	0.6170	0.0088	3099	14	3099	18	3098	35
58	100	118	0.85	0.0658	0.0016	1.1579	0.0288	0.1277	0.0019	799	28	781	14	775	11
59	273	296	0.92	0.1190	0.0047	5.7473	0.2064	0.3502	0.0055	1942	72	1939	31	1936	26
60	218	247	0.88	0.1814	0.0032	12.4466	0.2378	0.4974	0.0071	2666	15	2639	18	2603	30
61	99	112	0.88	0.0720	0.0015	1.6073	0.0343	0.1618	0.0024	987	22	973	13	967	13
62	133	306	0.43	0.0706	0.0013	1.5016	0.0300	0.1543	0.0022	945	20	931	12	925	12
63	335	445	0.75	0.1609	0.0029	10.4750	0.2025	0.4722	0.0067	2465	16	2478	18	2493	29
64	86	228	0.38	0.0746	0.0017	1.7985	0.0420	0.1748	0.0027	1058	24	1045	15	1038	15
65	160	84	1.92	0.1548	0.0031	10.0222	0.2098	0.4695	0.0072	2399	17	2437	19	2481	32
66	131	122	1.08	0.0597	0.0018	0.7366	0.0223	0.0895	0.0014	591	39	560	13	553	8
67	238	402	0.59	0.1579	0.0029	10.0135	0.1971	0.4598	0.0066	2434	16	2436	18	2439	29
68	34	38	0.92	0.1585	0.0038	9.8466	0.2388	0.4504	0.0078	2440	20	2421	22	2397	35

69	225	827	0.27	0.0714	0.0014	1.6495	0.0332	0.1675	0.0024	969	20	989	13	998	13
70	250	471	0.53	0.0634	0.0013	1.0252	0.0221	0.1173	0.0017	721	23	717	11	715	10
71	92	106	0.86	0.0608	0.0018	0.8694	0.0264	0.1037	0.0016	632	39	635	14	636	9
72	107	92	1.16	0.0648	0.0037	1.1005	0.0619	0.1232	0.0024	767	86	754	30	749	13
73	157	363	0.43	0.0753	0.0015	1.8952	0.0401	0.1825	0.0027	1077	21	1079	14	1081	14
74	97	192	0.50	0.0718	0.0016	1.6185	0.0374	0.1634	0.0024	981	24	977	15	975	13
75	122	378	0.32	0.0612	0.0013	0.8870	0.0195	0.1050	0.0015	647	24	645	10	644	9
76	121	213	0.57	0.0737	0.0016	1.7587	0.0387	0.1730	0.0025	1034	22	1030	14	1029	14
77	158	89	1.78	0.0714	0.0023	1.5824	0.0505	0.1607	0.0026	969	39	963	20	960	14
78	41	308	0.13	0.0608	0.0015	0.8366	0.0206	0.0998	0.0015	632	29	617	11	613	9
79	456	622	0.73	0.0586	0.0012	0.7281	0.0160	0.0901	0.0013	552	24	555	9	556	8
~~*80*~~	~~*53*~~	~~*123*~~	~~*0.43*~~	~~*0.0724*~~	~~*0.0023*~~	~~*0.7563*~~	~~*0.0237*~~	~~*0.0757*~~	~~*0.0012*~~	~~*998*~~	~~*38*~~	~~*572*~~	~~*14*~~	~~*470*~~	~~*7*~~
81	173	368	0.47	0.1552	0.0031	9.3997	0.1979	0.4392	0.0064	2404	18	2378	19	2347	29
82	137	277	0.49	0.1405	0.0028	8.1045	0.1714	0.4184	0.0061	2233	18	2243	19	2253	28
83	53	163	0.33	0.0797	0.0019	2.1504	0.0531	0.1956	0.0031	1191	26	1165	17	1151	16
84	87	109	0.80	0.0604	0.0018	0.8512	0.0257	0.1022	0.0016	618	39	625	14	627	9
85	124	291	0.42	0.0745	0.0016	1.7905	0.0401	0.1744	0.0026	1054	23	1042	15	1036	14
86	136	137	0.99	0.0767	0.0023	1.9265	0.0582	0.1820	0.0029	1114	36	1090	20	1078	16
87	16	32	0.52	0.0712	0.0033	1.5983	0.0728	0.1628	0.0029	963	64	970	28	972	16
88	95	434	0.22	0.1749	0.0037	11.7056	0.2540	0.4855	0.0071	2605	18	2581	20	2551	31
89	82	132	0.62	0.0714	0.0020	1.5371	0.0439	0.1561	0.0025	969	33	945	18	935	14
90	85	206	0.41	0.0655	0.0020	1.0834	0.0333	0.1199	0.0019	791	38	745	16	730	11
~~*91*~~	~~*10*~~	~~*11*~~	~~*0.95*~~	~~*0.0953*~~	~~*0.0141*~~	~~*2.0904*~~	~~*0.3034*~~	~~*0.1591*~~	~~*0.0063*~~	~~*1533*~~	~~*218*~~	~~*1146*~~	~~*100*~~	~~*952*~~	~~*35*~~
92	146	108	1.35	0.1592	0.0035	10.2245	0.2302	0.4658	0.0070	2447	19	2455	21	2465	31
93	34	63	0.53	0.0709	0.0022	1.5829	0.0496	0.1619	0.0026	954	38	964	19	968	15
94	194	251	0.77	0.1535	0.0034	9.4831	0.2139	0.4481	0.0067	2385	20	2386	21	2387	30
95	84	532	0.16	0.0619	0.0014	0.9363	0.0222	0.1096	0.0016	672	27	671	12	671	9
96	47	351	0.13	0.0790	0.0019	2.4259	0.0578	0.2226	0.0033	1173	25	1250	17	1296	18
97	173	141	1.23	0.0756	0.0019	1.7853	0.0455	0.1712	0.0026	1085	28	1040	17	1019	15
98	161	305	0.53	0.0696	0.0016	1.4858	0.0356	0.1548	0.0023	917	26	925	15	928	13
99	44	105	0.42	0.0626	0.0021	0.9536	0.0318	0.1105	0.0018	693	44	680	17	676	10
100	191	439	0.43	0.0760	0.0017	1.8974	0.0444	0.1810	0.0027	1096	24	1080	16	1072	15

Sample 10GD52-1, Middle Ordovician, Yulin

1	102	147	0.70	0.0700	0.0012	1.5095	0.0280	0.1563	0.0022	929	18	934	11	936	12
2	27	520	0.05	0.0746	0.0011	1.8011	0.0302	0.1750	0.0024	1059	15	1046	11	1040	13
3	308	734	0.42	0.0924	0.0013	3.2480	0.0536	0.2550	0.0036	1475	14	1469	13	1464	18
4	183	346	0.53	0.1149	0.0032	5.3233	0.1273	0.3359	0.0049	1879	52	1873	20	1867	24
5	163	244	0.67	0.0703	0.0011	1.5148	0.0267	0.1563	0.0022	937	17	936	11	936	12
6	1058	1555	0.68	0.0577	0.0009	0.6800	0.0115	0.0855	0.0012	517	17	527	7	529	7
7	343	1185	0.29	0.1749	0.0025	11.5485	0.1895	0.4788	0.0066	2605	12	2569	15	2522	29
8	238	411	0.58	0.0733	0.0011	1.7719	0.0306	0.1754	0.0025	1021	16	1035	11	1042	14
9	408	508	0.80	0.0939	0.0014	3.3439	0.0557	0.2584	0.0036	1505	14	1491	13	1481	18
10	99	161	0.61	0.1521	0.0023	9.4235	0.1619	0.4494	0.0064	2369	13	2380	16	2392	29
11	51	181	0.28	0.0735	0.0012	1.7473	0.0320	0.1724	0.0025	1028	17	1026	12	1025	13
12	51	85	0.60	0.0761	0.0015	1.9419	0.0416	0.1851	0.0027	1097	21	1096	14	1095	15
13	100	78	1.29	0.1674	0.0026	11.1807	0.1925	0.4844	0.0069	2532	13	2538	16	2546	30
14	56	136	0.42	0.0657	0.0015	1.0791	0.0253	0.1191	0.0018	797	26	743	12	725	10
15	39	116	0.34	0.2001	0.0030	15.0781	0.2551	0.5465	0.0077	2827	12	2820	16	2810	32
16	156	178	0.88	0.0647	0.0013	1.1424	0.0243	0.1281	0.0019	764	22	774	12	777	11
17	170	266	0.64	0.1824	0.0027	12.7054	0.2127	0.5050	0.0071	2675	13	2658	16	2635	30
18	130	214	0.61	0.1737	0.0026	11.9879	0.2015	0.5005	0.0070	2594	13	2603	16	2616	30
19	147	320	0.46	0.0792	0.0012	2.0691	0.0363	0.1894	0.0027	1178	16	1139	12	1118	14
20	71	667	0.11	0.0766	0.0012	2.0549	0.0356	0.1947	0.0027	1109	16	1134	12	1147	15
21	287	315	0.91	0.0593	0.0039	0.7375	0.0467	0.0903	0.0015	576	146	561	27	557	9
22	98	334	0.29	0.0761	0.0012	1.9508	0.0343	0.1858	0.0026	1099	16	1099	12	1099	14
23	415	1312	0.32	0.0732	0.0011	1.7407	0.0295	0.1723	0.0024	1021	16	1024	11	1025	13
24	373	376	0.99	0.0580	0.0011	0.7076	0.0142	0.0884	0.0013	531	21	543	8	546	7
25	40	360	0.11	0.0744	0.0012	1.8070	0.0320	0.1761	0.0025	1053	16	1048	12	1046	14
26	333	330	1.01	0.0575	0.0011	0.6723	0.0141	0.0848	0.0012	509	23	522	9	525	7
27	172	701	0.24	0.0588	0.0010	0.7446	0.0134	0.0918	0.0013	561	18	565	8	566	8
28	127	274	0.46	0.1147	0.0018	5.3022	0.0917	0.3354	0.0047	1874	14	1869	15	1864	23
29	106	206	0.52	0.0646	0.0012	1.1265	0.0217	0.1264	0.0018	762	19	766	10	767	10
30	222	327	0.68	0.0739	0.0012	1.7743	0.0317	0.1742	0.0025	1038	17	1036	12	1035	13

31	87	496	0.18	0.0682	0.0011	1.3694	0.0242	0.1456	0.0020	874	17	876	10	876	11
32	57	509	0.11	0.1031	0.0016	4.2273	0.0746	0.2972	0.0042	1681	15	1679	14	1678	21
33	102	166	0.62	0.0659	0.0013	1.2062	0.0249	0.1328	0.0019	803	21	803	11	804	11
34	26	163	0.16	0.0661	0.0013	1.2291	0.0259	0.1348	0.0019	810	22	814	12	815	11
35	251	569	0.44	0.0718	0.0011	1.6200	0.0288	0.1637	0.0023	980	17	978	11	977	13
36	165	350	0.47	0.0609	0.0011	0.8351	0.0167	0.0995	0.0014	635	21	616	9	611	8
37	88	430	0.21	0.0769	0.0013	2.1195	0.0388	0.1998	0.0028	1119	17	1155	13	1174	15
38	267	916	0.29	0.0748	0.0012	1.8775	0.0333	0.1820	0.0026	1063	16	1073	12	1078	14
39	6	21	0.27	0.0654	0.0054	1.1304	0.0917	0.1253	0.0025	787	138	768	44	761	14
40	64	128	0.50	0.0655	0.0014	1.1669	0.0258	0.1293	0.0019	789	23	785	12	784	11
41	101	122	0.83	0.0678	0.0016	1.3258	0.0324	0.1418	0.0021	863	27	857	14	855	12
42	14	271	0.05	0.0973	0.0016	3.9562	0.0719	0.2949	0.0042	1572	16	1625	15	1666	21
43	67	189	0.36	0.0593	0.0015	0.7753	0.0207	0.0948	0.0014	579	33	583	12	584	8
44	53	110	0.49	0.0607	0.0021	0.8559	0.0296	0.1022	0.0016	630	48	628	16	627	9
45	599	700	0.86	0.0695	0.0012	1.5378	0.0283	0.1605	0.0023	913	18	946	11	959	13
46	70	347	0.20	0.0610	0.0012	0.8775	0.0182	0.1043	0.0015	640	22	640	10	640	9
47	50	1715	0.03	0.0581	0.0010	0.8024	0.0148	0.1001	0.0014	534	19	598	8	615	8
48	291	786	0.37	0.0573	0.0010	0.7439	0.0142	0.0941	0.0013	503	20	565	8	580	8
49	201	379	0.53	0.1564	0.0026	9.8720	0.1796	0.4576	0.0064	2418	14	2423	17	2429	28
50	63	290	0.22	0.0616	0.0013	0.8996	0.0195	0.1059	0.0015	660	23	652	10	649	9
51	222	441	0.50	0.1026	0.0017	4.2885	0.0794	0.3030	0.0043	1672	16	1691	15	1706	21
52	191	348	0.55	0.1549	0.0026	9.7798	0.1806	0.4577	0.0065	2401	15	2414	17	2429	29
53	88	149	0.59	0.1609	0.0028	10.1045	0.1894	0.4554	0.0065	2465	15	2444	17	2419	29
54	84	94	0.89	0.1613	0.0028	10.3217	0.1958	0.4641	0.0067	2469	15	2464	18	2457	29
55	459	220	2.08	0.0714	0.0014	1.5894	0.0323	0.1614	0.0023	969	20	966	13	964	13
56	203	394	0.51	0.0602	0.0011	0.8287	0.0167	0.0998	0.0014	612	21	613	9	613	8
57	78	110	0.71	0.2368	0.0041	20.1536	0.3817	0.6170	0.0088	3099	14	3099	18	3098	35
58	100	118	0.85	0.0658	0.0016	1.1579	0.0288	0.1277	0.0019	799	28	781	14	775	11
59	273	296	0.92	0.1190	0.0047	5.7473	0.2064	0.3502	0.0055	1942	72	1939	31	1936	26
60	218	247	0.88	0.1814	0.0032	12.4466	0.2378	0.4974	0.0071	2666	15	2639	18	2603	30
61	99	112	0.88	0.0720	0.0015	1.6073	0.0343	0.1618	0.0024	987	22	973	13	967	13
62	133	306	0.43	0.0706	0.0013	1.5016	0.0300	0.1543	0.0022	945	20	931	12	925	12

63	335	445	0.75	0.1609	0.0029	10.4750	0.2025	0.4722	0.0067	2465	16	2478	18	2493	29
64	86	228	0.38	0.0746	0.0017	1.7985	0.0420	0.1748	0.0027	1058	24	1045	15	1038	15
65	160	84	1.92	0.1548	0.0031	10.0222	0.2098	0.4695	0.0072	2399	17	2437	19	2481	32
66	131	122	1.08	0.0597	0.0018	0.7366	0.0223	0.0895	0.0014	591	39	560	13	553	8
67	238	402	0.59	0.1579	0.0029	10.0135	0.1971	0.4598	0.0066	2434	16	2436	18	2439	29
68	34	38	0.92	0.1585	0.0038	9.8466	0.2388	0.4504	0.0078	2440	20	2421	22	2397	35
69	225	827	0.27	0.0714	0.0014	1.6495	0.0332	0.1675	0.0024	969	20	989	13	998	13
70	250	471	0.53	0.0634	0.0013	1.0252	0.0221	0.1173	0.0017	721	23	717	11	715	10
71	92	106	0.86	0.0608	0.0018	0.8694	0.0264	0.1037	0.0016	632	39	635	14	636	9
72	107	92	1.16	0.0648	0.0037	1.1005	0.0619	0.1232	0.0024	767	86	754	30	749	13
73	157	363	0.43	0.0753	0.0015	1.8952	0.0401	0.1825	0.0027	1077	21	1079	14	1081	14
74	97	192	0.50	0.0718	0.0016	1.6185	0.0374	0.1634	0.0024	981	24	977	15	975	13
75	122	378	0.32	0.0612	0.0013	0.8870	0.0195	0.1050	0.0015	647	24	645	10	644	9
76	121	213	0.57	0.0737	0.0016	1.7587	0.0387	0.1730	0.0025	1034	22	1030	14	1029	14
77	158	89	1.78	0.0714	0.0023	1.5824	0.0505	0.1607	0.0026	969	39	963	20	960	14
78	41	308	0.13	0.0608	0.0015	0.8366	0.0206	0.0998	0.0015	632	29	617	11	613	9
79	456	622	0.73	0.0586	0.0012	0.7281	0.0160	0.0901	0.0013	552	24	555	9	556	8
~~*80*~~	~~*53*~~	~~*123*~~	~~*0.43*~~	~~*0.0724*~~	~~*0.0023*~~	~~*0.7563*~~	~~*0.0237*~~	~~*0.0757*~~	~~*0.0012*~~	~~*998*~~	~~*38*~~	~~*572*~~	~~*14*~~	~~*470*~~	~~*7*~~
81	173	368	0.47	0.1552	0.0031	9.3997	0.1979	0.4392	0.0064	2404	18	2378	19	2347	29
82	137	277	0.49	0.1405	0.0028	8.1045	0.1714	0.4184	0.0061	2233	18	2243	19	2253	28
83	53	163	0.33	0.0797	0.0019	2.1504	0.0531	0.1956	0.0031	1191	26	1165	17	1151	16
84	87	109	0.80	0.0604	0.0018	0.8512	0.0257	0.1022	0.0016	618	39	625	14	627	9
85	124	291	0.42	0.0745	0.0016	1.7905	0.0401	0.1744	0.0026	1054	23	1042	15	1036	14
86	136	137	0.99	0.0767	0.0023	1.9265	0.0582	0.1820	0.0029	1114	36	1090	20	1078	16
87	16	32	0.52	0.0712	0.0033	1.5983	0.0728	0.1628	0.0029	963	64	970	28	972	16
88	95	434	0.22	0.1749	0.0037	11.7056	0.2540	0.4855	0.0071	2605	18	2581	20	2551	31
89	82	132	0.62	0.0714	0.0020	1.5371	0.0439	0.1561	0.0025	969	33	945	18	935	14
90	85	206	0.41	0.0655	0.0020	1.0834	0.0333	0.1199	0.0019	791	38	745	16	730	11
~~*91*~~	~~*10*~~	~~*11*~~	~~*0.95*~~	~~*0.0953*~~	~~*0.0141*~~	~~*2.0904*~~	~~*0.3034*~~	~~*0.1591*~~	~~*0.0063*~~	~~*1533*~~	~~*218*~~	~~*1146*~~	~~*100*~~	~~*952*~~	~~*35*~~
92	146	108	1.35	0.1592	0.0035	10.2245	0.2302	0.4658	0.0070	2447	19	2455	21	2465	31
93	34	63	0.53	0.0709	0.0022	1.5829	0.0496	0.1619	0.0026	954	38	964	19	968	15
94	194	251	0.77	0.1535	0.0034	9.4831	0.2139	0.4481	0.0067	2385	20	2386	21	2387	30

95	84	532	0.16	0.0619	0.0014	0.9363	0.0222	0.1096	0.0016	672	27	671	12	671	9
96	47	351	0.13	0.0790	0.0019	2.4259	0.0578	0.2226	0.0033	1173	25	1250	17	1296	18
97	173	141	1.23	0.0756	0.0019	1.7853	0.0455	0.1712	0.0026	1085	28	1040	17	1019	15
98	161	305	0.53	0.0696	0.0016	1.4858	0.0356	0.1548	0.0023	917	26	925	15	928	13
99	44	105	0.42	0.0626	0.0021	0.9536	0.0318	0.1105	0.0018	693	44	680	17	676	10
100	191	439	0.43	0.0760	0.0017	1.8974	0.0444	0.1810	0.0027	1096	24	1080	16	1072	15
Sample 10GD51, Upper Ordovician, Yulin															
1	504	218	2.31	0.0725	0.0012	1.6720	0.0303	0.1673	0.0024	999	17	998	12	997	13
2	130	187	0.69	0.0736	0.0012	1.7546	0.0327	0.1730	0.0025	1029	17	1029	12	1029	14
3	362	884	0.41	0.0591	0.0009	0.7469	0.0131	0.0917	0.0013	570	17	566	8	566	8
4	407	214	1.90	0.0686	0.0011	1.3940	0.0258	0.1473	0.0021	888	18	886	11	886	12
5	196	258	0.76	0.0736	0.0012	1.7552	0.0315	0.1730	0.0025	1030	17	1029	12	1029	14
6	23	510	0.05	0.0633	0.0010	1.0240	0.0183	0.1173	0.0017	719	17	716	9	715	10
7	75	82	0.91	0.0577	0.0014	0.6616	0.0169	0.0831	0.0013	520	30	516	10	515	8
8	120	72	1.68	0.0583	0.0017	0.7042	0.0207	0.0876	0.0014	541	37	541	12	541	8
9	1324	2065	0.64	0.0668	0.0010	1.2683	0.0218	0.1377	0.0020	832	16	832	10	831	11
10	120	305	0.39	0.0895	0.0014	2.9467	0.0518	0.2388	0.0034	1414	15	1394	13	1381	18
11	12	593	0.02	0.0598	0.0010	0.7592	0.0139	0.0920	0.0013	597	18	574	8	568	8
12	300	650	0.46	0.0653	0.0010	1.1830	0.0208	0.1314	0.0019	783	17	793	10	796	11
13	90	828	0.11	0.0614	0.0010	0.9035	0.0160	0.1068	0.0015	653	17	654	9	654	9
14	134	253	0.53	0.0695	0.0012	1.4674	0.0274	0.1532	0.0022	912	18	917	11	919	12
~~*15*~~	~~*363*~~	~~*191*~~	~~*1.90*~~	~~*0.0686*~~	~~*0.0061*~~	~~*0.7546*~~	~~*0.0655*~~	~~*0.0797*~~	~~*0.0015*~~	~~*888*~~	~~*190*~~	~~*571*~~	~~*38*~~	~~*495*~~	~~*9*~~
16	173	573	0.30	0.0918	0.0014	3.2212	0.0562	0.2545	0.0036	1463	15	1462	14	1462	19
17	178	188	0.94	0.0785	0.0013	2.1261	0.0387	0.1965	0.0028	1158	17	1157	13	1157	15
18	79	136	0.58	0.0576	0.0014	0.6526	0.0160	0.0822	0.0012	513	29	510	10	509	7
19	172	132	1.30	0.0582	0.0015	0.6962	0.0185	0.0868	0.0013	537	32	537	11	536	8
20	167	308	0.54	0.1586	0.0024	9.6990	0.1693	0.4436	0.0063	2440	13	2407	16	2367	28
21	88	190	0.46	0.0636	0.0011	1.0420	0.0202	0.1188	0.0017	728	19	725	10	724	10
22	176	143	1.23	0.0930	0.0015	3.2784	0.0598	0.2558	0.0037	1487	16	1476	14	1468	19
23	494	573	0.86	0.2469	0.0038	21.5327	0.3760	0.6324	0.0090	3165	13	3163	17	3159	35
24	53	52	1.01	0.0836	0.0025	2.6776	0.0804	0.2323	0.0043	1283	31	1322	22	1346	23

25	71	161	0.44	0.0611	0.0013	0.8817	0.0195	0.1046	0.0015	643	24	642	11	641	9
26	121	179	0.67	0.0704	0.0012	1.5278	0.0290	0.1573	0.0023	941	18	942	12	942	13
27	262	596	0.44	0.0578	0.0010	0.6759	0.0127	0.0848	0.0012	523	19	524	8	525	7
28	137	442	0.31	0.1609	0.0025	10.6642	0.1894	0.4806	0.0069	2465	14	2494	16	2530	30
29	169	280	0.60	0.1665	0.0026	11.0694	0.1973	0.4820	0.0069	2523	14	2529	17	2536	30
30	100	140	0.71	0.0738	0.0013	1.6286	0.0323	0.1600	0.0023	1036	19	981	12	957	13
31	179	690	0.26	0.0710	0.0012	1.5684	0.0286	0.1601	0.0023	958	17	958	11	958	13
32	200	183	1.09	0.0740	0.0013	1.7829	0.0350	0.1748	0.0025	1041	19	1039	13	1038	14
33	167	300	0.56	0.0579	0.0012	0.6718	0.0143	0.0841	0.0012	526	23	522	9	521	7
34	181	403	0.45	0.0580	0.0011	0.6764	0.0138	0.0846	0.0012	529	22	525	8	524	7
35	50	445	0.11	0.0684	0.0012	1.4057	0.0267	0.1490	0.0022	882	18	891	11	895	12
36	197	597	0.33	0.0718	0.0012	1.6095	0.0299	0.1626	0.0023	979	18	974	12	971	13
37	58	96	0.61	0.1356	0.0028	6.7092	0.1470	0.3588	0.0059	2172	18	2074	19	1977	28
38	142	275	0.52	0.0708	0.0013	1.5593	0.0307	0.1596	0.0023	953	19	954	12	955	13
39	67	291	0.23	0.0715	0.0013	1.5977	0.0312	0.1621	0.0024	971	19	969	12	968	13
40	221	348	0.64	0.0611	0.0013	0.8387	0.0187	0.0995	0.0015	643	24	618	10	611	9
41	200	313	0.64	0.0764	0.0013	1.9550	0.0377	0.1855	0.0027	1107	18	1100	13	1097	15
42	129	100	1.29	0.0776	0.0016	1.9424	0.0428	0.1815	0.0027	1137	22	1096	15	1075	15
43	51	704	0.07	0.1864	0.0031	13.4203	0.2490	0.5222	0.0075	2710	14	2710	18	2709	32
44	166	158	1.05	0.0986	0.0018	3.7677	0.0736	0.2772	0.0041	1597	17	1586	16	1577	20
45	74	90	0.82	0.1614	0.0028	10.3880	0.2002	0.4668	0.0069	2470	15	2470	18	2470	30
46	812	465	1.75	0.0716	0.0013	1.6048	0.0310	0.1626	0.0024	974	19	972	12	971	13
47	13	29	0.43	0.1298	0.0028	6.7549	0.1525	0.3773	0.0059	2096	20	2080	20	2063	28
48	213	264	0.81	0.0720	0.0013	1.6459	0.0331	0.1658	0.0024	986	20	988	13	989	13
49	27	74	0.36	0.0603	0.0021	0.8256	0.0285	0.0993	0.0016	615	47	611	16	610	9
50	148	127	1.17	0.0646	0.0015	1.1149	0.0274	0.1252	0.0019	761	28	761	13	760	11
51	292	320	0.91	0.0896	0.0016	3.0921	0.0605	0.2502	0.0036	1417	18	1431	15	1440	19
52	214	751	0.29	0.1798	0.0031	12.8540	0.2477	0.5185	0.0075	2651	15	2669	18	2693	32
53	94	86	1.09	0.1612	0.0029	10.2413	0.2029	0.4606	0.0068	2469	16	2457	18	2442	30
54	187	258	0.72	0.0719	0.0016	1.6372	0.0380	0.1651	0.0026	984	24	985	15	985	14
55	257	698	0.37	0.0746	0.0014	1.8276	0.0362	0.1776	0.0026	1059	19	1055	13	1054	14
56	208	330	0.63	0.0584	0.0012	0.7094	0.0156	0.0881	0.0013	544	24	544	9	544	8

57	52	138	0.38	0.1580	0.0029	10.1111	0.2029	0.4641	0.0069	2434	16	2445	19	2457	30
58	539	1116	0.48	0.0662	0.0012	1.2371	0.0247	0.1355	0.0020	814	20	818	11	819	11
59	49	80	0.61	0.0750	0.0019	1.8641	0.0490	0.1802	0.0028	1069	29	1068	17	1068	15
60	86	259	0.33	0.0698	0.0014	1.4791	0.0320	0.1537	0.0023	922	22	922	13	922	13
61	273	483	0.57	0.0585	0.0012	0.7059	0.0156	0.0875	0.0013	548	24	542	9	541	8
62	151	882	0.17	0.1672	0.0031	10.6262	0.2135	0.4610	0.0067	2529	16	2491	19	2444	30
63	30	29	1.02	0.1530	0.0032	9.4210	0.2077	0.4465	0.0070	2380	18	2380	20	2380	31
64	182	564	0.32	0.0717	0.0014	1.6197	0.0332	0.1639	0.0024	977	20	978	13	978	13
65	171	357	0.48	0.0767	0.0015	2.1558	0.0448	0.2037	0.0030	1114	20	1167	14	1195	16
66	81	138	0.59	0.0723	0.0016	1.5930	0.0363	0.1597	0.0024	996	24	967	14	955	13
67	151	488	0.31	0.0760	0.0015	1.8860	0.0395	0.1799	0.0027	1096	20	1076	14	1066	15
68	319	641	0.50	0.0710	0.0014	1.5802	0.0331	0.1615	0.0024	956	21	962	13	965	13
69	230	206	1.12	0.0586	0.0015	0.6854	0.0176	0.0848	0.0013	552	31	530	11	525	8
70	14	28	0.49	0.0752	0.0035	1.8766	0.0870	0.1809	0.0034	1075	63	1073	31	1072	18
71	35	55	0.64	0.0807	0.0019	2.2995	0.0566	0.2067	0.0032	1213	25	1212	17	1211	17
72	141	119	1.19	0.0603	0.0015	0.8286	0.0215	0.0997	0.0016	613	30	613	12	613	9
73	117	1032	0.11	0.0583	0.0012	0.7044	0.0152	0.0876	0.0013	543	23	541	9	541	8
74	473	491	0.96	0.0719	0.0015	1.6339	0.0354	0.1647	0.0025	984	22	983	14	983	14
75	108	72	1.50	0.0584	0.0026	0.7070	0.0312	0.0878	0.0015	544	67	543	19	543	9
76	250	419	0.60	0.1671	0.0034	11.0828	0.2382	0.4809	0.0071	2529	18	2530	20	2531	31
77	230	301	0.76	0.0771	0.0016	2.0652	0.0460	0.1942	0.0029	1124	22	1137	15	1144	16
78	265	310	0.86	0.0583	0.0014	0.7008	0.0169	0.0872	0.0013	540	28	539	10	539	8
79	94	439	0.21	0.0715	0.0015	1.6327	0.0363	0.1656	0.0025	972	23	983	14	988	14
80	171	409	0.42	0.1084	0.0023	5.0599	0.1126	0.3386	0.0051	1772	20	1829	19	1880	25
81	68	191	0.36	0.0609	0.0015	0.8666	0.0221	0.1032	0.0016	635	29	634	12	633	9
82	367	180	2.04	0.0635	0.0016	1.1326	0.0296	0.1294	0.0020	724	30	769	14	784	11
83	57	116	0.49	0.0595	0.0020	0.7609	0.0257	0.0927	0.0015	585	46	575	15	572	9
84	132	217	0.61	0.0720	0.0016	1.6169	0.0384	0.1629	0.0025	985	25	977	15	973	14
85	59	53	1.10	0.1721	0.0038	10.8404	0.2503	0.4567	0.0071	2579	19	2510	21	2425	31
86	307	546	0.56	0.0581	0.0014	0.6888	0.0174	0.0859	0.0013	535	29	532	10	531	8
87	70	42	1.68	0.0751	0.0027	1.9115	0.0692	0.1846	0.0031	1071	46	1085	24	1092	17
88	130	175	0.74	0.1140	0.0025	5.2049	0.1209	0.3311	0.0051	1864	21	1853	20	1844	25

89	81	210	0.38	0.0779	0.0018	2.0323	0.0490	0.1891	0.0029	1145	25	1126	16	1117	16
90	387	356	1.09	0.0586	0.0015	0.7033	0.0182	0.0870	0.0013	554	31	541	11	538	8
91	215	229	0.94	0.0689	0.0017	1.3773	0.0349	0.1450	0.0023	895	28	879	15	873	13
92	34	626	0.05	0.0688	0.0016	1.4180	0.0334	0.1495	0.0023	893	25	897	14	898	13
93	324	966	0.34	0.0733	0.0016	1.7294	0.0405	0.1712	0.0026	1021	24	1020	15	1019	14
94	265	749	0.35	0.0586	0.0014	0.7223	0.0180	0.0894	0.0014	551	29	552	11	552	8
95	29	34	0.85	0.0883	0.0037	2.8524	0.1186	0.2344	0.0043	1388	52	1369	31	1357	22
96	153	96	1.60	0.0595	0.0031	0.6817	0.0356	0.0831	0.0015	585	82	528	21	514	9
97	453	172	2.63	0.0596	0.0019	0.7702	0.0247	0.0938	0.0015	587	42	580	14	578	9
98	121	148	0.81	0.0719	0.0020	1.6431	0.0466	0.1656	0.0027	984	33	987	18	988	15
99	163	180	0.90	0.1625	0.0038	10.7362	0.2584	0.4791	0.0074	2482	21	2501	22	2523	32
100	155	271	0.57	0.1728	0.0040	11.3012	0.2723	0.4744	0.0073	2584	21	2548	22	2503	32
Sample 10GD56, Lower Silurian, Yulin															
1	152	217	0.70	0.0561	0.0013	0.5481	0.0127	0.0709	0.0010	455	27	444	8	442	6
2	45	103	0.43	0.0701	0.0013	1.5352	0.0275	0.1589	0.0023	931	17	945	11	950	13
3	71	236	0.30	0.0568	0.0013	0.5420	0.0125	0.0693	0.0010	482	27	440	8	432	6
4	176	304	0.58	0.0555	0.0012	0.5340	0.0115	0.0697	0.0010	434	24	434	8	435	6
5	238	639	0.37	0.0557	0.0009	0.5369	0.0086	0.0700	0.0010	438	16	436	6	436	6
6	28	214	0.13	0.0725	0.0015	1.6445	0.0319	0.1645	0.0025	1000	18	987	12	982	14
7	216	450	0.48	0.0557	0.0010	0.5480	0.0099	0.0714	0.0010	439	19	444	7	445	6
8	72	421	0.17	0.0555	0.0011	0.5348	0.0108	0.0699	0.0010	432	22	435	7	435	6
9	109	370	0.29	0.0529	0.0010	0.5119	0.0098	0.0701	0.0010	326	21	420	7	437	6
10	55	285	0.19	0.0548	0.0014	0.5389	0.0136	0.0713	0.0011	404	31	438	9	444	6
11	67	222	0.30	0.0557	0.0019	0.5426	0.0178	0.0707	0.0011	440	47	440	12	440	6
12	148	169	0.88	0.0558	0.0020	0.5185	0.0182	0.0674	0.0011	444	49	424	12	420	7
13	64	235	0.27	0.0558	0.0014	0.5352	0.0130	0.0696	0.0010	444	29	435	9	434	6
14	142	370	0.39	0.0557	0.0013	0.5297	0.0121	0.0690	0.0010	440	26	432	8	430	6
15	85	321	0.26	0.0557	0.0013	0.5477	0.0128	0.0714	0.0011	439	27	444	8	444	6
16	106	676	0.16	0.0556	0.0010	0.5383	0.0093	0.0702	0.0010	436	18	437	6	437	6
17	42	263	0.16	0.0557	0.0012	0.5417	0.0116	0.0705	0.0010	440	24	440	8	439	6
18	50	214	0.23	0.0600	0.0014	0.7733	0.0175	0.0935	0.0014	602	25	582	10	576	8

19	68	123	0.55	0.0607	0.0018	0.8077	0.0232	0.0965	0.0015	628	36	601	13	594	9
20	303	166	1.83	0.0773	0.0013	1.9841	0.0326	0.1862	0.0026	1128	15	1110	11	1101	14
21	159	183	0.87	0.0556	0.0020	0.5324	0.0187	0.0695	0.0011	436	51	433	12	433	6
22	89	172	0.52	0.0557	0.0018	0.5353	0.0165	0.0697	0.0011	439	42	435	11	435	6
23	63	266	0.24	0.0558	0.0014	0.5369	0.0134	0.0698	0.0010	443	31	436	9	435	6
24	54	389	0.14	0.0583	0.0012	0.7139	0.0141	0.0888	0.0013	542	21	547	8	548	8
25	138	376	0.37	0.0556	0.0011	0.5365	0.0106	0.0700	0.0010	436	21	436	7	436	6
26	63	360	0.18	0.0555	0.0012	0.5331	0.0111	0.0697	0.0010	432	23	434	7	434	6
27	128	240	0.53	0.0556	0.0017	0.5342	0.0158	0.0697	0.0010	438	40	435	10	434	6
28	86	259	0.33	0.0559	0.0016	0.5499	0.0154	0.0713	0.0011	450	36	445	10	444	6
29	102	299	0.34	0.0558	0.0015	0.5470	0.0141	0.0711	0.0010	444	32	443	9	443	6
30	96	477	0.20	0.0556	0.0011	0.5393	0.0100	0.0703	0.0010	437	19	438	7	438	6
31	745	826	0.90	0.0557	0.0010	0.5465	0.0097	0.0712	0.0010	438	18	443	6	443	6
32	48	241	0.20	0.0567	0.0019	0.5408	0.0181	0.0692	0.0011	479	47	439	12	431	6
33	54	559	0.10	0.0557	0.0012	0.5507	0.0111	0.0717	0.0010	440	22	445	7	447	6
34	93	161	0.58	0.0575	0.0021	0.6410	0.0223	0.0809	0.0013	509	48	503	14	502	8
35	109	232	0.47	0.0586	0.0013	0.7227	0.0160	0.0894	0.0013	552	25	552	9	552	8
36	193	302	0.64	0.1681	0.0026	11.0384	0.1673	0.4763	0.0066	2538	11	2526	14	2511	29
37	46	144	0.32	0.0688	0.0017	1.3536	0.0321	0.1427	0.0021	893	26	869	14	860	12
38	243	555	0.44	0.0556	0.0011	0.5325	0.0097	0.0695	0.0010	434	19	433	6	433	6
39	98	167	0.59	0.0555	0.0019	0.5309	0.0176	0.0694	0.0011	432	47	432	12	432	6
40	255	435	0.59	0.0557	0.0014	0.5325	0.0128	0.0694	0.0010	440	29	433	8	432	6
41	258	246	1.05	0.0557	0.0015	0.5311	0.0140	0.0692	0.0010	440	33	433	9	431	6
42	68	166	0.41	0.0556	0.0020	0.5396	0.0193	0.0705	0.0011	434	52	438	13	439	7
43	53	267	0.20	0.0559	0.0016	0.5450	0.0155	0.0707	0.0011	449	37	442	10	440	6
44	138	156	0.88	0.0558	0.0023	0.5392	0.0217	0.0701	0.0012	445	60	438	14	436	7
45	284	310	0.92	0.0555	0.0015	0.5411	0.0143	0.0707	0.0010	431	33	439	9	441	6
46	36	113	0.32	0.1406	0.0029	7.7187	0.1550	0.3982	0.0064	2234	16	2199	18	2161	29
47	75	223	0.34	0.0556	0.0020	0.5424	0.0189	0.0708	0.0011	435	50	440	12	441	7
48	131	423	0.31	0.0554	0.0012	0.5248	0.0110	0.0687	0.0010	430	23	428	7	428	6
49	143	146	0.98	0.0557	0.0023	0.5455	0.0222	0.0710	0.0011	440	63	442	15	442	7
50	136	210	0.65	0.0591	0.0016	0.6988	0.0184	0.0858	0.0013	570	32	538	11	530	8

51	593	565	1.05	0.0691	0.0013	1.3646	0.0245	0.1433	0.0020	900	17	874	11	863	11
52	43	248	0.17	0.0602	0.0017	0.8561	0.0230	0.1032	0.0016	609	32	628	13	633	10
53	90	224	0.40	0.0561	0.0016	0.5365	0.0144	0.0693	0.0010	458	34	436	10	432	6
54	60	195	0.31	0.0557	0.0017	0.5328	0.0160	0.0694	0.0010	441	40	434	11	432	6
55	75	319	0.24	0.0555	0.0013	0.5332	0.0124	0.0696	0.0010	433	27	434	8	434	6
56	84	477	0.18	0.0555	0.0012	0.5400	0.0114	0.0705	0.0010	434	24	438	8	439	6
57	70	343	0.20	0.0559	0.0013	0.5380	0.0122	0.0698	0.0010	449	26	437	8	435	6
58	44	84	0.53	0.0581	0.0029	0.6955	0.0341	0.0868	0.0017	535	73	536	20	536	10
59	377	531	0.71	0.0714	0.0014	1.5605	0.0291	0.1586	0.0022	968	18	955	12	949	12
60	51	290	0.17	0.0560	0.0014	0.5524	0.0130	0.0716	0.0011	452	27	447	8	446	6
61	122	541	0.22	0.0568	0.0013	0.5471	0.0123	0.0699	0.0010	483	26	443	8	435	6
62	300	758	0.40	0.0706	0.0014	1.5439	0.0291	0.1586	0.0023	946	18	948	12	949	13
63	65	243	0.27	0.0557	0.0016	0.5468	0.0151	0.0713	0.0011	438	35	443	10	444	6
64	103	288	0.36	0.0555	0.0019	0.5270	0.0174	0.0689	0.0011	432	46	430	12	429	6
65	71	122	0.58	0.0559	0.0024	0.5415	0.0222	0.0702	0.0012	449	62	439	15	438	7
66	84	418	0.20	0.0751	0.0017	1.7856	0.0394	0.1724	0.0026	1071	22	1040	14	1025	14
67	278	429	0.65	0.0556	0.0015	0.5357	0.0136	0.0699	0.0011	436	31	436	9	435	6
68	74	241	0.31	0.0558	0.0026	0.5540	0.0256	0.0720	0.0012	443	74	448	17	448	7
69	34	104	0.33	0.0602	0.0029	0.8245	0.0382	0.0993	0.0018	611	70	611	21	610	10
70	79	247	0.32	0.0555	0.0021	0.5278	0.0198	0.0690	0.0011	431	55	430	13	430	7
71	93	203	0.46	0.0558	0.0021	0.5389	0.0194	0.0700	0.0012	445	50	438	13	436	7
72	74	289	0.26	0.0559	0.0016	0.5516	0.0148	0.0716	0.0011	446	33	446	10	446	7
73	94	238	0.40	0.0555	0.0017	0.5302	0.0157	0.0693	0.0011	432	38	432	10	432	7
74	68	209	0.32	0.0606	0.0023	0.9113	0.0333	0.1090	0.0018	625	50	658	18	667	10
75	92	347	0.26	0.0558	0.0016	0.5457	0.0146	0.0710	0.0011	443	34	442	10	442	6
76	58	194	0.30	0.0556	0.0023	0.5342	0.0210	0.0697	0.0011	436	59	435	14	434	7
77	167	273	0.61	0.0555	0.0016	0.5362	0.0150	0.0701	0.0011	432	36	436	10	437	7
78	38	38	1.02	0.1961	0.0055	15.8678	0.5183	0.5867	0.0166	2794	24	2869	31	2976	67
79	48	284	0.17	0.0555	0.0017	0.5356	0.0155	0.0700	0.0011	433	38	436	10	436	6
80	72	366	0.20	0.0556	0.0014	0.5390	0.0132	0.0704	0.0011	435	29	438	9	438	6
81	104	162	0.64	0.0556	0.0022	0.5286	0.0205	0.0690	0.0011	435	58	431	14	430	7
82	109	309	0.35	0.0559	0.0018	0.5368	0.0163	0.0696	0.0011	450	40	436	11	434	6

83	46	421	0.11	0.0557	0.0015	0.5369	0.0140	0.0699	0.0011	441	32	436	9	435	6
84	116	303	0.38	0.0562	0.0019	0.5414	0.0175	0.0699	0.0011	459	44	439	12	435	7
85	108	171	0.63	0.0559	0.0025	0.5370	0.0233	0.0697	0.0012	448	67	436	15	434	7
86	124	489	0.25	0.0552	0.0015	0.5291	0.0141	0.0695	0.0011	421	33	431	9	433	6
87	96	443	0.22	0.0559	0.0015	0.5324	0.0139	0.0690	0.0011	450	32	433	9	430	6
88	72	586	0.12	0.0707	0.0017	1.5080	0.0353	0.1547	0.0023	949	25	934	14	927	13
89	842	1069	0.79	0.0586	0.0017	0.7349	0.0203	0.0910	0.0014	551	34	559	12	561	9
90	109	449	0.24	0.0556	0.0018	0.5373	0.0166	0.0701	0.0011	437	41	437	11	437	7
91	116	261	0.45	0.0554	0.0022	0.5384	0.0205	0.0705	0.0011	427	56	437	14	439	7
92	238	389	0.61	0.0557	0.0018	0.5401	0.0167	0.0704	0.0011	438	42	438	11	438	7
93	65	372	0.18	0.0570	0.0017	0.6235	0.0173	0.0793	0.0012	492	35	492	11	492	7
94	85	76	1.12	0.1041	0.0034	3.5360	0.1151	0.2463	0.0051	1698	31	1535	26	1420	26
95	102	269	0.38	0.0555	0.0020	0.5293	0.0187	0.0692	0.0011	431	50	431	12	431	7
96	104	292	0.36	0.0557	0.0019	0.5456	0.0177	0.0711	0.0011	439	44	442	12	443	7
97	86	372	0.23	0.0555	0.0018	0.5438	0.0166	0.0710	0.0011	433	40	441	11	442	7
98	171	255	0.67	0.0556	0.0018	0.5361	0.0165	0.0699	0.0011	438	40	436	11	435	7
99	101	287	0.35	0.0558	0.0020	0.5390	0.0184	0.0701	0.0011	444	48	438	12	437	7
100	68	137	0.50	0.0556	0.0025	0.5417	0.0238	0.0706	0.0012	438	67	440	16	440	7
Sample 10GD58, Middle-Upper Silurian, Yulin															
1	505	200	2.53	0.0730	0.0016	1.8255	0.0413	0.1813	0.0025	1015	24	1055	15	1074	14
2	27	76	0.36	0.0694	0.0022	1.4613	0.0468	0.1528	0.0023	909	41	915	19	916	13
3	513	1411	0.36	0.2241	0.0052	17.7735	0.3385	0.5753	0.0076	3010	38	2978	18	2929	31
4	14	203	0.07	0.0656	0.0017	1.1244	0.0288	0.1243	0.0018	793	30	765	14	755	10
5	19	61	0.32	0.1589	0.0033	9.7951	0.2086	0.4469	0.0069	2444	17	2416	20	2382	31
6	51	39	1.31	0.1719	0.0035	11.6291	0.2432	0.4906	0.0074	2576	17	2575	20	2573	32
7	211	282	0.75	0.0649	0.0015	1.0770	0.0253	0.1204	0.0017	770	27	742	12	733	9
8	22	428	0.05	0.0735	0.0014	1.7699	0.0348	0.1747	0.0024	1026	20	1034	13	1038	13
9	52	792	0.07	0.0815	0.0014	2.4259	0.0453	0.2158	0.0029	1234	18	1250	13	1260	15
10	249	132	1.88	0.0748	0.0020	1.8505	0.0487	0.1795	0.0027	1062	29	1064	17	1064	15
11	82	202	0.41	0.0687	0.0016	1.3717	0.0320	0.1448	0.0020	890	26	877	14	872	11
12	77	580	0.13	0.0693	0.0013	1.4741	0.0284	0.1541	0.0021	909	20	920	12	924	12

13	196	1013	0.19	0.0726	0.0013	1.7615	0.0324	0.1759	0.0023	1004	18	1031	12	1044	13
14	184	582	0.32	0.0747	0.0022	1.7785	0.0466	0.1727	0.0023	1060	61	1038	17	1027	13
15	61	75	0.81	0.0732	0.0024	1.7584	0.0570	0.1742	0.0028	1019	40	1030	21	1035	15
16	55	564	0.10	0.1861	0.0032	13.4588	0.2436	0.5244	0.0069	2708	14	2712	17	2718	29
17	111	205	0.54	0.0747	0.0015	1.7477	0.0368	0.1696	0.0023	1061	22	1026	14	1010	13
18	199	190	1.05	0.0661	0.0019	1.1334	0.0330	0.1244	0.0018	809	37	769	16	756	10
19	311	216	1.44	0.0707	0.0017	1.6048	0.0388	0.1647	0.0024	947	27	972	15	983	13
20	114	201	0.57	0.0666	0.0016	1.2694	0.0301	0.1382	0.0020	825	27	832	13	835	11
21	149	195	0.76	0.1636	0.0029	10.4888	0.1964	0.4648	0.0063	2494	15	2479	17	2461	28
22	118	163	0.73	0.0719	0.0017	1.5187	0.0362	0.1531	0.0022	984	26	938	15	918	12
23	194	313	0.62	0.1594	0.0028	10.1139	0.1892	0.4601	0.0062	2449	15	2445	17	2440	27
24	485	837	0.58	0.0672	0.0013	1.1484	0.0227	0.1239	0.0017	844	21	776	11	753	10
25	66	62	1.06	0.0694	0.0027	1.4483	0.0546	0.1514	0.0025	909	51	909	23	909	14
26	113	218	0.52	0.0723	0.0017	1.5363	0.0368	0.1541	0.0022	995	27	945	15	924	12
27	429	406	1.06	0.0573	0.0015	0.6464	0.0170	0.0819	0.0012	502	34	506	10	507	7
28	278	612	0.45	0.0783	0.0015	2.0417	0.0403	0.1891	0.0025	1154	20	1130	13	1116	14
29	104	78	1.34	0.0583	0.0042	0.7462	0.0530	0.0928	0.0018	542	122	566	31	572	11
30	163	339	0.48	0.0719	0.0015	1.5742	0.0343	0.1587	0.0022	983	23	960	14	950	12
31	148	688	0.22	0.0751	0.0014	1.7670	0.0349	0.1707	0.0023	1071	20	1033	13	1016	13
32	27	1387	0.02	0.1046	0.0019	4.3784	0.0829	0.3036	0.0040	1707	17	1708	16	1709	20
33	131	121	1.08	0.1127	0.0025	5.0260	0.1114	0.3234	0.0046	1843	21	1824	19	1806	22
34	175	139	1.26	0.0608	0.0039	0.8352	0.0536	0.0996	0.0017	633	109	616	30	612	10
35	188	293	0.64	0.0709	0.0017	1.5319	0.0368	0.1568	0.0022	953	27	943	15	939	12
36	538	495	1.09	0.0595	0.0018	0.7293	0.0217	0.0889	0.0013	585	40	556	13	549	8
37	94	142	0.66	0.0799	0.0022	2.1538	0.0602	0.1956	0.0029	1194	32	1166	19	1151	16
38	175	171	1.02	0.0654	0.0023	1.1270	0.0384	0.1250	0.0019	787	46	766	18	759	11
39	14	20	0.71	0.0669	0.0081	1.1196	0.1339	0.1214	0.0031	834	211	763	64	739	18
40	77	168	0.46	0.0616	0.0019	0.9009	0.0272	0.1061	0.0016	660	39	652	15	650	9
41	325	247	1.31	0.0580	0.0022	0.6701	0.0256	0.0837	0.0013	531	58	521	16	518	7
42	541	857	0.63	0.1000	0.0036	3.8526	0.1276	0.2795	0.0040	1623	69	1604	27	1589	20
43	70	1188	0.06	0.0730	0.0014	1.7132	0.0350	0.1703	0.0023	1013	21	1013	13	1014	13
44	147	395	0.37	0.1168	0.0034	5.4139	0.1387	0.3361	0.0047	1908	54	1887	22	1868	23

45	116	1078	0.11	0.0680	0.0014	1.3683	0.0284	0.1459	0.0020	869	22	875	12	878	11
46	259	335	0.77	0.0991	0.0020	3.8752	0.0820	0.2835	0.0039	1608	20	1609	17	1609	20
47	42	151	0.28	0.0752	0.0022	1.7581	0.0511	0.1695	0.0025	1075	35	1030	19	1009	14
48	390	698	0.56	0.0723	0.0015	1.6392	0.0348	0.1645	0.0023	994	22	985	13	982	12
49	96	325	0.30	0.0739	0.0017	1.7249	0.0400	0.1693	0.0024	1038	25	1018	15	1008	13
50	154	436	0.35	0.0714	0.0015	1.5807	0.0347	0.1607	0.0022	967	24	963	14	960	12
51	385	172	2.24	0.0777	0.0023	2.0882	0.0616	0.1949	0.0029	1139	35	1145	20	1148	16
52	1246	2923	0.43	0.0581	0.0012	0.7058	0.0148	0.0881	0.0012	534	24	542	9	544	7
53	60	164	0.36	0.1618	0.0034	10.4975	0.2255	0.4706	0.0067	2474	18	2480	20	2486	29
54	126	125	1.00	0.0569	0.0028	0.6213	0.0307	0.0792	0.0013	486	81	491	19	492	8
55	219	486	0.45	0.1717	0.0035	11.6577	0.2422	0.4923	0.0067	2575	18	2577	19	2580	29
56	210	435	0.48	0.0730	0.0016	1.6319	0.0360	0.1622	0.0022	1014	24	983	14	969	12
57	183	194	0.94	0.0707	0.0018	1.5102	0.0386	0.1548	0.0022	950	30	935	16	928	12
58	355	464	0.77	0.0747	0.0016	1.7531	0.0389	0.1703	0.0024	1059	24	1028	14	1014	13
59	898	1411	0.64	0.0581	0.0013	0.6798	0.0150	0.0849	0.0012	532	26	527	9	525	7
60	228	282	0.81	0.0743	0.0017	1.7384	0.0402	0.1697	0.0024	1050	25	1023	15	1010	13
61	25	532	0.05	0.0660	0.0015	1.1986	0.0279	0.1317	0.0019	807	26	800	13	797	11
62	129	649	0.20	0.1630	0.0034	10.4358	0.2248	0.4642	0.0064	2487	19	2474	20	2458	28
63	136	137	0.99	0.1812	0.0039	12.9334	0.2852	0.5177	0.0073	2664	19	2675	21	2689	31
64	58	484	0.12	0.0757	0.0017	1.8725	0.0423	0.1795	0.0025	1086	24	1071	15	1064	14
65	40	122	0.32	0.0692	0.0021	1.5797	0.0468	0.1654	0.0026	906	36	962	18	987	14
66	98	423	0.23	0.0598	0.0015	0.8025	0.0207	0.0973	0.0014	597	32	598	12	599	8
67	330	233	1.42	0.0659	0.0017	1.2018	0.0317	0.1323	0.0019	803	31	801	15	801	11
68	152	270	0.56	0.0977	0.0022	3.5514	0.0823	0.2637	0.0037	1580	23	1539	18	1509	19
69	167	896	0.19	0.0712	0.0016	1.5908	0.0364	0.1621	0.0023	963	25	967	14	968	13
70	494	651	0.76	0.0717	0.0017	1.5219	0.0356	0.1540	0.0022	977	26	939	14	923	12
71	221	1475	0.15	0.0725	0.0016	1.6863	0.0385	0.1686	0.0023	1001	25	1003	15	1005	13
72	154	273	0.56	0.0724	0.0019	1.6310	0.0422	0.1635	0.0024	996	30	982	16	976	13
73	237	510	0.46	0.0754	0.0018	1.8051	0.0429	0.1737	0.0025	1079	26	1047	16	1032	13
74	134	485	0.28	0.0626	0.0017	0.8819	0.0234	0.1022	0.0015	695	33	642	13	627	9
75	51	850	0.06	0.0711	0.0017	1.5008	0.0357	0.1531	0.0022	960	26	931	14	918	12
76	153	187	0.82	0.1582	0.0037	10.1539	0.2415	0.4656	0.0068	2436	22	2449	22	2464	30

77	195	288	0.68	0.0727	0.0020	1.5835	0.0441	0.1579	0.0023	1006	33	964	17	945	13
78	614	599	1.02	0.0740	0.0018	1.8072	0.0441	0.1772	0.0025	1040	27	1048	16	1052	14
79	315	561	0.56	0.1915	0.0045	13.9174	0.3267	0.5271	0.0074	2755	21	2744	22	2729	31
80	276	170	1.62	0.0576	0.0029	0.6602	0.0324	0.0832	0.0014	513	78	515	20	515	8
81	29	38	0.77	0.1325	0.0042	7.0215	0.2197	0.3842	0.0067	2132	31	2114	28	2096	31
82	240	586	0.41	0.0602	0.0017	0.8122	0.0227	0.0979	0.0014	610	36	604	13	602	8
83	162	258	0.63	0.0610	0.0022	0.8887	0.0310	0.1056	0.0016	640	48	646	17	647	10
84	343	340	1.01	0.0703	0.0019	1.5274	0.0414	0.1576	0.0023	937	32	941	17	943	13
85	41	580	0.07	0.0676	0.0018	1.3696	0.0362	0.1470	0.0022	855	31	876	16	884	12
86	138	229	0.60	0.0698	0.0021	1.5272	0.0451	0.1587	0.0024	922	36	941	18	950	13
87	114	399	0.29	0.1564	0.0039	9.6353	0.2387	0.4468	0.0064	2417	23	2401	23	2381	29
88	301	1144	0.26	0.1667	0.0041	10.7843	0.2661	0.4692	0.0067	2525	23	2505	23	2480	29
89	259	1423	0.18	0.1098	0.0027	4.8211	0.1197	0.3185	0.0046	1796	25	1789	21	1782	22
90	294	1001	0.29	0.0690	0.0018	1.4193	0.0364	0.1491	0.0022	900	30	897	15	896	12
91	221	967	0.23	0.0711	0.0018	1.5444	0.0399	0.1576	0.0023	960	30	948	16	943	13
92	128	192	0.67	0.1601	0.0041	10.3669	0.2654	0.4695	0.0069	2457	24	2468	24	2481	30
93	349	1385	0.25	0.0691	0.0018	1.4605	0.0375	0.1532	0.0022	903	30	914	15	919	12
94	122	258	0.47	0.0652	0.0022	1.1349	0.0376	0.1262	0.0020	781	43	770	18	766	11
95	132	447	0.29	0.1078	0.0028	4.7840	0.1258	0.3217	0.0049	1763	27	1782	22	1798	24
96	250	1107	0.23	0.0691	0.0018	1.4283	0.0376	0.1499	0.0022	901	31	901	16	901	12
97	128	317	0.40	0.1114	0.0030	4.8842	0.1295	0.3179	0.0047	1822	27	1800	22	1780	23
98	565	1333	0.42	0.0718	0.0019	1.6032	0.0422	0.1620	0.0024	979	30	971	16	968	13
99	190	978	0.19	0.0699	0.0019	1.5762	0.0422	0.1635	0.0024	925	32	961	17	976	13
100	734	942	0.78	0.1128	0.0030	4.8892	0.1284	0.3142	0.0046	1846	27	1800	22	1761	23
Sample 10GD60, Middle-Upper Silurian, Yulin															
1	73	409	0.18	0.0776	0.0011	1.9446	0.0255	0.1818	0.0024	1136	12	1097	9	1077	13
2	29	687	0.04	0.0849	0.0011	2.6141	0.0338	0.2233	0.0030	1313	12	1305	9	1299	16
3	84	140	0.60	0.2700	0.0034	24.7746	0.3030	0.6653	0.0090	3306	9	3299	12	3288	35
4	63	950	0.07	0.2831	0.0034	26.7735	0.3185	0.6858	0.0091	3380	9	3375	12	3366	35
5	95	151	0.63	0.0836	0.0013	2.5130	0.0384	0.2179	0.0030	1284	13	1276	11	1271	16
6	188	79	2.39	0.0941	0.0022	3.2170	0.0719	0.2479	0.0038	1510	21	1461	17	1428	20

7	259	479	0.54	0.0722	0.0010	1.5891	0.0220	0.1596	0.0022	991	13	966	9	955	12
8	457	411	1.11	0.0669	0.0010	1.1942	0.0178	0.1294	0.0018	836	14	798	8	784	10
9	158	229	0.69	0.0567	0.0016	0.5892	0.0156	0.0754	0.0011	479	33	470	10	468	7
10	71	104	0.68	0.1104	0.0018	4.8488	0.0743	0.3185	0.0045	1806	12	1793	13	1782	22
11	127	98	1.30	0.0650	0.0020	1.0922	0.0319	0.1218	0.0018	774	37	750	15	741	11
12	304	528	0.58	0.0772	0.0011	2.1591	0.0287	0.2028	0.0027	1126	12	1168	9	1190	15
13	17	25	0.68	0.0675	0.0056	1.2311	0.0994	0.1323	0.0030	852	131	815	45	801	17
14	220	463	0.48	0.0758	0.0011	1.9853	0.0274	0.1900	0.0026	1089	13	1111	9	1121	14
15	200	379	0.53	0.1589	0.0020	10.0797	0.1246	0.4599	0.0061	2444	10	2442	11	2439	27
16	66	144	0.46	0.0705	0.0017	1.5008	0.0347	0.1543	0.0024	944	24	931	14	925	13
17	120	222	0.54	0.0618	0.0017	0.8767	0.0233	0.1029	0.0015	667	32	639	13	631	9
18	63	117	0.54	0.0715	0.0017	1.6083	0.0376	0.1630	0.0024	973	25	973	15	974	13
19	360	531	0.68	0.0712	0.0011	1.5266	0.0227	0.1554	0.0021	964	14	941	9	931	12
20	233	324	0.72	0.0898	0.0013	3.1058	0.0436	0.2509	0.0034	1421	12	1434	11	1443	18
21	344	940	0.37	0.0750	0.0010	1.8767	0.0253	0.1815	0.0024	1068	12	1073	9	1075	13
22	73	326	0.22	0.0731	0.0012	1.7305	0.0278	0.1717	0.0024	1016	15	1020	10	1022	13
23	84	269	0.31	0.3566	0.0046	38.5705	0.4867	0.7842	0.0106	3736	9	3735	12	3732	38
24	566	162	3.50	0.0654	0.0018	1.1824	0.0319	0.1312	0.0019	786	33	792	15	795	11
25	93	771	0.12	0.0718	0.0010	1.7040	0.0234	0.1722	0.0023	980	13	1010	9	1024	13
26	443	671	0.66	0.1280	0.0017	6.5770	0.0851	0.3727	0.0050	2070	11	2056	11	2042	23
27	194	597	0.33	0.1758	0.0023	12.0625	0.1554	0.4974	0.0067	2614	10	2609	12	2603	29
28	216	211	1.02	0.0660	0.0013	1.2099	0.0228	0.1330	0.0019	806	19	805	10	805	11
29	82	877	0.09	0.0733	0.0011	1.7454	0.0243	0.1726	0.0023	1023	13	1025	9	1026	13
30	549	1279	0.43	0.1737	0.0023	11.6406	0.1520	0.4861	0.0065	2593	10	2576	12	2554	28
31	156	483	0.32	0.0681	0.0011	1.4133	0.0226	0.1505	0.0021	871	15	895	10	904	12
32	380	742	0.51	0.0721	0.0011	1.7032	0.0246	0.1713	0.0023	988	13	1010	9	1019	13
33	146	470	0.31	0.0757	0.0012	1.8187	0.0278	0.1743	0.0024	1087	14	1052	10	1036	13
34	65	345	0.19	0.1070	0.0016	4.6110	0.0650	0.3125	0.0043	1749	12	1751	12	1753	21
35	133	233	0.57	0.0701	0.0014	1.5137	0.0295	0.1567	0.0022	930	19	936	12	938	12
36	138	757	0.18	0.0733	0.0011	1.7414	0.0254	0.1724	0.0024	1021	13	1024	9	1025	13
37	1299	1581	0.82	0.0731	0.0012	1.6607	0.0253	0.1647	0.0023	1018	14	994	10	983	13
38	132	206	0.64	0.1492	0.0024	9.0020	0.1404	0.4377	0.0063	2336	12	2338	14	2340	28

39	172	170	1.01	0.0834	0.0015	2.5695	0.0443	0.2234	0.0032	1279	15	1292	13	1300	17
40	137	225	0.61	0.0835	0.0015	2.5062	0.0428	0.2178	0.0031	1280	15	1274	12	1270	16
41	189	630	0.30	0.1622	0.0023	10.5251	0.1469	0.4707	0.0064	2478	11	2482	13	2486	28
42	326	507	0.64	0.0716	0.0012	1.6487	0.0267	0.1669	0.0023	975	15	989	10	995	13
43	29	46	0.63	0.1618	0.0030	10.4008	0.1824	0.4663	0.0070	2474	13	2471	16	2467	31
44	218	685	0.32	0.0709	0.0012	1.5485	0.0244	0.1585	0.0022	954	14	950	10	948	12
45	168	494	0.34	0.0725	0.0013	1.6665	0.0278	0.1668	0.0023	999	15	996	11	994	13
46	259	395	0.65	0.0720	0.0013	1.6514	0.0296	0.1664	0.0024	986	17	990	11	992	13
47	230	642	0.36	0.0581	0.0012	0.6672	0.0128	0.0833	0.0012	532	20	519	8	516	7
48	13	819	0.02	0.0928	0.0014	3.2834	0.0491	0.2566	0.0035	1484	13	1477	12	1472	18
49	141	492	0.29	0.1555	0.0024	9.6747	0.1433	0.4512	0.0062	2407	11	2404	14	2401	28
50	249	695	0.36	0.0760	0.0012	1.9275	0.0297	0.1839	0.0025	1095	14	1091	10	1088	14
51	279	417	0.67	0.0666	0.0012	1.1222	0.0190	0.1222	0.0017	825	16	764	9	743	10
52	117	368	0.32	0.1609	0.0025	9.9055	0.1495	0.4464	0.0061	2465	11	2426	14	2379	27
53	278	840	0.33	0.0721	0.0012	1.6719	0.0260	0.1682	0.0023	989	14	998	10	1002	13
54	180	198	0.91	0.0753	0.0016	1.8871	0.0381	0.1818	0.0027	1076	19	1077	13	1077	15
55	163	300	0.55	0.0728	0.0013	1.7076	0.0293	0.1701	0.0024	1008	16	1011	11	1013	13
56	674	287	2.34	0.0583	0.0014	0.6548	0.0149	0.0814	0.0012	543	26	511	9	505	7
57	600	685	0.88	0.0615	0.0011	0.8892	0.0154	0.1049	0.0015	656	17	646	8	643	9
58	288	597	0.48	0.0761	0.0013	1.9043	0.0313	0.1814	0.0025	1099	15	1083	11	1075	14
59	46	97	0.47	0.0654	0.0023	1.1321	0.0385	0.1256	0.0020	787	45	769	18	763	11
60	80	118	0.68	0.0966	0.0037	3.6932	0.1294	0.2774	0.0043	1559	74	1570	28	1578	22
61	206	322	0.64	0.0802	0.0015	2.2457	0.0400	0.2032	0.0029	1201	16	1195	12	1193	15
62	228	315	0.72	0.1646	0.0028	10.3572	0.1690	0.4564	0.0064	2504	12	2467	15	2423	28
63	107	706	0.15	0.0715	0.0013	1.6430	0.0277	0.1668	0.0023	971	16	987	11	994	13
64	27	72	0.37	0.1763	0.0032	12.0695	0.2130	0.4965	0.0074	2619	13	2610	17	2599	32
65	32	49	0.65	0.1594	0.0031	9.9701	0.1861	0.4538	0.0068	2449	14	2432	17	2412	30
66	105	100	1.06	0.1649	0.0030	10.5290	0.1859	0.4632	0.0067	2506	13	2482	16	2454	30
67	509	658	0.77	0.0591	0.0012	0.7201	0.0142	0.0883	0.0013	572	21	551	8	546	8
68	147	429	0.34	0.0719	0.0014	1.6446	0.0309	0.1659	0.0024	983	18	987	12	989	13
69	77	134	0.57	0.0638	0.0021	1.1276	0.0365	0.1281	0.0020	736	43	767	17	777	11
70	154	790	0.20	0.0732	0.0015	1.8081	0.0351	0.1793	0.0026	1018	19	1048	13	1063	14

71	108	276	0.39	0.1138	0.0021	5.3837	0.0968	0.3431	0.0049	1861	15	1882	15	1901	24
72	213	375	0.57	0.0576	0.0014	0.6656	0.0152	0.0839	0.0013	514	26	518	9	519	7
73	943	1010	0.93	0.0705	0.0013	1.6057	0.0291	0.1653	0.0024	942	17	972	11	986	13
74	139	238	0.58	0.0974	0.0020	3.7951	0.0765	0.2826	0.0043	1575	18	1592	16	1604	22
75	110	145	0.76	0.0748	0.0021	1.8738	0.0497	0.1817	0.0028	1064	30	1072	18	1076	15
76	229	594	0.39	0.0761	0.0015	1.9162	0.0368	0.1828	0.0027	1096	18	1087	13	1082	14
77	116	152	0.77	0.0787	0.0018	2.1530	0.0480	0.1985	0.0030	1164	22	1166	15	1167	16
78	139	143	0.97	0.0707	0.0021	1.5998	0.0451	0.1640	0.0026	950	33	970	18	979	14
79	287	522	0.55	0.1881	0.0036	13.2604	0.2429	0.5115	0.0073	2725	14	2698	17	2663	31
80	498	777	0.64	0.0583	0.0012	0.7153	0.0146	0.0890	0.0013	542	22	548	9	549	8
81	87	410	0.21	0.0893	0.0018	3.0772	0.0599	0.2499	0.0036	1411	18	1427	15	1438	19
82	197	300	0.66	0.0897	0.0020	3.1746	0.0663	0.2567	0.0039	1420	19	1451	16	1473	20
83	99	185	0.54	0.1135	0.0024	5.0858	0.1029	0.3250	0.0048	1857	17	1834	17	1814	23
84	246	227	1.08	0.0691	0.0017	1.5066	0.0353	0.1582	0.0024	901	25	933	14	947	13
85	129	882	0.15	0.0826	0.0017	2.3714	0.0461	0.2084	0.0030	1259	18	1234	14	1220	16
86	64	658	0.10	0.0741	0.0015	1.8904	0.0379	0.1852	0.0027	1043	19	1078	13	1095	15
87	740	314	2.36	0.0580	0.0018	0.6764	0.0201	0.0847	0.0013	528	38	525	12	524	8
88	194	259	0.75	0.1115	0.0024	4.8344	0.0988	0.3144	0.0047	1825	18	1791	17	1762	23
89	128	188	0.68	0.0941	0.0021	3.3326	0.0728	0.2569	0.0039	1511	20	1489	17	1474	20
90	231	301	0.77	0.0924	0.0020	3.1882	0.0666	0.2502	0.0037	1476	19	1454	16	1440	19
91	140	455	0.31	0.0730	0.0016	1.7462	0.0372	0.1735	0.0026	1015	21	1026	14	1031	14
92	362	45	8.02	0.1574	0.0039	10.3317	0.2422	0.4761	0.0077	2428	20	2465	22	2510	33
93	360	494	0.73	0.0717	0.0016	1.5362	0.0339	0.1554	0.0023	978	23	945	14	931	13
94	144	298	0.48	0.0760	0.0017	1.9588	0.0429	0.1870	0.0028	1095	22	1101	15	1105	15
95	165	704	0.23	0.0723	0.0016	1.6649	0.0353	0.1671	0.0025	994	21	995	13	996	14
96	131	403	0.33	0.0729	0.0017	1.7778	0.0406	0.1768	0.0027	1012	23	1037	15	1050	15
97	194	189	1.03	0.1612	0.0036	10.4447	0.2220	0.4702	0.0071	2468	18	2475	20	2484	31
98	173	295	0.59	0.0990	0.0022	3.8869	0.0845	0.2848	0.0043	1606	20	1611	18	1616	21
99	347	620	0.56	0.0564	0.0016	0.5569	0.0154	0.0716	0.0011	469	34	449	10	446	7
100	486	1630	0.30	0.1527	0.0033	9.3588	0.1971	0.4447	0.0066	2376	18	2374	19	2372	29

Sample 10GD83-1, Upper Ordovician, Dongkou

1	76	1111	0.07	0.0611	0.0004	0.8440	0.0126	0.1002	0.0013	642	15	621	7	616	8
2	136	424	0.32	0.0675	0.0011	1.2252	0.0268	0.1316	0.0018	854	35	812	12	797	10
3	292	538	0.54	0.0766	0.0005	1.9147	0.0292	0.1813	0.0025	1111	12	1086	10	1074	14
4	72	130	0.55	0.0708	0.0018	1.5433	0.0470	0.1581	0.0027	952	52	948	19	946	15
5	312	413	0.76	0.0700	0.0006	1.4409	0.0236	0.1493	0.0021	928	17	906	10	897	12
6	62	2085	0.03	0.0988	0.0003	3.7082	0.0498	0.2722	0.0036	1602	5	1573	11	1552	18
7	122	1026	0.12	0.0697	0.0004	1.4576	0.0211	0.1517	0.0020	920	11	913	9	910	11
8	440	1148	0.38	0.0901	0.0010	2.3372	0.0960	0.1880	0.0075	1429	20	1224	29	1111	40
9	107	281	0.38	0.1155	0.0007	5.1227	0.0819	0.3218	0.0048	1887	10	1840	14	1799	23
10	107	999	0.11	0.0604	0.0006	0.8393	0.0137	0.1007	0.0014	619	20	619	8	619	8
11	131	775	0.17	0.0705	0.0004	1.5627	0.0232	0.1607	0.0022	944	11	956	9	960	12
12	470	271	1.73	0.1644	0.0007	9.2875	0.1430	0.4097	0.0061	2501	7	2367	14	2214	28
13	309	1347	0.23	0.0594	0.0004	0.7534	0.0113	0.0920	0.0012	581	15	570	7	568	7
14	237	355	0.67	0.0665	0.0007	1.2495	0.0224	0.1363	0.0020	821	21	823	10	824	11
15	98	644	0.15	0.1144	0.0004	5.3182	0.0780	0.3371	0.0048	1871	7	1872	13	1873	23
16	260	362	0.72	0.0784	0.0006	2.1542	0.0357	0.1993	0.0029	1157	15	1166	12	1172	16
17	149	305	0.49	0.0838	0.0007	2.4435	0.0419	0.2115	0.0032	1288	16	1256	12	1237	17
~~*18*~~	~~*299*~~	~~*1482*~~	~~*0.20*~~	~~*0.1532*~~	~~*0.0045*~~	~~*7.0612*~~	~~*0.2286*~~	~~*0.3344*~~	~~*0.0046*~~	~~*2381*~~	~~*50*~~	~~*2119*~~	~~*29*~~	~~*1860*~~	~~*22*~~
19	1815	1809	1.00	0.0680	0.0006	1.1164	0.0180	0.1191	0.0016	867	18	761	9	726	9
~~*20*~~	~~*38*~~	~~*2121*~~	~~*0.02*~~	~~*0.0791*~~	~~*0.0021*~~	~~*1.2552*~~	~~*0.0382*~~	~~*0.1151*~~	~~*0.0018*~~	~~*1175*~~	~~*52*~~	~~*826*~~	~~*17*~~	~~*702*~~	~~*10*~~
~~*21*~~	~~*110*~~	~~*1177*~~	~~*0.09*~~	~~*0.1539*~~	~~*0.0005*~~	~~*7.2578*~~	~~*0.1031*~~	~~*0.3421*~~	~~*0.0047*~~	~~*2389*~~	~~*5*~~	~~*2144*~~	~~*13*~~	~~*1897*~~	~~*23*~~
22	18	129	0.14	0.0621	0.0026	0.8918	0.0409	0.1041	0.0018	679	91	647	22	638	10
23	55	805	0.07	0.0602	0.0005	0.8017	0.0126	0.0966	0.0013	610	16	598	7	594	8
24	357	641	0.56	0.0586	0.0005	0.7163	0.0118	0.0887	0.0013	551	18	548	7	548	7
25	647	1772	0.37	0.1311	0.0003	6.6706	0.0927	0.3691	0.0050	2113	5	2069	12	2025	24
26	927	2786	0.33	0.0597	0.0006	0.5972	0.0102	0.0725	0.0010	593	23	475	6	451	6
27	282	1541	0.18	0.0727	0.0003	1.6586	0.0240	0.1654	0.0023	1006	9	993	9	987	13
28	368	909	0.40	0.0864	0.0005	2.4857	0.0391	0.2086	0.0030	1347	12	1268	11	1221	16
29	74	639	0.12	0.0704	0.0005	1.4620	0.0241	0.1507	0.0022	939	15	915	10	905	12
30	79	353	0.22	0.1713	0.0007	11.3785	0.1801	0.4817	0.0074	2571	6	2555	15	2535	32
31	135	769	0.18	0.1820	0.0007	11.9269	0.1811	0.4753	0.0070	2671	6	2599	14	2507	31
32	210	785	0.27	0.0693	0.0007	1.4328	0.0261	0.1499	0.0022	908	22	903	11	901	12

33	58	209	0.27	0.0644	0.0009	1.0033	0.0215	0.1130	0.0019	755	29	706	11	690	11
34	109	312	0.35	0.0601	0.0013	0.7254	0.0193	0.0875	0.0014	608	46	554	11	541	8
35	13	107	0.12	0.0592	0.0040	0.8282	0.0581	0.1015	0.0019	574	147	613	32	623	11
36	193	241	0.80	0.0612	0.0060	1.0733	0.1080	0.1272	0.0026	646	212	740	53	772	15
37	280	1101	0.25	0.0711	0.0004	1.5999	0.0250	0.1633	0.0024	959	11	970	10	975	13
39	186	659	0.28	0.0845	0.0020	2.2679	0.0650	0.1946	0.0031	1305	47	1202	20	1146	17
40	104	650	0.16	0.0702	0.0008	1.9057	0.0397	0.1968	0.0034	935	24	1083	14	1158	18
~~*41*~~	~~*248*~~	~~*1048*~~	~~*0.24*~~	~~*0.1054*~~	~~*0.0005*~~	~~*3.2007*~~	~~*0.0512*~~	~~*0.2202*~~	~~*0.0033*~~	~~*1721*~~	~~*9*~~	~~*1457*~~	~~*12*~~	~~*1283*~~	~~*18*~~
42	1874	2246	0.83	0.0665	0.0004	1.2309	0.0196	0.1343	0.0020	822	13	815	9	812	11
44	100	671	0.15	0.1250	0.0005	6.1872	0.0987	0.3589	0.0055	2029	7	2003	14	1977	26
45	16	1450	0.01	0.0624	0.0004	0.9941	0.0163	0.1156	0.0018	688	13	701	8	705	10
46	11	244	0.04	0.0588	0.0012	0.8003	0.0215	0.0987	0.0017	560	45	597	12	607	10
47	62	121	0.51	0.0706	0.0014	1.5765	0.0438	0.1620	0.0032	945	40	961	17	968	18
48	318	652	0.49	0.0785	0.0005	2.1182	0.0363	0.1956	0.0031	1160	13	1155	12	1152	17
49	48	550	0.09	0.0952	0.0005	3.2430	0.0557	0.2472	0.0040	1531	10	1468	13	1424	21
50	137	192	0.71	0.1538	0.0015	7.4404	0.1604	0.3509	0.0067	2388	17	2166	19	1939	32
51	2	131	0.01	0.0565	0.0036	0.6839	0.0461	0.0878	0.0018	471	142	529	28	543	10
52	113	193	0.59	0.0762	0.0009	1.9245	0.0423	0.1831	0.0033	1101	24	1090	15	1084	18
53	179	795	0.23	0.0777	0.0017	1.8110	0.0627	0.1691	0.0044	1138	45	1049	23	1007	25
54	882	928	0.95	0.0697	0.0009	1.4007	0.0258	0.1457	0.0020	920	26	889	11	877	11
55	75	192	0.39	0.0590	0.0014	0.7518	0.0213	0.0925	0.0015	566	52	569	12	570	9
56	88	267	0.33	0.0685	0.0007	1.2864	0.0231	0.1361	0.0020	885	21	840	10	823	12
57	505	250	2.02	0.0585	0.0012	0.7284	0.0182	0.0902	0.0014	550	43	556	11	557	8
58	330	1160	0.28	0.0625	0.0010	0.8490	0.0182	0.0985	0.0013	692	36	624	10	606	8
59	45	94	0.47	0.2276	0.0014	18.6587	0.3547	0.5947	0.0107	3035	10	3024	18	3008	43
~~*60*~~	~~*57*~~	~~*101*~~	~~*0.56*~~	~~*0.0511*~~	~~*0.0046*~~	~~*0.6376*~~	~~*0.0586*~~	~~*0.0905*~~	~~*0.0017*~~	~~*245*~~	~~*208*~~	~~*501*~~	~~*36*~~	~~*559*~~	~~*10*~~
61	282	447	0.63	0.1821	0.0006	13.2058	0.1968	0.5260	0.0076	2672	5	2694	14	2725	32
62	466	529	0.88	0.1513	0.0035	7.6224	0.2070	0.3655	0.0054	2360	39	2188	24	2008	25
63	429	470	0.91	0.1630	0.0006	10.6187	0.1579	0.4725	0.0068	2487	6	2490	14	2495	30
~~*64*~~	~~*115*~~	~~*699*~~	~~*0.16*~~	~~*0.1207*~~	~~*0.0009*~~	~~*2.8445*~~	~~*0.0482*~~	~~*0.1709*~~	~~*0.0026*~~	~~*1967*~~	~~*13*~~	~~*1367*~~	~~*13*~~	~~*1017*~~	~~*14*~~
65	11	669	0.02	0.0736	0.0004	1.7344	0.0268	0.1709	0.0025	1031	12	1021	10	1017	14
66	111	85	1.30	0.0731	0.0016	1.5666	0.0449	0.1555	0.0030	1016	43	957	18	931	17

67	59	115	0.51	0.1603	0.0011	10.5360	0.2003	0.4768	0.0084	2459	12	2483	18	2513	37
Sample 10GD84, Lower Silurian, Dongkou															
1	127	444	0.29	0.0706	0.0009	1.6405	0.0251	0.1685	0.0024	946	14	986	10	1004	13
2	221	441	0.50	0.0780	0.0009	2.0993	0.0320	0.1953	0.0028	1146	14	1149	10	1150	15
3	322	583	0.55	0.0693	0.0008	1.5581	0.0238	0.1631	0.0023	907	14	954	9	974	13
4	289	451	0.64	0.0704	0.0009	1.6823	0.0258	0.1734	0.0025	939	14	1002	10	1031	14
5	56	74	0.76	0.0669	0.0011	1.2690	0.0233	0.1375	0.0020	836	18	832	10	831	12
6	761	1206	0.63	0.0846	0.0010	2.7353	0.0413	0.2346	0.0033	1305	13	1338	11	1359	17
7	101	286	0.35	0.0730	0.0009	1.8129	0.0282	0.1802	0.0026	1013	14	1050	10	1068	14
~~*8*~~	~~*1508*~~	~~*879*~~	~~*1.72*~~	~~*0.0811*~~	~~*0.0010*~~	~~*1.5150*~~	~~*0.0231*~~	~~*0.1355*~~	~~*0.0019*~~	~~*1224*~~	~~*13*~~	~~*936*~~	~~*9*~~	~~*819*~~	~~*11*~~
9	199	912	0.22	0.1145	0.0014	5.3531	0.0808	0.3389	0.0048	1873	12	1877	13	1881	23
10	506	1835	0.28	0.1415	0.0017	7.5028	0.1141	0.3846	0.0055	2245	12	2173	14	2098	26
11	178	212	0.84	0.0557	0.0010	0.5416	0.0107	0.0706	0.0010	438	21	439	7	440	6
12	316	405	0.78	0.0662	0.0008	1.2339	0.0193	0.1352	0.0019	812	15	816	9	818	11
13	119	387	0.31	0.0718	0.0009	1.6465	0.0254	0.1663	0.0024	980	14	988	10	992	13
14	534	787	0.68	0.1857	0.0022	13.7573	0.2081	0.5371	0.0076	2705	11	2733	14	2771	32
15	345	608	0.57	0.0584	0.0007	0.7168	0.0112	0.0890	0.0013	546	15	549	7	549	8
16	483	908	0.53	0.0717	0.0009	1.6935	0.0265	0.1713	0.0025	977	14	1006	10	1019	13
17	290	213	1.36	0.1617	0.0020	10.4604	0.1597	0.4690	0.0067	2474	12	2476	14	2479	29
18	36	189	0.19	0.0647	0.0009	1.1243	0.0188	0.1259	0.0018	766	16	765	9	765	10
19	107	138	0.77	0.1562	0.0019	9.7642	0.1500	0.4533	0.0065	2415	12	2413	14	2410	29
20	266	597	0.45	0.0745	0.0009	1.8432	0.0284	0.1795	0.0026	1054	14	1061	10	1064	14
21	79	344	0.23	0.0764	0.0010	1.9736	0.0309	0.1874	0.0027	1104	14	1107	11	1107	14
22	277	283	0.98	0.1591	0.0020	10.1248	0.1554	0.4613	0.0066	2447	12	2446	14	2445	29
23	366	702	0.52	0.0611	0.0008	0.8764	0.0137	0.1041	0.0015	641	15	639	7	638	9
24	165	256	0.64	0.0806	0.0010	2.3125	0.0363	0.2080	0.0030	1212	14	1216	11	1218	16
25	194	650	0.30	0.0743	0.0009	1.8219	0.0282	0.1777	0.0025	1051	14	1053	10	1054	14
26	232	386	0.60	0.0764	0.0010	1.9850	0.0310	0.1883	0.0027	1107	14	1110	11	1112	14
27	959	1198	0.80	0.1597	0.0020	10.5163	0.1614	0.4774	0.0068	2453	12	2481	14	2516	29
28	141	518	0.27	0.0729	0.0009	1.7162	0.0269	0.1707	0.0024	1011	14	1015	10	1016	13
29	8	34	0.24	0.1595	0.0022	10.2206	0.1655	0.4646	0.0068	2450	12	2455	15	2460	30

30	95	515	0.18	0.0955	0.0012	3.3375	0.0520	0.2535	0.0036	1537	13	1490	12	1456	18
31	82	335	0.24	0.0744	0.0010	1.8216	0.0288	0.1774	0.0025	1053	14	1053	10	1053	14
32	225	612	0.37	0.0934	0.0012	3.4270	0.0533	0.2659	0.0038	1497	13	1511	12	1520	19
33	132	332	0.40	0.0736	0.0010	1.7283	0.0277	0.1702	0.0024	1031	14	1019	10	1013	13
34	95	353	0.27	0.0704	0.0009	1.5634	0.0252	0.1611	0.0023	939	15	956	10	963	13
35	147	337	0.44	0.0813	0.0024	2.2998	0.0588	0.2052	0.0030	1229	59	1212	18	1203	16
36	409	619	0.66	0.1402	0.0018	7.9045	0.1236	0.4088	0.0058	2229	12	2220	14	2210	26
37	141	386	0.37	0.0736	0.0010	1.7572	0.0279	0.1732	0.0025	1029	14	1030	10	1030	14
38	107	231	0.46	0.1252	0.0016	6.4052	0.1009	0.3708	0.0053	2032	12	2033	14	2033	25
39	396	596	0.66	0.0708	0.0009	1.6915	0.0268	0.1733	0.0025	951	14	1005	10	1030	13
40	97	454	0.21	0.0710	0.0009	1.6277	0.0260	0.1663	0.0024	956	15	981	10	992	13
41	82	311	0.26	0.0748	0.0010	1.8554	0.0299	0.1798	0.0026	1064	14	1065	11	1066	14
42	124	166	0.74	0.0648	0.0010	1.1718	0.0208	0.1311	0.0019	768	17	787	10	794	11
43	129	87	1.48	0.1623	0.0022	10.2527	0.1649	0.4581	0.0065	2479	12	2458	15	2431	29
44	183	974	0.19	0.0793	0.0010	2.2234	0.0353	0.2032	0.0029	1180	14	1188	11	1193	15
45	81	147	0.55	0.1140	0.0015	5.2112	0.0841	0.3313	0.0047	1865	13	1854	14	1845	23
46	357	236	1.51	0.1660	0.0022	10.7651	0.1719	0.4702	0.0066	2518	12	2503	15	2484	29
47	53	106	0.50	0.0989	0.0014	3.8486	0.0638	0.2823	0.0040	1603	14	1603	13	1603	20
48	180	192	0.93	0.0584	0.0009	0.6995	0.0125	0.0869	0.0013	543	18	538	7	537	7
49	139	262	0.53	0.0721	0.0010	1.5875	0.0263	0.1597	0.0023	988	15	965	10	955	13
50	294	306	0.96	0.0700	0.0010	1.4758	0.0251	0.1528	0.0022	929	16	921	10	917	12
51	93	110	0.85	0.0654	0.0011	1.1673	0.0225	0.1295	0.0019	786	19	785	11	785	11
52	54	266	0.20	0.1535	0.0021	9.6857	0.1568	0.4576	0.0065	2385	12	2405	15	2429	29
53	130	733	0.18	0.1469	0.0020	8.7990	0.1423	0.4343	0.0061	2310	12	2317	15	2325	28
54	304	335	0.91	0.0721	0.0010	1.6066	0.0267	0.1615	0.0023	990	15	973	10	965	13
55	118	341	0.35	0.0557	0.0009	0.5313	0.0099	0.0692	0.0010	440	19	433	7	431	6
56	338	335	1.01	0.0654	0.0010	1.1862	0.0200	0.1316	0.0019	786	16	794	9	797	11
57	135	1326	0.10	0.1540	0.0021	9.4978	0.1546	0.4472	0.0063	2391	12	2387	15	2383	28
58	390	297	1.32	0.0800	0.0011	2.2267	0.0371	0.2019	0.0029	1196	15	1189	12	1186	15
59	231	241	0.96	0.0915	0.0013	3.1506	0.0526	0.2498	0.0035	1456	14	1445	13	1437	18
60	276	589	0.47	0.1542	0.0022	9.1037	0.1495	0.4282	0.0060	2392	13	2348	15	2298	27
61	154	392	0.39	0.0676	0.0010	1.3352	0.0226	0.1433	0.0020	856	16	861	10	863	11

62	84	819	0.10	0.0797	0.0011	2.2281	0.0371	0.2027	0.0029	1190	15	1190	12	1190	15
63	147	504	0.29	0.0682	0.0010	1.4321	0.0241	0.1523	0.0022	873	16	902	10	914	12
64	211	308	0.68	0.0900	0.0013	3.1277	0.0525	0.2521	0.0036	1425	14	1440	13	1449	18
65	60	888	0.07	0.0705	0.0010	1.5612	0.0261	0.1607	0.0023	942	15	955	10	960	13
66	195	201	0.97	0.0668	0.0011	1.2715	0.0224	0.1381	0.0020	830	17	833	10	834	11
67	862	525	1.64	0.0763	0.0011	1.9527	0.0334	0.1855	0.0026	1103	15	1099	11	1097	14
68	152	220	0.69	0.0727	0.0011	1.6693	0.0295	0.1666	0.0024	1004	16	997	11	993	13
69	435	614	0.71	0.0721	0.0011	1.6539	0.0282	0.1663	0.0024	990	16	991	11	991	13
70	655	565	1.16	0.0580	0.0009	0.6818	0.0119	0.0853	0.0012	528	17	528	7	528	7
71	95	223	0.43	0.0774	0.0012	1.9509	0.0343	0.1827	0.0026	1132	16	1099	12	1082	14
72	328	517	0.63	0.0710	0.0011	1.5624	0.0269	0.1595	0.0023	959	16	955	11	954	13
73	329	213	1.54	0.0586	0.0010	0.7240	0.0137	0.0896	0.0013	553	19	553	8	553	8
74	29	38	0.75	0.0726	0.0018	1.7710	0.0458	0.1769	0.0027	1002	29	1035	17	1050	15
75	331	377	0.88	0.0989	0.0015	3.6219	0.0623	0.2656	0.0038	1603	15	1554	14	1518	19
76	190	416	0.46	0.0769	0.0012	2.0183	0.0352	0.1905	0.0027	1117	16	1122	12	1124	15
77	73	71	1.02	0.0658	0.0014	1.1921	0.0265	0.1314	0.0019	799	24	797	12	796	11
78	70	320	0.22	0.0748	0.0012	1.7893	0.0317	0.1736	0.0025	1062	16	1042	12	1032	14
79	76	114	0.67	0.1067	0.0017	4.5015	0.0808	0.3060	0.0044	1743	15	1731	15	1721	22
80	199	466	0.43	0.1061	0.0016	4.6085	0.0803	0.3151	0.0045	1733	15	1751	15	1766	22
81	338	227	1.49	0.0714	0.0012	1.5564	0.0283	0.1581	0.0023	969	17	953	11	946	13
82	199	273	0.73	0.0790	0.0013	1.9441	0.0348	0.1786	0.0025	1171	16	1096	12	1059	14
83	16	56	0.28	0.1723	0.0028	11.7968	0.2116	0.4964	0.0071	2580	14	2588	17	2598	31
84	384	316	1.21	0.0584	0.0010	0.6868	0.0132	0.0853	0.0012	546	20	531	8	527	7
85	453	611	0.74	0.0768	0.0012	1.9834	0.0353	0.1873	0.0027	1116	16	1110	12	1107	14
86	86	675	0.13	0.0802	0.0019	2.1600	0.0418	0.1953	0.0027	1202	48	1168	13	1150	15
87	317	268	1.18	0.0653	0.0011	1.1088	0.0208	0.1232	0.0018	784	18	758	10	749	10
88	306	402	0.76	0.1652	0.0027	10.7003	0.1907	0.4698	0.0066	2510	14	2497	17	2482	29
89	350	367	0.96	0.3173	0.0051	31.0134	0.5532	0.7089	0.0100	3557	13	3519	18	3454	38
90	172	206	0.83	0.1013	0.0017	3.9676	0.0721	0.2840	0.0040	1648	16	1628	15	1612	20
91	260	453	0.57	0.0687	0.0012	1.2853	0.0237	0.1358	0.0019	889	18	839	11	821	11
92	234	755	0.31	0.0684	0.0011	1.3772	0.0251	0.1462	0.0021	879	17	879	11	879	12
93	193	143	1.35	0.0659	0.0013	1.1852	0.0244	0.1305	0.0019	802	21	794	11	791	11

94	218	209	1.04	0.1654	0.0028	10.8754	0.1982	0.4771	0.0068	2511	14	2513	17	2515	30
95	166	209	0.80	0.0634	0.0012	1.0187	0.0201	0.1167	0.0017	720	20	713	10	711	10
96	216	150	1.44	0.1002	0.0017	3.9464	0.0736	0.2856	0.0041	1629	16	1623	15	1620	20
97	53	204	0.26	0.1098	0.0019	4.6509	0.0862	0.3074	0.0044	1796	16	1758	15	1728	22
98	167	248	0.67	0.2808	0.0047	25.7536	0.4730	0.6653	0.0094	3367	13	3337	18	3288	36
99	104	148	0.70	0.0660	0.0012	1.2059	0.0239	0.1326	0.0019	806	20	803	11	802	11
100	105	97	1.09	0.1627	0.0029	10.5905	0.2013	0.4724	0.0069	2483	15	2488	18	2494	30
Sample 10GD85, Middle-Upper Silurian, Dongkou															
1	193	863	0.22	0.0862	0.0012	2.8788	0.0477	0.2421	0.0034	1343	14	1376	12	1398	18
2	271	746	0.36	0.0776	0.0011	2.0699	0.0343	0.1935	0.0027	1136	15	1139	11	1140	15
3	420	523	0.80	0.1283	0.0019	5.3609	0.0915	0.3030	0.0044	2075	13	1879	15	1706	22
4	156	275	0.57	0.0781	0.0011	2.0653	0.0352	0.1918	0.0027	1149	15	1137	12	1131	15
5	462	886	0.52	0.0786	0.0012	2.0528	0.0350	0.1894	0.0027	1162	15	1133	12	1118	15
6	258	707	0.37	0.0770	0.0011	2.0613	0.0347	0.1942	0.0028	1120	15	1136	11	1144	15
7	93	157	0.59	0.0707	0.0012	1.5370	0.0294	0.1576	0.0023	949	18	945	12	943	13
8	135	398	0.34	0.1090	0.0015	4.8125	0.0796	0.3202	0.0045	1783	14	1787	14	1791	22
9	112	1273	0.09	0.0731	0.0010	1.7431	0.0292	0.1730	0.0025	1016	15	1025	11	1029	13
10	187	415	0.45	0.0774	0.0011	2.0403	0.0346	0.1911	0.0027	1132	15	1129	12	1127	15
11	754	989	0.76	0.0865	0.0012	2.7888	0.0460	0.2337	0.0033	1350	14	1353	12	1354	17
12	125	245	0.51	0.1062	0.0015	4.4998	0.0756	0.3072	0.0044	1736	14	1731	14	1727	21
13	262	473	0.56	0.0714	0.0011	1.6052	0.0278	0.1629	0.0023	970	16	972	11	973	13
14	227	496	0.46	0.1143	0.0016	5.2968	0.0878	0.3361	0.0047	1868	13	1868	14	1868	23
15	388	281	1.38	0.0728	0.0012	1.7824	0.0321	0.1775	0.0026	1009	17	1039	12	1053	14
16	191	367	0.52	0.0755	0.0013	1.9286	0.0363	0.1851	0.0027	1083	18	1091	13	1095	15
17	126	221	0.57	0.0752	0.0012	1.8893	0.0342	0.1821	0.0026	1074	17	1077	12	1079	14
18	353	765	0.46	0.0771	0.0011	2.0322	0.0340	0.1911	0.0027	1124	15	1126	11	1128	15
19	255	391	0.65	0.0721	0.0011	1.6514	0.0286	0.1660	0.0024	990	16	990	11	990	13
20	359	521	0.69	0.0635	0.0011	1.1467	0.0216	0.1310	0.0019	724	18	776	10	794	11
21	390	180	2.16	0.1585	0.0023	9.9524	0.1666	0.4553	0.0065	2440	13	2430	15	2419	29
22	114	89	1.28	0.0741	0.0015	1.7482	0.0380	0.1711	0.0026	1044	22	1026	14	1018	14
23	22	32	0.70	0.1746	0.0028	11.9682	0.2142	0.4970	0.0074	2602	13	2602	17	2601	32

24	184	183	1.01	0.0788	0.0025	2.1028	0.0657	0.1934	0.0037	1168	33	1150	21	1140	20
25	636	828	0.77	0.0721	0.0011	1.6506	0.0280	0.1660	0.0023	989	16	990	11	990	13
26	681	596	1.14	0.0796	0.0012	2.1226	0.0362	0.1934	0.0027	1186	15	1156	12	1140	15
27	128	1215	0.11	0.1767	0.0025	12.2198	0.2036	0.5014	0.0071	2622	12	2621	16	2620	30
28	264	477	0.55	0.0783	0.0012	2.2382	0.0393	0.2074	0.0030	1153	16	1193	12	1215	16
29	311	365	0.85	0.0729	0.0011	1.6812	0.0296	0.1672	0.0024	1011	16	1001	11	997	13
30	322	412	0.78	0.1480	0.0022	9.0766	0.1561	0.4446	0.0064	2323	13	2346	16	2371	28
31	239	144	1.66	0.0704	0.0012	1.5267	0.0288	0.1573	0.0023	939	18	941	12	942	13
32	112	136	0.83	0.0667	0.0013	1.3551	0.0286	0.1474	0.0022	828	22	870	12	886	12
33	175	185	0.95	0.1628	0.0024	10.4895	0.1794	0.4671	0.0067	2485	13	2479	16	2471	29
34	32	91	0.36	0.0721	0.0014	1.6587	0.0344	0.1669	0.0025	988	20	993	13	995	14
35	116	350	0.33	0.2493	0.0036	21.9036	0.3701	0.6371	0.0090	3180	12	3179	16	3178	35
36	105	369	0.28	0.0729	0.0011	1.6971	0.0300	0.1689	0.0024	1010	16	1007	11	1006	13
37	59	275	0.22	0.1470	0.0022	8.5910	0.1469	0.4239	0.0060	2311	13	2296	16	2278	27
38	344	713	0.48	0.0794	0.0012	2.1538	0.0372	0.1967	0.0028	1182	15	1166	12	1157	15
39	78	152	0.51	0.0891	0.0020	3.1689	0.0723	0.2578	0.0043	1407	21	1450	18	1478	22
40	136	617	0.22	0.0857	0.0014	2.7289	0.0492	0.2310	0.0034	1330	16	1336	13	1340	18
41	62	105	0.59	0.0725	0.0014	1.6160	0.0341	0.1616	0.0024	1001	21	976	13	965	13
42	171	176	0.97	0.1666	0.0025	11.3740	0.1976	0.4950	0.0071	2524	13	2554	16	2592	30
43	133	623	0.21	0.0748	0.0012	1.8741	0.0334	0.1816	0.0026	1064	16	1072	12	1076	14
44	374	539	0.69	0.0683	0.0011	1.2867	0.0230	0.1365	0.0020	879	17	840	10	825	11
45	70	185	0.38	0.1229	0.0019	6.0845	0.1071	0.3591	0.0051	1998	14	1988	15	1978	24
46	157	221	0.71	0.1104	0.0017	4.8772	0.0867	0.3203	0.0046	1806	15	1798	15	1791	22
47	253	455	0.56	0.2129	0.0032	16.9327	0.2951	0.5768	0.0082	2927	13	2931	17	2936	33
48	391	454	0.86	0.0815	0.0014	2.2270	0.0416	0.1981	0.0029	1234	17	1190	13	1165	15
49	90	740	0.12	0.1168	0.0018	5.4622	0.0957	0.3392	0.0048	1907	14	1895	15	1883	23
50	81	241	0.33	0.1079	0.0017	4.6111	0.0823	0.3100	0.0044	1764	15	1751	15	1741	22
51	233	424	0.55	0.0709	0.0012	1.5525	0.0283	0.1588	0.0023	954	17	951	11	950	13
52	304	630	0.48	0.0797	0.0013	2.1363	0.0386	0.1944	0.0028	1189	16	1161	12	1145	15
53	1278	576	2.22	0.0729	0.0012	1.7473	0.0316	0.1739	0.0025	1010	17	1026	12	1033	14
54	373	758	0.49	0.0747	0.0012	1.8043	0.0324	0.1752	0.0025	1060	17	1047	12	1040	14
55	320	520	0.62	0.0768	0.0013	2.0810	0.0379	0.1964	0.0028	1117	17	1143	12	1156	15

56	72	106	0.68	0.1034	0.0019	4.1902	0.0832	0.2938	0.0044	1687	17	1672	16	1660	22
57	25	87	0.28	0.0749	0.0028	1.7715	0.0657	0.1714	0.0034	1067	44	1035	24	1020	18
58	166	1213	0.14	0.0728	0.0012	1.7049	0.0309	0.1697	0.0024	1010	17	1010	12	1011	13
59	273	634	0.43	0.0712	0.0012	1.6145	0.0297	0.1644	0.0024	963	17	976	12	981	13
60	233	806	0.29	0.0904	0.0015	2.8563	0.0520	0.2292	0.0033	1434	16	1370	14	1330	17
61	462	437	1.06	0.1212	0.0020	6.0203	0.1100	0.3602	0.0052	1974	15	1979	16	1983	24
62	1455	2647	0.55	0.0685	0.0011	1.3562	0.0248	0.1435	0.0021	884	18	870	11	865	12
63	213	177	1.21	0.0653	0.0014	1.1683	0.0256	0.1298	0.0019	782	23	786	12	787	11
64	63	762	0.08	0.0846	0.0014	2.7129	0.0502	0.2326	0.0033	1306	17	1332	14	1348	17
65	87	686	0.13	0.0894	0.0015	2.9998	0.0555	0.2433	0.0035	1413	16	1408	14	1404	18
66	649	529	1.23	0.0758	0.0013	1.8295	0.0345	0.1749	0.0025	1091	18	1056	12	1039	14
67	9	964	0.01	0.0764	0.0013	1.9482	0.0365	0.1850	0.0027	1105	17	1098	13	1094	14
68	157	202	0.78	0.0722	0.0013	1.6668	0.0330	0.1673	0.0025	992	19	996	13	997	14
69	439	397	1.10	0.0768	0.0013	1.9977	0.0383	0.1887	0.0027	1115	18	1115	13	1114	15
70	138	131	1.05	0.0663	0.0014	1.2294	0.0281	0.1346	0.0020	814	24	814	13	814	11
71	26	60	0.44	0.0603	0.0026	0.8388	0.0362	0.1008	0.0017	615	65	618	20	619	10
72	367	759	0.48	0.0872	0.0016	2.8838	0.0571	0.2397	0.0035	1366	18	1378	15	1385	18
73	267	688	0.39	0.0692	0.0012	1.4222	0.0274	0.1491	0.0022	903	19	898	11	896	12
74	115	34	3.35	0.0645	0.0041	1.0549	0.0665	0.1185	0.0025	759	97	731	33	722	15
75	380	502	0.76	0.0970	0.0017	3.5705	0.0683	0.2669	0.0039	1567	17	1543	15	1525	20
76	294	202	1.46	0.0701	0.0014	1.5033	0.0312	0.1555	0.0023	931	21	932	13	932	13
77	148	250	0.59	0.1045	0.0020	4.2527	0.0864	0.2950	0.0044	1706	18	1684	17	1666	22
78	30	1582	0.02	0.0774	0.0014	2.0367	0.0393	0.1908	0.0028	1131	18	1128	13	1126	15
79	128	582	0.22	0.0709	0.0013	1.5558	0.0306	0.1591	0.0023	955	19	953	12	952	13
80	67	871	0.08	0.0691	0.0013	1.4353	0.0282	0.1506	0.0022	901	19	904	12	904	12
81	377	337	1.12	0.0574	0.0012	0.6411	0.0141	0.0811	0.0012	505	24	503	9	502	7
82	25	262	0.10	0.0743	0.0014	1.8715	0.0382	0.1827	0.0027	1049	20	1071	14	1082	15
83	145	256	0.57	0.0740	0.0014	1.8313	0.0375	0.1794	0.0026	1043	20	1057	13	1063	14
84	76	122	0.63	0.0632	0.0016	1.0487	0.0266	0.1204	0.0018	714	29	728	13	733	11
85	491	493	1.00	0.0690	0.0013	1.3692	0.0278	0.1439	0.0021	898	20	876	12	867	12
86	1	51	0.01	0.0604	0.0020	0.8389	0.0277	0.1008	0.0017	617	43	619	15	619	10
87	39	104	0.37	0.1695	0.0032	10.8960	0.2205	0.4661	0.0069	2553	16	2514	19	2467	30

88	57	135	0.42	0.0713	0.0016	1.5106	0.0344	0.1536	0.0023	966	24	935	14	921	13
89	48	833	0.06	0.0925	0.0017	3.2588	0.0658	0.2555	0.0037	1477	18	1471	16	1467	19
90	208	300	0.69	0.0554	0.0013	0.5288	0.0125	0.0692	0.0010	430	27	431	8	431	6
91	312	475	0.66	0.0716	0.0014	1.5873	0.0327	0.1608	0.0024	974	20	965	13	961	13
92	249	398	0.62	0.0592	0.0013	0.7699	0.0175	0.0943	0.0014	575	25	580	10	581	8
93	341	396	0.86	0.1456	0.0028	8.1891	0.1681	0.4079	0.0060	2295	17	2252	19	2205	27
94	338	500	0.68	0.0774	0.0015	2.1298	0.0441	0.1996	0.0029	1131	20	1159	14	1173	16
95	21	189	0.11	0.0706	0.0015	1.4377	0.0312	0.1478	0.0022	944	22	905	13	888	12
96	39	476	0.08	0.0713	0.0014	1.5551	0.0326	0.1582	0.0023	965	21	953	13	947	13
97	99	73	1.36	0.0848	0.0019	2.6170	0.0608	0.2238	0.0034	1311	23	1305	17	1302	18
98	65	264	0.25	0.1674	0.0033	11.1343	0.2321	0.4824	0.0071	2531	17	2534	19	2538	31
99	72	137	0.53	0.0742	0.0016	1.8116	0.0416	0.1770	0.0027	1047	24	1050	15	1051	15
100	155	428	0.36	0.0656	0.0014	1.1843	0.0260	0.1310	0.0020	793	23	793	12	793	11
Sample 10GD88, Middle Silurian, Zhangjiajie															
1	156	100	1.56	0.1164	0.0017	5.5281	0.0921	0.3443	0.0050	1902	13	1905	14	1907	24
2	53	186	0.28	0.1724	0.0023	12.0625	0.1955	0.5073	0.0072	2581	12	2609	15	2645	31
3	96	126	0.77	0.0600	0.0012	0.8135	0.0180	0.0983	0.0015	603	24	604	10	605	9
4	79	168	0.47	0.1634	0.0022	10.6426	0.1732	0.4724	0.0067	2491	12	2492	15	2494	29
5	130	250	0.52	0.0829	0.0027	2.3630	0.0691	0.2068	0.0031	1267	66	1232	21	1212	17
6	133	673	0.20	0.0693	0.0010	1.4452	0.0240	0.1512	0.0022	908	15	908	10	908	12
7	253	248	1.02	0.0620	0.0010	0.9405	0.0173	0.1101	0.0016	673	18	673	9	673	9
8	48	103	0.47	0.0993	0.0015	3.8876	0.0666	0.2839	0.0041	1611	14	1611	14	1611	21
9	120	265	0.45	0.0702	0.0011	1.4915	0.0260	0.1541	0.0022	934	16	927	11	924	12
10	69	116	0.60	0.0713	0.0012	1.5831	0.0299	0.1610	0.0024	966	18	964	12	962	13
11	146	106	1.38	0.0698	0.0012	1.4914	0.0294	0.1549	0.0023	923	19	927	12	928	13
12	89	122	0.73	0.0845	0.0013	2.6130	0.0463	0.2244	0.0033	1303	16	1304	13	1305	17
13	296	311	0.95	0.1558	0.0021	9.7717	0.1601	0.4550	0.0065	2410	12	2413	15	2417	29
14	56	89	0.64	0.0723	0.0013	1.6569	0.0324	0.1662	0.0025	994	19	992	12	991	14
15	79	123	0.64	0.1141	0.0016	5.2441	0.0887	0.3334	0.0048	1865	14	1860	14	1855	23
16	153	309	0.49	0.1045	0.0015	4.3212	0.0721	0.3000	0.0043	1705	14	1697	14	1691	21
17	83	208	0.40	0.1085	0.0016	4.7578	0.0801	0.3180	0.0046	1774	14	1777	14	1780	22

18	277	308	0.90	0.0716	0.0011	1.5924	0.0283	0.1613	0.0023	974	16	967	11	964	13
19	183	254	0.72	0.0902	0.0013	3.0961	0.0526	0.2489	0.0036	1430	15	1432	13	1433	18
20	40	50	0.80	0.1653	0.0025	10.8135	0.1868	0.4745	0.0070	2510	13	2507	16	2503	30
21	257	239	1.07	0.0714	0.0011	1.5683	0.0283	0.1594	0.0023	968	17	958	11	953	13
22	189	361	0.52	0.0757	0.0011	1.9062	0.0328	0.1827	0.0026	1086	16	1083	11	1082	14
23	510	794	0.64	0.0719	0.0010	1.6149	0.0274	0.1628	0.0023	984	16	976	11	972	13
24	426	416	1.03	0.1115	0.0016	4.9989	0.0842	0.3252	0.0047	1824	14	1819	14	1815	23
25	451	457	0.99	0.0751	0.0011	1.8852	0.0323	0.1821	0.0026	1071	16	1076	11	1078	14
26	214	521	0.41	0.1124	0.0017	5.0563	0.0875	0.3263	0.0047	1838	14	1829	15	1820	23
27	95	110	0.86	0.0583	0.0017	0.7071	0.0212	0.0880	0.0014	540	39	543	13	544	8
28	49	113	0.43	0.0747	0.0013	1.8223	0.0362	0.1770	0.0026	1060	19	1054	13	1050	14
29	285	290	0.98	0.1653	0.0024	10.8250	0.1842	0.4750	0.0068	2510	13	2508	16	2505	30
30	57	65	0.88	0.0728	0.0018	1.6050	0.0420	0.1600	0.0025	1008	29	972	16	957	14
31	135	369	0.37	0.0750	0.0012	1.8578	0.0331	0.1797	0.0026	1068	16	1066	12	1065	14
32	478	697	0.69	0.0970	0.0015	3.6435	0.0643	0.2725	0.0040	1567	15	1559	14	1553	20
33	87	236	0.37	0.0824	0.0013	2.4159	0.0434	0.2127	0.0031	1254	16	1247	13	1243	16
34	131	351	0.37	0.1560	0.0025	9.7576	0.1752	0.4536	0.0068	2413	14	2412	17	2411	30
35	324	277	1.17	0.0785	0.0013	2.1445	0.0390	0.1980	0.0029	1161	16	1163	13	1165	16
36	193	427	0.45	0.1311	0.0020	7.2665	0.1295	0.4020	0.0059	2113	14	2145	16	2178	27
37	95	427	0.22	0.0906	0.0014	3.1243	0.0557	0.2501	0.0036	1438	15	1439	14	1439	19
38	362	272	1.33	0.0731	0.0012	1.7154	0.0319	0.1703	0.0025	1016	17	1014	12	1013	14
39	251	222	1.13	0.0850	0.0014	2.6469	0.0484	0.2259	0.0033	1315	16	1314	13	1313	17
40	92	584	0.16	0.0712	0.0016	1.5533	0.0356	0.1582	0.0025	963	23	952	14	947	14
41	88	559	0.16	0.0712	0.0011	1.6016	0.0291	0.1630	0.0024	964	17	971	11	974	13
42	378	248	1.53	0.1251	0.0020	6.5013	0.1188	0.3770	0.0055	2030	15	2046	16	2062	26
43	100	272	0.37	0.0929	0.0015	3.3786	0.0616	0.2637	0.0039	1486	16	1499	14	1509	20
44	120	93	1.29	0.1624	0.0026	10.4602	0.1901	0.4671	0.0069	2481	14	2476	17	2471	30
45	93	74	1.26	0.1218	0.0020	6.0485	0.1127	0.3601	0.0053	1983	15	1983	16	1983	25
46	84	156	0.54	0.0666	0.0013	1.2430	0.0267	0.1354	0.0020	824	22	820	12	819	11
47	37	88	0.42	0.0719	0.0016	1.6289	0.0380	0.1643	0.0025	983	24	981	15	981	14
48	131	265	0.50	0.0655	0.0012	1.1915	0.0234	0.1320	0.0020	790	19	797	11	799	11
49	16	222	0.07	0.0592	0.0011	0.7642	0.0157	0.0936	0.0014	575	21	576	9	577	8

50	80	94	0.85	0.1259	0.0021	6.3461	0.1207	0.3656	0.0054	2041	16	2025	17	2009	26
51	154	419	0.37	0.0700	0.0012	1.4921	0.0286	0.1546	0.0023	929	18	927	12	926	13
52	26	26	0.99	0.0653	0.0024	1.1700	0.0427	0.1300	0.0023	783	47	787	20	788	13
53	111	186	0.60	0.2016	0.0034	15.3496	0.2902	0.5523	0.0083	2839	14	2837	18	2835	35
54	184	547	0.34	0.0723	0.0012	1.6673	0.0313	0.1671	0.0024	996	18	996	12	996	13
55	89	299	0.30	0.0715	0.0013	1.5959	0.0312	0.1619	0.0024	971	19	969	12	968	13
56	215	474	0.45	0.0716	0.0012	1.6032	0.0308	0.1624	0.0024	975	18	971	12	970	13
57	39	46	0.85	0.1941	0.0034	14.4510	0.2834	0.5398	0.0082	2777	15	2780	19	2783	34
58	210	502	0.42	0.0752	0.0013	1.8826	0.0361	0.1816	0.0027	1074	18	1075	13	1076	15
59	79	368	0.21	0.0622	0.0011	0.9786	0.0196	0.1141	0.0017	681	20	693	10	697	10
60	126	449	0.28	0.1436	0.0024	8.1997	0.1571	0.4142	0.0061	2270	15	2253	17	2234	28
61	161	332	0.48	0.0681	0.0012	1.3985	0.0276	0.1490	0.0022	870	19	888	12	896	12
62	169	312	0.54	0.0890	0.0015	3.1466	0.0612	0.2565	0.0038	1403	17	1444	15	1472	19
63	97	163	0.60	0.1137	0.0020	5.2182	0.1020	0.3329	0.0049	1859	17	1856	17	1852	24
64	329	426	0.77	0.0673	0.0012	1.3127	0.0266	0.1415	0.0021	846	20	851	12	853	12
65	69	67	1.03	0.1623	0.0029	10.3414	0.2046	0.4621	0.0069	2480	16	2466	18	2449	31
66	172	385	0.45	0.1825	0.0032	12.9457	0.2527	0.5144	0.0076	2676	15	2676	18	2675	32
67	246	477	0.52	0.0686	0.0012	1.4005	0.0280	0.1482	0.0022	885	20	889	12	891	12
~~*68*~~	~~*182*~~	~~*479*~~	~~*0.38*~~	~~*0.0679*~~	~~*0.0015*~~	~~*0.7929*~~	~~*0.0180*~~	~~*0.0847*~~	~~*0.0013*~~	~~*865*~~	~~*23*~~	~~*593*~~	~~*10*~~	~~*524*~~	~~*8*~~
~~*69*~~	~~*162*~~	~~*59*~~	~~*2.76*~~	~~*0.2098*~~	~~*0.0039*~~	~~*11.1862*~~	~~*0.2273*~~	~~*0.3867*~~	~~*0.0059*~~	~~*2904*~~	~~*16*~~	~~*2539*~~	~~*19*~~	~~*2108*~~	~~*27*~~
70	172	309	0.56	0.0842	0.0015	2.5656	0.0520	0.2209	0.0033	1298	19	1291	15	1287	17
71	56	134	0.42	0.1594	0.0029	10.1640	0.2046	0.4624	0.0069	2450	16	2450	19	2450	31
72	186	195	0.95	0.1612	0.0029	10.3096	0.2084	0.4639	0.0069	2468	16	2463	19	2457	31
73	69	79	0.86	0.1635	0.0032	10.7824	0.2262	0.4782	0.0074	2492	17	2505	19	2519	32
74	183	189	0.97	0.0993	0.0019	3.9064	0.0824	0.2854	0.0043	1610	19	1615	17	1619	22
75	591	247	2.40	0.0601	0.0014	0.8140	0.0199	0.0982	0.0015	608	28	605	11	604	9
76	180	497	0.36	0.1052	0.0020	4.4260	0.0920	0.3051	0.0046	1718	18	1717	17	1716	23
77	166	108	1.54	0.0799	0.0018	2.2459	0.0543	0.2039	0.0032	1194	25	1195	17	1196	17
78	320	313	1.02	0.0724	0.0016	1.6864	0.0384	0.1689	0.0026	997	23	1003	15	1006	14
79	70	135	0.52	0.0728	0.0017	1.6957	0.0419	0.1690	0.0026	1008	26	1007	16	1006	14
80	52	117	0.44	0.0661	0.0018	1.2122	0.0337	0.1330	0.0021	810	32	806	15	805	12
81	207	329	0.63	0.0703	0.0015	1.5187	0.0350	0.1566	0.0024	938	24	938	14	938	13

82	119	292	0.41	0.0661	0.0014	1.2253	0.0274	0.1344	0.0021	810	23	812	13	813	12
83	100	117	0.85	0.1187	0.0024	5.7185	0.1265	0.3494	0.0054	1937	19	1934	19	1932	26
84	144	193	0.75	0.0915	0.0018	3.1861	0.0693	0.2525	0.0038	1457	20	1454	17	1451	20
85	214	223	0.96	0.0697	0.0014	1.4653	0.0326	0.1525	0.0023	920	23	916	13	915	13
86	68	77	0.89	0.0754	0.0017	1.8888	0.0455	0.1817	0.0029	1078	25	1077	16	1076	16
87	793	74	10.64	0.0695	0.0018	1.4565	0.0387	0.1521	0.0024	912	30	913	16	913	13
88	74	160	0.46	0.1779	0.0035	12.4118	0.2684	0.5059	0.0077	2633	18	2636	20	2639	33
89	88	125	0.71	0.0665	0.0015	1.2663	0.0310	0.1380	0.0021	823	27	831	14	833	12
90	50	126	0.40	0.0712	0.0016	1.6300	0.0396	0.1661	0.0026	962	26	982	15	990	14
91	130	143	0.91	0.0709	0.0016	1.5526	0.0368	0.1588	0.0025	955	25	952	15	950	14
92	212	492	0.43	0.0601	0.0013	0.7827	0.0178	0.0944	0.0014	608	25	587	10	582	8
93	121	172	0.70	0.0753	0.0016	1.8863	0.0430	0.1816	0.0028	1077	23	1076	15	1076	15
94	166	113	1.47	0.0577	0.0017	0.6644	0.0202	0.0836	0.0013	516	39	517	12	517	8
95	187	371	0.50	0.0654	0.0014	1.1151	0.0254	0.1236	0.0019	788	24	761	12	751	11
96	128	328	0.39	0.0607	0.0013	0.8505	0.0197	0.1016	0.0016	629	25	625	11	624	9
97	209	104	2.01	0.0595	0.0018	0.7428	0.0231	0.0906	0.0015	585	40	564	13	559	9
98	535	870	0.62	0.0587	0.0012	0.7330	0.0167	0.0906	0.0014	556	25	558	10	559	8
99	279	216	1.29	0.0642	0.0014	1.0887	0.0260	0.1229	0.0019	749	26	748	13	747	11
100	146	400	0.36	0.0682	0.0015	1.3767	0.0318	0.1464	0.0023	874	24	879	14	881	13
Sample 10GD87, Upper Silurian, Zhangjiajie															
1	105	487	0.22	0.1224	0.0016	6.2621	0.0960	0.3711	0.0051	1991	12	2013	13	2035	24
2	64	262	0.24	0.2455	0.0031	21.6040	0.3318	0.6382	0.0088	3156	11	3166	15	3182	35
3	188	249	0.75	0.0723	0.0010	1.6741	0.0268	0.1680	0.0023	993	15	999	10	1001	13
4	222	384	0.58	0.0959	0.0017	3.7675	0.0741	0.2850	0.0044	1545	17	1586	16	1616	22
5	177	74	2.39	0.0713	0.0012	1.5731	0.0298	0.1601	0.0023	965	18	960	12	957	13
6	7	66	0.10	0.1787	0.0028	11.1968	0.1959	0.4545	0.0069	2640	13	2540	16	2415	31
7	184	159	1.15	0.0729	0.0011	1.6879	0.0285	0.1680	0.0024	1010	15	1004	11	1001	13
8	133	199	0.66	0.1321	0.0037	7.1394	0.1690	0.3921	0.0058	2126	50	2129	21	2132	27
9	80	157	0.51	0.0762	0.0011	2.0019	0.0330	0.1905	0.0027	1101	15	1116	11	1124	14
10	93	134	0.69	0.0781	0.0028	1.7837	0.0622	0.1657	0.0031	1149	40	1040	23	988	17
11	285	227	1.25	0.1153	0.0015	5.3964	0.0837	0.3395	0.0047	1884	12	1884	13	1884	23

12	149	173	0.86	0.0715	0.0010	1.4043	0.0236	0.1424	0.0020	971	16	891	10	858	11
13	134	160	0.84	0.0783	0.0011	2.0381	0.0339	0.1888	0.0027	1154	15	1128	11	1115	14
14	70	52	1.35	0.0641	0.0018	1.0418	0.0305	0.1180	0.0018	743	37	725	15	719	10
15	165	176	0.94	0.1505	0.0019	8.8714	0.1384	0.4276	0.0060	2351	12	2325	14	2295	27
16	17	91	0.19	0.0685	0.0012	1.3503	0.0267	0.1429	0.0020	884	20	868	12	861	12
17	380	435	0.87	0.1011	0.0013	3.9870	0.0620	0.2860	0.0040	1644	13	1632	13	1621	20
18	450	101	4.43	0.1198	0.0060	4.8011	0.2308	0.2905	0.0112	1954	39	1785	40	1644	56
19	170	230	0.74	0.0980	0.0014	3.7663	0.0608	0.2787	0.0039	1586	13	1586	13	1585	20
20	302	254	1.19	0.0934	0.0040	2.7665	0.1107	0.2148	0.0034	1497	83	1347	30	1254	18
21	56	166	0.34	0.1066	0.0014	4.6647	0.0740	0.3173	0.0044	1742	13	1761	13	1777	22
22	164	126	1.30	0.0659	0.0011	1.2101	0.0221	0.1333	0.0019	802	18	805	10	806	11
23	186	330	0.56	0.0663	0.0009	1.2302	0.0200	0.1345	0.0019	816	15	814	9	814	11
24	331	250	1.32	0.1808	0.0023	12.8739	0.2007	0.5163	0.0071	2660	12	2670	15	2684	30
25	103	321	0.32	0.0696	0.0010	1.4866	0.0240	0.1549	0.0022	916	15	925	10	928	12
~~*26*~~	~~*309*~~	~~*845*~~	~~*0.37*~~	~~*0.0886*~~	~~*0.0034*~~	~~*1.3884*~~	~~*0.0485*~~	~~*0.1136*~~	~~*0.0017*~~	~~*1396*~~	~~*75*~~	~~*884*~~	~~*21*~~	~~*694*~~	~~*10*~~
27	59	177	0.33	0.1322	0.0018	7.0853	0.1121	0.3886	0.0054	2128	12	2122	14	2116	25
28	241	268	0.90	0.1615	0.0021	10.3564	0.1626	0.4650	0.0064	2471	12	2467	15	2462	28
29	105	601	0.18	0.0629	0.0033	0.8753	0.0445	0.1010	0.0015	704	116	638	24	620	9
30	113	224	0.51	0.0747	0.0011	1.8113	0.0298	0.1760	0.0025	1059	15	1050	11	1045	13
31	189	210	0.90	0.0738	0.0011	1.6435	0.0275	0.1615	0.0023	1036	15	987	11	965	13
32	121	143	0.84	0.0673	0.0033	0.8113	0.0382	0.0874	0.0014	848	106	603	21	540	8
33	336	717	0.47	0.1499	0.0020	8.7056	0.1400	0.4213	0.0059	2344	12	2308	15	2266	27
34	61	56	1.09	0.0642	0.0023	1.2995	0.0455	0.1468	0.0027	748	44	845	20	883	15
35	36	303	0.12	0.1205	0.0016	5.9983	0.0954	0.3610	0.0050	1963	13	1976	14	1987	24
~~*36*~~	~~*203*~~	~~*239*~~	~~*0.85*~~	~~*0.0722*~~	~~*0.0012*~~	~~*0.9120*~~	~~*0.0163*~~	~~*0.0916*~~	~~*0.0013*~~	~~*990*~~	~~*17*~~	~~*658*~~	~~*9*~~	~~*565*~~	~~*8*~~
37	265	733	0.36	0.1656	0.0022	10.8321	0.1718	0.4744	0.0066	2513	12	2509	15	2503	29
38	150	674	0.22	0.0775	0.0011	1.7460	0.0281	0.1633	0.0023	1134	14	1026	10	975	13
39	72	45	1.58	0.0683	0.0033	1.4536	0.0710	0.1544	0.0027	877	72	911	29	925	15
40	181	235	0.77	0.0618	0.0015	0.8011	0.0197	0.0940	0.0015	668	27	597	11	579	9
41	110	220	0.50	0.0734	0.0011	1.7088	0.0290	0.1687	0.0024	1026	16	1012	11	1005	13
42	169	253	0.67	0.1694	0.0023	11.1762	0.1806	0.4785	0.0067	2552	12	2538	15	2521	29
43	54	89	0.60	0.0623	0.0014	0.8770	0.0203	0.1021	0.0015	683	26	639	11	627	9

44	47	69	0.69	0.0757	0.0013	1.9303	0.0361	0.1850	0.0027	1087	17	1092	13	1094	15
45	160	290	0.55	0.0861	0.0012	2.5252	0.0419	0.2126	0.0030	1341	14	1279	12	1242	16
46	187	126	1.48	0.0798	0.0012	2.2338	0.0386	0.2029	0.0029	1193	15	1192	12	1191	15
47	102	233	0.44	0.0933	0.0014	3.3445	0.0563	0.2600	0.0037	1494	14	1492	13	1490	19
48	157	439	0.36	0.0706	0.0026	1.0591	0.0358	0.1088	0.0016	946	77	733	18	666	9
49	278	462	0.60	0.1013	0.0014	4.0080	0.0657	0.2869	0.0040	1648	14	1636	13	1626	20
50	230	408	0.56	0.0727	0.0011	1.6187	0.0274	0.1615	0.0023	1006	16	977	11	965	13
51	1214	520	2.34	0.1029	0.0020	3.5215	0.0730	0.2482	0.0038	1677	18	1532	16	1429	20
52	26	318	0.08	0.2520	0.0035	21.8473	0.3588	0.6287	0.0088	3197	12	3177	16	3144	35
53	79	86	0.92	0.1663	0.0024	10.5680	0.1769	0.4609	0.0065	2520	13	2486	16	2444	29
54	107	146	0.74	0.2115	0.0030	16.2189	0.2683	0.5560	0.0078	2917	12	2890	16	2850	32
55	330	605	0.55	0.0858	0.0029	2.1952	0.0659	0.1856	0.0027	1333	66	1180	21	1097	15
56	242	301	0.81	0.1086	0.0016	4.7139	0.0791	0.3147	0.0044	1776	14	1770	14	1764	22
57	25	20	1.23	0.0662	0.0042	1.0043	0.0622	0.1101	0.0024	811	94	706	31	673	14
58	78	128	0.60	0.1798	0.0026	11.5335	0.1938	0.4652	0.0066	2651	13	2567	16	2462	29
59	96	106	0.90	0.0801	0.0014	1.9752	0.0380	0.1788	0.0026	1200	18	1107	13	1060	14
60	18	376	0.05	0.0718	0.0011	1.5201	0.0262	0.1535	0.0022	981	16	939	11	920	12
61	119	290	0.41	0.1323	0.0019	7.3757	0.1249	0.4041	0.0057	2129	13	2158	15	2188	26
62	127	271	0.47	0.1071	0.0016	4.5367	0.0773	0.3071	0.0043	1751	14	1738	14	1727	21
63	220	99	2.23	0.0592	0.0018	0.6800	0.0209	0.0833	0.0013	573	41	527	13	516	7
64	58	120	0.48	0.0711	0.0012	1.5528	0.0289	0.1584	0.0023	960	18	952	11	948	13
~~*65*~~	~~*370*~~	~~*461*~~	~~*0.80*~~	~~*0.0853*~~	~~*0.0013*~~	~~*1.4137*~~	~~*0.0246*~~	~~*0.1201*~~	~~*0.0017*~~	~~*1323*~~	~~*15*~~	~~*895*~~	~~*10*~~	~~*731*~~	~~*10*~~
66	81	100	0.81	0.1669	0.0025	10.8263	0.1875	0.4702	0.0067	2527	13	2508	16	2485	29
67	69	124	0.56	0.1096	0.0017	4.8568	0.0852	0.3213	0.0046	1793	15	1795	15	1796	22
68	247	236	1.05	0.1672	0.0025	11.1520	0.1926	0.4837	0.0068	2530	13	2536	16	2543	30
69	219	389	0.56	0.0711	0.0011	1.5952	0.0282	0.1628	0.0023	959	17	968	11	972	13
70	270	397	0.68	0.0793	0.0012	2.1388	0.0375	0.1955	0.0028	1180	16	1161	12	1151	15
71	280	460	0.61	0.0791	0.0012	1.8525	0.0325	0.1697	0.0024	1176	16	1064	12	1011	13
72	105	130	0.81	0.0783	0.0014	1.8762	0.0356	0.1739	0.0025	1153	18	1073	13	1033	14
73	63	305	0.21	0.1108	0.0017	4.7029	0.0824	0.3077	0.0044	1813	15	1768	15	1729	21
~~*74*~~	~~*824*~~	~~*501*~~	~~*1.64*~~	~~*0.1331*~~	~~*0.0066*~~	~~*2.1492*~~	~~*0.0996*~~	~~*0.1172*~~	~~*0.0021*~~	~~*2139*~~	~~*89*~~	~~*1165*~~	~~*32*~~	~~*714*~~	~~*12*~~
75	28	66	0.42	0.0723	0.0014	1.6676	0.0341	0.1672	0.0025	995	20	996	13	997	14

76	120	76	1.56	0.0666	0.0017	1.1481	0.0304	0.1250	0.0019	826	31	776	14	759	11
77	174	390	0.45	0.0705	0.0011	1.4981	0.0270	0.1540	0.0022	944	17	930	11	923	12
78	44	316	0.14	0.0622	0.0011	0.9258	0.0173	0.1079	0.0016	682	19	665	9	660	9
79	152	326	0.47	0.1033	0.0017	4.3520	0.0811	0.3055	0.0044	1684	16	1703	15	1718	22
80	38	215	0.18	0.0682	0.0012	1.2854	0.0240	0.1367	0.0020	875	18	839	11	826	11
81	317	256	1.24	0.1106	0.0019	4.9787	0.0926	0.3265	0.0047	1808	16	1816	16	1822	23
82	54	75	0.71	0.0777	0.0015	1.8988	0.0396	0.1772	0.0026	1139	20	1081	14	1052	14
83	280	240	1.16	0.0775	0.0016	2.1772	0.0465	0.2036	0.0031	1135	21	1174	15	1195	16
84	110	217	0.51	0.1036	0.0017	4.1649	0.0760	0.2914	0.0042	1690	16	1667	15	1649	21
85	275	580	0.47	0.0827	0.0014	2.5559	0.0469	0.2240	0.0032	1263	17	1288	13	1303	17
86	178	518	0.34	0.0758	0.0030	1.9514	0.0711	0.1868	0.0029	1089	81	1099	24	1104	16
87	237	348	0.68	0.0845	0.0014	2.5056	0.0473	0.2150	0.0031	1304	17	1274	14	1255	16
88	51	50	1.01	0.1689	0.0029	10.8025	0.2038	0.4637	0.0068	2547	15	2506	18	2456	30
89	45	231	0.20	0.2125	0.0035	16.7074	0.3063	0.5700	0.0082	2925	14	2918	18	2908	33
90	165	212	0.78	0.0705	0.0013	1.2204	0.0237	0.1255	0.0018	944	19	810	11	762	10
91	152	184	0.83	0.1659	0.0028	10.7062	0.1982	0.4678	0.0067	2517	14	2498	17	2474	29
92	41	65	0.63	0.0593	0.0019	0.7609	0.0244	0.0930	0.0015	578	43	575	14	573	9
93	42	88	0.48	0.1190	0.0021	5.6706	0.1078	0.3455	0.0050	1941	16	1927	16	1913	24
94	53	183	0.29	0.1016	0.0018	3.7088	0.0706	0.2647	0.0038	1653	17	1573	15	1514	20
95	78	320	0.24	0.0612	0.0060	0.7778	0.0736	0.0921	0.0031	647	146	584	42	568	18
96	180	393	0.46	0.0674	0.0013	1.2349	0.0249	0.1329	0.0020	850	20	817	11	804	11
97	355	220	1.62	0.0656	0.0012	1.1515	0.0228	0.1273	0.0019	794	20	778	11	772	11
98	42	93	0.45	0.0645	0.0014	1.0990	0.0245	0.1236	0.0019	757	24	753	12	751	11
99	272	331	0.82	0.0594	0.0011	0.6945	0.0139	0.0847	0.0012	583	21	536	8	524	7
100	137	131	1.05	0.0710	0.0014	1.5700	0.0322	0.1603	0.0024	958	20	958	13	958	13

Appendix C2 MC-ICP-MS zircon Lu–Hf isotope data for selected Cambrian–Silurian samples across the lower Palaeozoic Nanhua foreland basin, South China

Spot#	age	1σ	$^{176}Lu/^{177}Hf$	2σ	$^{176}Hf/^{177}Hf$	2σ	$\varepsilon_{Hf}(t)^{*}$	2σ	T_{DM} (Ma)†	T_{DM}^{C} (Ma)§	$f_{Lu/Hf}$
Sample 10GD37, Upper Cambrian, Yulin											
1	1534	17	0.000505	0.000005	0.281716	0.000021	-3.76	1.50	2125	2303	-0.98
2	1311	18	0.001217	0.000005	0.281969	0.000019	-0.38	1.48	1814	1954	-0.96
3	485	8	0.000255	0.000003	0.282107	0.000019	-12.93	1.29	1581	1921	-0.99
4	779	11	0.000559	0.000005	0.281987	0.000018	-10.87	1.31	1759	2052	-0.98
5	2316	16	0.000844	0.000015	0.281202	0.000019	-4.99	1.46	2844	2997	-0.97
6	523	8	0.000303	0.000001	0.282112	0.000017	-11.93	1.24	1576	1900	-0.99
7	787	12	0.000592	0.000008	0.281936	0.000019	-12.53	1.33	1830	2141	-0.98
8	3041	15	0.001803	0.000025	0.280893	0.000020	-1.61	1.50	3343	3421	-0.95
9	905	13	0.000655	0.000018	0.281947	0.000017	-9.57	1.32	1817	2087	-0.98
10	1404	84	0.000767	0.000012	0.281419	0.000020	-17.43	3.99	2544	2877	-0.98
11	2265	16	0.000787	0.000001	0.281993	0.000021	22.06	1.50	1761	1615	-0.98
12	2345	15	0.000495	0.000006	0.280937	0.000020	-13.18	1.46	3172	3421	-0.99
13	1567	15	0.000410	0.000002	0.280979	0.000018	-29.07	1.40	3109	3579	-0.99
14	781	12	0.001010	0.000017	0.282196	0.000021	-3.67	1.39	1490	1690	-0.97
15	1495	15	0.000619	0.000003	0.281512	0.000022	-11.98	1.46	2409	2680	-0.98
16	785	12	0.000461	0.000002	0.281964	0.000019	-11.49	1.35	1785	2088	-0.99
17	1009	14	0.000812	0.000004	0.281722	0.000017	-15.39	1.35	2134	2461	-0.98
18	2441	15	0.000434	0.000003	0.281287	0.000025	1.51	1.56	2701	2779	-0.99
19	1788	17	0.000855	0.000007	0.281502	0.000020	-6.09	1.49	2437	2624	-0.97
20	1043	15	0.000473	0.000001	0.282255	0.000020	4.48	1.43	1387	1491	-0.99
21	2113	16	0.000588	0.000005	0.281197	0.000023	-9.35	1.53	2833	3047	-0.98
22	665	10	0.001232	0.000003	0.282473	0.000066	3.57	2.58	1108	1230	-0.96

23	528	8	0.000608	0.000001	0.282437	0.000028	-0.44	1.47	1141	1323	-0.98
24	522	8	0.000426	0.000005	0.282083	0.000029	-13.03	1.49	1621	1955	-0.99
25	1510	16	0.000504	0.000003	0.281473	0.000023	-12.91	1.51	2454	2738	-0.98
26	1568	17	0.000754	0.000008	0.281814	0.000018	0.20	1.45	2005	2133	-0.98
27	655	10	0.000684	0.000015	0.282401	0.000027	1.03	1.48	1193	1351	-0.98
28	1498	17	0.001532	0.000031	0.281998	0.000020	4.40	1.48	1789	1866	-0.95
29	1016	16	0.000584	0.000012	0.282134	0.000026	-0.49	1.55	1558	1720	-0.98
30	610	9	0.000882	0.000003	0.282476	0.000022	2.62	1.35	1094	1233	-0.97
31	502	8	0.000611	0.000017	0.282130	0.000023	-11.88	1.36	1565	1881	-0.98
32	2452	15	0.000749	0.000011	0.281847	0.000020	21.17	1.48	1959	1815	-0.98
33	1390	17	0.000212	0.000001	0.280770	0.000019	-40.24	1.45	3370	3985	-0.99
34	941	14	0.000549	0.000002	0.282168	0.000019	-0.91	1.38	1510	1681	-0.98
35	965	15	0.000906	0.000007	0.282328	0.000023	5.06	1.47	1301	1398	-0.97
36	973	14	0.000830	0.000003	0.282293	0.000022	4.07	1.43	1347	1455	-0.97
37	1344	15	0.000867	0.000016	0.281994	0.000022	1.55	1.47	1763	1884	-0.97
38	983	16	0.000506	0.000007	0.281970	0.000022	-6.96	1.49	1779	2019	-0.98
39	954	14	0.000899	0.000003	0.282302	0.000018	3.93	1.37	1337	1447	-0.97
40	892	12	0.001065	0.000009	0.282258	0.000021	0.90	1.37	1405	1549	-0.97
41	2343	15	0.000287	0.000001	0.281076	0.000022	-7.97	1.50	2971	3165	-0.99
42	901	13	0.000173	0.000008	0.282043	0.000017	-6.00	1.33	1666	1904	-0.99
43	1020	18	0.000785	0.000004	0.281936	0.000024	-7.55	1.57	1839	2078	-0.98
44	633	9	0.000365	0.000003	0.282400	0.000020	0.64	1.31	1184	1353	-0.99
45	1556	17	0.000494	0.000003	0.281506	0.000018	-10.71	1.44	2409	2666	-0.99
46	1080	17	0.000843	0.000010	0.282017	0.000020	-3.42	1.47	1731	1919	-0.97
47	979	14	0.000490	0.000009	0.281997	0.000019	-6.07	1.39	1741	1971	-0.99
48	886	13	0.002971	0.000032	0.281889	0.000024	-13.41	1.46	2018	2263	-0.91
49	972	13	0.001947	0.000028	0.282368	0.000020	5.95	1.38	1281	1359	-0.94
50	1013	17	0.000802	0.000047	0.282019	0.000023	-4.77	1.52	1726	1933	-0.98
51	1196	18	0.000687	0.000008	0.281618	0.000021	-14.88	1.50	2269	2585	-0.98
52	841	12	0.000189	0.000004	0.281389	0.000020	-30.50	1.35	2547	3079	-0.99
53	955	13	0.000469	0.000002	0.281847	0.000016	-11.90	1.32	1945	2244	-0.99
54	1683	16	0.000662	0.000004	0.281636	0.000019	-3.46	1.45	2243	2409	-0.98

55	1683	16	0.001177	0.000006	0.281589	0.000023	-5.71	1.52	2338	2520	-0.96
56	521	8	0.000638	0.000013	0.281935	0.000022	-18.35	1.34	1833	2222	-0.98
57	875	14	0.000628	0.000003	0.282410	0.000016	6.17	1.33	1178	1268	-0.98
57	937	13	0.000485	0.000011	0.282147	0.000016	-1.70	1.31	1536	1717	-0.99
57	928	13	0.000056	0.000001	0.281949	0.000018	-8.65	1.34	1788	2060	-1.00
61	966	13	0.000981	0.000002	0.282137	0.000021	-1.71	1.41	1569	1741	-0.97
62	804	11	0.000688	0.000003	0.282180	0.000019	-3.56	1.33	1499	1703	-0.98
63	1337	16	0.000521	0.000009	0.281900	0.000017	-1.63	1.40	1876	2037	-0.98
64	2454	15	0.000186	0.000000	0.281264	0.000018	1.41	1.44	2714	2795	-0.99
65	522	8	0.000322	0.000005	0.282096	0.000018	-12.52	1.26	1598	1929	-0.99
66	2407	15	0.000386	0.000002	0.280763	0.000019	-17.82	1.45	3395	3696	-0.99
67	1420	17	0.000426	0.000005	0.282001	0.000016	3.87	1.42	1734	1829	-0.99
68	612	9	0.000654	0.000003	0.282468	0.000018	2.48	1.27	1098	1242	-0.98
69	882	13	0.001151	0.000034	0.282450	0.000021	7.43	1.40	1139	1210	-0.97
70	1670	17	0.001469	0.000010	0.281806	0.000016	1.40	1.43	2054	2156	-0.96
71	610	9	0.000632	0.000004	0.282419	0.000020	0.69	1.32	1166	1331	-0.98
72	2457	15	0.000598	0.000005	0.281164	0.000022	-2.75	1.50	2876	3001	-0.98
73	944	13	0.000346	0.000009	0.281951	0.000019	-8.38	1.37	1797	2059	-0.99
74	951	13	0.000806	0.000003	0.282206	0.000021	0.50	1.41	1467	1617	-0.98
75	1035	6	0.000592	0.000003	0.281914	0.000021	-7.86	1.31	1860	2106	-0.98
76	1686	17	0.000646	0.000008	0.281691	0.000019	-1.43	1.48	2168	2310	-0.98
77	1039	18	0.000586	0.000003	0.281924	0.000018	-7.43	1.47	1846	2087	-0.98
78	1368	16	0.000778	0.000014	0.281565	0.000021	-13.07	1.46	2347	2632	-0.98
79	2403	15	0.000377	0.000003	0.281032	0.000019	-8.33	1.46	3037	3231	-0.99
80	2413	15	0.000334	0.000002	0.281148	0.000021	-3.90	1.48	2879	3022	-0.99
81	642	9	0.001162	0.000009	0.282431	0.000020	1.60	1.31	1165	1311	-0.97
82	1674	16	0.000836	0.000025	0.281597	0.000020	-5.23	1.46	2306	2489	-0.97
83	2421	15	0.000521	0.000002	0.281185	0.000024	-2.70	1.55	2843	2970	-0.98
84	564	8	0.000481	0.000003	0.281682	0.000019	-26.33	1.28	2170	2655	-0.99
85	1079	17	0.000330	0.000001	0.281802	0.000016	-10.68	1.40	2000	2282	-0.99
86	907	13	0.000536	0.000001	0.282050	0.000022	-5.82	1.42	1671	1900	-0.98
87	1040	18	0.000919	0.000012	0.282030	0.000021	-3.86	1.51	1715	1909	-0.97

88	753	11	0.000795	0.000013	0.281909	0.000021	-14.32	1.37	1877	2204	-0.98
89	727	10	0.000858	0.000042	0.282203	0.000018	-4.49	1.29	1473	1688	-0.97
90	931	13	0.000810	0.000003	0.282080	0.000017	-4.41	1.33	1642	1849	-0.98
91	907	13	0.001063	0.000004	0.282381	0.000021	5.59	1.40	1232	1324	-0.97
92	1051	16	0.001037	0.000005	0.281843	0.000021	-10.33	1.47	1980	2242	-0.97
93	1015	14	0.001355	0.000016	0.282036	0.000023	-4.49	1.46	1727	1920	-0.96
94	834	12	0.000587	0.000001	0.282318	0.000021	2.03	1.38	1305	1445	-0.98
95	2362	15	0.000674	0.000019	0.281161	0.000020	-5.15	1.46	2887	3042	-0.98
96	967	13	0.000911	0.000026	0.282199	0.000018	0.55	1.35	1481	1628	-0.97
97	1764	16	0.001552	0.000020	0.281637	0.000020	-2.69	1.47	2295	2436	-0.95
98	1690	16	0.001215	0.000015	0.281570	0.000021	-6.29	1.47	2367	2555	-0.96
99	1072	18	0.000833	0.000013	0.282008	0.000016	-3.88	1.43	1742	1936	-0.97
100	1170	15	0.000908	0.000013	0.282175	0.000021	4.12	1.45	1514	1613	-0.97
101	872	12	0.001136	0.000023	0.282199	0.000018	-1.66	1.33	1490	1663	-0.97
102	1630	16	0.000738	0.000008	0.281793	0.000021	0.87	1.48	2032	2150	-0.98
103	498	7	0.001185	0.000005	0.282124	0.000020	-12.36	1.28	1597	1902	-0.96
104	1544	17	0.004329	0.000053	0.282160	0.000019	8.24	1.48	1687	1711	-0.87
105	900	13	0.000664	0.000002	0.281955	0.000017	-9.42	1.33	1807	2075	-0.98
106	802	11	0.000339	0.000025	0.281434	0.000020	-29.84	1.34	2497	3016	-0.99
107	1088	17	0.000998	0.000017	0.281987	0.000016	-4.41	1.40	1779	1976	-0.97
108	869	13	0.001120	0.000008	0.282360	0.000029	3.99	1.57	1264	1374	-0.97
109	998	14	0.001143	0.000008	0.281927	0.000019	-8.60	1.39	1870	2113	-0.97
110	2510	15	0.000543	0.000020	0.281282	0.000017	2.71	1.42	2715	2777	-0.98
111	495	7	0.000550	0.000037	0.282134	0.000025	-11.87	1.40	1557	1875	-0.98
112	955	13	0.000605	0.000006	0.282039	0.000021	-5.21	1.41	1690	1908	-0.98
113	2719	15	0.001356	0.000009	0.281075	0.000019	-1.38	1.47	3056	3147	-0.96
114	498	8	0.000480	0.000004	0.282031	0.000022	-15.40	1.33	1694	2055	-0.99
115	2356	15	0.000543	0.000004	0.281184	0.000021	-4.24	1.48	2846	2993	-0.98
116	557	8	0.000216	0.000002	0.282237	0.000017	-6.73	1.24	1402	1665	-0.99
117	796	11	0.000487	0.000006	0.282073	0.000015	-7.42	1.27	1638	1892	-0.99
118	2396	15	0.000347	0.000000	0.280835	0.000017	-15.43	1.41	3296	3571	-0.99
119	2654	15	0.001350	0.000004	0.281024	0.000022	-4.63	1.51	3125	3253	-0.96

120	855	12	0.000219	0.000002	0.281969	0.000019	-9.67	1.34	1768	2052	-0.99
Sample 10GD42-1, Lower Ordovician, Yulin											
1	491	8	0.000391	0.000005	0.282153	0.000015	-11.23	1.21	1525	1840	-0.99
2	2995	14	0.000614	0.000002	0.280874	0.000020	-0.85	1.46	3266	3347	-0.98
3	918	17	0.000817	0.000015	0.282175	0.000022	-1.32	1.50	1511	1683	-0.98
4	499	7	0.000453	0.000000	0.282201	0.000017	-9.36	1.23	1460	1751	-0.99
5	2403	16	0.001043	0.000009	0.281005	0.000015	-10.36	1.42	3126	3330	-0.97
6	637	9	0.000648	0.000002	0.282383	0.000020	0.00	1.31	1217	1388	-0.98
7	2358	15	0.000362	0.000003	0.280910	0.000016	-13.67	1.40	3198	3455	-0.99
8	1063	16	0.000493	0.000003	0.282123	0.000019	0.22	1.43	1570	1722	-0.99
9	1211	17	0.000710	0.000015	0.281664	0.000016	-12.95	1.41	2208	2501	-0.98
10	527	8	0.000373	0.000000	0.282111	0.000015	-11.91	1.21	1581	1902	-0.99
11	889	12	0.001169	0.000038	0.282160	0.000016	-2.71	1.30	1546	1729	-0.96
12	2053	16	0.000413	0.000001	0.280977	0.000018	-18.24	1.44	3112	3434	-0.99
13	520	7	0.000410	0.000002	0.282051	0.000017	-14.22	1.23	1665	2013	-0.99
14	979	14	0.000565	0.000004	0.281873	0.000019	-10.53	1.38	1915	2194	-0.98
15	932	13	0.000571	0.000001	0.282074	0.000017	-4.46	1.33	1640	1852	-0.98
16	1039	15	0.000547	0.000003	0.281861	0.000020	-9.60	1.43	1930	2196	-0.98
17	1696	17	0.000837	0.000007	0.281307	0.000017	-15.04	1.44	2701	2992	-0.97
18	2131	16	0.000664	0.000019	0.281189	0.000019	-9.32	1.45	2848	3060	-0.98
19	1134	16	0.000739	0.000020	0.281946	0.000016	-4.68	1.38	1824	2026	-0.98
20	858	13	0.001192	0.000006	0.282000	0.000020	-9.06	1.37	1771	2024	-0.96
21	902	13	0.001135	0.000007	0.282172	0.000018	-1.97	1.34	1528	1703	-0.97
22	896	13	0.000524	0.000001	0.281871	0.000015	-12.38	1.30	1915	2221	-0.98
23	1706	17	0.000408	0.000003	0.281311	0.000019	-14.17	1.47	2666	2957	-0.99
24	1152	18	0.001300	0.000009	0.281877	0.000020	-7.14	1.50	1946	2164	-0.96
25	1984	15	0.000575	0.000001	0.281156	0.000025	-13.66	1.54	2886	3155	-0.98
26	932	13	0.000836	0.000003	0.282301	0.000026	3.44	1.51	1336	1453	-0.97
27	2470	15	0.000410	0.000001	0.280772	0.000020	-16.10	1.48	3385	3663	-0.99
28	1008	18	0.000775	0.000003	0.281928	0.000021	-8.09	1.52	1850	2095	-0.98
29	908	13	0.000193	0.000005	0.281385	0.000018	-29.14	1.35	2552	3064	-0.99

30	930	13	0.000821	0.000015	0.281951	0.000022	-8.99	1.42	1820	2078	-0.98
31	958	13	0.001728	0.000044	0.282463	0.000020	9.17	1.39	1138	1184	-0.95
32	1281	17	0.000822	0.000003	0.282068	0.000019	2.81	1.46	1659	1769	-0.98
33	843	12	0.001310	0.000053	0.282326	0.000017	2.11	1.32	1318	1448	-0.96
34	953	14	0.000304	0.000004	0.282197	0.000022	0.54	1.45	1461	1617	-0.99
35	764	11	0.000325	0.000000	0.281958	0.000020	-12.09	1.34	1787	2101	-0.99
36	1047	15	0.000230	0.000006	0.281865	0.000017	-9.08	1.37	1909	2177	-0.99
37	1076	17	0.000619	0.000027	0.282011	0.000018	-3.56	1.44	1729	1923	-0.98
38	1132	17	0.001032	0.000002	0.281942	0.000019	-5.05	1.45	1842	2043	-0.97
39	999	14	0.001194	0.000014	0.282030	0.000022	-4.95	1.45	1728	1931	-0.96
40	513	7	0.000976	0.000007	0.281784	0.000020	-23.99	1.29	2058	2498	-0.97
41	1221	17	0.001137	0.000021	0.282232	0.000015	7.05	1.40	1444	1507	-0.97
42	1063	18	0.001384	0.000018	0.281861	0.000019	-9.69	1.47	1973	2220	-0.96
43	958	13	0.000157	0.000002	0.281946	0.000022	-8.15	1.42	1796	2059	-1.00
44	1035	18	0.000471	0.000001	0.281914	0.000020	-7.79	1.49	1855	2102	-0.99
45	525	8	0.000288	0.000002	0.282126	0.000017	-11.38	1.24	1556	1874	-0.99
46	2034	16	0.000577	0.000005	0.281454	0.000020	-1.97	1.48	2485	2619	-0.98
47	520	7	0.000581	0.000006	0.282147	0.000016	-10.86	1.21	1540	1844	-0.98
48	513	7	0.000494	0.000006	0.282081	0.000018	-13.33	1.24	1627	1963	-0.99
49	1067	17	0.000514	0.000002	0.282018	0.000018	-3.41	1.44	1714	1908	-0.98
50	556	8	0.001075	0.000006	0.282401	0.000019	-1.28	1.29	1205	1388	-0.97
51	525	8	0.000452	0.000001	0.282132	0.000015	-11.26	1.22	1556	1868	-0.99
52	951	13	0.000600	0.000002	0.282088	0.000016	-3.55	1.32	1622	1822	-0.98
53	1643	17	0.003265	0.000083	0.281902	0.000022	2.22	1.53	2016	2094	-0.90
54	1055	16	0.000240	0.000014	0.281979	0.000017	-4.87	1.40	1755	1972	-0.99
55	937	14	0.000345	0.000009	0.282060	0.000017	-4.69	1.35	1649	1868	-0.99
56	1118	61	0.001611	0.000008	0.282076	0.000018	-1.05	3.00	1683	1831	-0.95
57	522	8	0.000366	0.000001	0.282132	0.000016	-11.27	1.22	1552	1866	-0.99
58	1704	16	0.002562	0.000018	0.281613	0.000018	-6.00	1.43	2393	2551	-0.92
59	524	9	0.000283	0.000000	0.282109	0.000016	-12.02	1.24	1580	1906	-0.99
60	933	13	0.000754	0.000004	0.282091	0.000015	-3.92	1.29	1624	1826	-0.98
61	1040	17	0.001745	0.000010	0.282469	0.000014	11.13	1.39	1129	1152	-0.95

~~62~~	~~2175~~	~~40~~	~~0.001735~~	~~0.000021~~	~~0.281049~~	~~0.000019~~	~~14.91~~	~~2.23~~	~~3123~~	~~3369~~	~~0.95~~
63	1566	17	0.001741	0.000009	0.281944	0.000015	3.74	1.40	1875	1955	-0.95
64	507	7	0.001268	0.000012	0.281893	0.000016	-20.37	1.21	1923	2312	-0.96
65	750	11	0.000722	0.000013	0.282239	0.000018	-2.67	1.31	1419	1615	-0.98
66	1745	17	0.000959	0.000006	0.281615	0.000015	-3.19	1.41	2290	2445	-0.97
67	525	8	0.000460	0.000001	0.282158	0.000016	-10.33	1.23	1520	1821	-0.99
68	959	13	0.000688	0.000003	0.282079	0.000016	-3.75	1.32	1638	1838	-0.98
69	3063	15	0.000621	0.000005	0.280831	0.000018	-0.83	1.47	3324	3401	-0.98
70	510	8	0.000414	0.000002	0.282148	0.000014	-10.98	1.20	1531	1842	-0.99
71	912	14	0.000309	0.000002	0.281616	0.000022	-20.96	1.45	2250	2662	-0.99
72	513	8	0.000632	0.000016	0.282118	0.000018	-12.06	1.25	1582	1899	-0.98
73	1970	15	0.001049	0.000009	0.281905	0.000019	11.98	1.44	1895	1874	-0.97
74	1025	18	0.000381	0.000027	0.281908	0.000015	-8.14	1.42	1858	2112	-0.99
75	2509	15	0.000743	0.000029	0.280764	0.000017	-16.04	1.42	3424	3691	-0.98
76	943	13	0.000980	0.000008	0.282168	0.000017	-1.13	1.33	1527	1693	-0.97
77	508	7	0.000489	0.000006	0.282048	0.000016	-14.61	1.21	1672	2023	-0.99
78	1122	15	0.000395	0.000002	0.281810	0.000018	-9.48	1.39	1992	2257	-0.99
79	541	8	0.000364	0.000001	0.282081	0.000015	-12.67	1.21	1622	1952	-0.99
80	1265	17	0.000694	0.000019	0.281980	0.000014	-0.54	1.38	1774	1924	-0.98
81	893	14	0.000649	0.000002	0.282341	0.000018	4.13	1.37	1274	1387	-0.98
82	2268	16	0.000303	0.000016	0.281102	0.000024	-8.78	1.56	2938	3144	-0.99
83	920	13	0.000811	0.000013	0.282211	0.000025	0.00	1.49	1460	1617	-0.98
84	1034	14	0.001328	0.000005	0.281925	0.000019	-8.00	1.39	1881	2112	-0.96
85	2468	15	0.000547	0.000002	0.280899	0.000022	-11.86	1.50	3228	3455	-0.98
86	1109	16	0.000763	0.000021	0.282392	0.000020	10.60	1.46	1207	1235	-0.98
87	882	13	0.000574	0.000007	0.282187	0.000022	-1.55	1.42	1485	1665	-0.98
88	972	15	0.000594	0.000016	0.281841	0.000019	-11.85	1.40	1960	2255	-0.98
89	3314	14	0.000921	0.000002	0.280661	0.000017	-1.81	1.44	3578	3653	-0.97
90	2430	15	0.000444	0.000001	0.281134	0.000018	-4.17	1.44	2905	3049	-0.99
91	1163	16	0.000641	0.000012	0.282235	0.000018	6.30	1.42	1421	1497	-0.98
92	1121	15	0.000772	0.000006	0.281940	0.000020	-5.19	1.42	1833	2041	-0.98
93	519	8	0.000321	0.000002	0.282166	0.000021	-10.12	1.32	1503	1806	-0.99

94	1338	16	0.001375	0.000005	0.281821	0.000021	-5.16	1.47	2028	2215	-0.96
95	969	14	0.001687	0.000024	0.282426	0.000019	8.14	1.39	1188	1245	-0.95
96	958	13	0.001599	0.000003	0.282401	0.000020	7.07	1.38	1221	1291	-0.95
97	1701	16	0.000628	0.000005	0.281778	0.000021	2.02	1.48	2048	2151	-0.98
98	1086	17	0.000448	0.000002	0.281999	0.000017	-3.63	1.42	1738	1935	-0.99
99	922	14	0.000482	0.000001	0.282294	0.000023	3.20	1.46	1333	1457	-0.99
100	1250	16	0.001075	0.000007	0.281941	0.000021	-2.57	1.47	1846	2014	-0.97
102	906	13	0.000721	0.000006	0.282369	0.000019	5.37	1.37	1237	1335	-0.98
103	1062	17	0.000375	0.000006	0.281829	0.000017	-10.13	1.41	1965	2241	-0.99
104	913	13	0.000249	0.000004	0.282385	0.000017	6.36	1.34	1201	1290	-0.99
105	975	14	0.001926	0.000003	0.282339	0.000021	5.01	1.42	1322	1409	-0.94
106	807	13	0.000815	0.000007	0.282162	0.000020	-4.20	1.38	1529	1738	-0.98
107	945	14	0.000530	0.000002	0.282182	0.000017	-0.31	1.35	1490	1653	-0.98
108	953	13	0.000921	0.000004	0.282050	0.000016	-5.04	1.31	1688	1898	-0.97
109	1183	16	0.001552	0.000012	0.282152	0.000024	3.06	1.53	1573	1677	-0.95
110	967	14	0.000960	0.000036	0.282170	0.000018	-0.51	1.36	1523	1681	-0.97
111	511	8	0.000314	0.000004	0.282136	0.000020	-11.34	1.29	1544	1861	-0.99
~~*112*~~	~~*505*~~	~~*7*~~	~~*0.002182*~~	~~*0.000009*~~	~~*0.282266*~~	~~*0.000016*~~	~~*-7.50*~~	~~*1.21*~~	~~*1435*~~	~~*1662*~~	~~*-0.93*~~
113	989	14	0.002578	0.000003	0.282422	0.000018	7.82	1.38	1224	1278	-0.92
114	916	14	0.000684	0.000011	0.282101	0.000021	-3.90	1.41	1607	1811	-0.98
115	914	13	0.000329	0.000001	0.282243	0.000018	1.30	1.34	1399	1547	-0.99
116	1151	17	0.000465	0.000001	0.281863	0.000019	-7.02	1.45	1923	2157	-0.99
117	2463	15	0.000871	0.000012	0.281151	0.000018	-3.54	1.44	2915	3045	-0.97
118	932	13	0.000834	0.000006	0.282186	0.000017	-0.62	1.33	1496	1659	-0.97
119	957	14	0.000861	0.000007	0.282055	0.000015	-4.74	1.32	1678	1886	-0.97
120	983	15	0.000404	0.000005	0.282405	0.000019	8.50	1.41	1179	1238	-0.99
Sample 10GD41, Lower Ordovician, Yulin											
1	916	12	0.000741	0.000036	0.282051	0.000028	-5.73	1.52	1679	1903	-0.98
2	995	13	0.000888	0.000008	0.281996	0.000026	-6.02	1.51	1761	1981	-0.97
3	522	8	0.000212	0.000001	0.282110	0.000030	-12.01	1.52	1576	1904	-0.99
4	1594	16	0.001027	0.000009	0.281742	0.000029	-2.07	1.64	2119	2268	-0.97

5	1069	20	0.000604	0.000004	0.281908	0.000020	-7.33	1.54	1869	2106	-0.98
6	1634	15	0.000529	0.000003	0.281534	0.000026	-8.00	1.55	2373	2595	-0.98
7	2348	15	0.000304	0.000001	0.280998	0.000020	-10.65	1.46	3076	3300	-0.99
8	882	12	0.000677	0.000009	0.281776	0.000026	-16.17	1.49	2054	2399	-0.98
9	2330	15	0.000540	0.000001	0.281136	0.000029	-6.54	1.64	2910	3084	-0.98
10	566	9	0.000611	0.000003	0.282229	0.000030	-6.95	1.52	1427	1683	-0.98
11	509	7	0.000347	0.000003	0.282155	0.000027	-10.72	1.45	1519	1828	-0.99
12	512	7	0.000345	0.000003	0.282122	0.000030	-11.85	1.51	1565	1888	-0.99
13	2301	15	0.000782	0.000008	0.281189	0.000028	-5.69	1.62	2857	3019	-0.98
14	584	8	0.000344	0.000002	0.282266	0.000028	-5.17	1.47	1368	1608	-0.99
15	2397	15	0.000370	0.000002	0.281096	0.000026	-6.15	1.58	2950	3119	-0.99
16	739	11	0.000356	0.000001	0.282024	0.000023	-10.34	1.40	1699	1993	-0.99
17	978	14	0.001070	0.000001	0.282320	0.000031	4.98	1.64	1317	1413	-0.97
18	877	12	0.000470	0.000002	0.282226	0.000028	-0.22	1.54	1428	1594	-0.99
~~*19*~~	~~*640*~~	~~*14*~~	~~*0.000181*~~	~~*0.000003*~~	~~*0.282047*~~	~~*0.000032*~~	~~*-11.63*~~	~~*1.65*~~	~~*1660*~~	~~*1979*~~	~~*-0.99*~~
20	508	7	0.000351	0.000002	0.282141	0.000029	-11.24	1.48	1538	1854	-0.99
21	588	8	0.000240	0.000001	0.282477	0.000027	2.42	1.45	1075	1226	-0.99
22	2416	15	0.000794	0.000013	0.281241	0.000029	-1.26	1.64	2787	2895	-0.98
23	774	13	0.000443	0.000004	0.282080	0.000029	-7.62	1.57	1626	1884	-0.99
24	542	8	0.000376	0.000005	0.281659	0.000026	-27.57	1.41	2195	2700	-0.99
25	528	7	0.001232	0.000027	0.281963	0.000029	-17.45	1.49	1824	2182	-0.96
26	917	13	0.000009	0.000000	0.281754	0.000021	-15.77	1.41	2048	2407	-1.00
27	1029	14	0.000812	0.000015	0.281966	0.000023	-6.31	1.46	1799	2023	-0.98
28	771	11	0.000539	0.000002	0.282110	0.000027	-6.66	1.48	1588	1834	-0.98
29	503	7	0.000308	0.000003	0.282148	0.000028	-11.09	1.45	1527	1842	-0.99
30	1152	15	0.000510	0.000001	0.281635	0.000025	-15.11	1.53	2236	2561	-0.98
31	614	9	0.000538	0.000006	0.282429	0.000019	1.18	1.30	1149	1310	-0.98
32	942	13	0.002190	0.000009	0.282215	0.000026	-0.25	1.49	1510	1648	-0.93
33	3035	14	0.000634	0.000003	0.280815	0.000019	-2.09	1.46	3347	3440	-0.98
34	2369	15	0.001433	0.000011	0.281232	0.000026	-3.68	1.58	2847	2976	-0.96
35	535	10	0.000355	0.000002	0.282084	0.000026	-12.70	1.45	1617	1949	-0.99
36	1783	16	0.001515	0.000017	0.281435	0.000027	-9.38	1.59	2573	2783	-0.95

37	1020	16	0.000845	0.000010	0.282277	0.000021	4.49	1.47	1371	1472	-0.97
38	928	13	0.000872	0.000002	0.282165	0.000023	-1.48	1.43	1526	1699	-0.97
39	960	14	0.000066	0.000002	0.281715	0.000025	-16.22	1.50	2103	2464	-1.00
40	758	11	0.000664	0.000002	0.282300	0.000025	-0.29	1.45	1332	1501	-0.98
41	559	46	0.000309	0.000004	0.282281	0.000028	-5.18	2.49	1346	1588	-0.99
42	2382	15	0.000314	0.000001	0.281218	0.000023	-2.08	1.53	2784	2908	-0.99
43	650	9	0.000582	0.000031	0.282425	0.000029	1.81	1.51	1156	1307	-0.98
44	754	11	0.000261	0.000003	0.282113	0.000023	-6.81	1.40	1574	1827	-0.99
45	844	12	0.001158	0.000002	0.282333	0.000023	2.48	1.43	1303	1430	-0.97
46	494	8	0.000352	0.000002	0.282193	0.000027	-9.72	1.44	1468	1766	-0.99
47	558	8	0.000339	0.000001	0.282543	0.000028	4.07	1.47	986	1117	-0.99
48	556	8	0.001165	0.000002	0.282197	0.000027	-8.53	1.45	1494	1755	-0.96
49	636	9	0.000042	0.000001	0.282078	0.000029	-10.55	1.50	1612	1921	-1.00
50	906	14	0.000766	0.000005	0.282196	0.000030	-0.80	1.61	1479	1647	-0.98
51	953	13	0.000641	0.000002	0.282037	0.000030	-5.34	1.59	1694	1913	-0.98
52	799	13	0.000597	0.000005	0.282317	0.000026	1.25	1.50	1305	1456	-0.98
53	742	11	0.000412	0.000008	0.282007	0.000024	-10.90	1.43	1725	2023	-0.99
54	907	38	0.001722	0.000018	0.282244	0.000023	0.34	2.16	1449	1590	-0.95
55	2261	16	0.000026	0.000000	0.281055	0.000025	-10.19	1.58	2979	3207	-1.00
56	1184	15	0.000867	0.000004	0.281564	0.000027	-17.22	1.57	2354	2692	-0.97
57	916	13	0.000808	0.000004	0.282025	0.000026	-6.69	1.49	1718	1951	-0.98
58	920	13	0.000139	0.000005	0.282111	0.000020	-3.12	1.38	1571	1775	-1.00
59	2376	15	0.000348	0.000000	0.281192	0.000026	-3.19	1.59	2821	2957	-0.99
60	773	11	0.000038	0.000000	0.282022	0.000023	-9.50	1.39	1688	1978	-1.00
61	518	8	0.000538	0.000004	0.282073	0.000028	-13.50	1.47	1639	1975	-0.98
62	981	14	0.000706	0.000006	0.282262	0.000028	3.23	1.56	1385	1504	-0.98
63	2307	15	0.000517	0.000002	0.281015	0.000020	-11.31	1.47	3070	3299	-0.98
64	644	9	0.000467	0.000002	0.282478	0.000024	3.59	1.39	1080	1211	-0.99
65	2333	15	0.000401	0.000001	0.281063	0.000023	-8.83	1.51	2997	3199	-0.99
66	937	13	0.000153	0.000001	0.282053	0.000023	-4.81	1.43	1650	1874	-1.00
67	1020	14	0.001238	0.000008	0.282266	0.000027	3.86	1.54	1399	1504	-0.96
68	913	13	0.000587	0.000006	0.282347	0.000024	4.81	1.46	1264	1368	-0.98

69	841	16	0.000685	0.000007	0.282453	0.000026	6.93	1.55	1120	1202	-0.98
70	955	14	0.000038	0.000001	0.281963	0.000019	-7.54	1.38	1768	2025	-1.00
71	2401	16	0.001709	0.000085	0.281305	0.000021	-0.84	1.51	2767	2862	-0.95
72	888	12	0.000296	0.000003	0.281796	0.000018	-15.08	1.33	2006	2350	-0.99
73	575	9	0.000558	0.000002	0.282416	0.000020	-0.13	1.31	1168	1345	-0.98
74	2359	16	0.000846	0.000021	0.280708	0.000022	-21.58	1.52	3508	3840	-0.97
75	515	8	0.000539	0.000012	0.282175	0.000022	-9.95	1.33	1499	1794	-0.98
76	908	13	0.000777	0.000009	0.281973	0.000018	-8.68	1.35	1788	2045	-0.98
77	518	8	0.000010	0.000000	0.281461	0.000020	-35.00	1.29	2440	3051	-1.00
78	972	14	0.000500	0.000002	0.282076	0.000024	-3.43	1.48	1633	1833	-0.98
79	723	10	0.001297	0.000018	0.281950	0.000024	-13.74	1.41	1844	2151	-0.96
80	2343	15	0.000201	0.000001	0.281199	0.000020	-3.45	1.47	2801	2943	-0.99
81	959	14	0.000991	0.000011	0.282102	0.000019	-3.12	1.38	1619	1806	-0.97
82	885	13	0.000657	0.000004	0.282428	0.000024	7.03	1.45	1154	1233	-0.98
83	893	13	0.000153	0.000002	0.281923	0.000020	-10.40	1.38	1827	2119	-1.00
84	834	12	0.002353	0.000069	0.282320	0.000029	1.14	1.55	1364	1490	-0.93
85	779	12	0.001024	0.000009	0.281763	0.000027	-19.04	1.51	2089	2460	-0.97
86	822	12	0.000956	0.000002	0.281664	0.000026	-21.58	1.47	2222	2621	-0.97
87	529	8	0.000781	0.000002	0.282578	0.000028	4.52	1.48	949	1071	-0.98
88	731	11	0.000780	0.000002	0.282588	0.000028	9.26	1.51	935	994	-0.98
89	933	13	0.000663	0.000005	0.282367	0.000029	5.92	1.58	1238	1329	-0.98
90	775	11	0.000222	0.000001	0.281858	0.000026	-15.36	1.47	1919	2274	-0.99
91	1070	15	0.000867	0.000027	0.281932	0.000027	-6.63	1.56	1848	2072	-0.97
92	635	10	0.000446	0.000005	0.282594	0.000027	7.52	1.47	918	1004	-0.99
93	532	8	0.000274	0.000024	0.282277	0.000028	-5.88	1.48	1350	1602	-0.99
94	580	9	0.000796	0.000006	0.282423	0.000025	0.15	1.42	1164	1335	-0.98
95	784	11	0.001166	0.000008	0.281901	0.000024	-14.11	1.43	1906	2218	-0.96
96	901	14	0.001025	0.000020	0.282411	0.000032	6.56	1.65	1189	1270	-0.97
97	933	13	0.000294	0.000003	0.281889	0.000027	-10.81	1.51	1880	2172	-0.99
98	958	15	0.001064	0.000010	0.282375	0.000028	6.49	1.58	1241	1320	-0.97
99	2418	16	0.000196	0.000001	0.280921	0.000026	-11.64	1.61	3170	3404	-0.99
100	602	9	0.000495	0.000006	0.282418	0.000026	0.55	1.44	1163	1332	-0.99

101	583	9	0.000707	0.000003	0.282374	0.000033	-1.49	1.60	1230	1420	-0.98
102	1050	15	0.000427	0.000001	0.282186	0.000029	2.23	1.61	1480	1611	-0.99
103	603	9	0.000193	0.000001	0.282572	0.000026	6.16	1.44	942	1047	-0.99
104	1000	14	0.001017	0.000049	0.281913	0.000036	-8.97	1.77	1883	2133	-0.97
105	538	8	0.001389	0.000003	0.282480	0.000022	1.03	1.33	1103	1256	-0.96
106	1771	17	0.000734	0.000005	0.281289	0.000028	-13.89	1.64	2718	2995	-0.98
107	963	15	0.000908	0.000011	0.281963	0.000038	-7.92	1.81	1808	2051	-0.97
108	953	14	0.000549	0.000011	0.282268	0.000022	2.92	1.44	1371	1497	-0.98
109	998	14	0.000485	0.000004	0.282049	0.000022	-3.83	1.43	1671	1874	-0.99
110	500	8	0.000365	0.000002	0.282115	0.000023	-12.37	1.36	1575	1904	-0.99
111	2387	15	0.000215	0.000001	0.281225	0.000026	-1.55	1.58	2767	2886	-0.99
112	1082	15	0.000690	0.000013	0.282003	0.000024	-3.76	1.51	1743	1938	-0.98
113	777	11	0.000416	0.000005	0.282126	0.000024	-5.93	1.42	1563	1801	-0.99
114	528	8	0.000371	0.000003	0.282165	0.000019	-9.96	1.28	1506	1805	-0.99
115	733	11	0.000947	0.000005	0.281882	0.000021	-15.77	1.36	1921	2261	-0.97
116	1836	17	0.000918	0.000020	0.281391	0.000023	-9.06	1.55	2592	2809	-0.97
117	995	15	0.000848	0.000001	0.282341	0.000025	6.23	1.53	1281	1364	-0.97
118	904	14	0.000160	0.000001	0.281951	0.000016	-9.16	1.33	1789	2066	-1.00
119	2426	15	0.000366	0.000001	0.281204	0.000022	-1.66	1.50	2807	2923	-0.99
120	1764	16	0.000313	0.000004	0.281505	0.000018	-5.90	1.43	2400	2595	-0.99
Sample 10GD38-1, Lower Ordovician, Yulin											
1	690	10	0.001068	0.000020	0.282587	0.000020	8.21	1.33	943	1014	-0.97
2	2093	15	0.001268	0.000016	0.281447	0.000021	-1.85	1.47	2539	2662	-0.96
3	1411	15	0.002520	0.000004	0.281747	0.000016	-7.33	1.37	2199	2381	-0.92
4	1037	17	0.001139	0.000007	0.281976	0.000018	-6.01	1.44	1801	2014	-0.97
5	1074	16	0.000032	0.000001	0.281941	0.000014	-5.65	1.35	1797	2026	-1.00
6	1104	16	0.000997	0.000028	0.282047	0.000021	-1.91	1.47	1695	1863	-0.97
~~*7*~~	~~*2236*~~	~~*39*~~	~~*0.000433*~~	~~*0.000004*~~	~~*0.281139*~~	~~*0.000019*~~	~~*-8.40*~~	~~*2.19*~~	~~*2898*~~	~~*3099*~~	~~*-0.99*~~
8	858	12	0.000858	0.000008	0.281978	0.000017	-9.62	1.31	1784	2052	-0.97
9	603	9	0.000464	0.000002	0.282463	0.000017	2.18	1.25	1100	1250	-0.99
10	3455	14	0.000788	0.000007	0.280519	0.000020	-3.33	1.49	3754	3842	-0.98

11	1082	17	0.000737	0.000021	0.282130	0.000017	0.73	1.42	1569	1712	-0.98
12	2489	15	0.001109	0.000004	0.281265	0.000024	0.68	1.54	2778	2859	-0.97
13	930	13	0.001164	0.000004	0.282375	0.000018	5.82	1.35	1244	1331	-0.96
14	809	12	0.002776	0.000030	0.282369	0.000017	2.13	1.31	1308	1420	-0.92
15	2031	47	0.000443	0.000001	0.281318	0.000018	-6.69	2.48	2660	2850	-0.99
16	2421	15	0.000933	0.000009	0.281153	0.000021	-4.52	1.48	2917	3059	-0.97
17	2462	43	0.000590	0.000005	0.281304	0.000018	2.33	2.35	2689	2756	-0.98
18	707	10	0.001792	0.000017	0.282294	0.000018	-2.15	1.29	1381	1554	-0.95
19	941	13	0.000773	0.000009	0.282208	0.000016	0.39	1.32	1463	1615	-0.98
20	927	13	0.000297	0.000002	0.282120	0.000017	-2.76	1.33	1566	1763	-0.99
21	498	8	0.000584	0.000018	0.282136	0.000018	-11.73	1.26	1555	1870	-0.98
22	1092	16	0.000381	0.000003	0.281930	0.000017	-5.90	1.40	1829	2054	-0.99
23	625	9	0.001148	0.000004	0.282411	0.000019	0.53	1.30	1193	1352	-0.97
24	716	10	0.001441	0.000042	0.282184	0.000020	-5.70	1.33	1523	1740	-0.96
25	1018	18	0.001110	0.000001	0.282188	0.000019	1.11	1.48	1505	1641	-0.97
26	2346	15	0.000357	0.000007	0.281095	0.000018	-7.35	1.44	2952	3137	-0.99
27	601	13	0.000762	0.000004	0.281770	0.000017	-22.51	1.33	2066	2493	-0.98
28	783	11	0.000698	0.000007	0.281966	0.000021	-11.59	1.35	1793	2091	-0.98
29	563	8	0.001988	0.000036	0.282607	0.000019	5.83	1.29	938	1032	-0.94
30	560	8	0.000871	0.000007	0.282174	0.000019	-9.15	1.28	1515	1790	-0.97
31	491	7	0.000451	0.000001	0.282159	0.000017	-11.04	1.24	1519	1830	-0.99
32	1014	14	0.000859	0.000006	0.282108	0.000019	-1.64	1.39	1606	1776	-0.97
33	961	14	0.000776	0.000012	0.282071	0.000017	-4.02	1.36	1652	1854	-0.98
34	499	7	0.000310	0.000001	0.281216	0.000022	-44.17	1.33	2786	3489	-0.99
35	542	8	0.000301	0.000001	0.282135	0.000021	-10.69	1.31	1544	1853	-0.99
36	1068	17	0.001510	0.000019	0.282006	0.000020	-4.53	1.48	1776	1965	-0.95
37	2832	14	0.001190	0.000008	0.281087	0.000022	1.88	1.51	3027	3081	-0.96
38	618	9	0.000535	0.000001	0.281851	0.000019	-19.19	1.29	1943	2341	-0.98
39	2277	16	0.001038	0.000006	0.281347	0.000016	-0.99	1.43	2660	2769	-0.97
40	2390	15	0.000609	0.000006	0.281019	0.000019	-9.47	1.44	3073	3276	-0.98
41	784	11	0.000052	0.000002	0.281868	0.000019	-14.72	1.32	1897	2249	-1.00
42	611	10	0.000567	0.000009	0.282465	0.000026	2.40	1.44	1099	1245	-0.98

43	707	10	0.001064	0.000006	0.282138	0.000015	-7.33	1.24	1572	1816	-0.97
44	802	11	0.001418	0.000005	0.281769	0.000021	-18.54	1.35	2103	2454	-0.96
45	988	14	0.000618	0.000002	0.282046	0.000018	-4.23	1.37	1680	1886	-0.98
46	2308	16	0.000122	0.000008	0.281066	0.000016	-8.88	1.43	2972	3181	-1.00
47	1388	17	0.000768	0.000001	0.281749	0.000020	-6.09	1.47	2095	2302	-0.98
48	608	9	0.000794	0.000010	0.282216	0.000022	-6.60	1.34	1453	1699	-0.98
49	537	8	0.000269	0.000001	0.282131	0.000019	-10.95	1.27	1549	1862	-0.99
50	2629	43	0.000990	0.000014	0.281039	0.000019	-3.99	2.37	3075	3202	-0.97
51	877	13	0.000164	0.000012	0.281860	0.000017	-12.99	1.32	1913	2236	-1.00
52	500	7	0.000624	0.000008	0.282166	0.000015	-10.65	1.20	1516	1817	-0.98
53	962	14	0.000900	0.000048	0.282141	0.000019	-1.63	1.39	1562	1734	-0.97
54	1035	16	0.000436	0.000003	0.281948	0.000018	-6.55	1.41	1806	2040	-0.99
55	930	13	0.001178	0.000009	0.282272	0.000020	2.14	1.39	1390	1518	-0.96
56	988	14	0.000147	0.000003	0.282043	0.000015	-4.04	1.32	1664	1876	-1.00
57	2372	15	0.000484	0.000002	0.280971	0.000018	-11.36	1.43	3126	3354	-0.99
58	968	14	0.000778	0.000003	0.282035	0.000017	-5.18	1.34	1703	1917	-0.98
59	937	15	0.000902	0.000007	0.281972	0.000018	-8.13	1.39	1794	2041	-0.97
60	1530	16	0.000790	0.000022	0.281514	0.000018	-11.31	1.43	2417	2675	-0.98
61	848	13	0.000551	0.000002	0.282249	0.000018	-0.07	1.34	1398	1563	-0.98
62	942	13	0.000860	0.000031	0.282081	0.000017	-4.15	1.33	1643	1845	-0.97
63	1813	16	0.000462	0.000016	0.281368	0.000015	-9.84	1.39	2594	2830	-0.99
64	1094	17	0.000769	0.000007	0.281852	0.000017	-8.89	1.42	1954	2205	-0.98
65	505	7	0.000626	0.000011	0.281971	0.000016	-17.44	1.22	1784	2163	-0.98
66	1136	17	0.000512	0.000005	0.282172	0.000019	3.56	1.45	1503	1613	-0.98
67	2431	14	0.000375	0.000002	0.281119	0.000020	-4.58	1.44	2921	3070	-0.99
68	1103	18	0.000407	0.000025	0.281948	0.000017	-5.01	1.44	1804	2018	-0.99
69	735	11	0.000293	0.000009	0.282023	0.000019	-10.42	1.32	1697	1994	-0.99
70	937	15	0.000944	0.000021	0.282485	0.000018	10.01	1.39	1083	1124	-0.97
71	2742	15	0.000858	0.000007	0.281046	0.000018	-0.97	1.44	3056	3147	-0.97
72	936	13	0.000684	0.000006	0.282041	0.000014	-5.60	1.29	1690	1913	-0.98
73	1258	16	0.001251	0.000040	0.281643	0.000017	-13.12	1.40	2269	2547	-0.96
74	998	14	0.001499	0.000012	0.282147	0.000018	-1.03	1.37	1578	1733	-0.95

75	888	13	0.000786	0.000022	0.282077	0.000016	-5.43	1.32	1645	1865	-0.98
76	2062	33	0.001240	0.000014	0.281118	0.000025	-14.20	2.05	2988	3244	-0.96
77	502	7	0.000573	0.000001	0.282111	0.000018	-12.54	1.24	1590	1914	-0.98
78	972	14	0.000426	0.000011	0.282391	0.000016	7.76	1.34	1199	1267	-0.99
79	853	12	0.000143	0.000003	0.282144	0.000015	-3.46	1.28	1527	1738	-1.00
80	511	8	0.000590	0.000005	0.282175	0.000018	-10.08	1.25	1502	1797	-0.98
81	926	13	0.000906	0.000007	0.282465	0.000019	9.08	1.37	1110	1163	-0.97
82	975	14	0.000227	0.000004	0.281885	0.000017	-9.96	1.34	1882	2163	-0.99
83	945	13	0.000982	0.000039	0.282033	0.000017	-5.87	1.33	1714	1933	-0.97
84	2389	15	0.000468	0.000005	0.281079	0.000027	-7.11	1.60	2981	3160	-0.99
85	1429	17	0.000330	0.000012	0.281798	0.000019	-3.01	1.47	2004	2181	-0.99
86	531	8	0.000363	0.000002	0.282121	0.000018	-11.46	1.26	1566	1883	-0.99
87	1128	18	0.001074	0.000014	0.281953	0.000019	-4.80	1.48	1830	2027	-0.97
88	537	8	0.000466	0.000003	0.282047	0.000022	-14.00	1.34	1673	2016	-0.99
90	2417	15	0.000592	0.000004	0.281046	0.000020	-7.86	1.47	3035	3219	-0.98
91	1054	18	0.000838	0.000013	0.282052	0.000017	-2.74	1.44	1682	1864	-0.97
92	1147	16	0.000604	0.000003	0.282074	0.000019	0.26	1.43	1641	1788	-0.98
93	759	11	0.002719	0.000046	0.282400	0.000019	2.23	1.32	1261	1374	-0.92
94	1067	17	0.000713	0.000003	0.281999	0.000020	-4.25	1.47	1750	1950	-0.98
95	1860	16	0.000549	0.000002	0.281557	0.000021	-2.18	1.50	2344	2489	-0.98
96	869	13	0.000643	0.000030	0.281928	0.000019	-11.03	1.36	1843	2131	-0.98
~~*97*~~	~~*339*~~	~~*5*~~	~~*0.001719*~~	~~*0.000040*~~	~~*0.282080*~~	~~*0.000017*~~	~~*17.42*~~	~~*1.21*~~	~~*1682*~~	~~*2030*~~	~~*0.95*~~
98	1080	17	0.000145	0.000011	0.281610	0.000019	-17.34	1.45	2249	2615	-1.00
99	1106	17	0.000856	0.000007	0.281930	0.000018	-5.94	1.44	1851	2067	-0.97
100	906	13	0.000326	0.000009	0.281794	0.000020	-14.77	1.38	2010	2348	-0.99
101	2428	15	0.000383	0.000003	0.281096	0.000019	-5.48	1.45	2952	3112	-0.99
102	949	13	0.000776	0.000007	0.282032	0.000018	-5.69	1.34	1707	1928	-0.98
103	903	13	0.000048	0.000001	0.282094	0.000017	-4.06	1.33	1591	1809	-1.00
104	856	13	0.000510	0.000021	0.281882	0.000019	-12.88	1.37	1900	2214	-0.98
105	885	13	0.000516	0.000006	0.282080	0.000018	-5.22	1.35	1629	1852	-0.98
106	1076	16	0.000923	0.000003	0.282138	0.000019	0.73	1.43	1566	1707	-0.97
107	504	8	0.000393	0.000001	0.282142	0.000019	-11.32	1.28	1539	1855	-0.99

~~*108*~~	~~*629*~~	~~*9*~~	~~*0.001320*~~	~~*0.000006*~~	~~*0.282296*~~	~~*0.000017*~~	~~*-3.54*~~	~~*1.25*~~	~~*1361*~~	~~*1561*~~	~~*-0.96*~~
109	947	13	0.000057	0.000001	0.281635	0.000018	-19.33	1.35	2209	2608	-1.00
110	1188	17	0.001168	0.000016	0.281840	0.000021	-7.56	1.50	1990	2214	-0.96
111	754	10	0.000705	0.000009	0.281883	0.000017	-15.17	1.27	1908	2247	-0.98
112	991	14	0.000485	0.000010	0.281885	0.000019	-9.80	1.39	1895	2168	-0.99
113	1493	41	0.001570	0.000014	0.281633	0.000016	-8.68	2.21	2301	2515	-0.95
114	1070	16	0.000463	0.000002	0.281693	0.000020	-14.84	1.45	2155	2482	-0.99
115	902	13	0.000658	0.000006	0.281394	0.000020	-29.24	1.38	2571	3065	-0.98
116	964	14	0.000888	0.000008	0.281933	0.000017	-8.92	1.36	1848	2102	-0.97
117	2500	14	0.000744	0.000018	0.281274	0.000019	1.89	1.43	2739	2809	-0.98
118	929	13	0.000598	0.000040	0.282093	0.000019	-3.83	1.36	1614	1818	-0.98
119	885	13	0.000504	0.000012	0.281951	0.000013	-9.79	1.27	1805	2082	-0.98
120	737	12	0.000850	0.000008	0.281843	0.000020	-17.03	1.37	1970	2327	-0.97
Sample 10GD54, Middle Ordovician, Yulin											
1	803	26	0.000296	0.000004	0.281735	0.000017	-19.13	1.33	2088	2484	-0.99
2	2558	42	0.000189	0.000014	0.281323	0.000024	5.89	1.69	2636	2660	-0.99
3	1589	88	0.000375	0.000005	0.281795	0.000017	0.40	2.34	2011	2140	-0.99
4	1731	48	0.001094	0.000018	0.282056	0.000035	12.03	1.96	1687	1674	-0.97
5	2490	44	0.000510	0.000013	0.281563	0.000022	12.33	1.67	2333	2286	-0.98
6	1197	52	0.000375	0.000005	0.281795	0.000017	-8.34	1.68	2011	2260	-0.99
7	1712	48	0.000815	0.000013	0.282095	0.000022	13.30	1.71	1621	1595	-0.98
8	1085	54	0.000815	0.000013	0.282095	0.000022	-0.51	1.78	1621	1777	-0.98
9	1115	58	0.000815	0.000013	0.282095	0.000022	0.14	1.84	1621	1768	-0.98
10	761	24	0.001075	0.000057	0.282186	0.000027	-4.49	1.51	1506	1716	-0.97
11	701	20	0.003544	0.000153	0.282576	0.000034	6.91	1.64	1025	1089	-0.89
12	1682	62	0.001157	0.000011	0.282013	0.000024	9.34	1.95	1750	1769	-0.97
13	1284	52	0.000819	0.000014	0.281810	0.000022	-6.24	1.74	2013	2225	-0.98
14	1028	60	0.001066	0.000036	0.282163	0.000026	0.50	1.93	1537	1680	-0.97
15	1303	52	0.001417	0.000060	0.282005	0.000024	0.57	1.79	1773	1900	-0.96
16	2456	48	0.001980	0.000493	0.281380	0.000028	2.59	2.02	2682	2739	-0.94
17	1025	56	0.001025	0.000020	0.281826	0.000017	-11.48	1.74	2002	2279	-0.97

18	1042	64	0.001231	0.000008	0.281838	0.000111	-10.86	4.32	1998	2261	-0.96
19	1492	60	0.001162	0.000017	0.282033	0.000028	5.88	1.98	1723	1787	-0.96
20	1580	74	0.000283	0.000000	0.282011	0.000021	7.98	2.12	1713	1754	-0.99
21	945	26	0.001457	0.000027	0.281945	0.000018	-9.29	1.35	1860	2105	-0.96
22	2859	46	0.000970	0.000020	0.281198	0.000029	6.89	1.85	2858	2858	-0.97
23	1670	52	0.000700	0.000056	0.281569	0.000017	-6.16	1.70	2336	2533	-0.98
24	1097	66	0.000530	0.000051	0.282055	0.000014	-1.46	1.88	1664	1834	-0.98
25	938	28	0.000103	0.000006	0.281577	0.000024	-21.64	1.47	2291	2716	-1.00
26	2542	48	0.000679	0.000016	0.281221	0.000016	1.04	1.65	2807	2885	-0.98
27	2618	48	0.000669	0.000024	0.280672	0.000044	-16.74	2.21	3540	3813	-0.98
28	1097	74	0.002140	0.000020	0.282482	0.000019	12.51	2.08	1122	1129	-0.94
29	608	18	0.000385	0.000006	0.281991	0.000032	-14.39	1.59	1745	2092	-0.99
30	1278	64	0.000393	0.000052	0.281921	0.000028	-2.07	2.03	1840	2012	-0.99
31	613	18	0.000977	0.000016	0.282314	0.000019	-3.08	1.29	1323	1525	-0.97
32	1182	62	0.001544	0.000028	0.281954	0.000032	-3.97	2.07	1852	2029	-0.95
33	756	24	0.001299	0.000038	0.281649	0.000027	-23.73	1.50	2263	2676	-0.96
35	953	30	0.000602	0.000018	0.282412	0.000019	7.99	1.40	1174	1240	-0.98
35	886	26	0.000652	0.000048	0.282073	0.000015	-5.55	1.29	1645	1870	-0.98
35	1239	62	0.000424	0.000021	0.281675	0.000017	-11.72	1.85	2177	2462	-0.99
35	1001	70	0.000456	0.000031	0.282375	0.000017	7.84	1.98	1221	1287	-0.99
35	1173	64	0.000134	0.000007	0.281904	0.000016	-4.82	1.86	1852	2065	-1.00
35	1374	66	0.001059	0.000006	0.281855	0.000016	-2.92	1.91	1965	2132	-0.97
35	1266	68	0.000359	0.000013	0.282001	0.000028	0.50	2.11	1731	1873	-0.99
35	1206	68	0.001074	0.000014	0.282120	0.000019	2.80	1.97	1598	1708	-0.97
35	1053	70	0.000925	0.000004	0.282113	0.000016	-0.64	1.96	1601	1757	-0.97
35	1097	92	0.001094	0.000023	0.281818	0.000024	-10.25	2.46	2017	2275	-0.97
35	1062	70	0.001335	0.000046	0.282114	0.000021	-0.71	2.02	1617	1768	-0.96
35	2083	60	0.000261	0.000011	0.281487	0.000023	0.76	1.92	2420	2525	-0.99
48	1195	70	0.001114	0.000016	0.282067	0.000038	0.66	2.32	1673	1807	-0.97
49	1015	72	0.000911	0.000005	0.282074	0.000018	-2.84	2.02	1654	1837	-0.97
51	1189	72	0.001041	0.000058	0.281960	0.000032	-3.19	2.24	1818	1996	-0.97
52	1108	72	0.000715	0.000044	0.281906	0.000027	-6.63	2.14	1877	2103	-0.98

53	946	28	0.001310	0.000014	0.282315	0.000019	3.96	1.38	1333	1439	-0.96
54	1867	66	0.001682	0.000017	0.281620	0.000021	-1.20	1.99	2326	2446	-0.95
56	1551	74	0.001060	0.000099	0.281619	0.000032	-7.40	2.29	2290	2498	-0.97
57	626	20	0.000933	0.000011	0.281744	0.000025	-22.97	1.43	2111	2536	-0.97
58	960	30	0.004956	0.000957	0.282341	0.000071	2.83	2.87	1436	1507	-0.85
59	2824	62	0.001008	0.000073	0.281265	0.000029	8.40	2.09	2770	2755	-0.97
60	1206	80	0.002431	0.000039	0.281979	0.000032	-3.27	2.37	1860	2014	-0.93
61	1181	78	0.004978	0.000522	0.282051	0.000044	-3.25	2.62	1888	1992	-0.85
62	2419	70	0.000521	0.000008	0.280980	0.000026	-10.05	2.16	3118	3328	-0.98
63	1264	78	0.000665	0.000029	0.281946	0.000031	-1.73	2.32	1819	1983	-0.98
64	1205	86	0.000734	0.000021	0.282043	0.000033	0.35	2.49	1689	1831	-0.98
65	2435	68	0.000539	0.000008	0.281856	0.000022	21.45	2.06	1936	1787	-0.98
66	917	32	0.001657	0.000047	0.282343	0.000019	4.11	1.44	1306	1407	-0.95
68	3524	64	0.000549	0.000061	0.280433	0.000037	-4.23	2.30	3845	3941	-0.98
69	1041	88	0.000659	0.000018	0.282131	0.000028	-0.08	2.43	1565	1720	-0.98
70	613	22	0.001043	0.000007	0.282435	0.000170	1.17	6.13	1156	1309	-0.97
Sample 10GD51, Upper Ordovician, Yulin											
1	997	13	0.000893	0.000015	0.282148	0.000019	-0.59	1.36	1551	1710	-0.97
2	1029	17	0.001653	0.000011	0.282399	0.000021	8.47	1.48	1226	1278	-0.95
3	566	8	0.000672	0.000007	0.282549	0.000019	4.35	1.28	986	1110	-0.98
4	886	12	0.000115	0.000001	0.282199	0.000027	-0.73	1.51	1450	1627	-1.00
5	1030	17	0.001342	0.000003	0.282317	0.000017	5.79	1.42	1332	1414	-0.96
6	715	10	0.000433	0.000004	0.282558	0.000016	8.00	1.26	968	1045	-0.99
7	515	8	0.000223	0.000000	0.282116	0.000020	-11.95	1.30	1568	1895	-0.99
8	541	8	0.000347	0.000002	0.281741	0.000020	-24.69	1.29	2083	2555	-0.99
9	831	11	0.000680	0.000004	0.281749	0.000018	-18.22	1.31	2090	2461	-0.98
10	1414	15	0.000439	0.000002	0.282157	0.000013	9.27	1.33	1521	1553	-0.99
11	568	8	0.000046	0.000000	0.281831	0.000014	-20.80	1.20	1946	2382	-1.00
12	796	11	0.000379	0.000003	0.282031	0.000016	-8.83	1.28	1690	1963	-0.99
13	654	9	0.001251	0.000007	0.282511	0.000018	4.64	1.27	1056	1166	-0.96
14	919	12	0.000152	0.000001	0.281868	0.000013	-11.76	1.25	1901	2208	-1.00

~~15~~	~~495~~	~~9~~	~~0.000386~~	~~0.000001~~	~~0.282164~~	~~0.000014~~	~~-10.73~~	~~1.20~~	~~1509~~	~~1818~~	~~-0.99~~
16	1463	15	0.000927	0.000002	0.281936	0.000015	2.05	1.36	1846	1955	-0.97
17	1158	17	0.000707	0.000006	0.281807	0.000020	-9.03	1.46	2012	2263	-0.98
18	509	7	0.000433	0.000004	0.281973	0.000016	-17.21	1.22	1772	2155	-0.99
19	536	8	0.000231	0.000002	0.282156	0.000016	-10.07	1.22	1514	1817	-0.99
20	2440	13	0.000511	0.000011	0.281227	0.000017	-0.78	1.38	2787	2891	-0.98
21	724	10	0.000359	0.000002	0.282153	0.000017	-6.10	1.27	1523	1767	-0.99
22	1487	16	0.000521	0.000001	0.281655	0.000018	-7.00	1.43	2210	2427	-0.98
23	3165	13	0.000749	0.000005	0.280810	0.000018	0.48	1.42	3363	3421	-0.98
24	1283	31	0.001216	0.000039	0.282005	0.000021	0.30	1.89	1764	1897	-0.96
25	641	9	0.000565	0.000002	0.282500	0.000023	4.26	1.37	1052	1175	-0.98
26	942	13	0.000407	0.000008	0.281835	0.000016	-12.59	1.31	1959	2268	-0.99
27	525	7	0.000407	0.000031	0.282074	0.000019	-13.26	1.26	1632	1969	-0.99
28	2465	14	0.000390	0.000001	0.281204	0.000017	-0.79	1.40	2808	2912	-0.99
29	2523	14	0.000378	0.000003	0.281038	0.000016	-5.38	1.38	3029	3184	-0.99
30	957	13	0.000729	0.000011	0.282370	0.000018	6.50	1.35	1237	1319	-0.98
31	958	13	0.000371	0.000004	0.282032	0.000014	-5.21	1.29	1688	1911	-0.99
32	1041	19	0.001732	0.000027	0.282099	0.000018	-1.98	1.48	1656	1815	-0.95
33	521	7	0.000395	0.000001	0.282470	0.000015	0.65	1.20	1089	1262	-0.99
34	524	7	0.000384	0.000004	0.282196	0.000019	-8.95	1.27	1464	1751	-0.99
35	895	12	0.000192	0.000007	0.282001	0.000015	-7.60	1.29	1722	1980	-0.99
36	971	13	0.000891	0.000004	0.282097	0.000016	-2.97	1.32	1621	1809	-0.97
37	2172	18	0.000207	0.000014	0.280606	0.000015	-28.46	1.45	3585	4025	-0.99
38	955	13	0.000682	0.000004	0.282140	0.000016	-1.68	1.32	1554	1731	-0.98
39	968	13	0.000844	0.000024	0.282096	0.000015	-3.06	1.30	1622	1811	-0.97
40	611	9	0.000449	0.000005	0.282168	0.000015	-8.10	1.23	1506	1778	-0.99
41	1107	18	0.000587	0.000001	0.282173	0.000016	2.90	1.43	1505	1623	-0.98
42	1137	22	0.001125	0.000040	0.282124	0.000016	1.42	1.54	1594	1722	-0.97
43	2710	14	0.001230	0.000009	0.280921	0.000018	-6.82	1.42	3255	3405	-0.96
44	1597	17	0.000730	0.000009	0.281736	0.000016	-1.89	1.42	2110	2261	-0.98
45	2470	15	0.000567	0.000003	0.280987	0.000018	-8.72	1.43	3112	3304	-0.98
46	971	13	0.001198	0.000023	0.282136	0.000020	-1.79	1.39	1580	1749	-0.96

47	2096	20	0.000353	0.000004	0.281169	0.000021	-10.38	1.60	2852	3084	-0.99
48	989	13	0.001564	0.000045	0.282155	0.000017	-0.96	1.33	1569	1722	-0.95
49	610	9	0.000447	0.000005	0.282436	0.000019	1.38	1.28	1137	1296	-0.99
50	760	11	0.000752	0.000001	0.282224	0.000019	-2.97	1.33	1439	1638	-0.98
51	1417	18	0.000373	0.000001	0.281660	0.000017	-8.25	1.45	2195	2432	-0.99
52	2651	15	0.000702	0.000005	0.280738	0.000016	-13.70	1.41	3455	3692	-0.98
53	2469	16	0.000355	0.000001	0.280883	0.000020	-12.07	1.50	3233	3467	-0.99
54	985	14	0.000577	0.000004	0.281977	0.000018	-6.70	1.37	1773	2008	-0.98
55	1059	19	0.000444	0.000008	0.281916	0.000015	-7.17	1.45	1851	2091	-0.99
56	544	8	0.000373	0.000003	0.282173	0.000020	-9.35	1.30	1496	1787	-0.99
57	2434	16	0.000302	0.000002	0.281305	0.000022	2.23	1.53	2667	2738	-0.99
58	819	11	0.000824	0.000002	0.281705	0.000017	-20.12	1.29	2158	2546	-0.98
59	1069	29	0.000456	0.000018	0.282227	0.000023	4.07	1.85	1425	1533	-0.99
60	922	13	0.000110	0.000009	0.282099	0.000019	-3.50	1.36	1587	1796	-1.00
61	541	8	0.000840	0.000005	0.282587	0.000021	5.08	1.31	937	1052	-0.97
62	2529	16	0.000972	0.000007	0.281025	0.000022	-6.72	1.53	3093	3254	-0.97
63	2380	18	0.000580	0.000006	0.280990	0.000020	-10.68	1.54	3109	3327	-0.98
64	978	13	0.001231	0.000008	0.282164	0.000014	-0.66	1.29	1542	1698	-0.96
65	1114	20	0.000581	0.000001	0.281978	0.000017	-3.83	1.50	1771	1967	-0.98
66	955	13	0.000443	0.000012	0.281952	0.000017	-8.18	1.33	1801	2058	-0.99
67	1096	20	0.000698	0.000001	0.282312	0.000017	7.53	1.50	1316	1380	-0.98
68	965	13	0.000109	0.000001	0.281733	0.000015	-15.51	1.30	2081	2432	-1.00
69	525	8	0.000348	0.000011	0.282151	0.000015	-10.53	1.22	1525	1831	-0.99
70	1075	63	0.001845	0.000025	0.282382	0.000020	8.70	3.10	1257	1304	-0.94
71	1213	25	0.000522	0.000002	0.282058	0.000019	1.24	1.68	1659	1793	-0.98
72	613	9	0.000349	0.000001	0.282463	0.000020	2.44	1.31	1097	1245	-0.99
73	541	8	0.000352	0.000009	0.282125	0.000015	-11.11	1.22	1561	1873	-0.99
74	983	14	0.000820	0.000013	0.282347	0.000018	6.20	1.37	1272	1355	-0.98
75	543	9	0.000328	0.000002	0.282096	0.000018	-12.09	1.28	1600	1925	-0.99
76	2529	18	0.001260	0.000028	0.281274	0.000020	1.66	1.54	2776	2844	-0.96
77	1144	16	0.000546	0.000003	0.281923	0.000016	-5.11	1.39	1846	2056	-0.98
78	539	8	0.000467	0.000002	0.282113	0.000017	-11.61	1.24	1582	1897	-0.99

79	988	14	0.000515	0.000059	0.282125	0.000015	-1.38	1.32	1568	1742	-0.98
80	1772	20	0.000588	0.000003	0.281541	0.000016	-4.77	1.51	2368	2546	-0.98
81	633	9	0.000249	0.000001	0.282549	0.000017	5.96	1.25	976	1082	-0.99
82	784	11	0.000615	0.000022	0.281934	0.000016	-12.65	1.28	1833	2145	-0.98
83	572	9	0.000577	0.000007	0.282288	0.000021	-4.73	1.32	1345	1576	-0.98
84	973	14	0.000708	0.000002	0.282157	0.000015	-0.70	1.33	1532	1696	-0.98
85	2579	19	0.000334	0.000012	0.281221	0.000019	2.50	1.55	2781	2843	-0.99
86	531	8	0.000363	0.000001	0.282184	0.000018	-9.24	1.25	1481	1771	-0.99
87	1071	46	0.001207	0.000012	0.282168	0.000023	1.49	2.45	1536	1665	-0.96
88	1864	21	0.000341	0.000002	0.281410	0.000017	-7.03	1.55	2528	2732	-0.99
89	1145	25	0.000983	0.000023	0.281725	0.000017	-12.46	1.65	2140	2424	-0.97
90	538	8	0.000445	0.000006	0.282129	0.000017	-11.06	1.24	1559	1868	-0.99
91	873	13	0.000208	0.000003	0.282214	0.000020	-0.57	1.39	1434	1608	-0.99
92	898	13	0.000123	0.000016	0.281866	0.000017	-12.29	1.33	1903	2218	-1.00
93	1021	24	0.001473	0.000017	0.282395	0.000016	8.28	1.60	1226	1281	-0.96
94	552	8	0.000690	0.000002	0.281171	0.000018	-44.75	1.26	2874	3558	-0.98
95	1388	52	0.000881	0.000008	0.282048	0.000020	4.41	2.67	1689	1776	-0.97
96	514	9	0.000305	0.000001	0.282140	0.000018	-11.15	1.27	1539	1854	-0.99
97	578	9	0.001057	0.000033	0.282138	0.000024	-10.11	1.38	1572	1852	-0.97
98	988	15	0.000617	0.000014	0.281791	0.000019	-13.26	1.41	2029	2338	-0.98
99	2482	21	0.000662	0.000002	0.281231	0.000022	0.09	1.66	2791	2883	-0.98
100	2584	21	0.000466	0.000001	0.280684	0.000023	-16.72	1.66	3506	3785	-0.99
Sample 10GD56, Lower Silurian, Yulin											
1	442	6	0.001218	0.000025	0.282305	0.000022	-7.16	1.31	1345	1594	-0.96
2	950	13	0.001233	0.000013	0.282493	0.000022	10.38	1.41	1080	1116	-0.96
3	432	6	0.001550	0.000025	0.282380	0.000017	-4.80	1.21	1250	1466	-0.95
4	435	6	0.000969	0.000008	0.282356	0.000018	-5.44	1.24	1265	1501	-0.97
5	436	6	0.001874	0.000017	0.282300	0.000018	-7.63	1.24	1375	1613	-0.94
6	982	14	0.000846	0.000011	0.282372	0.000020	7.02	1.40	1238	1313	-0.97
7	445	6	0.001446	0.000027	0.282279	0.000020	-8.08	1.27	1390	1643	-0.96
8	435	6	0.002295	0.000078	0.282273	0.000020	-8.75	1.27	1430	1669	-0.93

9	437	6	0.002187	0.000021	0.282372	0.000018	-5.17	1.23	1283	1489	-0.93
10	444	6	0.001748	0.000018	0.282354	0.000018	-5.54	1.24	1294	1514	-0.95
11	440	6	0.001697	0.000013	0.282328	0.000019	-6.52	1.26	1329	1560	-0.95
12	420	7	0.000970	0.000018	0.282285	0.000017	-8.25	1.24	1363	1632	-0.97
13	434	6	0.001241	0.000059	0.282303	0.000017	-7.39	1.22	1348	1599	-0.96
14	430	6	0.001366	0.000042	0.282321	0.000021	-6.87	1.29	1327	1570	-0.96
15	444	6	0.001373	0.000022	0.282340	0.000018	-5.92	1.23	1301	1533	-0.96
16	437	6	0.002342	0.000062	0.282349	0.000018	-6.04	1.25	1323	1533	-0.93
17	439	6	0.001706	0.000011	0.282375	0.000017	-4.89	1.22	1263	1477	-0.95
18	576	8	0.001106	0.000017	0.282337	0.000019	-3.11	1.29	1295	1497	-0.97
19	594	9	0.001248	0.000011	0.282422	0.000016	0.22	1.24	1181	1343	-0.96
20	1128	15	0.000633	0.000042	0.281889	0.000017	-6.73	1.38	1896	2124	-0.98
21	433	6	0.000968	0.000032	0.282330	0.000016	-6.39	1.20	1301	1548	-0.97
22	435	6	0.001478	0.000007	0.282382	0.000019	-4.65	1.25	1245	1461	-0.96
23	435	6	0.002142	0.000044	0.282317	0.000017	-7.13	1.22	1360	1587	-0.94
24	548	8	0.000876	0.000005	0.282521	0.000016	2.88	1.23	1031	1170	-0.97
25	436	6	0.001055	0.000034	0.282248	0.000016	-9.26	1.20	1419	1696	-0.97
26	434	6	0.002276	0.000006	0.282359	0.000015	-5.70	1.19	1304	1514	-0.93
27	434	6	0.001522	0.000034	0.282307	0.000016	-7.35	1.21	1353	1597	-0.95
28	444	6	0.001664	0.000012	0.282356	0.000015	-5.45	1.19	1288	1509	-0.95
29	443	6	0.001676	0.000021	0.282329	0.000015	-6.42	1.19	1327	1558	-0.95
30	438	6	0.002376	0.000048	0.282350	0.000017	-5.98	1.21	1322	1531	-0.93
31	443	6	0.001718	0.000037	0.282417	0.000015	-3.31	1.19	1203	1400	-0.95
32	431	6	0.001464	0.000038	0.282320	0.000017	-6.92	1.21	1332	1573	-0.96
33	447	6	0.001272	0.000009	0.282284	0.000015	-7.80	1.18	1376	1631	-0.96
34	502	8	0.001216	0.000018	0.282322	0.000017	-5.25	1.25	1320	1546	-0.96
35	552	8	0.001240	0.000013	0.282449	0.000016	0.28	1.23	1142	1305	-0.96
36	2538	11	0.000494	0.000003	0.281063	0.000016	-4.34	1.33	3004	3145	-0.99
37	860	12	0.001046	0.000009	0.282459	0.000016	7.36	1.30	1122	1196	-0.97
38	433	6	0.001334	0.000047	0.282294	0.000016	-7.78	1.20	1364	1618	-0.96
39	432	6	0.001227	0.000012	0.282391	0.000019	-4.33	1.27	1224	1443	-0.96
40	432	6	0.001597	0.000045	0.282306	0.000018	-7.44	1.23	1357	1600	-0.95

41	431	6	0.001460	0.000044	0.282312	0.000017	-7.20	1.23	1343	1587	-0.96
42	439	7	0.001944	0.000035	0.282308	0.000016	-7.33	1.22	1367	1601	-0.94
43	440	6	0.000976	0.000024	0.281640	0.000026	-30.66	1.40	2256	2773	-0.97
44	436	7	0.001081	0.000023	0.282294	0.000019	-7.62	1.26	1354	1613	-0.97
45	441	6	0.001185	0.000018	0.282319	0.000018	-6.67	1.23	1324	1569	-0.96
46	2234	16	0.001541	0.000004	0.281547	0.000017	4.38	1.43	2419	2469	-0.95
47	441	7	0.001663	0.000024	0.282310	0.000017	-7.13	1.24	1353	1592	-0.95
48	428	6	0.002108	0.000025	0.282372	0.000017	-5.32	1.22	1280	1490	-0.94
49	442	7	0.001106	0.000006	0.282336	0.000017	-6.01	1.23	1297	1536	-0.97
50	530	8	0.001967	0.000040	0.282542	0.000021	2.86	1.31	1031	1156	-0.94
51	863	11	0.001069	0.000016	0.281933	0.000017	-11.24	1.29	1857	2137	-0.97
52	633	10	0.001463	0.000032	0.281928	0.000027	-16.51	1.47	1883	2218	-0.96
53	432	6	0.001405	0.000025	0.282322	0.000017	-6.80	1.23	1327	1568	-0.96
54	432	6	0.001072	0.000025	0.282364	0.000017	-5.22	1.23	1256	1488	-0.97
55	434	6	0.002108	0.000013	0.282326	0.000020	-6.83	1.27	1347	1571	-0.94
56	439	6	0.001978	0.000082	0.282311	0.000018	-7.23	1.24	1364	1595	-0.94
57	435	6	0.001639	0.000026	0.282316	0.000018	-7.02	1.25	1344	1582	-0.95
58	536	10	0.001368	0.000067	0.282361	0.000021	-3.22	1.35	1271	1470	-0.96
59	949	12	0.000575	0.000005	0.282007	0.000018	-6.46	1.33	1732	1966	-0.98
60	446	6	0.001609	0.000008	0.282137	0.000018	-13.14	1.24	1597	1900	-0.95
61	435	6	0.002551	0.000040	0.282311	0.000018	-7.48	1.24	1385	1605	-0.92
62	949	13	0.000504	0.000004	0.282155	0.000018	-1.15	1.35	1526	1699	-0.98
63	444	6	0.002757	0.000054	0.282357	0.000020	-5.72	1.27	1325	1523	-0.92
64	429	6	0.002026	0.000014	0.282347	0.000018	-6.19	1.24	1314	1534	-0.94
65	438	7	0.001446	0.000038	0.282231	0.000020	-9.91	1.28	1457	1730	-0.96
66	1071	22	0.000944	0.000007	0.281780	0.000019	-12.07	1.58	2062	2345	-0.97
67	435	6	0.000945	0.000004	0.282376	0.000018	-4.70	1.23	1235	1464	-0.97
68	448	7	0.001808	0.000017	0.282284	0.000019	-7.95	1.27	1396	1639	-0.95
69	610	10	0.000313	0.000001	0.282441	0.000019	1.61	1.30	1126	1285	-0.99
70	430	7	0.001657	0.000020	0.282384	0.000017	-4.73	1.23	1247	1461	-0.95
71	436	7	0.002072	0.000044	0.282361	0.000018	-5.53	1.24	1295	1507	-0.94
72	446	7	0.001723	0.000047	0.282359	0.000019	-5.29	1.27	1285	1503	-0.95

73	432	7	0.001015	0.000020	0.282236	0.000016	-9.73	1.22	1433	1717	-0.97
74	667	10	0.000496	0.000035	0.282128	0.000015	-8.29	1.25	1562	1832	-0.99
75	442	6	0.002571	0.000049	0.282381	0.000018	-4.85	1.24	1283	1477	-0.92
76	434	7	0.001853	0.000006	0.282331	0.000016	-6.58	1.21	1330	1558	-0.94
77	437	7	0.001857	0.000021	0.282346	0.000019	-5.98	1.27	1308	1530	-0.94
78	2794	24	0.000880	0.000024	0.280990	0.000059	-1.82	2.62	3132	3230	-0.97
79	436	6	0.001167	0.000042	0.282127	0.000025	-13.55	1.38	1591	1912	-0.96
80	438	6	0.002305	0.000029	0.282323	0.000014	-6.90	1.18	1358	1578	-0.93
81	430	7	0.000816	0.000042	0.282167	0.000021	-12.16	1.31	1521	1838	-0.98
82	434	6	0.001902	0.000020	0.282363	0.000016	-5.48	1.20	1287	1503	-0.94
83	435	6	0.002269	0.000008	0.282288	0.000018	-8.21	1.25	1407	1641	-0.93
84	435	7	0.001893	0.000008	0.282377	0.000015	-4.96	1.20	1266	1477	-0.94
85	434	7	0.001334	0.000006	0.282344	0.000017	-5.97	1.23	1293	1528	-0.96
86	433	6	0.001558	0.000037	0.282344	0.000016	-6.05	1.20	1301	1531	-0.95
87	430	6	0.001424	0.000046	0.282457	0.000017	-2.08	1.21	1136	1327	-0.96
88	927	13	0.000141	0.000002	0.282111	0.000013	-2.98	1.27	1571	1773	-1.00
89	561	9	0.001156	0.000015	0.282299	0.000017	-4.81	1.26	1351	1571	-0.97
90	437	7	0.001886	0.000067	0.282272	0.000017	-8.61	1.23	1415	1663	-0.94
91	439	7	0.001581	0.000015	0.282301	0.000017	-7.45	1.23	1363	1607	-0.95
92	438	7	0.001402	0.000032	0.282316	0.000013	-6.90	1.17	1335	1578	-0.96
93	492	7	0.001256	0.000031	0.282467	0.000016	-0.35	1.22	1117	1289	-0.96
94	1698	31	0.000953	0.000036	0.281927	0.000019	6.88	1.89	1860	1906	-0.97
95	431	7	0.001882	0.000008	0.282374	0.000016	-5.12	1.21	1269	1482	-0.94
96	443	7	0.001609	0.000026	0.282308	0.000019	-7.14	1.27	1354	1594	-0.95
97	442	7	0.001823	0.000027	0.282304	0.000017	-7.36	1.23	1368	1605	-0.95
98	435	7	0.000923	0.000018	0.282302	0.000016	-7.31	1.21	1338	1596	-0.97
99	437	7	0.000945	0.000032	0.282345	0.000016	-5.77	1.22	1279	1520	-0.97
100	440	7	0.001274	0.000011	0.282248	0.000019	-9.23	1.28	1427	1698	-0.96
Sample 10GD58, Middle-Upper Silurian, Yulin											
1	1015	24	0.000664	0.000010	0.281875	0.000017	-9.72	1.61	1916	2183	-0.98
2	916	13	0.000540	0.000003	0.281399	0.000019	-28.67	1.36	2556	3048	-0.98

3	3010	38	0.001390	0.000024	0.280884	0.000019	-1.75	2.20	3319	3403	-0.96
4	755	10	0.000592	0.000008	0.282535	0.000017	7.99	1.27	1004	1078	-0.98
5	2444	17	0.000340	0.000006	0.281335	0.000022	3.45	1.55	2629	2686	-0.99
6	2576	17	0.000378	0.000001	0.281234	0.000018	2.80	1.48	2768	2826	-0.99
7	733	9	0.001235	0.000013	0.282258	0.000019	-2.59	1.30	1411	1597	-0.96
8	1026	20	0.000591	0.000004	0.281279	0.000021	-30.57	1.55	2722	3227	-0.98
9	1234	18	0.000397	0.000008	0.281797	0.000022	-7.46	1.52	2010	2246	-0.99
10	1062	29	0.000713	0.000011	0.281789	0.000018	-11.78	1.78	2037	2324	-0.98
11	872	11	0.000612	0.000009	0.282343	0.000019	3.74	1.32	1271	1389	-0.98
12	924	12	0.000961	0.000038	0.281933	0.000020	-9.84	1.36	1851	2116	-0.97
13	1004	18	0.002089	0.000041	0.282186	0.000020	0.11	1.50	1546	1680	-0.94
14	1060	61	0.000596	0.000003	0.281951	0.000018	-6.00	2.99	1809	2032	-0.98
15	1019	40	0.000714	0.000003	0.282421	0.000015	9.68	2.14	1165	1208	-0.98
16	2708	14	0.000509	0.000011	0.280767	0.000024	-11.02	1.54	3400	3608	-0.98
17	1061	22	0.001459	0.000020	0.282095	0.000019	-1.51	1.59	1650	1808	-0.96
18	756	10	0.001126	0.000003	0.281790	0.000020	-18.62	1.32	2057	2421	-0.97
19	983	13	0.000074	0.000001	0.281977	0.000017	-6.43	1.33	1750	1992	-1.00
20	835	11	0.000483	0.000003	0.281874	0.000016	-13.61	1.28	1910	2234	-0.99
21	2494	15	0.000596	0.000007	0.280571	0.000024	-23.02	1.55	3668	4017	-0.98
22	918	12	0.001077	0.000015	0.282481	0.000018	9.37	1.34	1092	1141	-0.97
23	2449	15	0.000533	0.000001	0.281105	0.000018	-4.94	1.44	2952	3102	-0.98
24	753	10	0.000753	0.000004	0.282072	0.000015	-8.51	1.24	1650	1912	-0.98
25	909	14	0.000677	0.000019	0.282108	0.000017	-3.81	1.35	1598	1801	-0.98
26	924	12	0.000105	0.000002	0.282062	0.000016	-4.77	1.29	1637	1861	-1.00
27	507	7	0.000636	0.000009	0.282106	0.000017	-12.61	1.23	1598	1922	-0.98
28	1154	20	0.000564	0.000003	0.281936	0.000016	-4.43	1.49	1828	2030	-0.98
29	572	11	0.000347	0.000001	0.282129	0.000017	-10.27	1.29	1555	1856	-0.99
30	950	12	0.000522	0.000008	0.281864	0.000014	-11.47	1.27	1925	2218	-0.98
31	1071	20	0.000630	0.000042	0.282103	0.000015	-0.38	1.48	1602	1759	-0.98
32	1707	17	0.000566	0.000014	0.281459	0.000016	-9.11	1.43	2478	2708	-0.98
33	1843	21	0.000768	0.000039	0.281468	0.000015	-5.98	1.53	2478	2663	-0.98
34	612	10	0.000482	0.000004	0.282463	0.000017	2.38	1.28	1100	1247	-0.99

35	939	12	0.000356	0.000039	0.281908	0.000017	-10.04	1.31	1857	2138	-0.99
36	549	8	0.000423	0.000019	0.282410	0.000015	-0.87	1.21	1172	1362	-0.99
37	1194	32	0.000486	0.000025	0.282091	0.000016	2.00	1.86	1613	1739	-0.99
38	759	11	0.001359	0.000022	0.281935	0.000021	-13.54	1.37	1868	2169	-0.96
39	739	18	0.000116	0.000001	0.281909	0.000016	-14.27	1.42	1843	2191	-1.00
40	650	9	0.000410	0.000002	0.282330	0.000015	-1.49	1.23	1282	1474	-0.99
41	518	7	0.000295	0.000002	0.282134	0.000015	-11.25	1.20	1546	1862	-0.99
42	1623	69	0.001986	0.000032	0.281980	0.000019	5.96	3.38	1837	1890	-0.94
43	1013	21	0.000217	0.000013	0.281928	0.000013	-7.61	1.48	1823	2075	-0.99
44	1908	54	0.000248	0.000003	0.281384	0.000015	-6.86	2.73	2558	2759	-0.99
45	878	11	0.000033	0.000005	0.282050	0.000017	-6.17	1.28	1650	1895	-1.00
46	1608	20	0.000438	0.000016	0.281426	0.000016	-12.34	1.50	2514	2788	-0.99
47	1075	35	0.000706	0.000013	0.282340	0.000016	8.02	1.96	1278	1338	-0.98
48	982	12	0.000834	0.000004	0.282261	0.000015	3.12	1.28	1392	1510	-0.97
49	1038	25	0.000642	0.000024	0.282096	0.000014	-1.39	1.60	1613	1783	-0.98
50	960	12	0.000515	0.000001	0.282076	0.000015	-3.71	1.28	1634	1837	-0.98
51	1139	35	0.000215	0.000004	0.281959	0.000014	-3.68	1.94	1781	1980	-0.99
52	544	7	0.001007	0.000003	0.281897	0.000015	-19.34	1.20	1904	2289	-0.97
53	2474	18	0.002218	0.000020	0.281175	0.000021	-4.70	1.56	2987	3111	-0.93
54	492	8	0.000530	0.000005	0.282313	0.000019	-5.59	1.27	1310	1555	-0.98
55	2575	18	0.000697	0.000009	0.280986	0.000017	-6.59	1.49	3124	3285	-0.98
56	969	12	0.001030	0.000026	0.282373	0.000016	6.66	1.30	1243	1321	-0.97
57	928	12	0.001729	0.000022	0.282381	0.000020	5.64	1.37	1254	1339	-0.95
58	1059	24	0.000625	0.000010	0.281933	0.000017	-6.69	1.61	1836	2066	-0.98
59	525	7	0.000447	0.000014	0.282163	0.000018	-10.15	1.25	1513	1812	-0.99
60	1050	25	0.000483	0.000001	0.282033	0.000016	-3.25	1.63	1693	1886	-0.99
61	797	11	0.000641	0.000030	0.281922	0.000020	-12.80	1.34	1851	2163	-0.98
62	2487	19	0.000878	0.000006	0.281043	0.000019	-6.85	1.55	3061	3226	-0.97
63	2664	19	0.000427	0.000006	0.280758	0.000021	-12.18	1.58	3404	3629	-0.99
64	1086	24	0.000709	0.000013	0.281112	0.000020	-35.27	1.64	2956	3505	-0.98
65	987	14	0.000742	0.000002	0.282447	0.000016	9.86	1.34	1131	1173	-0.98
66	599	8	0.000393	0.000001	0.282422	0.000015	0.66	1.21	1155	1324	-0.99

67	801	11	0.000599	0.000006	0.281911	0.000019	-13.10	1.33	1864	2181	-0.98
68	1580	23	0.000509	0.000005	0.281498	0.000015	-10.48	1.57	2421	2674	-0.98
69	968	13	0.000780	0.000003	0.282149	0.000016	-1.11	1.31	1545	1713	-0.98
70	923	12	0.000810	0.000008	0.282340	0.000020	4.65	1.36	1281	1385	-0.98
71	1001	25	0.001603	0.000019	0.282111	0.000016	-2.30	1.63	1633	1799	-0.95
72	976	13	0.001506	0.000006	0.282055	0.000017	-4.77	1.33	1708	1903	-0.95
73	1079	26	0.001078	0.000005	0.282085	0.000025	-1.17	1.79	1646	1805	-0.97
74	627	9	0.000247	0.000007	0.282237	0.000013	-5.19	1.20	1403	1643	-0.99
75	918	12	0.000096	0.000009	0.282025	0.000017	-6.19	1.30	1686	1928	-1.00
76	2436	22	0.000483	0.000009	0.281084	0.000016	-5.89	1.59	2975	3138	-0.99
77	945	13	0.001086	0.000028	0.282270	0.000018	2.46	1.35	1389	1514	-0.97
78	1040	27	0.001636	0.000029	0.281973	0.000017	-6.39	1.70	1829	2036	-0.95
79	2755	21	0.000466	0.000023	0.280997	0.000016	-1.68	1.58	3090	3192	-0.99
80	515	8	0.000331	0.000000	0.282158	0.000015	-10.49	1.20	1515	1821	-0.99
81	2132	31	0.000447	0.000002	0.280975	0.000015	-16.61	1.86	3119	3417	-0.99
82	602	8	0.000615	0.000010	0.282439	0.000017	1.25	1.25	1137	1296	-0.98
83	647	10	0.000243	0.000001	0.282339	0.000017	-1.16	1.27	1264	1455	-0.99
84	943	13	0.000335	0.000007	0.282161	0.000018	-0.97	1.35	1511	1685	-0.99
85	884	12	0.000624	0.000024	0.281562	0.000016	-23.68	1.30	2342	2775	-0.98
86	950	13	0.000518	0.000004	0.282304	0.000015	4.15	1.31	1321	1432	-0.98
87	2417	23	0.000710	0.000015	0.281194	0.000015	-2.79	1.60	2845	2971	-0.98
88	2525	23	0.000631	0.000024	0.280915	0.000014	-10.12	1.60	3213	3417	-0.98
89	1796	25	0.001922	0.000036	0.281644	0.000025	-2.19	1.78	2308	2437	-0.94
90	896	12	0.000152	0.000003	0.282120	0.000015	-3.35	1.27	1559	1767	-1.00
91	943	13	0.000578	0.000006	0.282266	0.000013	2.60	1.28	1376	1505	-0.98
92	2457	24	0.000503	0.000001	0.281151	0.000016	-3.07	1.66	2888	3017	-0.98
93	919	12	0.000188	0.000004	0.281890	0.000013	-11.00	1.25	1873	2170	-0.99
94	766	11	0.000369	0.000001	0.281735	0.000014	-19.98	1.24	2092	2497	-0.99
95	1763	27	0.000884	0.000017	0.281173	0.000026	-18.37	1.86	2886	3209	-0.97
96	901	12	0.000096	0.000002	0.282329	0.000014	4.19	1.27	1273	1390	-1.00
97	1822	27	0.000420	0.000003	0.281366	0.000016	-9.64	1.71	2593	2827	-0.99
98	968	13	0.000648	0.000003	0.282018	0.000014	-5.68	1.29	1720	1943	-0.98

99	976	13	0.000593	0.000019	0.282067	0.000015	-3.75	1.30	1651	1852	-0.98
100	1846	27	0.000693	0.000022	0.281299	0.000017	-11.82	1.73	2702	2953	-0.98
Sample 10GD60, Middle-Upper Silurian, Yulin											
1	1136	12	0.000987	0.000042	0.281950	0.000015	-4.65	1.29	1829	2026	-0.97
2	1313	12	0.000321	0.000013	0.281782	0.000019	-6.16	1.36	2026	2245	-0.99
3	3306	9	0.001107	0.000006	0.280736	0.000019	0.27	1.39	3494	3547	-0.97
4	3380	9	0.001092	0.000004	0.280481	0.000020	-7.11	1.41	3835	3963	-0.97
5	1284	13	0.000830	0.000010	0.281847	0.000017	-4.96	1.34	1964	2161	-0.98
6	1510	21	0.000797	0.000006	0.281842	0.000020	-0.12	1.59	1969	2102	-0.98
7	955	12	0.001472	0.000012	0.282173	0.000018	-0.99	1.33	1539	1696	-0.96
8	784	10	0.002128	0.000052	0.281912	0.000019	-14.24	1.30	1940	2224	-0.94
9	468	7	0.000986	0.000016	0.282377	0.000021	-3.96	1.30	1235	1453	-0.97
10	1806	12	0.000559	0.000013	0.281298	0.000020	-12.60	1.38	2695	2960	-0.98
11	741	11	0.000493	0.000004	0.281996	0.000020	-11.33	1.35	1743	2044	-0.99
12	1126	12	0.000880	0.000005	0.281987	0.000018	-3.49	1.33	1773	1960	-0.97
13	801	17	0.000277	0.000003	0.282052	0.000027	-7.92	1.59	1657	1921	-0.99
14	1089	13	0.000926	0.000019	0.282003	0.000016	-3.77	1.32	1754	1944	-0.97
15	2444	10	0.000903	0.000002	0.281251	0.000019	-0.46	1.36	2782	2879	-0.97
16	925	13	0.000477	0.000009	0.282173	0.000022	-1.01	1.42	1499	1673	-0.99
17	631	9	0.001094	0.000016	0.282435	0.000019	1.52	1.30	1158	1306	-0.97
18	974	13	0.001440	0.000012	0.282111	0.000023	-2.77	1.44	1626	1801	-0.96
19	931	12	0.001041	0.000016	0.281903	0.000018	-10.81	1.33	1897	2170	-0.97
20	1421	12	0.000652	0.000004	0.281856	0.000017	-1.44	1.33	1942	2096	-0.98
21	1068	12	0.000587	0.000011	0.282210	0.000019	3.38	1.35	1453	1567	-0.98
22	1016	15	0.000508	0.000007	0.281907	0.000015	-8.47	1.35	1866	2121	-0.98
23	3736	9	0.001026	0.000044	0.280153	0.000017	-10.51	1.37	4264	4414	-0.97
24	795	11	0.002474	0.000007	0.281856	0.000023	-16.17	1.41	2039	2329	-0.93
25	1024	13	0.000803	0.000020	0.282163	0.000015	0.59	1.30	1526	1672	-0.98
26	2070	11	0.000669	0.000007	0.281385	0.000016	-3.73	1.30	2584	2735	-0.98
27	2614	10	0.000784	0.000013	0.281025	0.000017	-4.48	1.34	3078	3214	-0.98
28	805	11	0.000775	0.000008	0.282197	0.000017	-2.98	1.29	1479	1675	-0.98

29	1023	13	0.000284	0.000001	0.281886	0.000016	-8.92	1.31	1884	2149	-0.99
30	2593	10	0.001897	0.000052	0.281094	0.000015	-4.45	1.31	3073	3195	-0.94
31	904	12	0.000553	0.000017	0.282138	0.000020	-2.77	1.36	1551	1744	-0.98
32	1019	13	0.002326	0.000075	0.282372	0.000019	6.83	1.36	1289	1353	-0.93
33	1087	14	0.000324	0.000003	0.281948	0.000014	-5.32	1.31	1801	2020	-0.99
34	1749	12	0.001215	0.000009	0.281529	0.000015	-6.43	1.30	2423	2610	-0.96
35	938	12	0.000949	0.000004	0.282190	0.000014	-0.43	1.26	1495	1654	-0.97
36	1021	13	0.002243	0.000013	0.282446	0.000018	9.55	1.35	1178	1216	-0.93
37	1018	14	0.001142	0.000026	0.282021	0.000018	-4.82	1.36	1738	1940	-0.97
38	2336	12	0.000639	0.000010	0.281175	0.000024	-5.17	1.47	2865	3022	-0.98
39	1279	15	0.000899	0.000027	0.282013	0.000018	0.76	1.40	1739	1871	-0.97
40	1280	15	0.000787	0.000004	0.281964	0.000015	-0.84	1.35	1800	1952	-0.98
41	2478	11	0.000460	0.000010	0.281007	0.000016	-7.63	1.33	3076	3257	-0.99
42	995	13	0.000474	0.000005	0.282062	0.000016	-3.43	1.32	1653	1851	-0.99
43	2474	13	0.000370	0.000002	0.281395	0.000016	6.23	1.37	2550	2574	-0.99
44	948	12	0.000576	0.000016	0.282360	0.000017	6.05	1.32	1246	1334	-0.98
45	994	13	0.000675	0.000018	0.281947	0.000015	-7.66	1.30	1819	2063	-0.98
46	992	13	0.000469	0.000004	0.282154	0.000015	-0.23	1.31	1526	1687	-0.99
47	516	7	0.000525	0.000004	0.281810	0.000018	-22.88	1.25	1999	2445	-0.98
48	1484	13	0.000108	0.000003	0.281425	0.000013	-14.81	1.29	2494	2812	-1.00
49	2407	11	0.000639	0.000003	0.281292	0.000016	0.60	1.33	2707	2796	-0.98
50	1095	14	0.001069	0.000008	0.281880	0.000016	-8.08	1.34	1930	2165	-0.97
51	743	10	0.000610	0.000013	0.282161	0.000020	-5.52	1.33	1522	1753	-0.98
52	2465	11	0.000073	0.000007	0.280850	0.000015	-12.86	1.30	3253	3502	-1.00
53	1002	13	0.000510	0.000027	0.282072	0.000016	-2.92	1.31	1639	1831	-0.98
54	1076	19	0.000457	0.000007	0.281995	0.000017	-3.99	1.47	1743	1945	-0.99
55	1008	16	0.000660	0.000003	0.281920	0.000019	-8.30	1.43	1856	2106	-0.98
56	505	7	0.000540	0.000005	0.282169	0.000018	-10.41	1.25	1509	1809	-0.98
57	643	9	0.001219	0.000042	0.282508	0.000017	4.32	1.26	1059	1174	-0.96
58	1099	15	0.000534	0.000001	0.282035	0.000017	-2.14	1.38	1692	1870	-0.98
59	763	11	0.000515	0.000010	0.281895	0.000028	-14.44	1.52	1882	2218	-0.98
60	1559	74	0.000307	0.000008	0.281239	0.000017	-19.93	3.56	2755	3124	-0.99

61	1201	16	0.000809	0.000011	0.282022	0.000030	-0.55	1.65	1722	1873	-0.98
62	2504	12	0.000632	0.000009	0.281280	0.000020	2.36	1.41	2724	2789	-0.98
63	994	13	0.000446	0.000013	0.282010	0.000021	-5.25	1.41	1721	1942	-0.99
64	2619	13	0.001464	0.000018	0.281169	0.000023	-0.47	1.49	2936	3022	-0.96
65	2449	14	0.000307	0.000008	0.281239	0.000017	0.21	1.40	2755	2850	-0.99
66	2506	13	0.001294	0.000014	0.282064	0.000018	29.17	1.40	1685	1460	-0.96
67	546	8	0.000384	0.000003	0.282121	0.000015	-11.15	1.21	1568	1879	-0.99
68	989	13	0.001294	0.000014	0.282064	0.000018	-4.02	1.35	1685	1876	-0.96
69	777	11	0.000514	0.000008	0.281814	0.000018	-17.02	1.31	1993	2358	-0.98
70	1018	19	0.000365	0.000015	0.282042	0.000014	-3.55	1.43	1675	1876	-0.99
71	1861	15	0.000750	0.000033	0.281375	0.000016	-8.88	1.38	2604	2821	-0.98
72	519	7	0.000563	0.000002	0.282003	0.000014	-15.98	1.19	1737	2101	-0.98
73	986	13	0.001180	0.000026	0.281806	0.000018	-13.17	1.35	2039	2332	-0.96
74	1575	18	0.000505	0.000010	0.280990	0.000019	-28.62	1.48	3103	3562	-0.98
75	1064	30	0.000939	0.000003	0.282211	0.000019	3.07	1.82	1465	1579	-0.97
76	1096	18	0.000899	0.000017	0.282011	0.000015	-3.30	1.42	1741	1926	-0.97
77	1164	22	0.000577	0.000004	0.282035	0.000014	-0.73	1.52	1694	1852	-0.98
78	979	14	0.000264	0.000001	0.281903	0.000015	-9.27	1.33	1859	2132	-0.99
79	2725	14	0.000635	0.000003	0.280710	0.000017	-12.90	1.40	3487	3713	-0.98
80	549	8	0.000402	0.000002	0.282124	0.000017	-10.97	1.24	1564	1873	-0.99
81	1411	18	0.001592	0.000024	0.281813	0.000019	-4.08	1.48	2051	2220	-0.95
82	1420	19	0.000920	0.000003	0.281979	0.000015	2.62	1.45	1787	1892	-0.97
83	1857	17	0.000881	0.000006	0.281650	0.000016	0.63	1.43	2237	2347	-0.97
84	947	13	0.000904	0.000020	0.281858	0.000016	-11.98	1.31	1953	2242	-0.97
85	1259	18	0.000957	0.000008	0.281965	0.000015	-1.44	1.42	1808	1965	-0.97
86	1043	19	0.000678	0.000017	0.281973	0.000019	-5.65	1.50	1783	2001	-0.98
87	524	8	0.000916	0.000014	0.282158	0.000019	-10.50	1.27	1538	1829	-0.97
88	1825	18	0.001177	0.000010	0.281654	0.000016	-0.28	1.46	2248	2366	-0.96
89	1511	20	0.000823	0.000005	0.281456	0.000016	-13.83	1.50	2498	2785	-0.98
90	1476	19	0.000780	0.000007	0.281832	0.000016	-1.21	1.47	1982	2129	-0.98
91	1015	21	0.000744	0.000003	0.282408	0.000018	9.09	1.54	1185	1235	-0.98
92	2428	20	0.000396	0.000006	0.280595	0.000016	-23.31	1.54	3617	3979	-0.99

93	931	13	0.000824	0.000013	0.282235	0.000018	1.08	1.35	1428	1572	-0.98
94	1095	22	0.000677	0.000004	0.281923	0.000017	-6.30	1.56	1852	2076	-0.98
95	996	14	0.001056	0.000012	0.282101	0.000017	-2.40	1.35	1623	1800	-0.97
96	1012	23	0.000768	0.000009	0.282172	0.000017	0.67	1.58	1512	1658	-0.98
97	2468	18	0.000653	0.000007	0.281066	0.000022	-6.08	1.57	3012	3173	-0.98
98	1606	20	0.000721	0.000005	0.281468	0.000017	-11.20	1.51	2476	2731	-0.98
99	446	7	0.001305	0.000014	0.282386	0.000018	-4.22	1.25	1233	1448	-0.96
100	2376	18	0.000887	0.000050	0.281206	0.000017	-3.56	1.49	2841	2975	-0.97

Note: *$\varepsilon_{Hf}(t) = 10{,}000\times\{[(^{176}Hf/^{177}Hf)_S-(^{176}Lu/^{177}Hf)_S\times(e^{\lambda t}-1)] / [(^{176}Hf/^{177}Hf)_{CHUR,0}-(^{176}Lu/^{177}Hf)_{CHUR}\times(e^{\lambda t}-1)]-1\}$.
†$T_{DM} = 1/\lambda\times\ln\{1+[(^{176}Hf/^{177}Hf)_S-(^{176}Hf/^{177}Hf)_{DM}] /[(^{176}Lu/^{177}Hf)_S-(^{176}Lu/^{177}Hf)_{DM}]\}$.
§$T_{DM}^C = T_{DM}-(T_{DM}-t)\times[(f_{cc}-f_s)/(f_{cc}-f_{DM})]$. $f_{Lu/Hf} = (^{176}Lu/^{177}Hf)_S/(^{176}Lu/^{177}Hf)_{CHUR}-1$.
where, $\lambda = 1.867\times10^{-11}$ year^{-1} (Soderlund et al., 2004); $(^{176}Lu/^{177}Hf)_S$ and $(^{176}Hf/^{177}Hf)_S$ are the measured values of the samples; $(^{176}Lu/^{177}Hf)_{CHUR} = 0.0332$ and $(^{176}Hf/^{177}Hf)_{CHUR,0} = 0.28277$ (Blichert-Toft and Albarède, 1997);
$(^{176}Lu/^{177}Hf)_{DM} = 0.0384$ and $(^{176}Hf/^{177}Hf)_{DM} = 0.28325$ (Griffin et al., 2000); $(^{176}Lu/^{177}Hf)_{upper\ crust}=0.0093$ (Amelin et al., 1999);
$f_{cc} = [(^{176}Lu/^{177}Hf)_{upper\ crust}/(^{176}Lu/^{177}Hf)_{CHUR}]-1$; $f_s = f_{Lu/Hf}$; $f_{DM} = [(^{176}Lu/^{177}Hf)_{DM}/(^{176}Lu/^{177}Hf)_{CHUR}]-1$; t = zircon crystallization age.

Appendix C3 P and D values of two-sample Kolmogorov–Smirnov (K–S) Tests for Ediacaran–Silurian samples groups across the lower Palaeozoic Nanhua foreland basin, South China (samples groups correspond to those in Figure 4.8 a-g)

	Edia (Gp. 1)	$\in_1$ (Gp.2-2)	$\in_1$ (Gp.2-3)	$\in_{2+3}$ (Gp.2-2)	$\in_{2+3}$ (Gp.2-3)	O_1 (Gp.2-2)	O_1 (Gp.2-3)	O_{2+3} (Gp.2-1)	O_{2+3} (Gp.2-2)	O_{2+3} (Gp.2-3)	O_{2+3} (Gp.3)	S_1 (Gp.2-1)	S_1 (Gp.2-3)	S_1 (Gp.3)	S_1 (Gp.4)	S_{2+3} (Gp.2-1)	S_{2+3} (Gp.2-3)	S_{2+3} (Gp.3)	S_{2+3} (Gp.4)
Edia (Gp. 1)		0.107	0.145	0.098	0.120	0.179	0.134	0.103	0.075	0.092	0.121	0.121	0.753	0.193	0.309	0.147	0.126	0.238	0.198
$\in_1$ (Gp.2-2)	**0.139**		0.050	0.081	0.053	0.077	0.174	0.180	0.058	0.113	0.192	0.204	0.815	0.100	0.226	0.241	0.085	0.141	0.113
$\in_1$ (Gp.2-3)	**0.066**	**0.995**		0.115	0.063	0.108	0.218	0.195	0.080	0.126	0.207	0.233	0.783	0.072	0.186	0.279	0.129	0.101	0.102
$\in_{2+3}$ (Gp.2-2)	0.030	**0.276**	**0.151**		0.063	0.084	0.147	0.174	0.063	0.074	0.175	0.200	0.754	0.114	0.260	0.235	0.050	0.152	0.178
$\in_{2+3}$ (Gp.2-3)	0.044	**0.925**	**0.924**	**0.470**		0.068	0.170	0.174	0.054	0.103	0.185	0.202	0.777	0.075	0.228	0.248	0.068	0.117	0.124
O_1 (Gp.2-2)	0.001	**0.626**	**0.386**	**0.219**	**0.699**		0.228	0.239	0.115	0.120	0.245	0.271	0.797	0.063	0.235	0.311	0.093	0.068	0.177
O_1 (Gp.2-3)	0.003	0.001	0.000	0.000	0.000	0.000		0.180	0.143	0.141	0.096	0.129	0.750	0.242	0.383	0.156	0.176	0.287	0.279
O_{2+3} (Gp.2-1)	**0.086**	0.039	0.005	0.014	0.035	0.000	0.009		0.107	0.162	0.223	0.082	0.844	0.208	0.314	0.093	0.189	0.258	0.217
O_{2+3} (Gp.2-2)	**0.234**	**0.744**	**0.596**	**0.163**	**0.726**	0.046	0.000	0.006		0.081	0.144	0.157	0.764	0.122	0.250	0.201	0.064	0.163	0.144
O_{2+3} (Gp.2-3)	**0.160**	**0.106**	**0.152**	**0.189**	**0.124**	**0.069**	0.002	0.001	**0.166**		0.146	0.171	0.764	0.124	0.269	0.219	0.082	0.164	0.179
O_{2+3} (Gp.3)	**0.471**	**0.073**	**0.072**	**0.070**	**0.079**	0.009	**0.725**	0.016	**0.217**	**0.243**		0.165	0.757	0.230	0.338	0.183	0.195	0.276	0.230
S_1 (Gp.2-1)	0.006	0.003	0.000	0.000	0.001	0.000	0.000	**0.147**	0.000	0.000	**0.108**		0.764	0.249	0.340	0.071	0.221	0.301	0.255
S_1 (Gp.2-3)	0.000	0.000	0.000	0.000	0.000	0.000	0.000	0.000	0.000	0.000	0.000	0.000		0.789	0.825	0.767	0.754	0.820	0.797
S_1 (Gp.3)	0.008	**0.537**	**0.947**	**0.203**	**0.826**	**0.960**	0.000	0.003	**0.164**	**0.201**	0.041	0.000	0.000		0.208	0.301	0.093	0.090	0.131
S_1 (Gp.4)	0.000	0.001	0.034	0.000	0.000	0.000	0.000	0.000	0.000	0.000	0.000	0.000	0.000	0.017		0.404	0.291	0.233	0.114
S_{2+3} (Gp.2-1)	0.021	0.000	0.000	0.000	0.000	0.000	0.006	**0.329**	0.000	0.000	**0.110**	**0.543**	0.000	0.000	0.000		0.253	0.349	0.302
S_{2+3} (Gp.2-3)	0.044	**0.484**	**0.183**	**0.823**	**0.700**	**0.359**	0.000	0.000	**0.586**	**0.406**	**0.063**	0.000	0.000	**0.618**	0.000	0.000		0.125	0.191
S_{2+3} (Gp.3)	0.000	**0.150**	**0.662**	0.034	**0.288**	**0.923**	0.000	0.000	0.023	0.036	0.007	0.000	0.000	**0.810**	0.005	0.000	**0.251**		0.168
S_{2+3} (Gp.4)	0.000	**0.095**	**0.364**	0.000	0.030	0.001	0.000	0.000	0.000	0.000	0.010	0.000	0.000	**0.149**	**0.194**	0.000	0.000	0.027	

Note: The results reflect the input of both determined ages and errors for each zircon grain. All probabilities (P values) > 0.05 indicate that the confidence of which the pair of samples can be statistically distinguished is less than 95%.

Sample Groups:

EdiaGp.1 (Ediacaran samples in Group 1): XW-12, XN-2, NX-3-2, ZC-8, ZC-6, YK-27; ∈1Gp.2-2 (Lower Cambrian samples in Group 2-2): JX-16, HU-37, J200;
∈1Gp.2-3 (Lower Cambrian samples in Group 2-3): 11FS-1, 11FS-3; ∈2+3Gp.2-2 (Middle-Upper Cambrian samples in Group 2-2): 10GD19, 10GD17, 10GD16, HU-46, HU-54, J186, J188, J192, JX-12;
∈2+3Gp.2-3 (Middle-Upper Cambrian samples in Group 2-3): 11FS-6, 11FS-11, 10GD37; O1Gp.2-2 (Lower Ordovician samples in Group 2-2): 950, 950-1, 950-2;
O1Gp.2-3 (Lower Ordovician samples in Group 2-3): 10GD42-1, 10GD41, 10GD38-1, 10GD45; O2+3Gp.2-1 (Middle-Upper Ordovician samples in Group 2-1): 11QZ-7, 11QZ-8, S08-1, S09-1;
O2+3Gp.2-2 (Middle-Upper Ordovician samples in Group 2-2): 960, 960-1, 960-2, JX-4, JX-8, JX-25, JX-32, J191, HU-48; O2+3Gp.2-3 (Middle-Upper Ordovician samples in Group 2-3): 10GD54, 10GD52-1, 10GD51;
O2+3Gp.3 (Middle-Upper Ordovician samples in Group 3): 10GD83-1; S1Gp.2-1 (Lower Silurian samples in Group 2-1): 11QZ-5, 11QZ-6, JS01, S01-2, S16-1, S15-1, S14-2;
S1Gp.2-3 (Lower Silurian samples in Group 2-3): 10GD56; S1Gp.3 (Lower Silurian samples in Group 3): 10GD84;
S1Gp.4 (Lower Silurian samples in Group 4): HG-32, HG-47, HG-65, E-300; S2+3Gp.2-1 (Middle-Upper Silurian samples in Group 2-1): 11QZ-3, 11QZ-1;
S2+3Gp.2-3 (Middle-Upper Silurian samples in Group 2-3): 10GD58, 10GD60; S2+3Gp.3 (Middle-Upper Silurian samples in Group 3): 10GD85;
S2+3Gp.4 (Middle-Upper Silurian samples in Group 4): 10GD87, 10GD88, HG-46, HG-45, G-26a.

Appendix D1 SHRIMP and LA-ICP-MS zircon U–Pb data for Cambrian clastic samples from Xinhuang area and Xinning area, Hunan province

Spot#	Th (ppm)	U (ppm)	Th/U	Corrected Ratios						Corrected Ages (Ma)					
				$^{207}Pb/^{206}Pb$	1σ	$^{207}Pb/^{235}U$	1σ	$^{206}Pb/^{238}U$	1σ	$^{207}Pb/^{206}Pb$	1σ	$^{207}Pb/^{235}U$	1σ	$^{206}Pb/^{238}U$	1σ
Sample 12GH38 (N27°07′31.4″, E109°09′16.3″)															
1	29	29	1.01	0.0680	0.0049	1.2343	0.0925	0.1316	0.0030	869	148	816	90	797	17
2	79	156	0.50	0.0672	0.0011	1.1854	0.0239	0.1279	0.0014	844	35	794	24	776	8
3	246	221	1.11	0.1667	0.0007	10.5633	0.1118	0.4597	0.0044	2525	7	2485	108	2438	20
4	90	205	0.44	0.0671	0.0009	1.1822	0.0199	0.1278	0.0013	840	28	792	20	775	7
5	187	277	0.67	0.0647	0.0010	1.0156	0.0185	0.1138	0.0010	765	33	712	19	695	6
6	82	130	0.63	0.0670	0.0013	1.1701	0.0323	0.1267	0.0024	837	42	787	32	769	14
7	76	284	0.27	0.0668	0.0008	1.2504	0.0188	0.1357	0.0012	832	25	824	19	821	7
8	63	142	0.44	0.0644	0.0012	1.0949	0.0232	0.1233	0.0014	755	38	751	23	749	8
9	42	85	0.50	0.0820	0.0013	2.3237	0.0488	0.2054	0.0028	1247	31	1220	48	1204	15
10	279	633	0.44	0.0657	0.0011	1.1561	0.0206	0.1276	0.0009	797	34	780	21	774	5
11	201	175	1.15	0.0669	0.0012	1.2060	0.0244	0.1307	0.0014	835	36	803	24	792	8
12	114	232	0.49	0.1840	0.0015	12.7855	0.1590	0.5041	0.0048	2689	13	2664	150	2631	21
13	162	529	0.31	0.1132	0.0004	4.7471	0.0416	0.3042	0.0024	1851	7	1776	41	1712	12
14	142	246	0.58	0.0675	0.0014	1.2711	0.0289	0.1366	0.0013	852	43	833	29	826	7
15	55	76	0.73	0.0629	0.0021	1.1910	0.0555	0.1373	0.0044	705	73	796	55	830	25
16	218	459	0.48	0.0669	0.0006	1.2690	0.0155	0.1376	0.0012	834	18	832	16	831	7
17	56	92	0.61	0.1151	0.0011	5.1826	0.0849	0.3265	0.0044	1882	17	1850	83	1822	21
18	97	155	0.62	0.0645	0.0013	1.2091	0.0274	0.1360	0.0015	757	42	805	27	822	8
19	146	286	0.51	0.0663	0.0008	1.2601	0.0183	0.1379	0.0012	815	24	828	18	833	7
20	42	68	0.62	0.0675	0.0019	1.1396	0.0429	0.1225	0.0031	853	58	772	43	745	18
21	81	118	0.69	0.1617	0.0010	10.1015	0.1360	0.4529	0.0055	2474	10	2444	130	2408	24
22	100	240	0.42	0.0639	0.0011	1.0374	0.0208	0.1178	0.0011	738	37	723	21	718	6

23	72	577	0.12	0.0716	0.0004	1.6140	0.0158	0.1636	0.0012	974	13	976	16	977	7
24	74	118	0.62	0.0631	0.0019	1.0888	0.0396	0.1252	0.0024	710	66	748	39	761	14
25	261	440	0.59	0.0652	0.0005	1.1756	0.0133	0.1307	0.0010	782	17	789	13	792	6
26	45	92	0.49	0.0677	0.0026	1.2632	0.0506	0.1353	0.0018	860	78	829	50	818	10
27	165	236	0.70	0.0663	0.0008	1.2334	0.0190	0.1349	0.0012	816	26	816	19	816	7
28	108	264	0.41	0.0593	0.0013	0.7998	0.0188	0.0979	0.0009	578	47	597	19	602	5
29	223	435	0.51	0.1493	0.0005	8.9107	0.0768	0.4328	0.0035	2338	5	2329	75	2318	16
30	106	224	0.47	0.0636	0.0013	1.1224	0.0255	0.1281	0.0013	727	43	764	26	777	7
31	248	264	0.94	0.0671	0.0009	1.2314	0.0193	0.1330	0.0012	842	26	815	19	805	7
32	135	212	0.64	0.0658	0.0009	1.0960	0.0187	0.1207	0.0012	801	29	751	19	735	7
33	139	183	0.76	0.0664	0.0010	1.3171	0.0247	0.1438	0.0016	820	31	853	25	866	9
34	23	41	0.56	0.1939	0.0033	15.1582	0.3931	0.5671	0.0110	2775	28	2825	337	2896	45
35	152	183	0.83	0.0645	0.0010	1.1611	0.0223	0.1305	0.0014	759	34	782	22	791	8
36	73	106	0.69	0.0662	0.0011	1.2383	0.0262	0.1356	0.0017	813	35	818	26	820	10
37	59	66	0.89	0.0633	0.0024	1.1360	0.0474	0.1302	0.0020	718	82	771	47	789	12
38	42	50	0.83	0.0614	0.0049	1.1367	0.0939	0.1342	0.0025	655	173	771	91	812	14
39	304	500	0.61	0.0661	0.0005	1.2270	0.0143	0.1347	0.0011	809	17	813	14	814	6
40	77	149	0.52	0.0535	0.0020	0.6243	0.0242	0.0846	0.0010	350	84	493	24	524	6
41	95	151	0.63	0.0681	0.0012	1.3000	0.0268	0.1384	0.0016	873	35	846	27	835	9
42	54	78	0.70	0.0642	0.0018	1.1256	0.0350	0.1271	0.0019	749	58	766	35	771	11
43	33	50	0.66	0.0569	0.0040	0.9874	0.0712	0.1259	0.0024	486	154	697	70	765	14
44	79	136	0.58	0.0652	0.0027	1.1201	0.0482	0.1245	0.0015	782	87	763	48	757	8
45	156	207	0.75	0.0677	0.0011	1.1633	0.0226	0.1247	0.0013	859	34	784	23	757	7
46	214	323	0.66	0.0651	0.0007	1.1609	0.0167	0.1293	0.0012	778	24	782	17	784	7
47	*333*	*299*	*1.12*	*0.0679*	*0.0010*	*0.6831*	*0.0148*	*0.0730*	*0.0012*	*864*	*29*	*529*	*15*	*454*	*7*
48	147	165	0.89	0.0657	0.0030	1.1754	0.0556	0.1298	0.0015	797	96	789	55	787	9
49	200	278	0.72	0.0659	0.0007	1.1701	0.0172	0.1288	0.0012	803	23	787	17	781	7
50	83	136	0.61	0.0662	0.0020	1.1793	0.0380	0.1291	0.0015	814	63	791	38	783	9
51	171	220	0.78	0.0657	0.0009	1.1795	0.0205	0.1302	0.0014	796	29	791	21	789	8
52	61	106	0.58	0.0640	0.0018	1.2131	0.0369	0.1374	0.0018	742	58	807	37	830	10
53	78	159	0.49	0.0647	0.0011	1.1179	0.0221	0.1254	0.0014	764	34	762	22	761	8
54	177	318	0.56	0.0648	0.0007	1.1189	0.0155	0.1251	0.0012	769	22	762	16	760	7

55	264	665	0.40	0.0643	0.0005	1.1204	0.0121	0.1264	0.0010	751	16	763	12	767	6
56	102	220	0.46	0.1647	0.0009	9.6545	0.1106	0.4251	0.0043	2505	9	2402	106	2283	20
57	145	157	0.92	0.0642	0.0009	1.1147	0.0213	0.1259	0.0016	748	30	760	21	765	9
58	29	29	1.01	0.0664	0.0031	1.2314	0.0537	0.1346	0.0037	819	48	815	24	814	21
59	79	156	0.50	0.0669	0.0024	1.2584	0.0427	0.1366	0.0035	833	33	827	19	825	20
60	246	221	1.11	0.0667	0.0019	1.2399	0.0341	0.1348	0.0031	829	26	819	15	815	18
61	90	205	0.44	0.0675	0.0011	1.3118	0.0208	0.1410	0.0030	853	20	851	9	851	17
62	187	277	0.67	0.0674	0.0016	1.2940	0.0282	0.1393	0.0031	850	21	843	12	841	17
63	82	130	0.63	0.0658	0.0034	1.1827	0.0572	0.1305	0.0038	799	55	793	27	791	22
64	76	284	0.27	0.0639	0.0014	1.0500	0.0214	0.1192	0.0026	740	21	729	11	726	15
65	63	142	0.44	0.0644	0.0013	1.0930	0.0214	0.1231	0.0027	755	20	750	10	748	15
66	42	85	0.50	0.0707	0.0009	1.5245	0.0197	0.1565	0.0032	948	22	940	8	937	18
67	279	633	0.44	0.0662	0.0018	1.1770	0.0297	0.1290	0.0030	812	24	790	14	782	17
68	201	175	1.15	0.0811	0.0013	2.2607	0.0347	0.2023	0.0042	1224	20	1200	11	1188	23
69	114	232	0.49	0.0578	0.0022	0.6638	0.0243	0.0834	0.0020	520	41	517	15	516	12
70	162	529	0.31	0.1421	0.0019	8.1772	0.1066	0.4174	0.0088	2253	19	2251	12	2249	40
71	142	246	0.58	0.1995	0.0070	14.9758	0.5109	0.5446	0.0201	2822	27	2814	32	2803	84
72	55	76	0.73	0.0715	0.0009	1.5980	0.0194	0.1621	0.0033	972	22	969	8	968	18
73	218	459	0.48	0.0672	0.0025	1.2677	0.0439	0.1369	0.0036	844	34	831	20	827	21
74	56	92	0.61	0.0647	0.0012	1.0895	0.0188	0.1222	0.0026	765	20	748	9	743	15
75	97	155	0.62	0.0669	0.0021	1.2443	0.0368	0.1350	0.0033	834	28	821	17	816	19
76	146	286	0.51	0.2190	0.0024	17.5712	0.1935	0.5820	0.0118	2973	19	2967	11	2957	48
77	42	68	0.62	0.0656	0.0022	1.1569	0.0364	0.1280	0.0032	793	30	781	17	776	18
78	81	118	0.69	0.0638	0.0017	1.0413	0.0250	0.1183	0.0027	736	23	725	12	721	16
79	100	240	0.42	0.1432	0.0031	8.2053	0.1713	0.4155	0.0104	2267	19	2254	19	2240	47
80	72	577	0.12	0.0647	0.0022	1.0868	0.0343	0.1219	0.0031	764	30	747	17	741	18
81	74	118	0.62	0.0657	0.0016	1.1744	0.0274	0.1296	0.0029	797	22	789	13	786	17
82	261	440	0.59	0.0675	0.0027	1.3046	0.0493	0.1401	0.0036	854	39	848	22	845	20
Sample 12GH39 (N27°07′22.8″, E109°09′42.3″)															
1	73	140	0.52	0.0669	0.0016	1.2499	0.0407	0.1354	0.0031	836	48	823	41	819	18
2	92	122	0.76	0.0637	0.0020	1.2486	0.0496	0.1421	0.0034	733	68	823	49	857	19

3	*132*	*218*	*0.61*	*0.1668*	*0.0013*	*8.3967*	*0.1949*	*0.3651*	*0.0080*	*2526*	*13*	*2275*	*181*	*2006*	*38*
4	*48*	*83*	*0.58*	*0.0811*	*0.0063*	*1.4644*	*0.1204*	*0.1309*	*0.0038*	*1224*	*151*	*916*	*115*	*793*	*21*
5	57	72	0.79	0.0626	0.0030	1.0788	0.0599	0.1249	0.0034	696	103	743	59	759	20
6	235	244	0.96	0.0664	0.0019	1.1995	0.0433	0.1311	0.0028	818	61	800	43	794	16
7	161	336	0.48	0.1201	0.0021	6.6014	0.1854	0.3988	0.0088	1957	31	2060	173	2163	40
8	225	554	0.41	0.0589	0.0018	0.7033	0.0256	0.0866	0.0017	562	66	541	26	536	10
9	29	71	0.41	0.0657	0.0043	1.2551	0.0885	0.1386	0.0038	795	136	826	86	837	22
10	170	135	1.26	0.0985	0.0012	3.8578	0.0997	0.2841	0.0065	1596	22	1605	96	1612	33
11	61	139	0.44	0.0676	0.0016	1.1892	0.0395	0.1277	0.0029	855	50	796	39	775	17
12	16	37	0.44	0.0643	0.0048	1.2668	0.1040	0.1429	0.0047	751	159	831	100	861	27
13	322	325	0.99	0.0598	0.0010	0.7658	0.0204	0.0929	0.0019	596	37	577	20	573	11
14	92	181	0.51	0.0598	0.0022	0.7214	0.0308	0.0874	0.0019	598	79	551	31	540	11
15	*140*	*250*	*0.56*	*0.0738*	*0.0037*	*1.3109*	*0.0724*	*0.1288*	*0.0030*	*1036*	*101*	*851*	*71*	*781*	*17*
16	142	293	0.49	0.0591	0.0010	0.7059	0.0189	0.0866	0.0018	572	37	542	19	535	11
17	366	551	0.66	0.0680	0.0008	1.3019	0.0297	0.1389	0.0027	868	24	847	30	839	15
18	301	459	0.65	0.0599	0.0009	0.6899	0.0171	0.0836	0.0017	599	32	533	17	517	10
19	141	164	0.86	0.0675	0.0016	1.1844	0.0380	0.1272	0.0028	855	48	793	38	772	16
20	196	224	0.88	0.0669	0.0013	1.3068	0.0379	0.1416	0.0030	836	41	849	38	854	17
21	44	84	0.53	0.0530	0.0042	0.6385	0.0533	0.0873	0.0023	330	180	501	53	540	13
22	164	166	0.99	0.0648	0.0011	1.1938	0.0340	0.1335	0.0030	769	37	798	34	808	17
24	102	155	0.66	0.0649	0.0014	1.1920	0.0369	0.1332	0.0031	772	44	797	37	806	17
25	*509*	*712*	*0.72*	*0.0951*	*0.0079*	*0.7544*	*0.0648*	*0.0575*	*0.0013*	*1530*	*156*	*571*	*64*	*361*	*8*
26	*721*	*393*	*1.83*	*0.0677*	*0.0042*	*0.8286*	*0.0542*	*0.0888*	*0.0018*	*859*	*129*	*613*	*54*	*548*	*11*
27	118	225	0.52	0.0612	0.0024	0.9522	0.0433	0.1129	0.0024	646	86	679	43	689	14
28	112	152	0.74	0.0650	0.0030	1.1941	0.0620	0.1332	0.0030	774	98	798	61	806	17
29	86	125	0.68	0.0651	0.0014	1.1243	0.0355	0.1252	0.0029	779	45	765	35	760	17
30	263	303	0.87	0.0702	0.0009	1.2852	0.0318	0.1329	0.0028	933	28	839	32	804	16
31	*237*	*315*	*0.75*	*0.2846*	*0.0764*	*4.7453*	*1.4753*	*0.1209*	*0.0190*	*3388*	*418*	*1775*	*920*	*736*	*109*
32	97	179	0.54	0.0587	0.0025	0.6996	0.0342	0.0865	0.0020	555	94	539	34	535	12
33	1	87	0.02	0.2296	0.0018	20.0256	0.5312	0.6325	0.0161	3050	12	3093	433	3159	63
34	35	136	0.26	0.0629	0.0017	1.1279	0.0398	0.1301	0.0030	705	57	767	40	788	17
35	150	291	0.52	0.0724	0.0053	1.9119	0.1583	0.1914	0.0076	998	148	1085	149	1129	41

36	99	186	0.53	0.0608	0.0012	0.7484	0.0219	0.0893	0.0020	631	42	567	22	551	12
37	116	170	0.68	0.0664	0.0015	1.2133	0.0378	0.1325	0.0029	820	46	807	38	802	17
38	160	630	0.25	0.0603	0.0010	0.6769	0.0177	0.0813	0.0016	616	36	525	18	504	10
39	*46*	*86*	*0.53*	*0.0949*	*0.0257*	*1.2358*	*0.3377*	*0.0944*	*0.0032*	*1527*	*511*	*817*	*295*	*582*	*19*
40	155	266	0.58	0.0582	0.0023	0.7055	0.0310	0.0879	0.0018	537	85	542	31	543	11
41	703	893	0.79	0.0785	0.0031	1.9342	0.0871	0.1787	0.0037	1160	79	1093	85	1060	20
42	135	195	0.69	0.0664	0.0017	1.1257	0.0378	0.1230	0.0027	819	53	766	38	748	15
43	61	241	0.25	0.0749	0.0010	1.8415	0.0465	0.1782	0.0038	1067	27	1060	46	1057	21
44	83	137	0.61	0.1651	0.0022	10.6741	0.2848	0.4689	0.0108	2509	23	2495	254	2479	47
45	237	398	0.60	0.0735	0.0057	1.6090	0.1292	0.1589	0.0036	1027	156	974	123	950	20
46	211	330	0.64	0.0596	0.0016	0.6349	0.0216	0.0773	0.0016	589	59	499	22	480	10
47	305	288	1.06	0.0653	0.0018	1.0314	0.0362	0.1146	0.0024	783	59	720	36	700	14
48	123	209	0.59	0.0832	0.0011	2.0476	0.0518	0.1786	0.0039	1273	25	1131	51	1059	21
49	124	188	0.66	0.0676	0.0011	1.3405	0.0366	0.1439	0.0032	855	34	863	37	867	18
50	146	510	0.29	0.0662	0.0008	1.1923	0.0280	0.1307	0.0026	811	26	797	28	792	15
51	169	216	0.79	0.0801	0.0049	1.6743	0.1144	0.1517	0.0047	1199	120	999	110	910	26
52	145	230	0.63	0.0930	0.0129	1.0983	0.1566	0.0857	0.0029	1487	262	753	148	530	17
53	256	394	0.65	0.0663	0.0018	1.2313	0.0415	0.1347	0.0028	816	56	815	41	815	16
54	*78*	*90*	*0.86*	*0.0757*	*0.0028*	*1.3004*	*0.0596*	*0.1245*	*0.0033*	*1088*	*75*	*846*	*59*	*757*	*19*
55	405	391	1.03	0.0726	0.0020	1.7431	0.0608	0.1742	0.0038	1002	55	1025	60	1035	21
56	56	234	0.24	0.0709	0.0019	1.5341	0.0600	0.1569	0.0044	955	56	944	59	940	24
57	108	391	0.28	0.0622	0.0029	0.7438	0.0385	0.0868	0.0018	680	101	565	38	536	11
58	*289*	*526*	*0.55*	*0.0956*	*0.0089*	*1.1804*	*0.1153*	*0.0895*	*0.0025*	*1540*	*176*	*791*	*111*	*553*	*15*
59	53	68	0.78	0.0647	0.0023	1.0887	0.0598	0.1221	0.0052	763	74	748	59	743	30
60	355	218	1.63	0.0676	0.0016	1.2160	0.0392	0.1304	0.0028	857	49	808	39	790	16
61	293	444	0.66	0.0758	0.0026	1.5898	0.0744	0.1522	0.0048	1089	69	966	73	913	27
62	*336*	*720*	*0.47*	*0.0857*	*0.0054*	*1.2746*	*0.0918*	*0.1079*	*0.0039*	*1332*	*121*	*834*	*89*	*660*	*22*
63	178	354	0.50	0.0647	0.0020	0.7532	0.0284	0.0844	0.0017	765	66	570	28	523	10
64	*350*	*730*	*0.48*	*0.0684*	*0.0039*	*0.6672*	*0.0404*	*0.0707*	*0.0014*	*881*	*118*	*519*	*40*	*441*	*9*
65	122	215	0.57	0.0605	0.0015	0.7020	0.0232	0.0842	0.0018	621	54	540	23	521	11
66	134	393	0.34	0.0593	0.0021	0.6789	0.0280	0.0830	0.0017	580	78	526	28	514	10
67	398	785	0.51	0.0775	0.0046	0.6879	0.0433	0.0643	0.0013	1135	119	532	43	402	8

68	141	440	0.32	0.0719	0.0011	1.4695	0.0371	0.1481	0.0030	984	31	918	37	891	17
69	*1039*	*1192*	*0.87*	*0.1641*	*0.0085*	*1.3107*	*0.0739*	*0.0579*	*0.0013*	*2498*	*87*	*850*	*72*	*363*	*8*
70	240	253	0.95	0.0653	0.0020	1.0658	0.0394	0.1184	0.0026	783	63	737	39	722	15
71	66	233	0.28	0.1468	0.0029	7.0273	0.4035	0.3473	0.0187	2308	34	2115	344	1922	89
72	204	759	0.27	0.0730	0.0017	1.4147	0.0514	0.1406	0.0039	1013	47	895	51	848	22
73	188	531	0.35	0.0736	0.0017	1.6075	0.0484	0.1583	0.0032	1032	45	973	48	947	18
74	97	156	0.62	0.0671	0.0015	1.2130	0.0390	0.1312	0.0030	840	47	807	39	795	17
75	*1012*	*730*	*1.39*	*0.0862*	*0.0059*	*0.6366*	*0.0454*	*0.0536*	*0.0011*	*1342*	*132*	*500*	*45*	*336*	*7*
76	494	1009	0.49	0.0704	0.0091	1.2689	0.1658	0.1307	0.0027	940	265	832	156	792	15
77	*58*	*401*	*0.14*	*0.0665*	*0.0090*	*0.6834*	*0.0935*	*0.0745*	*0.0017*	*822*	*282*	*529*	*91*	*463*	*10*
78	107	224	0.48	0.0652	0.0061	0.7778	0.0747	0.0866	0.0019	780	196	584	73	535	11
79	81	242	0.33	0.0783	0.0009	2.0054	0.0489	0.1857	0.0040	1155	23	1117	48	1098	22
80	78	119	0.65	0.0619	0.0022	1.1375	0.0495	0.1333	0.0032	670	78	771	49	807	18
Sample 10GD77 (N26°33′35.9″, E110°59′34.0″)															
1	449	643	0.70	0.0783	0.0004	2.1453	0.0262	0.1986	0.0022	1155	11	1164	12	1168	12
2	31	1160	0.03	0.1655	0.0003	10.8274	0.1158	0.4744	0.0050	2513	3	2508	22	2503	22
3	12	993	0.01	0.0741	0.0003	1.8245	0.0210	0.1785	0.0019	1045	9	1054	10	1059	10
4	36	89	0.40	0.0695	0.0016	1.4957	0.0411	0.1561	0.0024	914	47	929	13	935	13
5	238	229	1.04	0.0568	0.0011	0.6678	0.0157	0.0853	0.0011	484	44	519	6	528	6
6	206	222	0.93	0.0978	0.0007	3.7724	0.1823	0.2798	0.0134	1583	12	1587	67	1590	67
7	126	377	0.33	0.0602	0.0029	0.8264	0.0411	0.0996	0.0011	610	104	612	7	612	7
8	501	714	0.70	0.0955	0.0004	3.5473	0.0407	0.2695	0.0029	1538	7	1538	15	1538	15
9	191	262	0.73	0.1618	0.0007	10.3236	0.1321	0.4627	0.0056	2475	7	2464	25	2451	25
10	448	519	0.86	0.0783	0.0004	2.0630	0.0257	0.1910	0.0021	1155	11	1137	11	1127	11
11	49	290	0.17	0.0581	0.0008	0.7073	0.0125	0.0883	0.0010	533	28	543	6	546	6
12	484	1354	0.36	0.0727	0.0003	1.6922	0.0188	0.1688	0.0018	1006	8	1006	10	1005	10
13	450	521	0.86	0.0792	0.0005	2.0932	0.0264	0.1918	0.0021	1176	12	1147	12	1131	12
14	199	349	0.57	0.1815	0.0006	12.4809	0.1503	0.4988	0.0058	2666	5	2641	25	2609	25
15	249	1244	0.20	0.0710	0.0003	1.6025	0.0180	0.1637	0.0017	958	8	971	9	977	9
16	302	22	14.02	0.1650	0.0019	11.0775	0.3077	0.4868	0.0123	2508	19	2530	53	2557	53
17	236	276	0.86	0.0565	0.0011	0.6734	0.0154	0.0864	0.0010	472	43	523	6	534	6

18	113	163	0.70	0.0706	0.0009	1.3643	0.0254	0.1402	0.0018	945	27	874	10	846	10
19	83	92	0.90	0.1676	0.0010	10.5004	0.1681	0.4545	0.0067	2534	10	2480	30	2415	30
20	281	748	0.38	0.0586	0.0005	0.6906	0.0097	0.0855	0.0009	551	20	533	5	529	5
21	376	1284	0.29	0.0739	0.0003	1.8230	0.0204	0.1789	0.0019	1039	8	1054	10	1061	10
22	148	256	0.58	0.0766	0.0007	1.9227	0.0297	0.1821	0.0022	1110	19	1089	12	1078	12
23	140	157	0.89	0.0765	0.0040	1.8651	0.1009	0.1767	0.0024	1109	105	1069	13	1049	13
24	67	244	0.27	0.0713	0.0006	1.6079	0.0239	0.1636	0.0020	966	18	973	11	977	11
25	551	531	1.04	0.0566	0.0007	0.6603	0.0113	0.0847	0.0009	475	29	515	6	524	6
26	125	262	0.48	0.0680	0.0007	1.4018	0.0227	0.1495	0.0018	868	22	890	10	898	10
27	185	498	0.37	0.1666	0.0053	9.7275	0.7367	0.4235	0.0291	2524	54	2409	132	2276	132
28	133	216	0.61	0.0874	0.0007	2.7497	0.0442	0.2281	0.0032	1370	14	1342	17	1325	17
29	256	248	1.03	0.0675	0.0007	1.1826	0.0191	0.1271	0.0015	852	22	793	9	771	9
30	123	163	0.76	0.0596	0.0016	0.7424	0.0225	0.0903	0.0012	591	59	564	7	557	7
31	219	387	0.57	0.1231	0.0024	5.5427	0.1255	0.3265	0.0037	2002	35	1907	18	1822	18
32	233	398	0.59	0.0902	0.0005	3.0455	0.0387	0.2450	0.0028	1429	11	1419	14	1412	14
33	487	1408	0.35	0.0695	0.0003	1.4018	0.0157	0.1463	0.0015	913	8	890	9	880	9
34	105	332	0.32	0.0754	0.0006	1.8234	0.0250	0.1753	0.0020	1080	15	1054	11	1041	11
35	*77*	*315*	*0.24*	*0.1571*	*0.0007*	*7.2472*	*0.0900*	*0.3346*	*0.0039*	*2425*	*7*	*2142*	*19*	*1860*	*19*
36	192	221	0.87	0.0731	0.0010	1.6725	0.0302	0.1660	0.0021	1017	27	998	11	990	11
37	50	85	0.59	0.0695	0.0012	1.5212	0.0350	0.1588	0.0025	913	35	939	14	950	14
38	98	193	0.51	0.1877	0.0009	13.4445	0.1833	0.5194	0.0066	2722	8	2711	28	2697	28
39	162	148	1.10	0.0600	0.0014	0.7492	0.0197	0.0906	0.0012	603	49	568	7	559	7
40	39	176	0.22	0.2357	0.0008	19.4921	0.2584	0.5999	0.0077	3091	5	3066	31	3029	31
41	136	225	0.61	0.0721	0.0008	1.6440	0.0277	0.1655	0.0020	988	23	987	11	987	11
42	52	281	0.18	0.0670	0.0008	1.5151	0.0624	0.1641	0.0065	837	24	937	36	979	36
43	425	1121	0.38	0.0717	0.0003	1.6214	0.0184	0.1640	0.0017	977	9	979	10	979	10
44	185	392	0.47	0.1904	0.0005	13.2510	0.1552	0.5047	0.0057	2746	5	2698	25	2634	25
45	850	982	0.86	0.0870	0.0003	2.8416	0.0318	0.2369	0.0025	1361	7	1367	13	1370	13
46	141	465	0.30	0.0696	0.0006	1.3943	0.0195	0.1453	0.0016	917	17	887	9	875	9
47	147	179	0.82	0.0700	0.0036	1.4822	0.0781	0.1536	0.0020	928	105	923	11	921	11
48	90	182	0.50	0.0666	0.0009	1.1860	0.0221	0.1292	0.0017	825	28	794	9	783	9
49	35	232	0.15	0.0694	0.0007	1.3772	0.0223	0.1439	0.0018	911	22	879	10	867	10

50	536	718	0.75	0.1578	0.0004	9.1750	0.1039	0.4217	0.0047	2432	4	2356	21	2268	21
51	100	453	0.22	0.0707	0.0005	1.5689	0.0428	0.1610	0.0043	948	14	958	24	962	24
52	422	670	0.63	0.1829	0.0004	12.2876	0.1356	0.4874	0.0053	2679	3	2627	23	2559	23
53	117	1615	0.07	0.1618	0.0002	10.0403	0.1054	0.4499	0.0047	2475	3	2438	21	2395	21
54	145	467	0.31	0.0750	0.0005	1.6651	0.0221	0.1611	0.0018	1067	14	995	10	963	10
55	91	224	0.41	0.0591	0.0010	0.8018	0.0168	0.0983	0.0012	572	37	598	7	605	7
56	327	326	1.00	0.1595	0.0006	9.6086	0.1177	0.4369	0.0051	2450	6	2398	23	2337	23
57	686	1447	0.47	0.0784	0.0003	2.0366	0.0235	0.1884	0.0020	1157	8	1128	11	1113	11
58	131	269	0.49	0.1804	0.0037	12.2424	0.2934	0.4923	0.0062	2656	34	2623	27	2580	27
59	253	380	0.67	0.0657	0.0006	1.1631	0.0175	0.1284	0.0015	797	20	783	8	779	8
60	45	54	0.83	0.1713	0.0014	10.7877	0.2095	0.4567	0.0081	2571	14	2505	36	2425	36
61	44	106	0.42	0.1999	0.0011	14.8349	0.2325	0.5383	0.0079	2825	9	2805	33	2776	33
62	66	662	0.10	0.1150	0.0004	5.2729	0.0603	0.3325	0.0036	1880	6	1864	18	1850	18
63	168	1006	0.17	0.0715	0.0003	1.5969	0.0186	0.1621	0.0017	971	10	969	10	968	10
64	170	313	0.54	0.2833	0.0007	22.6322	0.2719	0.5794	0.0068	3381	4	3211	28	2946	28
65	312	654	0.48	0.0870	0.0040	2.5872	0.1235	0.2156	0.0025	1361	89	1297	13	1258	13
Sample 10GD78 (N26°34′05.1″, E111°01′39.1″)															
1	333	297	1.12	0.1619	0.0006	10.6353	0.1320	0.4764	0.0057	2476	6	2492	25	2512	25
2	12	40	0.31	0.0844	0.0032	2.2939	0.0978	0.1970	0.0040	1303	73	1210	22	1159	22
3	240	727	0.33	0.0581	0.0006	0.6890	0.0105	0.0860	0.0010	534	23	532	6	532	6
4	110	158	0.69	0.0671	0.0016	1.2687	0.0665	0.1372	0.0064	840	50	832	36	829	36
5	75	156	0.48	0.1118	0.0011	4.7722	0.0805	0.3094	0.0043	1830	17	1780	21	1738	21
6	341	278	1.23	0.0591	0.0010	0.6686	0.0142	0.0821	0.0010	570	38	520	6	509	6
7	32	349	0.09	0.0693	0.0007	1.3644	0.0208	0.1428	0.0017	908	20	874	9	860	9
8	370	493	0.75	0.0590	0.0006	0.7563	0.0117	0.0930	0.0011	565	23	572	6	574	6
9	313	426	0.74	0.1045	0.0005	4.4169	0.0538	0.3065	0.0035	1706	8	1716	17	1724	17
10	86	149	0.58	0.0660	0.0011	1.1672	0.0251	0.1282	0.0017	807	35	785	10	778	10
11	41	204	0.20	0.0740	0.0010	1.6430	0.0300	0.1611	0.0020	1040	27	987	11	963	11
12	36	314	0.12	0.1376	0.0285	6.7596	0.4035	0.3563	0.0043	2197	36	2080	20	1965	20
13	246	893	0.28	0.2017	0.0122	16.2840	1.0032	0.5855	0.0065	2840	99	2894	27	2971	27
14	194	1032	0.19	0.0718	0.0003	1.5948	0.0184	0.1611	0.0017	980	10	968	9	963	9

15	771	2064	0.37	0.0965	0.0002	3.6103	0.0392	0.2713	0.0029	1558	4	1552	15	1547	15
16	268	209	1.28	0.0741	0.0009	1.7343	0.0298	0.1698	0.0021	1044	23	1021	12	1011	12
17	389	614	0.63	0.3212	0.0024	32.7118	0.4315	0.7385	0.0081	3576	11	3572	30	3565	30
18	81	68	1.19	0.0568	0.0026	0.7074	0.0341	0.0903	0.0015	485	100	543	9	557	9
19	628	645	0.97	0.0697	0.0005	1.5774	0.0205	0.1643	0.0018	918	15	961	10	980	10
20	159	481	0.33	0.0697	0.0005	1.5774	0.0215	0.1641	0.0018	920	16	961	10	980	10
21	95	93	1.03	0.0755	0.0014	1.7089	0.0411	0.1642	0.0025	1082	37	1012	14	980	14
22	61	358	0.17	0.1538	0.0005	9.3664	0.1174	0.4418	0.0053	2388	6	2375	24	2359	24
23	116	387	0.30	0.0702	0.0006	1.5101	0.0437	0.1559	0.0043	935	17	934	24	934	24
24	291	327	0.89	0.1047	0.0005	4.4108	0.0566	0.3057	0.0036	1708	10	1714	18	1719	18
25	93	272	0.34	0.0703	0.0007	1.7271	0.1377	0.1781	0.0141	938	22	1019	77	1057	77
26	151	540	0.28	0.1592	0.0249	12.2395	0.8919	0.5576	0.0198	2447	25	2623	33	2857	33
27	292	494	0.59	0.1054	0.0019	4.4366	0.0953	0.3053	0.0034	1721	34	1719	17	1717	17
28	89	210	0.42	0.0619	0.0012	0.8813	0.0204	0.1033	0.0013	670	42	642	8	634	8
29	377	773	0.49	0.0770	0.0005	2.0448	0.0257	0.1926	0.0021	1122	12	1131	11	1135	11
30	468	304	1.54	0.1629	0.0006	10.6421	0.1326	0.4739	0.0056	2486	6	2492	25	2501	25
31	105	611	0.17	0.0658	0.0005	1.1915	0.0159	0.1313	0.0014	800	16	797	8	795	8
32	169	1083	0.16	0.0582	0.0004	0.7211	0.0094	0.0899	0.0010	537	16	551	6	555	6
33	223	418	0.53	0.0789	0.0006	2.0104	0.0273	0.1848	0.0021	1170	15	1119	11	1093	11
34	743	418	1.78	0.0737	0.0005	1.7764	0.0240	0.1749	0.0020	1033	15	1037	11	1039	11
35	97	100	0.97	0.0630	0.0023	0.7338	0.0295	0.0844	0.0013	709	79	559	8	523	8
36	175	714	0.25	0.0787	0.0004	2.0725	0.0252	0.1911	0.0021	1164	10	1140	11	1127	11
37	1	821	0.00	0.0600	0.0005	0.7686	0.0102	0.0929	0.0010	604	17	579	6	573	6
38	75	355	0.21	0.0587	0.0008	0.7240	0.0134	0.0895	0.0010	554	31	553	6	553	6
39	149	482	0.31	0.0699	0.0005	1.5127	0.0198	0.1570	0.0018	925	14	936	10	940	10
40	85	98	0.86	0.0991	0.0010	3.8372	0.0699	0.2809	0.0042	1607	19	1601	21	1596	21
41	70	428	0.16	0.1578	0.0005	9.0247	0.3624	0.4147	0.0166	2432	5	2341	76	2237	76
42	125	510	0.24	0.0699	0.0006	1.4903	0.0204	0.1545	0.0017	927	16	926	10	926	10
43	290	429	0.68	0.0962	0.0006	4.1040	0.0536	0.3094	0.0035	1552	12	1655	17	1738	17
44	199	1065	0.19	0.0707	0.0003	1.6092	0.0187	0.1650	0.0017	950	10	974	10	984	10
45	85	349	0.24	0.0695	0.0027	1.4226	0.0870	0.1484	0.0071	914	79	898	40	892	40
46	418	812	0.51	0.0899	0.0003	3.0068	0.0344	0.2425	0.0026	1424	7	1409	14	1400	14

47	87	388	0.22	0.1595	0.0006	9.2635	0.1146	0.4212	0.0050	2450	6	2364	23	2266	23
48	204	406	0.50	0.1839	0.0005	13.1482	0.1547	0.5185	0.0059	2688	5	2690	25	2693	25
49	123	287	0.43	0.0716	0.0007	1.6562	0.0248	0.1679	0.0020	974	19	992	11	1000	11
50	98	220	0.44	0.1372	0.0008	7.5732	0.1056	0.4002	0.0050	2193	11	2182	23	2170	23
51	304	772	0.39	0.1613	0.0018	10.2468	0.1602	0.4609	0.0050	2469	19	2457	22	2443	22
52	121	368	0.33	0.0696	0.0006	1.4266	0.0208	0.1486	0.0017	918	18	900	10	893	10
53	225	433	0.52	0.1137	0.0005	5.3268	0.0648	0.3397	0.0039	1860	7	1873	19	1885	19
54	59	171	0.35	0.1619	0.0008	10.0119	0.1396	0.4485	0.0059	2476	8	2436	26	2388	26
55	341	378	0.90	0.0592	0.0009	0.6899	0.0135	0.0845	0.0010	576	35	533	6	523	6
56	39	92	0.42	0.1669	0.0010	10.8514	0.1770	0.4715	0.0071	2527	10	2510	31	2490	31
57	229	302	0.76	0.0958	0.0006	3.4866	0.2064	0.2639	0.0155	1544	12	1524	79	1510	79
58	91	320	0.28	0.0715	0.0007	1.5993	0.0241	0.1623	0.0019	971	19	970	11	969	11
59	193	249	0.77	0.0718	0.0007	1.5966	0.0919	0.1613	0.0091	981	21	969	51	964	51
60	36	105	0.34	0.0836	0.0013	2.3183	0.0509	0.2011	0.0030	1283	31	1218	16	1181	16
61	190	370	0.51	0.0984	0.0006	3.9389	0.1343	0.2903	0.0097	1594	12	1622	49	1643	49
62	205	451	0.45	0.0747	0.0005	1.7705	0.0239	0.1720	0.0020	1060	14	1035	11	1023	11
63	142	124	1.15	0.0700	0.0043	1.5459	0.0976	0.1602	0.0023	928	126	949	13	958	13
64	423	585	0.72	0.0754	0.0004	1.8343	0.0228	0.1764	0.0019	1080	12	1058	11	1047	11
65	47	691	0.07	0.0772	0.0004	1.9531	0.0463	0.1834	0.0042	1127	10	1100	23	1085	23
66	63	59	1.06	0.0582	0.0020	0.7267	0.0302	0.0906	0.0020	536	77	555	12	559	12
67	312	330	0.95	0.0720	0.0006	1.5644	0.0224	0.1576	0.0018	985	17	956	10	944	10
68	430	973	0.44	0.0945	0.0003	3.5325	0.0409	0.2710	0.0030	1519	6	1535	15	1546	15

Note: Concordance is calculated by using $^{206}Pb/^{238}U$ ages to $^{207}Pb/^{235}U$ ages. Analyses excluded for final probability plotting due to large discordance (>10%) are given in *italics*.

Appendix D2 P and D values of two-sample Kolmogorov–Smirnov (K–S) tests on Cambrian samples from central Yangtze (Xinhuang), southeastern Yangtze (Xinning) and northwestern Cathaysia (Shaoguan), South China

	Xinhuang	Xinning (Wang)	Xinning	Shaoguan (Yao)	Shaoguan (Wang)	
Xinhuang		0.157	0.531	0.486	0.547	D value
Xinning (Wang)	**0.158**		0.392	0.348	0.397	
Xinning	0.000	0.000		0.169	0.168	
Shaoguan (Yao)	0.000	0.000	0.011		0.144	
Shaoguan (Wang)	0.000	0.000	**0.354**	**0.462**		
	P value					

Note: The results reflect the input of both determined ages and errors for each zircon grain. All probabilities (*P* values) > 0.05 indicate that the confidence of which the pair of samples can be statistically distinguished is less than 95%.

Sample probability plots: Xinhuang – Figure 6.3a, Xinning (Wang) – Figure 6.3b, Xinning – Figure 6.3c, Shaoguan (Yao) – Figure 6.3d, Shaoguan (Wang) – Figure 6.3e

Appendix D3 Zircon U–Pb Concordia age diagrams and histogram plots of lower Cambrian clastic samples from the Xinhuang area (12GH38 and 12GH39) and the Xinning area (10GD77 and 10GD78)

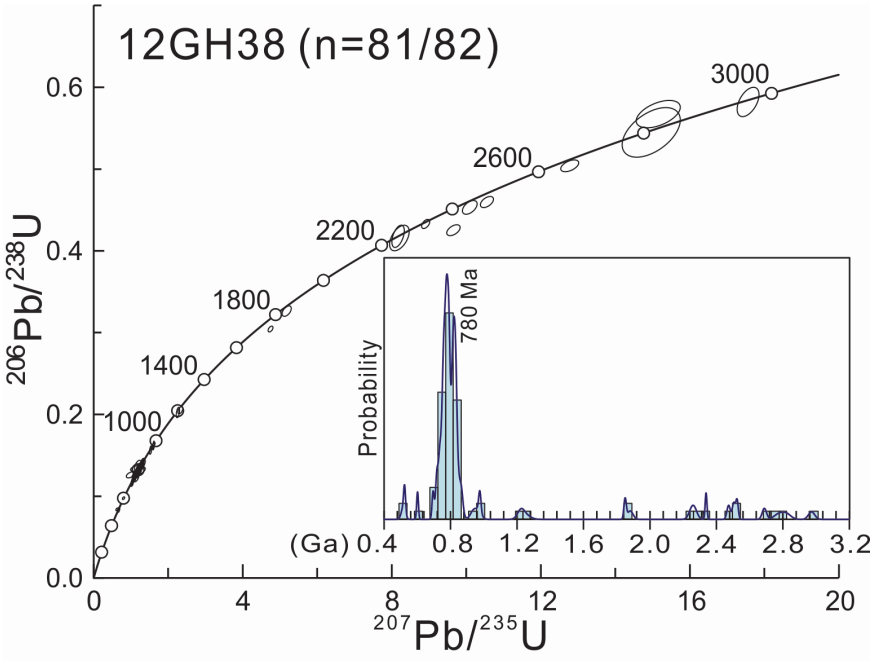

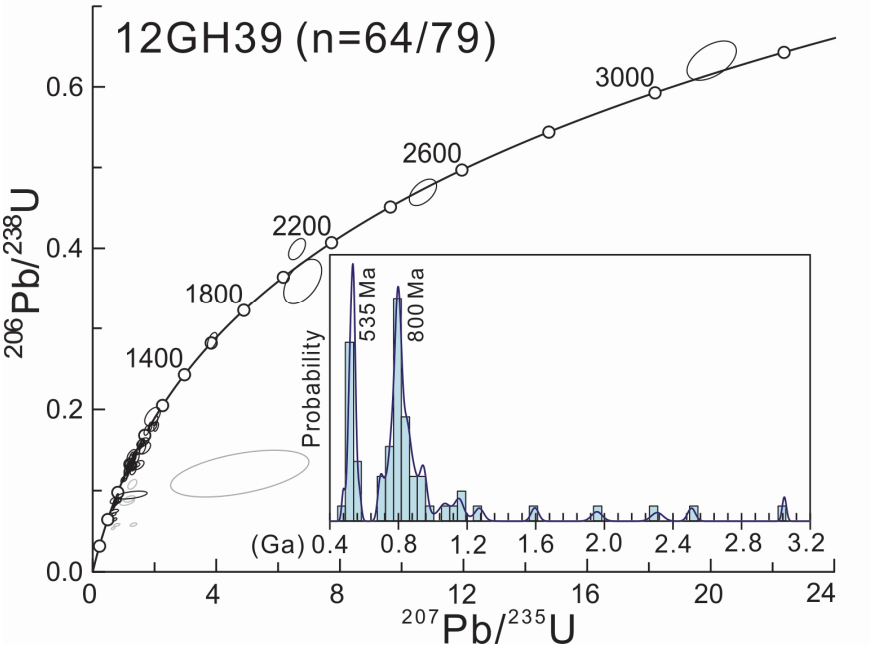

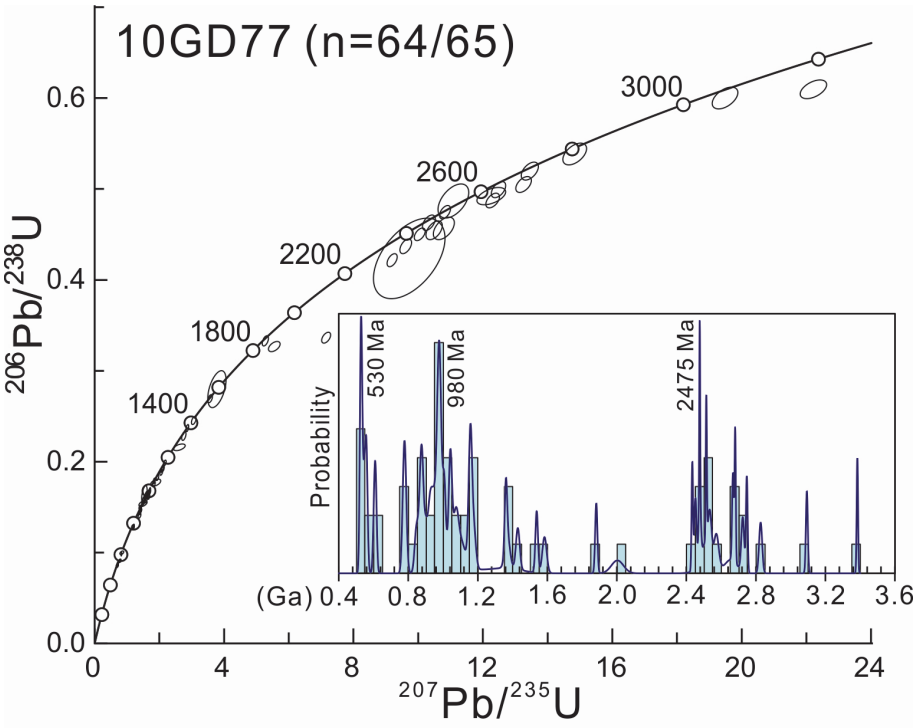
10GD77 (n=64/65)
3000
2600
2200
1800
1400
530 Ma
980 Ma
2475 Ma
Probability
(Ga) 0.4 0.8 1.2 1.6 2.0 2.4 2.8 3.2 3.6
0.0 0.2 0.4 0.6
0 4 8 12 16 20 24
$^{206}Pb/^{238}U$
$^{207}Pb/^{235}U$

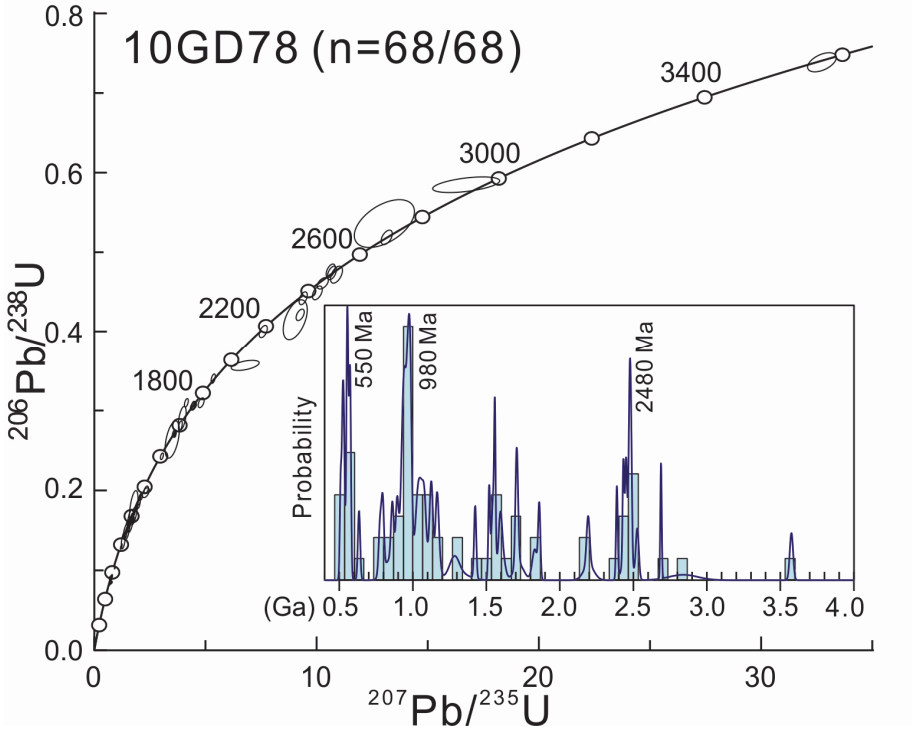
10GD78 (n=68/68)
3400
3000
2600
2200
1800
550 Ma
980 Ma
2480 Ma
Probability
(Ga) 0.5 1.0 1.5 2.0 2.5 3.0 3.5 4.0
0.0 0.2 0.4 0.6 0.8
0 10 20 30
$^{206}Pb/^{238}U$
$^{207}Pb/^{235}U$

Appendix E Statement of Contributions of Others

To whom it may concern,

I, **Wei-Hua Yao**, contributed to all aspects of research reported in this thesis, including, but not limited to, primary data collection both in the field and laboratories, data interpretation, and writing up the following published or draft research papers:

Paper 1: Yao, W.H., Li, Z.X., Li, W.X., Wang, X.C., Li, X.H., and Yang, J.H., 2012. Post-kinematic lithospheric delamination of the Wuyi–Yunkai orogen in South China: Evidence from *ca.* 435 Ma high-Mg basalts. Lithos 154, 115–129.

Paper 2: Yao, W.H., Li, Z.X., Li, W.X., Li, X.H., and Yang, J.H., 2014. From Rodinia to Gondwanaland: a tale of detrital zircon provenance analyses from the southern Nanhua Basin, South China. American Journal of Science 314, 278–313.

Paper 3: Yao, W.H., and Li, Z.X., 2014 (to be submitted). Stratigraphic history of the lower Palaeozoic Nanhua foreland basin in South China: Response to two successive orogenies.

Paper 4: Yao, W.H., Li, Z.X., Li, W.X., Su, L., and Yang, J.H., 2014 (to be submitted). Detrital provenance evolution of the lower Palaeozoic Nanhua foreland basin, South China.

Paper 5: Yao, W.H., Li, Z.X., and Li, W.X., 2014 (in press). Was there a Cambrian ocean in South China? – Insight from detrital provenance analyses.

A breakdown of percentage contributions by each co-author to these papers are given in the following pages, signed by all co-authors.

WEI-HUA YAO Weihua Yao

DATE: 11/03/2014

A realistic breakdown of the percentage contributions by each author:

Paper 1:

Title: Post-kinematic lithospheric delamination of the Wuyi–Yunkai orogen in South China: Evidence from *ca.* 435 Ma high-Mg basalts.

Journal: Lithos, Year: 2012, Volume: 154, Pages: 115–129.

Author list (and contribution): Wei-Hua Yao (60%), Zheng-Xiang Li (10%), Wu-Xian Li (10%), Xuan-Ce Wang (10%), Xian-Hua Li (5%), Jin-Hui Yang (5%)

Paper 2:

Title: From Rodinia to Gondwanaland: a tale of detrital zircon provenance analyses from the southern Nanhua Basin, South China.

Journal: American Journal of Science, Year: 2014, Volume: 314, Pages: 278–313.

Author list (and contribution): Wei-Hua Yao (60%), Zheng-Xiang Li (20%), Wu-Xian Li (10%), Xian-Hua Li (5%), Jin-Hui Yang (5%)

Paper 3:

Title: Stratigraphic history of the lower Palaeozoic Nanhua foreland basin in South China: Response to two successive orogenies (*to be submitted*).

Author list (and contribution): Wei-Hua Yao (90%), Zheng-Xiang Li (10%)

Paper 4:

Title: Detrital provenance evolution of the lower Palaeozoic Nanhua foreland basin, South China (*to be submitted*).

Author list (and contribution): Wei-Hua Yao (75%), Zheng-Xiang Li (10%), Wu-Xian Li (5%), Li Su (5%), Jin-Hui Yang (5%)

Paper 5:

Title: Was there a Cambrian ocean in South China? – Insight from detrital provenance analyses (*in press*).

Author list (and contribution): Wei-Hua Yao (85%), Zheng-Xiang Li (10%), Wu-Xian Li (5%)

I, **Zheng-Xiang Li**, as one of the co-authors and Wei-Hua's PhD supervisor, endorse that the level of contribution indicated above are appropriate.

PROF. ZHENG-XIANG LI

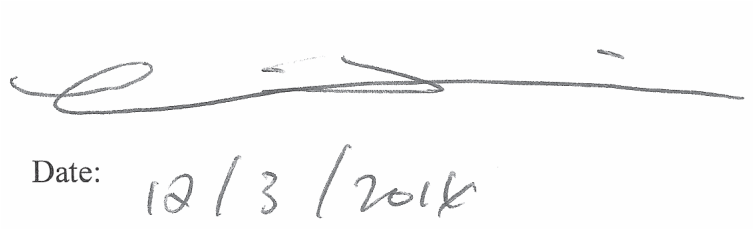

Date: 12/3/2014

I, **Wu-Xian Li**, as one of the co-authors, endorse that the level of contribution indicated above are appropriate.

PROF. WU-XIAN LI

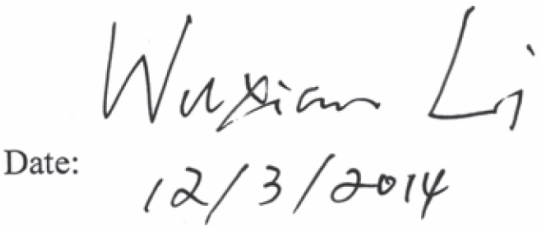

Date: 12/3/2014

I, **Xuan-Ce Wang**, as one of the co-authors, endorse that the level of contribution indicated above are appropriate.

DR. XUAN-CE WANG

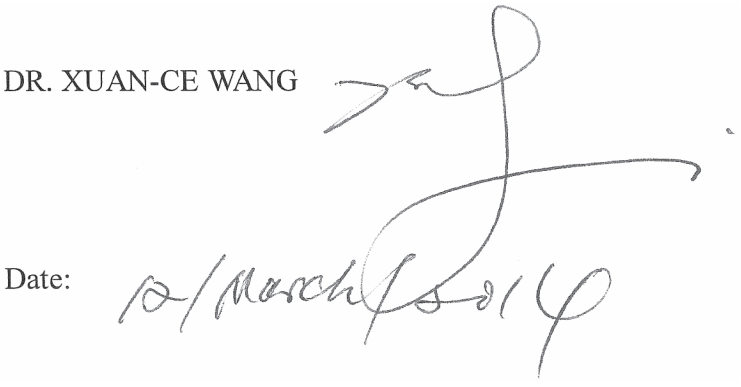

Date: 12/March/2014

I, **Xian-Hua Li**, as one of the co-authors and one of Wei-Hua's PhD associate supervisors, endorse that the level of contribution indicated above are appropriate.

PROF. XIAN-HUA LI 

Date: 14-03-2014

I, **Jin-Hui Yang**, as one of the co-authors, endorse that the level of contribution indicated above are appropriate.

PROF. JIN-HUI YANG

Date: 14-03-2014

I, **Li Su**, as a one of the co-authors, endorse that the level of contribution indicated above are appropriate.

DR. LI SU 

Date: 13-03-2014

Appendix F Permission of Copyright from Third Parties

Estimated size (number of pages)	480
Elsevier VAT number	GB 494 6272 12
Permissions price	0.00 USD
VAT/Local Sales Tax	0.00 USD / 0.00 GBP
Total	0.00 USD
Terms and Conditions	

INTRODUCTION

1. The publisher for this copyrighted material is Elsevier. Byclicking "accept" in connection with completing this licensingtransaction, you agree that the following terms and conditions apply to thistransaction (along with the Billing and Payment terms and conditionsestablished by Copyright Clearance Center, Inc. ("CCC"), at the timethat you opened your Rightslink account and that are available at any time at http://myaccount.copyright.com).

GENERAL TERMS

2. Elsevier hereby grants you permission to reproduce the aforementionedmaterial subject to the terms and conditions indicated.

3. Acknowledgement: If any part of the material to be used (for example,figures) has appeared in our publication with credit or acknowledgement toanother source, permission must also be sought from that source. If suchpermission is not obtained then that material may not be included in yourpublication/copies. Suitable acknowledgement to the source must be made, eitheras a footnote or in a reference list at the end of your publication, asfollows:

"Reprinted from Publication title, Vol /edition number, Author(s), Title ofarticle / title of chapter, Pages No., Copyright (Year), with permission fromElsevier [OR APPLICABLE SOCIETY COPYRIGHT OWNER]." Also Lancet special credit - "Reprinted from The Lancet, Vol. number, Author(s), Title of article, PagesNo., Copyright (Year), with permission from Elsevier."

4. Reproduction of this material is confined to the purpose and/or media forwhich permission is hereby given.

5. Altering/Modifying Material: Not Permitted. However figures andillustrations may be altered/adapted minimally to serve your work. Any otherabbreviations, additions, deletions and/or any other alterations shall be madeonly with prior written authorization of Elsevier Ltd. (Please contact Elsevierat permissions@elsevier.com)

6. If the permission fee for the requested use of our material is waived inthis instance, please be advised that your future requests for Elseviermaterials may attract a fee.

7. Reservation of Rights: Publisher reserves all rights not specificallygranted in the combination of (i) the license details provided by you andaccepted in the course of this licensing transaction, (ii) these terms andconditions and (iii) CCC's Billing and Payment terms and conditions.

8. License Contingent Upon Payment: While you may exercise the rightslicensed immediately upon issuance of the license at the end of the licensingprocess for the transaction, provided that you have disclosed complete andaccurate details of your proposed use, no license is finally effective unlessand until full payment is received from you (either by publisher or by CCC) asprovided in

CCC's Billing and Payment terms and conditions. If fullpayment is not received on a timely basis, then any license preliminarilygranted shall be deemed automatically revoked and shall be void as if nevergranted. Further, in the event that you breach any of these terms andconditions or any of CCC's Billing and Payment terms and conditions, thelicense is automatically revoked and shall be void as if never granted. Use of materials as described in a revoked license, as well as any use of thematerials beyond the scope of an unrevoked license, may constitute copyrightinfringement and publisher reserves the right to take any and all action toprotect its copyright in the materials.

9. Warranties: Publisher makes no representations or warranties with respectto the licensed material.

10. Indemnity: You hereby indemnify and agree to hold harmless publisher andCCC, and their respective officers, directors, employees and agents, from andagainst any and all claims arising out of your use of the licensed materialother than as specifically authorized pursuant to this license.

11. No Transfer of License: This license is personal to you and may not besublicensed, assigned, or transferred by you to any other person withoutpublisher's written permission.

12. No Amendment Except in Writing: This license may not be amended exceptin a writing signed by both parties (or, in the case of publisher, by CCC onpublisher's behalf).

13. Objection to Contrary Terms: Publisher hereby objects to any termscontained in any purchase order, acknowledgment, check endorsement or otherwriting prepared by you, which terms are inconsistent with these terms andconditions or CCC's Billing and Payment terms and conditions. These termsand conditions, together with CCC's Billing and Payment terms and conditions(which are incorporated herein), comprise the entire agreement between you andpublisher (and CCC) concerning this licensing transaction. In the eventof any conflict between your obligations established by these terms andconditions and those established by CCC's Billing and Payment terms andconditions, these terms and conditions shall control.

14. Revocation: Elsevier or Copyright Clearance Center may deny thepermissions described in this License at their sole discretion, for any reasonor no reason, with a full refund payable to you. Notice of such denialwill be made using the contact information provided by you. Failure toreceive such notice will not alter or invalidate the denial. In no eventwill Elsevier or Copyright Clearance Center be responsible or liable for anycosts, expenses or damage incurred by you as a result of a denial of yourpermission request, other than a refund of the amount(s) paid by you toElsevier and/or Copyright Clearance Center for denied permissions.

LIMITED LICENSE

The following terms and conditions apply only to specific license types:

15. **Translation**: This permission is granted fornon-exclusive world **English** rights only unless yourlicense was granted for translation rights. If you licensed translation rightsyou may only translate this content into the languages you requested. Aprofessional translator must perform all translations and reproduce the contentword for word preserving the integrity of the article. If this license is tore-use 1 or 2 figures then permission is granted for non-exclusive world rightsin all languages.

16. **Posting licensed content on any Website**: The followingterms and conditions apply as follows: Licensing material from an Elsevierjournal: All content posted to the web site must maintain the copyright informationline on the bottom of each image; A hyper-text must be included to the

Homepageof the journal from which you are licensing at http://www.sciencedirect.com/science/journal/xxxxx orthe Elsevier homepage for books at http://www.elsevier.com; CentralStorage: This license does not include permission for a scanned version of thematerial to be stored in a central repository such as that provided byHeron/XanEdu.

Licensing material from an Elsevier book: A hyper-text link must be includedto the Elsevier homepage at http://www.elsevier.com . Allcontent posted to the web site must maintain the copyright information line onthe bottom of each image.

Posting licensed content on Electronic reserve: In addition to the above the following clausesare applicable: The web site must be password-protected and made available onlyto bona fide students registered on a relevant course. This permission isgranted for 1 year only. You may obtain a new license for future websiteposting.

For journal authors: the following clauses are applicable inaddition to the above: Permission granted is limited to the author acceptedmanuscript version* of your paper.

***Accepted Author Manuscript (AAM) Definition:** An accepted authormanuscript (AAM) is the author's version of the manuscript of an article thathas been accepted for publication and which may include any author-incorporatedchanges suggested through the processes of submission processing, peer review,and editor-author communications. AAMs do not include other publishervalue-added contributions such as copy-editing, formatting, technicalenhancements and (if relevant) pagination.

You are not allowed to download and post the published journal article (whetherPDF or HTML, proof or final version), nor may you scan the printed edition tocreate an electronic version. A hyper-text must be included to the Homepage ofthe journal from which you are licensing at http://www.sciencedirect.com/science/journal/xxxxx. As part of our normal production process, you will receive an e-mail noticewhen your article appears on Elsevier's online service ScienceDirect(www.sciencedirect.com). That e-mail will include the article's Digital ObjectIdentifier (DOI). This number provides the electronic link to the publishedarticle and should be included in the posting of your personal version. We askthat you wait until you receive this e-mail and have the DOI to do any posting.

Posting to a repository: Authorsmay post their AAM immediately to their employer's institutional repository forinternal use only and may make their manuscript publically available after thejournal-specific embargo period has ended.

Please also refer to Elsevier'sArticle Posting Policy for further information.

18. **For book authors** the following clauses are applicable in addition tothe above: Authors are permitted to place a briefsummary of their work online only.. You are notallowed to download and post the published electronic version of your chapter,nor may you scan the printed edition to create an electronic version. Posting to a repository: Authors arepermitted to post a summary of their chapter only in their institution'srepository.

20. **Thesis/Dissertation**: If your license is for use in athesis/dissertation your thesis may be submitted to your institution in eitherprint or electronic form. Should your thesis be published commercially, pleasereapply for permission. These requirements include permission for the Libraryand Archives of Canada to supply single copies, on demand, of the completethesis and include permission for UMI to supply single copies, on demand, ofthe complete thesis. Should your

thesis be published commercially, pleasereapply for permission.

Elsevier Open Access Terms andConditions

Elsevier publishes Open Access articles in both its Open Access journals andvia its Open Access articles option in subscription journals.

Authors publishing in an Open Access journal or who choose to make theirarticle Open Access in an Elsevier subscription journal select one of thefollowing Creative Commons user licenses, which define how a reader may reusetheir work: Creative Commons Attribution License (CC BY), Creative CommonsAttribution – Non Commercial - ShareAlike (CC BY NCSA) and Creative Commons Attribution – Non Commercial – No Derivatives (CC BYNC ND)

Terms & Conditions applicable toall Elsevier Open Access articles:

Any reuse of the article must not represent the author as endorsing theadaptation of the article nor should the article be modified in such a way asto damage the author's honour or reputation.

The author(s) must be appropriately credited.

If any part of the material to be used (for example, figures) has appearedin our publication with credit or acknowledgement to another source it is theresponsibility of the user to ensure their reuse complies with the terms andconditions determined by the rights holder.

Additional Terms & Conditionsapplicable to each Creative Commons user license:

CC BY: You may distribute andcopy the article, create extracts, abstracts, and other revised versions,adaptations or derivative works of or from an article (such as a translation),to include in a collective work (such as an anthology), to text or data minethe article, including for commercial purposes without permission from Elsevier

CC BY NC SA: For non-commercialpurposes you may distribute and copy the article, create extracts, abstractsand other revised versions, adaptations or derivative works of or from anarticle (such as a translation), to include in a collective work (such as ananthology), to text and data mine the article and license new adaptations or creationsunder identical terms without permission from Elsevier

CC BY NC ND: For non-commercialpurposes you may distribute and copy the article and include it in a collectivework (such as an anthology), provided you do not alter or modify the article,without permission from Elsevier

Any commercial reuse of Open Access articles published with a CC BY NC SA or CC BY NC NDlicense requires permission from Elsevier and will be subject to a fee.

Commercial reuse includes:

- Promotional purposes (advertising or marketing)
- Commercial exploitation (e.g. a product forsale or loan)

- Systematic distribution (for a fee or free ofcharge)

Please refer to Elsevier'sOpen Access Policy for further information.

21. **Other Conditions**:

v1.7

If you would like to pay for this license now, please remit this license along with your payment made payable to "COPYRIGHT CLEARANCE CENTER" otherwise you will be invoiced within 48 hours of the license date. Payment should be in the form of a check or money order referencing your account number and this invoice number RLNK501239821. Once you receive your invoice for this order, you may pay your invoice by credit card. Please follow instructions provided at that time.

Make Payment To:
Copyright Clearance Center
Dept 001
P.O. Box 843006
Boston, MA 02284-3006

For suggestions or comments regarding this order, contact RightsLink Customer Support: customercare@copyright.com or +1-877-622-5543 (toll free in the US) or +1-978-646-2777.

Gratis licenses (referencing $0 in the Total field) are free. Please retain this printable license for your reference. No payment is required.

American Journal of Science

217 Kline Geology Laboratory
Yale University
P.O. Box 208109
New Haven, Connecticut 06520-8109
Email: ajs@yale.edu

Campus address:
Kline Geology Laboratory
210 Whitney Avenue
Telephones:
203 432-3131
203 432-5668
FAX: 203 432-5668

1st July 2014

Wei-Hua Yao
Department of Applied Geology
Curtin University
Kent Street
Bentley, WA 6102 Australia

Dear Ms. Yao,

We understand that you are publishing a doctoral thesis titled "Evolution of the Lower Palaeozoic Nanhua Foreland Basin and Nature of the Wuyi-Yunkai Orogeny, South China." You are requesting permission to publish the following paper in the thesis.

Yao, W.H., Li, Z. X., Li, W.X., Li, X.H., and Yang, J.H., 2014, From Rodinia to Gondwanaland: a tale of detrital zircon provenance analyses from the southern Nanhua Basin, South China: American Journal of Science, v. 314, p. 278-313, doi:10.2475/01.2014.08

Permission is granted for Wei-Hua Yao to include the above-mentioned material in her higher degree thesis for Curtin University, and to communicate this material via the Australasian Digital Thesis Program. This permission is granted on a non-exclusive basis and for an indefinite period.

We ask that you give credit to the American Journal of Science for the original work and permission for its use.

If material appears in our book with credit given to another source, authorization from that source is required.

Sincerely,

Danny M. Rye, Editor

American Journal of Science